

**Remote asymmetric induction in the organocatalytic aza-Darzens synthesis of peptide aziridines: towards the assembly of new glycopeptide antibiotic analogues**

**Polly-Anna Ashford**

Thesis submitted in part fulfillment of the requirements for the degree of Doctor of  
Philosophy

Supervisor: Dr Sean P. Bew



School of Chemistry

University of East Anglia

Norwich Research Park

September 2014

This copy of the thesis has been supplied on condition that anyone who consults it is understood to recognise that its copyright rests with the author and that use of any information derived there from must be in accordance with current UK Copyright Law. In addition, any quotation or extract must include full attribution.

## **Declaration**

The research presented in this thesis is, to the best of my knowledge, original except where due reference is made.

*Polly-Anna Ashford*

## **Abstract**

The widespread development of bacterial resistance to antibiotics is an ongoing process which represents a growing problem for modern medicine. Vancomycin is used as a drug of last resort against methicillin-resistant *Staphylococcus aureus* (MRSA), but the increasing prevalence of vancomycin-resistant bacteria has intensified the search for new antibiotics. The introductory chapter of this thesis presents an overview of publications reporting the synthesis of glycopeptide analogues and derivatives in the last decade, highlighting the successful approaches which have brought new pharmaceutical drugs to the market.

The results and discussion section of this work focusses first on the synthesis of a triaryl biether structure, which is a common feature of the glycopeptide antibiotic family and represents the beginning of a versatile synthetic approach towards natural products like orienticin C and vancomycin. The second discussion chapter describes the development of an asymmetric organocatalytic aza-Darzens aziridination protocol using diazo peptides and amino acid imines as substrates. A structurally diverse range of peptide aziridines are reported in yields and diastereoselectivity of up to 99%.

It is anticipated that the remote asymmetric induction methodology described in this thesis will be applicable not only to the synthesis of novel glycopeptide antibiotics and other peptide-based pharmaceutical compounds, but also to the more general asymmetric synthesis of natural and unnatural amino acids.

### **Publications arising from this research**

“Recent advances in the synthesis of new glycopeptide antibiotics”

Polly-Anna Ashford and Sean P. Bew, *Chem. Soc. Rev.*, **2012**, *41*, 957.

“Synthesis of Structure and Function Diverse  $\alpha$ -D-Diazoacetates,  $\alpha$ -D-Diazoacetamides,  $\alpha$ -D-Diazoketones, and the Antibiotic  $\alpha$ -D-Azaserine”

Sean P. Bew, Polly-Anna Ashford and Dominika U. Bachera, *Synthesis*, **2013**, *45*, 903.



## **Acknowledgements**

Out of a department full of friends and colleagues, my particular thanks go to the most recent bunch of Bew lab misfits: Glyn, Little Sean, Dominika, Victor, Deeptee, and Wilf. I've been very lucky to have your support and company during my PhD. Thank you also to my supervisor Dr Sean Bew for never running out of ideas or enthusiasm for the research, and for always finding the funding.

My parents have helped in every way they could, and their emotional and financial support has been invaluable. Thank you mum, for looking after me in the little cottage in Lyng, and thank you to the Norfolk and Norwich University Hospital for my NMR-friendly titanium plate.

Last but not least... Thank you Andy, for putting up with me in the final throes of my thesis writing, for providing unlimited tofu and cider, and for always finding ways to make me smile.

### List of Abbreviations

AA	amino acid
Ac	acetyl
ADME	absorption, distribution, metabolism and excretion
Aib	$\alpha$ -aminoisobutyric acid
Ar	aryl
BINAP	2,2'-bis(diphenylphosphino)-1,1'-binaphthyl
BINOL	1,1'-bi-2-naphthol
Bn	benzyl
Boc	<i>tert</i> -butoxycarbonyl
Bu	butyl
Bz	benzoyl
CAN	cerium(IV) ammonium nitrate
Cbz	carboxybenzyl
cod	1,5-cyclooctadiene
CTAB	cetyltrimethylammonium bromide
Cy	cyclohexyl
DABCO	1,4-diazabicyclo[2.2.2]octane
DBU	1,8-diazabicyclo[5.4.0]undec-7-ene
DCC	<i>N,N'</i> -dicyclohexylcarbodiimide
DCM	dichloromethane
DCU	<i>N,N'</i> -dicyclohexylurea
de	diastereomeric excess
DIBAL-H	diisobutylaluminium hydride
DIPEA	<i>N,N</i> -diisopropylethylamine
DMA	<i>N,N</i> -dimethylacetamide
DMF	<i>N,N</i> -dimethylformamide
DMSO	dimethyl sulfoxide
DPPA	diphenylphosphoryl azide
dr	diastereomeric ratio
DtBPF	1,10- <i>bis</i> (di- <i>tert</i> -butylphosphino)ferrocene
EC <sub>50</sub>	median effective concentration
EDCI	1-ethyl-3-(3-dimethylaminopropyl)carbodiimide

ee	enantiomeric excess
Et	ethyl
FT-IR	Fourier transform infrared spectroscopy
h	hour(s)
HATU	1-[bis(dimethylamino)methylene]-1H-1,2,3-triazolo[4,5-b]pyridinium 3-oxid hexafluorophosphate
HBTU	<i>O</i> -benzotriazole- <i>N,N,N',N'</i> -tetramethyluronium hexafluorophosphate
HNESP	high-resolution nanoelectrospray
HPLC	high performance liquid chromatography
LA	Lewis acid
MALDI-TOF	matrix-assisted laser desorption/ionization – time of flight
MeCN	acetonitrile
MIC	minimum inhibitory concentration
MRSA	methicillin-resistant <i>Staphylococcus aureus</i>
MS	molecular sieves
NBS	<i>N</i> -bromosuccinimide
NMR	nuclear magnetic resonance
Ph	phenyl
PG	peptidoglycan
PMP	<i>para</i> -methoxyphenyl
pMZ	9-methoxybenzyloxycarbonyl
ppm	parts per million
Pt	protecting group
pTSA	<i>para</i> -toluenesulfonic acid
PyrHOTf	pyridinium triflate
RAI	remote asymmetric induction
rt	room temperature
<i>S. aureus</i>	<i>Staphylococcus aureus</i>
S <sub>N</sub> Ar	nucleophilic aromatic substitution
SPhos	2-dicyclohexylphosphino-2',6'-dimethoxybiphenyl
TBAF	tetra- <i>n</i> -butylammonium fluoride
TBDPS	<i>tert</i> -butyldiphenylsilyl
TBTU	<i>O</i> -(benzotriazol-1-yl)- <i>N,N,N',N'</i> -tetramethyluronium

	tetrafluoroborate
<sup>t</sup> Bu	<i>tert</i> -butyl
TBDA	<i>tert</i> -butyl diazoacetate
TES	triethylsilyl
Tf	triflyl
TFA	trifluoroacetic acid
THF	tetrahydrofuran
TLC	thin layer chromatography
TMG	1,1,3,3-tetramethylguanidine
TMS	trimethylsilyl
Ts	tosyl
VANOL	3,3'-diphenyl-2,2'-bi-1-naphthol
VAPOL	2,2'-diphenyl-(4-biphenanthrol)
VRE	vancomycin-resistant <i>enterococci</i>
VRSA	vancomycin-resistant <i>Staphylococcus aureus</i>

## Contents

### **Introduction**

#### ***Chapter 1: Synthesis of new glycopeptide antibiotics***

1.1: History of vancomycin	1
1.2: Structure of the glycopeptide antibiotics	3
1.3: Mode of action	4
1.4: Semi-synthetic glycopeptide antibiotics	6
1.4.1 Oritavancin, telavancin and dalbavancin	6
1.4.2: Modification of the amino acids within the polypeptide chain	7
1.4.3: Introduction of hydrophobic side chains to the peripheral glycopeptide structure	15
1.5: Glycopeptide dimerisation studies	24
1.6: Synthesis of complestatin	36
1.7: Latest developments in the synthesis of new glycopeptide antibiotic Analogues	43
1.8: Conclusions	47

#### ***Chapter 2: Remote asymmetric induction (>1,5-stereocontrol)***

2.1 Introduction	49
2.2 Overview of remote stereocontrol	50
2.3 Cyclic substrates in remote asymmetric induction	54
2.3.1 Steric control in cyclisation reactions	54
2.3.2 Remote stereocontrol by the $\pi$ -allyltricarboxyliron lactone chiral auxiliary	57
2.3.3 Asymmetric keto boronate reduction	59
2.3.4 Chiral sulfoxides in remote asymmetric induction	60
2.4 Acyclic substrates in remote asymmetric induction	63
2.4.1 Remote asymmetric induction in the aldol addition reaction	64
2.4.2 Allylstannanes in remote asymmetric induction	69
2.4.3 Remote asymmetric induction in the Grignard reaction	72
2.4.4 Organolithium reagents in remote asymmetric induction	74

2.5 Atropisomeric and helical chiral substrates for RAI	77
2.6 Conclusions	81
2.7 Project aims	82
<b>Results and Discussion</b>	
<i><b>Chapter 3: Construction of the orienticin C backbone</b></i>	
3.1: Introduction	85
3.2: Diaryl ether coupling	86
3.2.1: S <sub>N</sub> Ar synthesis of triaryl biether and diaryl ether aldehydes	89
3.2.2: Mechanistic rationale and spectroscopic analysis	91
3.2.3: Diaryl ether coupling under continuous flow conditions	95
3.3: Synthesis of the ring <b>D</b> amino acid moiety of orienticin C	98
<i><b>Chapter 4: Synthesis of peptide aziridines via the aza-Darzens reaction</b></i>	
4.1: Racemic aza-Darzens aziridination of diaryl and triaryl ether aldehydes	108
4.2: Asymmetric, organocatalytic synthesis of peptide aziridines <i>via</i> remote chiral induction	113
4.2.1 Synthesis of diazopeptides using <i>N,N'</i> -ditosylhydrazine	115
4.2.2 Synthesis of diazopeptides using succinimidyl diazoacetate	118
4.2.3 Asymmetric organocatalytic aza-Darzens aziridination of non-chiral aryl imines with diazopeptides	120
4.2.4 One-pot asymmetric organocatalytic aza-Darzens reaction of peptide imines with diazopeptides	126
4.2.5 Asymmetric synthesis of <i>N</i> - $\alpha$ -methylbenzyl peptide aziridine <b>455</b>	132
4.2.6 Investigating the effect of temperature and chiral distance on stereoselectivity	135
4.2.7 Assigning the absolute stereochemistry of <i>cis</i> -aziridine <b>427</b>	139
4.3: Conclusions	143
4.4: Future work	144
<b>Experimental Section</b>	<b>146</b>
<b>Bibliography</b>	<b>220</b>
<b>Appendix: X-ray crystallographic data for compounds <b>305</b> and <b>406a</b></b>	<b>235</b>

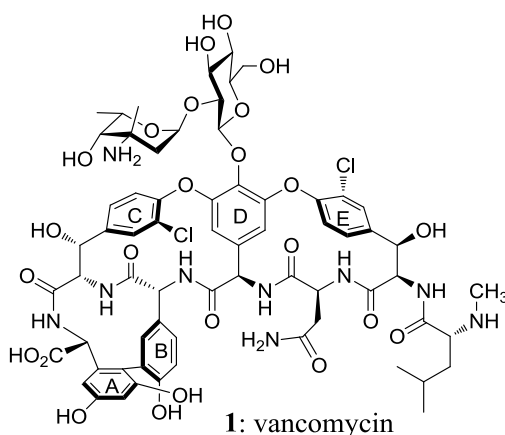
## CHAPTER ONE

### Synthesis of new glycopeptide antibiotics

Note: Section 1.1-1.6 published as “Recent advances in the synthesis of new glycopeptide antibiotics”, P. Ashford and S. P. Bew, *Chem. Soc. Rev.*, **2012**, *41*, 957. Reproduced by permission of the Royal Society of Chemistry.

## 1.1 History of vancomycin

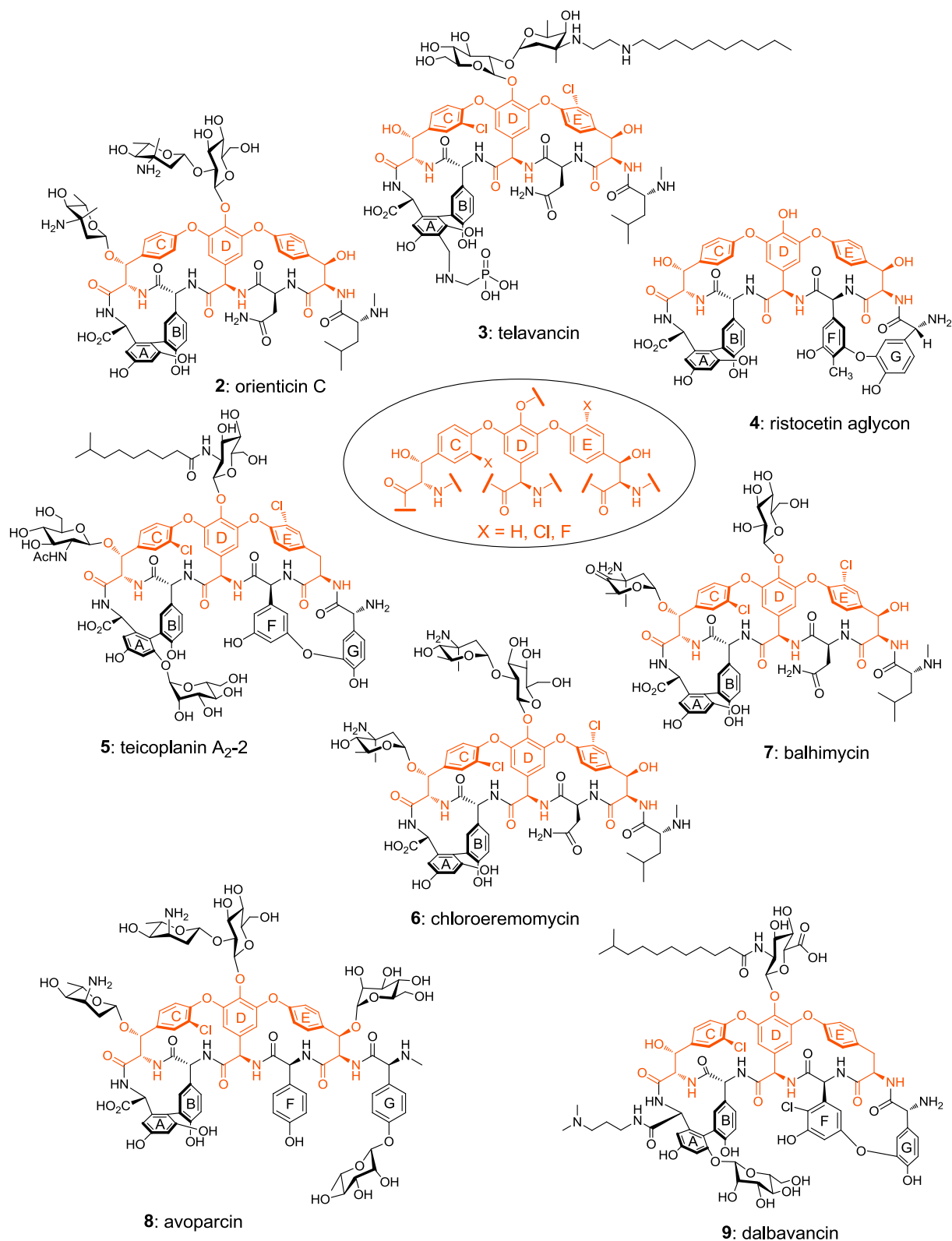
The discovery of vancomycin in 1956 was the dawn of a new age for antibacterial research, and over the last 50 years has led to the formation of a large class of compounds, natural and synthetic, known as the glycopeptide antibiotics. Scientists at Eli Lilly isolated vancomycin from the fermentation broth of *Streptomyces orientalis*, grown from a soil sample originating in the jungles of Borneo.<sup>1</sup> It displays potent activity against a range of Gram-positive bacteria, with an *in vitro* minimum inhibitory concentration (MIC) of 0.25–10.0  $\mu\text{g mL}^{-1}$  against *Staphylococcus aureus*.<sup>2</sup> Vancomycin was approved by the FDA in 1958, but was initially limited in clinical use due to its apparent side effects,<sup>3</sup> with methicillin becoming the antibiotic of choice against *S. aureus*. However, the sharp rise in drug-resistant strains, in particular the deadly methicillin-resistant *Staphylococcus aureus* (MRSA), has brought vancomycin back into the limelight, prompting a new wave of research into the chemistry and biology of this natural product.



**Figure 1.1 •** Molecular structure of vancomycin (**1**)

By 1989, a handful of glycopeptide antibiotics had been isolated and characterised. Among them, ristocetin (**4**) and teicoplanin (**5**) displayed antibacterial activity comparable to that of vancomycin (Figure 1.2).<sup>4</sup> Avoparcin (**8**) was widely used as a growth promoter in animal feed until a link was established between its use and the increased prevalence of vancomycin-resistant *enterococci* (VRE) in the food industry.<sup>5</sup> The use of avoparcin was banned in all EU countries by 1997.





**Figure 1.2 • The vancomycin family of glycopeptide antibiotics**

While vancomycin continues to be a crucial drug of last resort, the rise in geographically isolated human cases of VRE and the appearance of vancomycin-resistant *Staphylococcus aureus* (VRSA)<sup>6</sup> has signalled urgent research into the development of potent glycopeptide-based antibiotics in both an academic setting and in pharmaceutical and medicinal laboratories within industry. In the last ten years there has been increasing global interest in the design and development of semi-synthetic variants of natural product glycopeptides which have been aimed at providing a solution to this problem, either by modification of the existing scaffold, by the introduction of hydrophobic moieties or by dimerisation.<sup>7</sup> From recent reports, patterns of activity have emerged that may influence and direct future studies.

## 1.2 Structure of the glycopeptide antibiotics

Notable early attempts to elucidate the structure of vancomycin included rigorous NMR experiments carried out by D. H. Williams,<sup>8</sup> and X-ray crystallography of a less complex degradation product by G. Sheldrick,<sup>9</sup> but the precise structure was finally confirmed in 1982 by Harris and Harris.<sup>10</sup> Further NMR studies in 1993 showed that the glycopeptide exists mainly as a dimer in solution,<sup>11</sup> and thanks to advances in X-ray crystallography this observation was confirmed by a full crystal structure of vancomycin in 1996, which also gave an accurate picture of the stereochemistry.<sup>12</sup> The molecular structure of vancomycin consists of the **C-O-D-O-E** triaryl biether backbone forming two 16-membered ring macrocycles with a heptapeptide framework (Figure 1.1). A 12-membered ring comprising the **A-B** biaryl system forms a third macrocycle. It is interesting to note the conserved triaryl biether moiety in this class of compounds (Figure 1.2).

Chloro substitution of aromatic rings **C** and **E** and the strained nature of the macrocyclic systems causes vancomycin to adopt the low energy conformation (atropisomer) shown in Figure 1.1. There is no rotation of the **C** or **D** rings about the adjacent C–C and C–O bonds at ambient temperature; a study by Boger showed that **D-O-E** ring of vancomycin algycon is able to undergo thermal interconversion to the unnatural atropisomer at 110 °C in *o*-dichlorobenzene with a half-life of 94 h.<sup>13</sup>

There is a second region of atropisomerism associated with the **A-B** biaryl system, giving a total of 8 possible atropisomers and 18 chiral carbon centres. Selecting the natural

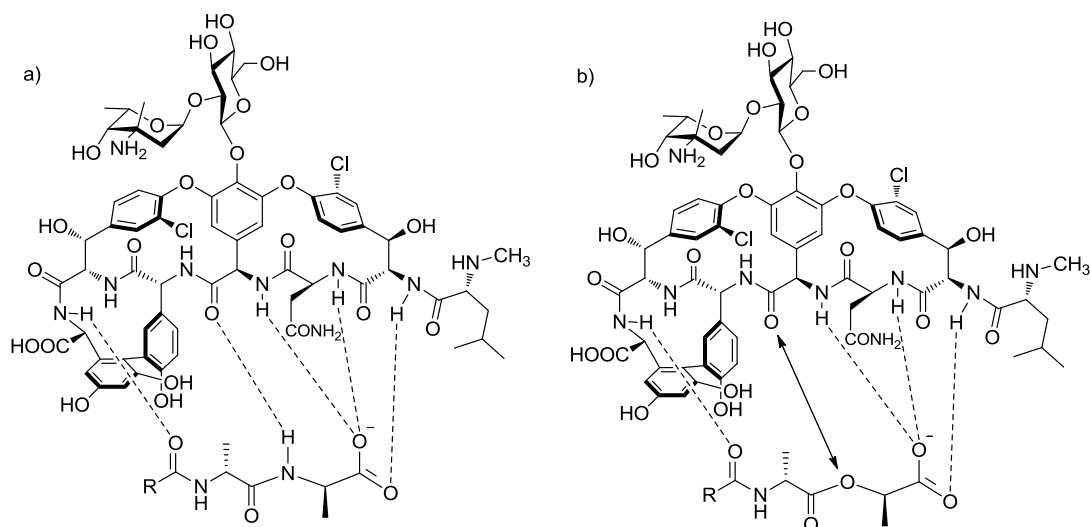
product atropisomer is therefore an important consideration when constructing these large ring systems.

A characteristic vancomycin feature is the disaccharide moiety mounted on the **D** ring, which consists of a  $\beta$ -D-glucose unit attached to a unique amino-sugar, vancosamine. Of the naturally-occurring glycopeptides, orienticin **C** (**2**), chloroeremomycin (**6**) and balhimycin (**7**) possess an additional carbohydrate unit on amino acid residue 6,  $\beta$ -hydroxytyrosine, (L-vancosamine, L-4-epivancosamine and 4-oxovancosamine respectively). Teicoplanin (**5**) is one of the most complex members of the vancomycin family, with *N*-acetyl- $\beta$ -D-glucosamine and D-mannose at residue 6 and 7 respectively, and a nine-carbon chain appended to the top of the molecule, as well as an additional 14-membered macrocycle (**F-O-G**). The complestatin sub-group discussed later in this review contains a tryptophan moiety in place of the **D-O-E** macrocycle.

### 1.3 Mode of action

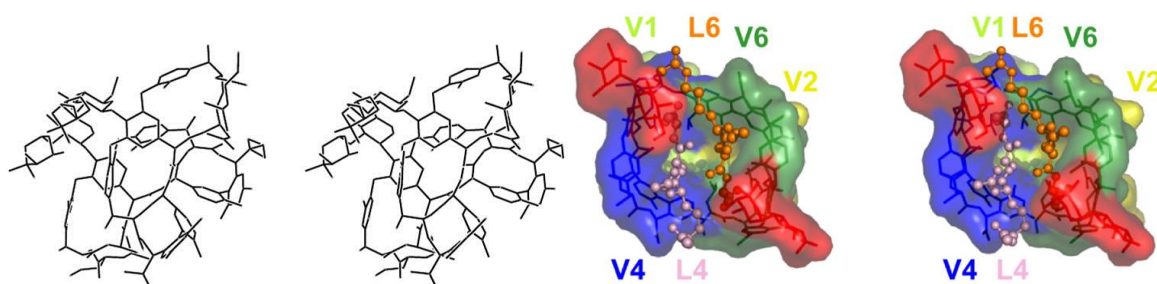
Bacterial cell walls contain a semi-rigid polymer called peptidoglycan, or murein, which acts as a structural support. The peptidoglycan monomers consist of peptide and disaccharide units that are joined in long chains by glycosidic bonds *via* transglycosidation. Cross-linking of the chains, or transpeptidation, affords the polymer a rigid framework. The glycopeptide antibiotics are able to pass through the peptidoglycan layer to the site of polymerisation, whereupon they form non-covalent bonds with the terminal carbohydrates, in a process that ultimately inhibits cross-linking by the transpeptidase enzyme. The weakened cell wall is no longer able to withstand the positive osmotic pressure within the cell, leading to cytolysis and bacteria death.

Previous NMR and X-ray studies<sup>14</sup> indicate that vancomycin binds to the L-Lys-D-Ala-D-Ala terminus of the peptidoglycan precursor *via* five hydrogen bonds (Figure 1.3a). It is interesting to note that a number of glycopeptides, such as vancomycin and ristocetin, have the ability to dimerise in aqueous solution. Dimerisation is of particular importance because glycopeptides such as eremomycin, with a high dimerisation constant (*ca.*  $106 \text{ M}^{-1}$ ) are potent antibiotics even though binding to cell wall analogs is only moderate ( $K_b$  *ca.*  $104 \text{ M}^{-1}$ ).<sup>15</sup>



**Figure 1.3** • Vancomycin binding to a) D-Ala-D-Ala terminus of susceptible bacteria and b) D-Ala-D-Lac terminus of resistant strains

X-ray crystallographic investigations by Sheldrick *et al.* in 1996 revealed the dimerisation activity of vancomycin (Figure 1.4), but recent X-ray crystal structures by Nitnai *et al.* provide a more detailed picture of the “back-to-back”, “face-to-face” and “side-to-side” arrangements observed in vancomycin binding to analogues of the peptidoglycan terminus (Figure 1.4). Teicoplanin (**5**) is unable to dimerise in solution, but contains a structural feature that is absent in vancomycin: an *N*-acylglucosamine moiety containing a 2-methyloctanyl chain (in the dominant component, teicoplanin A<sub>2</sub>-2). It has been shown that this lipophilic tail anchors the antibiotic to the phospholipid bilayer of the bacterial cell membrane.<sup>15</sup>



**Figure 1.4** • Stereoview of the vancomycin dimer by Sheldrick *et al.*<sup>12</sup> (left) Stereoview by Nitnai *et al.* showing the vancomycin dimer-to-dimer structure in the L-Lys-D-Ala-D-Ala complex.<sup>18</sup> (right)

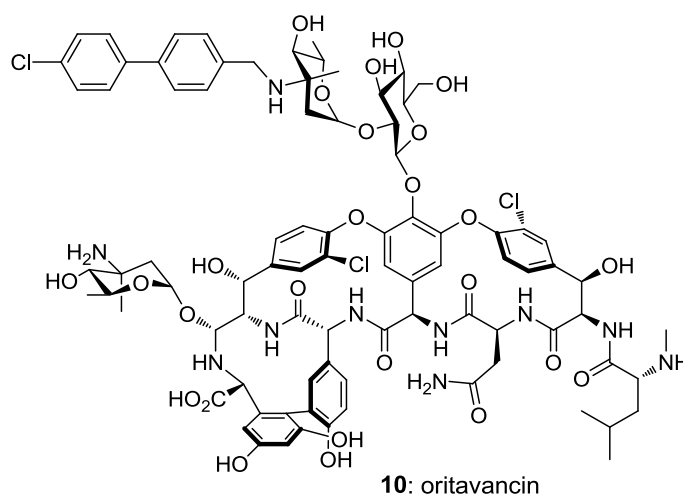
Changes in the structure of the peptidoglycan termini lead to vancomycin resistance. The most common phenotypes of vancomycin-resistant *enterococci* (VRE), VanA and VanB,

were found to have a D-lactate terminus in place of D-alanine.<sup>16</sup> This removes one of the hydrogen bonding interactions and leads to lone pair-lone pair repulsion (Figure 1.3b). A comprehensive review covering the mode of action of the glycopeptides antibiotics and the mechanisms of bacterial resistance has been compiled by Walsh and Kahne *et al.*<sup>17</sup>

## 1.4 Semi-synthetic glycopeptide antibiotics

### 1.4.1 Oritavancin, telavancin and dalbavancin

Early studies by Nagarajan *et al.* into the development of semi-synthetic glycopeptide antibiotics focused on utilizing vancomycin as a structural starting point, but the inadequate activity of vancomycin analogues<sup>19</sup> led to the selection of alternatives like teicoplanin (**5**) and chloroeremomycin (**6**) as platforms for novel glycopeptide elaboration. Structurally similar to teicoplanin (**5**) is the semi-synthetic compound dalbavancin (**9**) which is appended with an additional amide group at the C-terminus. Dalbavancin has come close to clinical success, and is currently undergoing phase III clinical trials funded by Durata Therapeutics.<sup>i</sup> Although its activity is similar to that of teicoplanin, the semi-synthetic compound has a remarkably long half-life of *ca.* 7 days as a result of strong binding to serum proteins.<sup>20</sup> By comparison, vancomycin has an elimination half-life of 3–9 h.<sup>21</sup> A drug that remains in the blood plasma for longer requires less frequent dosing, and is therefore clinically and economically advantageous.



**Figure 1.5 •** Molecular structure of oritavancin (**10**)

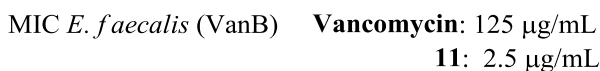
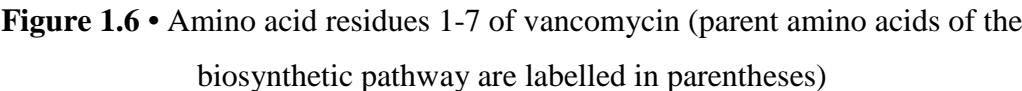
<sup>i</sup> Since publication of this review, Dalbavancin has been approved by the FDA for the treatment of bacterial skin infections (May 2014).

Oritavancin (**10**) (Figure 1.5) is derived from chloroeremomycin (**6**) (Figure 1.2). The key modification of natural product **6** was the installation of a 4'-chlorobiphenylmethylene group, which affords oritavancin an additional mode of action that is absent from vancomycin; recent investigations have shown that this biaryl group is involved in cell membrane depolarisation and an increase in membrane permeability.<sup>22</sup> As a consequence of this dual-action mechanism, oritavancin has excellent *in vitro* activity against gram positive bacteria, with MICs in the range of 0.004–1  $\mu\text{g mL}^{-1}$  against VRE,<sup>23</sup> and is currently in phase III clinical trials funded by The Medicines Company for the treatment of acute bacterial skin and skin structure infections (ABSSSIs).

A derivative of vancomycin, telavancin (**3**) (Figure 1.2) also follows the pattern of *N*-alkylation of the vancosamine moiety with a hydrophobic chain, in this case a decylaminoethyl group. In addition, a methylaminophosphonate group was installed on the **A**-ring of the **A-B** biaryl region for its hydrophilic properties, which improved the absorption, distribution, metabolism and excretion (ADME) profile of the compound.<sup>24</sup> With excellent activity against both VRE and VRSA, telavancin was approved by the FDA in September 2009 for complicated skin and skin structure infections (cSSSI). The success of these three semi-synthetic glycopeptides as drug candidates and their potent antibacterial activities in comparison to vancomycin,<sup>25</sup> has encouraged further research in the field of glycopeptide modification. The structure–activity relationships of telavancin, dalbavancin and oritavancin have provided valuable information about the modes of action that this class of compounds possess, with the results having a significant influence on future drug design.

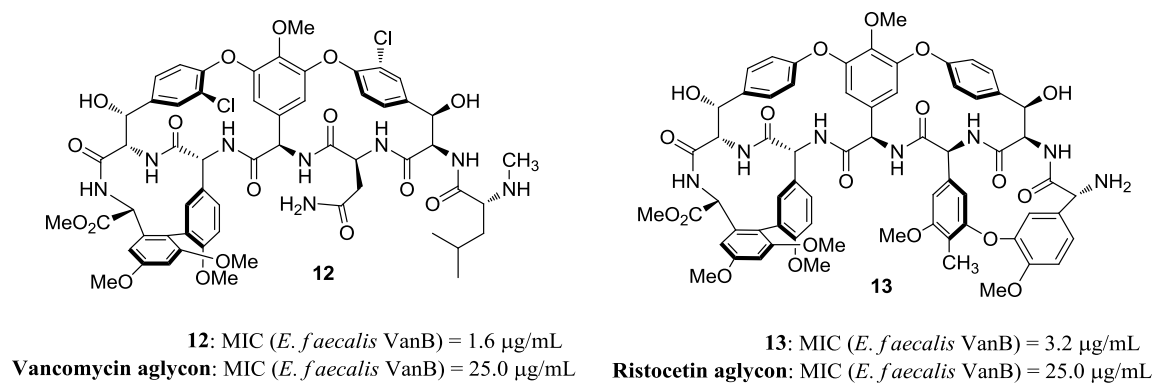
#### 1.4.2 Modification of the amino acids within the polypeptide chain

The challenge of where and how to successfully modify existing natural products can be approached in different ways. The glycopeptide antibiotics are large, complex molecules with plenty of potential for *N*- and *O*-alkylation as well as changes to the component amino acids of the heptapeptide chain. Even the chloro substituents of the triaryl biether backbone can be envisaged as sites of reactivity and as such are viable sites for chemical transformation.



However, despite the promising antibacterial activity of compound **11**, the nitrile derivatives were generally less active than the corresponding carboxamide. Crucially, removal of the four methyl ether modifications of **11** as well as hydrolysis of the methyl ester resulted in significantly lower activity, with an increase in the MIC against *S. aureus* from 0.625 to 10  $\mu\text{g mL}^{-1}$ . The effect of methylation is therefore clearly more pronounced than that of amino acid modification. When subjected to D-Ala-D-Ala peptide binding tests, nitrile derivative **11** and its corresponding carboxamide showed binding constants that were comparable to vancomycin ( $K_a = 9.9 \times 10^5$ ,  $2.0 \times 10^5$  and  $2.3\text{--}3.9 \times 10^5$  respectively). Boger suggested that this result may be due to the increased hydrophobicity of these compounds, mimicking the effect of the hydrophobic chain in teicoplanin.

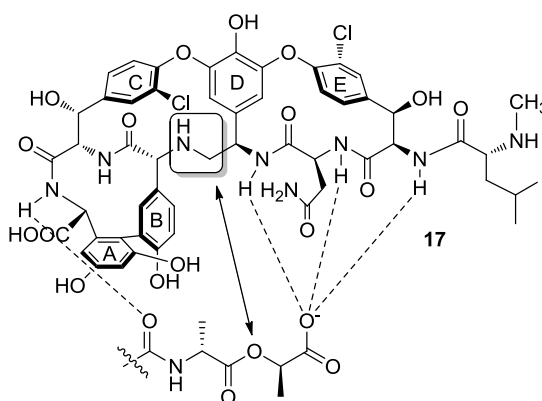
A subsequent study on the activity of vancomycin-derived methyl ether analogues demonstrated that *O*-methylation of the phenolic hydroxyl groups can have mixed results with regard to the biological activity.<sup>28</sup> *O*-methylated derivatives of vancomycin, teicoplanin and ristocetin were prepared from the corresponding aglycons using the following general procedure: *N*-Boc protection of the amine terminus followed by *O*-methylation by trimethylsilyldiazomethane and removal of the Boc group by 4*N* hydrochloric acid in dioxane. Activity against *S. aureus* by **12** decreased by half compared to vancomycin and its aglycon, but a significant improvement in activity was observed against the VRE VanB phenotype (Figure 1.8). Similarly, compound **13** performed better against VRE (VanB) than the parent compound, ristocetin, but was less active against *S. aureus*. In all cases the improvements in antibacterial activity afforded by methyl ether derivatisation clearly demonstrated the potential of *O*-alkylation as a protocol for the development of more potent vancomycin analogues.



**Figure 1.8 •** Methyl ether derivatives of a) vancomycin aglycon and b) ristocetin aglycon by Boger *et al.*

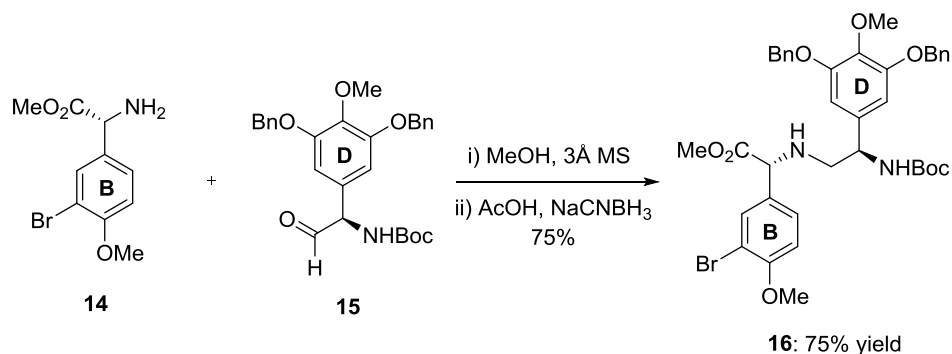


While many of the novel vancomycin derivatives discussed later in this review rely on the addition of groups by alkylation etc., a limited amount of work has been undertaken on modifying the peptide backbone of vancomycin itself. Modification of the peptide backbone presents a considerable synthetic challenge, as changes to the internal peptide structure may involve a full synthesis of the compound rather than simple manipulation of naturally sourced material. Using their experience of vancomycin total synthesis, the Boger group developed an analogue that was specifically designed to target vancomycin resistant organisms (Figure 1.9).<sup>16</sup> Compound **17** contains a modification in amino acid residue 4 (boxed), which is equipped with a methylene group in place of an amide carbonyl. The effect of this small change is to remove the oxygen-oxygen repulsion responsible for the observed decrease in binding affinity of vancomycin for the D-Ala-D-Lac terminus in the peptidoglycan of VRE type A and B.



**Figure 1.9** • Predicted interaction between vancomycin aglycon derivative **17** and the D-Ala-D-Lac peptidoglycan terminus (Boger *et al.*).

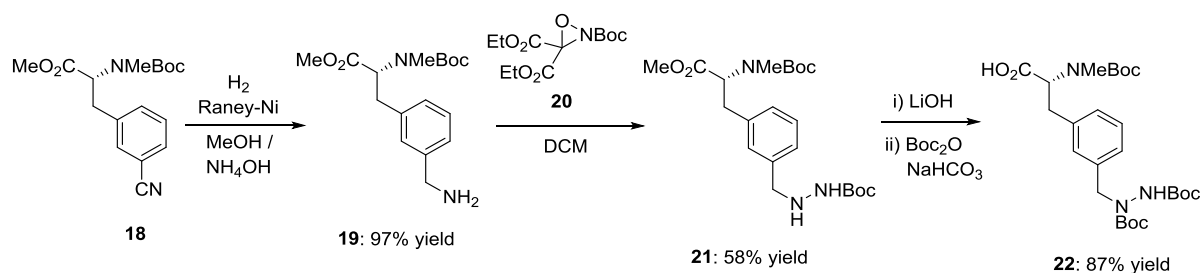
Analogue **17** was prepared by a similar route to the previously reported total synthesis of vancomycin, with changes to the synthesis of the **B** and **D**-ring regions (Scheme 1.1). Thus intermediate **16** was synthesised via a reductive amination reaction between (*R*)-methyl 2-amino-2-(3-bromo-4-methoxyphenyl)acetate **14** and (*R*)-tert-butyl-(1-(3,5-bis(benzyloxy)-4-methoxyphenyl)-2-oxoethyl)carbamate **15** in place of the standard peptide coupling procedure.



**Scheme 1.1** • Construction of a modified polypeptide chain for incorporation into vancomycin derivative **17** (Boger *et al.*)

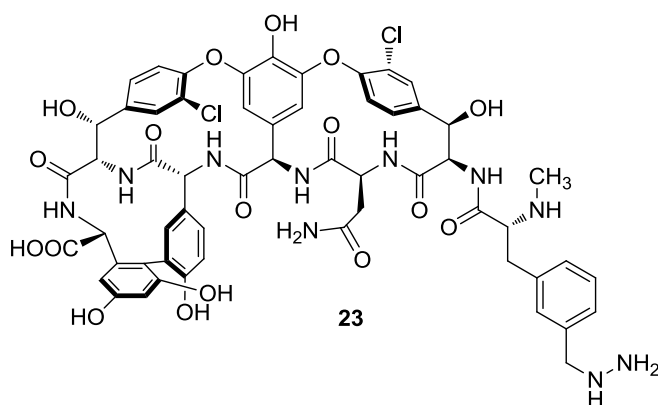
Gratifyingly, the design of analogue **17** improved affinity by removing lone pair repulsion, but relies on the strength of the four remaining hydrogen bonds involved in the interaction. Boger recognised that while affinity for D-Ala-D-Lac could be improved further by engineering a reverse hydrogen bond into the molecule, this may be clinically disadvantageous as it would disrupt H-bonding to D-Ala-D-Ala. The result would therefore be reduced activity against vancomycin-sensitive bacteria as well as resistant strains such as VanA that initially use the D-Ala-D-Ala terminus.

In binding tests, compound **17** proved to exhibit the desired dual-binding properties, with a 40-fold increase in affinity for D-Ala-D-Lac compared to vancomycin and conversely a 35-fold decrease in affinity for D-Ala-D-Ala, giving it the potential to be equally effective against both vancomycin-sensitive and resistant bacteria. Crucially, this analogue has an MIC of  $31 \mu\text{g mL}^{-1}$  against VRE (VanA), the most challenging of the resistant bacteria to combat by synthetic design. This compares favourably to the values for vancomycin ( $2000 \mu\text{g mL}^{-1}$ ) and the aglycon ( $640 \mu\text{g mL}^{-1}$ ) but remains higher than the MIC of  $<1 \mu\text{g mL}^{-1}$  generally required for clinical applications.



**Scheme 1.2** • Synthesis of protected hydrazine-containing amino acid **22** reported by Boger and Crane

The Boger group turned next to the *N*-methyl-L-leucine residue of vancomycin (residue 1). The aim of this investigation was to introduce additional hydrogen bonding to the peptidoglycan terminus away from the binding pocket of the molecule. Taking this idea further, they predicted that nucleophilic substituents might form a covalent attachment to D-Ala-D-Ala or D-Ala-D-Lac. With this in mind, a series of hydrazine-containing derivatives of vancomycin were synthesised and tested for their antibacterial activity.<sup>29</sup> Preparation of the modified amino acid is shown in Scheme 1.2. Reduction of (*R*)-Boc-*N*-methyl-3-cyanophenylalanine methyl ester **18** by RANEY<sup>®</sup> Ni, hydrogen and 28% aqueous ammonium hydroxide in methanol afforded the corresponding methylamine **19**. Amination with oxaziridine **20** afforded *N*-Boc protected hydrazine **21** in a 58% yield. Finally, lithium hydroxide hydrolysis of the methyl ester (and a second *N*-Boc protection) afforded **22**, the free acid substrate for peptide coupling.

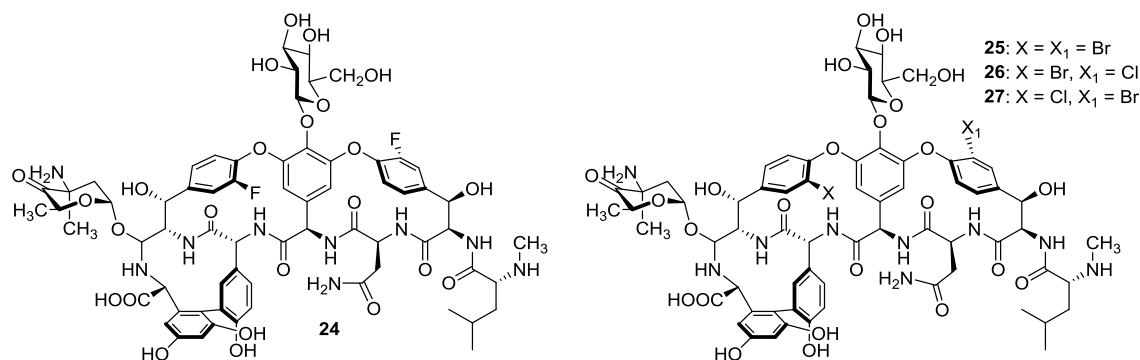


**Figure 1.10 •** Vancomycin benzylhydrazine derivative generated by Boger *et al.*

Compound **23** (Figure 1.10) had the same activity against *S. aureus* as vancomycin (MIC = 1.23  $\mu\text{g mL}^{-1}$ ), and activity against VRE remained poor. There was no evidence of a general trend in the activity of the hydrazine-containing derivatives or of an improvement in activity arising from exchange of the natural product *N*-terminal amino acid for those containing H-bond donors or reactive nucleophiles. Attempts to use the hydrazine group to form a covalent adduct between the vancomycin derivatives and the *C*-terminal ester of D-Ala-D-Lac were unsuccessful, even though this reaction could be carried out between the peptidoglycan chain and phenyl hydrazine.

Several members of the glycopeptide antibiotic family are appended with chlorine substituents on the aryl ring of  $\beta$ -hydroxytyrosine amino acid residues 2 and 6 (Figure 1.6), and the significance of these halogen atoms has been examined through structure–

activity relationship (SAR) studies. The presence of chlorine atoms has been shown to strongly enhance the potency of the compounds, probably as a result of their stabilising role in dimerisation.<sup>12</sup> In order to investigate the importance of the chlorine atoms further, Süssmuth *et al.* synthesised a series of balhimycin variants containing chlorine, bromine and fluorine substituents (Figure 1.11).<sup>30,31</sup>



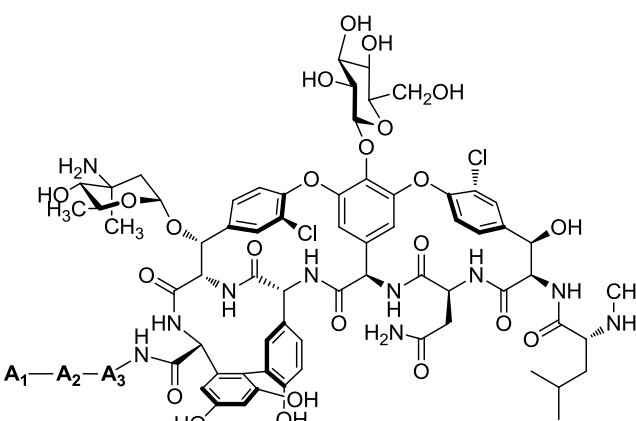
**Figure 1.11** • Fluorobalhimycin **24** (top), bromobalhimycin **25** and chlorobromobalhimycins **26** and **27** by Süssmuth *et al.*

Fluorobalhimycin (**24**) was produced *via* an enzymatic procedure to incorporate 3-fluoro- $\beta$ -hydroxytyrosine into the glycopeptide in place of the chlorinated amino acid. In a subsequent report, calcium chloride and magnesium chloride (1:1 ratio) were substituted by the corresponding bromide salts in the culture media of the balhimycin-producing *Amycolatopsis balhimycina*, resulting in the synthesis of bromobalhimycin **25**. Attempts to incorporate fluoride and iodide atoms by this method failed due to the toxicity of the salts. When equimolar amounts of bromide and chloride salts were added, a product with one bromine and one chlorine atom was observed in addition to the balhimycin and bromobalhimycin products. The hetero-halogen species was shown by mass spectrometry to be present as positional isomers **26** and **27** (1:1 ratio). Bromobalhimycin **25** showed similar *in vitro* antibacterial activity to balhimycin, with the exception of an 8-fold increase in MIC against *S. aureus*. Balhimycin **24** and bromobalhimycin **25** both performed up to 16 times better than dechlorobalhimycin against Gram-positive bacteria, confirming the important role that halogen substituents play within the glycopeptide family.

Following earlier work on the synthesis of chloroorienticin B derivatives,<sup>32</sup> Yasukata *et al.* turned to extending the heptapeptide chain as a possible method of improving antibiotic activity. Chloroorienticin B derivatives bearing a tripeptide chain at the C-

terminus were prepared by solid-phase parallel synthesis, allowing fast access to a library of over 80 compounds.<sup>33</sup> These compounds were tested for antibacterial activity against MRSA and VRE; a selection of the data is presented in Table 1.1. Compounds that incorporated tryptophan and tyrosine residues, such as **28** and **29**, were found to exhibit activity against VRE as well as matching the activity of the parent compound against MRSA. As a general rule, the tryptophan residue in particular was crucial for activity against VRE. The introduction of glutamic acid totally removed anti-VRE properties of the compound. Yasukata *et al.* concluded that amino acid residues with basic and hydrophobic character provided the most potent derivatives.

**Table 1.1** • MICs ( $\mu\text{g mL}^{-1}$ ) of chloroorienticin B tripeptide derivatives by Yasukata *et al.*

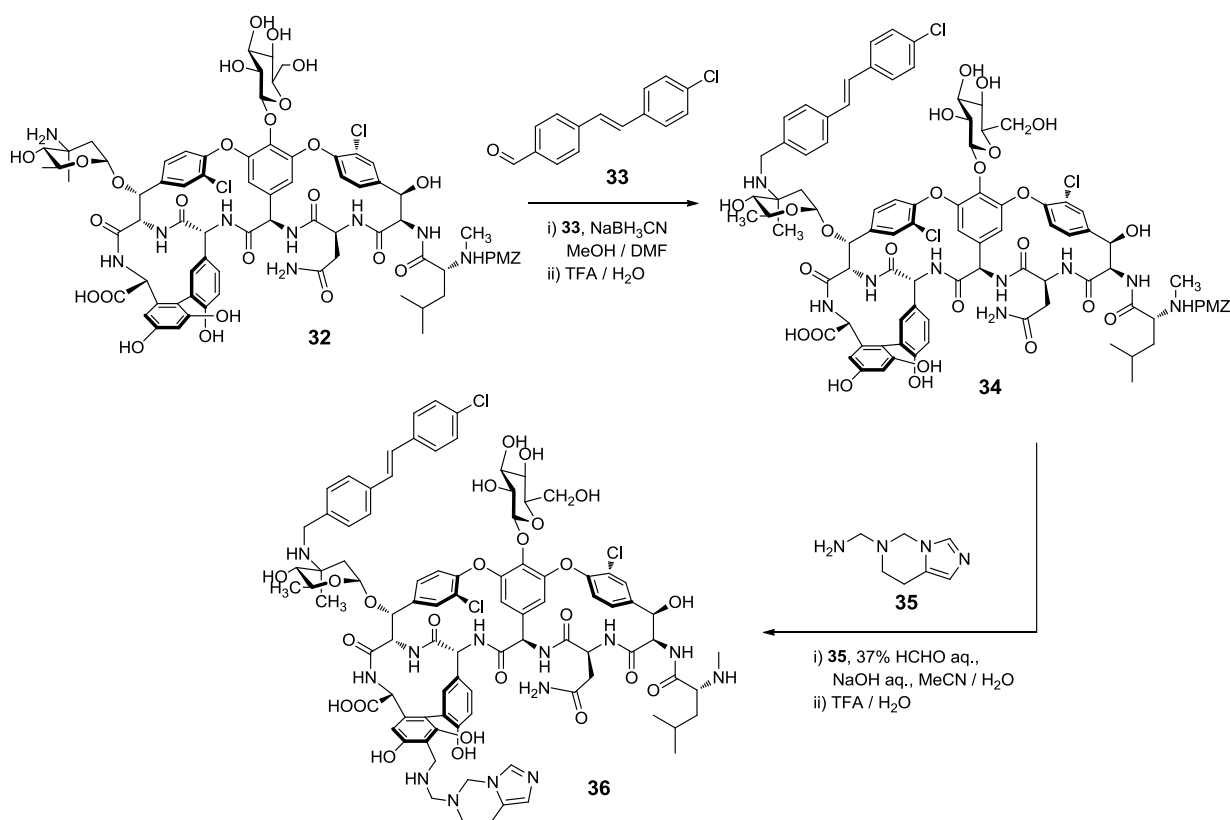


A <sub>1</sub> -A <sub>2</sub> -A <sub>3</sub>	<i>Staph. aureus</i> SR3637 (MRSA)	<i>E. faecalis</i> SR7914 <sup>a</sup>	<i>E. faecium</i> SR7917 <sup>a</sup>
<b>28</b> : Leu-Trp-Tyr	0.5	16	8
<b>29</b> : Tyr-Trp-His	0.5	16	8
<b>30</b> : Trp-Lys-His	<0.125	64	8
<b>31</b> : Glu-Trp-Tyr	8	>128	>128
Chloroorienticin B	0.5	>128	>128

<sup>a</sup> Vancomycin-resistant *enterococci* (VanA)

### 1.4.3 Introduction of hydrophobic side chains to the peripheral glycopeptide structure

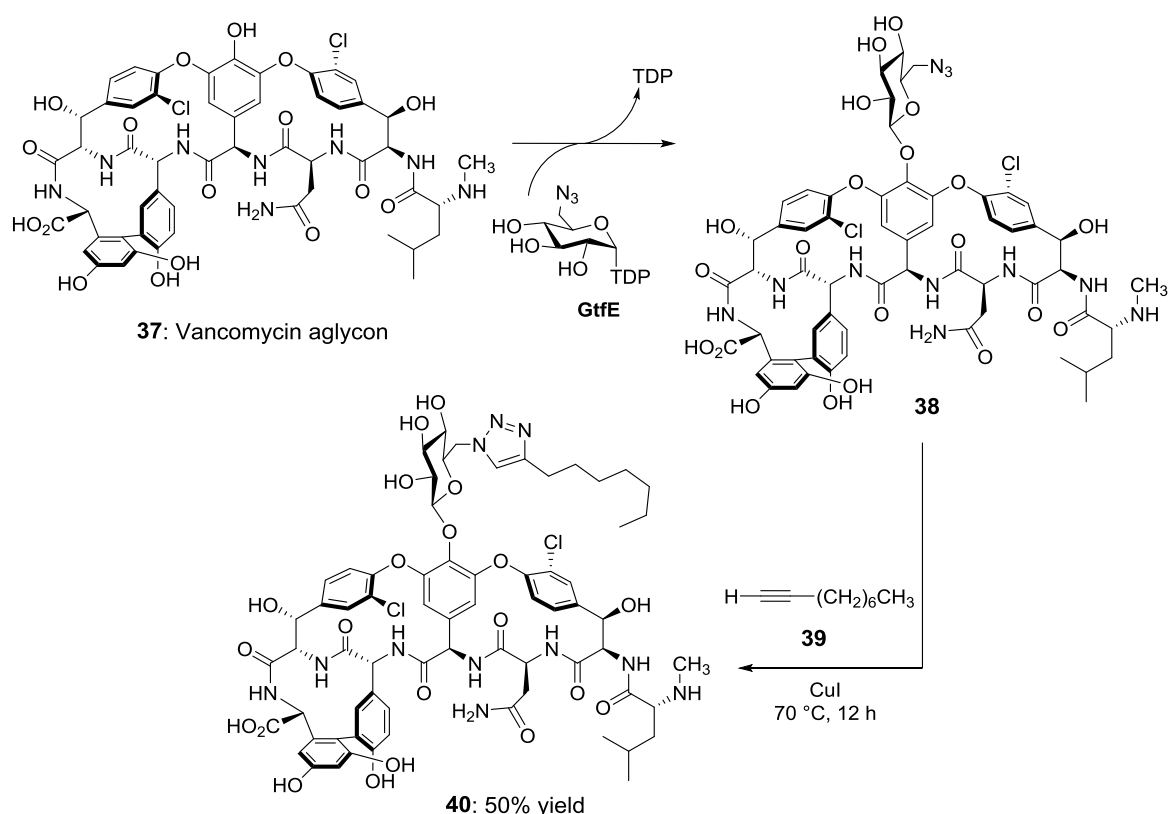
Many of the early modifications of vancomycin and the glycopeptide family involved the addition of hydrophobic chains to the molecule, frequently at the vancosamine nitrogen atom.<sup>34</sup> These derivatives mimicked the natural hydrophobic character of teicoplanin (**5**) (Figure 1.2), but alkylation of the polar hydroxyl, acid and amino groups can compromise the naturally high aqueous solubility of the parent compound.



**Scheme 1.3** • Double modification of chloroorienticin B by Yasukata *et al.*

Yasukata *et al.*<sup>35</sup> proposed a solution to this problem with a double modification of chloroorienticin B, inspired by earlier work on the double modification of teicoplanin by Preobrazhenskaya *et al.*<sup>36</sup> In the first step, protection of the amino peptide terminal with a *para*-methoxybenzyloxycarbonyl (pMZ) group was followed by *N*-alkylation of the amino sugar with (*E*)-4-(4-chlorostyryl)benzaldehyde **33** (Scheme 1.3). Subsequent pMZ removal afforded **34**. This compound has a higher antibacterial activity than chloroorienticin B or vancomycin but the hydrochloride salt has <1% solubility in water, compared to that of vancomycin, which is >99% soluble in water. The second step

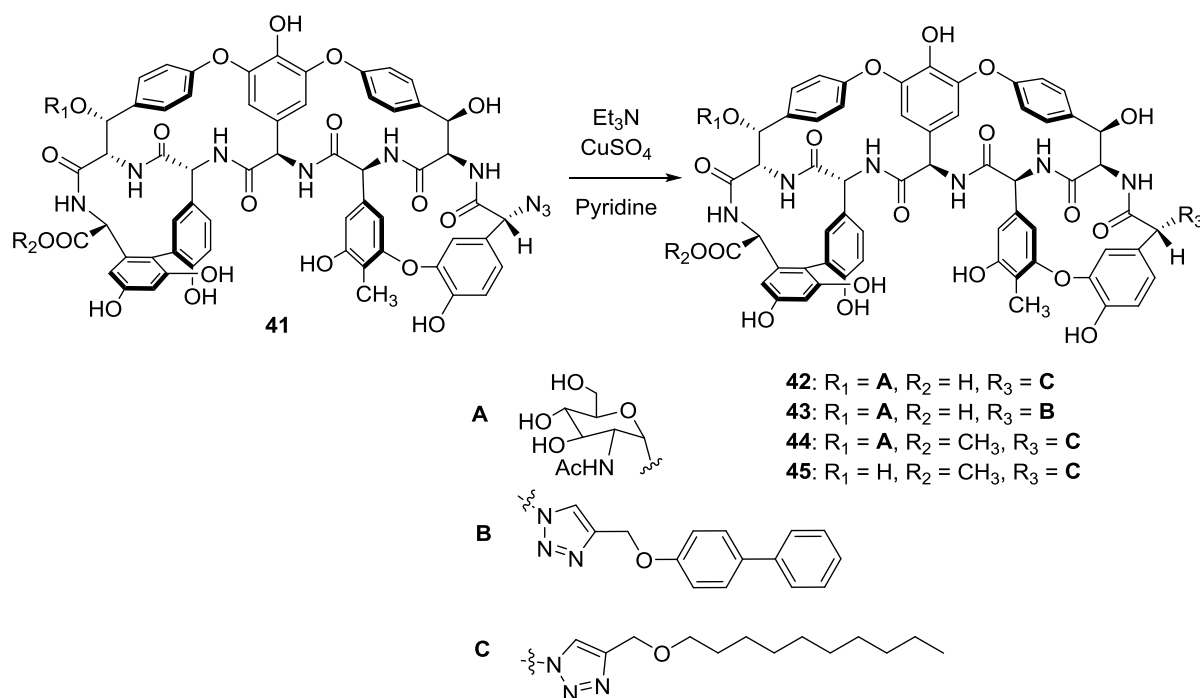
employed a Mannich reaction previously reported by the Preobrazhenskaya group<sup>37</sup> to introduce a hydrophilic aminoalkyl group into the **A-B** biaryl region of the molecule. Thus the reaction of **34** with 5,6,7,8-tetrahydroimidazo[1,5-c]pyrimidine-6-methylamine **35** under Mannich conditions afforded doubly-modified derivative **36**. Compound **36** exhibited MICs of 0.78  $\mu\text{g mL}^{-1}$  against MRSA (compared to 1.56  $\mu\text{g mL}^{-1}$  for vancomycin) and 3.13–6.25  $\mu\text{g mL}^{-1}$  against VRE (VanA). Crucially, the aqueous solubility of the hydrochloride salt was increased to 10% by the second modification.



**Scheme 1.4** • Vancomycin glycorandomisation process by Thorson *et al.*

Vancomycin derivatives that contain hydrophobic side chains are disadvantaged by their poor solubility. Yasukata *et al.* have demonstrated that secondary modifications on these glycopeptides can successfully increase solubility, hence making them more suitable for clinical use. One of the most versatile and currently widely employed methods of ligation is the Huisgen or Click reaction; a copper catalysed 1,3-dipolar cycloaddition reaction between an azide and an alkyne. The application of Click chemistry for glycopeptides modification was first reported in 2005 by Thorson *et al.*, who used a chemoenzymatic approach to install 6-azido glucose onto the vancomycin aglycon for subsequent

glycorandomization (Scheme 1.4).<sup>38</sup> Batta and Herczegh employed the Click reaction for the synthesis of ristocetin and teicoplanin aglycon derivatives bearing a hydrophobic side chain.<sup>39</sup> The *N*-termini of the glycopeptide aglycons were converted to an azide functionality *via* a diazo transfer reaction of the amine with triflic azide and catalytic amounts of copper(II) sulfate in pyridine. The alkyne substrates were prepared by propargylation of the corresponding alcohols (Scheme 1.5).

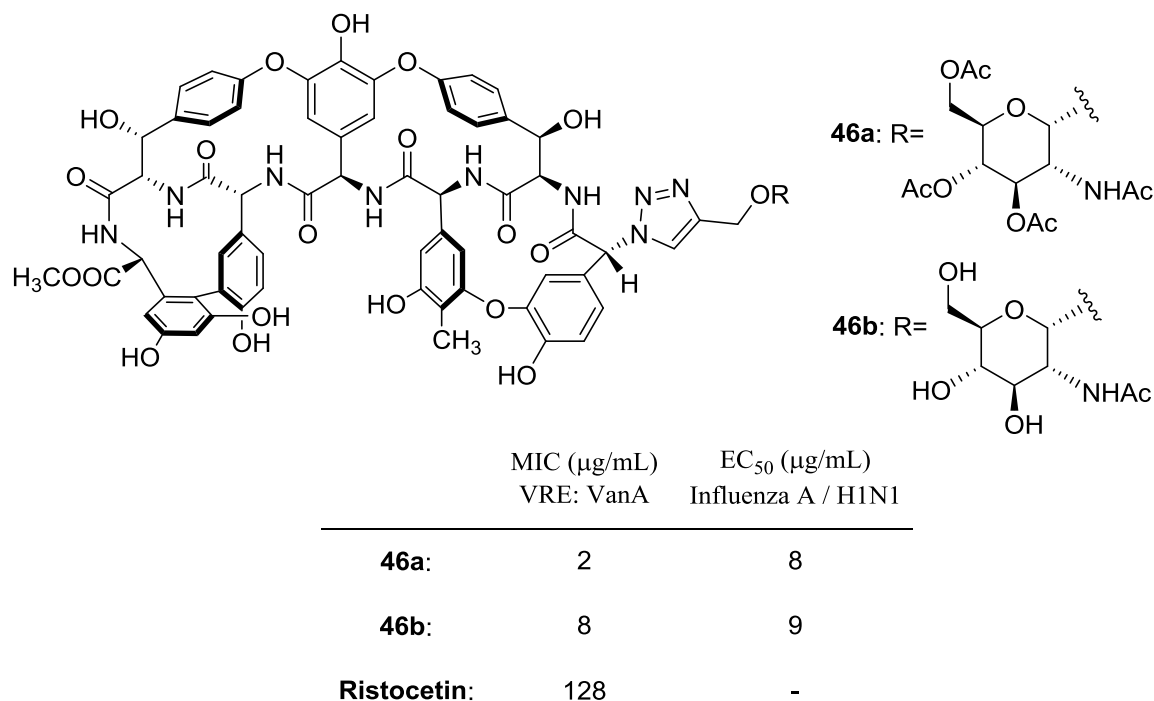


**Scheme 1.5** • Click chemistry for the generation of novel teicoplanin aglycon derivatives by Batta and Herczegh *et al.* (2009)

Reaction between the azide and alkyne with 10% CuI and triethylamine at room temperature afforded the 1,4-substituted 1,2,3-triazoles in 44–71% yield. The teicoplanin derivatives showed much higher activity than the parent compound, with **42** and **43** being potent against both VanA and VanB phenotypes of resistant *enterococci* (MICs of 0.5  $\mu\text{g mL}^{-1}$  in both cases). Batta and Herczegh postulated that the amphiphilic nature of these derivatives (the presence of the carboxylate group and a lipophilic side chain) favours the formation of a multivalent aggregate in aqueous medium, contributing to increased antibacterial activity. Compound **44**, a product of esterification at the *C*-terminus, showed decreased activity overall, and removal of the *N*-acetyl glucosamyl group at R<sub>1</sub> (compound **45**) drastically reduced potency against vancomycin-resistant and susceptible



strains. The presence of this sugar is key to the biological activity of these compounds. The ristocetin derivatives lost all antibacterial activity, although the ristocetin azide intermediate matched the activity of vancomycin against MRSA ( $\text{MIC} = 2 \mu\text{g mL}^{-1}$ ). Further work by Herczegh *et al.* employed the Click reaction to add a saccharide moiety to the *N*-terminus of ristocetin aglycon (Figure 1.12).<sup>40</sup> This modification was shown to improve both antibacterial and anti-influenza activity of the glycopeptide.

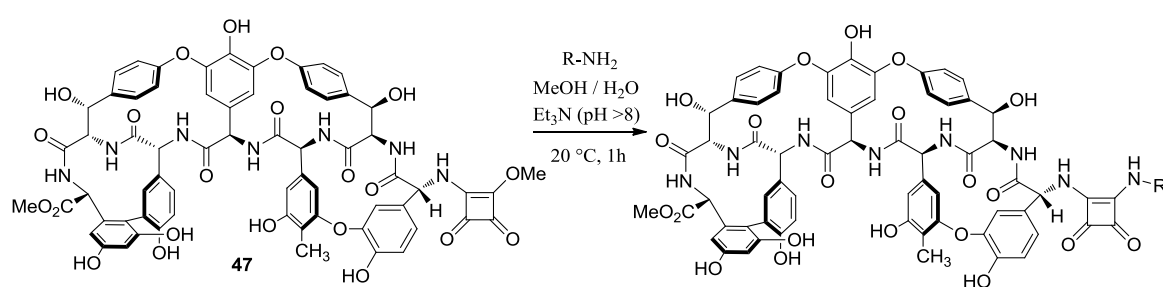


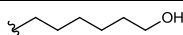
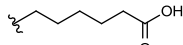
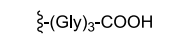
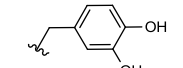
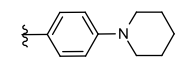
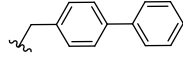
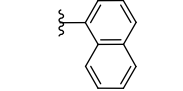
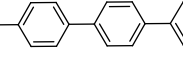
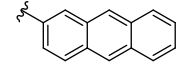
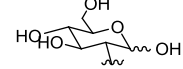
**Figure 1.12 •** Ristocetin triazole saccharide derivatives generated by Herczegh *et al.*

The anti-influenza virus properties of ristocetin aglycon derivatives were reported by Sztaricskai and Naesens in 2009, with the synthesis of a series of compounds bearing hydrophobic chains *via* a cyclobutenedione linker (Table 1.2).<sup>41</sup> Coupling of the ristocetin aglycon with dimethyl squarate and subsequent reaction with various primary amines afforded the corresponding asymmetric squaric diamides. The mild reaction conditions are a notable advantage of this ligation method. Furthermore, the lead compound in the series, 4-phenylbenzyl derivative **53**, showed excellent anti-viral activity against influenza A and B strains, with an average EC<sub>50</sub> of 0.4  $\mu\text{M}$ , which compares favourably with anti-influenza drugs currently on the market, including ribavirin (8.4  $\mu\text{M}$ ) and oseltamivir (2.8  $\mu\text{M}$ ).

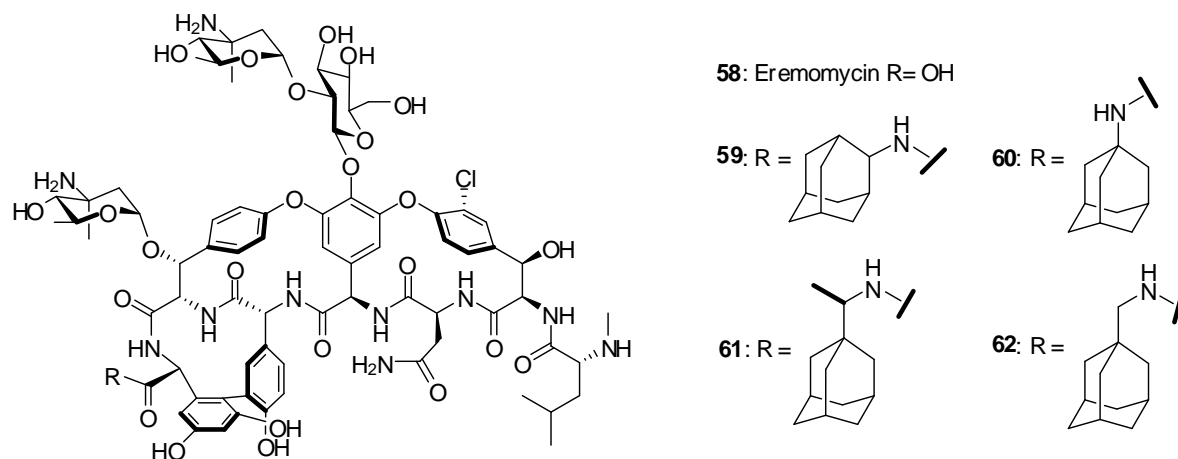
Interestingly, the corresponding aglycovancomycin derivatives showed no antiviral activity, suggesting that the core aglycoristocetin structure is essential for antiviral activity. There are a number of differences between the two compounds; ristocetin contains additional aromatic rings **F** and **G**, connected *via* a diphenylether linkage, and features a methyl ester at the C-terminus instead of the free carboxylic acid, but lacks the chloro substituents of lvancomycin. It is unclear which of these properties contributes to the antiviral characteristics of aglycoristocetin derivatives.

**Table 1.2 •** Squaric diamide derivatives of ristocetin aglycon by Naesens and Sztaricskai *et al.*



	R	Yield (%)	EC <sub>50</sub> (μM) <sup>a</sup>
48		72	1.0
49		38	>100
50		62	4.6
51		87	2.3
52		73	>100
53		68	0.36
54		54	0.50
55		42	>100
56		62	>100
57		75	>100

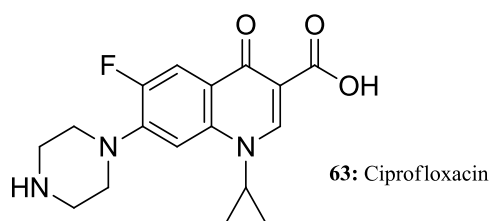
<sup>a</sup> Influenza A/H3N2



**Figure 1.13** • Adamantyl-containing eremomycin amides generated by Preobrazhenskaya *et al.*

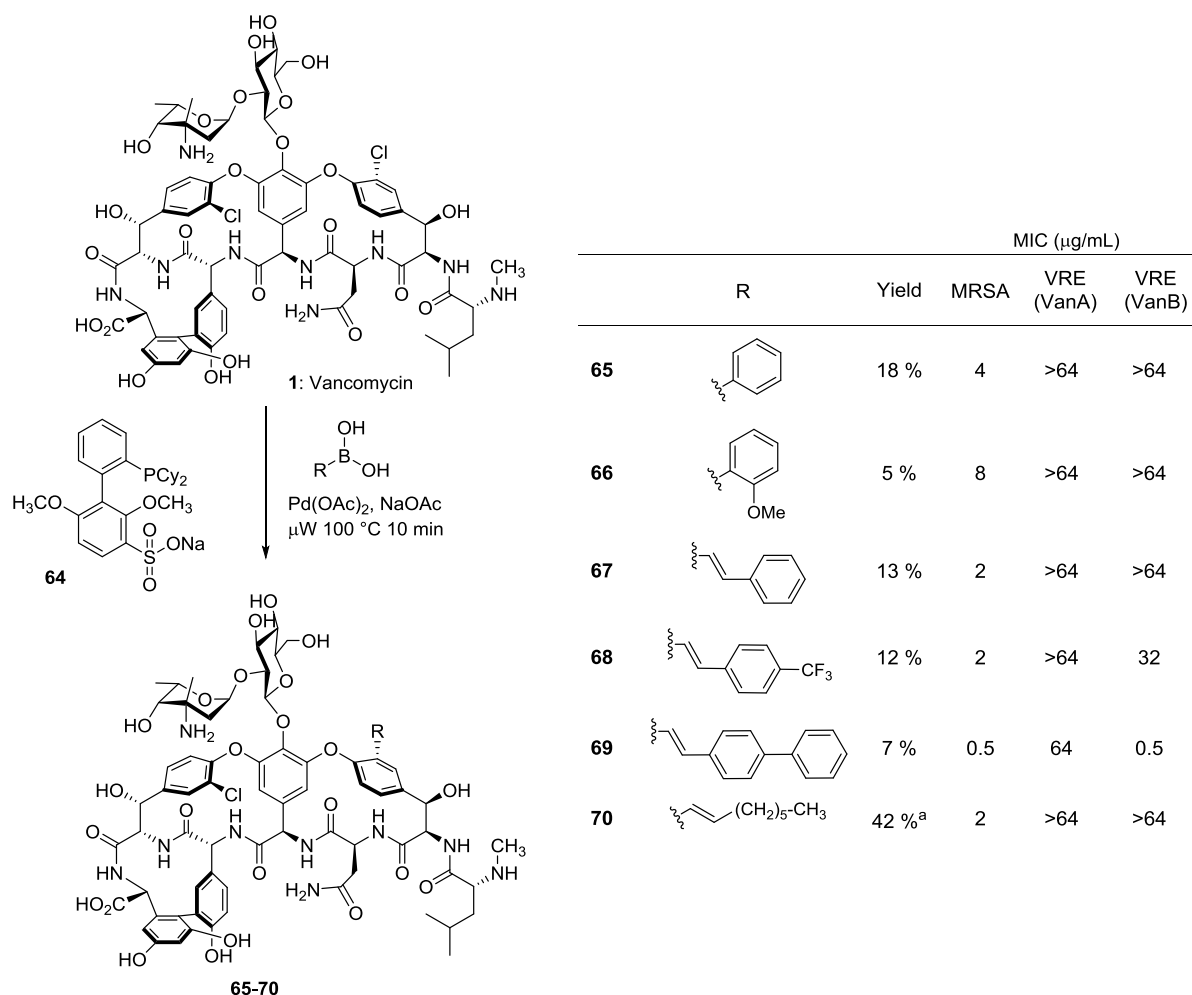
Following work on the modification of eremomycin by the incorporation of hydrophobic sugar substituents,<sup>42</sup> Preobrazhenskaya *et al.* turned their attention to glycopeptides derivatives that were active against *Bacillus anthracis*. With this in mind they generated a series of eremomycin and vancomycin derivatives appended with an adamantyl amide moiety (Figure 1.13).<sup>43</sup>

Anthrax has attracted much attention in the media as a biological weapon, and the mortality rate of patients who are infected by inhalation remains high. The appearance of drug-resistant strains of *Bacillus anthracis* indicates a particular need for the development of new compounds that are effective against these bacteria. The most potent compound in the series, adamantyl-2-amide eremomycin derivative **59** (Figure 1.13) showed wide-ranging potency against vancomycin-susceptible, intermediate and resistant strains of *S. aureus*, *E. faecalis* and *E. faecium* (MIC = 0.25–8  $\mu\text{g mL}^{-1}$ ).



**Figure 1.14** • Structure of anti-anthrax drug ciprofloxacin (**63**)

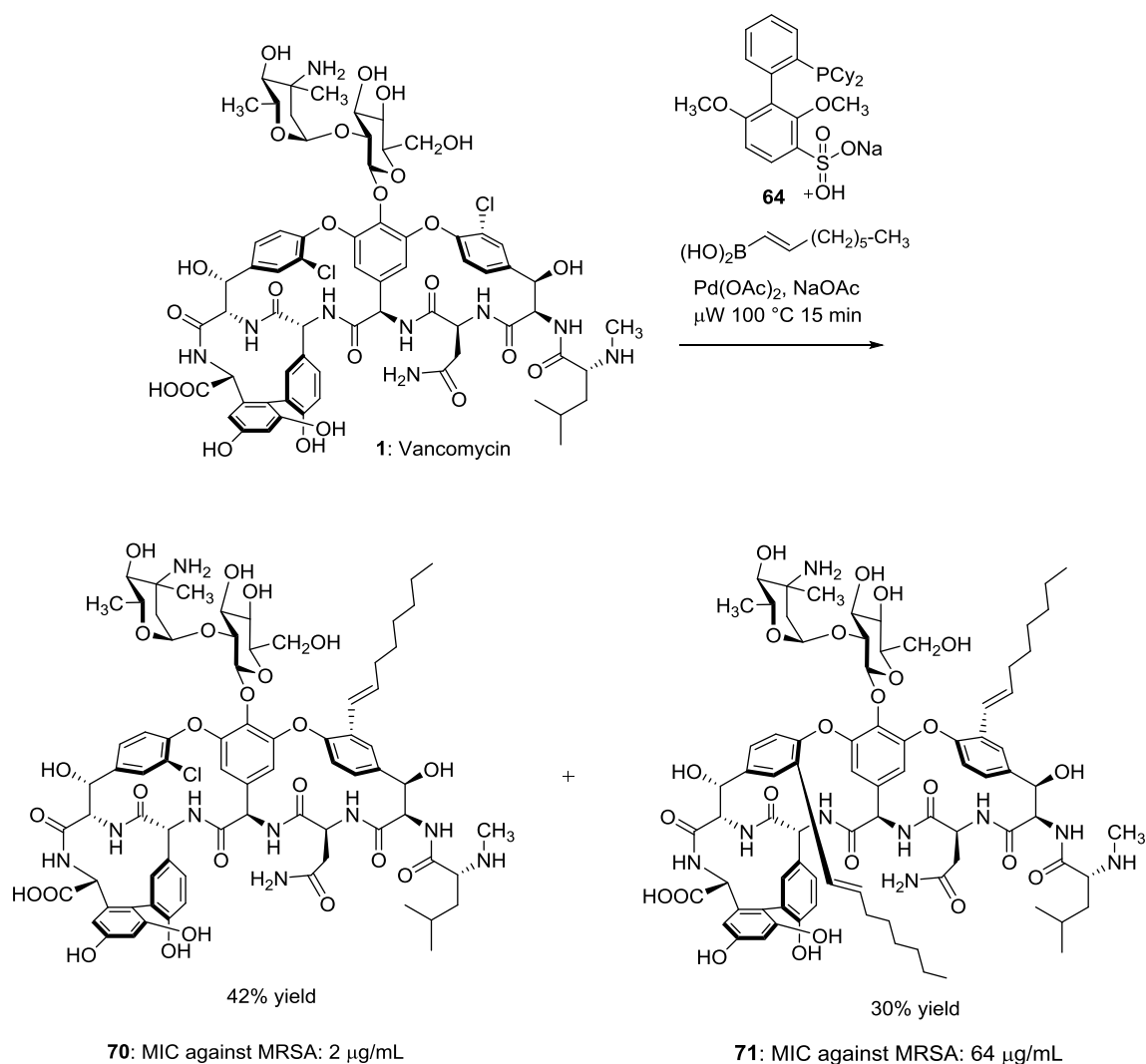
Compound **59** also proved to be very effective against *Bacillus anthracis* in *in vivo* testing, while it showed excellent *in vitro* activity against strains that are resistant to ciprofloxacin (**63**), the current drug of choice for treatment of anthrax poisoning (Figure 1.14).



**Scheme 1.6** • Application of the Suzuki-Miyaura cross-coupling on vancomycin by Arimoto *et al.*

Given the importance of the aryl halide derived glycopeptides and the multitude of transition metal-based protocols available to the chemist, it is interesting to note that it was not until 2010 that investigations probing their chemical transformation were undertaken. Focusing on amino acid residues 2 and 6, Arimoto *et al.* reported the application of a Suzuki-Miyaura coupling procedure using *trans*-2-(4-biphenyl)vinylboronic acid as the key coupling agent.<sup>44</sup>

Vancomycin has poor solubility in most organic solvents but high solubility in water. In a procedure that did not require any protecting group strategies Arimoto *et al.* reported the first example of a Suzuki coupling conducted in aqueous solution on a complex natural product. The protocol utilises a water-soluble catalyst combination using ligand **64**, originally developed for the Suzuki-Miyaura coupling reaction by Buchwald *et al.*<sup>45</sup> The synthesis of derivatives **65–70** was readily performed in the presence of the corresponding boronic acid, 20 mol% of palladium(II) acetate, sodium acetate (10 equiv.) and water soluble phosphine ligand sodium 2-dicyclohexylphosphino-2,6,0-dimethoxybiphenyl-30-sulfonate **64** (0.4 equiv.) (Scheme 1.6).



**Scheme 1.7** • Suzuki-Miyaura coupling of vancomycin with octenylboronic acid by Arimoto *et al.*

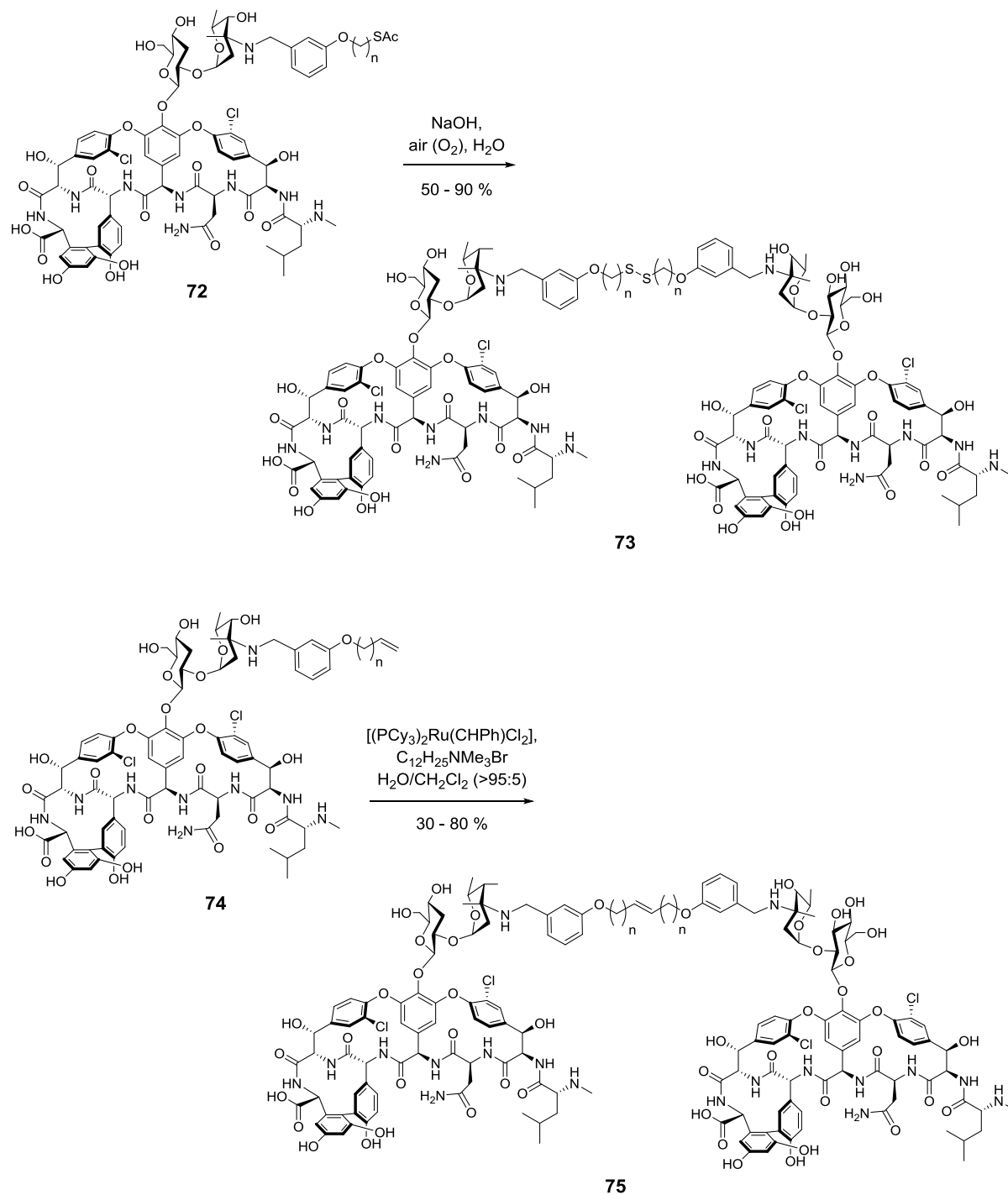
Although the aryl boronic acids used to generate derivatives **65–69** were found to have low reactivity towards vancomycin, those that did react did so with good selectivity. 2D  $^1\text{H}$ -NMR studies showed that C–C bond formation occurred only at residue 2, where the chloro substituent is on the less-hindered side of the molecule. Alkenylboronic acids were found to be more reactive; the reaction between vancomycin and octenylboronic acid afforded mono-substituted product **70** in a 42% yield, and di-substituted product **71** in a 30% yield (Scheme 1.7).

Novel vancomycin derivatives **65–71** were tested for their biological activity against a range of vancomycin resistant and susceptible bacteria. Simple aryl substitution of vancomycin at residue 2 (compounds **65** and **66**) gave a minor decrease in activity against vancomycin-susceptible bacteria and these derivatives remained inactive against VRE and VRSA. Styryl derivative **67** showed activity against VRSA ( $16\ \mu\text{g mL}^{-1}$ ) but this property was lost as the size of the substituent increased; **68** and **69** were inactive against VRSA but did exhibit activity against VRE (VanB). The overall antibacterial activity of compound **69** was particularly promising, with better activity against MRSA than vancomycin, and excellent activity against the VanB phenotype of vancomycin resistant *E. faecium* ( $\text{MIC } 0.5\ \mu\text{g mL}^{-1}$ ). Disubstituted products showed no activity against vancomycin-resistant bacteria, and importantly, also lost activity against vancomycin-susceptible strains. Arimoto *et al.* concluded that this behaviour is due to unfavourable steric interactions between the large substituent on residue 6 and the D-Ala-D-Ala peptide terminus, citing the reduced binding affinity of **71** for the D-Ala-D-Ala dipeptide compared to mono-substituted product **70** ( $K_D = 11.6\ \mu\text{M}$  and  $3.77\ \mu\text{M}$  respectively).

### 1.5 Glycopeptide dimerisation studies

Glycopeptide antibiotics are known to dimerise spontaneously in aqueous solution. Furthermore, dimerisation contributes to their potency. A 1999 study by Williams and Cooper used Surface Plasmon Resonance analysis to show that vancomycin, which dimerises weakly, has a low binding affinity for –Lys-D-Ala-D-Lac peptides found in VRE, whereas strongly dimerising antibiotics like chloroeremomycin had a higher binding affinity for the VRE mimic.<sup>46</sup> In the search for improved biological activity, a number of investigations have aimed to harness or exploit this characteristic by synthesizing covalently-linked glycopeptide dimers. In the design of effective dimers there are a number of options to consider: the site of dimerisation, the length and nature of the bridge, and the reaction employed for ligation.

Following a successful total synthesis of vancomycin, the Nicolaou group began to investigate the efficient synthesis of covalently-linked vancomycin dimers using target-accelerated combinatorial synthesis (TACS).<sup>47</sup> TACS allows the simultaneous evaluation of the effect of both the length of the linker and modifications in the binding pocket on the activity of the novel compounds produced. Initiating this study, the nitrogen atom of the vancosamine sugar was chosen as the linking site of dimerisation, and two ligation methods were tested; disulfide formation and olefin metathesis (Scheme 1.8). Saponification of thioacetate **72** in aqueous sodium hydroxide at 23 °C gave the corresponding disulfide **73**, one of the most biologically active in a series consisting of tether lengths  $n = 3-9$ . Finding suitable conditions for an aqueous olefin metathesis proved more challenging, but the reaction proceeded smoothly in a mixed solvent system (H<sub>2</sub>O/DCM 95:5) with a phase transfer catalyst, trimethyldodecylammonium bromide, and Grubbs 1st generation catalyst, at room temperature. In each case the dimer was isolated as a 1:1 mix of *cis* and *trans* isomers in the olefin bridge in a 30–80% yield. The novel dimers were tested for activity against a range of vancomycin-susceptible and resistant strains of bacteria, and a number of general structure–activity trends were observed.



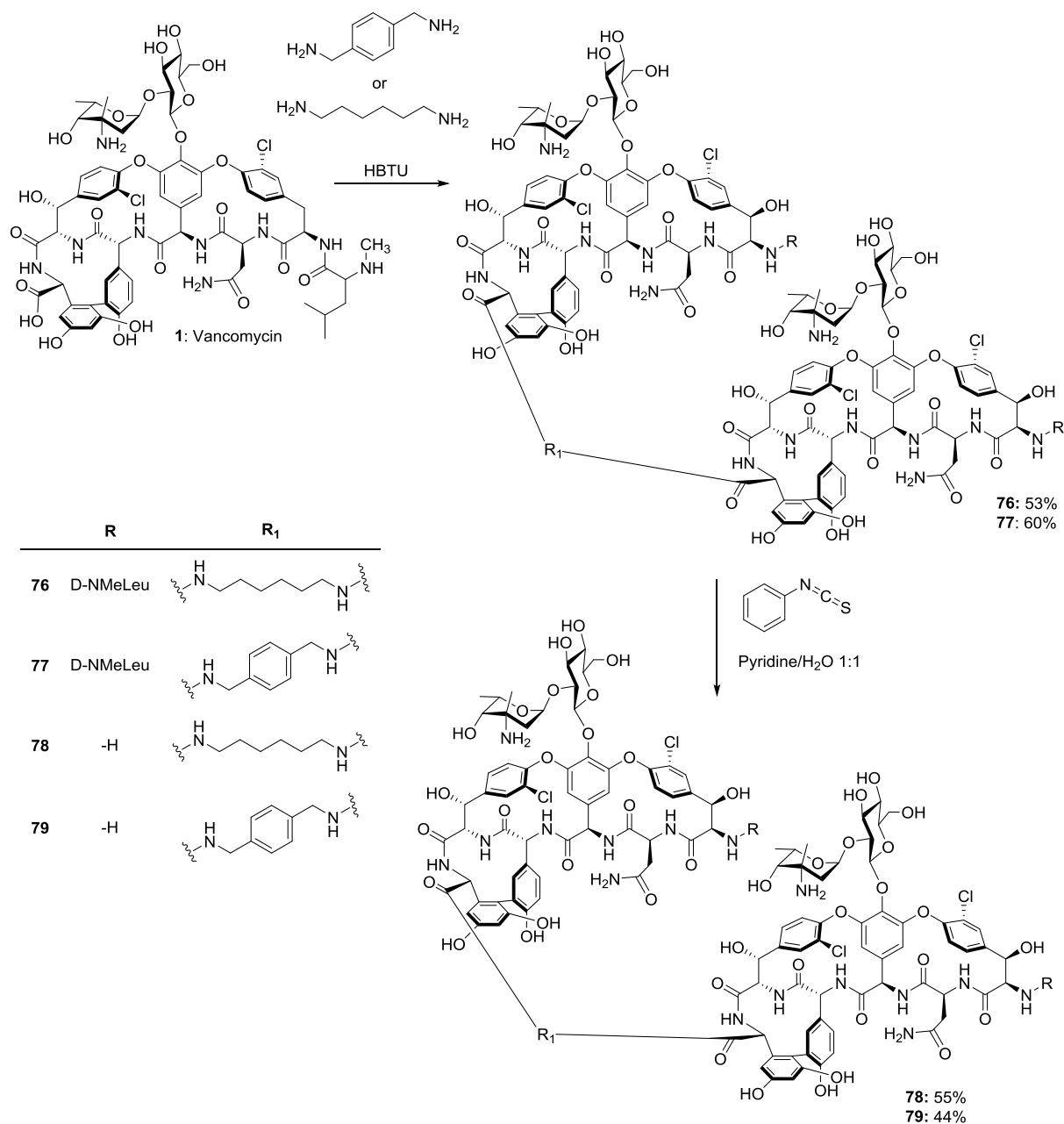
**Scheme 1.8** • Vancomycin dimers by disulfide formation  $n = 3$  (top) and olefin metathesis  $n = 2$  (bottom) by Nicolaou *et al.*



The antibacterial activity of both classes of dimer was found to be strongly dependant on the length of the tether employed, especially for the olefin-bridged dimers, where the optimum length was sixteen atoms between the vancosamine nitrogens (compound **75**). Dimer **75** had MICs of 1–2  $\mu\text{g mL}^{-1}$  against VRE (VanA) and vancomycin-intermediate *S. Aureus*, but antibacterial activity was lost on removal of the residue 1 D-leucine from the binding pocket. Of the disulfide dimers, compound **73** was particularly effective against VRE (VanA) with MICs of 0.06–0.5  $\mu\text{g mL}^{-1}$  compared to the vancomycin MIC of 50–100  $\mu\text{g/mL}$ . In this case, removal of amino acid residue 1 did not remove all antibacterial activity of the dimer, which retained MICs of 2  $\mu\text{g mL}^{-1}$  against vancomycin susceptible *enterococci* and 2–16  $\mu\text{g mL}^{-1}$  against VRE (VanA).

With promising biological results using the traditional synthetic approach described above, the Nicolaou group turned to applying a combinatorial methodology that allows an array of building blocks to assemble and react in the presence of a biological target. The biologically optimal combination of building blocks is then generated as the most prevalent species. For this study, three vancomycin analogues with tethers of different lengths were mixed, and under olefin metathesis conditions the reaction was monitored by mass spectrometry. In the presence of the peptide terminus analogue (Ac<sub>2</sub>-L-Lys-D-Ala-D-Ala), dimers with shorter tethers were formed preferentially, a result which matched the outcome of the antibacterial activity study. In conducting this study the Nicolaou group has therefore demonstrated that target induced rate acceleration is a powerful method for the rapid generation of biologically active dimers in the vancomycin family. The application of this approach to other biologically active systems would seem to hold promise for the development of more potent bioactive compounds.

The precise mode of action of vancomycin dimers has been called into question by Ellman *et al.*,<sup>48</sup> who compared the antibacterial activities of vancomycin and a series of tail-to-tail dimers with the corresponding desleucyl compounds, which were prepared by double Edman degradation (Scheme 1.9). Desleucyl vancomycin is unable to bind to L-Lys-D-Ala- D-Ala, a fact that is attributed to the lack of the leucine amino acid in the binding pocket, and it is therefore inactive against vancomycin-susceptible or resistant bacteria. However, the desleucyl dimers performed well against VRE (VanA) strains, and showed only a 3.5-8-fold increase in MIC over the vancomycin dimers (Table 1.3).



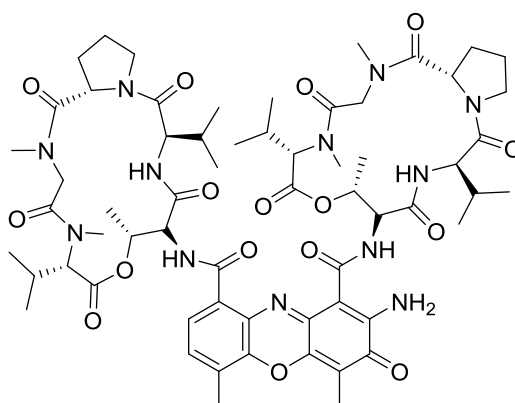
**Scheme 1.9** • Vancomycin tail-to-tail dimers, **76,77** and the corresponding desleucyl dimers **78,79** generated by Ellman *et al.*

**Table 1.3** *In vitro* antibacterial activity and peptide model binding affinity (Ellman *et al.*)

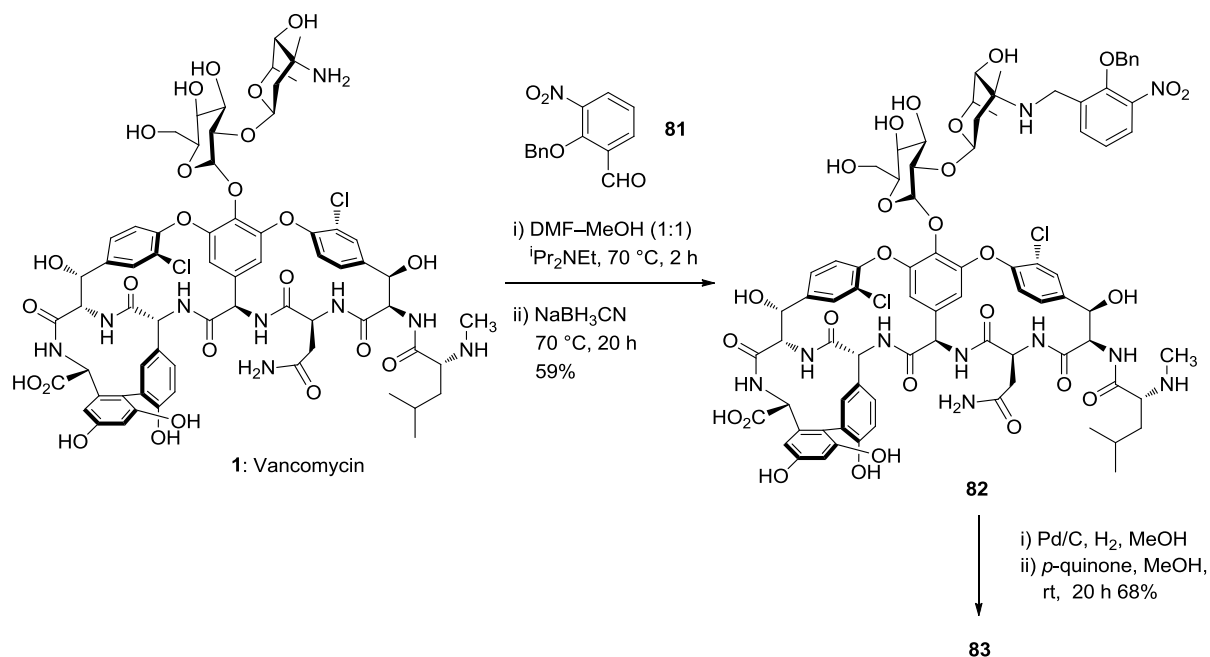
Compound	MIC ( $\mu\text{g/mL}$ ) <sup>a</sup>	K <sub>d</sub> ( $\mu\text{M}$ ) <sup>b</sup>
<b>Vancomycin</b>	1200	1.3
<b>Desleucylvancomycin</b>	>1200	>60
<b>76</b>	1.5	1.1
<b>77</b>	1.5	2.1
<b>78</b>	12	>60
<b>79</b>	5.8	>60

<sup>a</sup> Against *E. Faecium* (VanA). <sup>b</sup> Binding to dansyl-Lys(Ac)-D-Ala-D-Ala.

Crucially, a binding affinity study showed that **79** did not bind to the peptide model dansyl-Lys(Ac)-D-Ala-D-Ala or to surface-immobilised L-Lys-D-Ala-D-Lac. This indicates that the *in vitro* behaviour of vancomycin dimers is due to an alternative mechanism.

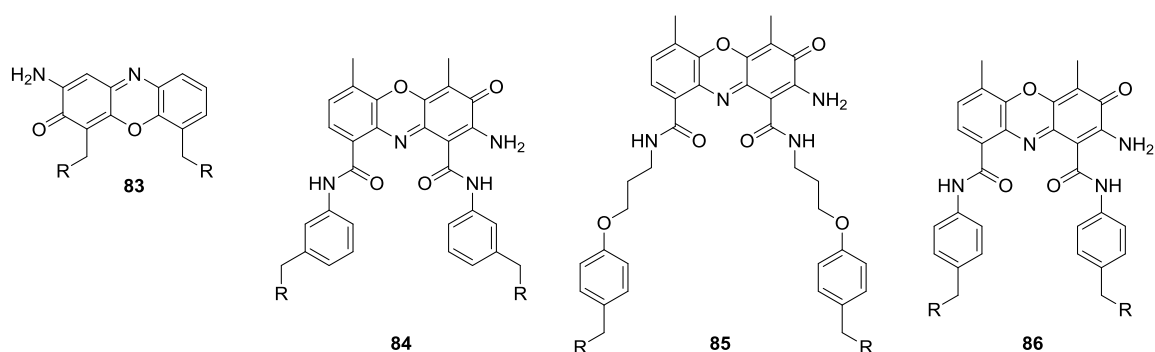
**80:** Actinomycin D**Figure 1.15 •** Molecular structure of actinomycin D (**80**)

Many of the previously reported dimers have been connected by long, flexible tethers, but a review of polyvalent interactions by Whitesides *et al.* highlighted the entropic disadvantages of such flexible linkers.<sup>49</sup> Changing tack, Arimoto *et al.* investigated the effect that incorporating a rigid natural product scaffold from actinomycin **80** (Figure 1.15) would have on the biological activity of vancomycin.<sup>50</sup> Reductive alkylation of vancomycin with 2-benzyloxy-3-nitrobenzaldehyde **81** was followed by a one-pot catalytic hydrogenation that removed the benzyl protecting group and reduced the nitro group to an amine (Scheme 1.10).



**Scheme 1.10** • Synthesis of actinomycin-inspired vancomycin dimers by Arimoto *et al.*

The unstable product was subjected to dimerisation using quinone in methanol, and afforded dimer **83** in a good yield (68%). This procedure benefits from mild reaction conditions, good selectivity and high yields. Actinocin-based dimers **83–86** were prepared with variations in linker length and character (Figure 1.16), all of which showed good stability *in vivo*.



**Figure 1.16** • Structure of actinomycin-inspired dimers by Arimoto *et al.* (R = vancomycin)

Dimers **83–86** were tested for biological activity against a range of vancomycin-susceptible and resistant bacteria (Table 1.4). As predicted, the short, rigid linker gave the best activity; compound **83** showed particularly promising activity against VRE but somewhat lower potency against MRSA than vancomycin.

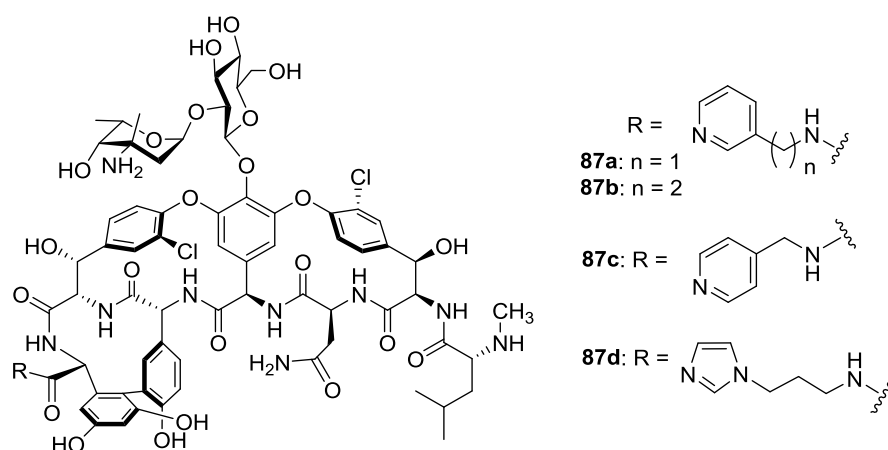
The low potency problem was overcome by changing the trifluoroacetate salt for the hydrochloride salt. This simple “anion switch” increased activity up to 32-fold. Furthermore, an *in vivo* study indicated that dimer **83** rivals the activity of the currently employed anti-pneumonia drug, linezolid, against *S. pneumoniae*.

**Table 1.4** Antibacterial activity of novel vancomycin dimers by Arimoto *et al.*

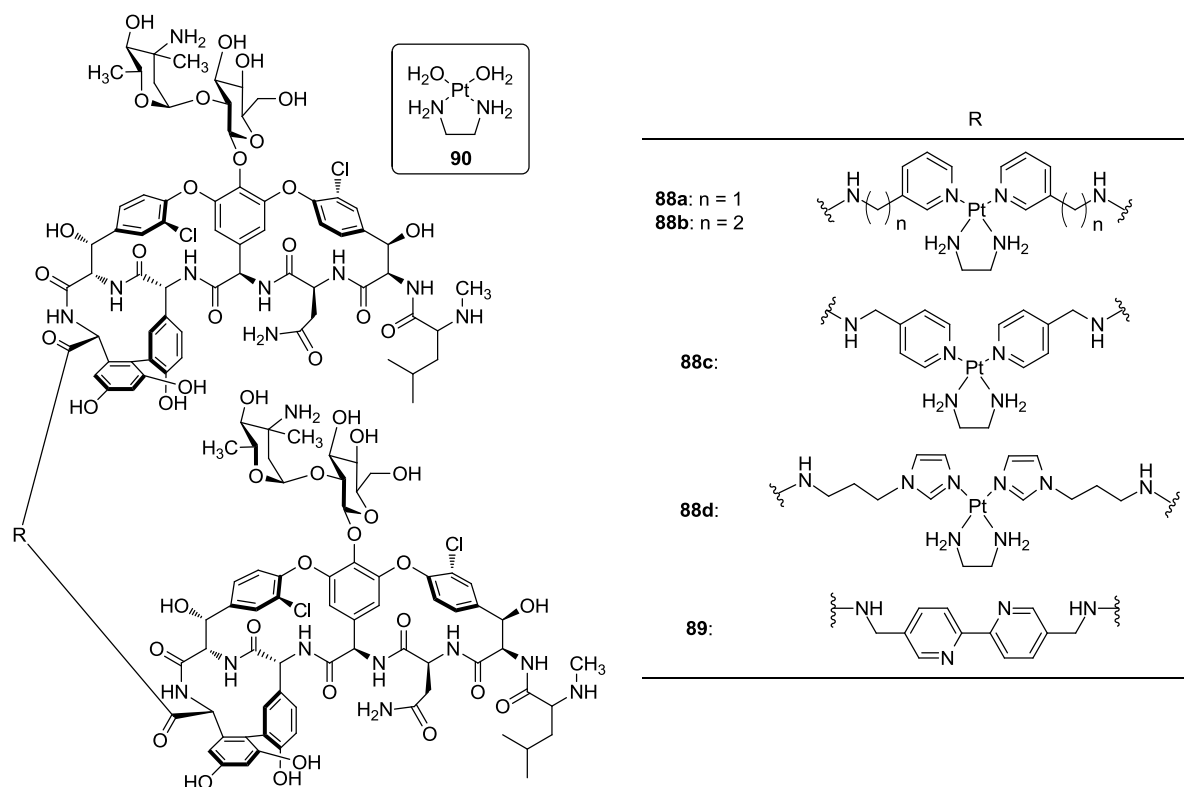
	<b>1</b>	<b>83</b>	<b>84</b>	<b>85</b>	<b>86</b>
<i>S. aureus</i> (MRSA)	1	16 (8)	32	16 (2)	32
<i>E. faecium</i>	0.5	0.5	1	2	0.5
<i>E. faecium</i> (VanA)	>64	32	2	8	32
<i>E. faecium</i> (VanB)	>64	1 (0.25)	1	2 (0.5)	1
<i>S. aureus</i> VRSA-2	>64	8 (4)	-	32 (1)	-
<i>S. pneumonia</i> Type 1	0.5	0.125 ( $\leq 0.063$ )	-	1 (0.25)	-

<sup>a</sup> MICs of the HCl salt shown in parentheses.

Acknowledging that the synthesis of covalently-linked dimers can be time-consuming and problematic, the Xu group have focussed on developing a different strategy based on self-assembly<sup>51</sup> and coordination chemistry. In 2003 Xu *et al.* reported on the exploitation of the unique structural geometry and stability that metal complexes can afford in the formation of vancomycin dimers.<sup>52</sup> Vancomycin reacted with the corresponding amine to give carboxamide derivatives **87a–d** in high yields (>65%) (Figure 1.17).



**Figure 1.17** • Vancomycin carboxamide derivatives generated by Xu *et al.*



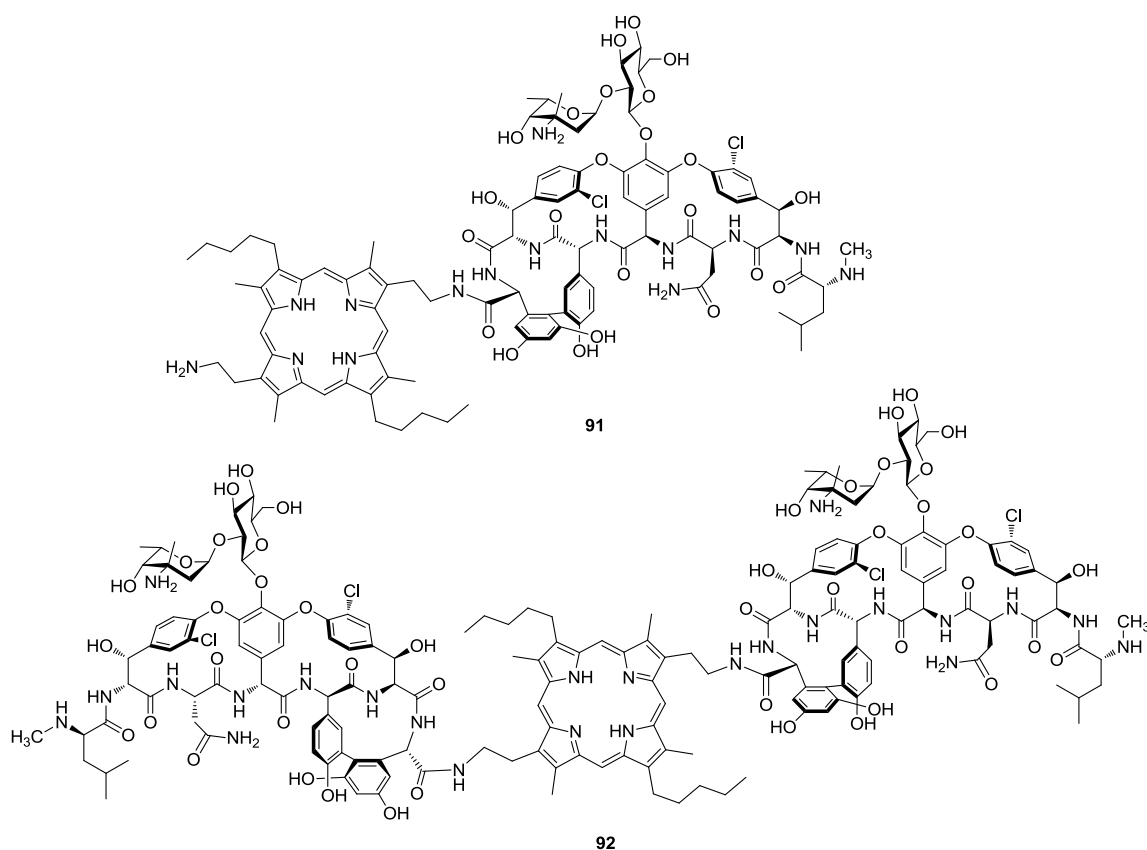
**Figure 1.18 •** Platinum-based vancomycin dimers by Xu *et al.*

Subsequent co-ordination with *cis*-platin derivative  $[Pt(en)(H_2O)_2]^{2+}$  in DMSO (20 h, rt, no light) afforded the dimeric complexes **88a–d** (Figure 1.18). Platinum complex-based vancomycin dimers **88a–d** exhibited higher biological activity against VRE than vancomycin itself, while retaining activity against vancomycin-susceptible *enterococci* (Table 1.5). Compounds **88a** and **88c**, with short chains, performed particularly well against a range of VRE, with MICs of 0.03–3.3  $\mu\text{g mL}^{-1}$ . Conversely, the more flexible dimers **88b** and **88d** lost activity against VRE (VanA) but remained relatively active against the VanB and VanC phenotypes, with MICs in the range of 0.05–4.8  $\mu\text{g mL}^{-1}$ . Crucially, platinum complex precursor **90** was completely inactive against gram positive bacteria, and vancomycin carboxamide derivatives **87a–d** only showed activity against vancomycin-susceptible *enterococci* and VRE (VanC).

**Table 1.5** • Antibacterial activity of Pt-based vancomycin dimers by Xu *et al.*

	1: Vancomycin	88a	88b	88c	88d
<i>E. faecalis</i> TCC29212	2	1	1	1	1
<i>E. faecalis</i> (VanA)	576	0.8	14	3.3	38
<i>E. faecium</i> (VanB)	102	0.28	2	1.2	4.8
<i>E. gallinarum</i> (VanC)	8	0.03	0.05	1	1

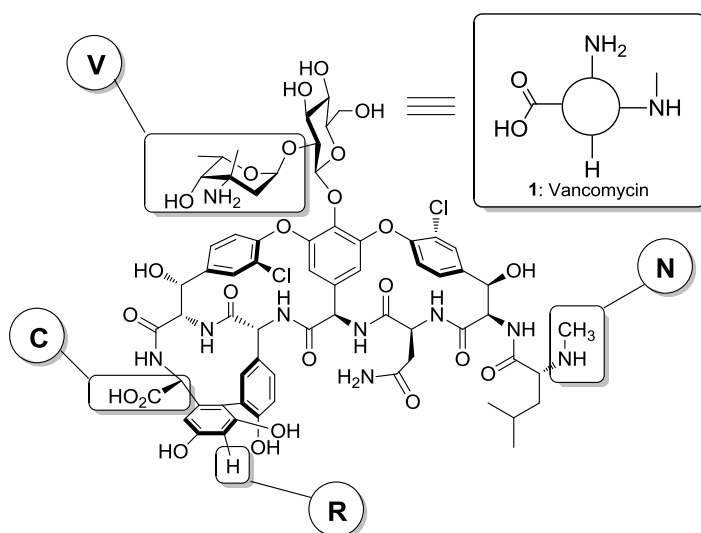
In this preliminary study, Xu *et al.* have shown that the rigid platinum complexes work well as linkers for the construction of multivalent inhibitors, but the cytotoxicity of such metal complexes is a factor that would need further investigation if the compounds were to find use in a clinical setting.

**Figure 1.19** • Mono- and divalent vancomycin-porphyrin conjugates generated by Xu *et al.*

In a more recent study, Xu *et al.* demonstrated the potential for application of a divalent vancomycin-porphyrin conjugate within photodynamic antimicrobial chemotherapy (PACT).<sup>53</sup> Porphyrin acts as a photosensitizer that generates a reactive oxygen species (ROS) on exposure to a suitable wavelength of light. The ROS causes cell death by attacking cell walls and membranes. The synthesis of a vancomycin-porphyrin conjugate

allowed PACT to accurately target areas of bacterial infection. Thus vancomycin was coupled to porphyrin using HBTU affording divalent conjugate **92** in a 54% yield (Figure 1.19). The use of excess quantities of porphyrin afforded monovalent conjugate **91** in a 53% yield. Both conjugates performed poorly against VRE (VanA and VanB) in the *in vitro* testing, with MICs in excess of  $32 \mu\text{g mL}^{-1}$ . However, divalent vancomycin-porphyrin conjugate **92** proved to be a successful affinity ligand in PACT evaluation, efficiently directing the porphyrin moiety to the surface of vancomycin-resistant bacteria.

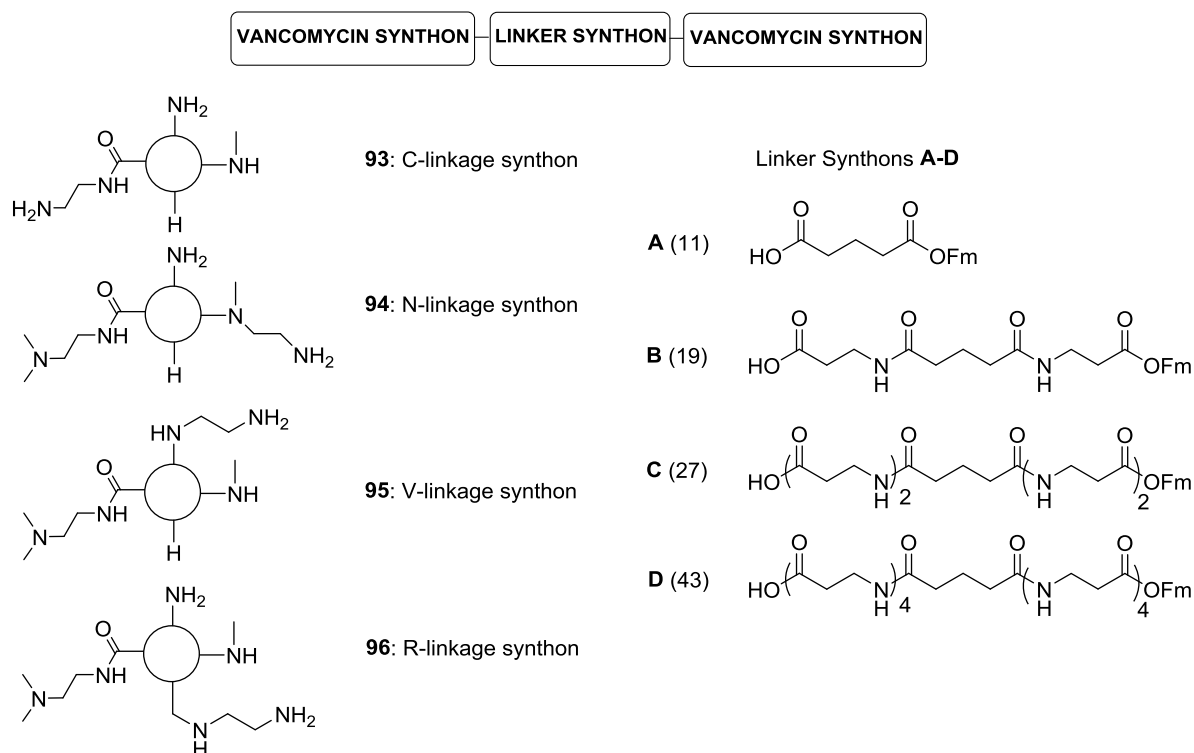
The majority of studies investigating glycopeptide dimerisation use vancomycin as the parent compound because of its proven activity against Gram-positive bacteria, and because dimers of other members of the glycopeptide family are rarely seen in the literature.<sup>54</sup> The exact structural requirements for good dimer activity remain elusive, though attempts to clarify patterns and trends have been made.



**Figure 1.20** Four sites of vancomycin ligation; vancosamine (V), N-terminus (N), C-terminus (C) and resorcinol ring (R).

Griffin *et al.* took a systematic approach to dimer design, identifying four sites of ligation; the C-terminus (C), N-terminus (N), vancosamine residue (V) and resorcinol ring (R) (Figure 1.20). Vancomycin synthons **93–96** were prepared using appropriate procedures; reductive alkylation was employed for preparation of the N and V synthons, amide bond formation for the C synthon and Mannich aminomethylation for the R synthon. The four vancomycin synthons **93–96** were connected in 10 unique combinations by linker synthons A-E to build an array of 40 dimers (Figure 1.21).<sup>55</sup>





**Figure 1.21** • Synthons for an array of vancomycin dimers by Griffin *et al.*

The V-V series was the most effective against vancomycin susceptible bacteria and the VRE *E. faecalis* VanB phenotype, whereas C-C, C-V and V-R combinations afforded broad spectrum activity, with MICs as low as  $9.4 \mu\text{g mL}^{-1}$  against the VanA resistant strain. The shortest linker, A, which placed a total of 11 atoms between the vancomycin molecules, was preferred for activity against VRE (VanA and VanB), whereas activity against vancomycin-susceptible *enterococci* was generally unaffected by linker length. Ultimately, this comprehensive study did not reveal many easily comprehensible structure–activity relationships for the vancomycin dimers; potency remained highly dependent on the strain of bacteria.

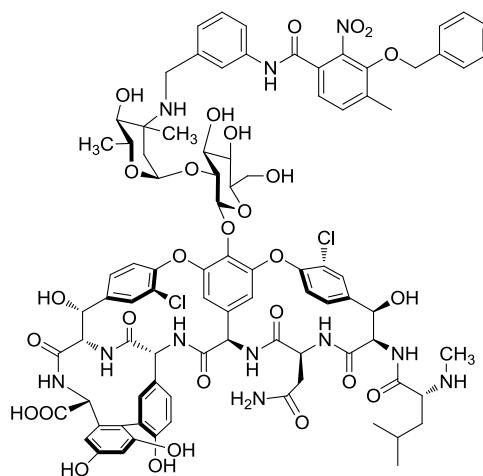
A key problem with the design of effective dimers is the ambiguity over the nature of the interactions between the dimers and the bacterial cells at a molecular level. The precise mode of action of the dimers has been called into question by several groups over the last decade, but there has been little investigation into the subject until earlier this year. The Arimoto group have recently reported the first biochemical study of the mechanism for vancomycin dimer activity.<sup>56</sup> Previously reported actinocin-based dimers **83** and **84** (Figure 1.16) were evaluated for their inhibitory action against bacterial macromolecules such as proteins, RNA, DNA, peptidoglycan and lipid biosynthesis. Vancomycin dimers

joined by the C-terminus of each monomer by the same actinocin linkers were also tested. The incorporation of radio-isotope-labelled precursors was used as a measure of activity for each process; protein synthesis ( $^{14}\text{C}$ -leucine), DNA synthesis ( $^{14}\text{C}$ -thymidine), RNA synthesis ( $^3\text{H}$ -uracil) and fatty acid synthesis ( $^{14}\text{C}$ -acetic acid) were unaffected by the presence of the vancomycin dimers, which exhibited selective inhibition of peptidoglycan synthesis ( $^3\text{H}$ -*N*-acetyl-D-glucosamine). This represents the first experimental evidence that vancomycin and the dimers that are formed act as VRE cell wall synthesis suppressors.

**Table 1.6** Inhibition of lipid intermediate (LI) and peptidoglycan (PG) synthesis by vancomycin dimers (Arimoto *et al.*)

	Susceptible Model <sup>a</sup>		Resistant Model <sup>a</sup>	
	LI	PG	LI	PG
<b>Vancomycin</b>	180	4.5	2300	85
<b>83</b>	98	2.2	700	31
<b>84</b>	74	11	300	61
<b>Van-M-02</b>	32	4.2	76	36

<sup>a</sup> IC50 ( $\mu\text{g}/\text{mL}$ )

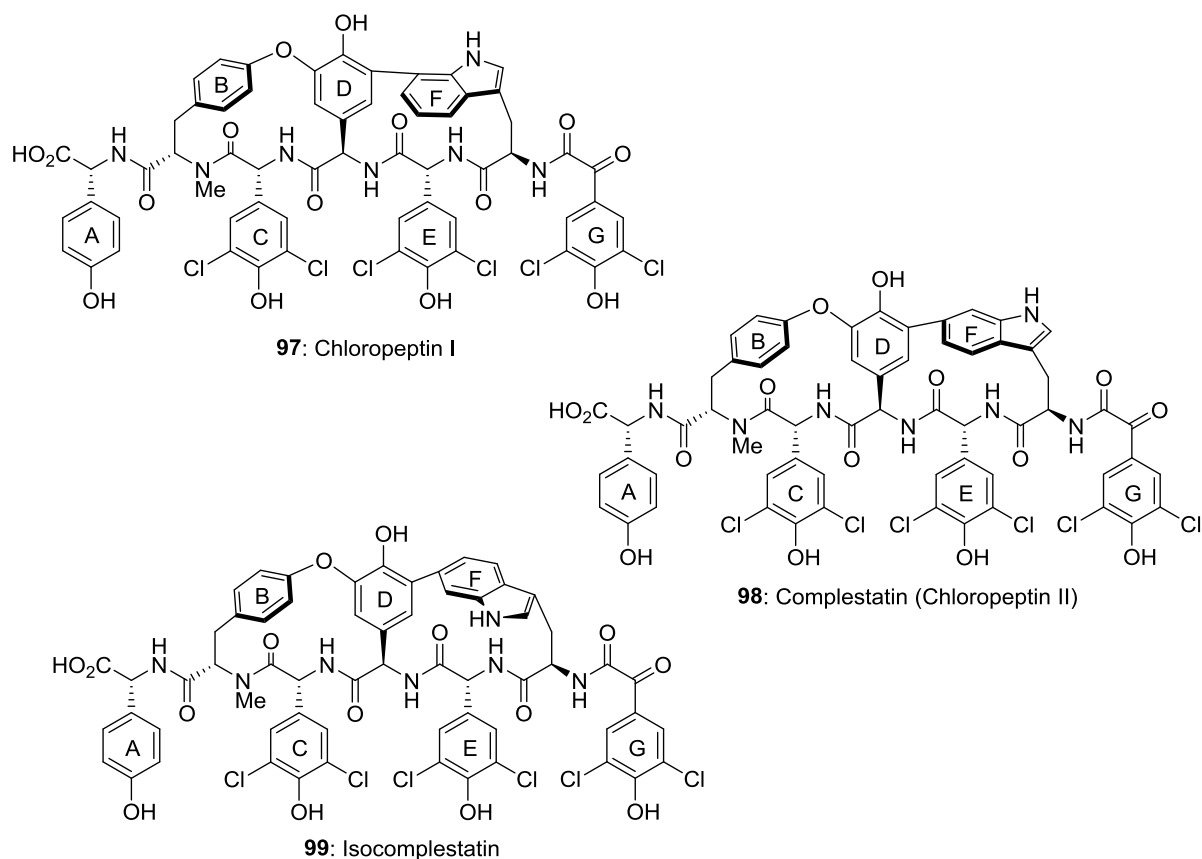


**Figure 1.22 •** Structure of novel vancomycin derivative Van-M-02 generated by Arimoto *et al.*

A sophisticated *in vitro* cell wall synthesis assay was then used to establish the effect of these compounds on the two stages in this process: lipid intermediate (LI) synthesis and peptidoglycan (PG) synthesis (Figure 1.23).



chloropeptin I (**97**) were isolated from *Streptomyces* sp. WK3419 in 1997, and the full stereochemistry of these compounds were elucidated from NMR data.<sup>59</sup>

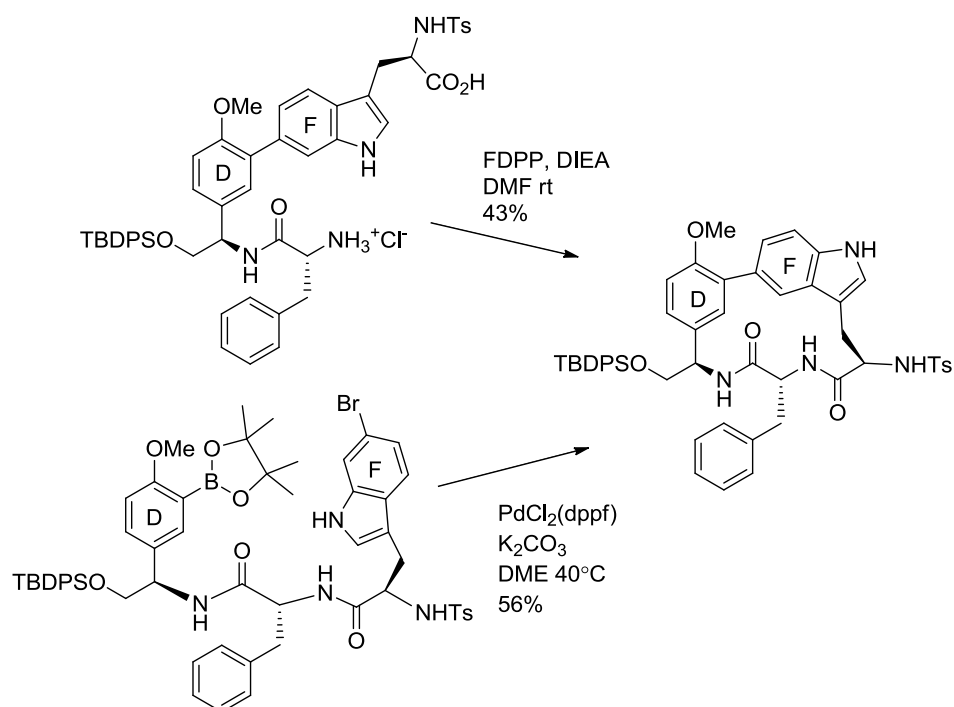


**Figure 1.24** Structure of the chloropeptins: chloropeptin I, complestatin (or chloropeptin II) and isocomplestatin

The structure of the chloropeptins is reminiscent of the glycopeptides antibiotics, with two macrocycles formed by coupling of the amino acid groups in the linear peptide chain. While the left hand side of the molecule shares the characteristic biaryl ether linkage of the vancomycin family, the second macrocycle is formed by a tryptophan indole ring. Restricted axial rotation about the indole means that there are two possible atropisomers of each compound, and while the natural products **97** and **98** consist only of the (*R*)-atropisomer, an (*S*)-atropisomer, isocomplestatin (**99**), has also been synthesised.<sup>60</sup> Compounds **97** and **98** differ only in the position of the junction between phenyl ring **D** and the indole ring **E**. Complestatin (**98**) can be easily converted to the less strained isomer, chloropeptin I (**97**), by an acid-catalysed rearrangement.<sup>61</sup> Also of note is the  $\alpha$ -

keto amide moiety connecting aryl ring G to the polypeptide chain, a structural feature which is not present in the vancomycin family.

Unlike the glycopeptide antibiotics, the chloropeptins show no activity against gram-positive bacteria, but they have attracted considerable interest for their significant activity against HIV. Studies have shown that this class of compounds inhibits binding of the HIV gp-120 glycoprotein to the CD4 receptor of T-lymphocytes, thus preventing HIV infection of the cells.<sup>62</sup> Isocomplestatin has also been shown to have activity against HIV integrase, the enzyme responsible for integration of viral DNA into the DNA of the infected cell.<sup>63</sup>

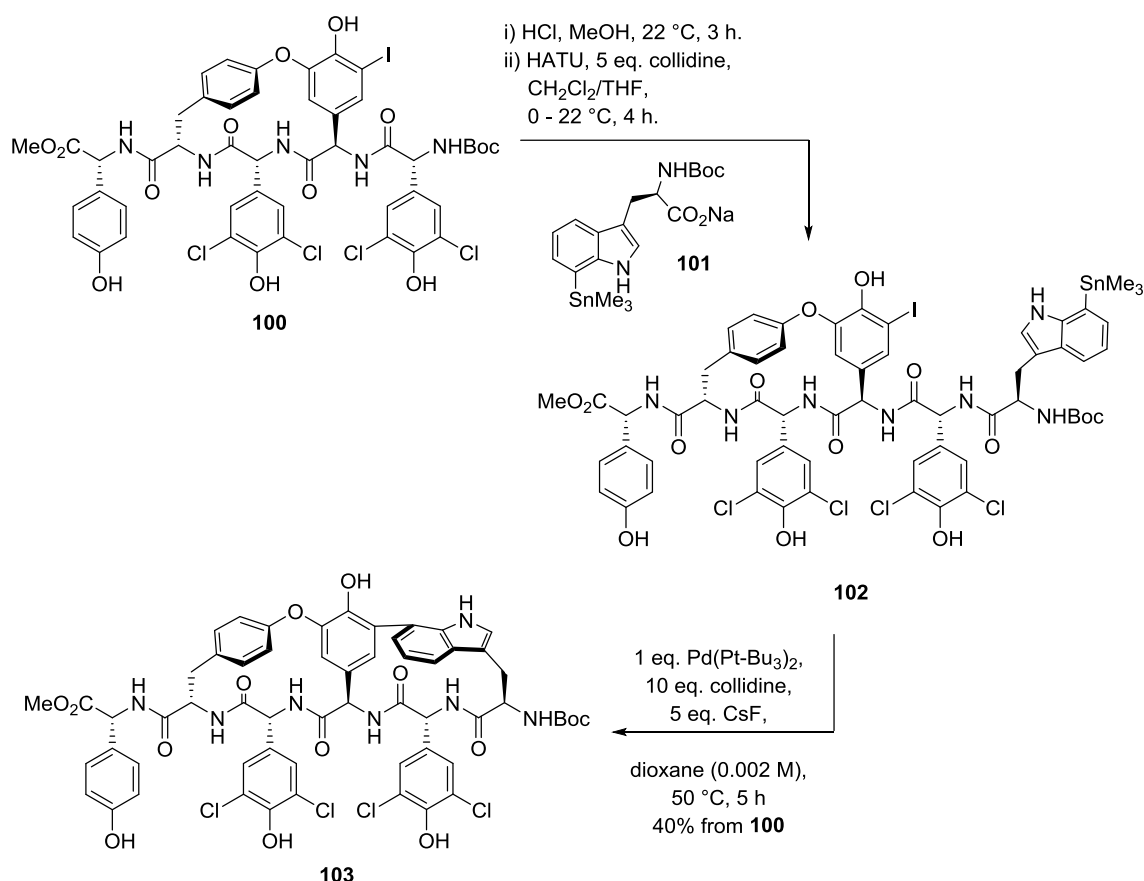


**Scheme 1.11** • Two macrocyclisation procedures for construction of the **D-F** ring of complestatin by Rich and Elder.

While complestatin was isolated and characterised in the 1980s, synthetic studies have been slow to emerge. The challenges presented by this compound are centred around the atropisomerism of the **D-F** macrocycle and, as with vancomycin, finding an effective solution to the problematic biaryl ether formation/cyclisation step. Until 2000, only a handful of complestatin fragments had been synthesised.<sup>64</sup> In the first of these, Gurjar *et al.* employed a Suzuki-Miyaura cross-coupling method to construct the aryl-indole C-C bond prior to cyclisation, but discovered that subsequent peptide coupling protocols could

not be used to complete this macrocycle.<sup>65</sup> The problem was overcome by Rich and Elder two years later (Scheme 1.11).<sup>66</sup>

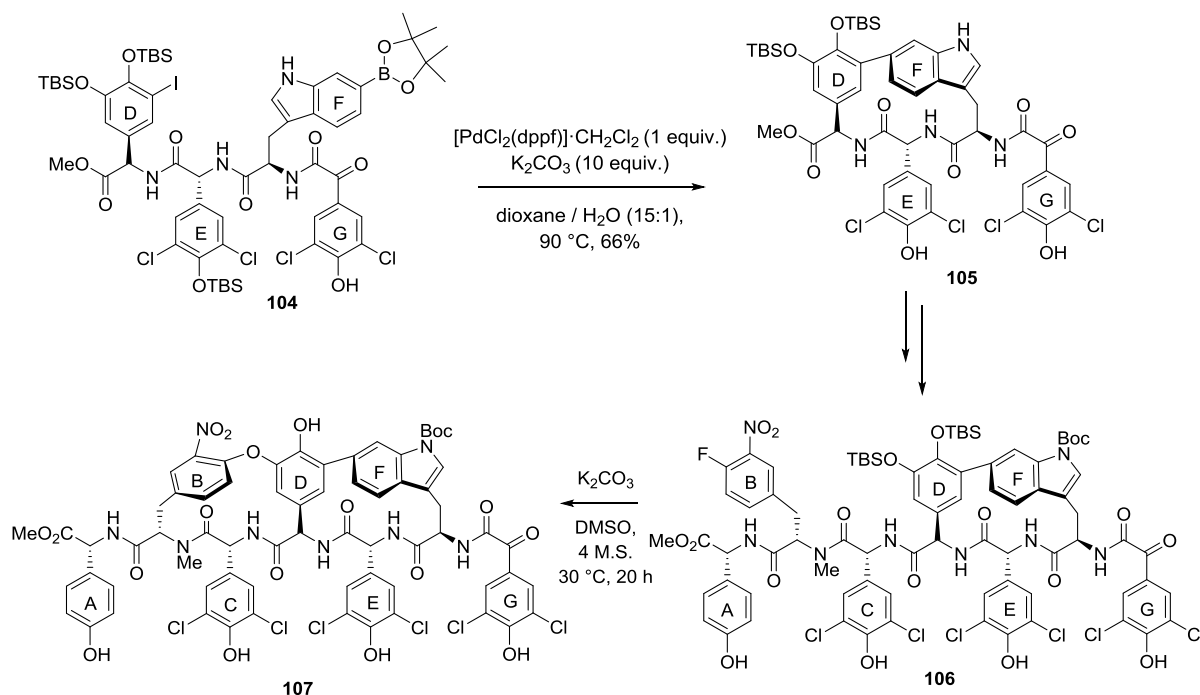
The first stereoselective total synthesis of chloropectin I was published in 2003 by Snapper and Hoveyda.<sup>67</sup> The synthetic design involved a copper-mediated biaryl ether formation to close the **B-O-D** macrocycle followed by palladium-mediated cross-coupling to generate the **D-F** macrocycle (Scheme 1.12).



**Scheme 1.12 • D-F macrocyclisation step in the synthesis of Chloropectin I reported by Snapper and Hoveyda**

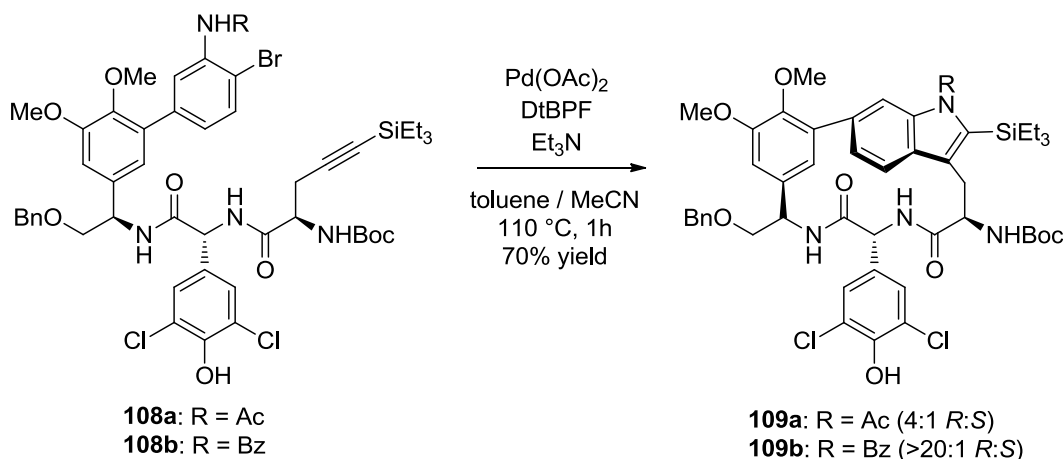
For this key step, stannyl tryptophane **101** was incorporated *via* peptide coupling, affording intermediate **102**. The subsequent cyclisation step was achieved with one equivalent of bis(tri-tertbutylphosphine) palladium(0), 10 equivalents of collidine and cesium fluoride (5 equiv.). The macrocyclisation product **103** was obtained in a 40% yield from **100**. The addition of collidine (10 equiv.) to the standard conditions previously reported<sup>68</sup> for this Stille-type C–C bond formation proved crucial to the efficiency of the reaction; in the absence of this additional base the reaction ceased after 30 minutes and

the solution turned black. Snapper and Hoveyda speculated that collidine has a role in the stabilization of the active palladium complex.



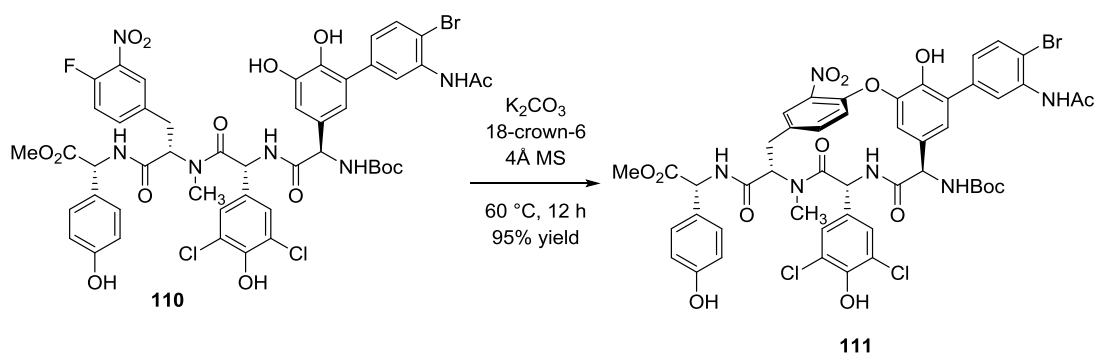
**Scheme 1.13** • Intramolecular Suzuki-Miyaura coupling and S<sub>N</sub>Ar macrocyclisation steps by Zhu *et al.*

After chloropeptin I, complestatin (chloropeptide II) became the next target for total synthesis. The Zhu group first chose to apply the well-used nucleophilic aromatic substitution reaction promoted by a nitro substituent on the aromatic ring to close the **B-O-D** macrocycle (Scheme 1.13).<sup>69</sup> The right hand side of the molecule was then constructed *via* an intramolecular Suzuki-Miyaura coupling reaction that completed assembly of the **D-F** macrocycle. It was during this study that Zhu *et al.* discovered that this approach resulted in the synthesis of the unnatural (*S*)-atropisomer, isocomplestatin. Reversing the order of cyclisation favoured the correct (*R*)-atropisomer, a conclusion also reached by the Boger group in their publication of the same year.<sup>70</sup> Preparation of linear peptide **104** afforded the substrate for intramolecular Suzuki-Miyaura coupling with 1,10-bis(diphenylphosphino)-ferrocene-palladium(II)dichloride, which afforded **105** in a 66% yield. NOE studies confirmed the (*R*) axial chirality of **105**. The intramolecular S<sub>N</sub>Ar reaction of **106** for the formation of the **B-O-D** biaryl ether linkage in **107** was achieved in a pleasing 62% yield under mild conditions.



**Scheme 1.14** • Larock macrocyclisation by Boger *et al.*

In a unique approach to the challenge of the **D-F** ring system of complestatin, Boger *et al.* investigated the use of an intramolecular Larock indole synthesis<sup>71</sup> that would provide simultaneous construction of both the right-hand macrocycle and the five-membered indole ring (Scheme 1.14).<sup>70</sup> Studies by Larock *et al.* indicated that the steric influence of a large terminal alkyne substituent, such as a triethylsilyl group, would induce the correct regioselectivity in the indole cyclisation process.<sup>72</sup> The reaction was found to benefit from the incorporation of an electron-rich bidentate phosphine ligand, 1,10-bis(di-tertbutylphosphino) ferrocene (DtBPF). Yields of up to 89% were obtained with aniline acetamide **108a**, with 4:1 (*R:S*) atropodistatereoselectivity. However, incorporating the larger benzamide group, intermediate **108b**, afforded >95% of the (*R*)-atropisomer in a 70% yield.

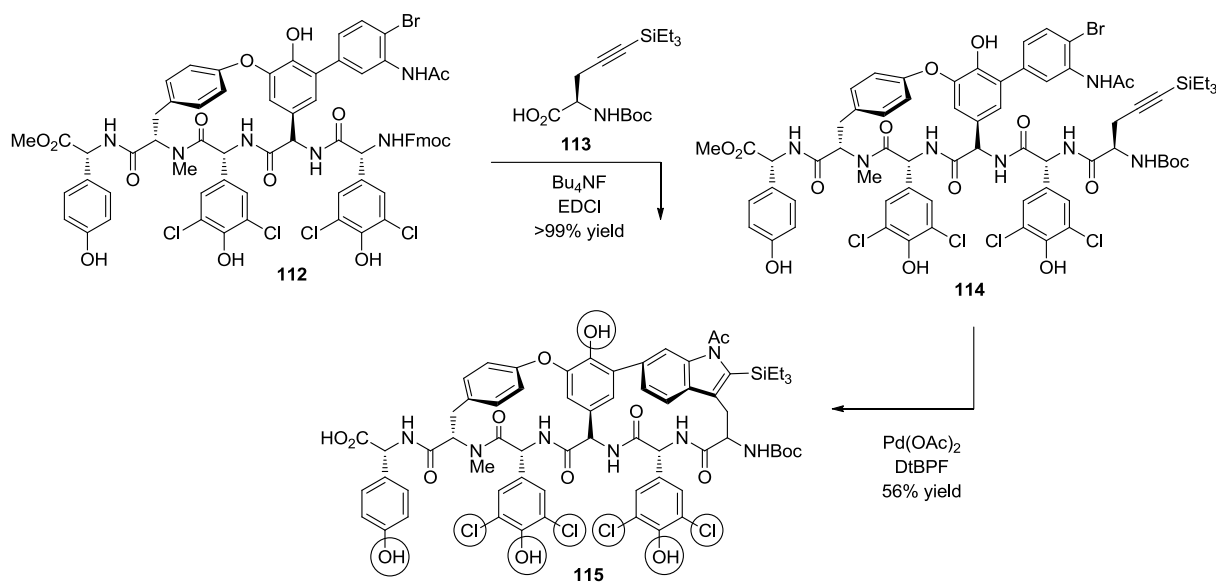


**Scheme 1.15** • Intramolecular  $S_NAr$  macrocyclisation for formation of the **B-O-D** biaryl ether linkage of complestatin (Boger *et al.*)

These promising results were applied to a total synthesis of complestatin with great success. Taking a reverse approach to the order of macrocyclisation chosen by the Zhu group, the Boger group found that construction of the **B-O-D** ring system before indole



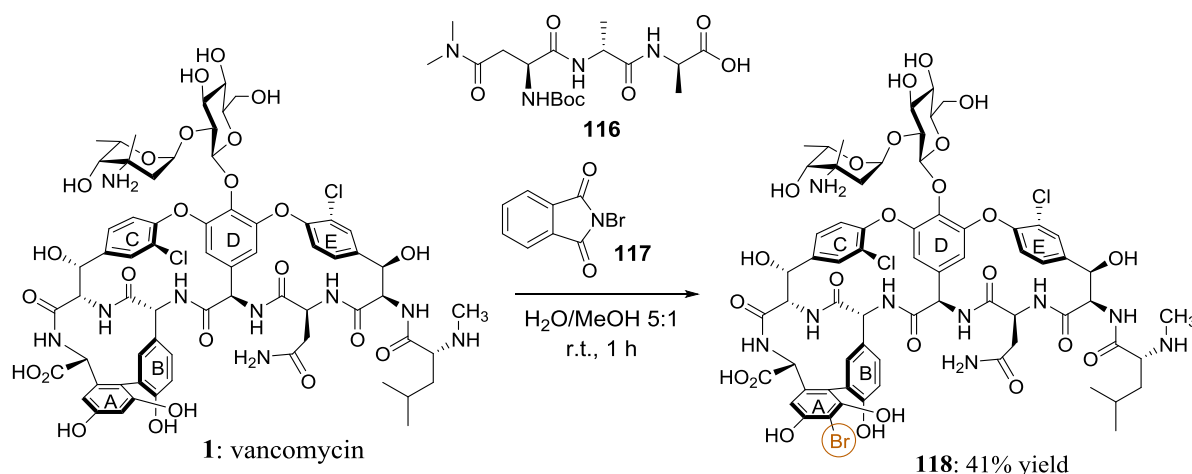
macrocyclisation produced better results. Thus intramolecular nucleophilic aromatic substitution of **110** with potassium carbonate at 60 °C for 12 h in the presence of 4 Å molecular sieves and 18-crown-6 afforded **111** in an excellent 95% yield (Scheme 1.15). The nitro substituent used as a promoter for this step was subsequently removed by a previously reported same two-step procedure.<sup>73</sup> The alkyne required for Larock cyclisation, with its triethylsilyl substituent, was introduced as amino acid component **113** (Scheme 1.16). Fmoc deprotection followed by peptide coupling afforded **114** in a quantitative yield ready for subsequent indole synthesis. Unlike analogue **108** on which the reaction conditions were developed, the substrate in the total synthesis contained a number of potentially problematic functional groups: notably the four unprotected phenols and “four labile aryl chlorides” (circled in Scheme 1.16).<sup>70</sup> However, the intramolecular Larock cyclisation afforded **115** as a single (*R*)-atropisomer, in an unoptimised yield of 56%. The remaining triethylsilyl substituent was easily removed from the indole ring using dilute hydrochloric acid.



**Scheme 1.16** • Intramolecular Larock indole synthesis applied to the total synthesis of complestatin by Boger *et al.*

## 1.7 Latest developments in the synthesis of new glycopeptide antibiotic analogues<sup>ii</sup>

Employing their expertise in the area of functionalisation of complex molecules,<sup>74</sup> the Miller group investigated the site-selective bromination of the **A-B** ring of vancomycin (**1**) (Scheme 1.17), with the expectation that incorporating bromine into the binding pocket region of **1** would have an impact on its biological activity.<sup>75</sup> To this end, peptide catalyst **116** was designed around the D-Ala-D-Ala dipeptide moiety known to have a good binding affinity for vancomycin (see Section 1.3). Catalyst **116** also features the *N,N'*-dimethylamido functionality which was anticipated to accelerate the rate of bromination in these reactions based on the observed efficiency and selectivity of the NBS-DMF reagent reported by Mitchell *et al.*<sup>76</sup>

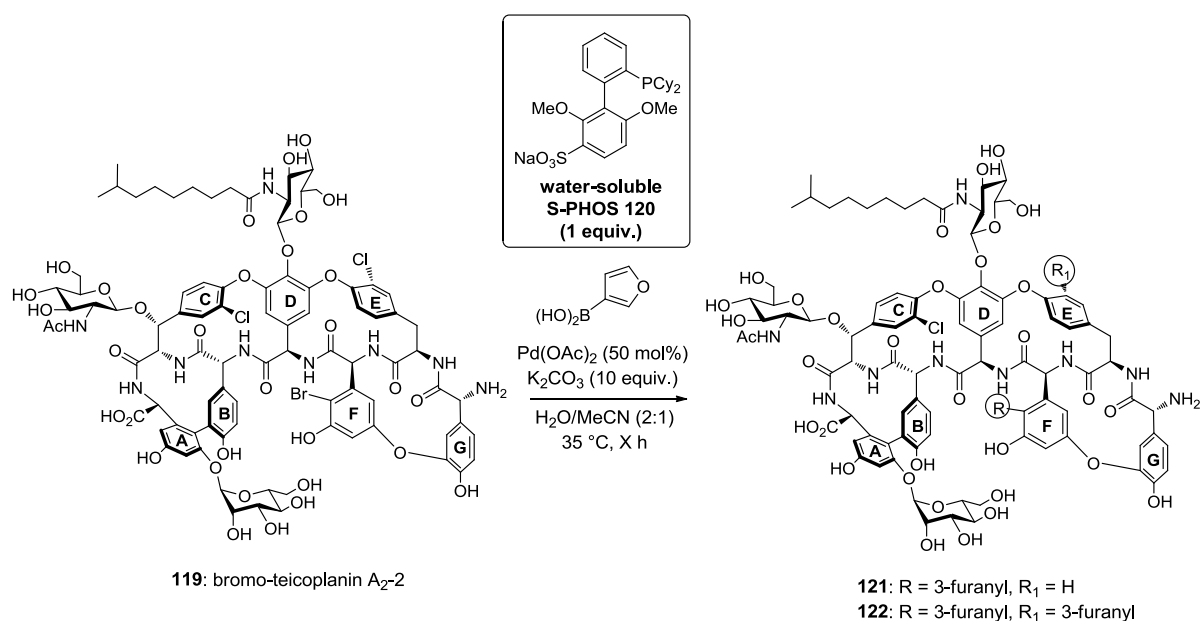


**Scheme 1.17 • Site-selective monobromination of vancomycin reported by Miller and Pathak**

While the uncatalysed bromination of vancomycin with *N*-bromophthalimide **117** afforded a 1:1 ratio of monobromination at the two available positions on ring **A**, the addition of catalyst **116** afforded compound **118** in a 41% yield on a preparative 100 mg scale. Dibromination of ring **A** was observed to be the major byproduct by HPLC analysis of the reaction mixture. Antibacterial studies carried out on these compounds showed that bromination of ring **A** failed to improve the biological activity of vancomycin against gram-positive bacteria.

ii Section 1.7 presents an overview of research reported in this area since publication of the following review: P. Ashford and S. P. Bew, *Chem. Soc. Rev.*, **2012**, *41*, 957.

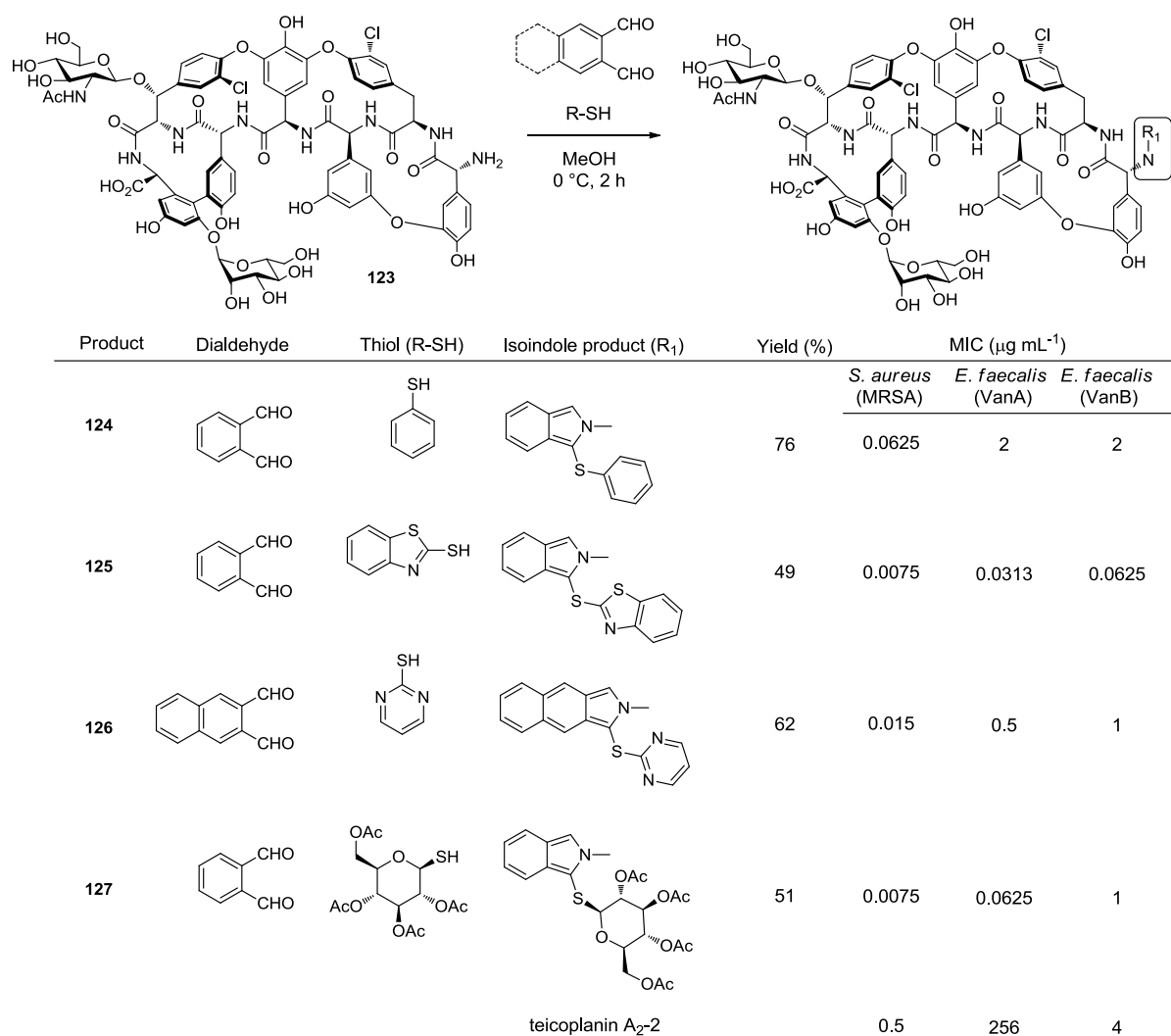
A similar approach to the “chemical tailoring” of teicoplanin (**5**) afforded a series of brominated derivatives with potential as substrates for metal-catalysed cross-coupling reactions.<sup>77</sup> With this in mind, the palladium(II) acetate catalysed Suzuki coupling of compound **119** with a series of aryl and alkyl boronic acids was carried out (Scheme 1.18). The Suzuki reaction was initially unsuccessful, and [substrate+Pd] molecular ions were observed by LC-MS, indicating that the palladium species in the reaction was able to bind to teicoplanin, inhibiting catalysis. An unusually high catalyst loading of 50 mol% was therefore required for these reactions to take place. Thus compound **119** was coupled with 3-furanylboronic acid in the presence of water-soluble *S*-PHOS ligand **120** (1 equiv.) at 35 °C to afford product **121** in a 28% yield. Employing a higher temperature of 50 °C brought about a second Suzuki coupling reaction at the C-Cl bond on ring **E** to afford compound **122**.



**Scheme 1.18** • Suzuki cross-coupling reaction of bromo-teicoplanin **119** reported by Miller and Pathak

3-Furanyl substituted derivatives **121** and **122** showed slightly improved activity against MRSA compared to teicoplanin (MIC = 0.25 µg mL<sup>-1</sup> compared to 0.5 µg mL<sup>-1</sup> for teicoplanin A<sub>2</sub>-2) but were equally inactive against the VanE strain of vancomycin-resistant *enterococci*.

Following their earlier work on the application of the Click reaction to the synthesis of novel teicoplanin derivatives (Section 1.4.3), Herczegh *et al.* set out to synthesise a series of fluorescent teicoplanin and ristocetin derivatives which could be used to elucidate their mode of action at the bacterial cell wall.<sup>78</sup> Inspired by the early studies of Nagarajan *et al.* on the *N*-alkylation of glycopeptides described earlier in this review (Section 1.4.1), Herczegh *et al.* employed a three-component isoindole formation to tag the *N*-terminus of the peptide chain with a fluorescent moiety (Scheme 1.19).

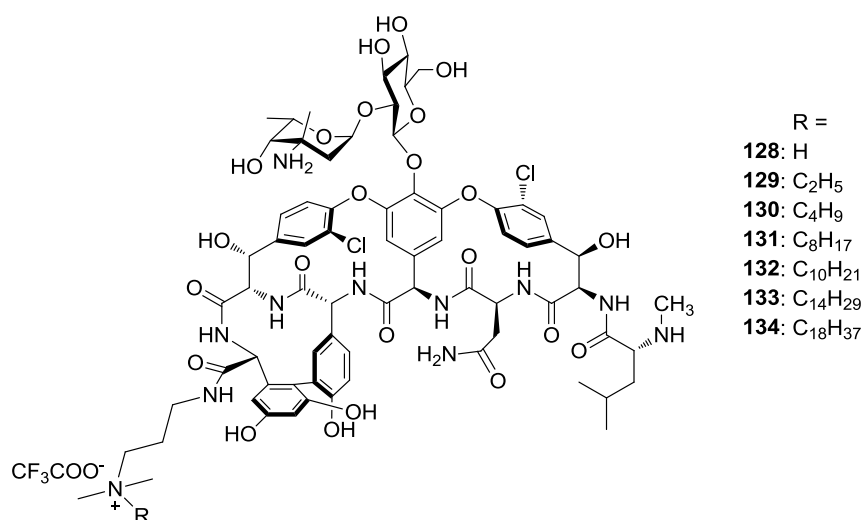


**Scheme 1.20** • Synthesis of isoindole and benzoisoindole derivatives of teicoplanin aglycon reported by Herczegh *et al.*

Thus teicoplanin pseudoaglycon **123** reacted with *o*-phthalaldehyde and an aryl or alkyl thiol at the *N*-terminus, affording a series of isoindole and benzoisoindole derivatives **124–127** in moderate to good yields of 31–76%. The new compounds were tested against

a range of resistant and non-resistant bacteria, and almost all exhibited better MICs than the parent natural product, teicoplanin. Compound **125** in particular shows excellent broad activity against both VanA and VanB strains of resistant bacteria, with MICs of  $0.0313 \mu\text{g mL}^{-1}$  and  $0.0625 \mu\text{g mL}^{-1}$  respectively, compared to values of  $>256 \mu\text{g mL}^{-1}$  and  $4 \mu\text{g mL}^{-1}$  for teicoplanin A<sub>2</sub>-2.

Bacteria are known to be slow in developing resistance to cell membrane disrupting agents such as antimicrobial peptides.<sup>79</sup> In order to counter bacterial resistance to vancomycin as well as increase its potency, Haldar *et al.* designed a series of derivatives bearing a permanent cationic quaternary ammonium moiety at the C-terminus (Figure 1.25).<sup>80</sup> These new glycopeptides were synthesised by coupling the carboxylic acid group of vancomycin with the desired amine using HBTU. This peptide coupling step was achieved in yields of 70-80% to afford compounds **128-134** bearing alkyl chains between 2 and 18 carbons in length.



**Figure 1.25 •** Alkyl quaternary ammonium trifluoroacetate derivatives of vancomycin reported by Haldar *et al.*

Haldar *et al.* propose that the lipophilicity of the added alkyl chain disrupts the integrity of the bacterial cell membrane, while the permanent positive charge may strengthen the interaction between the antibiotic and the negatively charged bacterial membrane, “anchoring” the drug in place. By adding a secondary mode of action to the inherent antibacterial activity of vancomycin, Haldar *et al.* have synthesised a highly potent broad-spectrum antibiotic (compound **133**) which shows 25-fold improvement in activity against VRE compared to the second generation glycopeptide dalbavancin **9**.

Furthermore, the repeated exposure of MRSA to compounds **131** and **133** resulted in no change in MIC after 52 days, compared to a 20-fold increase in MIC for vancomycin, indicating that they are slow to induce bacterial resistance in this strain.

## 1.8 Conclusions

It is clear that the race to complete a total synthesis of vancomycin in the late 1990s was not the end of the glycopeptide story; the 21st century demand for effective novel antibiotics is reflected in the plethora of articles published in this field. This review has brought together the many and varied approaches to vancomycin modification; in particular the alkylation of oxygen and nitrogen-containing groups has been shown to significantly increase antibacterial activity. Other modifications take their cues from nature, with the construction of covalent dimers mimicking the dimerisation of vancomycin in aqueous solution, and the addition of long tethers similar to the hydrophobic “anchor” of teicoplanin.

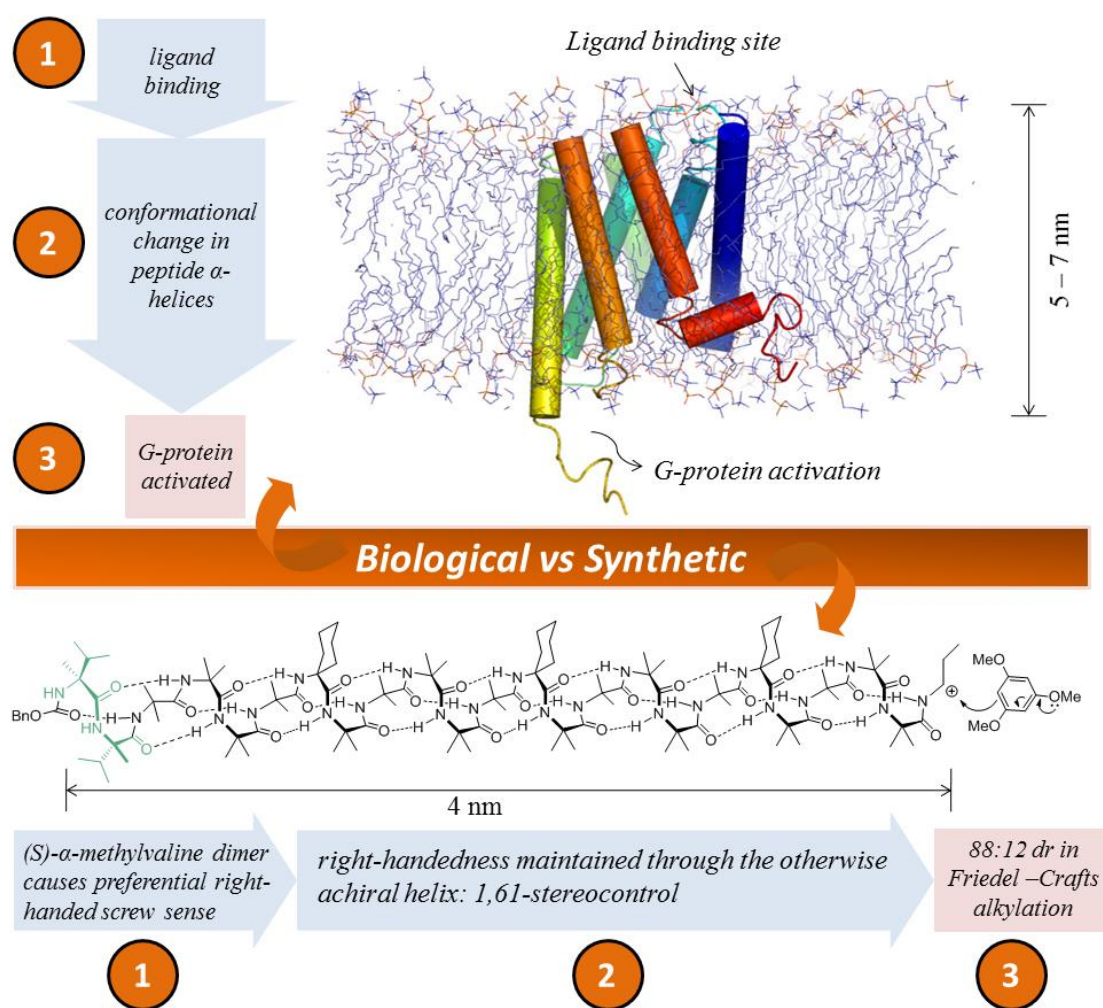
The importance of a tandem approach to drug design and biochemical investigation is particularly highlighted by recent research into the mode of action of glycopeptide dimers, and stronger links forged between antibiotic design and the nature of the intended target will undoubtedly lead to further reports of biologically active molecules. Alongside these ongoing investigations, the total synthesis of the closely-related complestatin family has been completed by a number of research groups in the last decade. Following the success of vancomycin modification, it may well be that future publications will report the design and discovery of highly biologically active analogs and derivatives of complestatin, a natural product whose full potential has yet to be explored.

## CHAPTER TWO

Remote asymmetric induction (>1,5-stereocontrol)

## 2.1 Introduction

Remote stereocontrol, or remote asymmetric induction, occurs when the existing stereochemical centre or axis of the substrate molecule in a chemical reaction influences the formation of a new stereochemical feature in the product through more than five covalent bonds, equivalent to a through-space distance of  $>0.7$  nm.<sup>111</sup>



**Figure 2.1** Comparison of cross-membrane communication by the  $\beta$ -adrenergic G-protein-coupled receptor<sup>i</sup> (top) with state of the art remote asymmetric induction by a helical peptide foldamer, reported by Clayden *et al.*, 2014 (bottom)

Long-range communication of stereochemical information is common in biological systems. A particularly well understood example is the structure and mechanism of the  $\beta$ -2 adrenergic G-protein-coupled receptor (GPCR) which takes part in cell signaling by spanning the width of the phospholipid bilayer (Figure 2.1).<sup>81</sup> When a ligand such as (*R*)-

<sup>i</sup>Figure 2.1 image top right adapted and reproduced by permission of MacMillan Publishers Ltd: Nature,<sup>81</sup> copyright 2008.

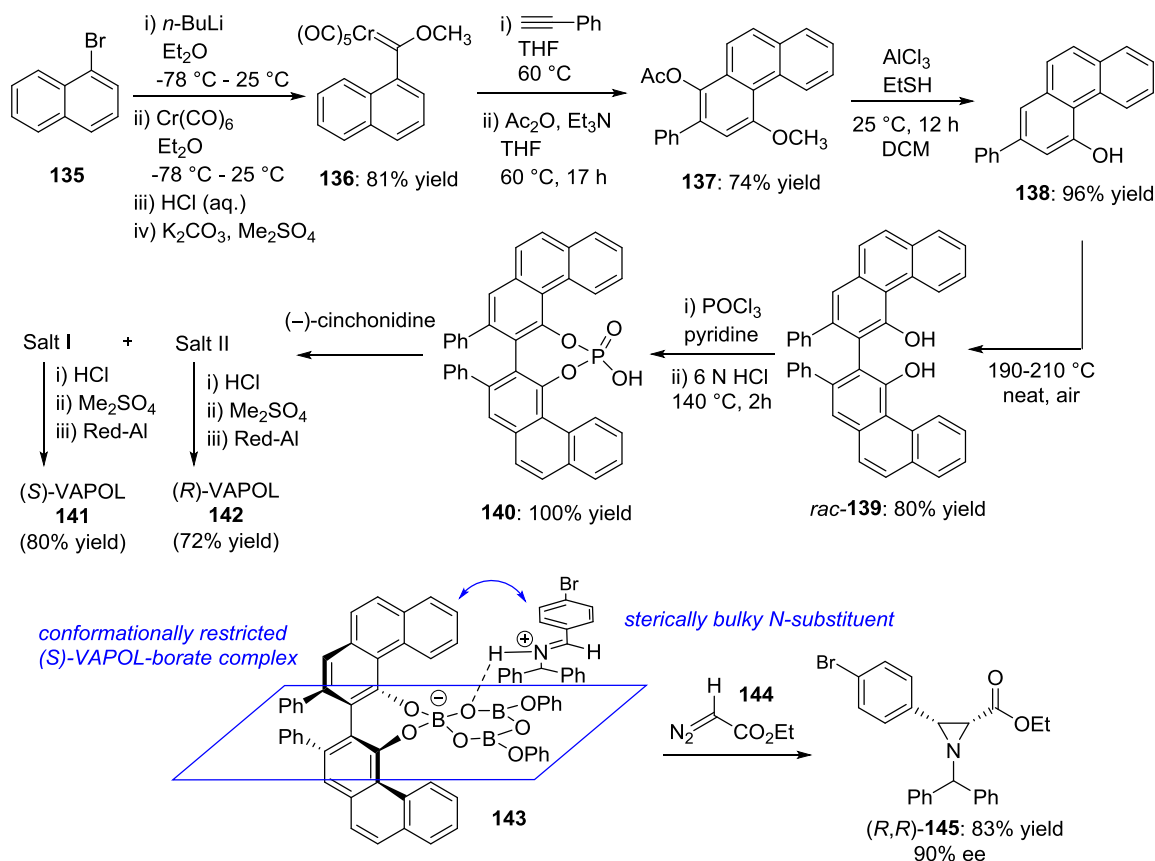


epinephrine (adrenaline) binds to the  $\beta$ -2 adrenergic receptor outside the cell, a conformational change takes place in the peptide structure which activates G-proteins within the cell, leading to changes in the levels of intracellular messengers such as  $\text{Ca}^{2+}$  ions. By the long-range communication of stereochemical information, the  $\beta$ -2 adrenergic receptor therefore effects a change in cell processes across an impressive distance of 5 - 7 nm from the ligand binding site.

Remote stereocontrol in synthetic chemistry has generally been limited to a distance of 5 to 8 covalent bonds by the need for rigidity in the reaction transition states. However, research by Clayden and co-workers over the last five years has pushed the boundaries of remote asymmetric induction to through-space distances of up to 4 nm.<sup>82</sup> This advance makes synthetic remote stereocontrol comparable to biological systems. The recent high-impact publications by Clayden *et al.* have led to a renewed interest in the development of the long-range communication of stereochemical information associated with remote asymmetric induction for potential new applications in the design of artificial peptide-based cell structures such as synthetic receptors.<sup>83</sup>

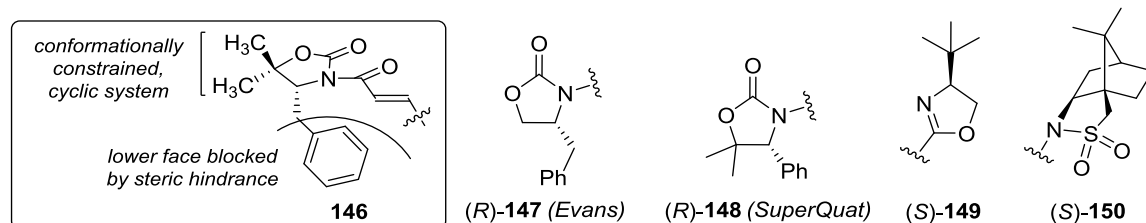
## 2.2 Overview of remote stereocontrol

The stereoselective synthesis of a new chiral centre in an organic compound can be achieved either by reagent control (i.e. using a chiral catalyst or additive) or by substrate control, in which existing chiral information is relayed through the covalent bonds of the compound to the site of reactivity. In organocatalysis,  $\text{C}_2$ -symmetric chiral catalysts based on rigid frameworks such as BINOL and BINAP have become increasingly popular in the synthesis of aziridines, epoxides, and for asymmetric hydrogenation.<sup>84</sup> They are efficient with regard to the amount of chiral material used, and the stereochemistry (*R* / *S*, or *M* / *P* in the case of helical compounds) of the catalyst can be selected to obtain the desired enantiomer of the reaction product. However, such catalysts can be expensive to purchase and time-consuming to make. As a typical example, (*S*)-VAPOL **141**, employed as a catalyst in asymmetric aziridination,<sup>85</sup> can be purchased at a cost of £104 per mg. The first reported synthesis of (*S*)-VAPOL by Wulff *et al.* was achieved in a 37% yield over 7 steps (Scheme 2.1).<sup>86</sup> An (*S*)-VAPOL-borate complex (10 mol%) catalysed the asymmetric aza-Darzens reaction of *N*-benzylidene-1,1-diphenylmethanamine with ethyl diazoacetate **144** to afford aziridine (*R,R*)-**145** in an 83% yield and with 90% ee.



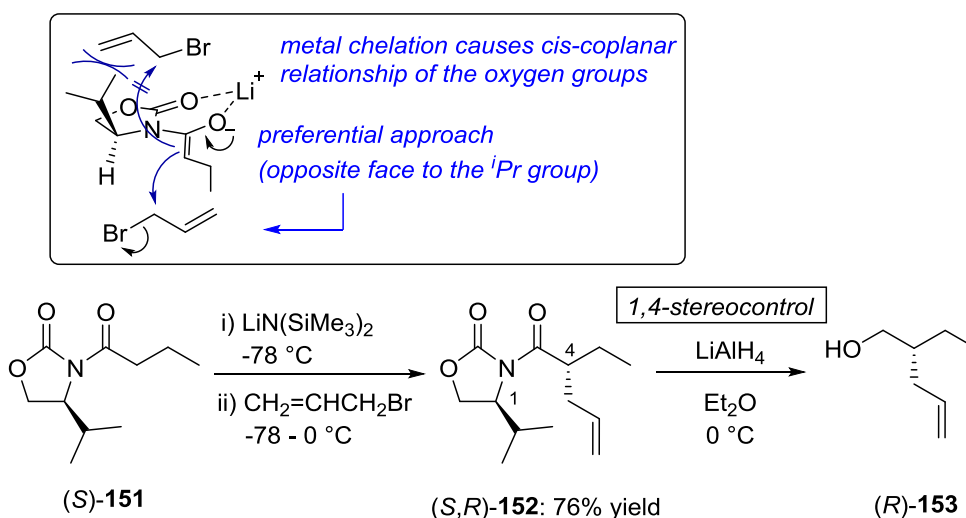
**Scheme 2.1** • Synthesis of *(R)*- and *(S)*-VAPOL reported by Wulff *et al.* and the Brønsted acid complex formed between the *(S)*-VAPOL-borate active catalyst and *N*-benzylidene-1,1-diphenylmethanamine (**143**) in the asymmetric synthesis of *cis*-aziridine *(R,R)*-**145**

The transmission of stereochemical information through distances of three or more bonds has been a particularly useful synthetic tool since the development of chiral auxiliaries by Corey and Evans in the 1980s.<sup>87</sup> Amongst these, the oxazolidinone (**147**, **148**),<sup>88</sup> oxazoline (**149**)<sup>89</sup> and camphorsultam (**150**)<sup>90</sup> “chiral auxiliaries” have received the most attention (Figure 2.2). The chiral auxiliaries listed above share key structural features: they are conformationally constrained, cyclic systems bearing a sterically bulky chiral group, such as the benzyl substituent in example **146**.



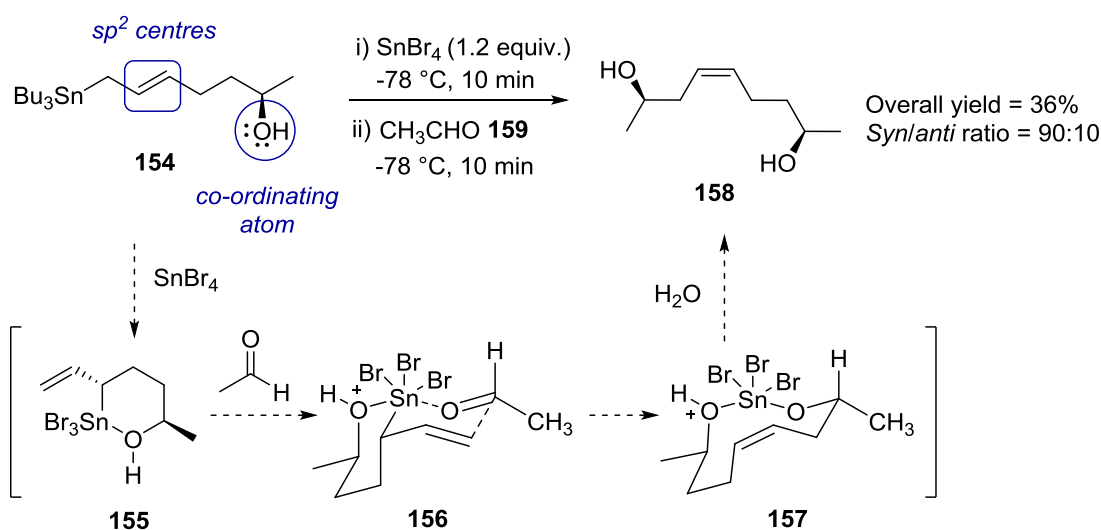
**Figure 2.2** • Oxazolidinone (Evans-type and SuperQuat<sup>91</sup>), oxazoline and camphorsultam chiral auxiliaries

The Evans oxazolidinone chiral auxiliary is commercially available and has been employed in a number of landmark total syntheses, including the synthesis of talaromycins A and B reported by Smith *et al.* in 1984, in which (*S,R*)-**152** was obtained as a single diastereomer in a 76% yield (Scheme 2.2).<sup>92</sup> The ability to easily remove the chiral auxiliary from the product makes this method particularly versatile and applicable to a wide range of substrates. 1,4-Stereocontrol of the type shown in Scheme 2.2 is frequently found in the literature, and a number of comprehensive reviews have been published on the subject.<sup>93</sup>



**Scheme 2.2** • Use of the Evans chiral auxiliary in the synthesis of talaromycins A and B reported by Smith *et al.*

Acyclic substrates such as allylstannane **154** (Scheme 2.3) lack the rigid conformation of a 5- or 6-membered ring, and tend to rely on self-assembly of the reagents by chelation with a metal reagent *via* oxygen or nitrogen lone pairs, forming a highly ordered, conformationally constrained complex. In transition state **156**, co-ordination of both the alcohol and aldehyde oxygen atoms to the metal centre (*via* their lone pairs) bring the existing chiral centre and the newly forming chiral centre into close proximity, bringing about a 1,5- steric induction. Hydrolysis of intermediate **157** releases diol **158**, with a 1,7-*cis* relationship. Despite the restricted conformation of the transition state, Lewis acid-mediated remote asymmetric induction reactions of acyclic substrates generally proceed with moderate yield and diastereomeric excess. As Scheme 2.3 shows, diol **158** (the major *syn* product of the reaction) was obtained in a low 36% yield, and with a *syn/anti* ratio of 90:10.



**Scheme 2.3** • Structural features influencing stereoselectivity in the reaction between acetaldehyde **159** and acyclic allylstannane **154**

Metal-free acyclic systems lack the conformational constraint of a cyclic co-ordination complex in the transition state and are therefore extremely rare. Indeed a comprehensive review of “substrate-directable chemical reactions” by Evans *et al.* published in 1993 contained no examples of organocatalytic substrate-controlled chiral induction reactions, and a search of the literature from 1993-2015 revealed no subsequent examples.<sup>94</sup> A review of stereochemical communication “over nanometer distances” published by Clayden in 2009 found that such transformations were limited to transition metal-catalysed, Lewis acid-mediated, and Grignard reactions.<sup>95</sup>

This introductory chapter will present an overview of the major advances made in remote asymmetric induction (RAI) over the last 30 years, with a particular focus on examples where the stereocentre of the chiral substrate is more than 3 covalent bonds from the newly formed chiral centre in the product. Examples of 1,5- to 1,8-asymmetric induction and beyond, including those comparable to enzyme-catalysed reactions, are rare and particularly difficult to achieve with good diastereoselectivity. Exploring the structural features and mechanisms of these reactions will provide insight and inspiration for the design of future RAI transformations. Achieving absolute communication of stereochemical information on a nanometer scale within a biologically relevant architecture is a challenge that has not yet been met by synthetic chemistry.

### 2.3 Cyclic substrates in remote asymmetric induction

Substrates with a 5- or 6-membered ring cyclic structure are generally conformationally restricted and inflexible. As a result, the angle of approach of a second molecule to the site of reactivity is limited, causing the preferential formation of a single diastereomer in the product. This is the classical approach to remote asymmetric induction led by the use of the chiral auxiliaries illustrated in Figure 2.2 (Section 2.2). Examining the mechanism of stereocontrol in these examples, and the success of various approaches to improving the diastereomeric ratio of the product, will inform substrate design and optimization of stereoselectivity in future remote asymmetric induction reactions.

#### 2.3.1 Steric control in cyclisation reactions

The Nazarov cyclisation involves the Lewis acid activation of a divinyl ketone followed by the  $4\pi$  electrocyclic ring closure of a pentadienyl cation.<sup>96</sup> Very few diastereoselective examples of this cyclisation exist. However, in 1999 Pridgen *et al.* reported a remarkable 1,5-asymmetric induction methodology in the Nazarov cyclisation for the synthesis of non-racemic indanes, which were found to be effective as endothelin receptor antagonists.<sup>97</sup> Substrate **160**, bearing the Evans chiral auxiliary, underwent Lewis acid-mediated cyclisation to afford two products, diastereomers *trans*-**161** and *cis*-**162** (Table 2.1).

**Table 2.1** • Diastereoselective Nazarov cyclisation reported by Pridgen *et al.*

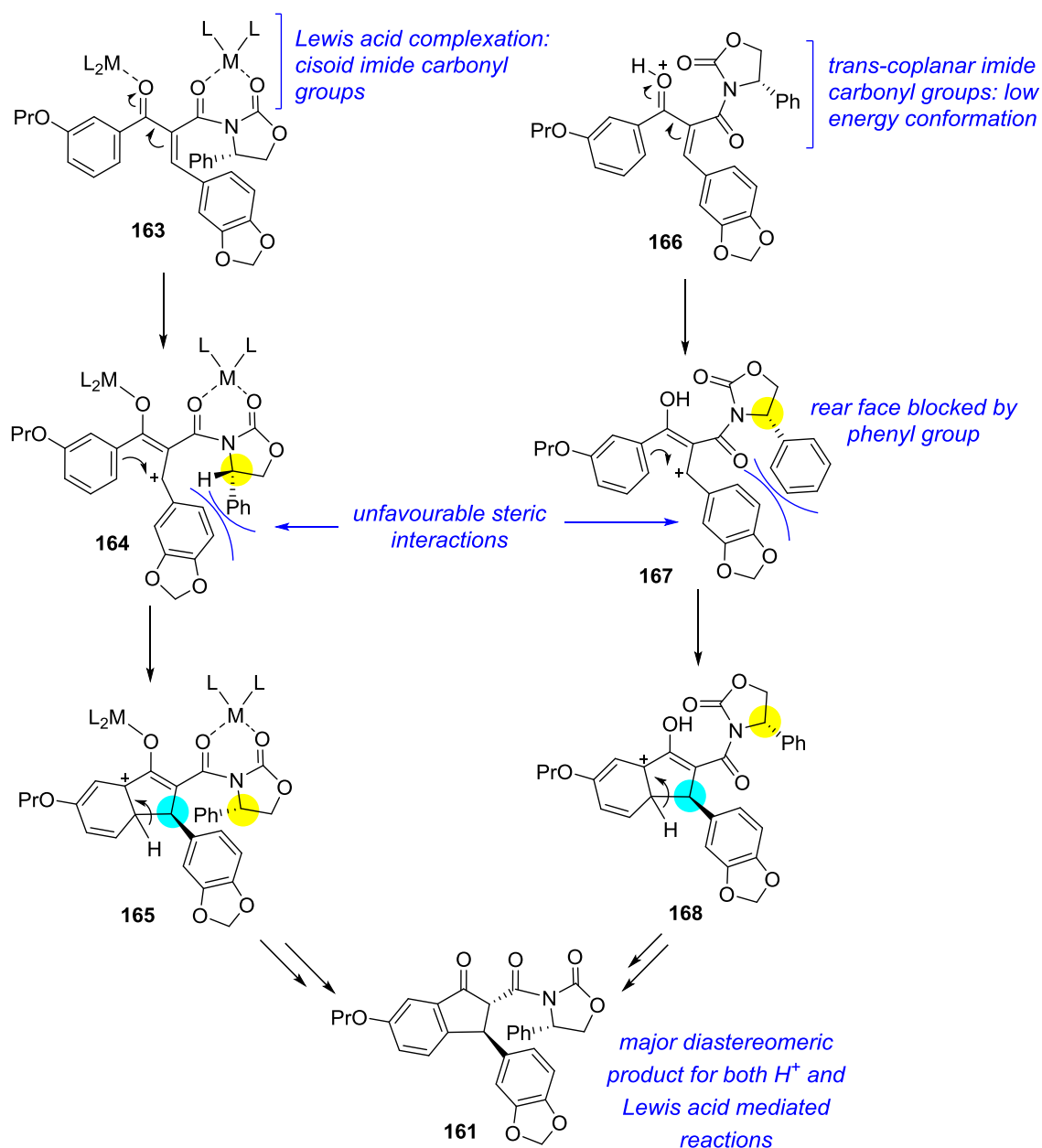
	Acid	Yield (%)	Isomer ratio 161:162
Lewis acid	SnCl <sub>4</sub>	85	88:12
Lewis acid	TiCl <sub>4</sub>	60	70:30
Brønsted acid	CH <sub>3</sub> SO <sub>3</sub> H	88	85:15

When the cyclisation was carried out with Lewis acids tin(IV) tetrachloride and titanium(IV) chloride, indane **161** was obtained as the major diastereomer, with ratios

(**161:162**) of 88:12 and 70:30 respectively. This moderate diastereoselectivity was thought to result from the formation of reaction intermediate **163** (Figure 2.3), in which Lewis acid complexation restricts the conformation of the substrate with a temporary 6-membered ring. However, one of the highest diastereomeric ratios (85:15, *trans*-**161**:*cis*-**162**) was obtained using methanesulfonic acid rather than a Lewis acid, which surprisingly suggests that metal-carbonyl complexation is not crucial for a stereoselective cyclisation in this case.

**Lewis acid-mediated reaction:**

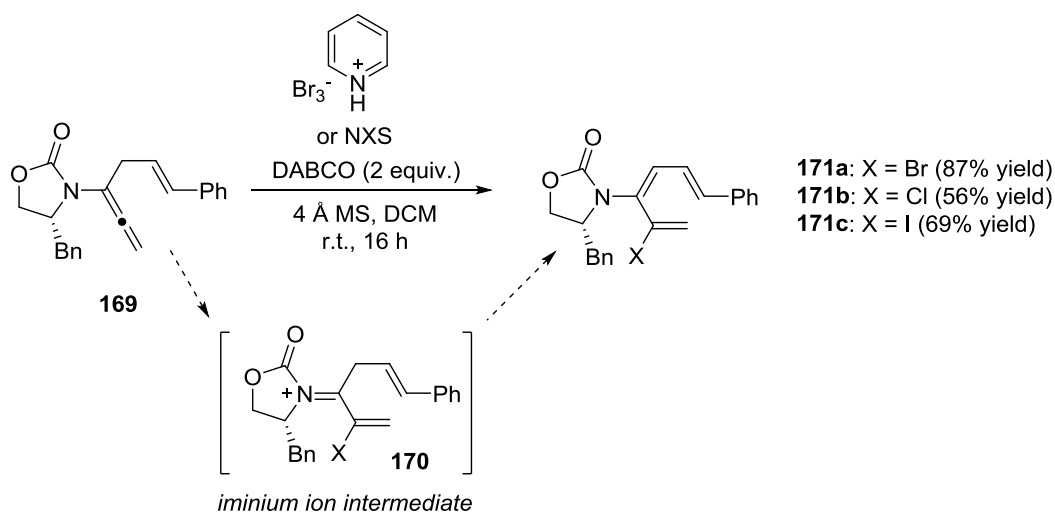
**Brønsted acid-catalysed reaction:**



**Figure 2.3** • Mechanistic comparison of the Lewis acid and Brønsted acid mediated Nazarov cyclisation reported by Pridgen *et al.*

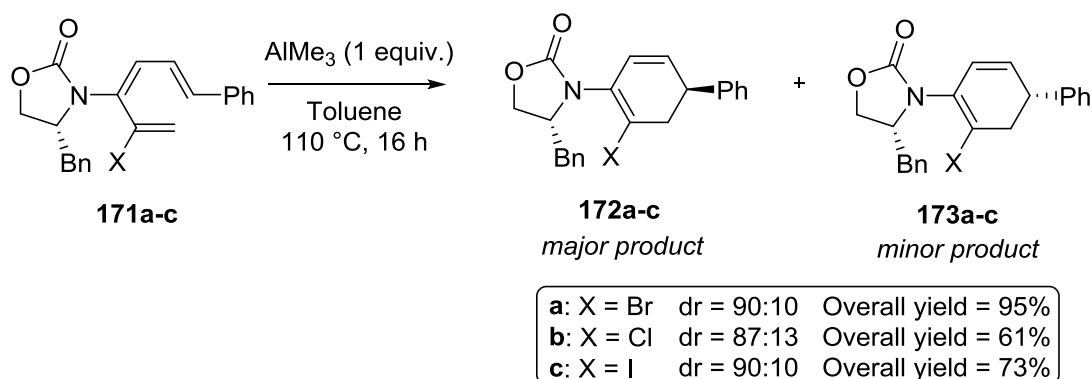
In fact, computational calculations suggested that the lowest energy conformation of the starting material **166** without Lewis acid complexation has a *trans*-coplanar geometry of the imide carbonyls, as represented in Figure 2.3. In this conformation, steric demands alone bring the alkene into sufficiently close proximity to the aromatic ring for  $\pi$ - $\pi$  interaction and the formation of a new covalent bond. Thus both the Lewis and Brønsted acid mediated reactions proceed with diastereoselectivity in favour of *trans* product **161**.

An Evans chiral auxiliary was also used by Hsung *et al.* for a 1,6-asymmetric induction in the stereoselective  $6\pi$  electrocyclic ring closure of 2-halo-amidotrienes (Scheme 2.5).<sup>98</sup> Substrates **171a-c** were synthesised by the electrophilic isomerization of allenamide **169** with an  $X^+$  source of the halogen (pyridinium bromide, NCS or NIS) in the presence of two equivalents of DABCO and 4 Å molecular sieves (Scheme 2.4). After 16 hours at room temperature, the 1,3,5-hexatrienes **171a-c** were obtained, *via* deprotonation of the acyliminium ion intermediate **170** ( $X = \text{Cl}, \text{Br}, \text{I}$ ).



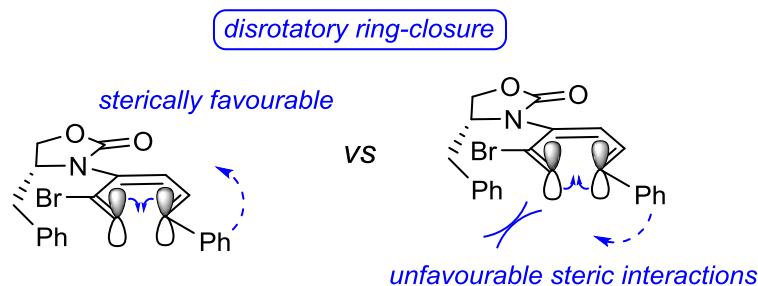
**Scheme 2.4** • Synthesis of 2-halo-amidotrienes **171a-c** reported by Hsung *et al.*

The  $6\pi$ -electron electrocyclicalisation of **171a-c** proceeded with good yields of up to 95%, and diastereomeric ratios of up to 90:10 (where  $X = \text{bromine or chlorine}$ , major product **172a** and **172c**) (Scheme 2.5). The choice of halogen did not appear to have a significant effect on the diastereomeric ratio, although the yield of the cyclisation was lower where  $X$  was chlorine or iodine, affording **172b+173b** and **172c+173c** in 61% and 73% overall yields respectively. The newly installed vinyl halide was shown to play an important role in relaying the chirality of the Evans auxiliary in the 1,6-asymmetric induction as well as being a site of possible functionalization in subsequent reactions.



**Scheme 2.5** • Diastereoselective cyclisation of 1,3,5-hexatrienes **171a-c** reported by Hsung *et al.*

The mechanism of the thermally allowed disrotatory ring-closure provides an explanation for the selective formation of **172a-c** over **173a-c** (Figure 2.4). Clockwise rotation of the  $\text{sp}^2$  orbital of the carbon bearing the phenyl substituent (right) would bring this group into proximity of the benzyl group of the Evans auxiliary, whereas anticlockwise rotation (left) has no such unfavourable steric interactions.

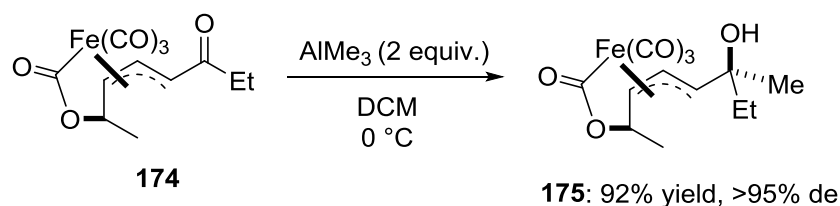


**Figure 2.4** • Mechanistic explanation for the diastereoselective synthesis of 1,3,5-hexatrienes **172a-c**

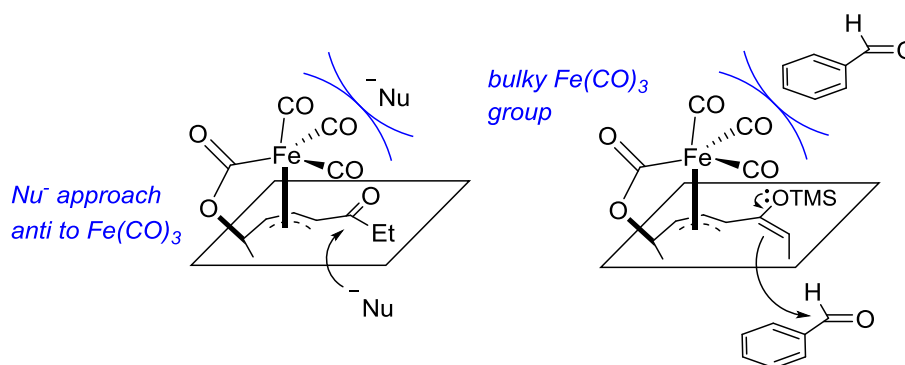
### 2.3.2 Remote stereocontrol by the $\pi$ -allyltricarboxyliron lactone chiral auxiliary

Ley *et al.* have investigated the effect of a  $\pi$ -allyltricarboxyliron lactone complex as a chiral auxiliary, for example in the addition of trimethylaluminium to ketone **174** (Scheme 2.6).<sup>99</sup> The synthesis of **174** was achieved in 4 steps from the commercially available starting material (*E,E*)-hexa-2,4-dienoic acid, (employing the toxic, highly flammable solid iron source diiron nonacarbonyl) with an overall yield of just 23%. In the reaction between ketone **174** and two equivalents of trimethylaluminium, tertiary alcohol **175** was obtained in an excellent 92% yield, and with >95% diastereomeric excess. The high diastereoselectivity of this reaction is thought to be due to a combination of the stability of the lactone tether, and the steric bulk of the irontricarbonyl group, blocking one face of the ketone against nucleophilic attack (Figure 2.5).



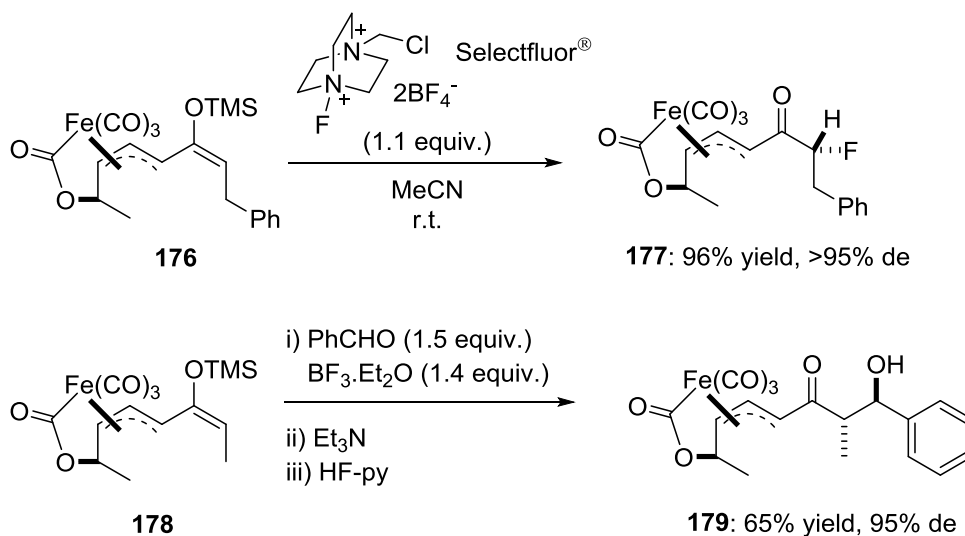


**Scheme 2.6** • A  $\pi$ -allyltricarbonyliron lactone complex as a chiral auxiliary, reported by Evans *et al.*



**Figure 2.5** •  $\pi$ -Allyltricarbonyl group blocking one face of the substrate from nucleophilic addition (left) and Mukaiyama aldol addition (right)

Similarly, the C-F bond formation resulting from the reaction between silyl enol ether **176** and Selectfluor® proceeded with >95 diastereomeric excess (Scheme 2.7).<sup>100</sup> The same  $\pi$ -allyltricarbonyliron lactone moiety also directed a 1,7-stereocontrol in the Mukaiyama aldol reaction of **178** with benzaldehyde, affording  $\beta$ -hydroxycarbonyl **179** in a 95% de and an overall yield of 65% after desilylation.

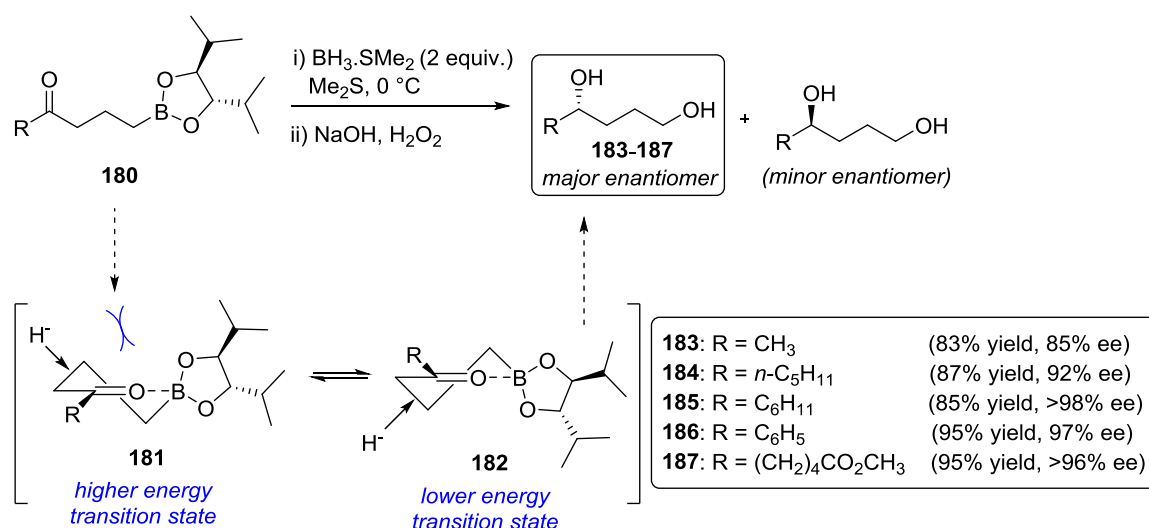


**Scheme 2.7** • Asymmetric fluorination (above) and Mukaiyama aldol reaction (below) reported by Evans *et al.*

Ley *et al.* have shown that the use of a  $\pi$ -allyltricarbonyliron lactone auxiliary is applicable to a range of reactions, with the benefit of releasing the free (*E,E*)-diene on decomplexation.<sup>101</sup> As a chiral auxiliary, the  $\pi$ -allyltricarbonyliron lactone is therefore highly reliable and cheap, although synthesis of the lactone itself is low yielding and employs reagents which may be difficult to handle.

### 2.3.3 Asymmetric keto boronate reduction

Reactions which progress *via* a highly ordered cyclic transition state have excellent potential for remote chiral induction. In a particularly successful example, Molander *et al.* achieved a 1,7-induction in the reduction of keto boronates (**180**) under optimized conditions of borane-dimethylsulfide (2 equivalents) in dimethylsulfide at 0 °C (Scheme 2.8).<sup>102</sup> The diol products **183-187** were obtained in high yields of 81-95% and with excellent enantioselectivity (85-98% ee).



**Scheme 2.8** • Asymmetric keto boronate reduction reported by Molander *et al.*

Molander *et al.* proposed that the steric interactions between the approaching nucleophile and the isopropyl group of boronate **180** result in a preferred face of attack, in what is thought to be a 6-membered cyclic transition state (represented by **181** and **182**). The basic solvent, dimethyl sulfide, is also likely to form a sterically bulky complex with the borane reducing agent, further limiting the possible trajectory of the nucleophilic attack. This method provides a straightforward way to synthesise chiral non-racemic secondary alcohols bearing sterically and electronically similar alkyl substituents. In terms of remote asymmetric induction, the synthesis of non-racemic diols **183-187** was achieved by a combination of a cyclic chiral substrate and a conformationally restricted cyclic transition

state – an approach which is also common to the transformations described in Section 2.3.4.

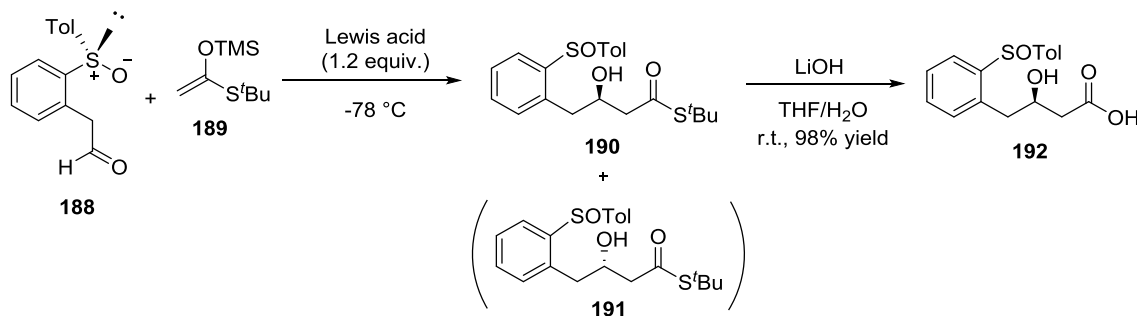
### 2.3.4 Chiral sulfoxides in remote asymmetric induction

The sulfoxide group is generally represented in Lewis structures as being analogous to a carbonyl moiety. However, when the R substituents are not equivalent, the sulfur atom is a stereogenic centre (Figure 2.6). The energy barrier to interconversion of the two enantiomers is around 40 kcal/mol, meaning that they are conformationally stable at room temperature and will only racemise under harsh conditions of high temperature or irradiation.<sup>103</sup>



**Figure 2.6** • Chirality of a disubstituted sulfinyl group, where  $R_1 \neq R_2$

Optically active sulfoxides have been employed as chiral auxiliaries in a diverse range of diastereoselective transformations, particularly those involving 1,3- and 1,4-stereocontrol. Examples of dihydroxylation,<sup>104</sup> reduction,<sup>105</sup> halogenation<sup>106</sup> and ring cleavage<sup>107</sup> using substrates bearing chiral sulfoxides can be readily located in the literature. The popularity of the sulfur-based chiral auxiliaries can be explained by three key points: sulfur lone pairs are able to coordinate to Lewis acids, promoting highly ordered transition states, the large steric difference between the substituents (eg. lone pair, phenyl group, oxygen) results in good differentiation of the faces of the sulfoxide, and the chiral sulfoxides are straightforward to prepare in very high enantiomeric excess. The stereoselective Mukaiyama aldol reaction of (*S*)-2-(2-(*p*-tolylsulfinyl)phenyl)acetaldehyde **188** and *O*-silylated ketenethioacetal **189** was reported by Ruano and Maestro *et al.* in 2006 (Scheme 2.9).<sup>108</sup>



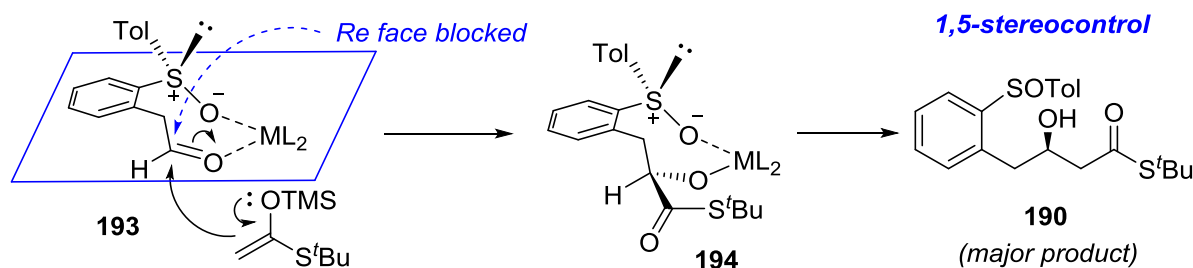
**Scheme 2.9** • 1,5-Asymmetric induction in the Mukaiyama aldol reaction and subsequent hydrolysis of thioester **190** to β-hydroxy carboxylic acid **192**

Aldehyde **188** was prepared in 4 steps from 2-bromobenzaldehyde and (*S*)-(-)-methyl *p*-toluenesulfinate with an overall yield of 55%.<sup>109</sup> The chiral sulfoxide group of **188** exerted a clear 1,5-stereocontrol in the Mukaiyama aldol reaction, which was found to be influenced by the choice of Lewis acid (Table 2.2). Ytterbium(III) triflate (1.2 equiv) gave the highest diastereoselectivity of the series, affording **190** and **191** in a ratio of 88:12, which increased to 96:4 when the reaction was carried out in acetonitrile at -40 °C instead of dichloromethane at -78 °C. Utilising the optimised conditions, this asymmetric Mukaiyama aldol reaction, followed by desulfinylation and further transformations, proved to be an effective route to 1,3-diols and beta-hydroxy acids with >98% ee.

**Table 2.2** • Asymmetric Mukaiyama aldol reaction reported by Ruano *et al.*

Lewis acid	Conversion (%)	Ratio <b>190:191</b>
TiCl <sub>4</sub>	87	61:39
AlCl <sub>3</sub>	34	66:34
ZnI <sub>2</sub>	72	72:28
Yb(OTf) <sub>3</sub>	60	88:12

A mechanistic explanation for the diastereoselective synthesis of  $\beta$ -hydroxythioester **190** is presented in Figure 2.7. Bidentate co-ordination of the sulfoxide and aldehyde oxygen atoms of substrate **188** to the metal centre of the Lewis acid creates cyclic complex **193**. Steric interactions therefore limit attack of the aldehyde carbonyl to the exposed *Si* face. However, the degree of stereocontrol was only moderate, with a maximum 76% de in the synthesis of **190**. This may be due to the inherent size and flexibility of the 8-membered ring in intermediate **193**.



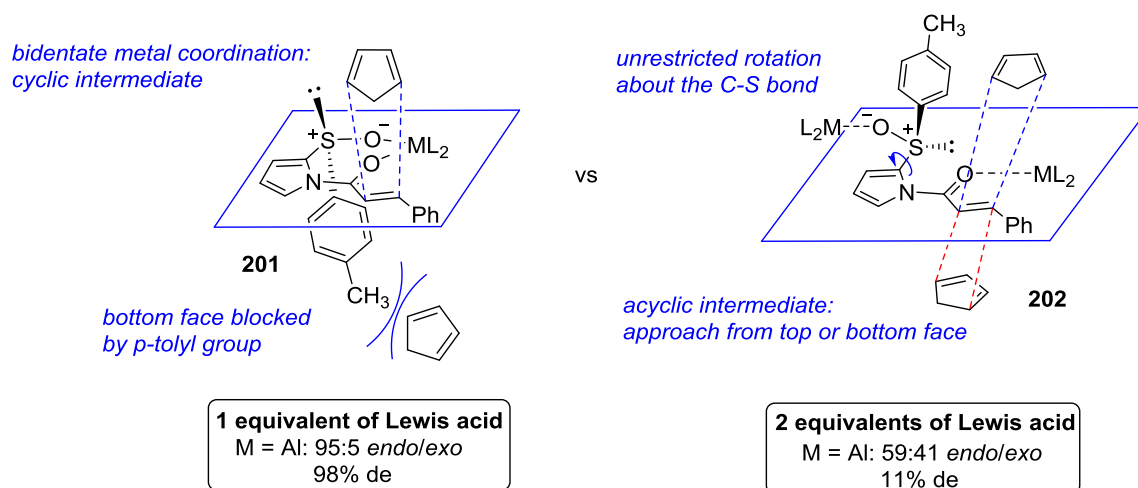
**Figure 2.7** • Reaction intermediates in the Mukaiyama aldol reaction

Arai *et al.* then turned their attention to the Diels-Alder reaction, employing  $\alpha,\beta$ -unsaturated amide **195** as a chiral dienophile in the reaction with cyclopentadiene **196** (Table 2.3).<sup>110</sup> Where the Mukaiyama aldol addition had an 8-membered ring intermediate, the Diels-Alder reaction proceeded *via* the more conformationally restricted

7-membered ring complex **201** (Figure 2.8). This Lewis acid-promoted [4+2] cycloaddition proceeded smoothly at room temperature in overall yields of up to 99% and favoured the *endo* product in each case. The *endo/exo* ratio depended on the Lewis acid used: zinc chloride and the lanthanum triflates gave moderate *endo* selectivity, while aluminium trichloride gave a 95:5 ratio of *endo/exo* products and an excellent *endo* de of 98%.

**Table 2.3** • Diels-Alder reaction of chiral sulfinyl dienophile **195** reported by Arai *et al.*

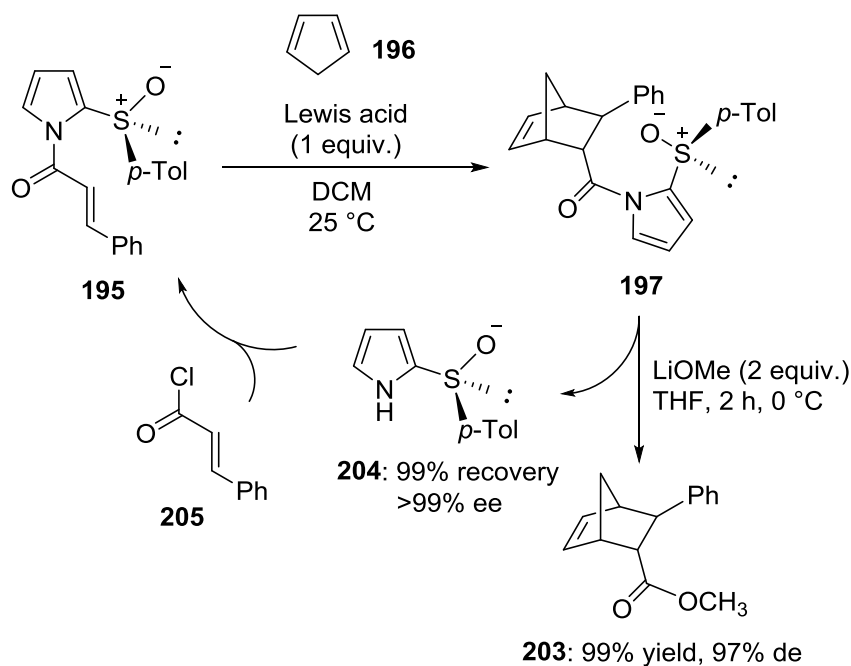
Lewis Acid	Time (h)	Yield (%)	Ratio <i>endo/exo</i> (197+198) / (199+200)	<i>endo</i> de (%)
ZnCl <sub>2</sub>	29	60	77/23	38
AlCl <sub>3</sub>	13	99	95/5	98
Yb(OTf) <sub>3</sub>	45	61	69/31	89



**Figure 2.8** • Reaction transition states in the Diels-Alder addition using 1 equivalent of Lewis acid (left) and two equivalents of Lewis acid (right), reported by Arai *et al.*

When the synthesis of **197** was attempted with two equivalents of Lewis acid (for example aluminium trichloride), the *endo/exo* selectivity dropped dramatically from 95:5 to 59:41, with a similar decrease in diastereomeric excess of the *endo* product from 98% to 11%. With more than one equivalent of Lewis acid, the reaction proceeds *via* transition state **202**, which lacks the conformational restraint of the 7-membered ring found in **201** (Figure 2.8).

Following its use in asymmetric reactions, the chiral sulfoxide group is usually cleaved by the reaction with activated Raney nickel,<sup>109</sup> releasing the unstable sulfenic acid, which prevents recycling of the chiral material. Arai *et al.* demonstrated the recycling of the chiral sulfoxide following the Diels-Alder reaction by treatment of **197** with two equivalents of lithium methanolate to afford methyl ester **203** in a 99% yield (Scheme 2.10).<sup>111</sup> (*S*)-2-(*p*-Tolylsulfinyl)-1*H*-pyrrole **204** was recovered in a 99% yield, and with >99% optical purity, making it economically viable as a reusable chiral auxiliary.



**Scheme 2.10** • Recycling of the (*S*)-2-(*p*-Tolylsulfinyl)-1*H*-pyrrole chiral auxiliary **204** in the asymmetric Diels-Alder reaction, reported by Arai *et al.*

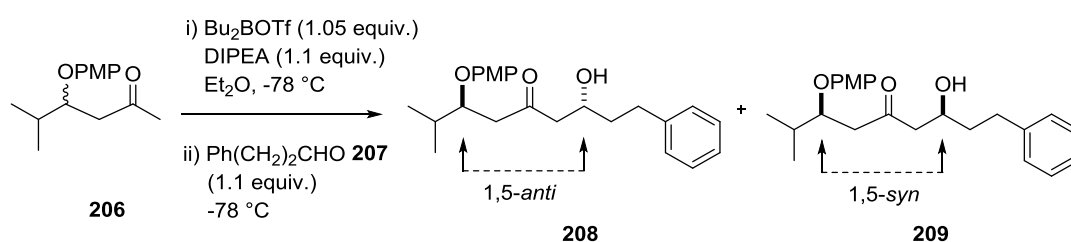
## 2.4 Acyclic substrates in remote asymmetric induction

In their 2001 review of acyclic remote stereocontrol,<sup>111</sup> Mikami and Maryanoff identified common structural features which have been used to improve enantioselectivity in substrate-controlled chiral induction: i)  $sp^2$  centres, such as C=C bonds and amide groups, which restrict rotation of the molecule and provide planarity, ii) biasing substituents, i.e.

sterically bulky nitrogen or oxygen protecting groups, which restrict the conformation of the molecule, and iii) alcohol or amino functional groups capable of coordinating metals *via* oxygen or nitrogen lone pairs. These characteristics are also desirable for the control of regio- and stereoselectivity in the field of supramolecular chemistry, and are found in architectures such as metal-organic frameworks (MOFs),<sup>112</sup> calixarenes<sup>113</sup> and dendrimers.<sup>114</sup> In the following reports of remote asymmetric induction, the acyclic reaction substrates all bear at least one of the structural features described by Mikami and Maryanoff. In many cases the remarkable through-bond distance over which stereochemical information appears to be communicated can be explained by the formation of highly ordered, cyclic reaction transition states in which the through-bond and through-space distance between the existing and forming chiral centres is in fact shorter than it first appears.

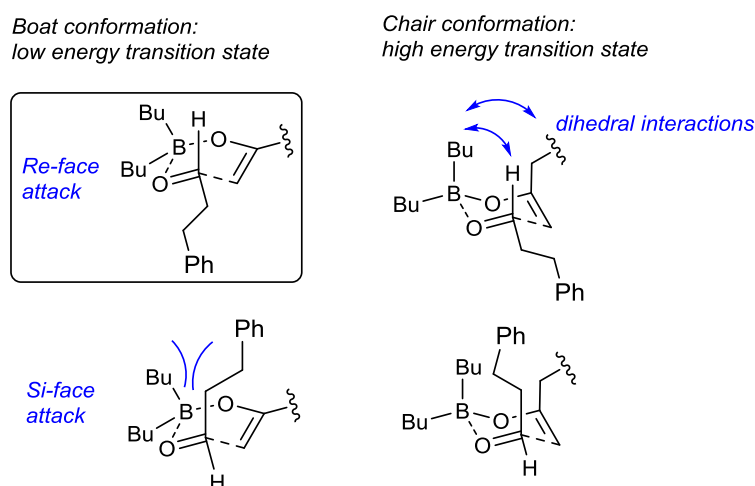
#### 2.4.1 Remote asymmetric induction in the aldol addition reaction

The aldol addition of an enolate to an aldehyde or ketone is one of the most powerful reactions in organic synthesis, and the “primary engine” of C-C bond formation in nature.<sup>115</sup> The  $\beta$ -hydroxy carbonyl functionality resulting from the aldol addition is a precursor of the 1,3-diol relationship commonly found in natural products, particularly the polyketides.<sup>116</sup> The low natural abundance of marine-derived polyketides has placed great emphasis on the ability of total synthesis to provide enantiopure samples of these compounds in sufficient quantity for structure elucidation, biological evaluation and possible clinical development.<sup>117</sup> Stereoselective 1,5-*anti* aldol reactions are a particularly well investigated class of remote asymmetric induction, following boron-mediated aldol methodology developed by Evans and Paterson in the 1990s,<sup>118</sup> which has since been employed in a number of natural product total syntheses.<sup>119</sup> Following their previous work on 1,3-induction in the boron-mediated asymmetric aldol reaction,<sup>120</sup> Evans and co-workers investigated the reaction of an achiral aldehyde with a ketone enolate substrate bearing a chiral  $\beta$ -alkoxy substituent (Scheme 2.11).<sup>121</sup>



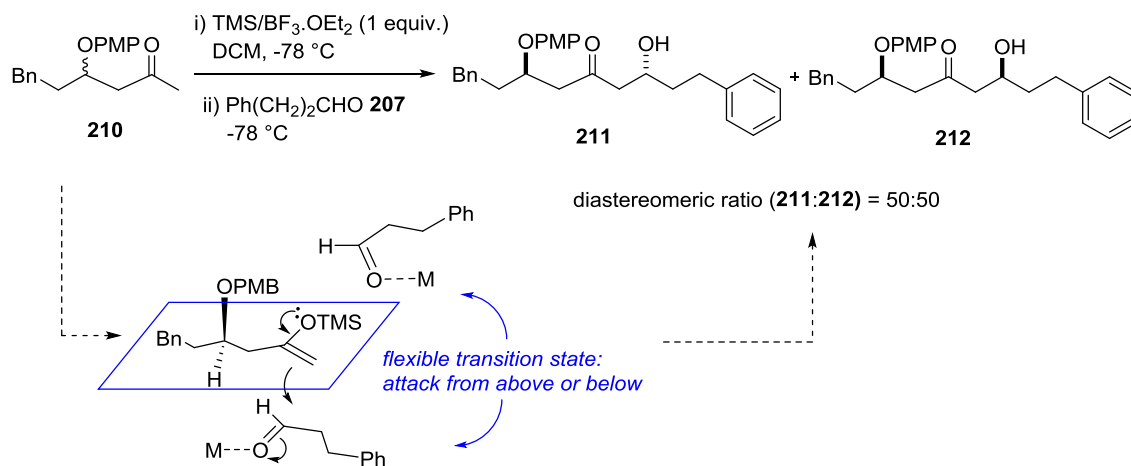
**Scheme 2.11** • 1,5-Stereocontrol in the boron-mediated aldol reaction, by Evans *et al.*

Ketone **206** first reacted with 1.05 equivalents of dibutylboron triflate in the presence of Hunig's base at  $-78\text{ }^{\circ}\text{C}$  to form a boron enolate intermediate. The subsequent addition of dihydrocinnamaldehyde **207** (1.1 equivalents) afforded 1,5-*anti* diastereomer **208** as the major product, with an *anti/syn* ratio of 95:5 and a good overall yield of 89%. The high stereoselectivity of the boron-mediated aldol reaction is thought to be the result of the short boron-oxygen bond in the enolate, giving rise to a tight cyclic transition state (Figure 2.9).<sup>122</sup>



**Figure 2.9** • Cyclic transition states for the boron-mediated asymmetric aldol reaction: boat conformations (left) and chair conformations (right), by Goodman *et al.*

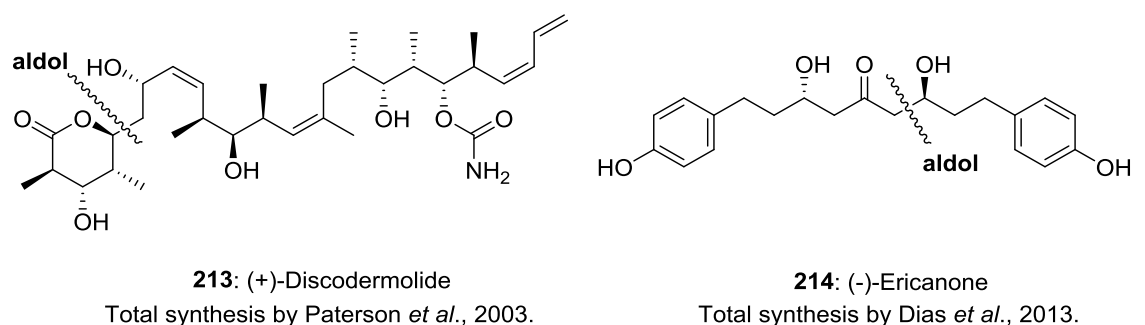
By contrast, Evans *et al.* found that a Lewis-acid catalyzed enol silane addition protocol removed any 1,5-stereocontrol by ketone substrate **210** (Scheme 2.12), affording the *anti* and *syn* products **211** and **212** in a 1:1 ratio. Effectively “switching off” the 1,5-influence, this route would therefore allow a dominant 1,3-stereocontrol from a chiral aldehyde if desired.



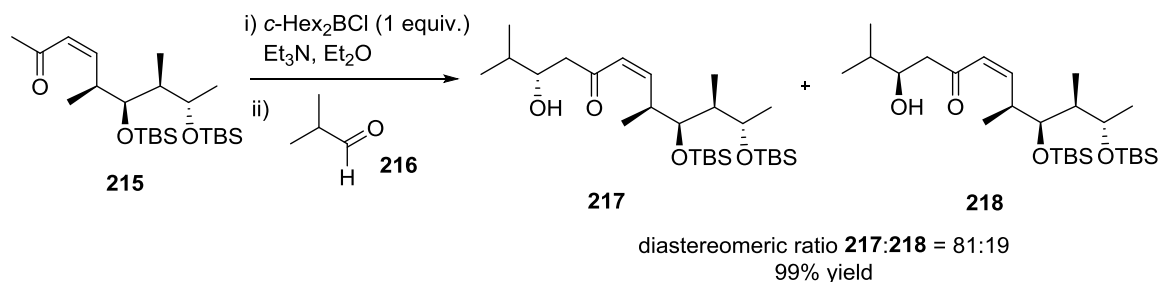
**Scheme 2.12** • Lewis acid-catalysed enol silane aldol addition reported by Evans *et al.*



A comprehensive investigation into the full scope and limitations of these reactions was published by Evans *et al.* in 2003.<sup>123</sup> In their total synthesis of the anti-cancer polyketide (+)-discodermolide **213** (Figure 2.10), Paterson *et al.* were able to extend the stereocontrol of the boron-mediated aldol reaction to a 1,6-induction.<sup>124</sup> Model studies demonstrated that the boron enolate of (*Z*)-enone **215** reacted with isobutyraldehyde **216** to afford 1,6-*anti* aldol product **217** as the major diastereomer, with an *anti/syn* ratio of 81:19 (Scheme 2.13).



**Figure 2.10** • Molecular structure of (+)-discodermolide **213** (left) and (-)-ericanone **214** (right) showing the aldol disconnection.



**Scheme 2.13** • 1,6-Stereocontrol in the boron-mediated aldol reaction, reported by Paterson *et al.*

This test reaction was successfully exploited in the synthesis of (+)-discodermolide **213**, in which the key aldol addition step proceeded with a total yield of 64% and an excellent diastereomeric ratio of >95:5 in favour of the desired natural product isomer. The same boron reagent, chlorodicyclohexylborane, was also used by Dias *et al.* in their 2013 total synthesis of the natural product (-)-ericanone (**214**, Figure 2.10), in which the key aldol addition step afforded the desired 1,5-*anti* diol relationship in the product with a diastereomeric ratio of 94:6 (*anti/syn*).<sup>125</sup>

The absence of 1,5-stereocontrol encountered by Evans *et al.* in the enol silane aldol addition reaction (Scheme 2.12) indicated that the boron-mediated aldol methodology was unsuitable for such substrates. Following investigations into this limitation, Yamamoto *et*

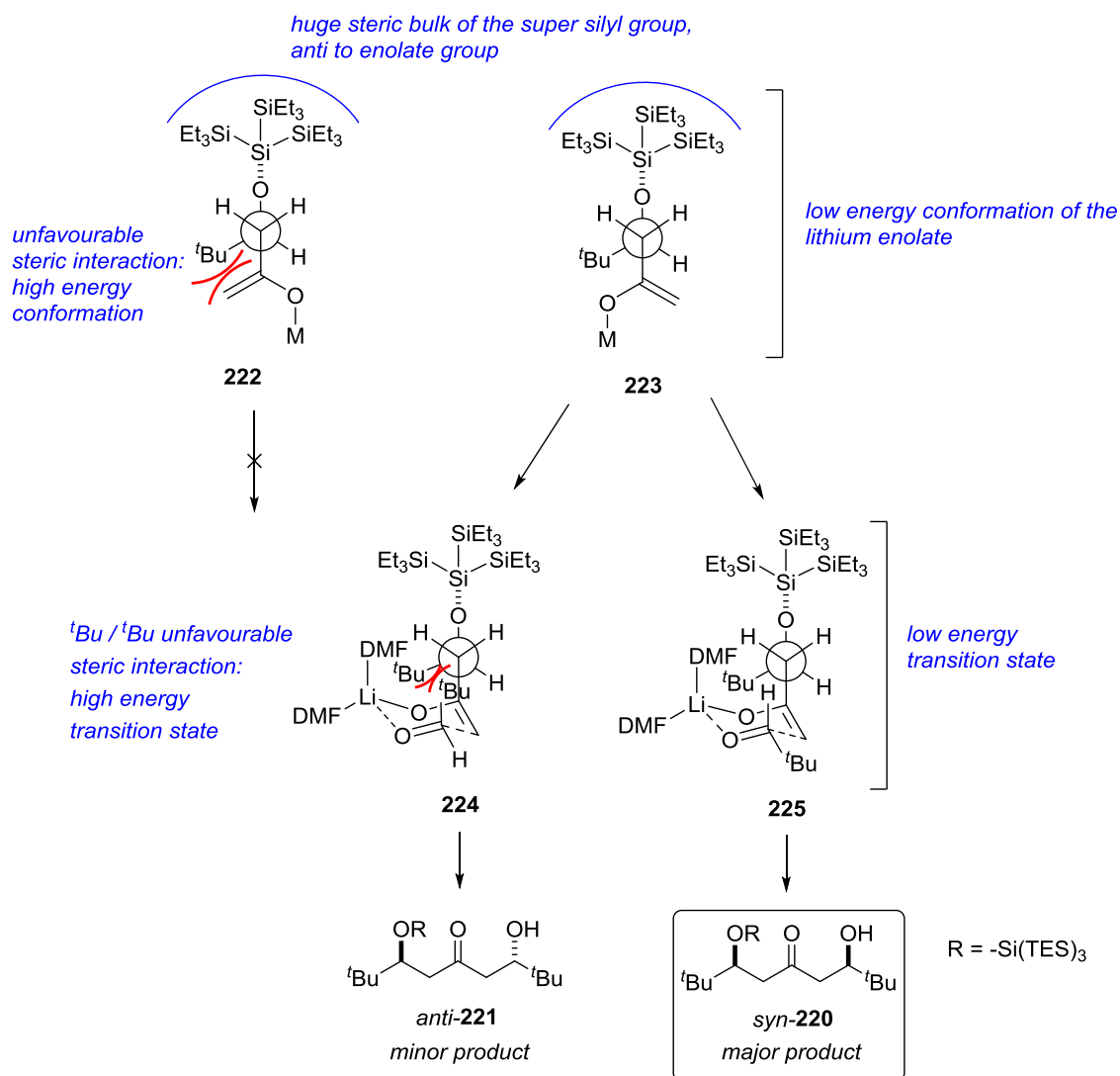
*al.* reported the use of “super silyl” protecting groups<sup>126</sup> in the aldol reaction of  $\beta$ -siloxy methyl ketones with pivalaldehyde (Table 2.4).<sup>127</sup>

**Table 2.4** • Asymmetric aldol reaction reported by Yamamoto *et al.*

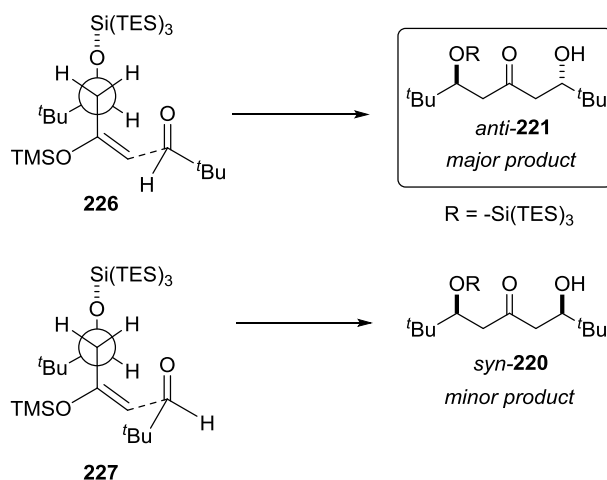
	<b>219</b>		<b>220</b>		<b>221</b>
R =	Enolisation reagent	<i>T</i> (°C)	Solvent	Yield (%)	dr ( <i>syn/anti</i> )
Si(TMS) <sub>3</sub>	LiHMDS	-60	DCM	50	60:40
Si(TMS) <sub>3</sub>	LiHMDS	-60	Toluene	70	60:40
Si(TMS) <sub>3</sub>	LiHMDS	-60	DMF	94	87:13
Si(TES) <sub>3</sub>	LiHMDS	-60	DMF	82	<b>96:4</b>
Si(TES) <sub>3</sub>	TMSOTf/Et <sub>3</sub> N	-78	Toluene	79	<b>2:98</b>

The extraordinary steric bulk of the super silyl group was found to bring about high selectivity in this reaction, favouring a 1,5-*syn* product **220** when lithium hexamethyldisilazide was used as the enolisation reagent. The stereoselectivity of the reaction was found to be highly solvent dependent, with non-coordinating solvents such as dichloromethane and toluene leading to a moderate diastereomeric ratio of 60:40 (**220:221**) compared with a ratio of 87:13 when the reaction was carried out in *N,N'*-dimethylformamide. This can be explained by the formation of a cyclic transition state in which co-ordination of two molecules of *N,N'*-dimethylformamide to the lithium centre stabilizes the conformation of the 6-membered ring (Figure 2.11).

Changing the protecting group from a TMS-type super silyl to the bulkier TES-type brought about the highest diastereomeric ratio of 96:4 (**220:221**). Yamamoto *et al.* found that the favoured diastereomer of the product could be switched from *syn* to *anti* by employing a silyl enol ether in place of the lithium enolate, with a resulting dr of 2:98 (*syn/anti* **220:221**) (Table 2.4, entry 5). Without the formation of a conformationally restricted cyclic transition state around a metal centre, the direction of approach of pivaldehyde to the silyl enol ether in transition states **226** and **227** is influenced by steric interactions only, leading to a preferential formation of the 1,5-*anti* product **221** (Figure 2.12).



**Figure 2.11** • Transition states of the lithium mediated aldol reaction reported by Yamamoto *et al.*

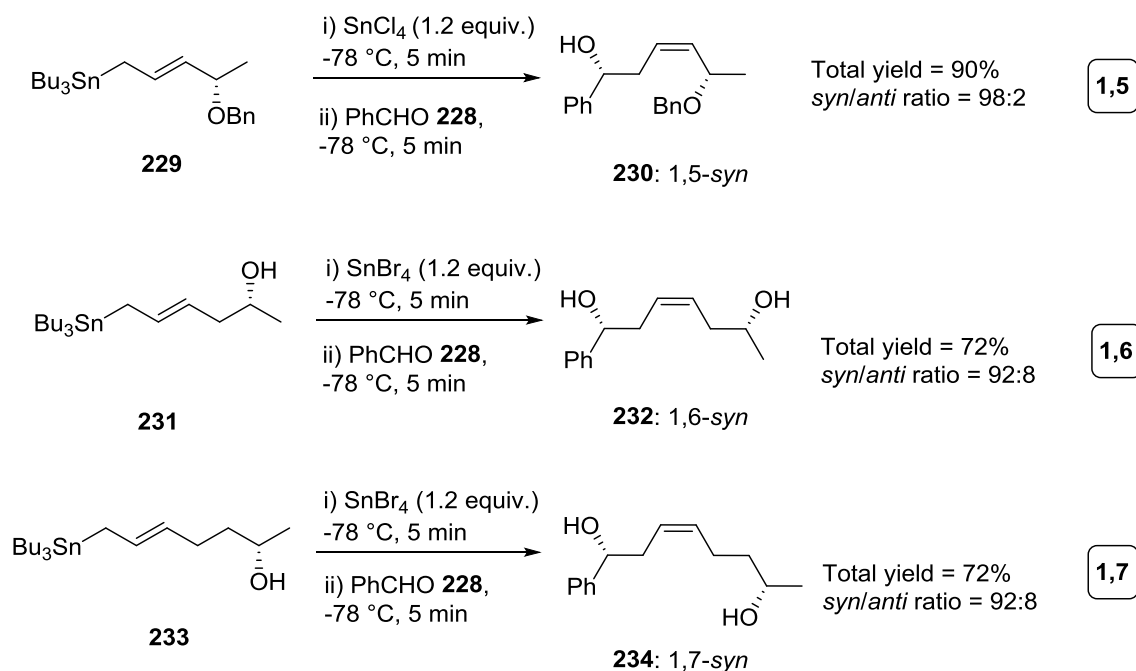


**Figure 2.12** • Transition states in the Mukaiyama aldol synthesis: 1,5-*anti* diastereoselectivity, reported by Yamamoto *et al.*

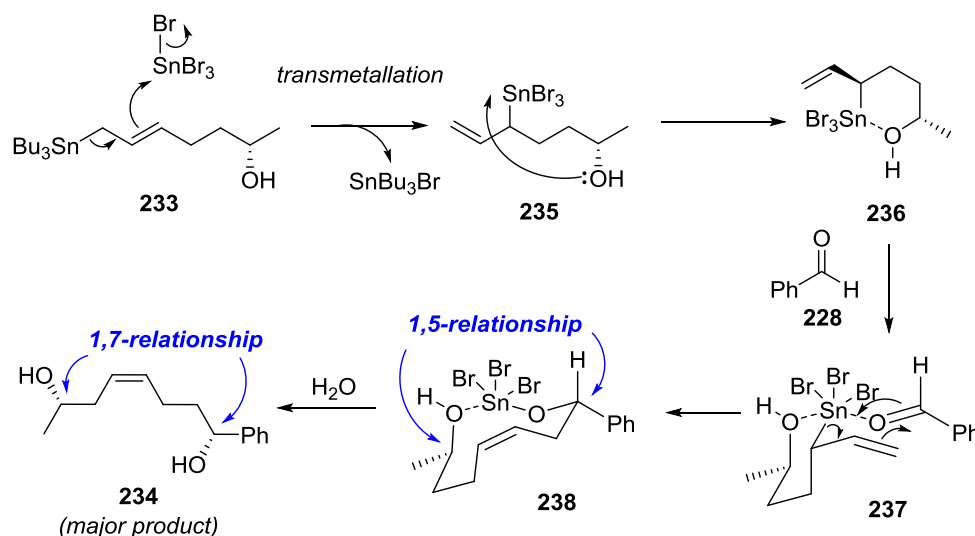
In each case (*syn* or *anti* favoured) the reaction was found to tolerate a wide range of aldehydes (RCHO where R = cyclohexyl, isopropyl, 4-methoxyphenyl, 4-nitrophenyl) with excellent diastereomeric ratios of between 85:15 and 98:2.

### 2.4.2 Allylstannanes in remote asymmetric induction

The addition of allylstannanes to aldehydes, promoted by the addition of a tin(IV) halide reagent, has been found to afford homoallylic alcohols with high enantioselectivity.<sup>128</sup> Much of the investigation into remote asymmetric induction in this reaction has been carried out by E. J. Thomas and coworkers over the last 25 years.<sup>129</sup> Thomas *et al.* found that the addition of 4-, 5-, and 6-substituted allylstannanes to benzaldehyde **228** favoured the *syn* product in each case (Scheme 2.14).<sup>130</sup> The addition of **229** to benzaldehyde proceeded *via* a transmetallation between stannane **229** and tin(IV) chloride. After five minutes, the addition of benzaldehyde **228** afforded the 1,5-*syn*-(*Z*) isomer of allylic alcohol **156** as the major product. The excellent diastereomeric ratio of 98:2 (*syn/anti*) in the 1,5-asymmetric induction dropped slightly with extension of the substrate carbon chain. Thus, the reaction between stannane **231** and benzaldehyde **228** afforded 1,6-*syn* product **232** with a diastereomeric ratio of 92:8, which was matched by the corresponding 1,7-induction (addition product **234**).



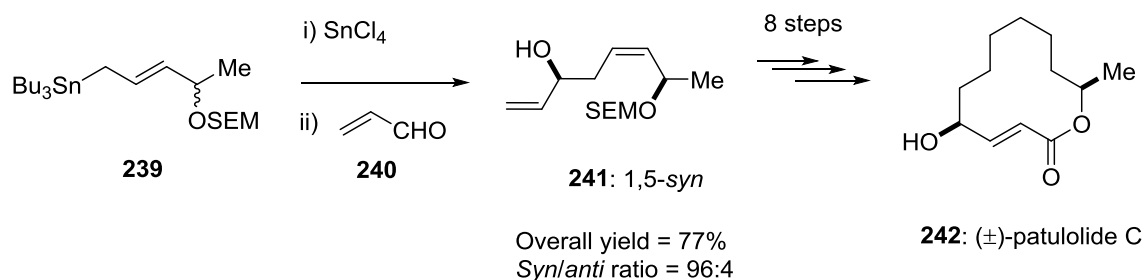
**Scheme 2.14** • 1,5- to 1,7-stereocontrol in the addition of benzaldehyde **228** to allylstannanes **229**, **231** and **233**, reported by Thomas *et al.*



**Figure 2.13 • Mechanism of the Lewis acid-mediated reaction between allylstannane **233** and benzaldehyde **228****

The mechanism of the reaction between allylstannane **233** and benzaldehyde **228** reveals the source of the high degree of stereocontrol (Figure 2.13). Following the transmetalation step, the alcohol group is able to co-ordinate to the tin centre *via* an oxygen lone pair. As a result, 6-membered ring intermediate **236** is formed, in which the vinyl and methyl substituents have an *anti*-relationship across the ring to achieve the lowest energy conformation. The approach of benzaldehyde is further limited by co-ordination of the carbonyl oxygen atom to the metal centre (**237**). Consequently, the addition reaction that follows actually occurs *via* a 1,5-asymmetric induction through the co-ordinated tin atom, despite the 1,7-relationship in the free diol (**234**).

The remote stereocontrol shown by the tin(IV) halide mediated addition of substituted allylstannanes to simple aldehydes (Scheme 2.14) has led to the development of new strategies in the synthesis of various natural products. For example, the total synthesis of the antibacterial macrolide ( $\pm$ )-patulolide C **163** by Thomas *et al.* (Scheme 2.15) featured a 1,5- remote asymmetric induction in the reaction between tributylstannane **239** and acrolein **240** to afford alcohol **241** with a diastereomeric ratio of 96:4 in favour of the *syn* product, and a good overall yield of 77%.<sup>131</sup> An Ireland-Claisen rearrangement was then used to relay the stereochemical information down the chain, resulting in the 1,6-*syn* relationship found in the natural product (**242**).



**Scheme 2.15** • 1,5-Stereocontrol in the synthesis of (±)-patulolide C, reported by Thomas *et al.*

While the organotin chemistry described above provided a reliable method for acyclic remote stereocontrol, the reactions require very low temperatures ( $-78\text{ }^{\circ}\text{C}$ ) and anhydrous conditions. Organotin compounds are also notoriously toxic, and cause well-documented damage to the environment.<sup>132</sup> Finally, the removal of tin residues such as tributyltin chloride from the final product of the reaction can be very challenging. In order to overcome these limitations, Thomas *et al.* turned to allylgermane substrates in place of the allylstannanes (Table 2.5).<sup>133</sup>

**Table 2.5** • 1,6-Stereocontrol in the addition of aldehydes to allylgermane **243**

Germane E/Z	Aldehyde R	Isolated Yield (%)	Ratio <b>244:245</b>
( <i>E</i> )- <b>243</b>	Ph	63	89:11
( <i>Z</i> )- <b>243</b>	Ph	80	94:6
( <i>Z</i> )- <b>243</b>	(CH <sub>3</sub> ) <sub>2</sub> CH	82	93:7
( <i>Z</i> )- <b>243</b>	4-ClC <sub>6</sub> H <sub>4</sub>	81	92:8
( <i>Z</i> )- <b>243</b>	3-ClC <sub>6</sub> H <sub>4</sub>	83	93:7
( <i>Z</i> )- <b>243</b>	4-NO <sub>2</sub> C <sub>6</sub> H <sub>4</sub>	81	91:9

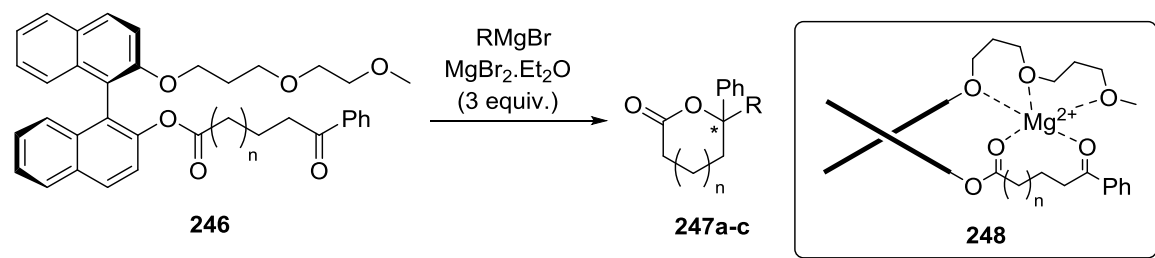
(*E*)-**243** was found to react with tin(IV) tetrabromide and then benzaldehyde **263** with promising 1,6-stereocontrol to afford diol **244** as the major product, with a diastereomeric ratio of 89:11 (**244:245**). This diastereomeric ratio, as well as the overall yield, was found to improve when the (*Z*)-isomer of **243** was used, increasing the dr to 94:6 in favour of the *syn* product **244**. The reaction shown in Table 2.5 was also able to tolerate a range of

aldehyde substrates including those bearing aliphatic chains (entry 3) and substituted benzaldehydes (entries 4-6, Table 2.5).

### 2.4.3 Remote asymmetric induction in the Grignard reaction

Tamai *et al.* employed (*R*)-BINOL as the chiral auxiliary in the Grignard reaction of ketoester **246** (Table 2.6).<sup>134</sup> By extending the carbon chain of the ketoacid starting material, they were able to achieve up to 1,12-asymmetric induction with significant enantiomeric excess. However, the ee decreased with increasing length of the carbon chain, with an optimum of  $n = 1$  (1,8-stereocontrol), which afforded the (*R*)-isomer **247a** as the major product with 97% ee and an overall yield of 82%.

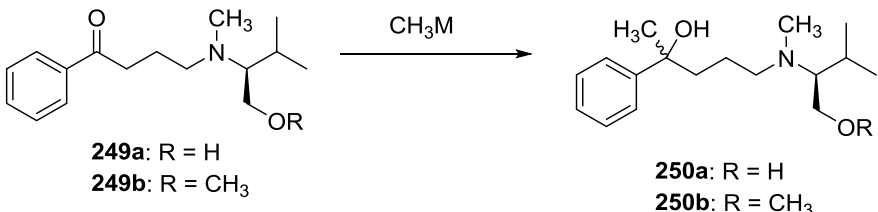
**Table 2.6** • 1,8- to 1,10-stereocontrol in the Grignard reaction, reported by Tamai *et al.*



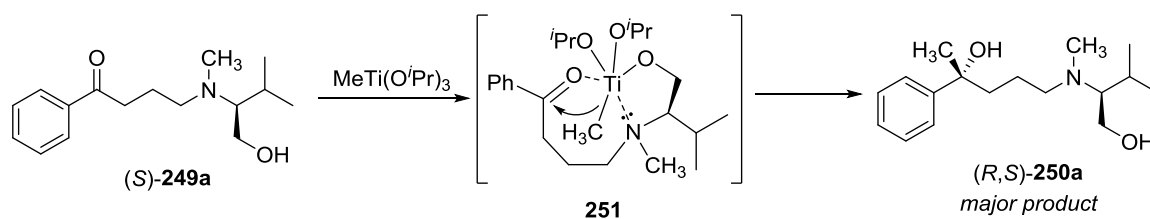
Product	n	R	1,X-induction	Yield (%)	ee (%)
( <i>R</i> )- <b>247a</b>	1	-C <sub>9</sub> H <sub>19</sub>	1,8	82	97
( <i>S</i> )- <b>247b</b>	2	-CH <sub>3</sub>	1,9	90	82
( <i>S</i> )- <b>247c</b>	3	-CH <sub>3</sub>	1,10	89	4

The reaction was thought to proceed *via* a pseudo-macroscopic chelate such as **248**, where the oligoether substituent functions as a podand around the Mg<sup>2+</sup> centre. The stability of this complex fixes the orientation of the ketone carbonyl group, allowing nucleophilic attack only from the outside of the macrocycle. A short chain ketoester, where  $n = 1$ , appears to hinder the formation of complex **248**, and no enantioselectivity was observed in the product. As the chain extends beyond  $n = 3$ , the complex becomes too flexible to limit the direction of nucleophilic attack. The stability of the pseudo-macroscopic intermediate therefore governs the stereoselectivity of this reaction. The *in situ* lactonisation means that the (*R*)-BINOL chiral framework is released during the reaction, and could therefore be recovered and re-used if desired.

**Table 2.7** • 1,6-Stereocontrol in the nucleophilic addition to ketones, reported by Takahashi *et al.*

						
	MeLi		MeMgBr		MeTi(O <sup><i>i</i></sup> Pr) <sub>3</sub>	
Product	Yield (%)	dr ( <i>SS:RS</i> )	Yield (%)	dr ( <i>SS:RS</i> )	Yield (%)	dr ( <i>SS:RS</i> )
<b>250a</b>	53	55:45	63	54:46	27	<b>11:89</b>
<b>250b</b>	63	51:49	53	68:32	34	49:51

Following their earlier work on the 1,5-asymmetric induction in the diastereoselective reaction of carbonyl compounds with organotitanium reagents,<sup>135</sup> Takahashi *et al.* reported a comparison of the 1,6 remote asymmetric induction achieved using three different organometallic reagents: the Grignard reagent methylmagnesium bromide, methyllithium, and methyltitanium triisopropoxide (Table 2.7).<sup>136</sup> Valinol-derived (*S*)-4-amino-1-phenylbutanones **249a** and **249b** reacted with methyltitanium triisopropoxide in tetrahydrofuran at room temperature to afford diastereomeric mixtures of products **250a** and **250b**. When the same reaction was carried out with methyllithium or methylmagnesium bromide as the organometallic reagent, little diastereoselectivity was observed.

**Scheme 2.16** • Cyclic reaction intermediate complex **251** in the methylation of ketone (*S*)-**249a**, reported by Takahashi *et al.*

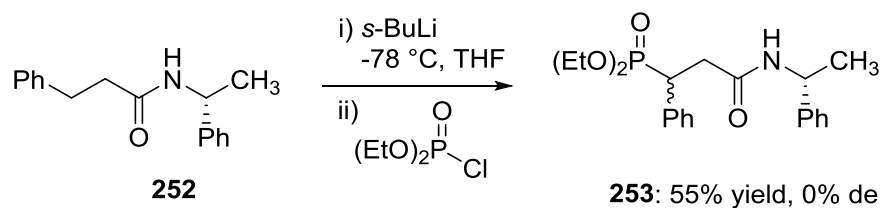
With methyltitanium triisopropoxide, moderate diastereoselectivity was achieved in the synthesis of **250a**, favouring the *R,S* diastereomer in a ratio of 89:11 (*R,S*: *S,S*). However, there was no stereocontrol observed in the synthesis of **250b** (where R = -CH<sub>3</sub>), suggesting that the free hydroxyl group is necessary for a cyclic chiral reaction intermediate. To explain the reagent- and substrate-dependent diastereoselectivity of the



reaction, Takahashi *et al.* proposed the formation of transition state **251** (Scheme 2.16), in which co-ordination of the carbonyl and hydroxyl oxygen atoms to the titanium centre brought the existing and forming chiral centres into close proximity - a conformation further stabilized by the possible co-ordination of the tertiary amine *via* the nitrogen lone pair. The steric bulk of the isopropoxy ligands compared to the methyl ligand would give rise to preferential addition of the methyl group to the same face as the existing chiral centre. Methylmagnesium bromide and methyl lithium are stronger nucleophiles than methyltitanium triisopropoxide, as reflected in the yield of the reactions (63% and 53% yield respectively, compared to 27% with  $\text{MeTi}(\text{O}^i\text{Pr})_3$ ). When these reagents are used, methylation occurs before the formation of a highly ordered metal complex can take place.

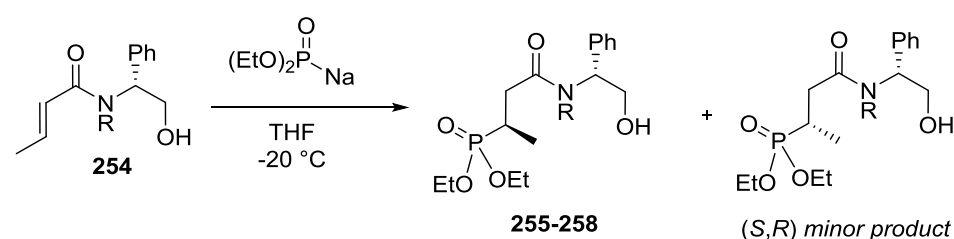
#### 2.4.4 Organolithium reagents in remote asymmetric induction

Phosphorylated amino acids are found in a range of antibiotics, antivirals, and enzyme inhibitors as well as natural products.<sup>137</sup> In their 2001 synthesis of  $\beta$ -amidophosphonates, Quirion *et al.* compared a number of synthetic routes, each involving a 1,5-asymmetric induction.<sup>138</sup> In the first approach,  $\beta$ -amidobenzene **252** was deprotonated at the benzylic carbon by *s*-butyllithium, before the addition of diethyl chlorophosphite as an electrophile (Scheme 2.17). While compound **253** was obtained in a 55% yield, no diastereoselectivity was observed for this reaction due to the flexibility of the substrate molecule.



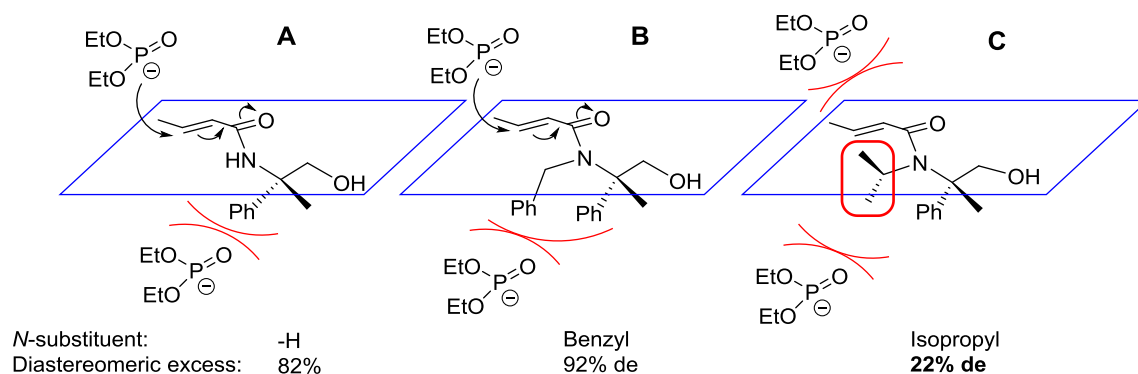
**Scheme 2.17** • Synthesis of  $\beta$ -amidophosphonates **253** reported by Quirion *et al.*

However, in a more successful approach, diethylphosphite reacted with a series of  $\alpha,\beta$ -unsaturated chiral amide **254** *via* a Michael addition (Table 2.8). The diastereoselectivity of this reaction was found to be particularly dependant on the nitrogen protecting group, with an *N*-benzyl group affording the highest de of 92%, and the more hindered *N*-isopropyl group resulted in a significant loss of selectivity, with a de of just 22%. A mechanistic rationale for this effect is presented in Figure 2.14. In **A**, where there is no *N*-substituent, the molecule is largely flat due to the planarity of the alkene and amide bonds.

**Table 2.8** • Asymmetric synthesis of  $\beta$ -amidophosphonates, reported by Quirion *et al.*


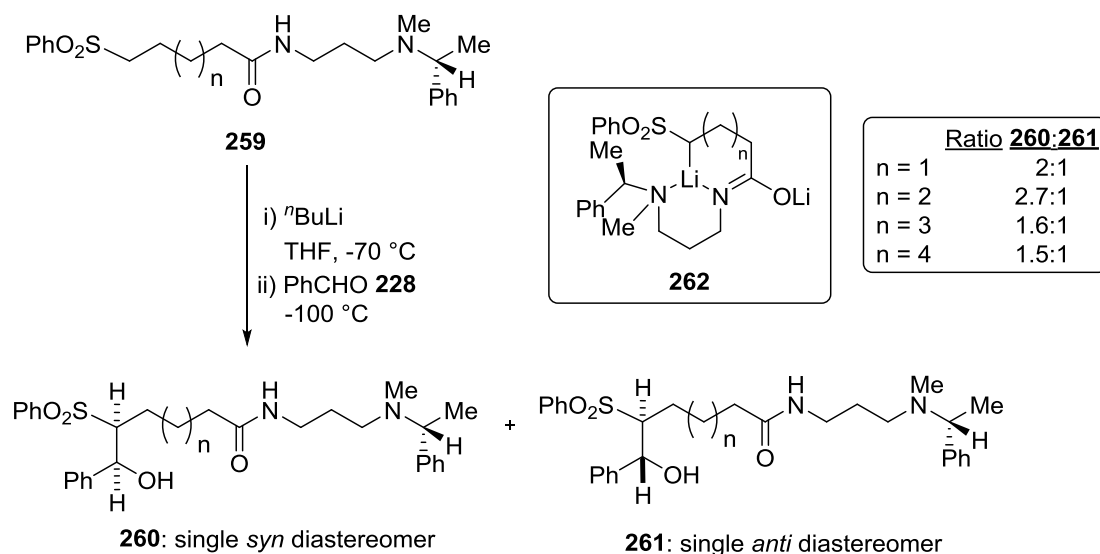
Major Product	R	Yield (%)	de (%)
( <i>R,R</i> )- <b>255</b>	H	55	82
( <i>R,R</i> )- <b>256</b>	Me	60	76
( <i>R,R</i> )- <b>257</b>	<i>i</i> Pr	45	22
( <i>R,R</i> )- <b>258</b>	Bn	50	92

Diethyl phosphite therefore preferentially approaches the upper face of the alkene to avoid interactions with the phenyl ring. Similarly in **B**, the lower face is blocked by the phenyl group, and further steric interactions with the *N*'-benzyl substituent also limit the trajectory of the nucleophile, leading to a slight increase in diastereomeric excess from 82% to 92%. Finally, the *N*'-isopropyl substituent in **C** lies perpendicular to the plane of the amide, cause steric hindrance on both the upper and lower face of the alkene substrate which is reflected the lower de of 22%.

**Figure 2.14** • Mechanistic explanation for the diastereoselectivity in the Michael addition of diethylphosphite to  $\alpha,\beta$ -unsaturated chiral amides, reported by Quirion *et al.*

Examples of remote chiral induction beyond a distance of 8 covalent bonds are extremely rare – only a handful exist, and these tend to rely on supramolecular complexation of an acyclic substrate (bearing a chiral auxiliary) around a metal centre, such as the work by Magnus *et al.* described below.

In 1997, following earlier investigations into 1,9-stereocontrol for the same methodology,<sup>139</sup> Magnus and Magnus reported a 1,13- and 1,14-asymmetric induction in the synthesis of linear chiral sulfones (Scheme 2.18).<sup>140</sup> Substrate **259**, bearing the (*R*)- $\alpha$ -methylbenzylamine chiral auxiliary, was deprotonated by *n*-butyllithium at -70 °C before the addition of benzaldehyde **228** at -100 °C. There are four possible diastereomeric products of this reaction: two *syn*-isomers (*R,R,R/S,S,R*) and two *anti*-isomers (*R,S,R/S,R,R*). However, only two diastereomers were observed in the <sup>1</sup>H-NMR of the impure reaction mixture: one *syn*, and one *anti*.



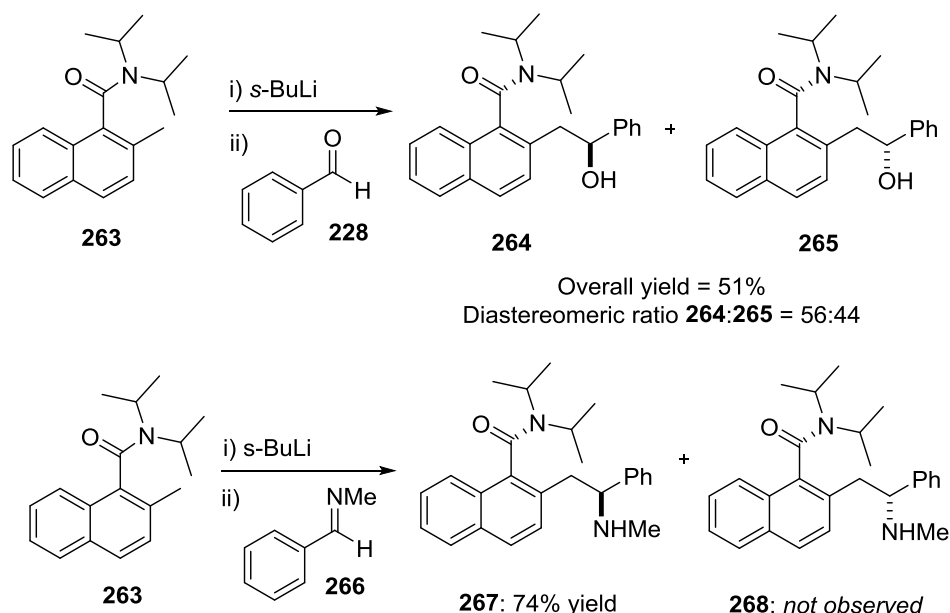
**Scheme 2.18** • 1,13 and 1,14-asymmetric induction in the synthesis of chiral sulfones, reported by Magnus and Magnus.

Magnus and Magnus proposed that the unexpected long-range stereoselectivity of this reaction may be due to the formation of bicyclic chelate intermediate **262**, in which the chiral centre of the starting material is only three atoms from the C-Li bond. The stereocontrol therefore operates over a much shorter distance than it would appear from the long-chain structure of starting material **259**, being a 1,4- rather than a 1,14- remote asymmetric induction. The ratio of **260:261** deteriorated as the chain length increased from  $n = 2$  to  $n = 4$ , as the corresponding change in ring size from 7 to 9 atoms increased the flexibility of the transition state.

Taking a highly flexible substrate such as **259**, with no C=C bonds, alcohol groups or cyclic features, and achieving an apparent 1,14-stereocontrol is undoubtedly a significant achievement. However, the examples of RAI described so far in this review lack truly impressive *through-space* distance in the chiral induction.

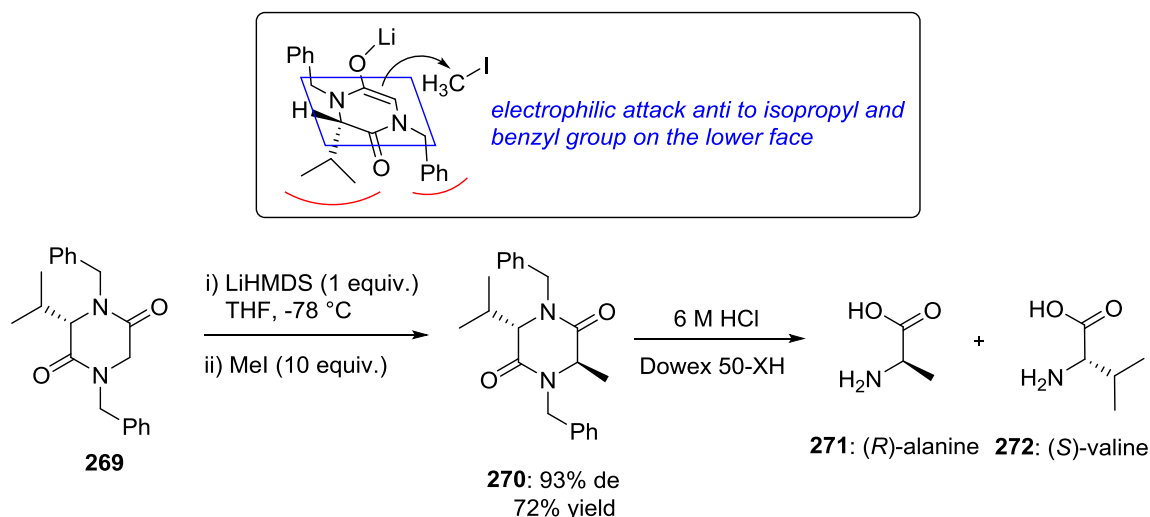
## 2.5 Atropisomeric and helical chiral substrates for RAI

In order to achieve the long-range communication of stereochemical information over nanometer distances, it is necessary to employ a substrate which is structurally linear and has a global conformational constraint. Clayden and co-workers initially investigated the use of atropisomeric amide compounds for this purpose, and in 1997 they reported a rare case of remote chiral induction by a rotationally restricted amide (Scheme 2.19).<sup>141</sup> Naphthamide **263** was deprotonated by *s*-butyl lithium before the addition of benzaldehyde **228**, to afford secondary alcohol diastereomers **264** and **265** in an overall yield of 51%. Unfortunately, no significant diastereoselectivity was observed in this reaction. However, when an *N*-benzylidenemethylamine **266** was employed as the electrophile, secondary amine **267** was obtained as a single diastereomer in a 74% yield.



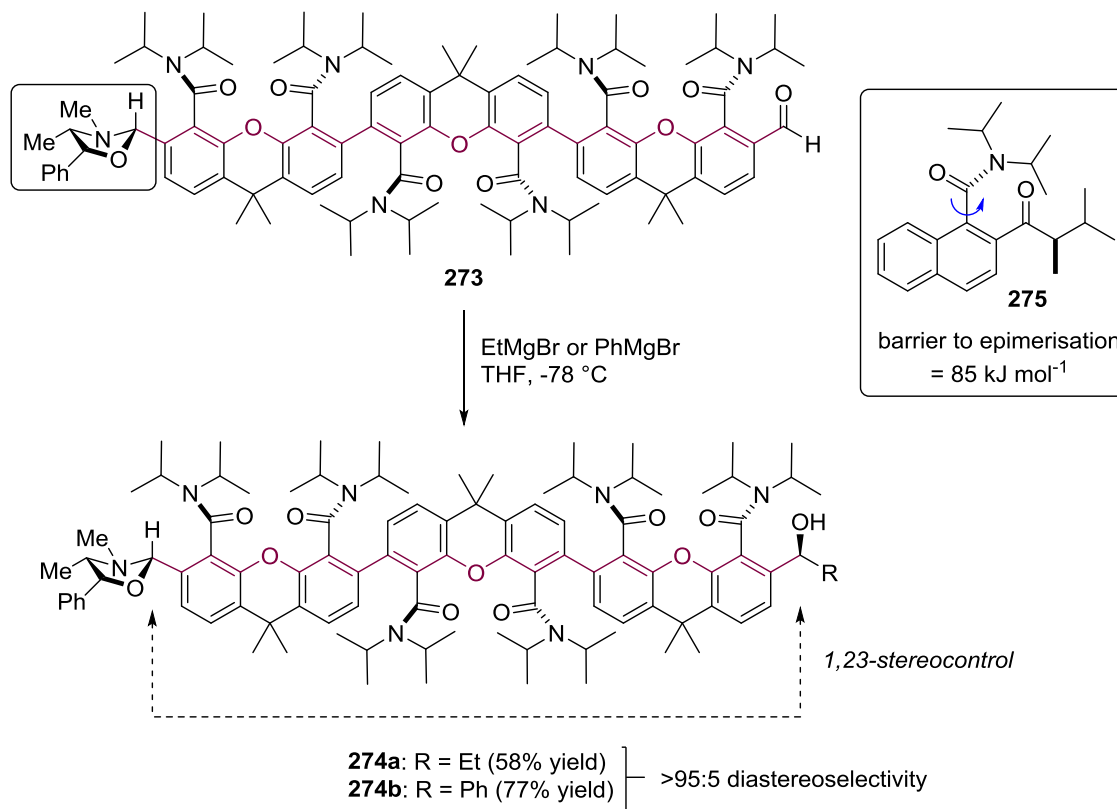
**Scheme 2.19** • 1,5-Stereocontrol by atropisomerism, reported by Clayden *et al.*

The conformation of amides can be controlled by nearby stereogenic centres, and can further influence the conformation of neighbouring amide groups.<sup>142</sup> This approach mirrors the “chiral relay” methodology introduced by Davies *et al.* in the synthesis of enantiomerically pure  $\alpha$ -amino acids (Scheme 2.20).<sup>143</sup> Sterically bulky groups such as the *N*-benzyl substituents of cyclic amide **269** can increase the influence of the existing chiral centre on the remote site of reactivity. Thus diastereomer **270** was obtained by 1,4-stereocontrol with 93% de and an overall yield of 72%.



**Scheme 2.20** • Chiral relay auxiliary for the synthesis of optically active  $\alpha$ -amino acids  
 (R)-alanine **271** and (S)-valine **272**, reported by Davies *et al.*

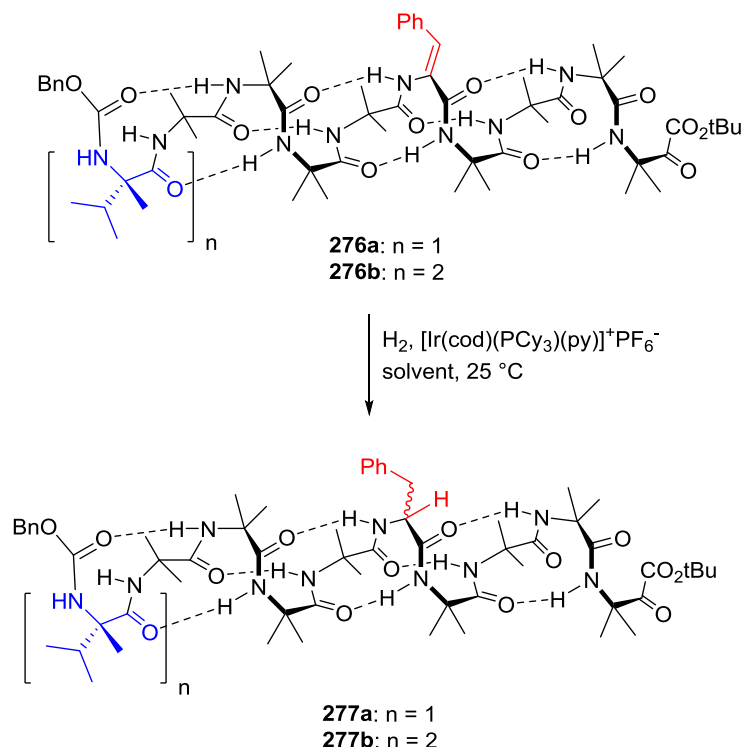
Viewing substrate **263** as a promising building block, Clayden *et al.* constructed a highly rigid polyxanthene structure (**273**) bearing rotationally restricted amides whose atropisomeric stereochemistry was fixed by a (1*S*,2*R*)-ephedrine moiety (Scheme 2.21).<sup>144</sup> At the far end of the molecule, an aldehyde group provided a target for asymmetric nucleophilic attack by a suitable Grignard reagent.



**Scheme 2.21** • 1,23-Stereocontrol in a polyxanthene structure, reported by Clayden *et al.*

The conformationally constrained nature of compound **273** meant that the chiral centre was both spatially remote from the aldehyde carbonyl group as well as separated by the chain of covalent bonds (coloured purple, Scheme 2.21). The energy barrier to epimerization of this class of compounds, such as amide **275** ( $85 \text{ kJ mol}^{-1}$ ) is sufficiently high to prevent changes in conformation through the structure, and each amide substituent is angled *anti* to its neighbours. Remarkably, Clayden *et al.* found that the distance of the stereocontrol was limited by difficulties in synthesis of suitable substrates rather than the reliability of the chiral relay, as they were unable to synthesise a tetraxanthene starting material.

In a change of strategy, Clayden *et al.* instead built substrate **276**: a peptide chain consisting of multiple aminoisobutyric acid (Aib) subunits, which adopts a helical conformation.<sup>145</sup> The direction of the helix was established by either one or two (*S*)- $\alpha$ -methyl valine residues at one end (**276a** and **276b** respectively). Under hydrogenation conditions of Crabtree's catalyst<sup>146</sup> (10% w/w) and a hydrogen atmosphere, peptides **277a** and **277b** were obtained as the major diastereomers, featuring (*S*)-phenylalanine residues highlighted in red.

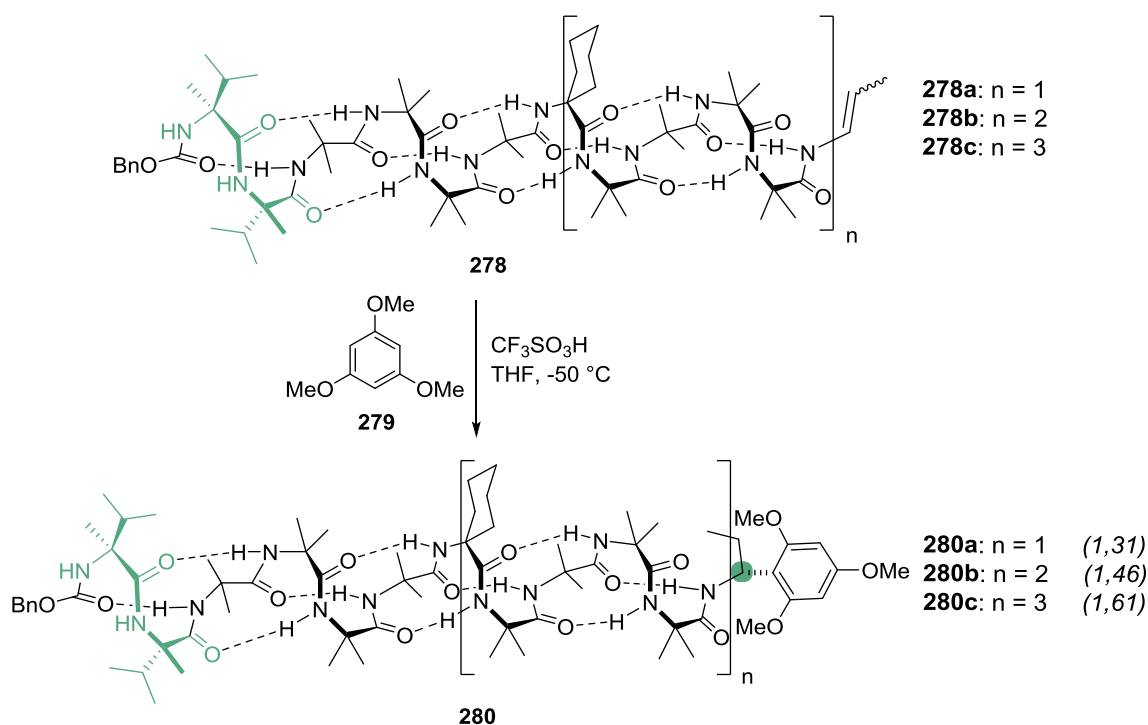


**Scheme 2.22** • Asymmetric hydrogenation for the synthesis of an (*S*)-phenylalanine residue within a right-handed helical peptide foldamer: 1,16-asymmetric induction, reported by Clayden *et al.*

**Table 2.9** • Asymmetric hydrogenation in a peptide foldamer reported by Clayden *et al.*

Product	n	solvent	dr ( <i>S</i> )-Phe- <b>277</b> : ( <i>R</i> )-Phe- <b>277</b>
<b>277a</b>	1	EtOH	79:21
<b>277a</b>	1	CH <sub>2</sub> Cl <sub>2</sub>	88:12
<b>277b</b>	2	EtOH	89:11
<b>277b</b>	2	CH <sub>2</sub> Cl <sub>2</sub>	>95:5

The diastereoselectivity of the hydrogenation reaction was improved by using dichloromethane as the solvent rather than ethanol, with an increase in dr from 79:21 to 88:12 in the synthesis of **277a**. This can be explained by the ability of polar protic solvents such as ethanol and methanol to disrupt hydrogen bonding, which would compromise the conformational integrity of right-handed helical foldamer **276a**. The highest dr (>95:5) was achieved with two units of (*S*)- $\alpha$ -methyl valine in the substrate ( $n = 2$ , compound **276b**).

**Scheme 2.23** • Foldamer-mediated remote stereocontrol reported by Clayden *et al.*

Aiming to improve on the 1,16-asymmetric induction achieved for the hydrogenation reaction (Scheme 2.22), Clayden *et al.* increased the length of the peptide chain, maintaining the ordered helix by the incorporation of cyclohexane (Ac6c) residues (compound **278**, Scheme 2.23).<sup>145</sup> The resulting peptide formed a helical foldamer at low

temperatures (down to -50 °C) held in a stable conformation by multiple hydrogen bonds. The chiral centres of the (*S*)- $\alpha$ -methyl valine dimer again influenced a preference for a right-handed screw-sense of the helix. Thus chiral information could be relayed through up to 60 covalent bonds to the site of reactivity. In the Friedel-Crafts reaction between *N*-alkenes **278a-c** and 1,3,5-trimethoxybenzene **279** in the presence of trifluoromethanesulfonic acid in THF at -50 °C, a mixture of two diastereomers were formed, where (*S,S,R*)-**280** was the major product. In the 1,31-induction (*n* = 1), a diastereomeric ratio of 92:8 was achieved in favour of **280a**, which dropped only slightly to 90:10 for the 1,46-induction (**280b**) and 88:12 for the 1,61-induction (**280c**). The yields of the reactions also remained high, with an overall range of 78-91%.

The 1,61-asymmetric induction described in Scheme 2.23 represents the communication of stereochemical information over a distance of around 4 nm,<sup>146</sup> which is far greater than any remote stereocontrol reaction previously reported. The mode of chiral induction showcased by this peptide foldamer is comparable to the stereoselectivity shown by enzymes, and may therefore find potential use in artificial cell structures for biological applications.

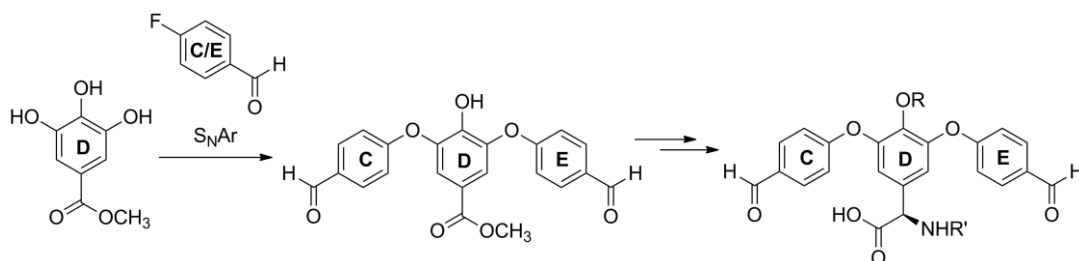
## 2.6 Conclusions

Remote asymmetric induction is a concept that has been used by organic chemists for half a century. Chiral auxiliaries have been widely employed in the synthesis of chiral non-racemic small compounds and in large natural products total syntheses. They are efficient, commercially available, and in many cases recyclable. However, the future of remote asymmetric induction lies beyond the synthesis of isolated small molecules. Mastering the transfer of information *via* remotely-triggered conformational changes in large molecules, particularly peptides, opens up the possibility of designing and manipulating artificial trans-membrane receptors in human cells.



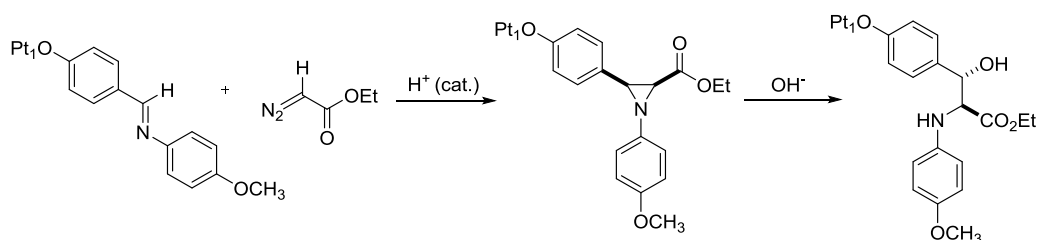
## 2.7 Project Aims

In the first chapter of this thesis, an introductory review of previously published work on the synthesis and biological activity of glycopeptide antibiotic analogues showed that this is an important class of antibiotics to pursue, and that an efficient, low cost route to the triaryl biether backbone (**C-O-D-O-E**) would be highly desirable for future syntheses of compounds featuring this structural motif. To this end, the early aim of this project (presented in Chapter 3) was to investigate the feasibility of a double nucleophilic aromatic substitution between methyl gallate and 4-fluorobenzaldehyde, and to then employ previously reported transformations for the synthesis of the ring **D**  $\alpha$ -amino acid moiety of orienticin **C** (Scheme 2.24).



**Scheme 2.24** • Plan for the construction of the **C-O-D-O-E** triaryl biether backbone of the glycopeptide antibiotic family

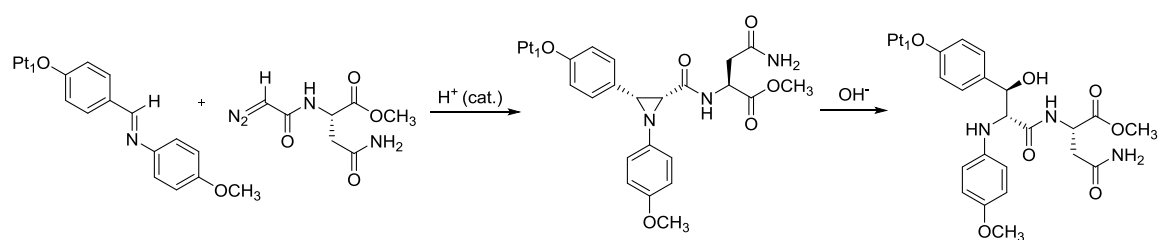
In a parallel study, the aldehyde functional group of the **C-O-D-O-E** backbone would be subject to imine condensation and aza-Darzens aziridination, with the intention of ring-opening a suitable aziridine to afford the functional group protected  $\beta$ -hydroxy  $\alpha$ -amino acid (Scheme 2.25), which is a key component of the **D-O-E** macrocycle of orienticin **C**.



**Scheme 2.25** • Proposed aza-Darzens aziridination for the synthesis of the  $\beta$ -hydroxy  $\alpha$ -amino acid moiety of orienticin **C**

In order to increase the efficiency of this approach in the synthesis of glycopeptide antibiotic analogues, the direct synthesis of peptide from amino acid-based precursors was also investigated. As the literature review of remote asymmetric induction in Chapter 2 shows, existing chiral centres in reaction substrates can influence the stereochemical outcome of a reaction, even when the substrates are acyclic. It was anticipated that amino

acid derived imines or diazoacetamides might exert a 1,3- or 1,5-induction in the Brønsted acid catalyzed aza-Darzens aziridination reaction (Scheme 2.26).



**Scheme 2.26** • Brønsted acid catalyzed aza-Darzens synthesis of a peptide aziridine precursor to the  $\beta$ -hydroxy  $\alpha$ -amino acid moiety of orienticin C

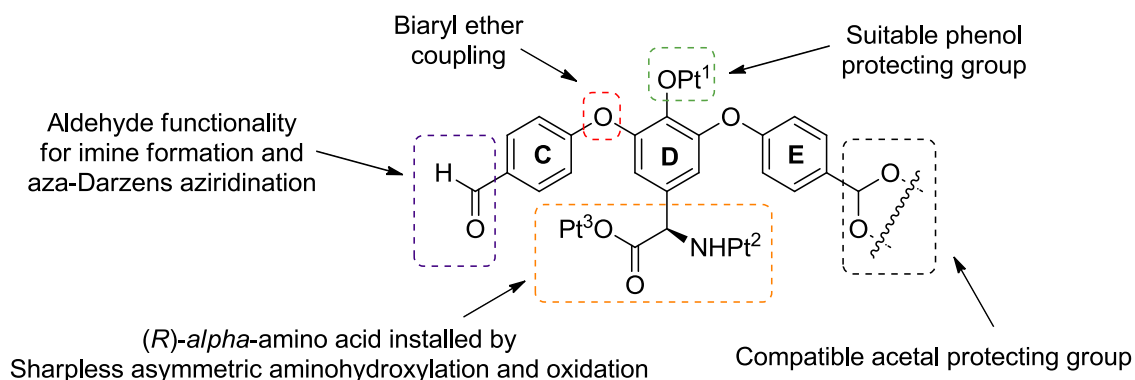
As well as being investigated for the synthesis of glycopeptide antibiotic analogues, the remote chiral induction strategy described in Chapter 4 may prove more generally useful in the synthesis of chiral non-racemic peptide aziridines as precursors for unnatural dipeptides and  $\alpha$ -amino acids.

## CHAPTER THREE

### Construction of the orienticin C backbone

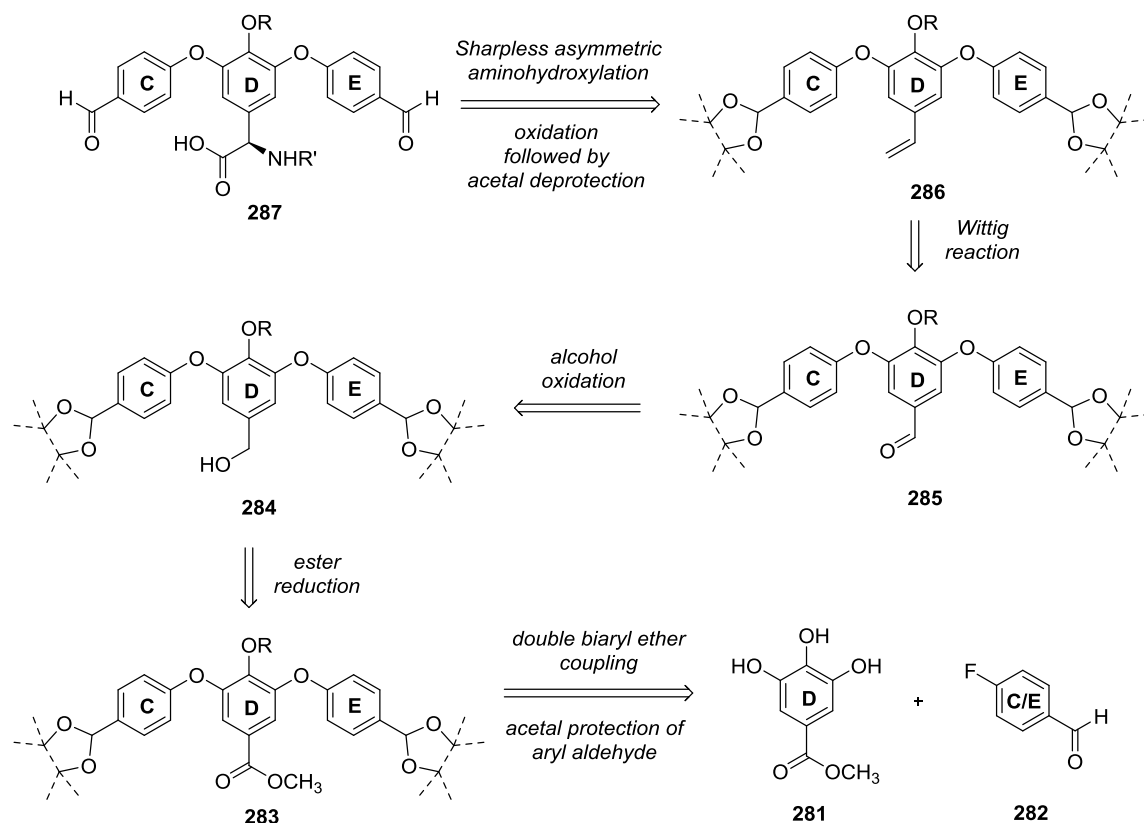
### 3.1 Introduction

In order to explore the application of an organocatalytic asymmetric aza-Darzens reaction to the synthesis of vancomycin-type compounds, an aldehyde-functionalised core starting point for the **C-O-D-O-E** backbone was required (Figure 3.1). Ideally this would feature the central (*R*)-3,4,5-trihydroxyphenylglycine derivative (ring **D**) already in place. Protecting group  $Pt^2$  at the amino acid on ring **D** will be necessary to prevent an unwanted imine condensation at this position during subsequent aziridination steps, and protecting group  $Pt^3$  will be required for ease of purification. Phenol derivatives are poor nucleophiles, but still under specific conditions are able to ring-open substituted aziridines.<sup>147</sup> This potential side reaction will be prevented by incorporating a phenol protecting group on ring **D** ( $Pt^1$ ).



**Figure 3.1** • Summary of project aims for construction of the triaryl vancomycin backbone

The initial starting material for the synthesis of the **C-O-D-O-E** backbone, methyl gallate **281**, is commercially available and can be easily obtained by esterification of gallic acid,<sup>148</sup> an inexpensive natural product found in a range of plant sources including acacia bark and grape seeds.<sup>149</sup> It was anticipated that the ester functionality of compound **281** would influence the chemoselectivity of the  $S_NAr$  reaction with 4-fluorobenzaldehyde **282**, leading to coupling only at the 3- and 5-hydroxy positions of **281** (Scheme 3.1). Protection of the dialdehyde functionality on **283** in the form of a cyclic or acyclic acetal is necessary during the reduction of the methyl ester to primary alcohol **284** and the subsequent oxidation that leads to the formation of the Wittig reaction precursor, aldehyde **285**.

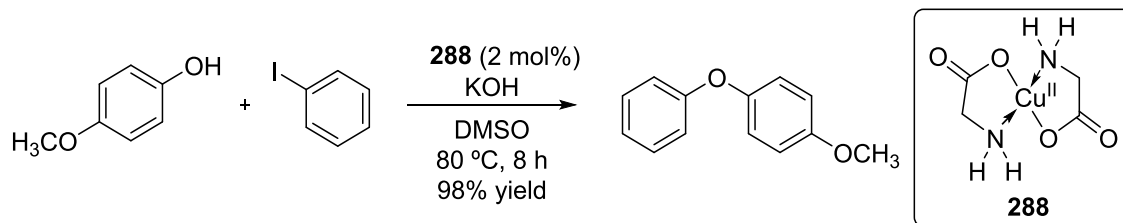


**Scheme 3.1** • Retrosynthetic analysis for the construction of the triaryl biether core **287** of orienticin C ( $R = -CH_3, -Bn$ ;  $R' = -Cbz, -Boc$ )

With the styrene moiety of **286** in place, a Sharpless asymmetric aminohydroxylation reaction should afford an amino alcohol which could be oxidised to **287**, completing the synthesis of the (*R*)- $\alpha$ -amino acid of ring **D**. Acid-catalysed hydrolysis of the two acetal protecting groups on rings **C** and **E** would restore the aldehyde functionality in preparation for imine condensation and subsequent asymmetric aza-Darzens aziridination.

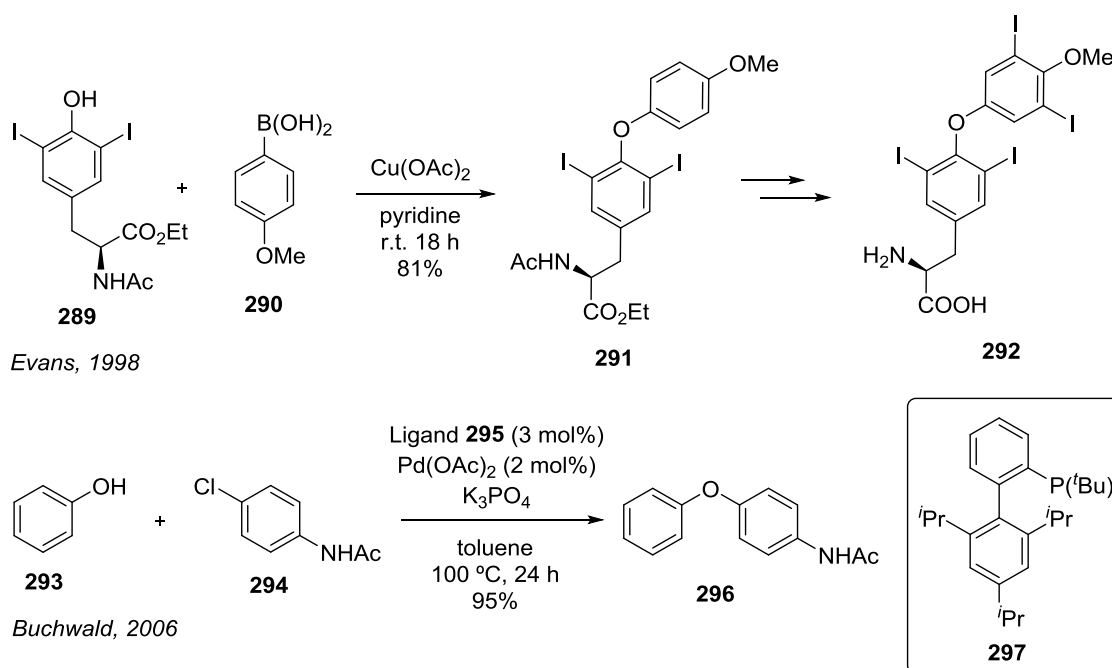
### 3.2 Diaryl ether coupling

Since Fritz Ullmann reported the copper(0)-catalysed reaction between phenol and bromobenzene in 1905,<sup>150</sup> a myriad of methods have been developed for diaryl ether synthesis. Traditionally, the Ullmann ether synthesis uses high temperatures (100–300 °C), long reaction times (48–72 hours) and stoichiometric metal reagents or high catalyst loading.<sup>151</sup> Modern variations include the use of 2 mol% of copper(II) *trans*-bis-(glycinato) catalyst **288** by Jain *et al.*, which enables lower reaction temperatures, shorter reaction times and lower catalyst loading than previous protocols (Scheme 3.2).<sup>152</sup>



**Scheme 3.2** • Copper(II)-catalysed diaryl ether coupling reported by Jain *et al.*, 2012.

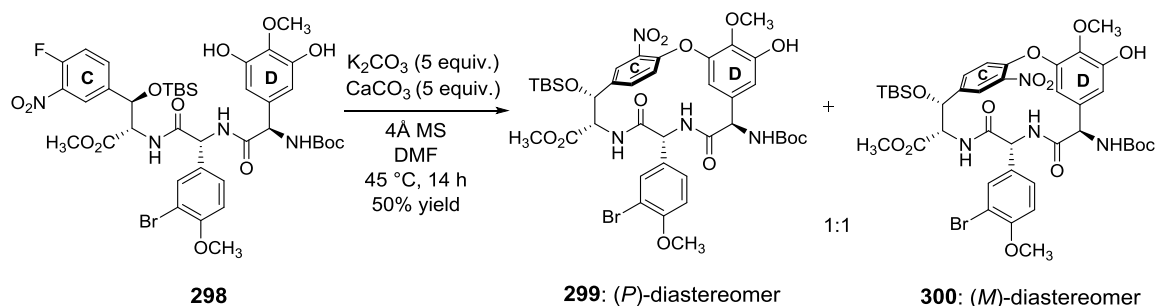
The copper(II)-mediated Chan-Lam coupling of a hydroxyl group with 4-methoxyphenylboronic acid **290** was employed by Evans *et al.* in their 1998 formal synthesis of L-thyroxine **292** from (*S*)-ethyl 2-acetamido-3-(4-hydroxy-3,5-diiodophenyl)propanoate **289** (Scheme 3.3).<sup>153</sup> A range of palladium(II)-catalysed protocols have also been reported, exploiting the recent interest in using platinum-group metals in coupling methodologies, such as that of Buchwald *et al.* which employed the bulky and sterically hindered phosphorus diaryl ligand, *t*BuXPhos **297** (Scheme 3.3).<sup>154</sup>



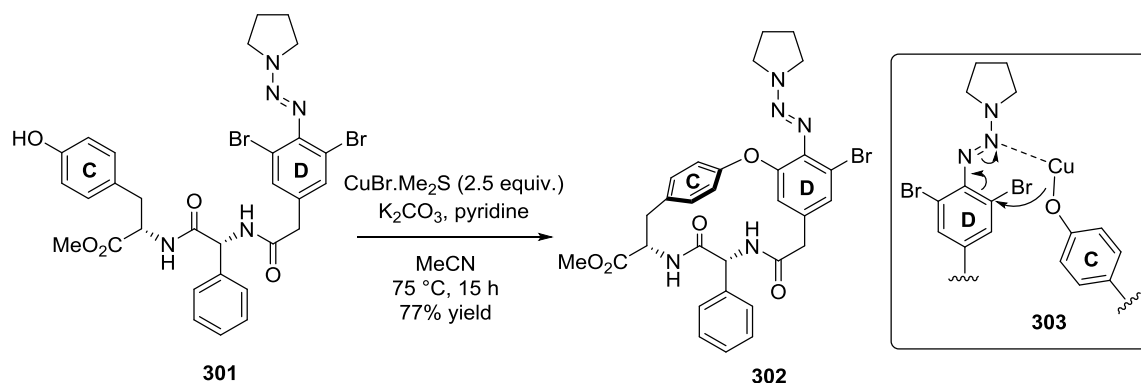
**Scheme 3.3** • Copper(II)-catalysed arylboronic acid coupling reported by Evans *et al.*, 1998; palladium(II)-catalysed coupling reported by Buchwald *et al.*, 2006.

Previous syntheses of vancomycin and its analogues have employed as key strategies either copper(I)-catalysed or transition metal-free coupling methods. In their 1997 synthesis of monomacrocylic vancomycin analogues, the Boger group performed a nucleophilic aromatic substitution to generate the C-O-D macrocycles **299** and **300** (atropisomers which were separable by flash column chromatography) (Scheme 3.4).<sup>155</sup>

The presence of an electron withdrawing nitro group *ortho* to the fluoro substituent (compound **298**, ring C) has previously been shown to activate the halogen towards nucleophilic attack.<sup>156</sup> The macrocyclisation of **298** proceeded in a moderate 50% yield overall, although there was no selectivity for the natural (*M*)-diastereomer **300** over the unnatural (*P*)-diastereomer **299** in this case. The nitro group of **300** was converted in three steps to the chloro substituent found in vancomycin (**1**, p. 1) later in the synthesis.



**Scheme 3.4** • Synthesis of vancomycin C-O-D ring analogues reported by Boger *et al.*

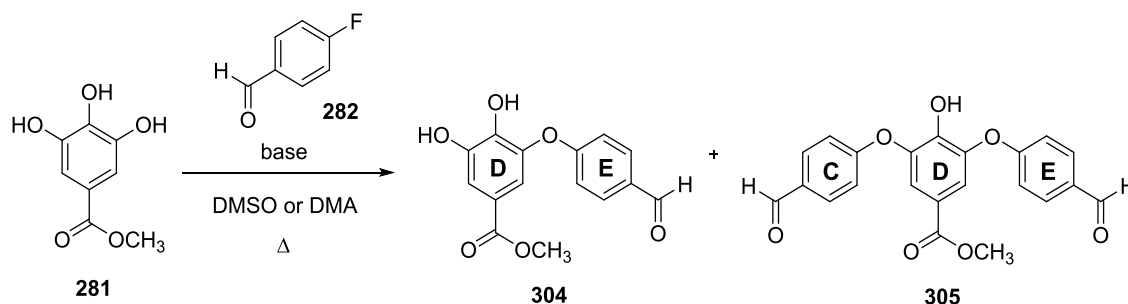


**Scheme 3.5** • Triazene-based 16 atom macrocyclisation reported by Nicolaou *et al.*

Taking a novel approach to this problem for their 1998 total synthesis of vancomycin, the Nicolaou group developed a triazene-based macrocyclisation reaction which employed an excess of a copper(I) bromide dimethyl sulfide complex (Scheme 3.5).<sup>157</sup> It was proposed that the reaction proceeded *via* intermediate **303**, in which the attacking nucleophile was brought into the proximity of the aryl bromide by coordination of the metal counterion to the triazene functionality of ring D, which itself became an “electron sink” for the nucleophilic substitution. Following the synthesis of model C-O-D ring **302** in a 77% yield, this methodology also proved to be moderately efficient in the synthesis of vancomycin, closing the D-O-E macrocycle in a 60% yield.<sup>158</sup>

### 3.2.1 S<sub>N</sub>Ar synthesis of triaryl biether and diaryl ether aldehydes

An aldehyde-functionalised triaryl biether was required as the starting point for our synthesis of the **C-O-D-O-E** backbone of orienticin C. With this in mind, a double nucleophilic aromatic substitution reaction between methyl gallate **281** and 4-fluorobenzaldehyde **282** (Scheme 3.6) was investigated, exploring a range of reaction conditions (Table 3.1 and 3.2).



**Scheme 3.6** • General scheme for the S<sub>N</sub>Ar reaction between methyl gallate **281** and 4-fluorobenzaldehyde **282**

At room temperature, no reaction was observed between methyl gallate **281** and 4-fluorobenzaldehyde **282** in the presence of 2.5 equivalents of potassium carbonate (Table 3.1). Increasing the temperature to 70 °C afforded **304** in a poor 20% yield after prolonged heating for 48 hours.

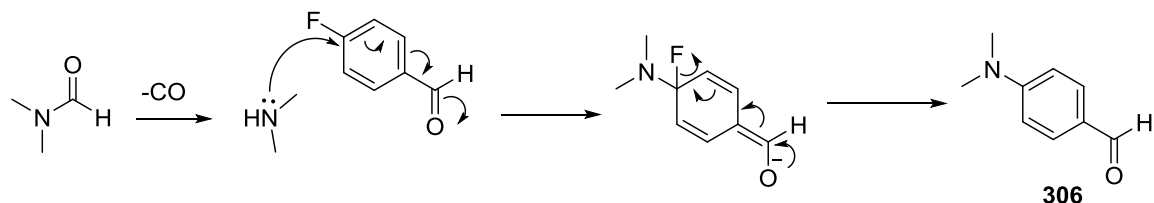
**Table 3.1** Attempted synthesis of **304** and **305** (oil bath heating)

Base	Solvent	4-Fluoro- benzaldehyde (equiv)	Temp. (°C)	Time (h)	Yield <b>304</b> mono (%)	Yield <b>305</b> di (%)	Total Yield (%)
K <sub>2</sub> CO <sub>3</sub>	DMF	1.1	25	24	0	0	0
K <sub>2</sub> CO <sub>3</sub>	DMA	2	70	48	20	-	20
K <sub>2</sub> CO <sub>3</sub>	DMF	2	160	4	<5	-	0

In an attempt to reduce the reaction time, the flask was heated to reflux (~160 °C) in DMF. After four hours, a white crystalline precipitate was observed, whose physicochemical properties matched those of 1-(4-(dimethylamino)phenyl)ethanone **306**. Formation of **306** was undoubtedly due to the *in situ* decomposition of DMF into dimethylamine and carbon monoxide. Presumably the dimethylamine underwent a nucleophilic aromatic substitution with 4-fluorobenzaldehyde (Scheme 3.7). Indeed this



reaction has recently been exploited by Ulven *et al.* in a flow chemistry protocol using a range of aryl halides.<sup>159</sup> DMF was therefore deemed an unsuitable solvent for this reaction at the temperature indicated. Instead, using DMA or DMSO as the reaction solvent for the synthesis of **304** and **305** prevented the formation of byproduct **306**.



**Scheme 3.7** • Mechanism for the  $S_NAr$  reaction between dimethylamine and 4-fluorobenzaldehyde following the *in situ* decomposition of DMF

Compared to the low yield, high temperature and long reaction time of using a conventional oil bath set-up, the application of microwave irradiation offered several significant advantages for this reaction. A comparable 21% yield of **304** was obtained in just 30 minutes by changing the heating method to microwave irradiation at the same temperature (160 °C), in DMA (Table 3.2). Changing the base to cesium carbonate and the solvent to DMSO increased the yield of **304** to 32%, and triaryl biether **305** was observed for the first time in a 5% yield. By adding 3.2 equivalents of 4-fluorobenzaldehyde, dialdehyde **305** could be obtained in a 56% yield, with a total reaction yield of compounds **304** and **305** of 77%.

**Table 3.2** Base and solvent study for the synthesis of **304** and **305** (microwave irradiation)

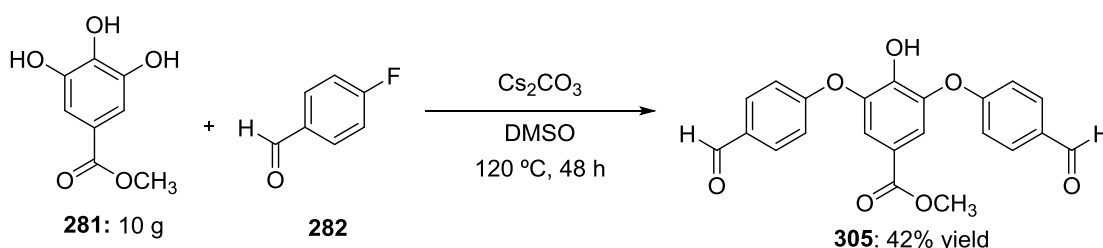
Base	Solvent	4-Fluoro- benzaldehyde (equiv)	Temp. (°C)	Time (h)	Yield <b>304</b> mono (%)	Yield <b>305</b> di (%)	Total Yield (%)
K <sub>2</sub> CO <sub>3</sub>	DMA	1	160	0.5	21	-	21
K <sub>2</sub> CO <sub>3</sub>	DMSO	1	160	2	<5	-	0
Cs <sub>2</sub> CO <sub>3</sub>	DMSO	1	160	2	32	5	37
Cs <sub>2</sub> CO <sub>3</sub>	DMSO	1.2	160	1	42	<5	42
Cs <sub>2</sub> CO <sub>3</sub>	DMSO	3.2	160	2	21	56	77

Increasing the reaction time, temperature or number of equivalents beyond those reported in Table 3.2 did not increase the yield of either **304** or **305**. Instead only decomposition of

the starting materials and products was observed, presumably by base-mediated hydrolysis of the methyl ester. The marked increase in yield of **304** on switching from potassium carbonate to cesium carbonate in DMSO (Table 3.2, entries 2 and 3) may be a result of the “cesium effect”, a term which refers to the large electronic polarizability and cationic radius (1.67 Å vs. 1.33 Å for K<sup>+</sup>) of Cs<sup>+</sup> compared to other alkali metal ions.<sup>160</sup> Cesium carbonate therefore releases the “naked” carbonate anion more readily. In addition, cesium carbonate has a much higher solubility in DMSO, DMF, and DMA than potassium carbonate (Table 3.3).<sup>161</sup>

**Table 3.3** Solubility of alkali carbonates determined by Cella *et al.* (g/10 mL)

Solvent	Cs <sub>2</sub> CO <sub>3</sub>	K <sub>2</sub> CO <sub>3</sub>	Li <sub>2</sub> CO <sub>3</sub>	Na <sub>2</sub> CO <sub>3</sub>
DMF	1.195	0.075	0.003	0.038
DMSO	3.625	0.470	0.014	0.143
DMA	0.490	0.047	0.004	0.021



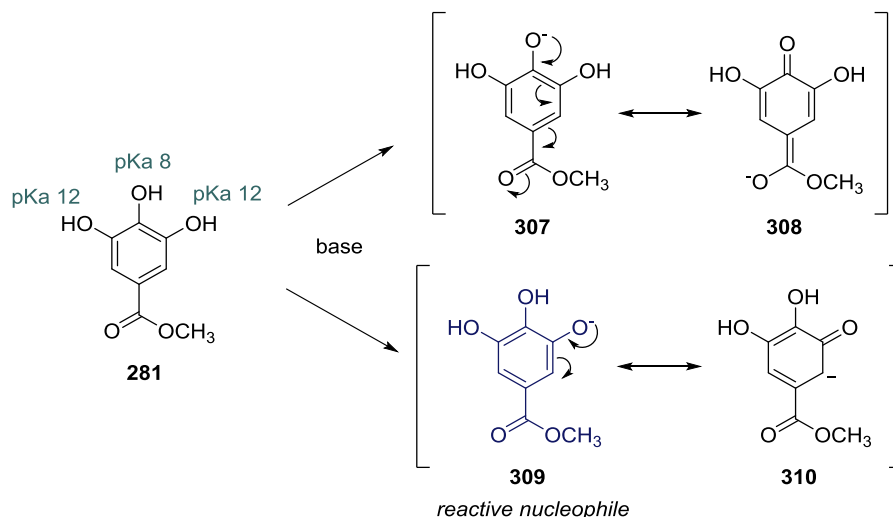
**Scheme 3.8** • Synthesis of dialdehyde **305** on a 10 g scale by oil bath heating

Though the microwave reactor provided a relatively fast and efficient route to **305**, the key aldehyde starting material of the orienticin C backbone, the scale was limited to a ‘batch synthesis’ using 500 mg of methyl gallate. Fortunately, the improved reaction conditions could be applied to a 10 g scale oil bath protocol with a minimal reduction in yield (Scheme 3.8). In this case, the impure reaction product could be brought to 98% purity (estimated by <sup>1</sup>H-NMR) without column chromatography by washing the orange solid with cold diethyl ether.

### 3.2.2 Mechanistic rationale and spectroscopic analysis of diaryl ether **304** and triaryl diether **305**

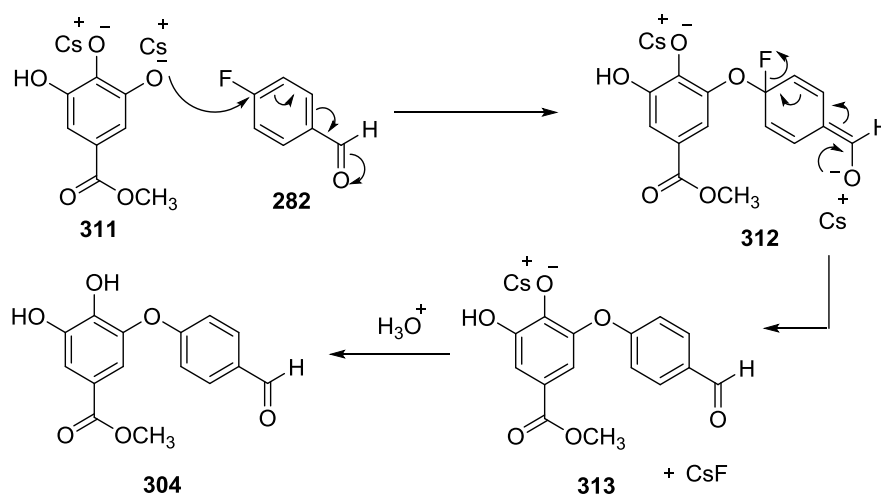
The nucleophilic aromatic substitution described above (Scheme 3.7) shows chemoselectivity for the 3- and 5-hydroxy positions of methyl gallate **281**. The most

acidic proton is at the 4-hydroxy position, with a calculated pKa of 8 compared to a pKa of 12 for the 3- and 5-hydroxy positions.<sup>162</sup> Deprotonation at the 4-hydroxy position of **281** results in anion **307** which is stabilised by conjugation with the ester group *para* to the phenoxide (Figure 3.2). By contrast, the anion formed by deprotonation at the 3-hydroxy position (**309**) is not stabilised by the ester, making intermediate **309** the more reactive nucleophile.



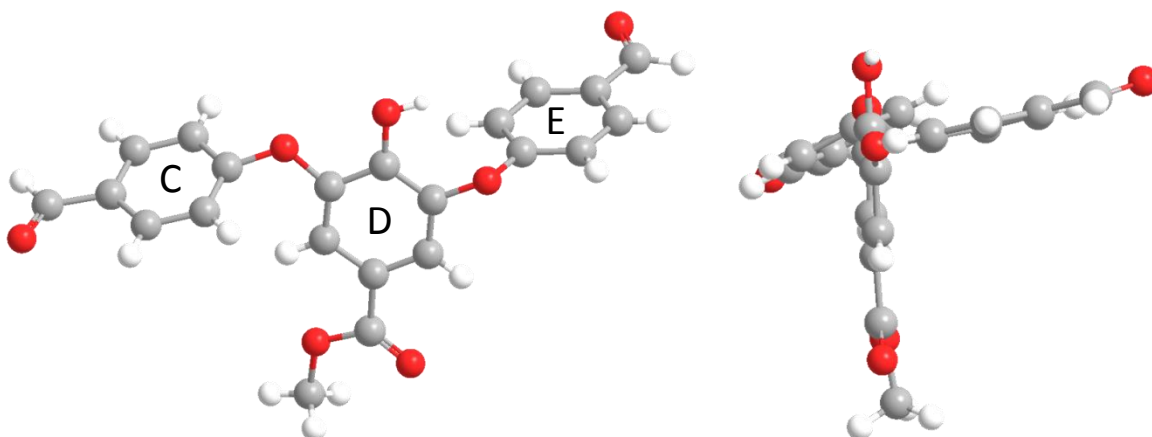
**Figure 3.2** • Resonance stabilisation of the reaction intermediates formed by deprotonation of methyl gallate **281**

This analysis indicates that two equivalents of base are required for the first S<sub>N</sub>Ar. Deprotonation is followed by an addition-elimination mechanism (Scheme 3.9) in which the electron-withdrawing aldehyde *para* to the halide provides stabilisation of anion **312**.

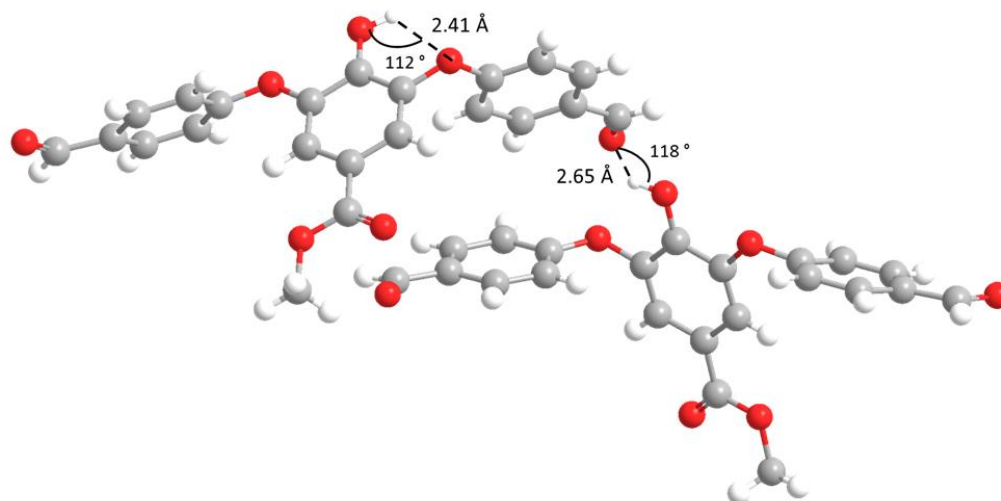


**Scheme 3.9** • Postulated mechanism of the S<sub>N</sub>Ar reaction between deprotonated methyl gallate **281** and 4-fluorobenzaldehyde **282**

The carbon-fluorine bond has been referred to as “the strongest single bond in organic chemistry”.<sup>163</sup> The short C-F bond length (1.4 Å compared to 1.9 Å for C-Br)<sup>164</sup> and high bond dissociation energy (averaging around 500 kJ mol<sup>-1</sup> compared to 290 kJ mol<sup>-1</sup> for C-Br)<sup>165</sup> are due to the large difference in electronegativity between carbon and fluorine (2.5 vs. 4.0).<sup>166</sup> Consequently the C-F bond is highly polar, and the electron-poor carbon makes an excellent electrophile in the rate-determining addition step of the S<sub>N</sub>Ar reaction. Re-aromatisation of the benzene ring in **312** is sufficiently exothermic to permit the energetically disfavoured breaking of the strong C-F bond.



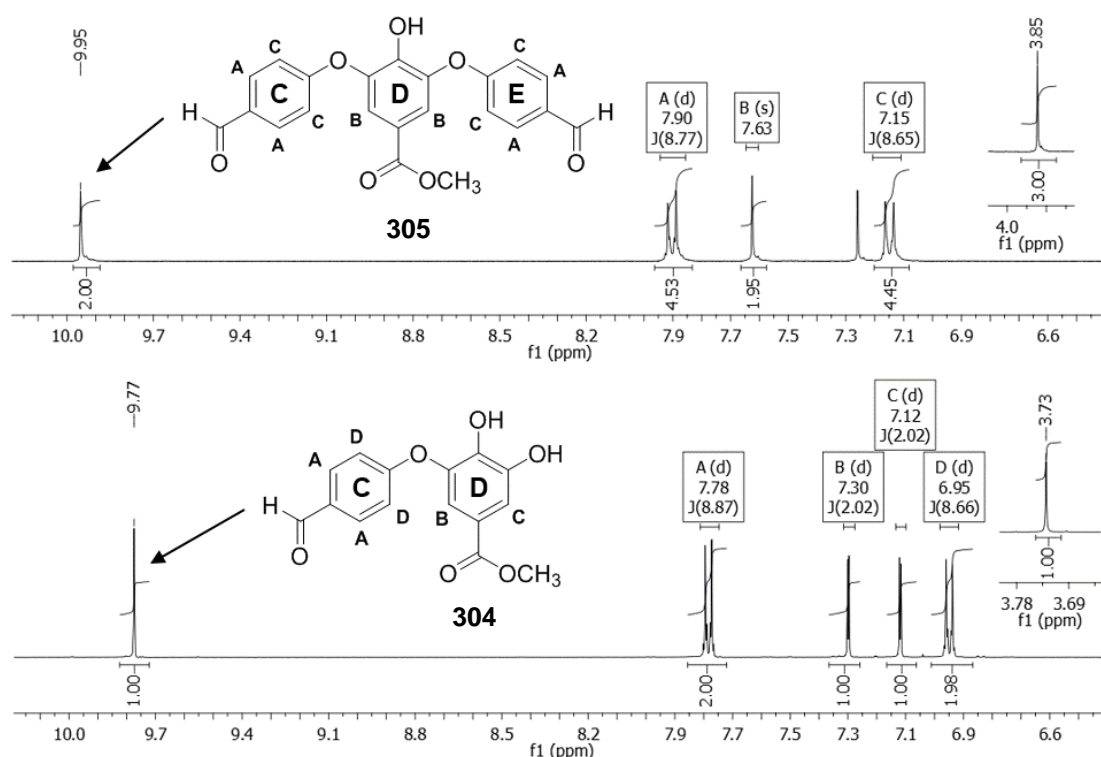
**Figure 3.3** • X-ray crystal structure of dialdehyde **305**: front view (left) and side view (right)



**Figure 3.4** • Intra- and intermolecular hydrogen bonding in the X-ray crystal structure of dialdehyde **305**

Pale brown crystals of dialdehyde **305** were obtained by crystallisation from diethyl ether and subjected to X-ray crystallographic analysis. This confirmed the symmetry of the

double nucleophilic aromatic substitution product (Figure 3.3). In the monoclinic crystal, compound **305** has a non-planar conformation where aryl rings **C** and **E** are tilted at an angle of approximately  $70^\circ$  to the central **D**-ring, compared to  $80^\circ$  in the crystal structure of vancomycin **1**.<sup>167</sup> There is evidence of intermolecular hydrogen bonding between the hydroxyl group on ring **D** and the aldehyde carbonyl of ring **E**, with a bond length of 2.65 Å and an angle of  $118^\circ$  (O—H---O, Figure 3.4). A possible intramolecular hydrogen bond was also identified between the hydroxyl on ring **D** and the oxygen of the neighbouring diaryl ether, with a bond length of 2.41 Å compared to 0.84 Å for the O-H covalent bond.



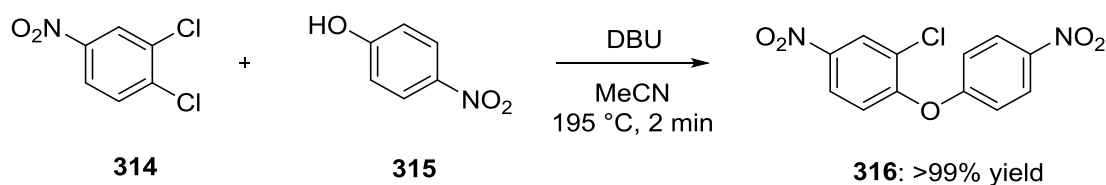
**Figure 3.5** • Partial  $^1\text{H}$ -NMR spectra of **305** (300 MHz,  $\text{CDCl}_3$ ) and **304** (400 MHz,  $\text{CD}_3\text{OD}$ )

The  $^1\text{H}$ -NMR spectrum supported our hypothesis that aldehyde **304** is substituted only at the 3-hydroxy position (Figure 3.5). The non-equivalent aromatic protons of the **D** ring appear as doublets at 7.30 and 7.12 ppm. The coupling constant  $^4J = 2$  Hz is consistent with *meta* proton-proton coupling across an aromatic ring.<sup>168</sup> By contrast, the magnetically equivalent **D**-ring protons in dialdehyde **305** appear as one peak: a singlet at 7.62 ppm. In each case the aldehyde protons appear at 9.95 ppm (di-**305**,  $\text{CDCl}_3$ ) and 9.77 ppm (mono-**304**,  $\text{CD}_3\text{OD}$ ) and the methyl ester signals appear in the appropriate region at

3.85 ppm (**305**) and 3.73 ppm (**304**). The FT-IR spectrum confirmed the presence of the aldehyde and ester functional groups, with carbonyl stretch bands at 1692 and 1669  $\text{cm}^{-1}$  for dialdehyde **305** and an overlapping band at 1686  $\text{cm}^{-1}$  for mono-aldehyde **304**. The C=O signals appear at a lower frequency than the expected range for carbonyl stretch bands due to the conjugation in these molecules.<sup>169</sup>

### 3.2.3 Diaryl ether coupling under continuous flow conditions

Continuous processes in the synthesis of fine chemicals and pharmaceuticals have grown increasingly sophisticated over the last three decades, and versatile modular flow systems are now commercially available and within the reach of both academic and industrial laboratories. Chemical reactions conducted in flow micro-reactors benefit from rapid heat transfer, increased safety and the ability to handle unstable reaction species.<sup>170</sup> On an industrial scale, continuous flow processes have attractive economic and environmental benefits due to their high energy efficiency and reduced consumption of resources compared with batch processes.<sup>171</sup> Flow system software offers precise control over reaction conditions and continuous measurement of temperature and pressure inside the reactor. Flow systems are therefore also highly compatible with continuous in-line and on-line reaction monitoring by analytical techniques such as ReactIR infrared spectroscopy and flow NMR spectroscopy.<sup>172,173</sup> The differences in mass and heat transfer, surface area, catalyst exposure and reaction concentration between flow systems and corresponding batch processes can have profound effects on the efficiency and selectivity of a chemical reaction.<sup>174</sup> This so-called “flash chemistry” concept coined by Jun-ichi Yoshida<sup>175</sup> was applied to the synthesis of diaryl ethers by Wiles and Watts in 2011 (Scheme 3.10).<sup>176</sup>

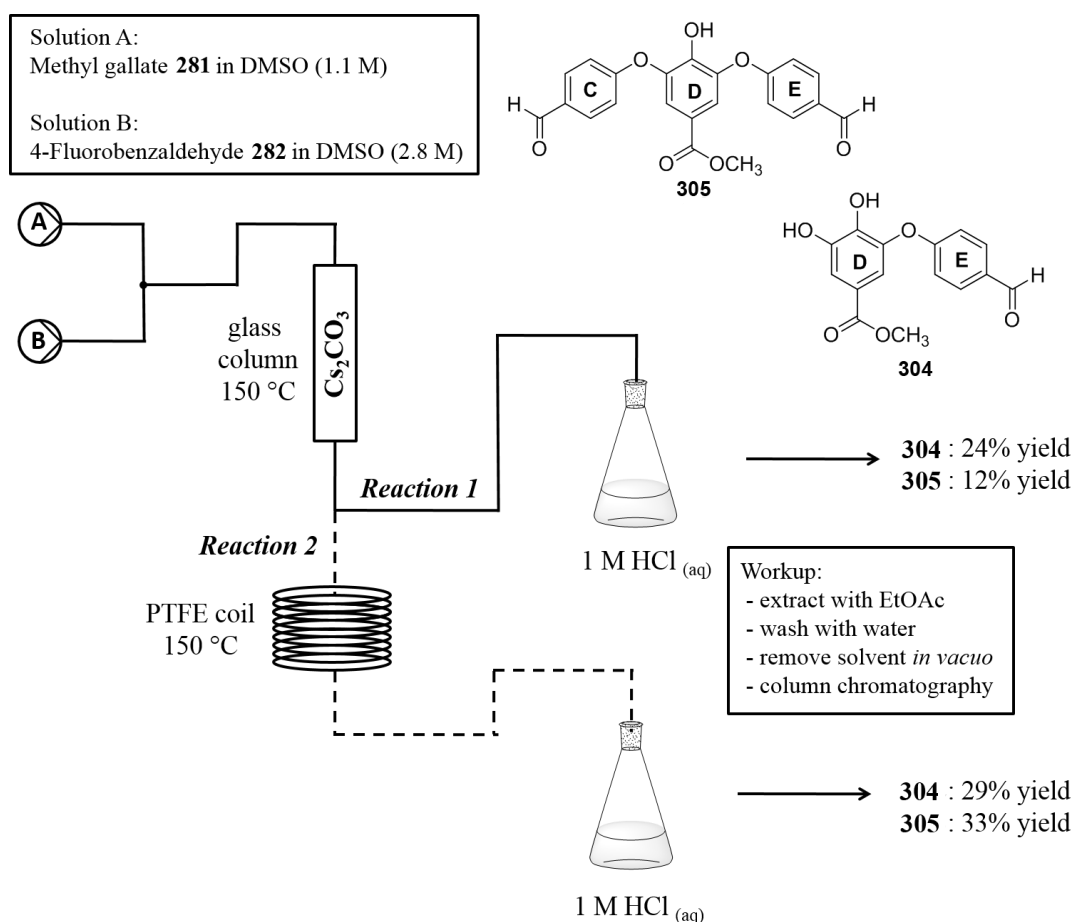


**Scheme 3.10** • Continuous flow synthesis of 1-chloro-4-nitro-2-(4-nitrophenoxy)benzene **316** reported by Wiles *et al.*

Using an organic base, DBU, to ensure the reaction was homogenous, 1,2-dichloro-4-nitrobenzene **314** was coupled with 4-hydroxynitrobenzene **315** in acetonitrile at 195 °C to afford diaryl ether **316**. Employing this flow protocol reduced the reaction time from

ten minutes to two minutes compared to the microwave-assisted reaction reported by Moseley *et al.* in 2010, with an accompanying increase in yield from 70% to >99%.<sup>177</sup> Subsequent investigation into the use of a biphasic aqueous potassium carbonate / acetonitrile mixture within the micro-reactor indicated that inorganic bases could be used in place of DBU, which significantly reduced the costs of the reaction.<sup>i</sup>

Preliminary investigations into the continuous flow synthesis of dialdehyde **305** were carried out using a Uniqsis FlowSyn reactor. Employing the most favourable base/solvent conditions (outlined in Section 3.2.1, Table 3.2) of cesium carbonate in DMSO, a system was devised in which separate solutions of methyl gallate **281** and 4-fluorobenzaldehyde **282** in DMSO were simultaneously pumped at a flow rate of 1 mL/min *via* a static mixer through a preheated glass column packed with cesium carbonate (Figure 3.6).

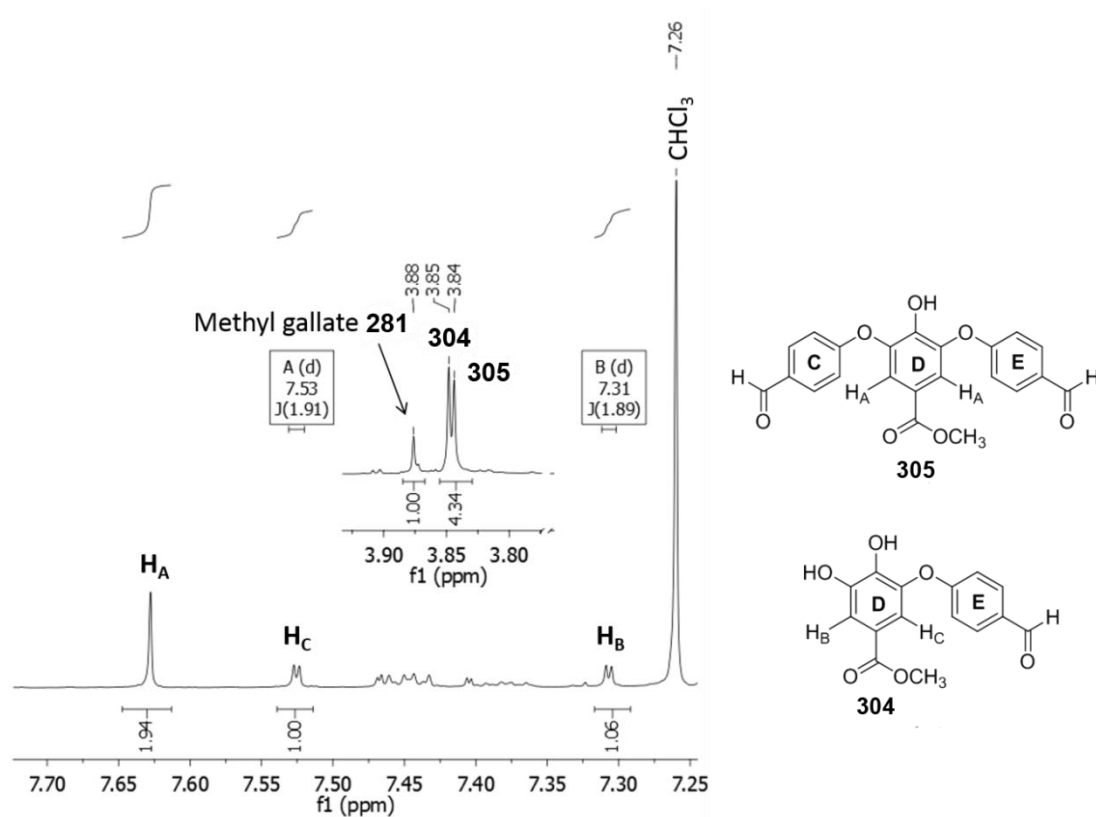


**Figure 3.6** • Continuous flow synthesis of triaryl biether **305** and diaryl ether **304**; 1) using a heated column only and 2) with an additional 20 mL heated coil

<sup>i</sup> Potassium carbonate ~£20 per kg compared to DBU ~£400 per kg based on current prices from Sigma-Aldrich Co.

The concentrations of the organic starting materials were such that 2.5 equivalents of 4-fluorobenzaldehyde **282** were present to one equivalent of methyl gallate **281**. It was anticipated that the presence of the inorganic base cesium carbonate in a large excess relative to the amount of methyl gallate flowing through the column would increase the efficiency of the diaryl ether coupling. The amount of base inside the column decreased slightly over the course of the reaction, partly due to the slight solubility of cesium carbonate in DMSO (Section 3.2.1, Table 3.3) but mainly due to reaction with methyl gallate to form the soluble cesium salt **311** (Scheme 3.9, Section 3.2.2). However, the high temperature and high polarity of the solvent ensured that no precipitation of the intermediates or byproducts occurred inside the PTFE tubing of the reactor.

In an attempt to improve the yield of dialdehyde **305**, a 20 mL PTFE coil reactor heated to 150 °C was added to the FlowSyn set-up between the glass column and the collection flask (Figure 3.6). This increased the reaction time by 10 minutes and changed the ratio of the mono- and di-substitution products **304** and **305** to ~1:1 by <sup>1</sup>H-NMR spectroscopy of the impure reaction mixture (Figure 3.7).



**Figure 3.7** • Partial <sup>1</sup>H-NMR spectra of the impure reaction mixture of flow synthesis reaction 2 (Figure 3.6) (CDCl<sub>3</sub>, 500 MHz)



Measuring the integration of the methyl ester  $-OCH_3$  protons shows a total conversion of 81% from the starting material methyl gallate **281** to products **304** and **305**. However, the isolated yields of **304** and **305** (29% and 33% respectively) add up to an overall reaction yield of 62%, indicating some loss of material due to base hydrolysis of the methyl ester moiety. The yield of the diaryl ether coupling step using a flow reactor is comparable to (but no better than) the yield of the corresponding microwave-assisted reaction discussed in Section 3.2.1, but these initial studies demonstrate the potential of continuous flow systems for the fast automated synthesis of the triaryl biether core of orienticin C.

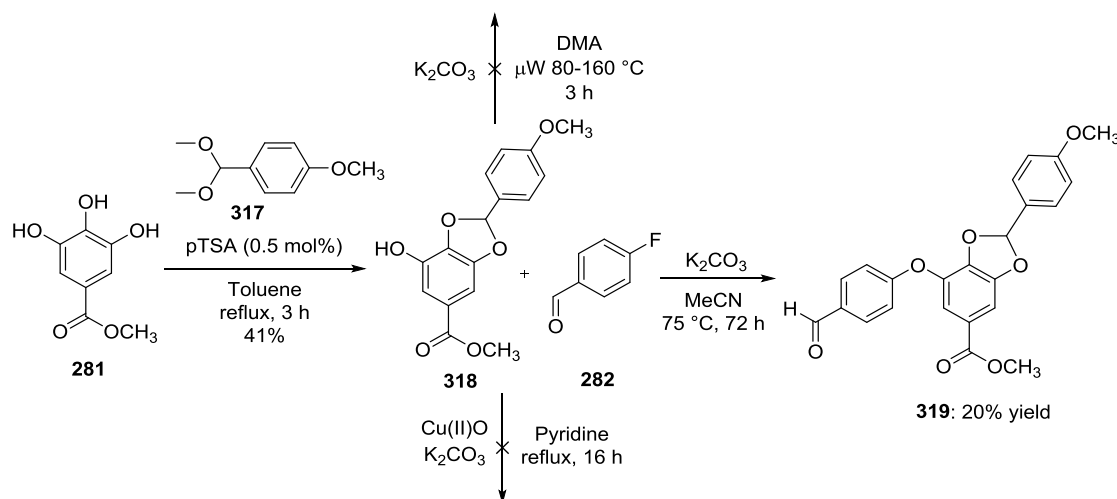
In the microwave irradiation, flow synthesis and conventional oil bath procedures discussed above, the yield of the desired dialdehyde **305** remained frustratingly low. It is likely that employing an *ortho* nitro electron-withdrawing group on the electrophile (as demonstrated by both Evans and Boger, Section 3.2) would increase the yield of the reaction. There is also the possibility of switching to a transition metal-catalysed reaction such as that developed by Nicolaou *et al.* (Scheme 3.4, Section 3.2). However, the commercial availability and low cost of methyl gallate (and its precursor gallic acid) make our nucleophilic aromatic substitution route more appealing in terms of minimising the time and number of synthetic steps required. The byproduct of the  $S_NAr$  discussed above, diaryl ether **304**, is extremely useful as the starting material for the single-ring glycopeptide analogues which could be employed as test systems for new macrocyclisation chemistry in this field.<sup>178</sup> Alternatively, diaryl ether **304** could be resubmitted to the  $S_NAr$  reaction conditions for triaryl biether formation.

### 3.3 Towards the synthesis of the ring D $\alpha$ -amino acid

Aldehydes **304** and **305** described in Section 3.2 contain phenolic hydroxyl groups which required functional group protection at this stage to prevent possible ring-opening of the aziridines later in the synthesis. The phenol functional group can be routinely protected by a methyl, benzyl or allyl ether.<sup>179</sup> The synthesis of a cyclic *para*-methoxybenzylidene acetal of methyl gallate, compound **281**, was reported simultaneously by the groups of S. Tsuboi<sup>180</sup> and T. H. Chan<sup>181</sup> in 2005.

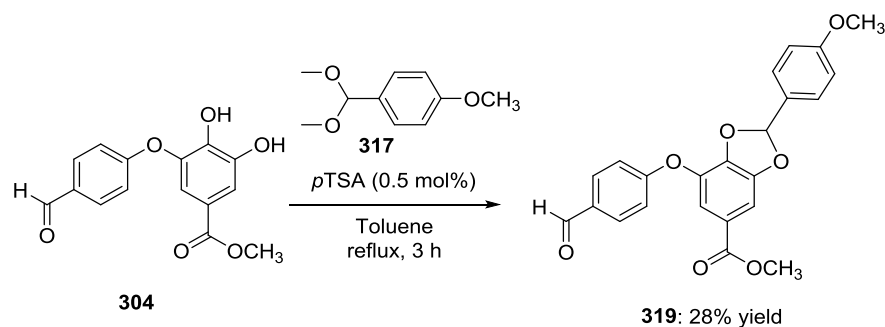
Following a similar procedure to Chan *et al.*, the transacetalisation reaction of methyl gallate **281** with *para*-methoxybenzaldehyde dimethyl acetal **317**<sup>182</sup> was carried out in toluene under reflux conditions, with a catalytic amount (0.5 mol%) of *para*-

toluenesulfonic acid (Scheme 3.11). The round-bottom flask was fitted with a Soxhlet apparatus containing flame-dried 4Å molecular sieves to remove methanol from the reaction, and cyclic acetal **318** was obtained in a 41% yield. Methyl gallate **281** was recovered in a 47% yield after purification by flash column chromatography.



**Scheme 3.11** • Protection of methyl gallate **281** as PMB acetal **318**, and subsequent  $S_NAr$  diaryl ether coupling with 4-fluorobenzaldehyde

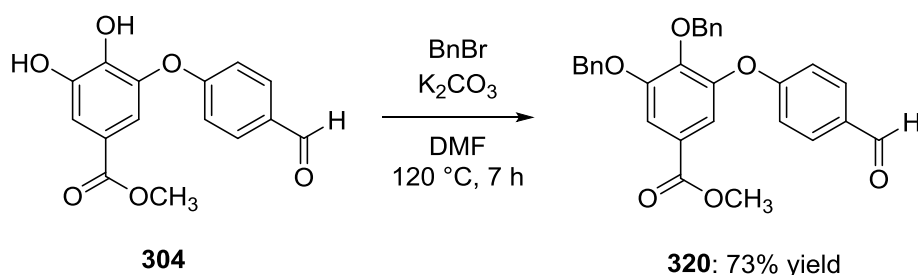
Coupling of acetal **318** with 4-fluorobenzaldehyde **282** under the conditions described in Section 3.2.1 was initially unsuccessful (Scheme 3.11); microwave irradiation at 80-120 °C for several hours produced no change by thin layer chromatography. After further heating at 160 °C for one hour the starting material was consumed and the reaction was quenched with distilled water. However, the  $^1H$ -NMR spectrum of the impure reaction mixture contained a mixture of 4-fluorobenzaldehyde **282**, methyl gallate **281** and *para*-methoxybenzaldehyde, indicating that hydrolysis of the acetal occurred during the workup. The same result was obtained using a copper(II) oxide coupling protocol reported by Kodama *et al.*<sup>183</sup>



**Scheme 3.12** • Protection of compound **304** as *para*-methoxybenzylidene acetal **319**

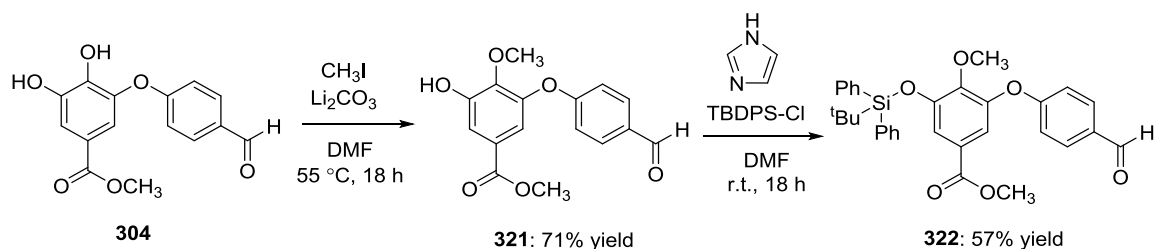
Compound **319** was finally obtained in a poor 20% yield by oil bath heating at 75 °C over a period of three days, employing potassium carbonate as the base and acetonitrile as the solvent (Scheme 3.11). Compound **319** could also be obtained by transacetalisation of diaryl ether **304** with *para*-methoxybenzaldehyde dimethyl acetal **317** (Scheme 3.12). However the overall yield of this two-step synthesis from methyl gallate **281** was only 11%, and with an 8% overall yield for the reactions described in Scheme 3.10, neither route is suitable for this synthesis.

Protecting the catechol functional group as the *O*-benzyl ether was more successful (Scheme 3.13). The reaction of diaryl ether **304** with benzyl bromide and potassium carbonate in DMF at 120 °C for 7 hours afforded compound **320** in a 73% yield.<sup>184</sup> The mono-protected product was not observed in a quantity large enough to isolate.



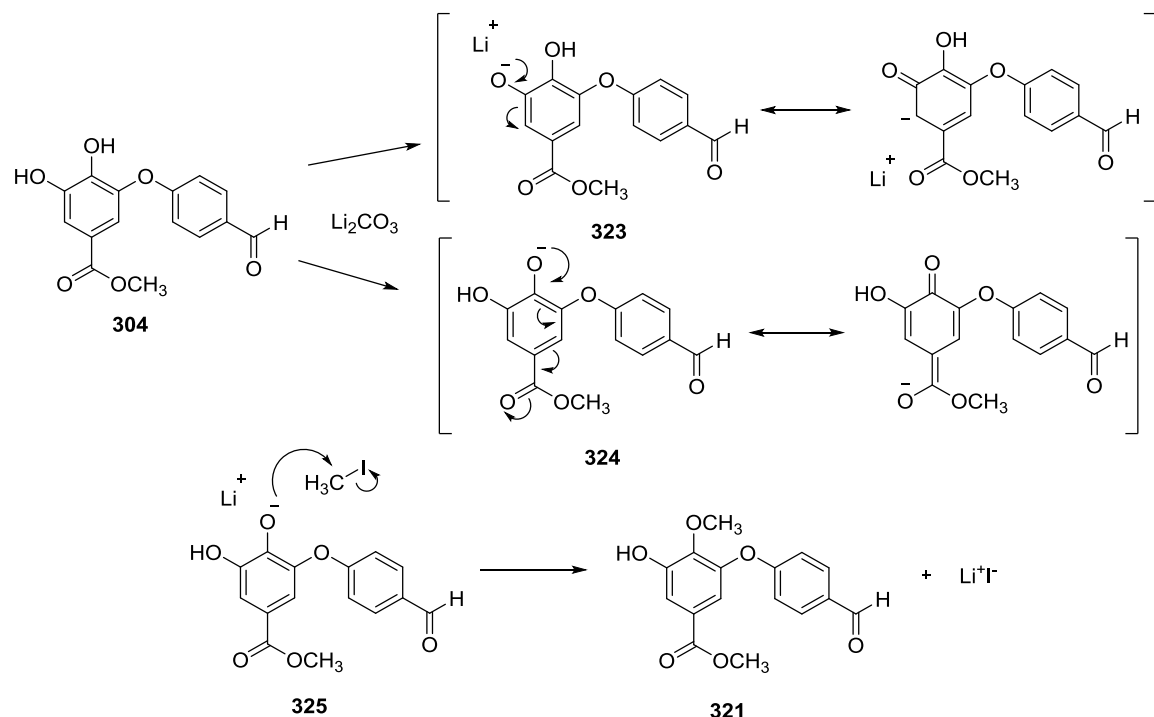
**Scheme 3.13** • *O*-Benzyl protection of the 1,2-diol functionality of diaryl ether **304**

Cleavage of a benzyl ether is generally carried out *via* hydrogenation in the presence of a catalytic amount of palladium on carbon.<sup>185</sup> In the case of diaryl ether **320** it is unlikely that any chemoselectivity would be shown, and both benzyl groups would be removed simultaneously under these conditions. To achieve a chemoselective deprotection, two protecting groups of differing reactivity were required. The 4-hydroxyl group (*para* to the methyl ester) of compound **304** is present in the aglycon of orienticin C (Chapter 1, Figure 1.2) and may remain protected until the end of the synthesis. In their 1999 synthesis of vancomycin, Boger *et al.* chose to install a methyl ether at the 4-hydroxyl position; a highly robust group which was removed only by a global demethylation in the final stages of the synthesis using aluminium tribromide and ethanethiol.<sup>13</sup> Following a procedure by Nishiyama *et al.*,<sup>186</sup> the reaction of compound **304** with one equivalent of lithium carbonate and one equivalent of iodomethane in DMF chemoselectively protected the 4-hydroxy group, affording compound **321** in a 71% yield (Scheme 3.14).



**Scheme 3.14** • Phenolic hydroxyl protection of **304** as i) methyl ether **321** and ii) TBDPS ether **322**

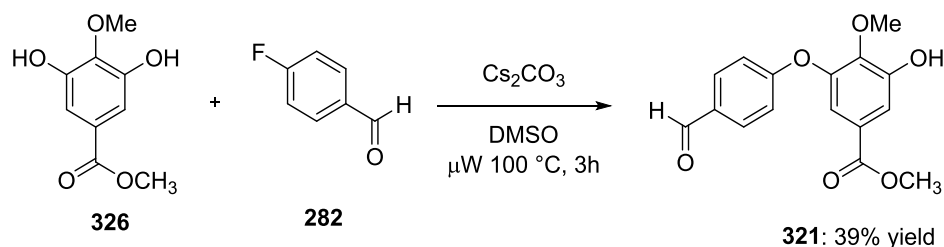
The chemoselectivity of this reaction is likely to be due to the influence of the electron withdrawing methyl ester on the acidity of the hydroxyl groups of compound **304**. Deprotonation by lithium carbonate at the more acidic 4-hydroxy position on **304** results in anion **323** which is stabilised by conjugation with the ester group *para* to the phenoxide (Scheme 3.15). By contrast, deprotonation at the 3-hydroxy position of **323** is not stabilised by the ester, resulting in a higher pKa. As only one equivalent of base was been added, anion **323** will be the major deprotonated species and will further react with iodomethane *via* an S<sub>N</sub>2 mechanism to generate compound **321**.



**Scheme 3.15** • Mechanism of the S<sub>N</sub>2 nucleophilic substitution of iodomethane with diaryl ether **304**

To confirm that the methyl ether was located *para* to the methyl ester, a second reaction was carried out, in which methyl 3,5-dihydroxy-4-methoxybenzoate **326**<sup>38</sup> was coupled

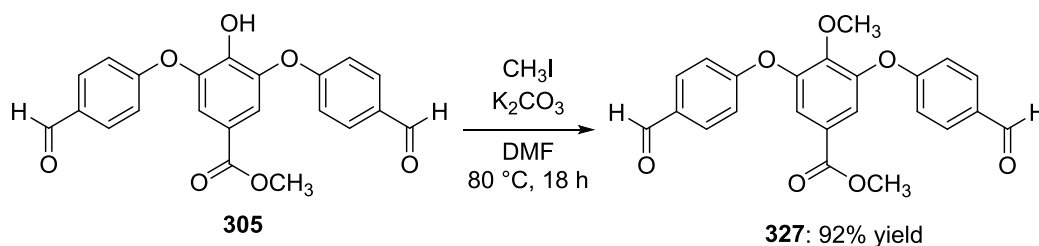
with one equivalent of 4-fluorobenzaldehyde **282** under the  $S_NAr$  reaction conditions described in Section 3.2.1 (Scheme 3.16). The  $^1H$ - and  $^{13}C$ -NMR spectra of the resulting product matched those of compound **321** obtained by the alternative route illustrated by Scheme 3.14.



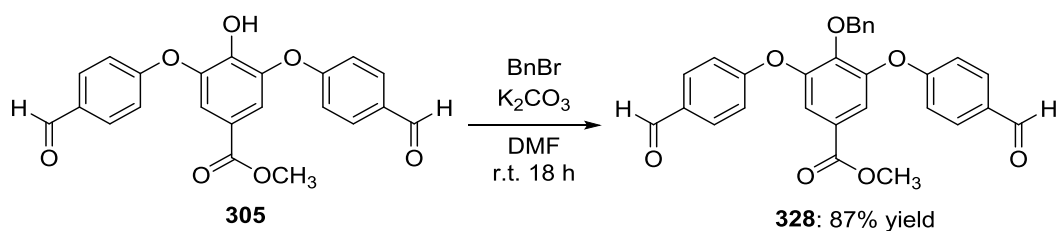
**Scheme 3.16** •  $S_NAr$  reaction of 4-fluorobenzaldehyde **282** with methyl 3,5-dihydroxy-4-methoxybenzoate **326**

A *tert*-butyldiphenylsilyl (TBDPS) group was chosen for protection of the remaining phenolic hydroxyl of compound **321**. More robust than the trimethyl silyl (TMS) ether group, aryl TBDPS ethers are stable towards weak acid, such as 1 M hydrochloric acid at room temperature, and can be selectively deprotected using TBAF<sup>187</sup> or DBU.<sup>188</sup> Following a procedure by Coelho *et al.*, compound **321** was added to a mixture of *tert*-butyldiphenylsilyl chloride (1.1 equiv.) and imidazole (2.2 equiv.) in DMF at room temperature (Scheme 3.14).<sup>189</sup> After 18 hours, TBDPS ether **322** was obtained in a moderate 57% yield after flash column chromatography. The yield of **322** is comparable to those reported by Coelho *et al.*, however it has since been found that the addition of 3 equivalents of iodine dramatically accelerates the reaction between aryl alcohols and TBDPS-Cl by the formation of a polyhalide  $I_2Cl^-$  anion, so there is potential to reduce the reaction time of the protection described in Scheme 3.14.<sup>190</sup>

The methyl ether and benzyl ether protections described in Section 3.3.1 above were also applied to triaryl biether **305** in excellent yields of 92% and 87% respectively (Schemes 3.17 and 3.18).



**Scheme 3.17** • Reaction of triaryl diether **305** with iodomethane to form methyl ether **327**

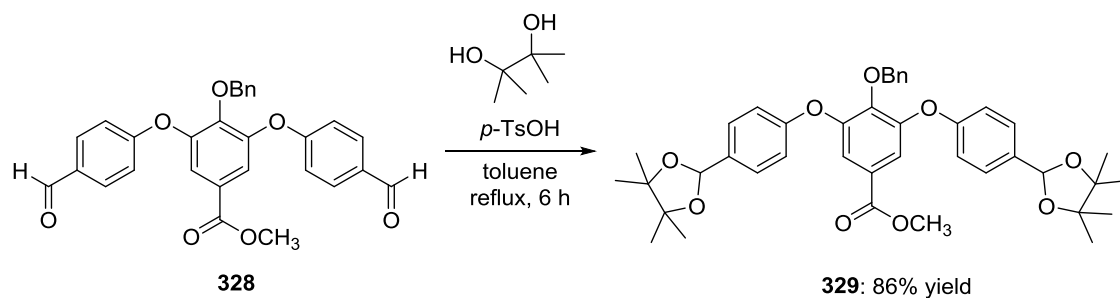


**Scheme 3.18 • Reaction of phenoxide **305** with benzyl bromide to form benzyl ether **328****

The benzyl ether was ultimately chosen as a convenient group to both synthesise and cleave later in the synthesis, as benzyl ethers can be efficiently removed by hydrogenation with palladium on carbon but are stable towards standard reduction and oxidation reactions as well as the mildly acidic conditions of the aza-Darzens aziridination reaction.<sup>37</sup>

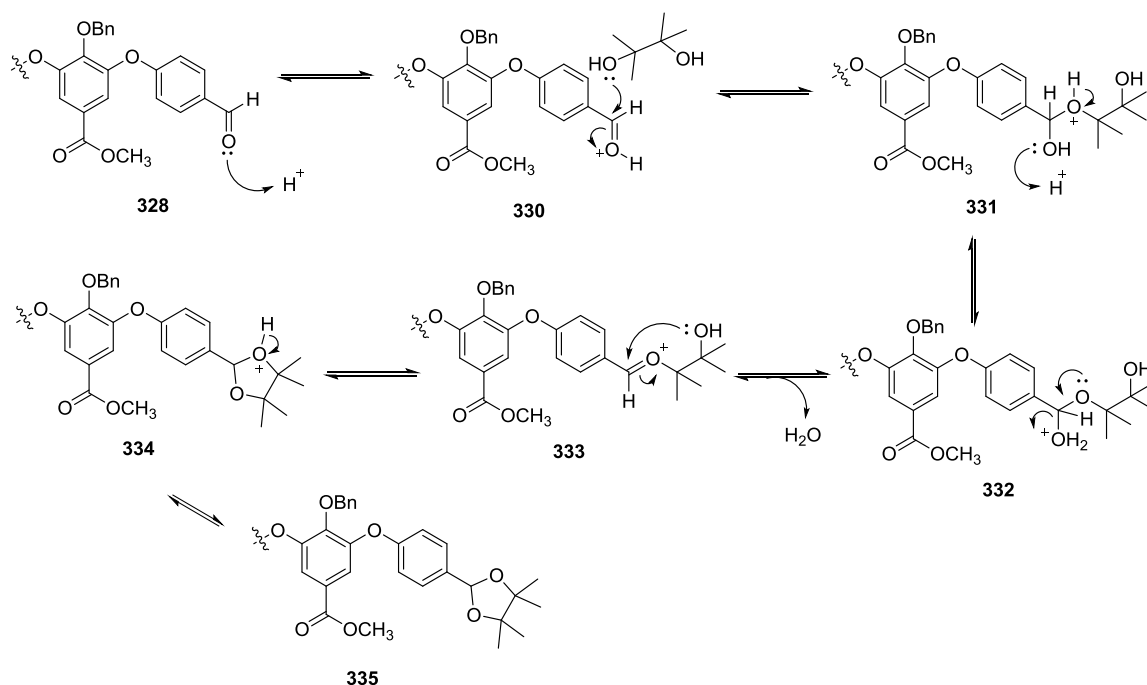
As it was decided to focus initially on conversion of the methyl ester of compound **328** to an  $\alpha$ -amino acid (analogous to the core ring **D** of orienticin C), it was necessary to protect the aldehyde functionality of **328**, which would be incompatible with subsequent reduction and oxidation steps. The acetal moiety is a widely used protecting group of the aldehyde carbonyl, and can be synthesised by the acid-catalysed reaction of an aldehyde with an alcohol, as discussed previously in this section.

Dimethyl acetals can be readily synthesised by the reaction of aldehydes with trimethyl orthoformate in methanol with a catalytic amount of *p*-toluenesulfonic acid.<sup>191</sup> However, they are prone to hydrolysis during aqueous reaction work-ups, and can be challenging to purify using flash column chromatography due to the slightly acidic nature of silica gel.<sup>192</sup> Cyclic acetals tend to be more stable towards hydrolysis than acyclic acetals, for entropic reasons (two compounds are obtained by hydrolysis of a cyclic acetal compared with three compounds for an acyclic acetal), and steric hindrance in the case of substituted cyclic acetals, which increases resistance to nucleophilic attack.<sup>193</sup>



**Scheme 3.19 • Protection of dialdehyde **328** as pinacol acetal **329****

Following a similar procedure originally reported by Ovaa *et al.*,<sup>194</sup> compound **328** reacted with 2.3 equivalents of pinacol in refluxing toluene in the presence of 0.5 mol% *p*-toluenesulfonic acid to afford the *bis*-acetal **329** in an 86% yield (Scheme 3.19). A Dean-Stark apparatus was used to collect the water produced in the reaction. The formation of a cyclic acetal is accelerated by the kinetically favourable intramolecular ring-closing step (intermediate **333**, Scheme 3.20). In the case of pinacol, the *gem*-dimethyl groups may aid the cyclisation step due to the Thorpe-Ingold effect, by which the size of the methyl substituents compresses the angle of the neighbouring substituents, bringing the nucleophilic alcohol group into closer proximity to the electrophilic carbon reaction site.<sup>195</sup>

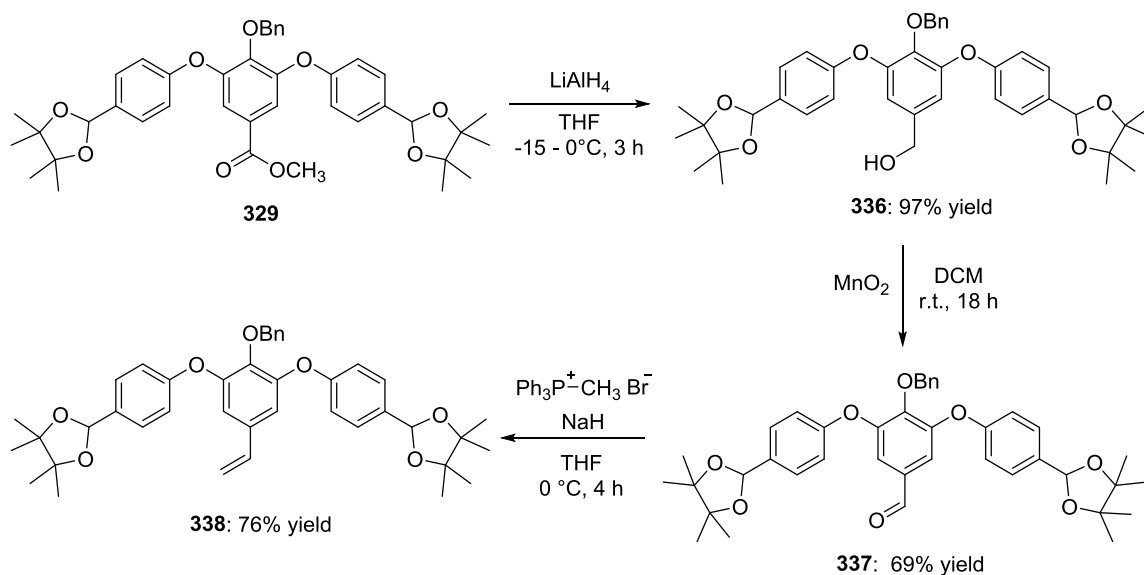


**Scheme 3.20** • Mechanism of acetal condensation between dialdehyde **328** and pinacol

With the acetal protecting groups in place, methyl ester **329** was reduced to primary alcohol **336** using 2.5 equivalents of lithium aluminium hydride in an excellent 97% yield following a similar procedure reported by Percec *et al.*<sup>196</sup> Oxidation of the alcohol **336** proceeded smoothly using 20 equivalents of activated manganese(II) dioxide to afford aldehyde **337** in a moderate yield of 69% after 18 hours at room temperature. The reduction of a methyl ester to an aldehyde has previously been achieved in one step using diisobutylaluminium hydride (DIBAL-H), which would be an advantage in this synthesis.<sup>197</sup> However, significant over-reduction of the ester to alcohol **336** was observed

by thin layer chromatography during the reaction between **329** and one equivalent of DIBAL-H at  $-78\text{ }^{\circ}\text{C}$ . This route was therefore disregarded in favour of the less efficient but more reliable two-step process shown in Scheme 3.21.

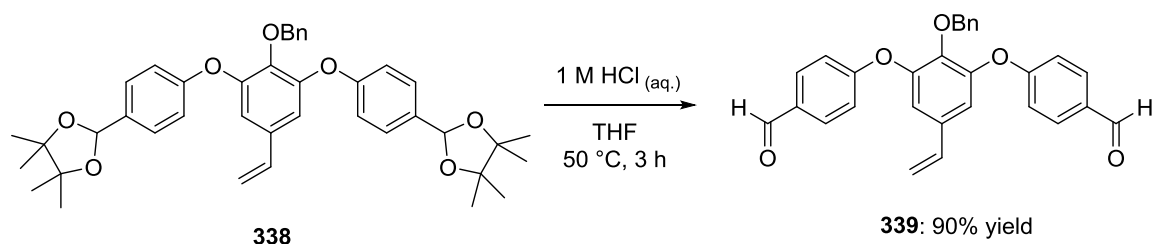
The Wittig reaction of aldehyde **337** to form styrene **338** was carried out using standard conditions, in which 3 equivalents of sodium hydride reacted with an equimolar amount of methyltriphenylphosphonium bromide (initially at a reaction temperature of  $-25\text{ }^{\circ}\text{C}$ ) to form a phosphorus ylide which then reacted with aldehyde **337** to afford styrene **338** in a 51% yield.



**Scheme 3.21** • Functional group interconversions from ester **329** to aldehyde **337** and subsequent Wittig olefination

The initially disappointing yield and slow rate of this reaction was thought to be a result of the low temperature employed. Indeed, maintaining the reaction temperature at  $0\text{ }^{\circ}\text{C}$  afforded compound **338** in a much improved 76% yield. Cyclic acetals such as those on **338** can be challenging to remove, often requiring strongly acidic conditions (10% aqueous hydrochloric acid / THF<sup>198</sup> or 50% aqueous trifluoroacetic acid<sup>199</sup>). In order to be sure that the pinacol acetals of **338** could be hydrolysed when required, a test deprotection was carried out (Scheme 3.22). The deprotection of a pinacol acetal in the presence of a 1,2-disubstituted alkene with similar success has been reported on multiple occasions in the literature, with no reports of alkene polymerisation.<sup>200</sup>





**Scheme 3.22** • Test hydrolysis of pinacol acetal **338** using 1 M aqueous hydrochloric acid in THF

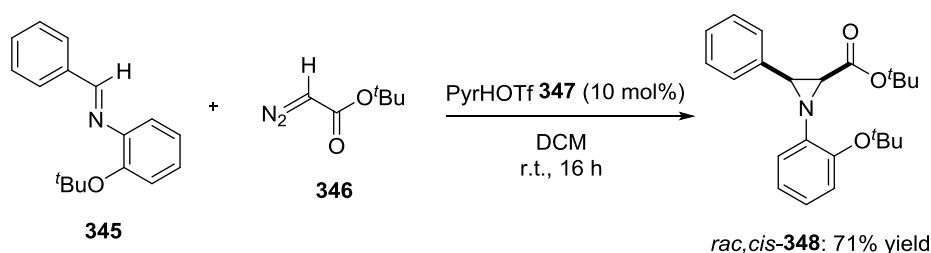
Following a procedure adapted from Eichen *et al.*,<sup>201</sup> acetal **338** was dissolved in a 1:1 homogeneous mixture of tetrahydrofuran and 1 M aqueous hydrochloric acid. The reaction was monitored regularly by thin layer chromatography. After stirring at room temperature for 2 hours no change was observed. The reaction temperature was increased to 50 °C, and after 3 hours the starting material was completely consumed. <sup>1</sup>H-NMR analysis of the impure reaction mixture indicated that the pinacol deprotection was complete. A small amount of the corresponding mono-aldehyde was observed by <sup>1</sup>H-NMR (400 MHz) but was not isolated in this case. Dialdehyde **339** was obtained in an excellent 90% yield after purification by flash column chromatography on silica gel.

## CHAPTER FOUR

Synthesis of peptide aziridines *via* the aza-Darzens reaction

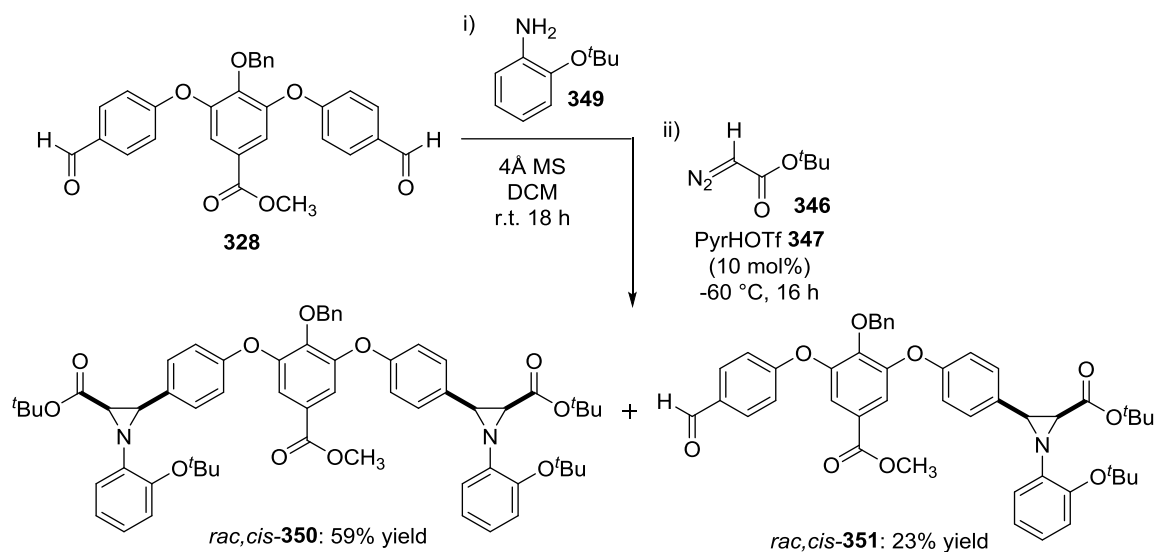
## 4.1 Racemic aza-Darzens aziridination of biaryl and triaryl ether aldehydes

Initial attempts to synthesise *N*-aryl aziridines from the triaryl and biaryl ether aldehydes described in chapter 2 were based on racemic organocatalytic methodology previously established within the Bew group (Scheme 4.1).<sup>202</sup> The reaction between imine **345** and *tert*-butyl diazoacetate (TBDA) **346** was catalysed by 10 mol% of pyridinium triflate **347** to afford racemic *cis*-aziridine **348** in a 71% yield. This reaction was also reported as a one-pot procedure from benzaldehyde, with the addition of 4Å molecular sieves to facilitate the initial imine condensation.



**Scheme 4.1** • Pyridinium triflate-catalysed aza-Darzens synthesis of racemic *cis*-aziridine **348** reported by Bew *et al.*, 2009

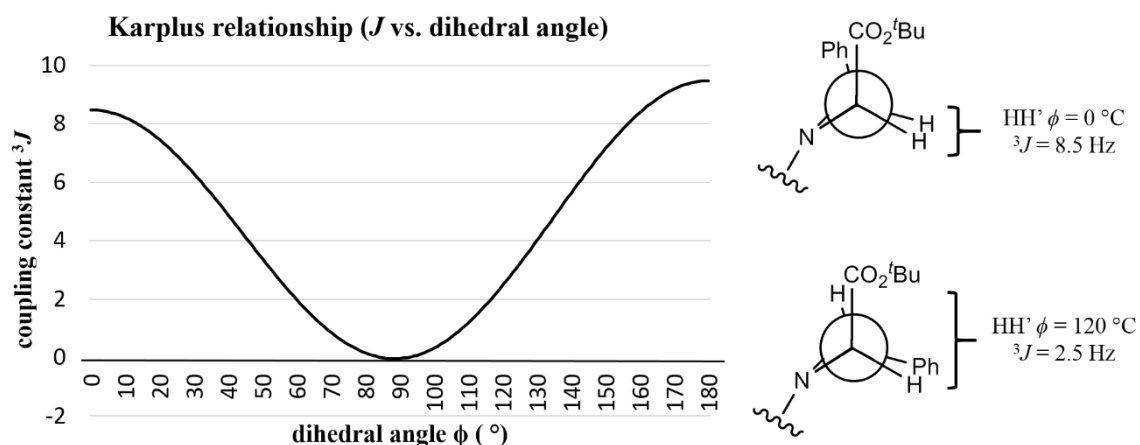
Applying this methodology to the triaryl biether system, a three-component one-pot reaction between aldehyde **328**, 2-*tert*-butoxyaniline **349** and *tert*-butyl diazoacetate **346** was catalysed by pyridinium triflate **347** (10 mol%) at -60 °C, affording *bis*-aziridine *cis*-**350** in a 59% yield. Byproduct racemic, *cis*-**351** was isolated in a 23% yield (Scheme 4.2).



**Scheme 4.2** • One-pot imine condensation / racemic aza-Darzens aziridination reaction of aldehyde **328** catalysed by pyridinium triflate **347**

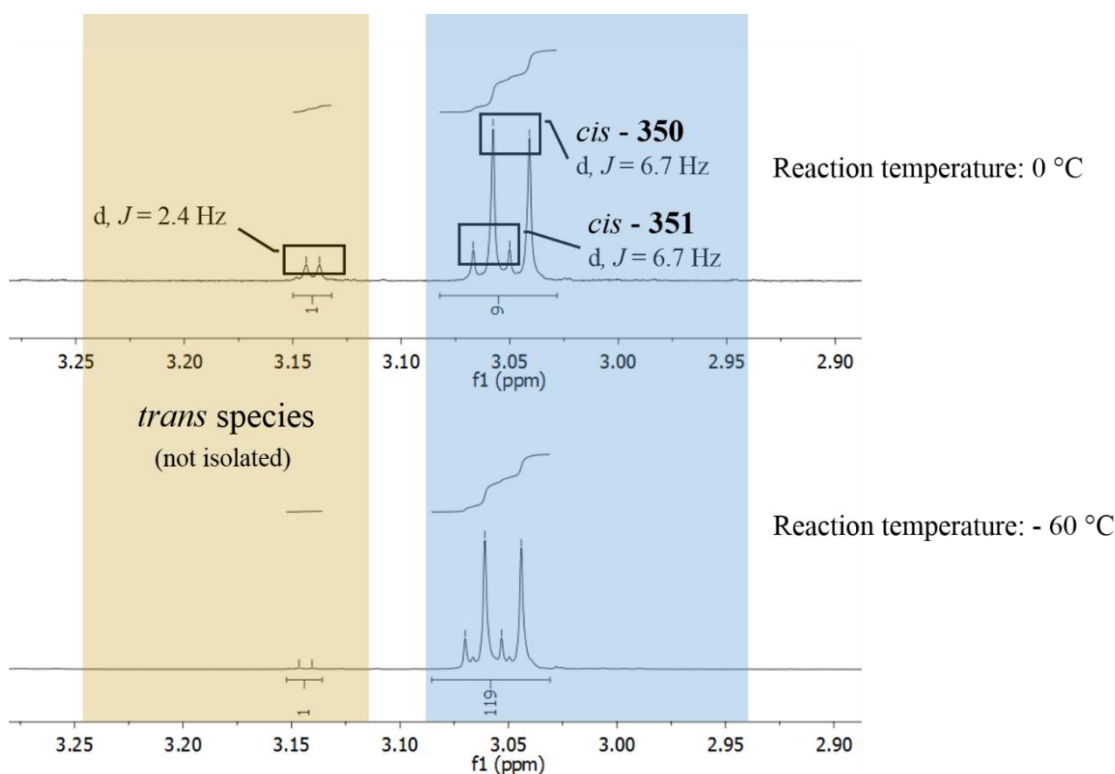
The one-pot protocol shown in Scheme 4.2 is a reaction in two parts; first the imine condensation between aldehyde **328** and 2-*tert*-butoxyaniline **349**, which took place at room temperature. Only 1.95 equivalents of **349** were added, to ensure complete consumption of the amine, which would otherwise be protonated by the pyridinium triflate catalyst and slow down the reaction. For the second part, the aza-Darzens reaction of the activated imine with a diazo compound, catalyst pyridinium triflate (**347**) was added at room temperature, and the sealed vial was cooled to -60 °C before the addition of *tert*-butyl diazoacetate **346**.

$C_{2,3}$ -disubstituted aziridines can be identified as their *cis* or *trans* diastereomer by their  $^1\text{H}$ -NMR doublet coupling constant.<sup>203</sup> The Karplus equation provides a relationship between the three-bond coupling constant ( $^3J$ ) and the H-C-C-H dihedral angle (Figure 4.1).<sup>204</sup> In the *cis*-aziridine, the protons are eclipsed, where the dihedral angle  $\phi = 0^\circ$ , therefore coupling constant  $^3J = \sim 7\text{--}11\text{ Hz}$ . In the *trans*-aziridine, the dihedral angle  $\phi = 120^\circ$ , giving a coupling constant of  $^3J = \sim 2\text{--}4\text{ Hz}$ .



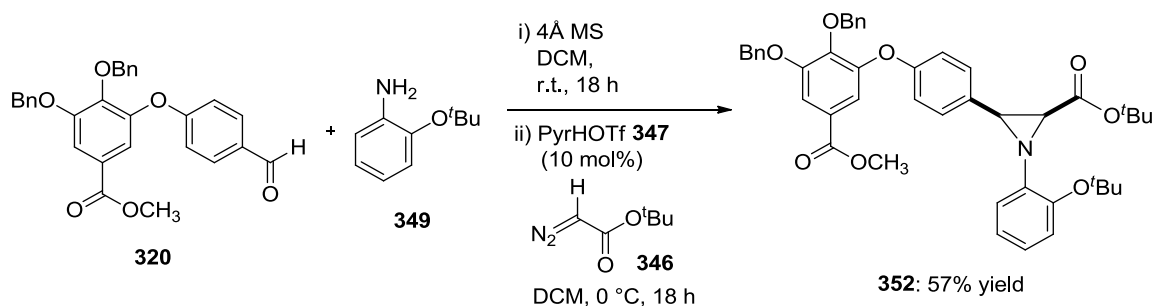
**Figure 4.1** • The Karplus relationship applied to *cis* and *trans*  $C_{2,3}$ -disubstituted aziridines

Compounds **350** and **351** isolated from the reaction in Scheme 4.2 have aziridine C-H doublets with coupling constants of 6.7 Hz, which is consistent with a *cis* configuration. An overall diastereoselectivity of  $>99:1$  (*cis:trans*) was observed by  $^1\text{H}$ -NMR analysis of the impure reaction mixture (Figure 4.2). When the same reaction was conducted at room temperature rather than -60 °C, the overall *cis/trans* ratio dropped to 90:10, although the ratio of *mono:bis* aziridines (**351:350**) remained approximately the same.



**Figure 4.2** • Partial <sup>1</sup>H-NMR spectra of the impure reaction mixtures in the formation of aziridines **350** and **351**

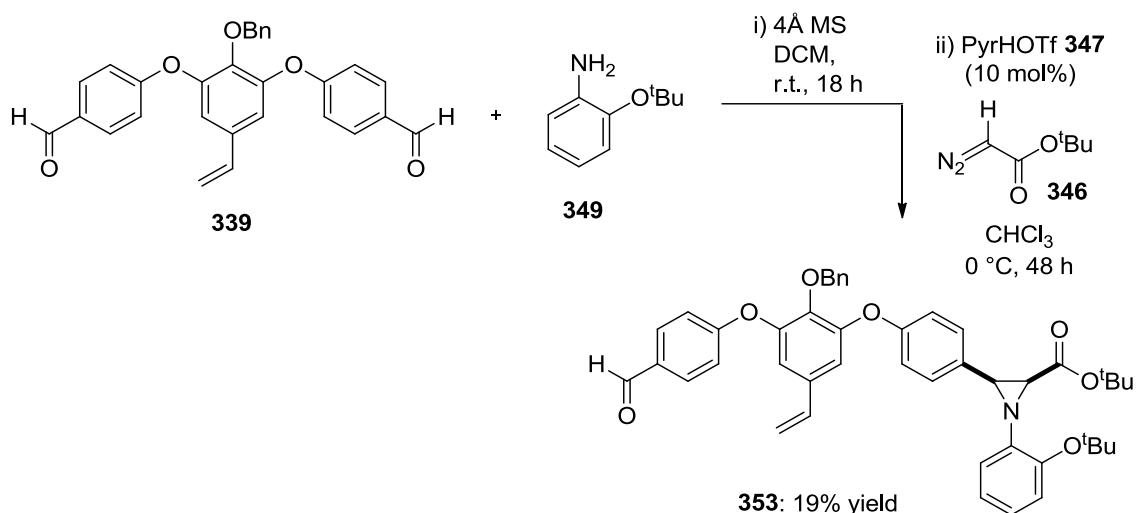
The reaction conditions outlined in Scheme 4.2 were applied to biaryl ether aldehyde **320** with similar success (Scheme 4.3). It was found that the one-pot imine condensation / racemic aza-Darzens aziridination reaction between **320**, 2-*tert*-butoxyaniline **349** and TBDA **346** could be carried out at 0 °C rather than -60 °C, affording racemic *cis*-aziridine **352** in a moderate 57% yield. The *trans* aziridine diastereomer was not observed in this case.



**Scheme 4.3** • One-pot imine condensation / racemic aza-Darzens reaction of aldehyde **320** with 2-*tert*-butoxyaniline **349** and *tert*-butyl diazoacetate **346**

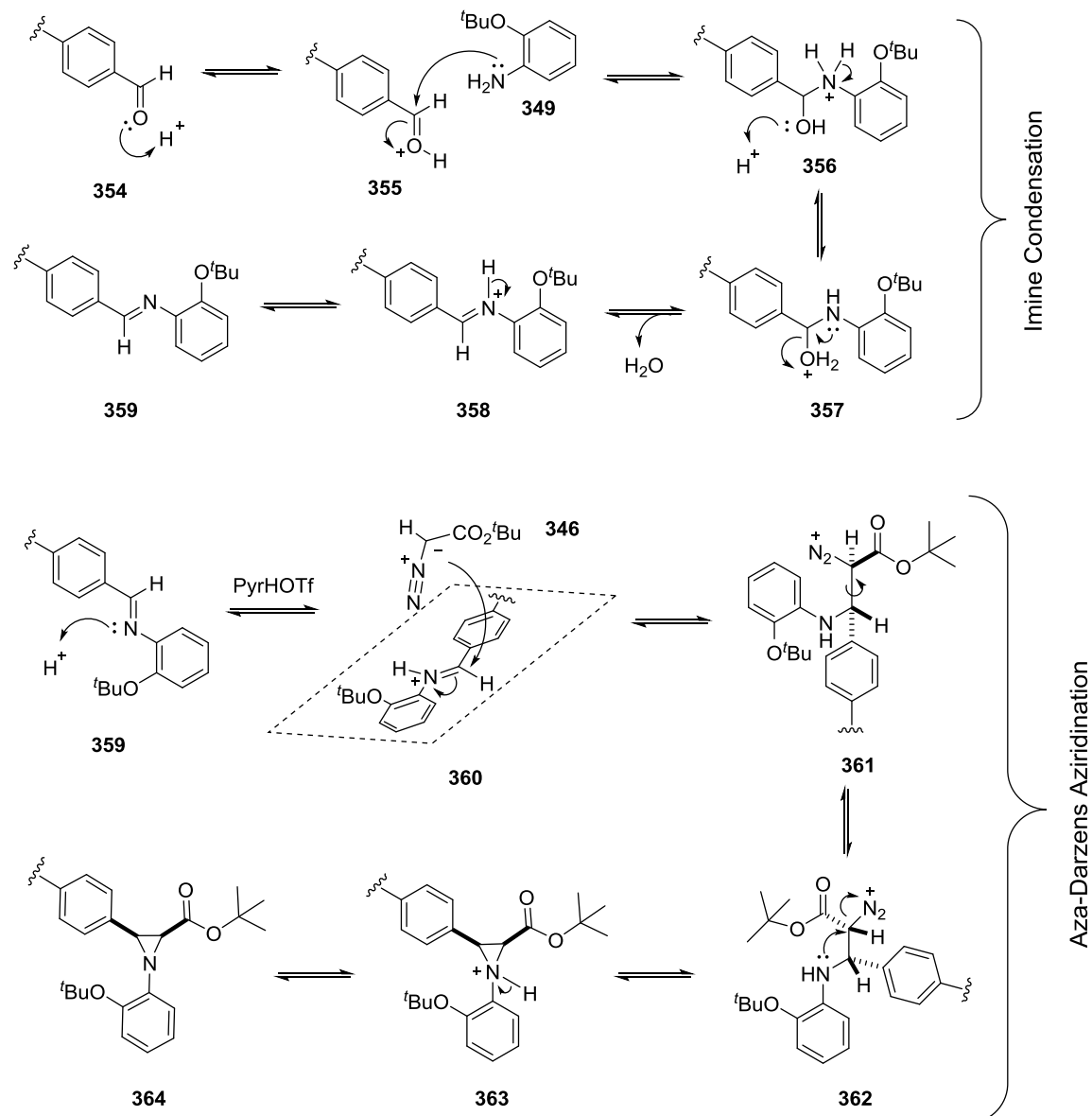
Attempting to carry out a selective mono-aziridination of aldehyde **339** using one equivalent of *tert*-butyl diazoacetate **346** proved more problematic (Scheme 4.4). *Cis*-

aziridine **353** was isolated in a poor 19% yield after purification by flash column chromatography, which is unlikely to reflect the true outcome of the reaction, as compound **353** was very difficult to separate from 2-*tert*-butoxyaniline **349** which was present in the impure reaction mixture. 2-*tert*-Butoxyaniline **349** was likely to have been produced by hydrolysis of the unreacted imine intermediate upon removal of the 4Å molecular sieves by filtration, or during the flash column chromatography itself.



**Scheme 4.4 •** One-pot imine condensation / racemic aza-Darzens reaction of aldehyde **339** with 2-*tert*-butoxyaniline **349** and *tert*-butyl diazoacetate **346**

The *cis*-selectivity of the racemic pyridinium triflate-catalysed aza-Darzens reactions described above are consistent with previous findings by the Bew group.<sup>202</sup> Wulff *et al.* have put forth a number of mechanistic explanations for this selectivity in relation to their VANOL/VAPOL-boroxinate catalyst.<sup>244</sup> With regard to the pyridinium triflate-catalysed reactions described above, a possible mechanism is proposed in Scheme 4.5. Aldehyde **354** first reacts with 2-*tert*-butoxyaniline **349** in a condensation reaction to form imine **359** *in situ*. On the addition of pyridinium triflate **347**, imine **359** is in equilibrium with protonated species **360**, which now is activated towards attack at the electrophilic sp<sup>2</sup>-hybridised carbon. Due to the difference in pK<sub>a</sub> of the imine (pK<sub>a</sub> around 7-8)<sup>205</sup> and pyridinium triflate **347** (pK<sub>a</sub> = 5.2),<sup>206</sup> the equilibrium lies towards the protonated imine species **358**. Diazoacetate **346** is nucleophilic at the –CHN<sub>2</sub> carbon due to resonance of the diazocarbonyl group,<sup>207</sup> and can attack either the top or bottom face of the imine on **360**.



**Scheme 4.5** • Proposed mechanism of the one-pot pyridinium triflate-catalysed aza-Darzens aziridination reaction

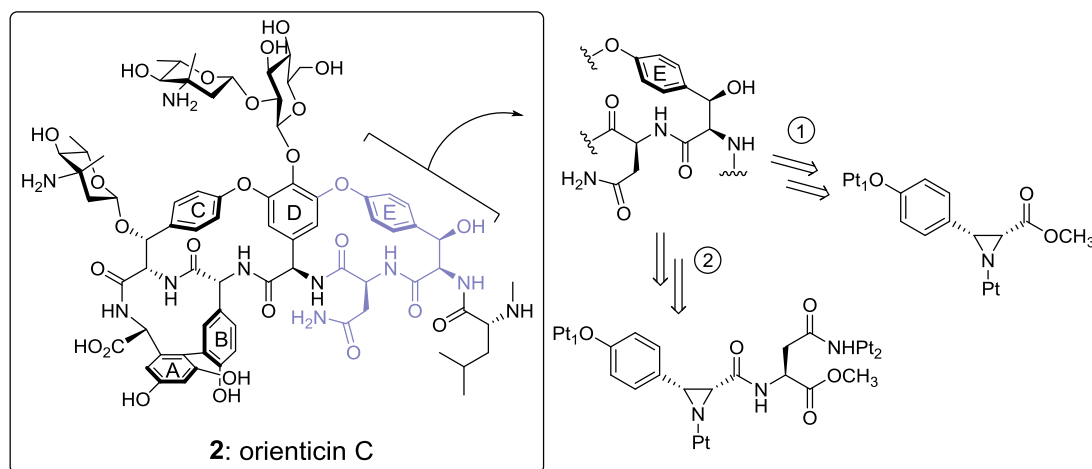
The orientation of the diazoacetate relative to the imine as it approaches defines the stereochemistry of the chiral centre in intermediate **361** produced by C-C bond formation. The approach of diazoacetate **346** to imine **360** is drawn such that the diazo group is in close proximity to the imine bond, which is consistent with tentative evidence that the reaction may alternatively proceed *via* a concerted cycloaddition mechanism.<sup>208</sup> In intermediate **361** the bulky *tert*-butyl group occupies the least sterically hindered position relative to the phenyl group of the imine. The ring-closing step requires a rotation of the bond indicated in **361** so that the nitrogen lone pair overlaps with the empty  $\sigma^*$  orbital of

the electrophilic carbon in a “backside attack” mechanism. The  $-N_2^+$  group leaves irreversibly as nitrogen gas, observed as bubbles produced during the reaction.

Overall, the results of the racemic aza-Darzens aziridination reactions described in this section were encouraging; the triaryl biether aldehydes **328** and **339** and biaryl ether **320** all reacted successfully in a one-pot procedure. These reactions all produced the *cis*-aziridine and little or no *trans*-aziridine. The yields of the aziridination reaction were poor to moderate, however, mainly due to problems with purification. 2-*tert*-Butoxyaniline **349** and its decomposition products proved difficult to remove from the *cis*-aziridine by column chromatography. The 2-*tert*-butoxyphenyl group has been found to enhance the enantioselectivity of the non-racemic version of the organocatalytic aza-Darzens reaction catalysed by BINOL-derived triflamides.<sup>209</sup> However, there have so far been no reports of methods to cleave the 2-*tert*-butoxyphenyl group from an amine, making it an undesirable protecting group for this multi-step synthesis. Following these initial investigations it was clear that a higher yielding, more flexible, and crucially non-racemic aza-Darzens aziridination route was required.

#### 4.2 Remote asymmetric induction in the organocatalytic synthesis of peptide aziridines

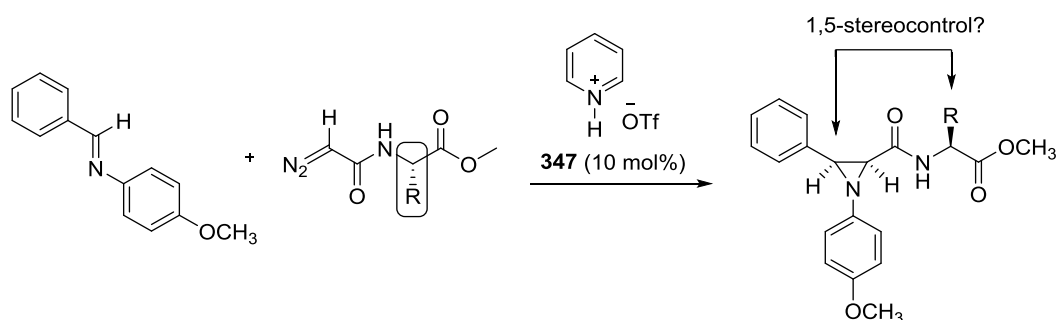
The initial approach to the synthesis of orienticin C described in this work involved the construction of (*S*)-phenylalanine derivative ring **E** as a protected  $\alpha$ -amino acid which would be subsequently deprotected by hydrolysis of the ester ready for peptide coupling with the asparagine residue of the peptide chain (Route 1, Figure 4.3).



**Figure 4.3** • Retrosynthetic analysis outlining the construction of the **E**-ring of orienticin C via a peptide aziridine



However, an approach involving the synthesis of a peptide aziridine (Route 2) would remove the need for a deprotection and peptide coupling step, making this route more efficient. The synthesis of *N*-aryl  $C_{2,3}$ -disubstituted  $\alpha$ -amino acid derived aziridines by aza-Darzens reaction of an imine with a diazopeptide has not yet been reported in the literature. Diazo substrates have so far been restricted to diazoacetates and simple phenyl diazoacetamides. It was anticipated that the reaction illustrated by Scheme 4.7 would be catalysed by achiral Brønsted acid pyridinium triflate **347** as in Section 4.1.

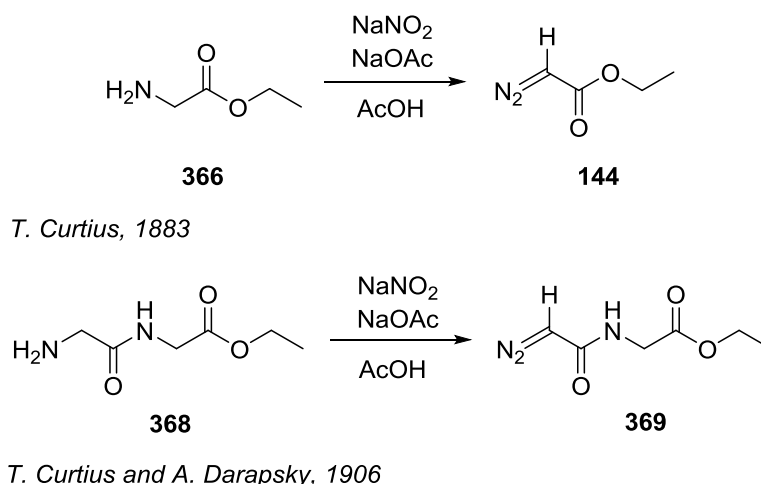


**Scheme 4.7** • General scheme for the pyridinium triflate-catalysed aza-Darzens reaction of an imine with a diazopeptide to afford a peptide-derived *cis*-aziridine

However, the influence of an  $\alpha$ -amino acid chiral centre in the diazoacetamide starting material may result in a diastereoselective reaction, due to a 1,5-asymmetric induction (Scheme 4.7). In order to investigate this hypothesis, a series of chiral non-racemic diazopeptides were required. Their synthesis and characterisation are described in Section 4.2.1.

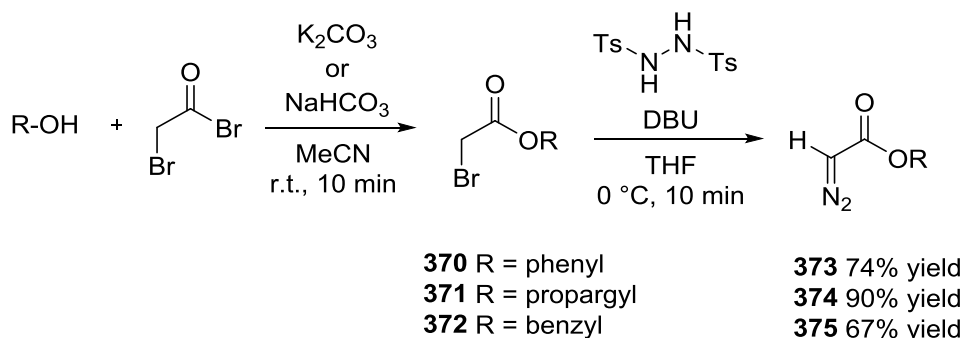
#### 4.2.1 Synthesis of diazopeptides using *N,N'*-ditosylhydrazine

$\alpha$ -Diazocarbonyl compounds have found a wide range of applications since the work of Theodor Curtius on their synthesis in the late 19<sup>th</sup> century (Scheme 4.8).<sup>210</sup> Diazopeptides exhibit biological activity in a number of areas, and notably they have been shown to display antibacterial<sup>211</sup> and anti-cancer properties.<sup>212</sup> Ethyl diazoacetate **144** was first synthesised by Curtius in 1883 by diazotisation of glycine methyl ester **366** in aqueous acid.<sup>210</sup> *N*-(Diazoacetamido)glycine ethyl ester **369** was subsequently synthesised from *N*-glycylglycine ethyl ester **368** employing the same conditions.<sup>213</sup> Despite the early synthesis of **369**, only a small number of diazopeptides have been reported, of which the majority are benzyl, benzoyl and methyl ester variants of *N*-(diazoacetamido)- glycine and phenylalanine.<sup>214</sup>

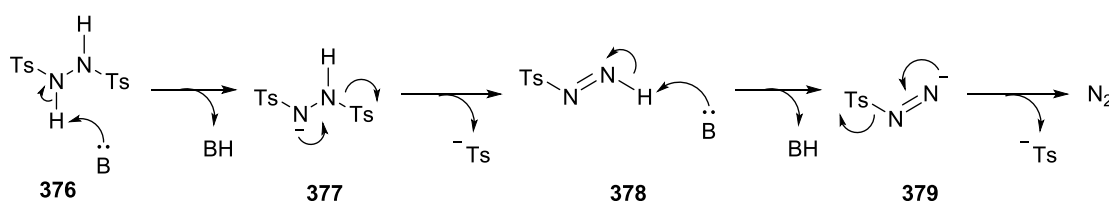


**Scheme 4.8** • Synthesis of ethyl diazoacetate **144** and *N*-(diazoacetamido)glycine ethyl ester **369** reported by Curtius *et al.*

In 2007, Fukuyama *et al.* reported the synthesis of diazoacetates from the corresponding alcohol in two steps using *N,N'*-ditosylhydrazine as the diazoacetylating reagent (Scheme 4.9).<sup>215</sup> This method represented a significant improvement on the conventional diazotisation route, affording a diverse range of phenyl, alkyl, allyl and benzyl diazoacetates in yields of 52-90%. *N,N'*-Ditosylhydrazine reacts with organic bases such as DBU and TMG according to the mechanism in Scheme 4.9 put forth by Ragnarsson *et al.* to afford nitrogen gas and two equivalents of a tosylate salt.<sup>216</sup>

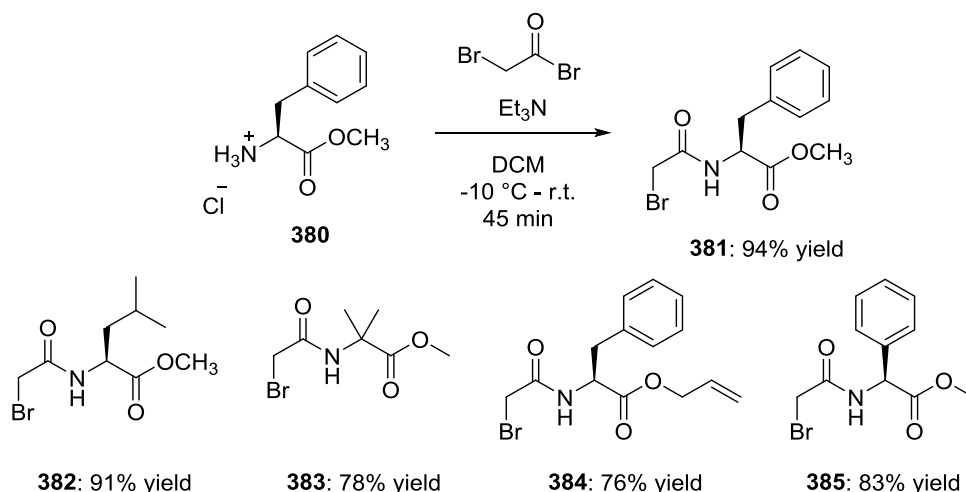


**Scheme 4.9** • Synthesis of diazoacetates reported by Fukuyama *et al.*



**Scheme 4.10** • Mechanism of reaction between *N,N'*-ditosylhydrazine **376** and a base (B), where B = DBU, TMG postulated by Ragnarsson and Grehn.

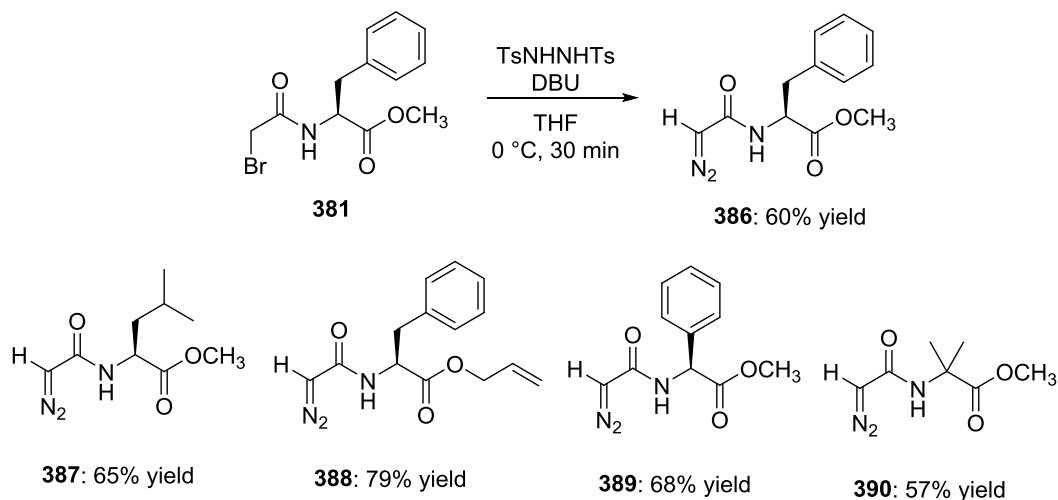
However, in the presence of an alkyl bromide, the deprotonated species **377** acts as a nucleophile, and a diazo compound is formed as the major product. In order to synthesise *N*-(diazooacetamido)-L-phenylalanine methyl ester **386** by the method reported by Fukuyama *et al.*, the corresponding bromoacetamide **381** was first made according to a procedure by Calorini *et al* (Scheme 4.11).<sup>217</sup>



**Scheme 4.11 • Synthesis of  $\alpha$ -amino acid bromoacetamides **381-385****

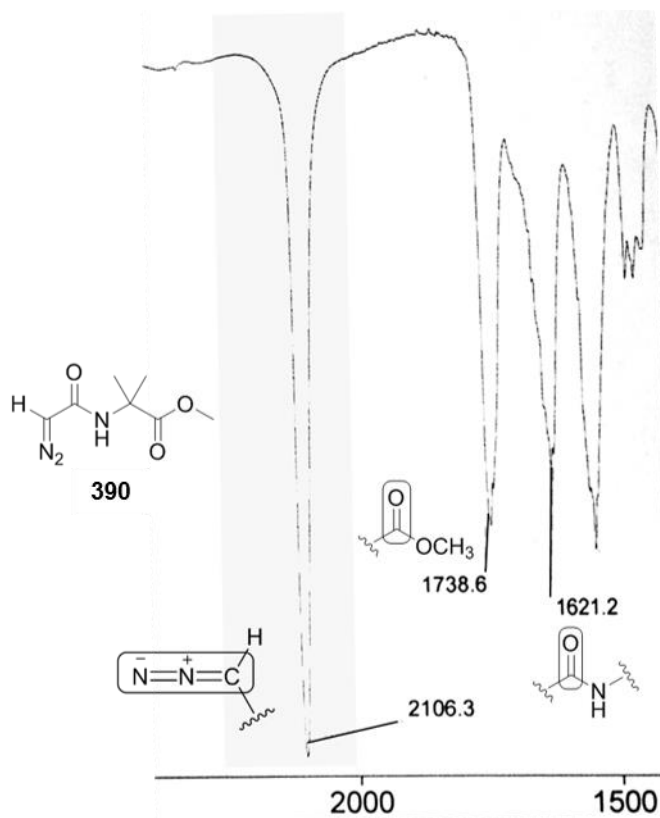
L-Phenylalanine methyl ester hydrochloride **380** reacted with one equivalent of triethylamine at room temperature to release the free amine *in situ* before the flask was cooled to -10 °C for the addition of one equivalent of bromoacetyl bromide and a further one equivalent of triethylamine to react with the HBr produced in the reaction. Gratifyingly, *N*-(bromoacetamido)-L-phenylalanine methyl ester **381** was obtained in an excellent 94% yield and could be used in the next step without further purification. These reaction conditions were applied to a further five  $\alpha$ -amino acids, affording compounds **382-385** in yields of 76-91%.  $\alpha$ -Amino acid bromoacetamides **381**, **382** and **385** are known compounds, and their physicochemical properties (<sup>1</sup>H-NMR, FT-IR, and MS) were consistent with those reported previously.<sup>218, 219, 220</sup>

The conversion of bromoacetamide **381** to *N*-(diazooacetamido)-L-phenylalanine methyl ester **386** proceeded smoothly at 0 °C in a 60% yield (Scheme 4.12). The product was isolated as a bright yellow solid, and the physicochemical data was consistent with that published for *rac*-**386** reported previously by Lowe *et al.* Diazopeptides **387-390** were also synthesised by this method in moderate yields of 57-79%.



**Scheme 4.12 • Synthesis of  $\alpha$ -amino acid diazoacetamides **386-390****

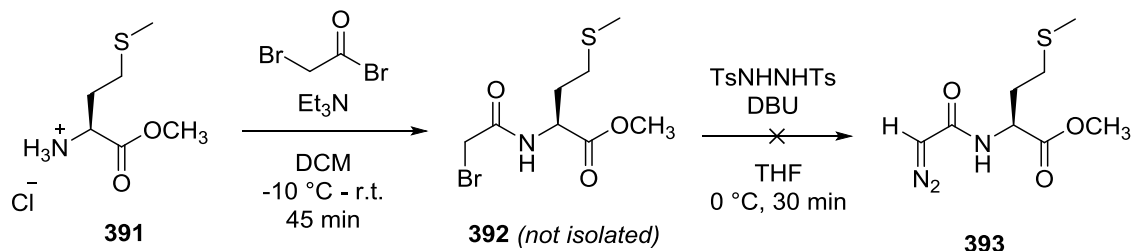
The striking yellow colour is common to compounds containing the diazo functional group, which also has a characteristic peak of strong intensity known as the “diazoband” at around  $2106\text{ cm}^{-1}$  in the FT-IR spectrum (Figure 4.3). This has been attributed to the effect of the  $\text{--C=N=N}$  cumulative double bond, as the stretching frequency of diazomethane in the gas phase is  $3712\text{ cm}^{-1}$ . Figure 4.3 also shows the ester and amide carbonyl stretch of diazopeptide **390** at  $1738.6$  and  $1621.2\text{ cm}^{-1}$  respectively.



**Figure 4.3 • FT-IR (thin film) spectrum of compound **390****

In the case of *N*-(diazooacetamido)-(*S*)-phenylalanine methyl ester **386**, which was reported previously by Lowe *et al.*, the specific rotation is comparable to the literature value:  $[\alpha]_D^{21} +175.0$  (c 1.0, CHCl<sub>3</sub>) *cf.*  $[\alpha]_D^{20} +186.0$  (c 1.0, CHCl<sub>3</sub>).<sup>221</sup>

Unfortunately, the Fukuyama diazoacetate synthesis described above could not be applied successfully to the synthesis of diazo peptide with side-chains bearing more reactive functional groups such as *N*-(diazooacetamido)-(*S*)-methionine methyl ester **393** (Scheme 4.13). A <sup>1</sup>H-NMR of the impure bromoacetamide **392** was obtained which appeared to show a successful reaction between (*S*)-methionine methyl ester hydrochloride **391** and bromoacetyl bromide to afford **392** as the major product.<sup>i</sup> However, this compound proved to be very unstable and could not be fully characterised. Consequently, an impure sample of **392** was submitted to the Fukuyama reaction conditions (*N,N'*-ditosylhydrazine / DBU) immediately after workup. The impure <sup>1</sup>H-NMR of diazo peptide **393** contained no peaks that could be identified as corresponding either to the starting material **392** or the product **393**. In order to obtain a diazo peptide with a methionine side-chain such as **393**, an alternative method of synthesis was investigated, which is described in section 4.2.2.



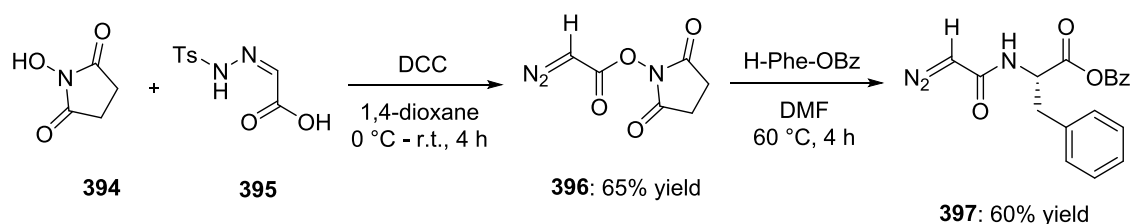
**Scheme 4.13** • Attempted synthesis of *N*-(diazooacetamido)-(*S*)-methionine methyl ester **393**

#### 4.2.2 Synthesis of $\alpha$ -amino acid diazo peptides using succinimidyl diazoacetate

Succinimidyl diazoacetate **396** was first synthesised in 1993 by Badet *et al.* as a convenient and versatile reagent for diazoacylation.<sup>222</sup> The Steiglich esterification of *N*-hydroxysuccinimide **394** with glyoxylic acid tosylhydrazine **395** using DCC in 1,4-dioxane afforded succinimidyl diazoacetate **396** in a reported yield of 65%. Compound **396** reacted with a range of aliphatic and aromatic amine nucleophiles, displacing *N*-hydroxysuccinimide to afford the corresponding *N*-diazo peptides in yields of 30-98%. A

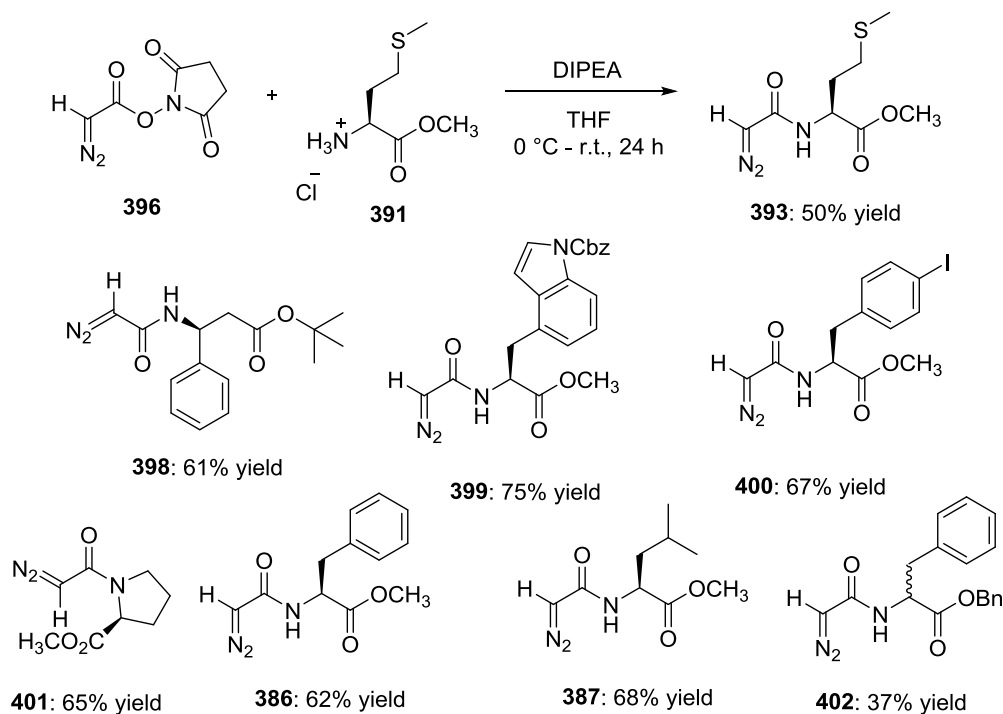
<sup>i</sup> Attempted synthesis of **393** (Scheme 4.13) carried out by Miss Haseena Seylani, BSc Chemistry final year dissertation (University of East Anglia)

number of novel *N*-diazopeptides were reported, including *N*-diazacetamido-(*S*)-phenylalanine benzoyl ester **397**.



**Scheme 4.14** • Synthesis of succinimidyl diazoacetate **396** and *N*-(diazacetamido)-(*S*)-phenylalanine benzoyl ester **397** by Badet *et al.*

The yield of succinimidyl diazoacetate **396** reported by Badet proved challenging to reproduce on a large (5-10 g) scale, partly due to the difficulty of removing unreacted DCC and the byproduct DCU from the product by column chromatography on silica gel. A 47% yield of **396** was the highest achieved. The reaction of compound **396** with (*S*)-methionine methyl ester hydrochloride **391** was carried out in THF at room temperature with three equivalents of Hünig's base (ethyl diisopropylamine or DIPEA), to afford **393** in 50% yield (Scheme 4.15).



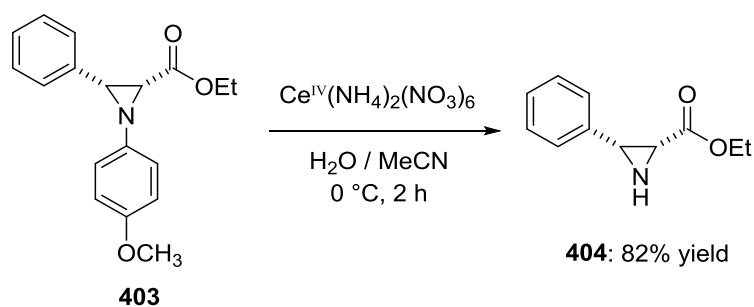
**Scheme 4.15** • Synthesis of amino acid diazoacetamides **393**, **386**, **387** and **398-402** using succinimidyl diazoacetate **396**

This method was used to synthesise novel *N*-(diazooacetamido)- $\alpha$ -amino acids **238-240** in moderate to good yields of 65-75%. The  $\beta$ -amino acid diazoacetamide **237** was obtained in a 61% yield from the commercially available free amine *tert*-butyl (3*S*)-3-amino-3-phenylpropanoate.

The poor yield of *N*-(diazooacetamido)-(*R,S*)-phenylalanine benzyl ester **402** can be explained by problems with purification. Overall the reaction was consistently reliable, with  $\alpha$ -amino acid diazopeptides **386** and **387** obtained in similar yields to those observed using the *N,N'*-ditosylhydrazine method described in Section 3.2.2. The disadvantages of the succinimidyl diazoacetate (**396**) route are the long reaction times (<24 hours) and the low yield of the **396** itself, which invariably required more than one purification by column chromatography following the DCC-mediated esterification (Scheme 4.14).

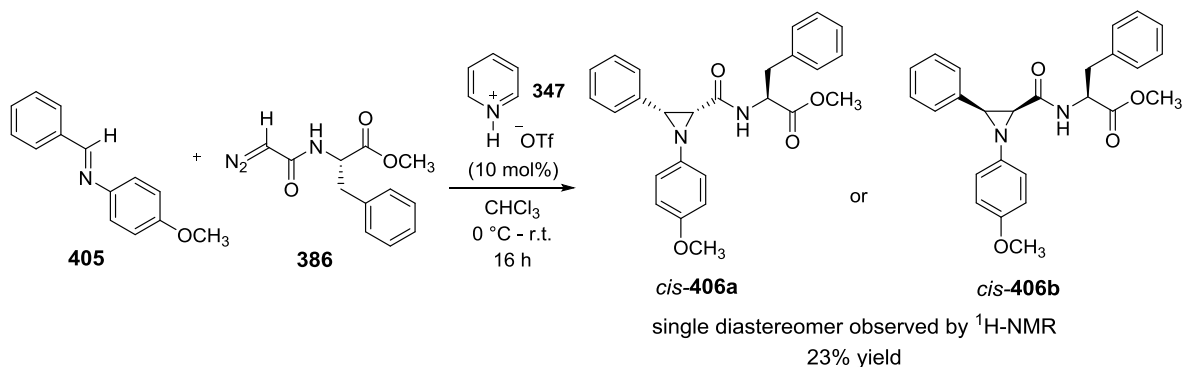
#### 4.2.3 Asymmetric organocatalytic aza-Darzens aziridination of non-chiral *N*-aryl imines with $\alpha$ -amino acid diazopeptides

*N*-Benzylidene-4-methoxyaniline **405** was chosen as the achiral imine substrate for our initial investigations into the asymmetric synthesis of peptide aziridines (Scheme 4.17). Compound **405** has previously been found by the Bew group to react successfully with ethyl diazoacetate **144** to afford a *cis*-aziridine.<sup>223</sup> Mayer *et al.* have established that the *p*-methoxyphenyl nitrogen protecting group can be removed with relative ease using cerium(IV) ammonium nitrate (CAN) (Scheme 4.16).<sup>224</sup>



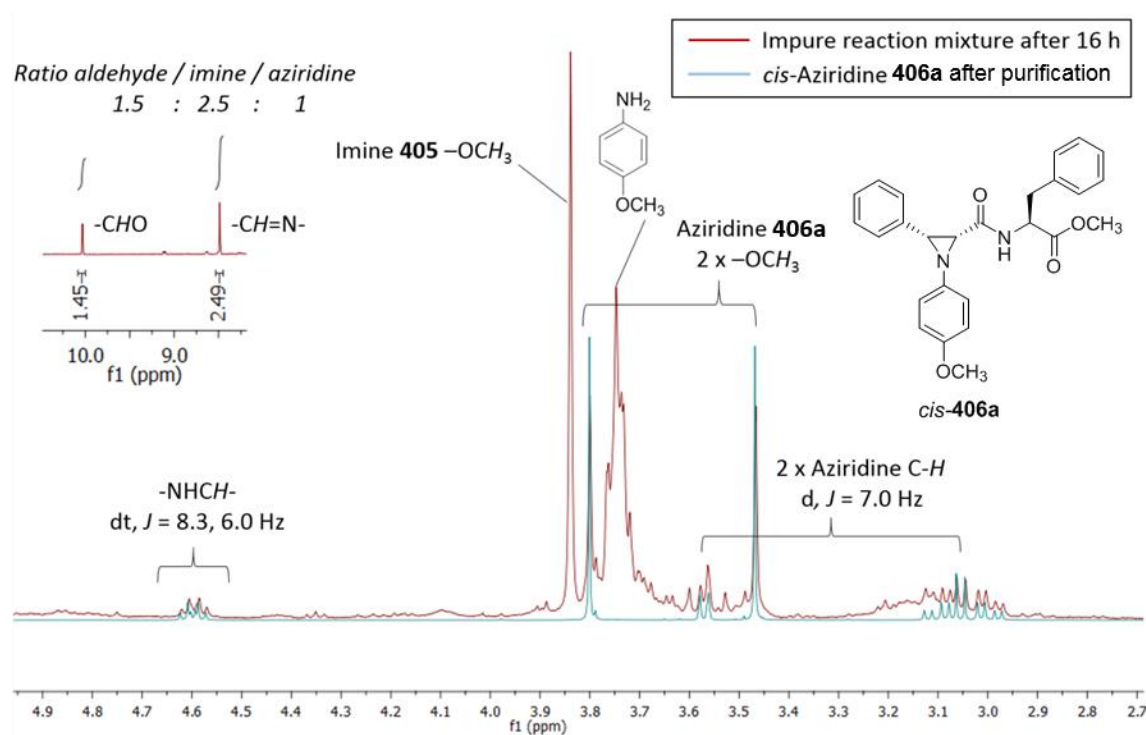
**Scheme 4.16** • CAN-mediated cleavage of the *N*-*p*-methoxyphenyl group from aziridine **242** reported by Mayer *et al.*

Employing similar conditions to the aza-Darzens reactions described in Section 3.1, imine **405** was cooled to  $0^\circ\text{C}$  in an ice bath before the addition of 10 mol% pyridinium triflate **347** and 1.2 equivalents of *N*-(diazooacetamido)-(*S*)-phenylalanine methyl ester **386** (Scheme 4.17). The sealed reaction vial was allowed to warm slowly to room temperature over 16 hours.



**Scheme 4.17** • Pyridinium triflate-catalysed aza-Darzens synthesis of *cis*-aziridine **406a**<sup>ii</sup>

The  $^1\text{H-NMR}$  of the impure reaction mixture shows poor conversion of imine **405** to aziridine **406a** (Figure 4.4). There is also a singlet peak at 10 ppm consistent with the  $-\text{CHO}$  proton of benzaldehyde, indicating partial hydrolysis of the imine during the reaction. Overall the reaction mixture contains benzaldehyde, imine **405** and aziridine **406a** in a ratio of approximately 1.5:2.5:1, which is consistent with the 23% isolated yield of **406a**.



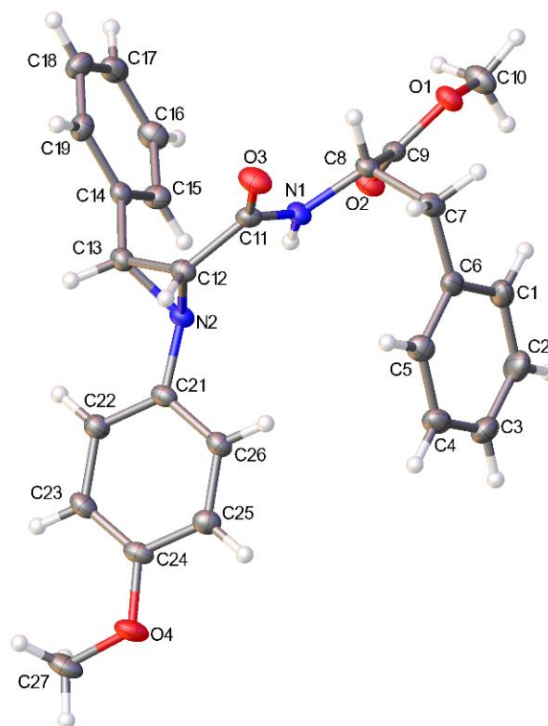
**Figure 4.4** • Partial  $^1\text{H-NMR}$  of *cis*-aziridine **406a** (blue) overlaid with the impure reaction mixture (red)

<sup>ii</sup> Absolute stereochemistry of **406a** inferred from x-ray crystal structure, Figure 4.5



The  $^1\text{H}$ -NMR of compound **406a** has aziridine C-H doublet peaks at 3.57 ppm and 3.05 ppm with coupling constants of 7.0 Hz, which is characteristic of a *cis*-aziridine. *N*-(Diazoacetamido)-(*S*)-phenylalanine methyl ester **386** is absent from the  $^1\text{H}$ -NMR of the impure reaction, which would prevent further conversion of imine **405** to product **406a**. It is likely that compound **386** decomposed during the course of the reaction; diazo compounds are known to be both light and acid sensitive.<sup>149</sup> In the synthesis of **406a** it may be that the rate of decomposition of **386** is faster than the rate of aziridination.

A small sample of aziridine **406a** crystallised in the eluent of the column chromatography during purification (petroleum ether / diethyl ether 1:1). X-ray crystallographic analysis revealed that compound **406a** crystallised in the centrosymmetric spacegroup triclinic *P*-1, indicating a racemic mixture of the *cis*-enantiomers (*R,R,S*) and (*S,S,R*) (Figure 4.5).

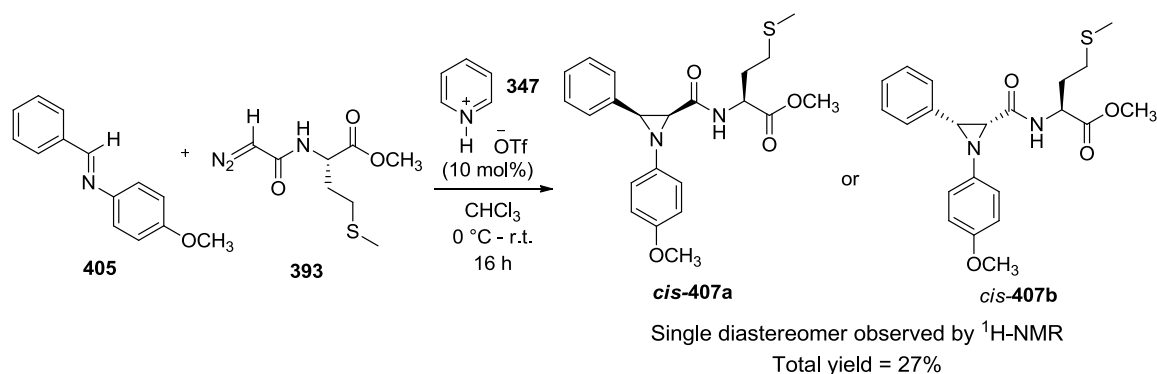


**Figure 4.5** • X-ray crystal structure of racemic *cis*-aziridine **406a**

The diazo peptide substrate **386** was synthesised with the *S* configuration (as supported by the specific rotation), but the ee was not confirmed by chiral HPLC, so either a small amount of the *R* configuration was present in the sample, or some racemisation of **386** occurred during the reaction. The two or three crystals formed during column chromatography may not be representative of the whole sample, as opposite enantiomers can have a greater affinity for each other than the same enantiomer, resulting in a small

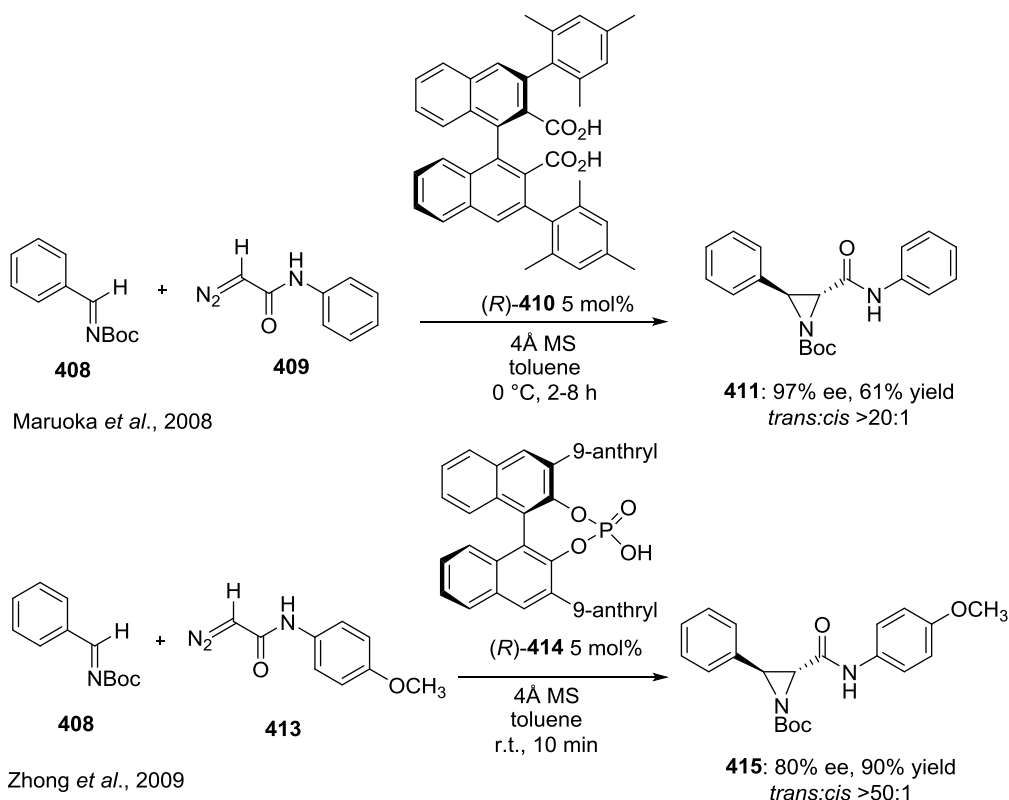
amount of the “true racemate” crystals.<sup>225</sup> Taking this into account, from the crystal structure of **406a** we can still infer that for the 1,5-induction there is a mismatch in the stereochemical outcome of the aziridination reaction: an *S* configuration in the diazo peptide substrate leads to an *R,R* configuration in the aziridine ring.

A second reaction was attempted under the same conditions using *N*-(diazooacetamido)-(*S*)-methionine methyl ester **393** (Scheme 4.18). Again only a single *cis*-aziridine product was obtained, according to the <sup>1</sup>H-NMR of the isolated product, **407a** or **407b**, which showed an aziridine C-H doublet coupling constant of 7.0 Hz. However, the yield was poor at 27% and the <sup>1</sup>H-NMR of the impure reaction mixture did not conclusively confirm the diastereoselectivity of this reaction. No crystals of the aziridine product were obtained in this case. The *cis*-selectivity of the aziridination reactions in Scheme 4.17 and 4.18 is surprising in the context of similar research reported in the literature. It has been generally accepted that acid catalysed aza-Darzens reactions with a diazoacetate substrate afford a *cis*-aziridine as the major product, while diazoacetamides generally afford a *trans* aziridine.<sup>226</sup>



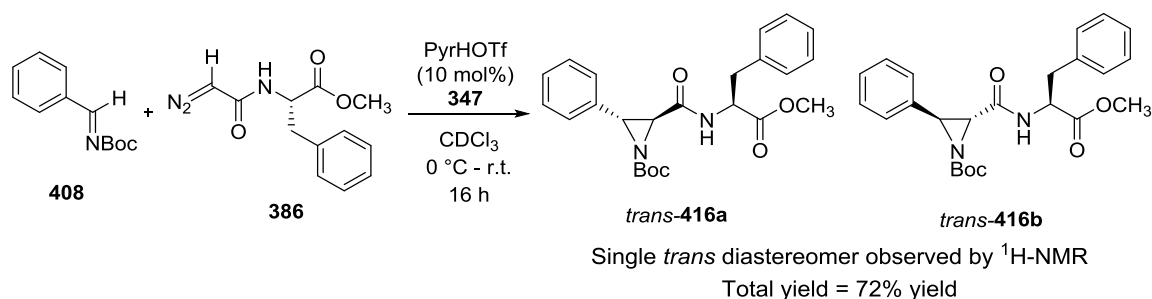
**Scheme 4.18** • Pyridinium triflate-catalysed synthesis of *cis*-aziridine **407**

In 2008 Maruoka *et al.* reported the use of BINOL-based dicarboxylic acid catalyst (*R*)-**410** for the *trans*-selective asymmetric aziridination of phenyl diazoacetamide **409** and *N*-Boc imine **408** (Scheme 4.19).<sup>227</sup> Aziridine (*R,S*)-**411** was isolated in a 61% yield, with an excellent 97% ee determined by chiral HPLC and a *trans*:*cis* ratio of >20:1. Similarly, Zhong *et al.* used BINOL-phosphoric acid catalyst (*R*)-**414** for the synthesis of *p*-methoxyphenyl aziridine (*R,S*)-**415** with a *trans*:*cis* ratio of >50:1.



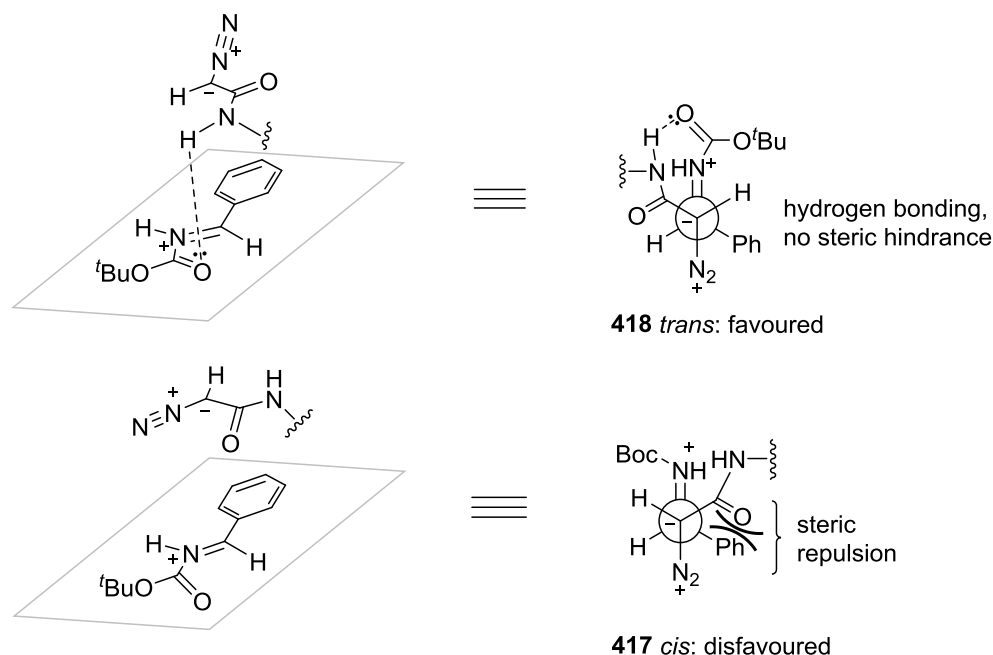
**Scheme 4.19** • BINOL-derived Bronsted acid-catalysed aza-Darzens aziridinations reported by Maruoka *et al.* (top) and Zhong *et al.* (bottom)

In order to make a comparison to the work by Maruoka and Zhong, *N*-Boc imine **408**<sup>iii</sup> was reacted with *N*-(diazooacetamido)-(*S*)-phenylalanine methyl ester **386** by the addition of 10 mol% of pyridinium triflate **347** (Scheme 4.20). Contrary to the outcome of the reactions using *p*-anisidine imine **405**, *trans*-aziridine **416** (**a** or **b**) was obtained in an isolated yield of 72% as the only product observed by <sup>1</sup>H-NMR of the impure reaction mixture (Scheme 4.20).



**Scheme 4.20** • Pyridinium triflate-catalysed *trans*-selective aza-Darzens aziridination between *N*-Boc imine **408** and diazo peptide **386**

<sup>iii</sup> Kindly provided by postgraduate research student Mr Victor Zdorichenko, University of East Anglia.

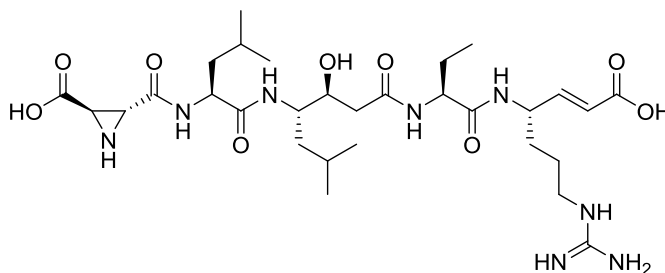


**Figure 4.6** • Possible explanation for the *trans* selectivity of the reaction between *N*-Boc imine **408** and *N*-(diazooacetamido)-(*S*)-phenylalanine **386**

Thus replacing the *p*-methoxyphenyl group on the imine with a Boc group resulted in a switch from *cis* selectivity to *trans* selectivity, showing that the nitrogen protecting group significantly influences the reaction. An explanation for the formation of a *trans* aziridine is presented in Figure 4.6. For the *trans* isomer (right), the approach of the diazoacetamide is influenced by hydrogen bonding between the amide –NH– and the carbonyl of the Boc group on the imine, affording intermediate **418** which is free from steric repulsion. Conversely reaction transition state **417** for the *cis* isomer (left) is made unfavourable by steric repulsion between the amide and the phenyl group. A single set of peaks corresponding to a *trans* aziridine was observed in the crude <sup>1</sup>H-NMR of **416**, indicating that there is excellent 1,5-stereocontrol in this reaction, although the absolute stereochemistry of **416** (either **a** or **b**) cannot be assigned without further investigation.

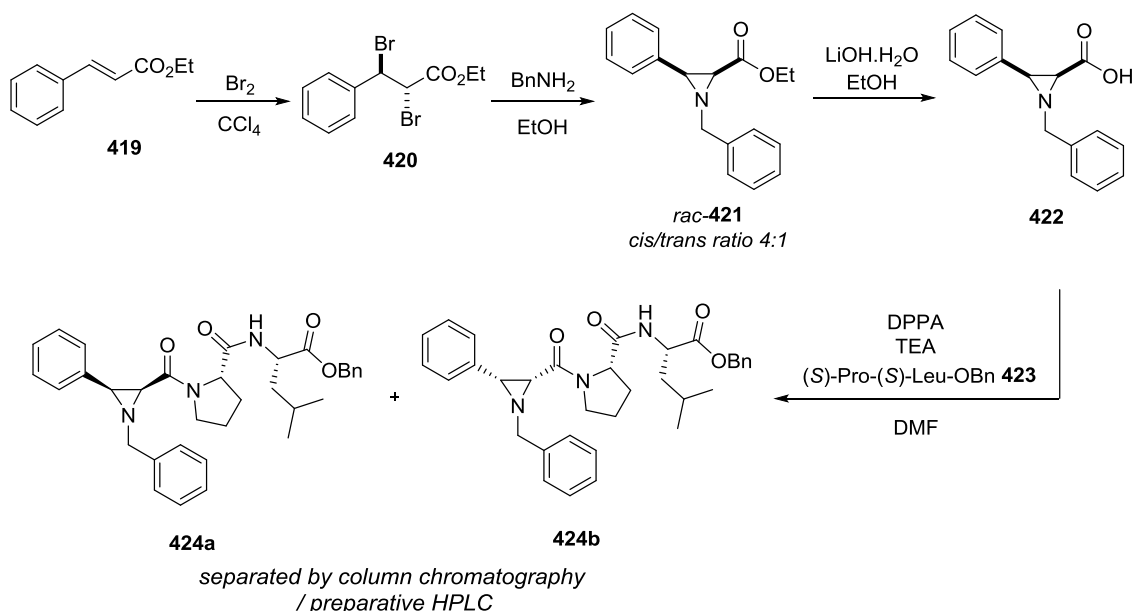
#### 4.2.4 One-pot asymmetric organocatalytic aza-Darzens reaction of peptide imines with diazopeptides

Peptide aziridines have attracted particular interest over the last 15 years as protease enzyme inhibitors.<sup>228</sup> The natural product miraziridine A, for example, is a cysteine protease inhibitor isolated from a marine sponge found in the Japanese archipelago (Figure 4.7).<sup>229</sup>



**Figure 4.7** • Molecular structure of miraziridine A

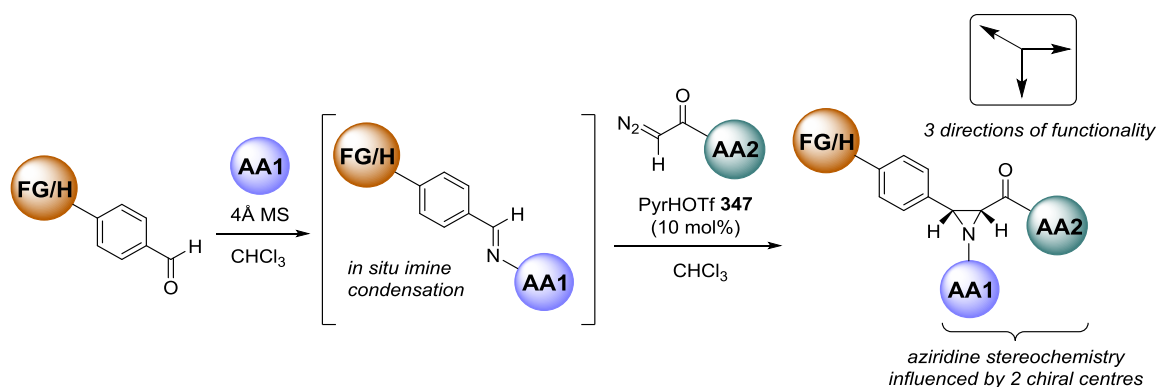
Recent work by the Yudin group has highlighted the use of aziridines in peptide ligation and macrocyclisation.<sup>230</sup> The chemical synthesis of peptide aziridines reported in the literature largely relies on peptide coupling reagents to bring together simple carboxylate aziridines and amino acids or peptide chains.<sup>231</sup> For example, T. Schirmeister *et al.* reported the synthesis of *cis*-aziridine **424** as a potential inhibitor of the secreted aspartic protease 2 (SAP2) of *Candida albicans* (Scheme 4.21).<sup>232</sup>



**Scheme 4.21** • Synthesis of peptide aziridine *cis*-**424** reported by Schirmeister *et al.*

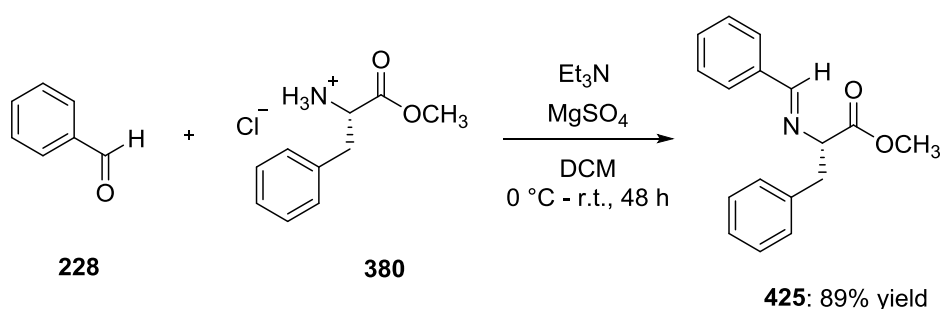
Racemic aziridine **421** was synthesised from *trans*-**420** as a mixture of two enantiomers (*R,R*) and (*S,S*). Hydrolysis of the ethyl ester of **421** afforded carboxylic acid **422** ready for DPPA coupling with dipeptide **423**. The resulting mixture of two diastereomers of *cis*-**424** could then be separated by a combination of column chromatography and preparative HPLC.

Following the initial work on the synthesis of  $\alpha$ -amino acid derived *cis*-aziridines by an aza-Darzens route presented in section 3.3.4, it was decided that to be practical and useful this route needed improved flexibility and higher yields. To this end, the *N*-aryl group would be replaced by an  $\alpha$ -amino acid, and functional groups introduced on the aldehyde substrate (Scheme 4.22). This approach was designed to install three directions of functionality, with the aziridine ring as the “connector” scaffold.



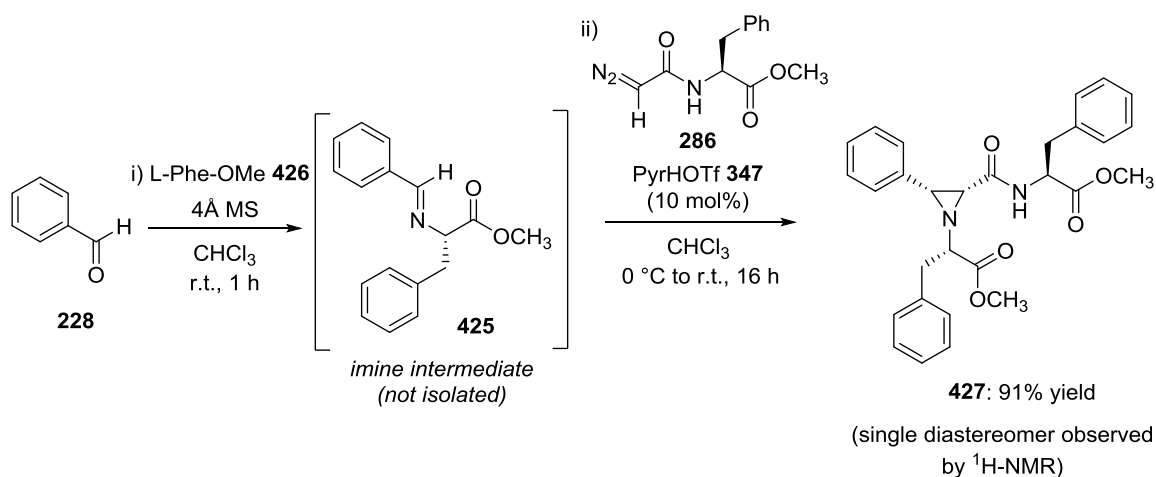
**Scheme 4.22** • Summary of the one-pot asymmetric aza-Darzens synthesis of peptide aziridines

The route illustrated in Scheme 4.22 offers considerable advantages over the conventional stepwise approach outlined in Scheme 4.21; there are significantly fewer steps required, and crucially the chirality of the  $\alpha$ -amino acid substrates were anticipated to influence the stereochemistry of the aziridine formation by both 1,3- and possibly 1,5-asymmetric induction.



**Scheme 4.23** • Synthesis of  $\alpha$ -amino acid imine **425** reported by Spring *et al.*

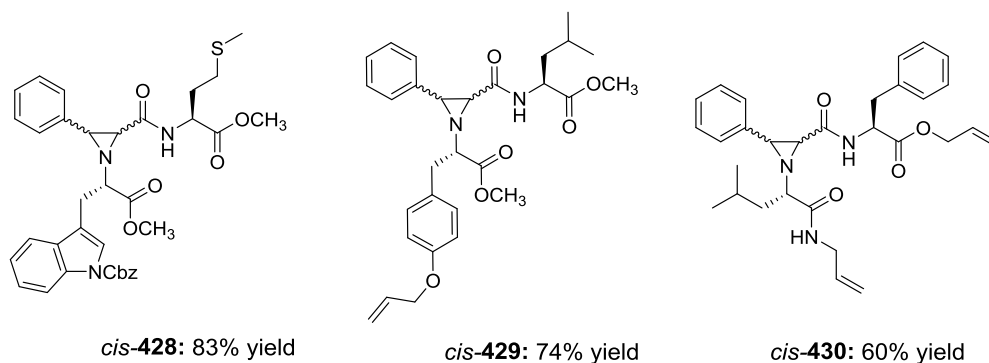
The imine condensation reaction between benzaldehyde **228** and (*S*)-phenylalanine methyl ester hydrochloride **380** was reported previously by Spring *et al.* (Scheme 4.23).<sup>233</sup> This reaction was successfully reproduced, and imine **425** was obtained in a 90% yield. The optical rotation of **425**,  $[\alpha]_{\text{D}}^{25}$  -198.5 (c 0.92, CHCl<sub>3</sub>), was close to the literature value of  $[\alpha]_{\text{D}}^{25}$  -206.7 (c 0.92, CHCl<sub>3</sub>). However, despite being stored at low temperature, the rotation was found to have dropped to  $[\alpha]_{\text{D}}^{25}$  -11.2 (c 1.0, CHCl<sub>3</sub>) after 24 hours, possibly due to isomerism of the imine. It was important to avoid racemisation of **425** prior to the aziridination step, so the synthesis of **425** was carried out *in situ* from benzaldehyde **228** and (*S*)-phenylalanine methyl ester **426** (Scheme 4.24). After one hour, 10 mol% of pyridinium triflate **347** and 1.2 equivalents of *N*-(diazooacetamido)-(*S*)-phenylalanine methyl ester **386** were added to the vial at 0 °C.



**Scheme 4.24** • Synthesis of peptide aziridine *cis*-**427**<sup>iv</sup> via a one-pot pyridinium triflate-catalysed aza-Darzens reaction

Gratifyingly, the <sup>1</sup>H-NMR of the impure reaction mixture after 16 hours showed complete consumption of benzaldehyde **228** and imine intermediate **425**, with the exclusive formation of a single *cis*-aziridine product **427** (where the aziridine doublet coupling constant  $J = 7.2$  Hz) which was isolated in an excellent 91% yield. The same reaction conditions were applied to the synthesis of a further three peptide aziridines **428–430** which bear  $\alpha$ -amino acid side-chains including *N*-Cbz-(*S*)-tryptophan, (*S*)-methionine, (*S*)-leucine and *O*-allyl-(*S*)-tyrosine (Figure 4.8). In each case, a single *cis* aziridine diastereomer was observed in the <sup>1</sup>H-NMR of the crude reaction mixture, where the absolute stereochemistry has not yet been determined.

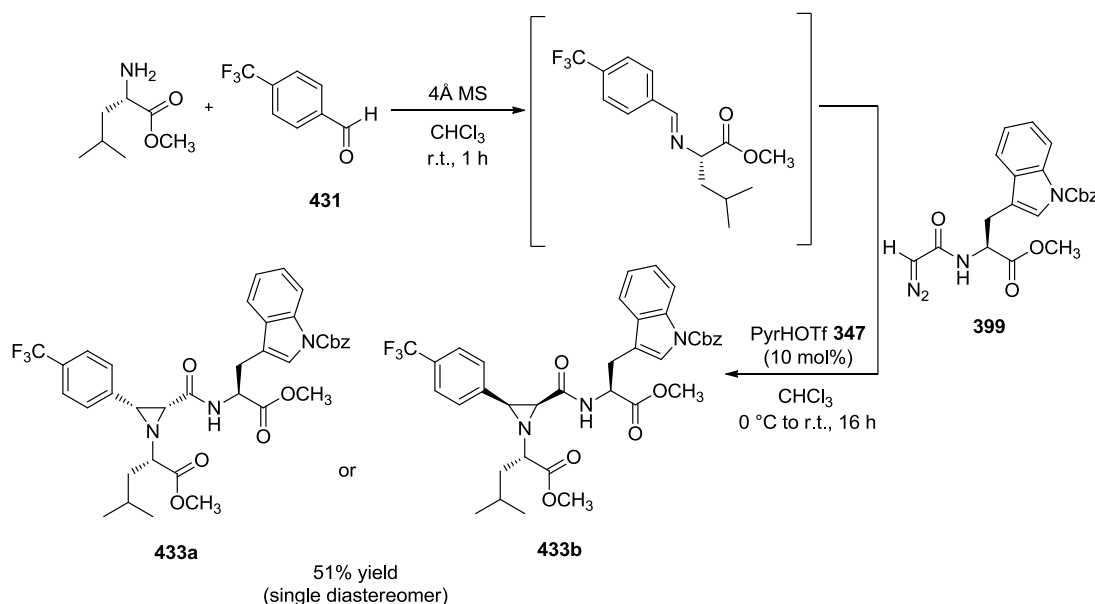
<sup>iv</sup> Absolute stereochemistry established in Section 4.2.7



**Figure 4.8** • Peptide aziridines **428–430** synthesised by a pyridinium triflate-catalysed aza-Darzens methodology

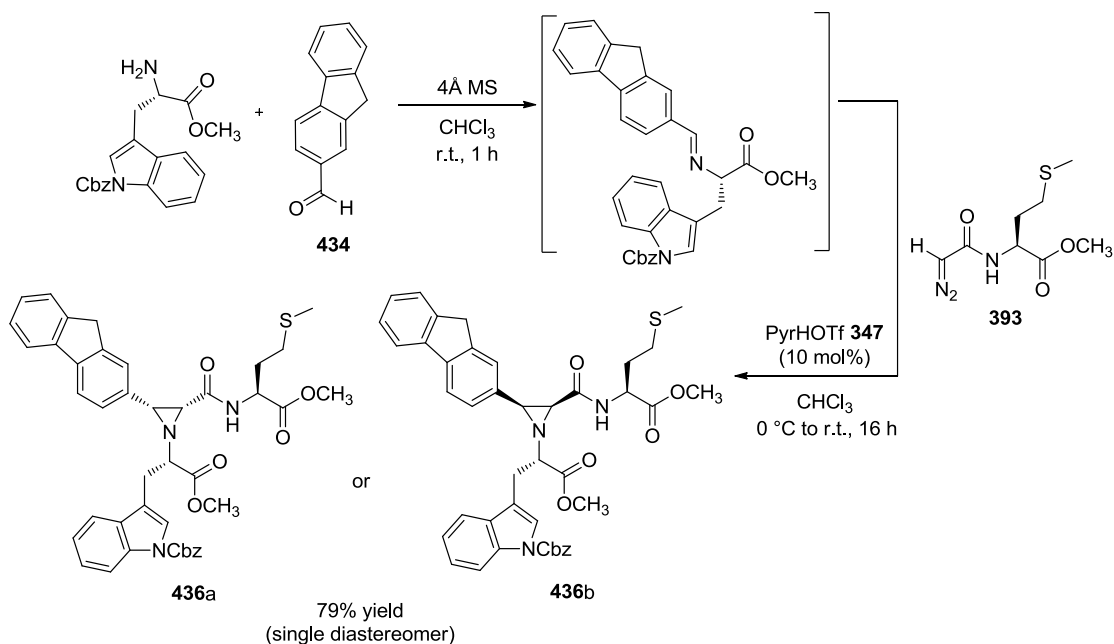
Aziridine **429**, featuring allyl ester and allyl amide functional groups, was designed as a potential precursor for transition metal-catalysed ring-closing metathesis to form a peptide macrocycle.

To achieve the “three directional” functionality described in Scheme 4.22, benzaldehyde **228** was replaced by commercial available aldehydes 4-trifluoromethylbenzaldehyde **431** and fluorene-2-carboxaldehyde **434** (Scheme 4.25). The incorporation of trifluoromethyl groups into peptides as a labelling technique in  $^{19}\text{F}$ -NMR is a key tool in structural biology.<sup>234</sup> Fluorene derivatives have been employed as fluorescent probes in two photon fluorescence microscopy.<sup>235</sup>



**Scheme 4.25** • Synthesis of CF<sub>3</sub>-bearing peptide aziridine *cis*-**433a/b** via a pyridinium triflate-catalysed aza-Darzens methodology

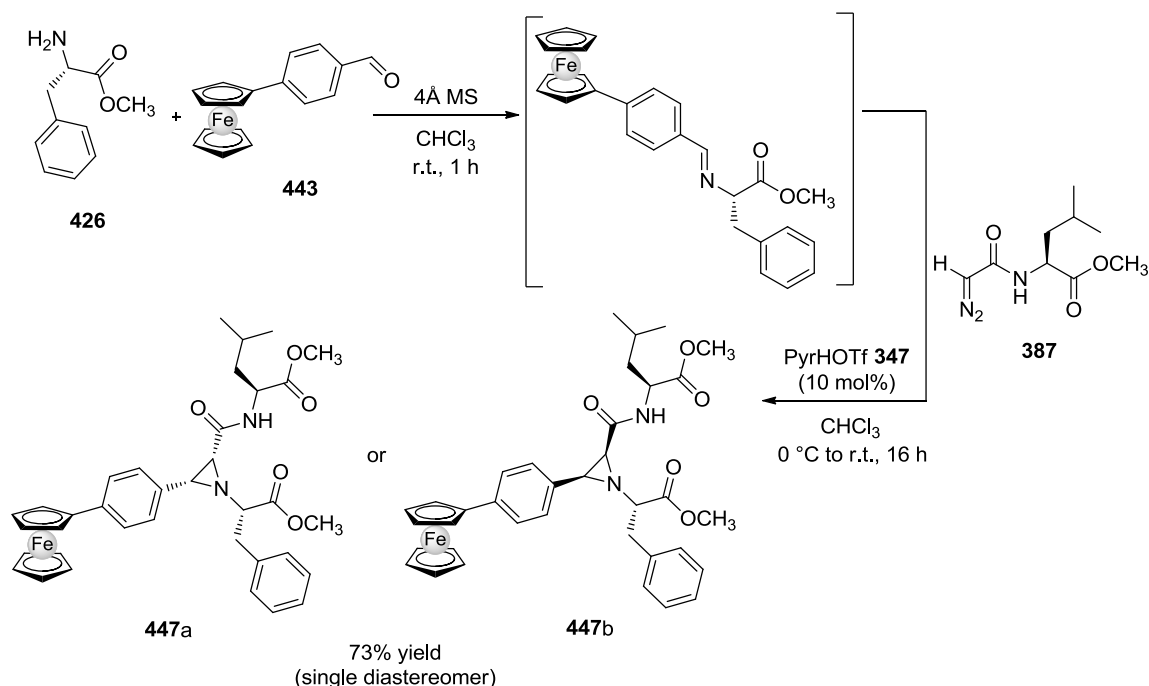




**Scheme 4.26** • Synthesis of fluorene-based peptide aziridine *cis*-**436a/b** via a pyridinium triflate-catalysed aza-Darzens methodology

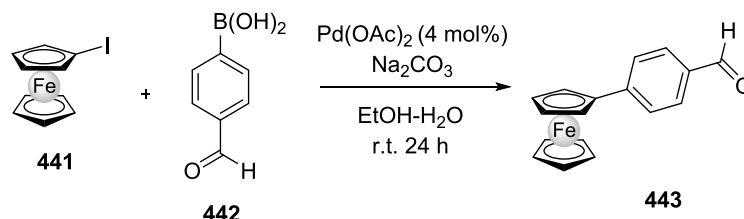
CF<sub>3</sub>-bearing *cis*-aziridine **433** was obtained in a disappointing 49% yield, indicating that this methodology may be less able to tolerate strongly electron withdrawing groups on the aldehyde substrate. The one-pot imine condensation / aziridination of fluorene-2-carboxaldehyde **434**, by contrast, afforded *cis*-aziridine **436** in a 79% yield after purification.

Ferrocenecarboxaldehyde **438** (Scheme 4.26) was identified as a potentially useful substrate for the aza-Darzens reaction due to the redox activity of ferrocene in biochemical processes.<sup>236</sup> For example, ferrocene-peptide conjugates have been used in the electrochemical probing of HIV enzymes.<sup>237</sup> Aldehyde **276** has been previously reported to react successfully with amines to form stable Schiff base ligands for transition metal complexes.<sup>238</sup> Indeed <sup>1</sup>H-NMR analysis of intermediate **277** contained a singlet peak at 8.16 ppm consistent with the imine –CH=N– proton. However, on the addition of catalyst **347** and *N*-(diazoacetamido)-(S)-leucine methyl ester **387** there was no further reaction observed. This may be due to stabilisation of the partial positive charge of the α-carbon attached to the Cp ring by the iron(II) centre – a recognised property of substituted ferrocene compounds.<sup>239</sup> In order to obtain a ferrocene-based peptide aziridine, therefore, a spacer was required between the Cp and the aziridine ring.



**Scheme 4.26** • Attempted aza-Darzens synthesis of ferrocenyl aziridine **440a/b** from ferrocenecarboxaldehyde **438**

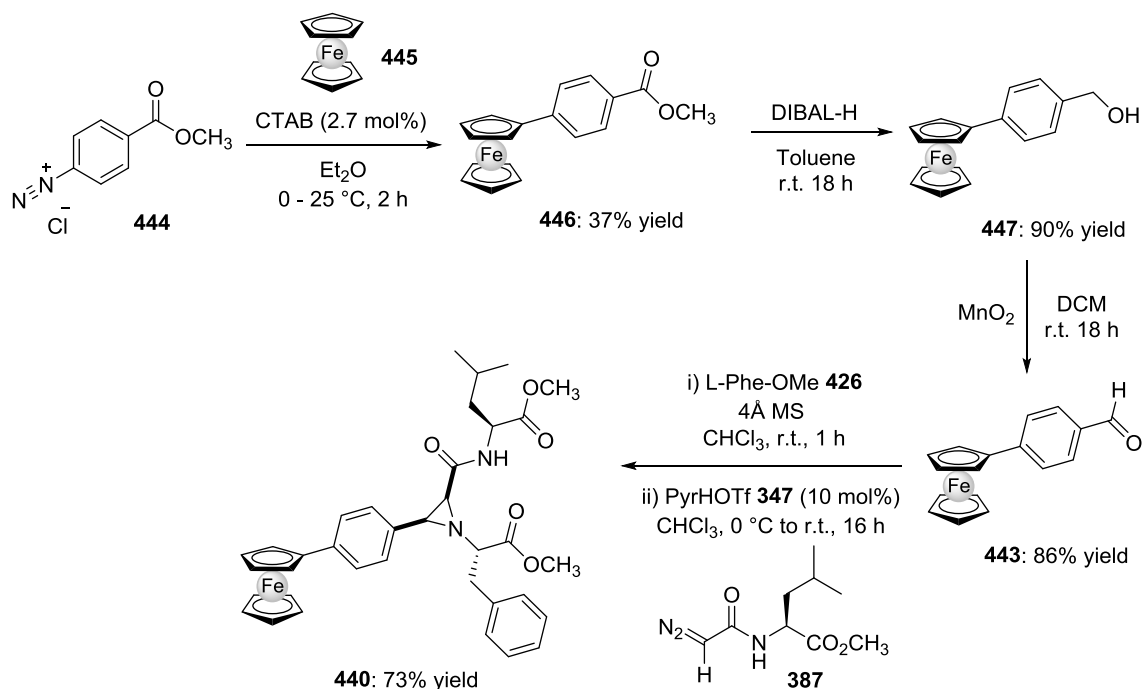
Imrie *et al.* synthesised 4-(ferrocenyl)benzaldehyde **443** by a Suzuki coupling reaction between iodoferrocene **441** and 4-formylphenylboronic acid **442** (Scheme 4.27).<sup>240</sup> However, the yield of this reaction was just 13%, and iodoferrocene **441** is not commercially available; it had to be synthesised in 2 steps from ferrocene in an overall 31% yield.



**Scheme 4.27** • Synthesis of 4-(ferrocenyl)benzaldehyde **443** reported by Imrie *et al.*

In order to obtain 4-(ferrocenyl)benzaldehyde **443** in a reasonable quantity, an alternative synthesis was designed in which methyl 4-aminobenzoate first reacted with sodium nitrite in a solution of aqueous hydrochloric acid to afford diazonium salt **444** *in situ* (Scheme 4.28). The addition of ferrocene **445** afforded methyl 4-(ferrocenyl)benzoate **446** as a deep red solid in a 37% yield. Subsequent DIBAL-H reduction of the ester group of **446** to alcohol **447** proceeded in an excellent 90% yield, and a manganese(IV) oxide oxidation of **447** afforded the desired aldehyde **443** in an 86% yield.

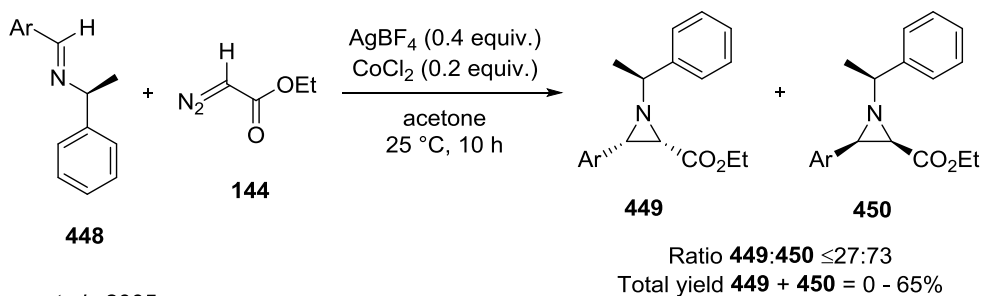
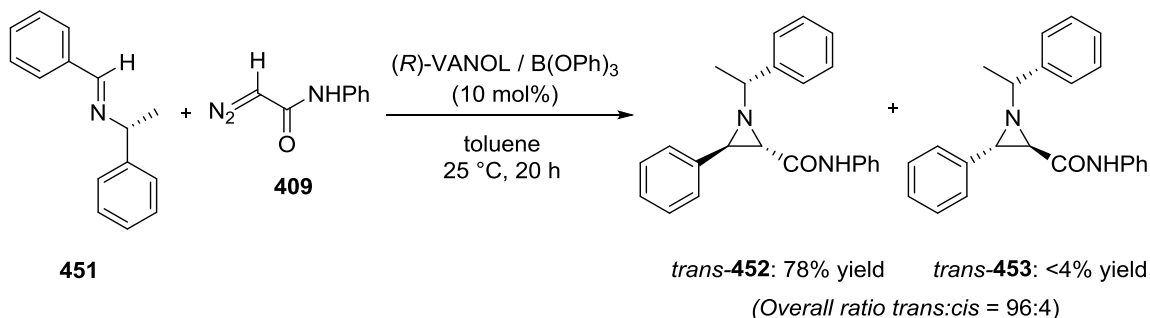
Unlike ferrocenecarboxaldehyde **438**, 4-(ferrocenyl)benzaldehyde **443** formed an imine with (*S*)-phenylalanine methyl ester **426** and then reacted successfully with *N*-(diazooacetamido)-(*S*)-leucine methyl ester **387** in the presence of 10 mol% of pyridinium triflate **347** to afford *cis*-aziridine **440** in a 73% yield.



**Scheme 4.28** • Four step synthesis of ferrocene-based peptide aziridine **440** from ferrocene **445** and diazoester **444**

#### 4.2.5 Asymmetric synthesis of *N*- $\alpha$ -methylbenzyl peptide aziridine **455**

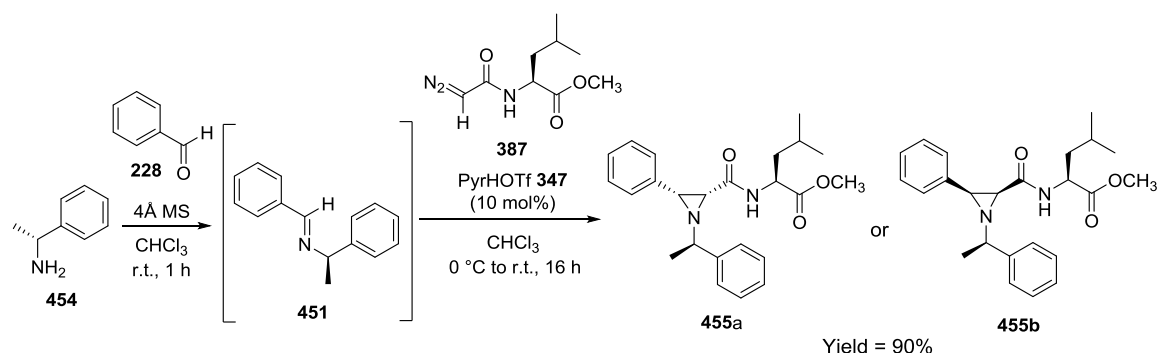
The  $\alpha$ -methylbenzyl group is a highly useful nitrogen protecting group; it has found numerous applications in remote chiral induction,<sup>241</sup> for example in the synthesis of isoquinoline alkaloids by Czarnocki *et al.*<sup>242</sup> After use as a chiral auxiliary the group can be subsequently cleaved under Pd/C hydrogenation conditions.<sup>243</sup> The asymmetric synthesis of aziridines bearing an (*R*)- or (*S*)-*N*- $\alpha$ -methylbenzyl group has been reported by the groups of Wulff and Lee (Scheme 4.29). Lee *et al.* investigated the Lewis acid-catalysed aza-Darzens reaction of ethyl diazoacetate **144** with a series of (*S*)-*N*- $\alpha$ -methylbenzyl imines using a combination of 20 mol% cobalt chloride and 40 mol% silver tetrafluoroborate.<sup>244</sup>

Lee *et al.*, 2005Wulff *et al.*, 2012

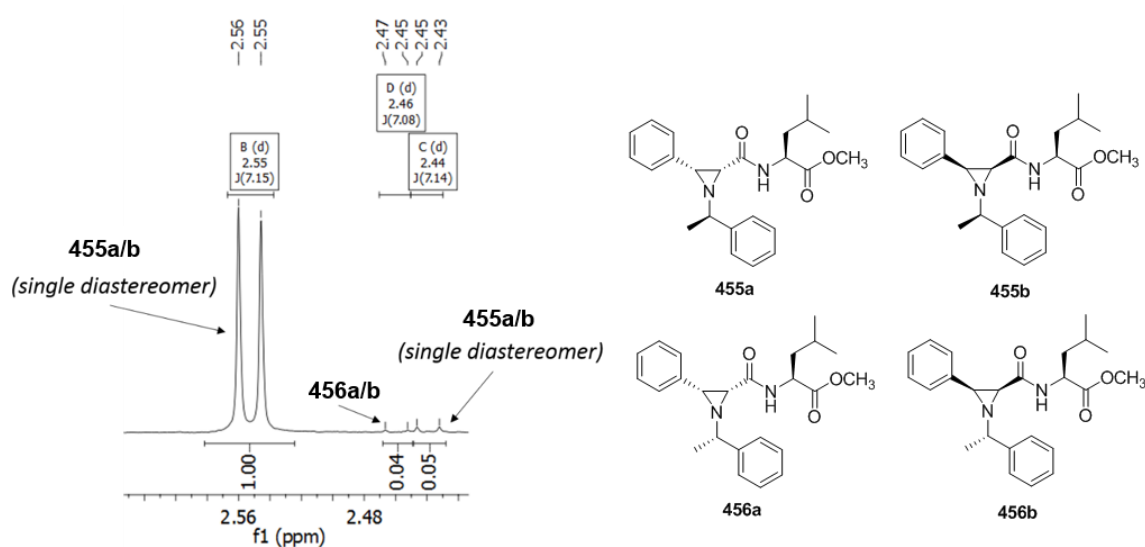
**Scheme 4.29** • Synthesis of aziridines bearing the *N*- $\alpha$ -methylbenzyl protecting group reported by Lee *et al.*, 2005, and Wulff *et al.*, 2012.

*Cis* diastereomers **449** and **450** were obtained in yields of up to 65%, however the diastereomeric ratio was generally poor ( $\leq 27:73$  in favour of **450**). Wulff *et al.* employed a double stereodifferentiation approach, using the chiral (*R*)-VANOL boroxinate catalyst for the reaction between (*R*)-*N*- $\alpha$ -methylbenzyl imine **451** and phenyl diazoacetamide **409**.<sup>245</sup> They reported a *trans/cis* ratio of 96:4 by this method, and ratio of the two *trans* diastereomers **452** and **453** of 95:5 (diastereomeric ratios obtained from the <sup>1</sup>H-NMR spectrum of the impure reaction mixture).

The pyridinium triflate-catalysed aza-Darzens reaction described in section 4.3.5 was applied to the synthesis of *N*- $\alpha$ -methylbenzyl aziridine **451** as a comparison to the work by Wulff *et al.* In the one-pot protocol (Scheme 4.30), benzaldehyde **228** reacted with (*R*)- $\alpha$ -methylbenzyl amine **454** to form imine intermediate **451** by a condensation reaction. Following the addition of 10 mol% of achiral catalyst **347** and 1.2 equivalents of *N*-(diazoacetamido)-(*S*)-leucine methyl ester **387**, <sup>1</sup>H-NMR analysis of the impure reaction mixture after 16 hours (Figure 4.9) showed the formation of a single major *cis*-aziridine product **455**, which was isolated in a 90% yield.



**Scheme 4.30** • One-pot pyridinium triflate-catalysed synthesis of *N*- $\alpha$ -methylbenzyl aziridine **455** (a or b)



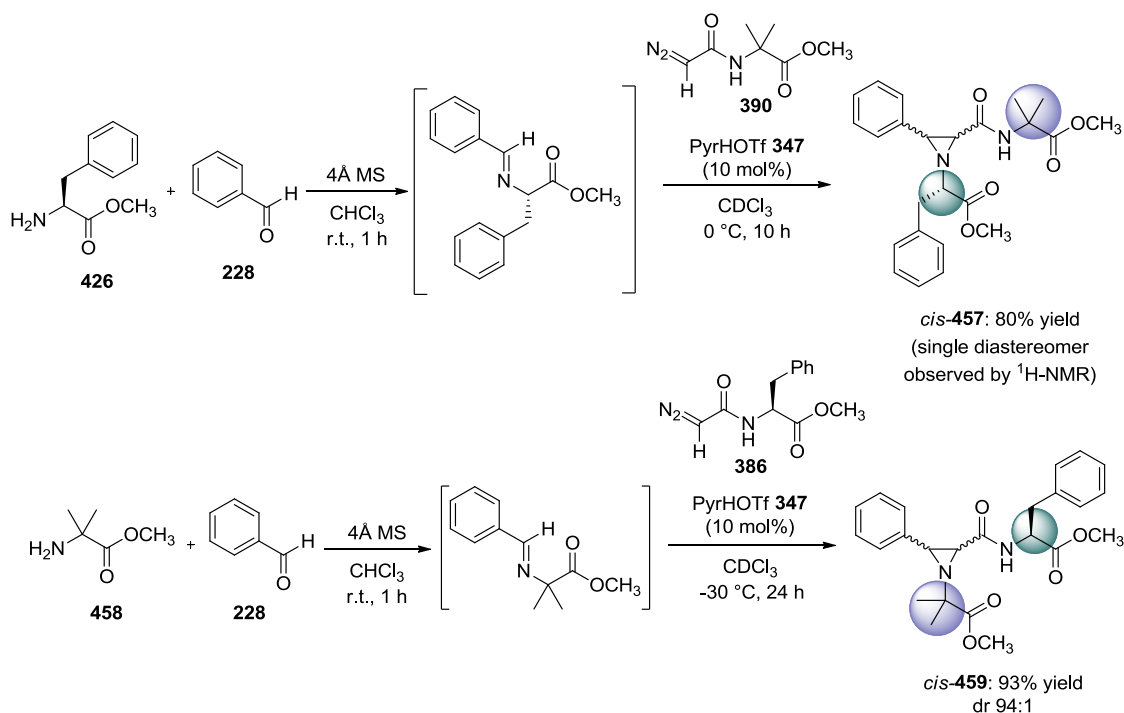
**Figure 4.9** • Partial  $^1\text{H}$ -NMR of the impure reaction mixture (Scheme 4.30)

Figure 4.9 shows the presence of two further doublets in the aziridine ring C-*H* region, with similar coupling constants to that of **455** ( $J = 7.1$  Hz). It is presumed that the doublet at 2.44 ppm (far right) represents a diastereomer of **455**, giving a *dr* of 95:5. The starting material for this reaction, (*R*)- $\alpha$ -methylbenzylamine **454**, was purchased at reagent grade, with an *ee* of 96% by GLC (see Experimental section for details). This may account for the presence of a third diastereomer **456** indicated by the doublet at 2.46 ppm, and the peak integration of 0.04 (4% of the reaction products) supports this theory.

Employing the remote chiral induction protocol in this way removes the need for expensive catalysts and introduces more functionality into the molecule in a single step than the reactions shown in Scheme 4.29. Isolated as a single isomer, **455** is potentially a direct precursor to a range of natural and unnatural, nitrogen-protected, non-racemic dipeptides accessible *via* nucleophilic ring opening of the *cis*-aziridine moiety.

## 4.2.6 Investigating the effect of temperature and chiral distance on stereoselectivity

The peptide aziridines described in Section 4.2.5 contain two  $\alpha$ -amino acid chiral centres – the first directly connected to the nitrogen of the aziridine ring, and the second separated from the aziridine ring by a single amide bond. In order to establish the degree of influence of each chiral centre on the stereochemistry of the aziridine ring being formed, a comparison was made between aziridines **457** and **459**, which feature the achiral  $\alpha$ -aminoisobutyric acid (Aib) amino acid (Scheme 4.31).

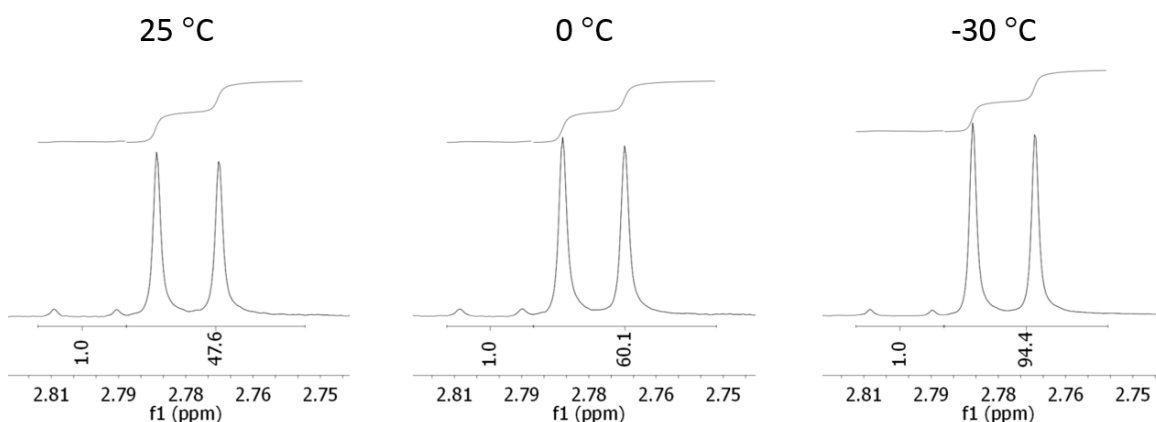


**Scheme 4.31** • Pyridinium triflate-catalysed aza-Darzens synthesis of aziridines **457** and **459**

The synthesis of *cis*-**457** (where the aziridine doublet coupling constant  $J = 7.2$  Hz) was carried out at  $0^\circ\text{C}$  using the protocol described previously (Section 4.3.5). The solvent was changed from chloroform to chloroform- $d_3$  to make monitoring the reaction by  $^1\text{H-NMR}$  more convenient. The reaction was complete after 10 hours, and a single aziridine product **457** was observed in the  $^1\text{H-NMR}$  of the impure reaction mixture, which was isolated in an 80% yield.

In the synthesis of *cis*-**459**, the formation of a major aziridine product was observed, with a set of doublets at 2.78 ppm ( $J = 6.9$  Hz) and 3.27 ppm ( $J = 6.9$  Hz) corresponding to the aziridine C-H protons. However, a second minor set of doublets was observed with an identical coupling constant of 6.9 Hz. It is presumed that these peaks correspond to the

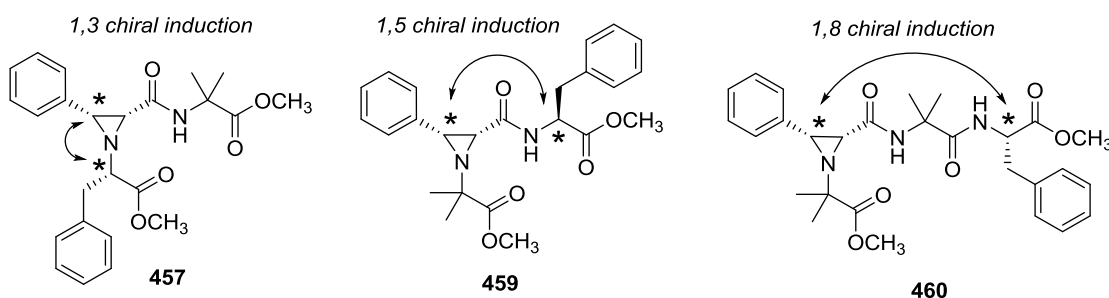
second diastereomer of **459**. A temperature study showed that the ratio of the two diastereomers was influenced by the reaction temperature (Figure 4.10).



**Figure 4.10** • Partial  $^1\text{H}$ -NMR of the impure reaction mixture in the synthesis of *cis*-aziridine **459** carried out at 25 °C, 0 °C, and -30 °C

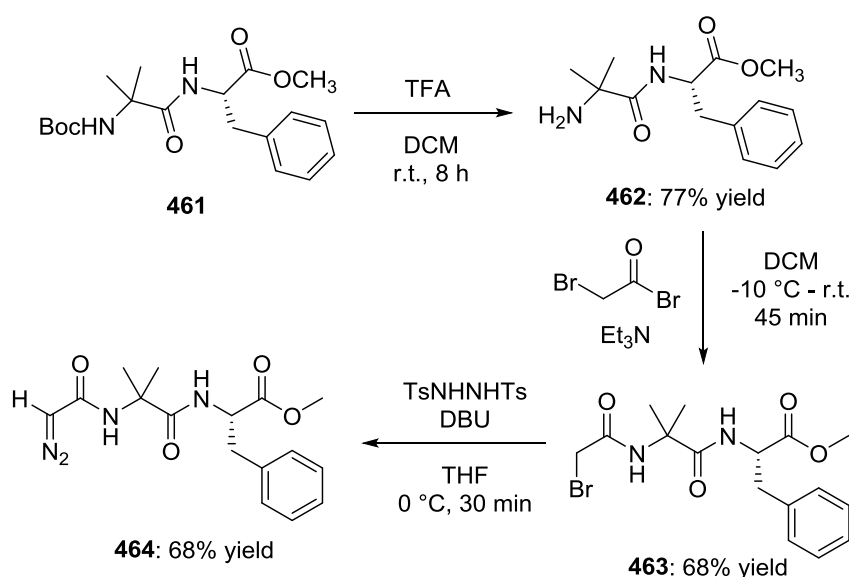
When the reaction was carried out at room temperature (25 °C), the ratio of major:minor diastereomers (measured by integration of the C-H doublets in the  $^1\text{H}$ -NMR) was 47.6:1, increasing to 60.1:1 when a 0 °C chiller bath was used. The optimum temperature for the synthesis of **459** was -30 °C, achieving a diastereomeric ratio of 94.4:1. Below this temperature, precipitation of *N*-(diazooacetamido)-(*S*)-phenylalanine methyl ester **386** was observed and the reaction failed.

The findings from the synthesis of **457** and **459** are consistent with the expectation in remote chiral induction reactions that the closer the chiral centre of the starting material to the chiral centre formed during the reaction, the stronger the influence, and the higher the stereoselectivity.



**Figure 4.11** • Comparison of the distance between the two key chiral centres of aziridines **457**, **459** and **460**

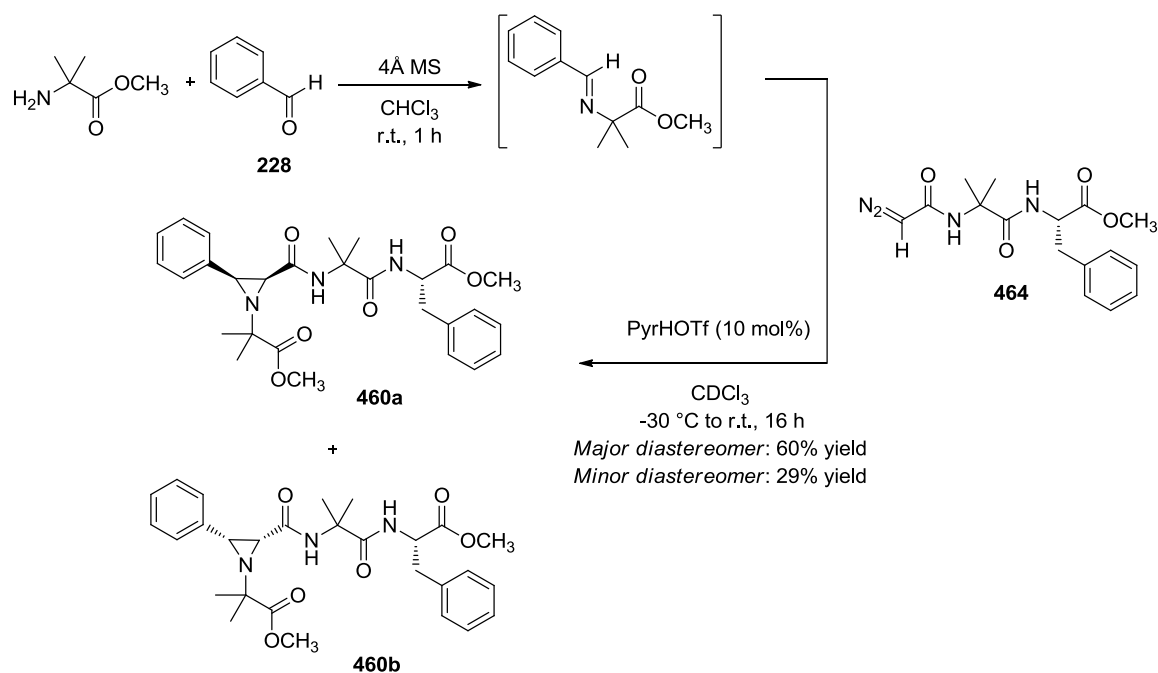
Thus in aziridine **457**, the (*S*)-phenylalanine chiral centre is two bonds from the first aziridine chiral centre formed during the aza-Darzens reaction (Figure 4.11), and a single diastereomer product is observed. In the synthesis of compound **459**, a 1,5-chiral induction takes place through four bonds, and selectivity is slightly lower, with a maximum *dr* of 94:1. It was hoped that inserting an Aib unit between the phenylalanine chiral centre and the aziridine ring would still result in a degree of stereoselectivity. This would be a 1,8 chiral induction (compound **460**, Figure 4.11). To this end, diazodipeptide **464** was synthesised from Boc-Aib-(*S*)-phenylalanine methyl ester **461** in three steps with an overall yield of 36% (Scheme 4.32).



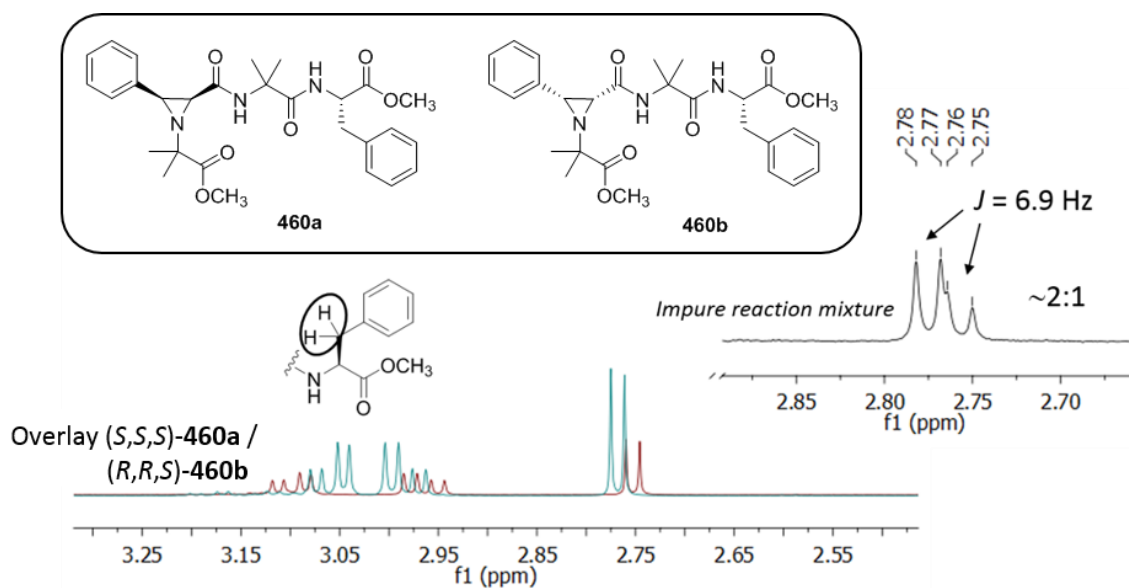
**Scheme 4.32 • Synthesis of diazoacetamide dipeptide **464****

Compound **464** was found to be poorly soluble in chloroform at low temperature, so for the one-pot aziridination step (Scheme 4.33) the reaction was cooled to -30 °C for the addition of **464** using a dry ice bath, which was allowed to warm slowly to room temperature overnight. Two *cis*-aziridine diastereomers were identified in the <sup>1</sup>H-NMR of the impure reaction mixture and were subsequently separated by column chromatography (Figure 4.12). The *dr* based on <sup>1</sup>H-NMR integration of the aziridine C-H doublets and the isolated yields were in close agreement at 2:1.





**Scheme 4.33** • One-pot pyridinium triflate-catalysed aza-Darzens synthesis of *cis*-aziridine **460a** and **460b**



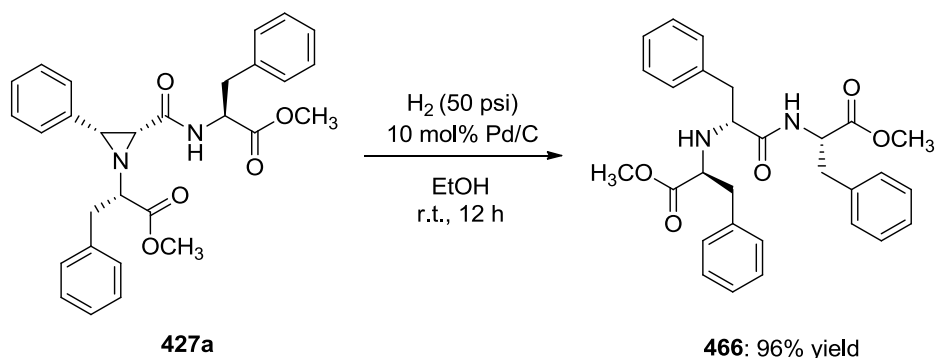
**Figure 4.12** • Partial  $^1\text{H}$ -NMR of i) the impure reaction mixture and ii) an overlay of separated, pure *cis* diastereomers **460a** and **460b**

It is clear that despite the conformationally restricted nature of the Aib unit, the 1,8 chiral induction was much less successful in terms of stereoselectivity than the 1,5- and 1,3-chiral induction reactions. Further work to increase the 2:1 ratio obtained in Scheme 4.33 may include changing the Aib unit for a cyclohexyl group or a dehydro amino acid, as

sections of fixed planarity and restricted rotation are known to relay chiral information over longer distances.<sup>246</sup>

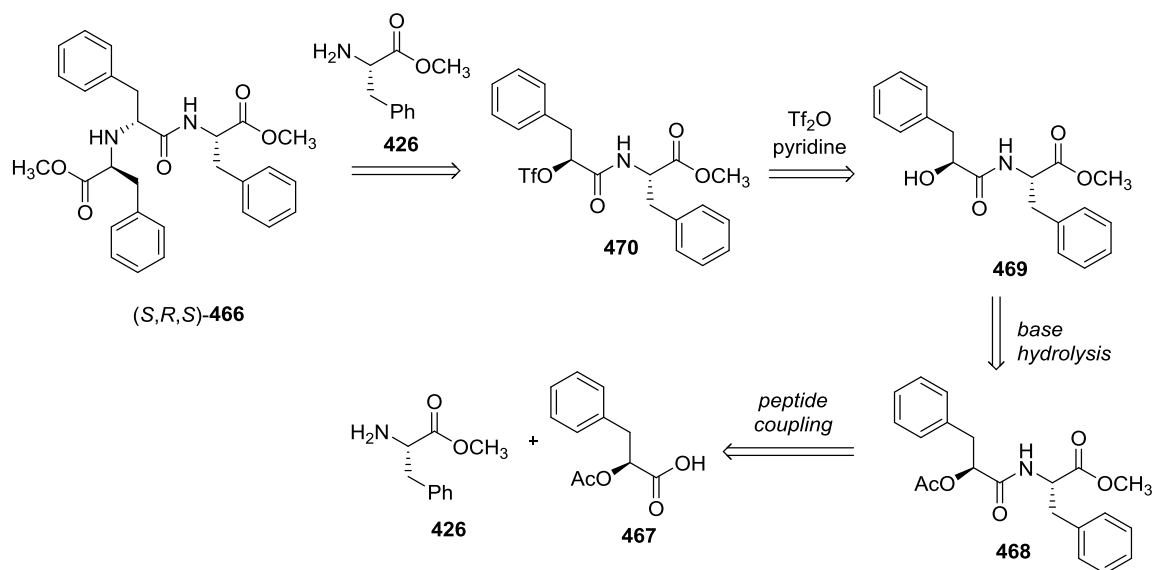
#### 4.2.7 Assigning the absolute stereochemistry of *cis*-aziridine **427a**

The peptide aziridines described in Section 4.3.5 were isolated and characterised as single *cis* diastereoisomers. However, it was not possible to assign the absolute stereochemistry of the aziridine ring in these compounds without further investigation. An alternative method of synthesis was required in which these unknown chiral centres would be derived from known enantiomerically pure starting materials. To simplify this process, the *cis*-aziridine would first be submitted to palladium(0)-catalysed hydrogenation, affording a pseudopeptide with just three chiral centres; a more convenient target for synthesis from commercially available amino acid starting materials (Scheme 4.34). Thus palladium on carbon (10 mol%) was added to a solution of aziridine **427a** in ethanol and the reaction pressurised to 50 psi with hydrogen in a Biotage Endeavour system to afford compound **466** in a 96% yield.



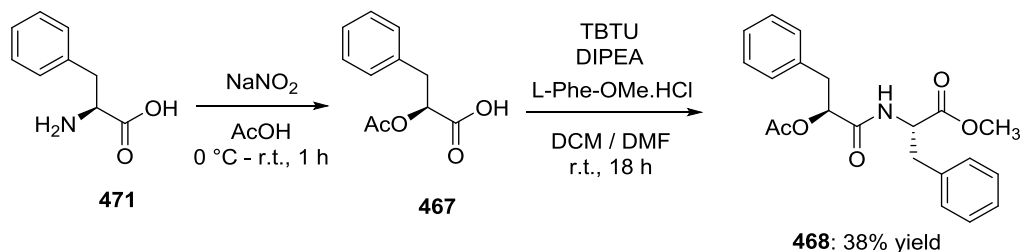
**Scheme 4.34** • Hydrogenation of the aziridine ring of **427** catalysed by palladium on carbon

A retrosynthetic summary of the alternative route to (*S,R,S*)-**466** is presented in Scheme 4.35. Peptide coupling of *O*-acetyl-(*S*)-phenyllactic acid **467** with (*S*)-phenylalanine methyl ester **426** affords compound **468**, which can be deprotected under basic conditions to afford alcohol **469**. The corresponding triflate **470** will then be displaced by (*S*)-phenylalanine methyl ester **426** via an S<sub>N</sub>2 mechanism to afford compound **466**.

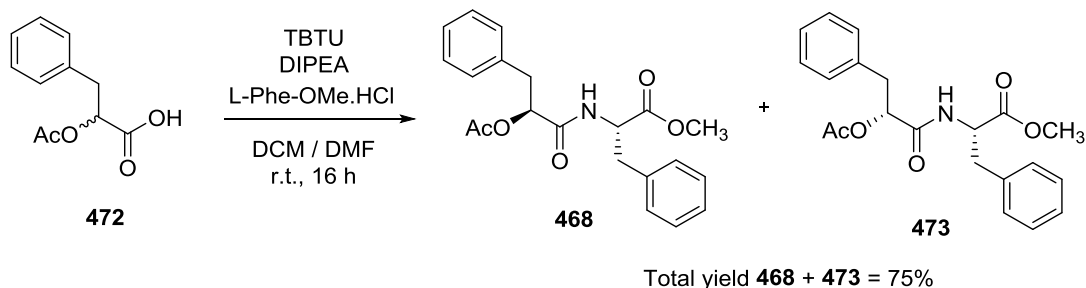


**Scheme 4.35** • Retrosynthetic analysis of the synthesis of pseudopeptide (S,R,S)-**466**

*O*-Acetyl-(*S*)-phenyllactic acid **467** was prepared from (*S*)-phenylalanine **471** according to a procedure by Pleniewicz *et al.*,<sup>247</sup> a reaction in which the (*S*) stereochemistry is retained in the product (Scheme 4.36). Subsequent coupling of **467** with (*S*)-phenylalanine methyl ester hydrochloride was achieved using TBTU, affording compound **468** in a 38% yield.



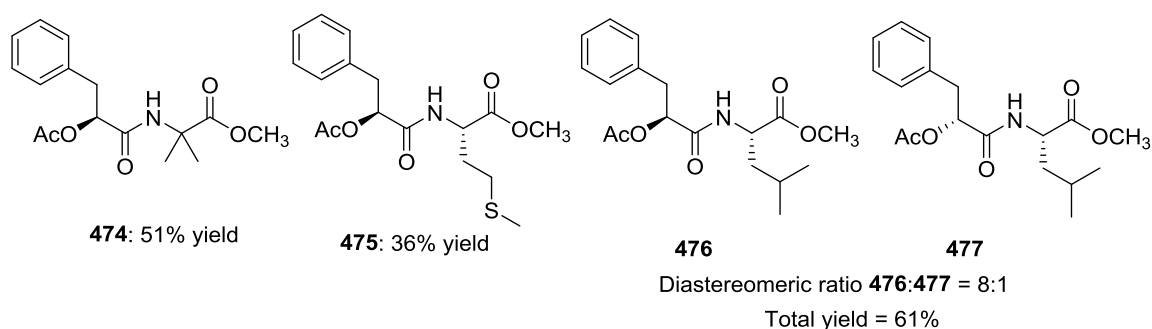
**Scheme 4.36** • Synthesis of (*S*)-methyl 2-((*S*)-2-acetoxy-3-phenylpropanamido)-3-phenylpropanoate **468** from (*S*)-phenylalanine **471**



**Scheme 4.37** • Synthesis of **468** and **473** as a mixture of two diastereomers: (*S,S*) and (*R,S*)

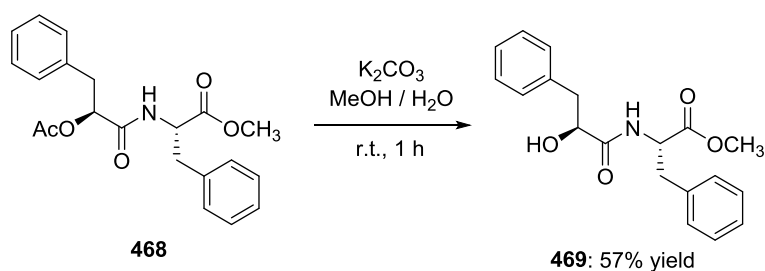
These reactions were repeated using *rac*-phenylalanine as the initial starting material to obtain diastereomers **468** and **473** (Scheme 4.37) from *O*-acetyl-(*R,S*)-phenyllactic acid **472**. Compounds **468** and **473** could not be separated by column chromatography and were used in the next step of the synthesis as a 1:1 mixture of the two diastereomers.

The TBTU-mediated coupling steps in Scheme 4.36 and 4.37 were repeated with the hydrochloride salts of (*S*)-methionine methyl ester, (*S*)-leucine methyl ester and  $\alpha$ -aminoisobutyric acid methyl ester to afford compounds **474–477** (Figure 4.13), with the intention of assigning the stereochemistry of a further range of peptide aziridines. In the synthesis of **476**, a minor diastereomer **477** was also formed, in a ratio of 8:1 (**476**:**477**). This indicates that the *O*-Acetyl-(*S*)-phenyllactic acid **467** was not enantiomerically pure, and diastereomers **476** and **477** proved impossible to separate by flash column chromatography.



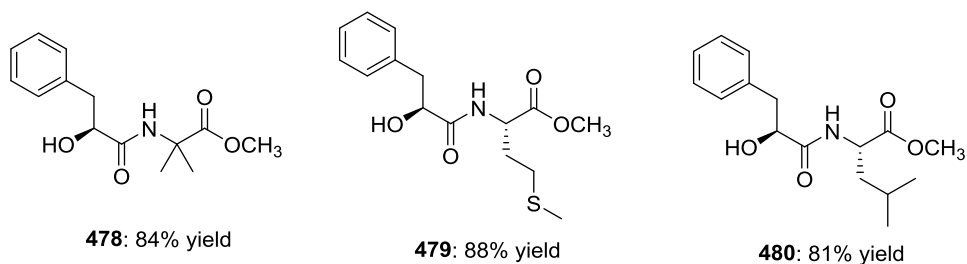
**Figure 4.13** • Compounds **474–477** synthesised by TBTU-mediated coupling illustrated by Scheme 4.37

Hydrolysis of the acetyl protecting group of compound **468** was achieved under basic conditions using 0.25 equivalents of potassium carbonate in aqueous methanol, following a procedure by Yang *et al.*<sup>248</sup> Complete consumption of the starting material was observed by thin layer chromatography after one hour, however the moderate 57% yield of the reaction indicates that some material may be lost by hydrolysis of the methyl ester.

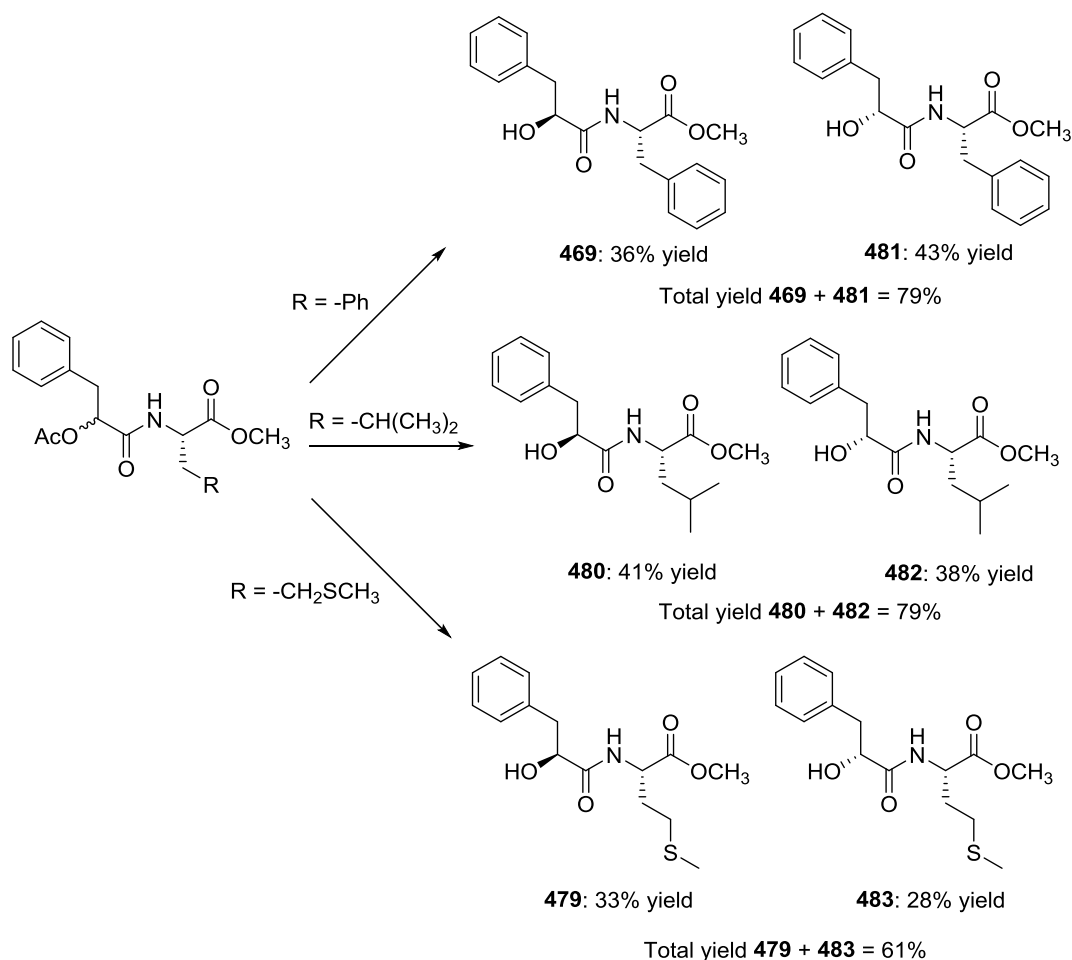


**Scheme 4.38** • Base hydrolysis of acetate **468** to afford alcohol **469**

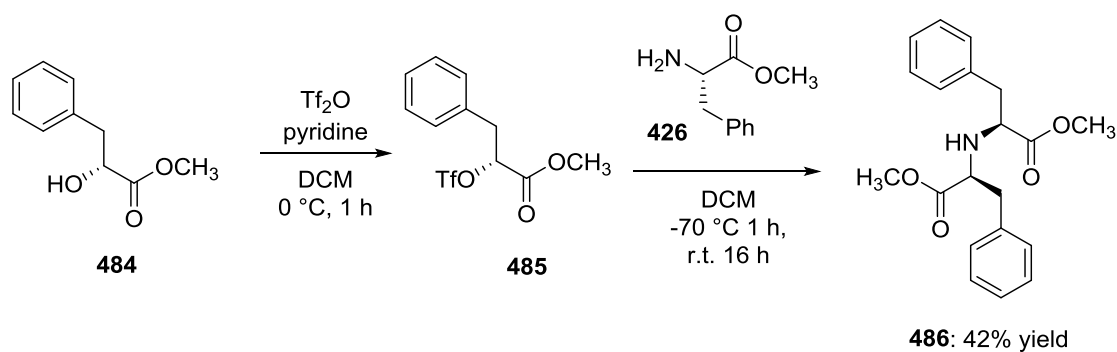
The acetate hydrolysis reaction was carried out on compounds **474-476**, affording peptide alcohols **478-480** as a single (*S,S*) diastereomer (Figure 4.14). Racemic mixtures of (*R,S*) and (*S,S*) acetate diastereomers were hydrolysed by the method shown in Scheme 4.36 to afford the corresponding alcohols, which could be separated easily by column chromatography on silica gel (Scheme 4.37).



**Figure 4.14** • Alcohols **478-480** synthesised by base hydrolysis of acetates **474-476**

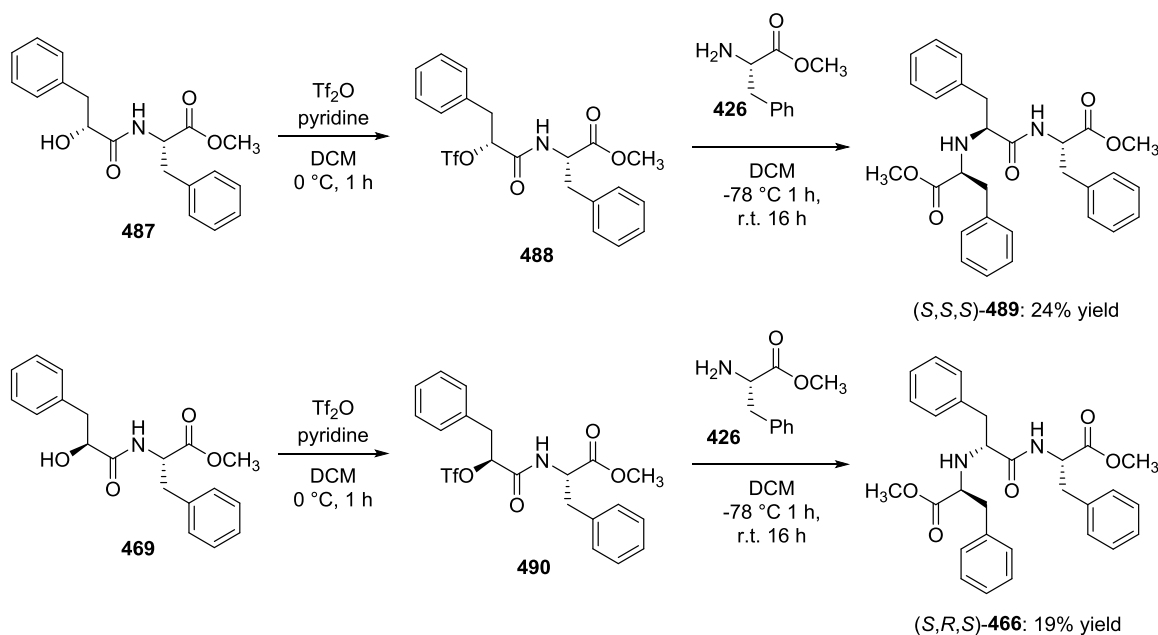


**Scheme 4.39** • Hydrolysis of racemic acetates to afford separable (*R,S*) and (*S,S*) diastereomers **469, 479** and **480-483**

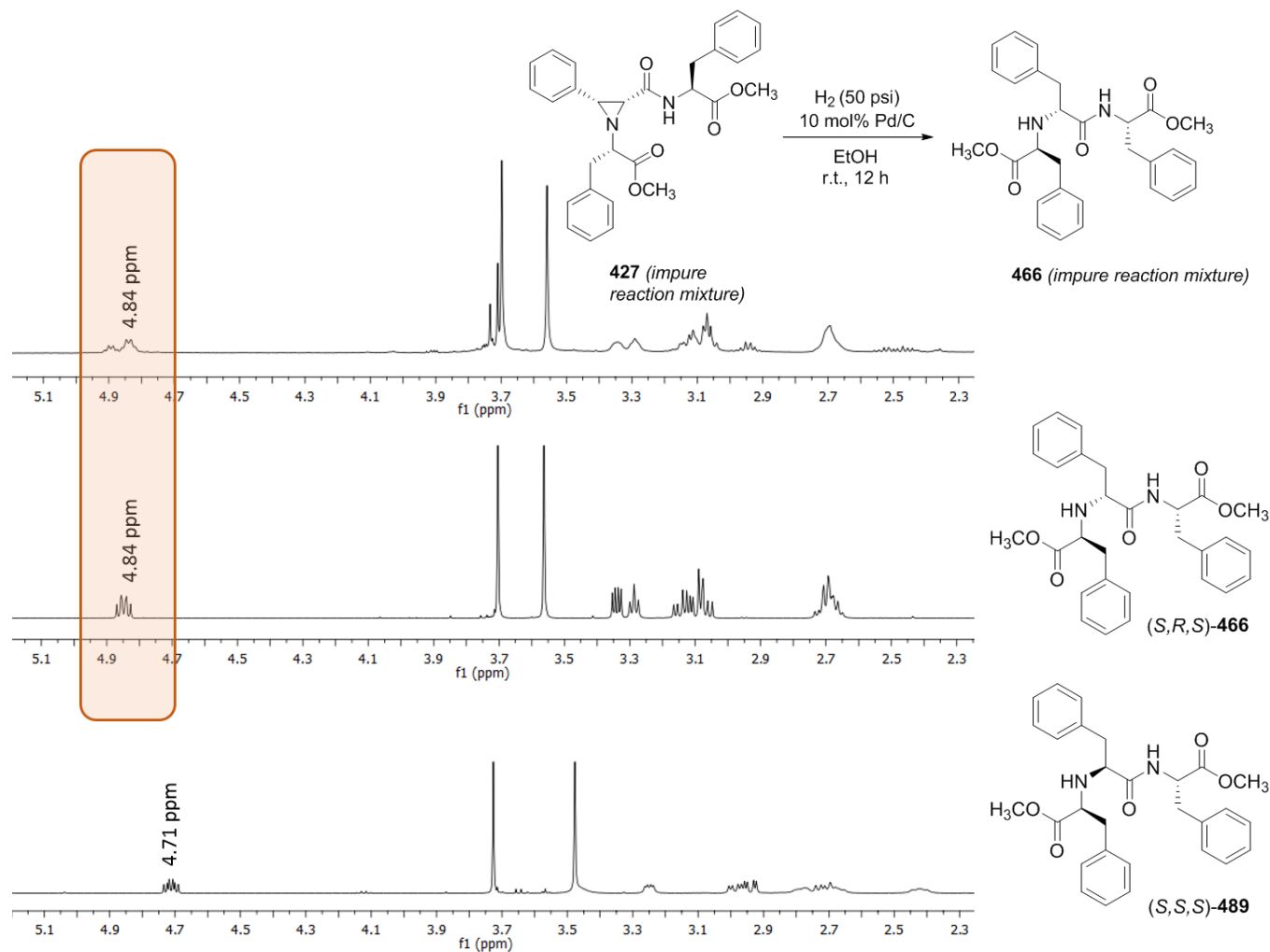


**Scheme 4.40** • Synthesis of methyl iminodiacetic derivative **486** reported by Langlois *et al.*

In their 2008 publication on the synthesis of iminodiacetic acid derivatives as potential inhibitors of HIV-1 aspartyl protease, Langlois *et al.* reported the reaction between triflate **485** and (*S*)-phenylalanine methyl ester **426** to afford compound **486** in a 42% yield (Scheme 4.40).<sup>249</sup> This route was applied to the synthesis of peptides **305** and **328** (Scheme 4.41). It was found that triflates **488** and **490** were highly unstable and had to be used immediately in the second step without purification. Despite careful handling, and the low reaction temperature of -78 °C, compounds **489** and **466** were obtained in low yields of 19% and 24% respectively. Fortunately, for the purposes of assigning absolute stereochemistry only pure samples of **489** and **466** were required for characterisation, and the yield was of less importance.



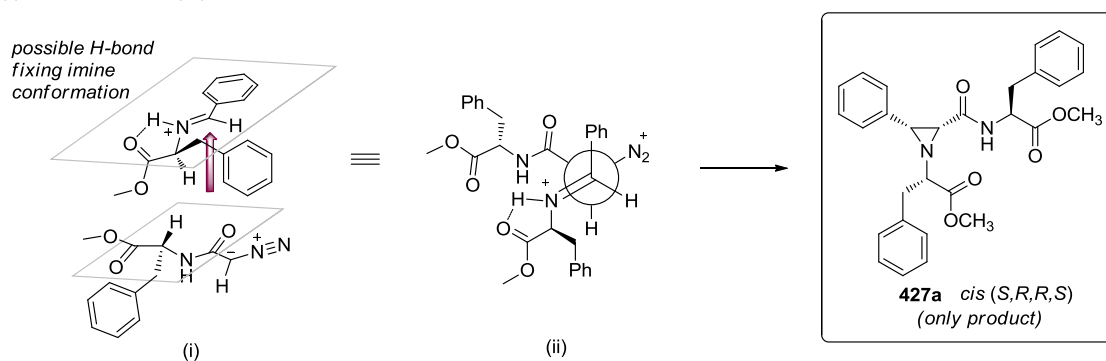
**Scheme 4.41** • Synthesis of pseudopeptide diastereomers **489** and **466** from phenyllactic acid derivatives **487** and **469**



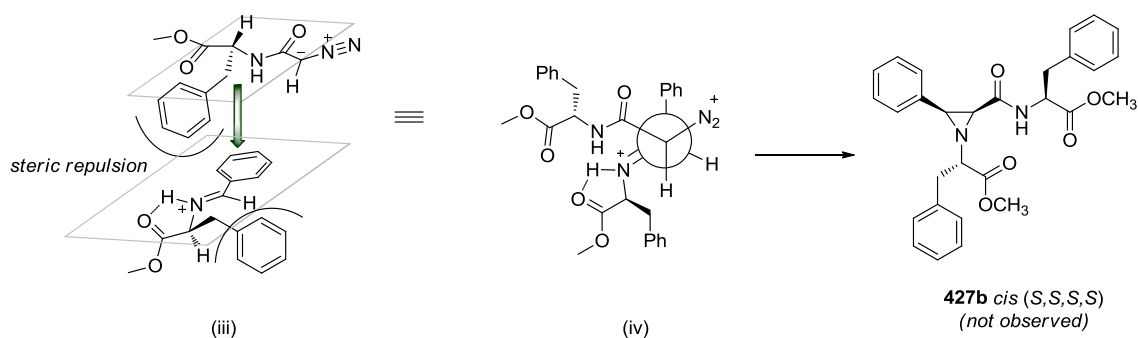
**Figure 4.15** • Partial  $^1\text{H}$ -NMR of the crude reaction mixture of hydrogenation of aziridine **427a** (top), pure diastereomer **466** (middle) and pure diastereomer **489** (bottom)

The impure reaction mixture of the aza-Darzens reaction for the synthesis of aziridine **427a** was submitted for hydrogenation by palladium on carbon in a vial pressurised with hydrogen (50 psi). Purification of **427a** by column chromatography was avoided to prevent enrichment of the diastereomeric ratio. The  $^1\text{H}$ -NMR spectrum of the impure hydrogenation reaction mixture was compared with the spectra of pure diastereomers **466** and **489** (Figure 4.15), and there is a clear match to (*S,R,S*) diastereomer **466**. The (*S,S,S*) diastereomer **489** is not visible in the  $^1\text{H}$ -NMR of the impure reaction mixture, indicating that the diastereoselectivity of the aziridination reaction is >99%. *Cis*-aziridine **427a** therefore has (*R,R*) stereochemistry at the chiral centres of the three-membered ring. A proposed mechanistic rationale for the formation of **427a** as the only product is presented in Figure 4.16.

a) Approach of the diazopeptide to the bottom face of the imine:



b) Approach of the diazopeptide to the top face of the imine:



**Figure 4.16** • Mechanistic rationale for the selective synthesis of *cis*-(*S,R,R,S*) diastereomer **427a** over *cis*-(*S,S,S,S*) **427b**

In Figure 4.16a (above), the *N*-diazopeptide is shown approaching the bottom face of the imine, in a suitable orientation for the addition of the diazo group to the protonated imine



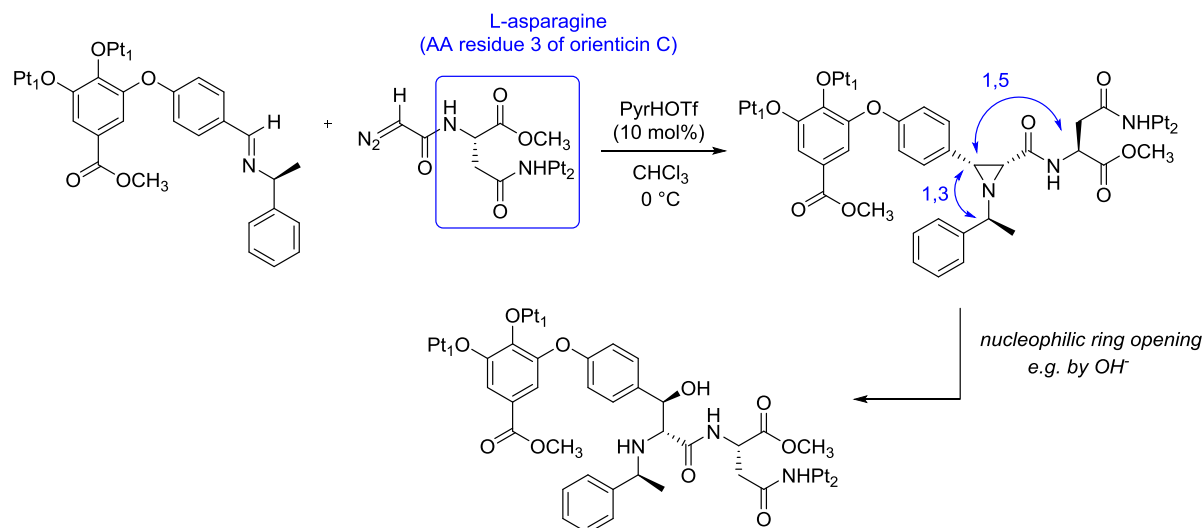
(as discussed in Section 4.1). In this proposed orientation of the two substrates (ii), the phenyl rings of the amino acid side chains are directed away from each other, minimising unfavourable steric interactions. Conversely, the approach of the diazo peptide to the top face of the imine in representations (iii) and (iv) brings the benzyl side chains into close proximity, leading to unfavourable steric interactions which prevent the formation of diastereomer **427b**.

### 4.3 Conclusions

The peptide aziridines described in this chapter were prepared by a previously unreported Bronsted acid-catalysed remote asymmetric induction methodology, achieving a 2:1 diastereomeric ratio in the 1,8-asymmetric induction which increased to 94:1 in the 1,5-induction, and >99:1 in the 1,3-induction, where only a single stereoisomer of the product was observed. The absolute stereochemistry of *cis*-aziridine **427** was established by hydrogenation of the three-membered ring to afford pseudopeptide **466**. It was revealed that the natural (*S*)-stereochemistry of the phenylalanine imine and diazoacetamide starting materials influenced the formation of the (*R,R*) stereochemistry in the aziridine product. This methodology therefore provides access not only to the synthesis of simple (*R,S*)-dipeptides, but also to the incorporation of unnatural, functionalised (*R*)-amino acid residues into an existing peptide chain, with potential applications in synthesis of the artificial cell structures discussed in Chapter 2.

#### 4.4 Future work

Taking the conclusions from the work described in chapters 3 and 4, the next step would be to apply the aza-Darzens remote asymmetric induction methodology to the synthesis of a glycopeptide antibiotic analogue. A proposed strategy is presented in Scheme 4.42, in which the (*S*)- $\alpha$ -methylbenzylamine group is employed as both a chiral auxiliary for 1,3-stereocontrol in the aza-Darzens reaction, and an easily cleaved nitrogen protecting group.



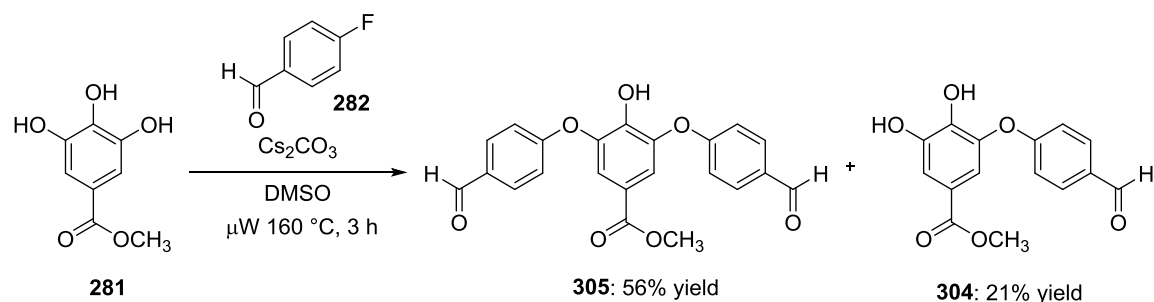
**Scheme 4.42** • Application of aza-Darzens remote asymmetric induction methodology to the synthesis of an orienticin C analogue

In order to further investigate the mechanism of the asymmetric aza-Darzens aziridination, it would be useful to establish the effect of different stereochemical configurations in the reaction substrates on the diastereoselectivity of the reaction. In the examples presented in Chapter 4, the (*S*)-amino acids were used exclusively to prepare both the imine and diazo peptide starting materials. This led to a mis-matched stereochemistry in the product, with *cis*-(*R,R*) configuration of the aziridine ring. Changing the configuration of the stereocentre in one or both of the substrates may produce the opposite diastereomer, or have a detrimental effect on the diastereoselectivity of the reaction, which may provide useful information about the competing or synergistic effect of combining 1,3- and 1,5- remote asymmetric induction in this context.

## EXPERIMENTAL SECTION

## General Information

Air and water-sensitive reactions were carried out under a nitrogen atmosphere and anhydrous conditions with magnetic stirring unless otherwise stated. Analytical thin-layer chromatography (TLC) was performed on Merck silica gel 60 F<sub>254</sub> plates (0.2 mm), with visualization by UV light and/or potassium permanganate stain followed by heating. Flash column chromatography was performed using Davisil silica gel 60 (40-63  $\mu$ m). <sup>1</sup>H- and <sup>13</sup>C-NMR spectra were recorded on a Bruker Avance spectrometer 500 (500 MHz), an Oxford Gemini 400 spectrometer (400 MHz) or an Oxford Gemini 300 spectrometer (300 MHz). Chemical shifts are reported in  $\delta$  (ppm) and referenced to residual solvent signals (<sup>1</sup>H-NMR: CDCl<sub>3</sub> at 7.26 ppm, CD<sub>3</sub>CN at 1.94 ppm; <sup>13</sup>C-NMR: CDCl<sub>3</sub> at 77.16 ppm, CD<sub>3</sub>CN at 1.32, 118.26 ppm). Signal multiplicities are described as follows: s = singlet, d = doublet, dd = doublet of doublets, t = triplet, q = quartet, m = multiplet, br = broad. FT-IR spectra were recorded on a Perkin Elmer Spectrum 100 spectrometer as thin films on sodium chloride plates and are reported in wavenumbers (cm<sup>-1</sup>). Optical rotations were measured using a Perkin Elmer 241 polarimeter with a 1 mL cell (path length 1 dm) and are reported as follows:  $[\alpha]_D^{T/^{\circ}\text{C}}$  concentration (c = g / 100 mL, solvent). MALDI-TOF mass spectra were recorded on a Shimadzu Axima-CFR spectrometer. High resolution mass spectrometry (HRMS) was carried out by the EPSRC National Mass Spectrometry Facility (Swansea, UK). Melting points of crystalline solids were recorded using a Stuart Scientific SMP1 apparatus (solvent of crystallization in brackets) and are uncorrected. Percentage yield refers to the isolated yield of analytically pure material unless otherwise stated. Dichloromethane was distilled from calcium hydride before use. Chloroform and *d*-chloroform were filtered through basic alumina and stored over 4Å molecular sieves. Tetrahydrofuran was distilled from sodium/benzophenone prior to use. All other solvents and reagents were purchased from commercial sources (Sigma-Aldrich, Alfa Aesar, Fluorochem and Fisher Scientific) and used as received.

**Methyl 3,5-bis(4-formylphenoxy)-4-hydroxybenzoate (305)****Synthesis A: Microwave irradiation**

To a 15 mL microwave vial under a nitrogen atmosphere was added methyl 3,4,5-trihydroxybenzoate **281** (500 mg, 2.72 mmol, 1 equiv.), cesium carbonate (2.41 g, 7.40 mmol, 2.7 equiv.) and a magnetic stirrer bar. Dimethyl sulfoxide (7 mL) was added, and the resulting mixture stirred vigorously for 10 minutes at room temperature before the addition of 4-fluorobenzaldehyde (0.93 mL, 8.69 mmol, 3.2 equiv.) *via* a 2.5 mL syringe. The vial was sealed with a PTFE-lined aluminium crimp cap and the dark red suspension heated at 160 °C in a Biotage microwave reactor for three hours, after which the reaction mixture was allowed to cool to room temperature and poured into a 250 mL separating funnel containing 1 M aqueous hydrochloric acid (50 mL). The aqueous mixture was extracted with ethyl acetate (2 x 50 mL) and the combined organic extracts were washed with distilled water (3 x 50 mL) and then brine (50 mL). The solution was dried over magnesium sulfate, filtered, and the solvent removed *in vacuo* to afford a dark brown residue. Purification *via* flash column chromatography on silica gel (eluent: dichloromethane / ethyl acetate 9:1;  $R_f$  = 0.30) afforded a pale yellow solid (600 mg, 1.53 mmol, 56% yield) whose physicochemical characteristics were consistent with those of the title compound (**305**).

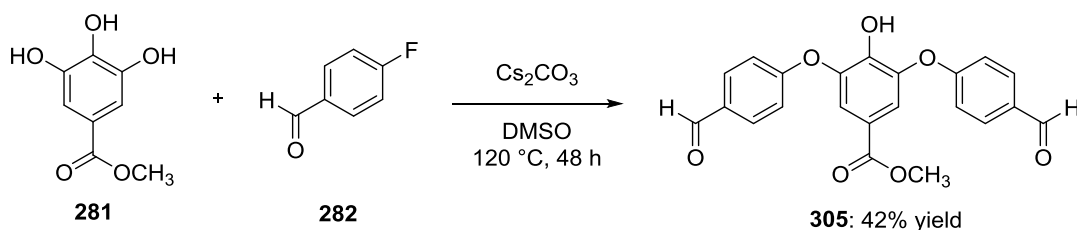
M.p. 161–162 °C;  $^1\text{H}$ -NMR (300 MHz,  $\text{CDCl}_3$ )  $\delta$  = 9.93 (s, 2H,  $-\text{CHO}$ ), 7.88 (d,  $J$  = 8.7 Hz, 4H, Ar- $H$ ), 7.62 (s, 2H, Ar- $H$ ), 7.13 (d, 4H,  $J$  = 8.8 Hz, Ar- $H$ ), 6.44 (s, 1H,  $-\text{OH}$ ), 3.84 (s, 3H,  $-\text{CO}_2\text{CH}_3$ );  $^{13}\text{C}$ -NMR (125 MHz,  $\text{CDCl}_3$ )  $\delta$  = 190.8 ( $-\text{CHO}$ ), 165.5 ( $-\text{CO}_2\text{CH}_3$ ), 161.8, 144.8, 143.1, 132.3(1), 132.2(7), 122.9, 119.1, 117.6, 52.6 ( $-\text{CO}_2\text{CH}_3$ ); FT-IR (ATR):  $\nu$  ( $\text{cm}^{-1}$ ) = 3079 (O-H), 2846 (C-H), 1692 (*ester* C=O), 1669 (*aldehyde* C=O), 1578, 1502, 1423, 1341, 1194; MS (MALDI-TOF):  $m/z$  414.82  $[\text{M}+\text{Na}]^+$ ; HRMS (APCI) exact mass calculated for  $\text{C}_{22}\text{H}_{17}\text{O}_7$  requires  $m/z$  393.0969, found  $m/z$  393.0965  $[\text{M}+\text{H}]^+$ .

A byproduct was isolated during the column chromatography ( $R_f = 0.60$ ; dichloromethane / methanol 2%); this was identified as methyl 3-(4-formylphenoxy)-4,5-dihydroxybenzoate **304** (165 mg, 0.57 mmol, 21% yield).

M.p. 191–193 °C (chloroform);  $^1\text{H-NMR}$  (300 MHz,  $\text{CD}_3\text{OD}$ )  $\delta = 9.87$  (s, 1H,  $-\text{CHO}$ ), 7.88 (d,  $J = 8.8$  Hz, 2H, Ar- $H$ ), 7.40 (d,  $J = 2.0$  Hz, 1H, Ar- $H$ ), 7.22 (d,  $J = 2.0$  Hz, 1H, Ar- $H$ ), 7.05 (d,  $J = 8.8$  Hz, 2H, Ar- $H$ ), 3.83 (s, 3H,  $-\text{CO}_2\text{CH}_3$ );  $^{13}\text{C-NMR}$  (125 MHz,  $\text{CD}_3\text{OD}$ )  $\delta = 192.8$  ( $-\text{CHO}$ ), 168.0 ( $-\text{CO}_2\text{CH}_3$ ), 164.7, 148.2, 144.3, 143.2, 133.0, 132.7, 122.2, 117.7, 116.0, 114.6, 52.5 ( $-\text{CO}_2\text{CH}_3$ ); FT-IR (thin film):  $\nu$  ( $\text{cm}^{-1}$ ) = 3217 (O-H), 1686 (C=O), 1593, 1504, 1439, 1319, 1224, 1156; MS (MALDI-TOF)  $m/z$  311.12  $[\text{M}+\text{Na}]^+$ ; HRMS (NESI) exact mass calculated for  $\text{C}_{15}\text{H}_{11}\text{O}_6$  requires  $m/z$  287.0561, found  $m/z$  287.0566  $[\text{M}-\text{H}]^-$ .

### Methyl 3,5-bis(4-formylphenoxy)-4-hydroxybenzoate (**305**)

Synthesis B: Conventional heating

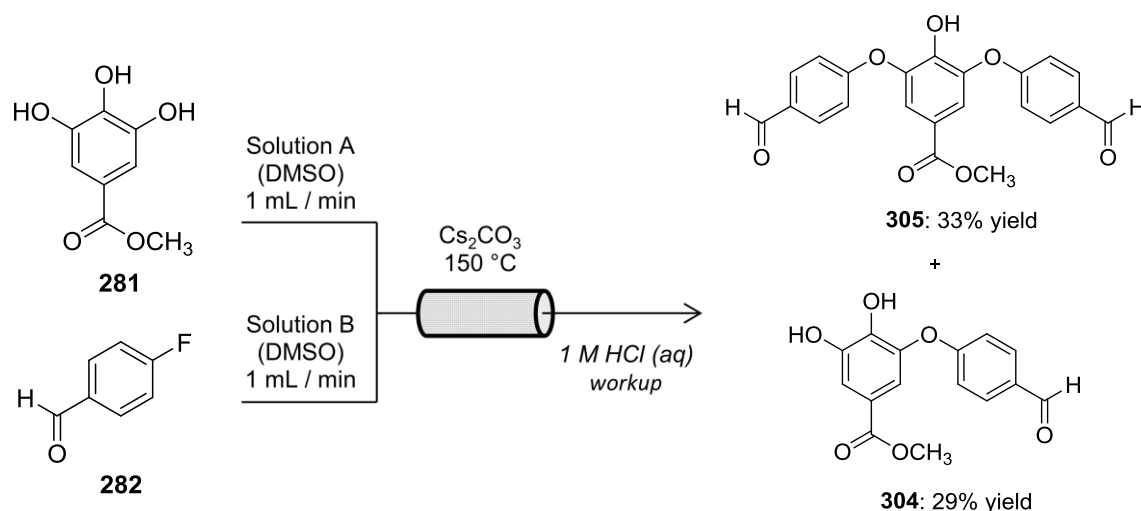


To a 500 mL two-necked round-bottom flask was added methyl 3,4,5-trihydroxybenzoate **281** (9.93 g, 53.9 mmol, 1 equiv.) and a magnetic stirrer bar. The white solid was dissolved in dimethyl sulfoxide (160 mL) under a nitrogen atmosphere. Cesium carbonate (52.7 g, 162 mmol, 3 equiv.) was added in one portion and the resulting mixture stirred at room temperature for 15 minutes before the addition of 4-fluorobenzaldehyde (14.4 mL, 135 mmol, 2.5 equiv.) *via* a 25 mL syringe. The flask was fitted with a reflux condenser and the reaction mixture heated at 120 °C for 48 hours using an aluminium heating block mounted on a hotplate magnetic stirrer. When no further conversion from **281** to **305** was observed by thin layer chromatography (eluent: dichloromethane / ethyl acetate 9:1), the reaction mixture was cooled to 0 °C, quenched with 1 M aqueous hydrochloric acid (200 mL) and poured into a 2 L separating funnel. The aqueous mixture was extracted with ethyl acetate (2 x 200 mL) and the combined organic extracts were washed with distilled water (3 x 300 mL) and then brine (250 mL). The solution was dried over magnesium sulfate, filtered, and the solvent removed *in vacuo* to afford a dark brown solid.

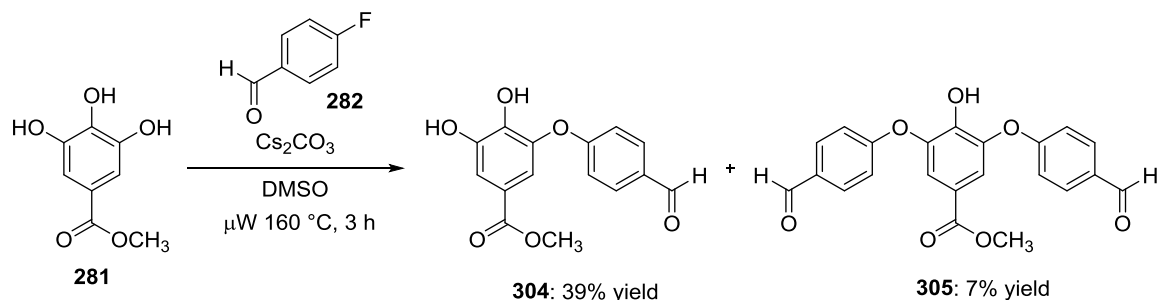
Trituration with diethyl ether afforded a cream solid (8.89 g, 22.7 mmol, 42% yield) whose physicochemical properties were consistent with those of the title compound (**305**) described previously.

### Methyl 3,5-bis(4-formylphenoxy)-4-hydroxybenzoate (**305**)

Synthesis C: Flow reactor

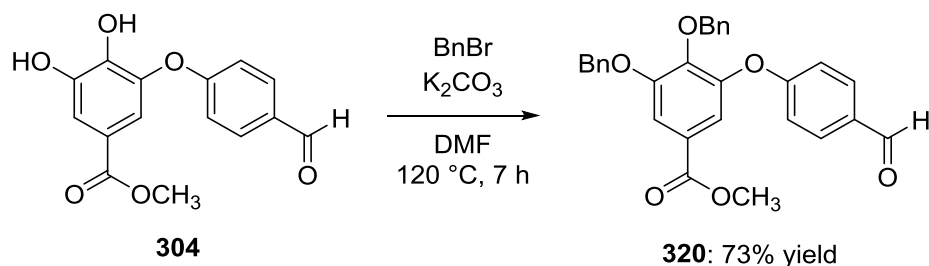


A Uniqsis Flow Syn reactor was fitted with a 6.6 x 100 mm glass column packed with cesium carbonate (5 g). The column was pre-heated to 150 °C. A solution of methyl 3,4,5-trihydroxybenzoate **281** (200 mg, 1.09 mmol, 1 equiv.) in dimethyl sulfoxide (2 mL), solution A, and a solution of 4-fluorobenzaldehyde **282** (0.4 mL, 2.78 mmol, 2.5 equiv.) in dimethyl sulfoxide (2 mL), solution B, were pumped simultaneously through the glass column, each with a flow rate of 1 mL / min. The dark red solution was collected in a 250 mL separating funnel containing 1 M hydrochloric acid (50 mL) at room temperature. The aqueous mixture was extracted with ethyl acetate (3 x 30 mL) and the combined organic layers were washed with distilled water (3 x 50 mL) and then brine (50 mL). The organic solution was dried over magnesium sulfate, filtered, and the solvent removed *in vacuo*. Purification *via* flash column chromatography on silica gel (eluent: dichloromethane / ethyl acetate 9:1) afforded **305** as a pale yellow solid (141 mg, 0.36 mmol, 33% yield) and **304** as a light brown solid (91 mg, 0.32 mmol, 29% yield). The physicochemical properties of these compounds matched the data obtained from the microwave-promoted synthesis outlined above.

**Methyl 3-(4-formylphenoxy)-4,5-dihydroxybenzoate (304)**

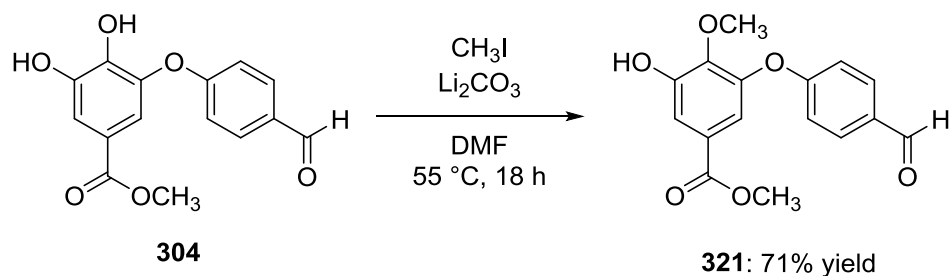
To a 15 mL microwave vial was added methyl 3,4,5-trihydroxybenzoate **281** (1 g, 5.43 mmol, 1 equiv.), cesium carbonate (3.89 g, 11.9 mmol, 2.2 equiv.) and a magnetic stirrer bar. The vial was purged with nitrogen, sealed with a PTFE-lined aluminium crimp cap and dimethyl sulfoxide (10 mL) was added *via* a 20 mL syringe. The resulting reaction mixture was stirred vigorously for 10 minutes at room temperature before the addition of 4-fluorobenzaldehyde (0.7 mL, 6.53 mmol, 1.2 equiv.) *via* a 2 mL syringe. The dark red suspension was heated to  $120^\circ\text{C}$  in a Biotage microwave reactor for 90 minutes. The reaction mixture was allowed to cool to room temperature and poured into a 250 mL separating funnel containing 1 M aqueous hydrochloric acid (50 mL). The aqueous mixture was extracted with ethyl acetate (2 x 50 mL) and the combined organic extracts were washed with distilled water (2 x 100 mL) and then brine (100 mL). The resulting solution was dried over magnesium sulfate, filtered, and the solvent removed *in vacuo* to afford a dark brown residue. Purification *via* flash column chromatography on silica gel (eluent: dichloromethane / ethyl acetate 9:1) afforded a yellow solid (603 mg, 2.09 mmol, 39% yield) whose physicochemical properties matched those of the title compound (**304**). Byproduct **305** was isolated in a 7% yield (149 mg, 0.38 mmol); the physicochemical properties were as outlined previously.



**Methyl 3,4-bis(benzyloxy)-5-(4-formylphenoxy)benzoate (320)**

To a 250 mL round-bottom flask containing methyl 3-(4-formylphenoxy)-4,5-dihydroxybenzoate **304** (333 mg, 1.16 mmol, 1 equiv.) under a nitrogen atmosphere was added *N,N*-dimethylformamide (35 mL) and a magnetic stirrer bar. Potassium carbonate (481 mg, 3.48 mmol, 3 equiv.) was added to the stirred orange solution in one portion, following by the addition of benzyl bromide (0.41 mL, 3.48 mmol, 3 equiv.) *via* a 1 mL syringe. The resulting suspension was heated to 120 °C for 7 hours. After cooling to room temperature, distilled water (30 mL) was added, followed by 1 M aqueous hydrochloric acid (40 mL). The mixture was extracted with ethyl acetate (2 x 50 mL) and the combined organic layers were washed with distilled water (2 x 100 mL) and then brine (100 mL) before being dried over magnesium sulfate, filtered, and the solvent removed *in vacuo*. Purification *via* flash column chromatography on silica gel (eluent: petroleum ether / diethyl ether 7:3;  $R_f$  = 0.20) afforded a cream solid whose physicochemical properties were consistent with those of the title compound **320** (398 mg, 0.85 mmol, 73% yield).

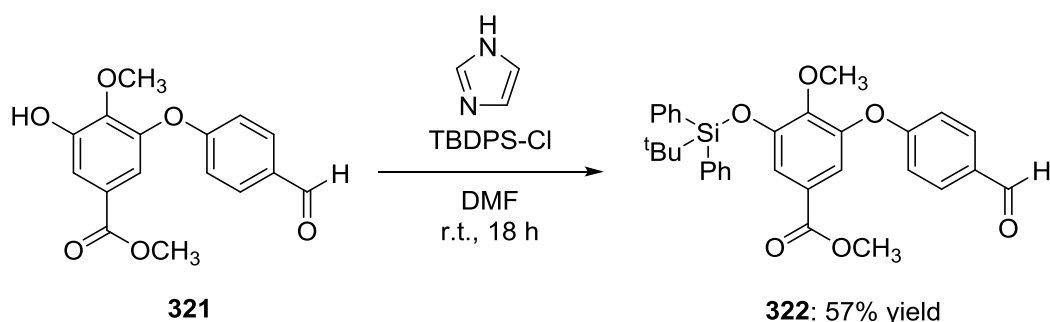
M.p. 88–90 °C (hexane / dichloromethane);  $^1\text{H-NMR}$  (400 MHz,  $\text{CDCl}_3$ )  $\delta$  9.91 (s, 1H, -CHO), 7.81 (d,  $J$  = 8.6 Hz, 2H, Ar-*H*), 7.62 (s, 1H, Ar-*H*), 7.49 – 7.33 (m, 6H, Ar-*H*), 7.24 – 7.14 (m, 5H, Ar-*H*), 6.96 (d,  $J$  = 8.6 Hz, 2H, Ar-*H*), 5.20 (s, 2H, -CH<sub>2</sub>Ph), 5.07 (s, 2H, -CH<sub>2</sub>Ph), 3.89 (s, 3H, -CO<sub>2</sub>CH<sub>3</sub>);  $^{13}\text{C-NMR}$  (126 MHz,  $\text{CDCl}_3$ )  $\delta$  190.9 (-CHO), 166.1 (-CO<sub>2</sub>CH<sub>3</sub>), 163.0, 153.3, 147.9, 144.8, 136.7, 136.2, 132.1, 131.5, 128.8, 128.5, 128.4, 128.3, 127.8, 126.0, 116.8, 116.8, 112.2, 75.4 (-CH<sub>2</sub>Ph), 71.5 (-CH<sub>2</sub>Ph), 52.5 (-CO<sub>2</sub>CH<sub>3</sub>); FT-IR (thin film):  $\nu$  (cm<sup>-1</sup>) = 3064 (O-H), 3033, 2952, 2736 (C-H), 1724 (C=O), 1697, 1584, 1503, 1427, 1341, 1220, 1157, 1076; MS (MALDI-TOF)  $m/z$  491.05 [M+Na]<sup>+</sup>, 507.00 [M+K]<sup>+</sup>; HRMS (HNESF) exact mass calculated for C<sub>29</sub>H<sub>25</sub>O<sub>6</sub> requires  $m/z$  469.1646, found  $m/z$  469.1642 [M+H]<sup>+</sup>.

**Methyl 3-(4-formylphenoxy)-5-hydroxy-4-methoxybenzoate (321)**

To a 15 mL microwave vial containing methyl 3-(4-formylphenoxy)-4,5-dihydroxybenzoate **304** (603 mg, 2.09 mmol, 1 equiv.) and a magnetic stirrer bar under a nitrogen atmosphere was added *N,N*-dimethylformamide (10 mL). To the stirred orange solution was added lithium carbonate (155 mg, 2.09 mmol, 1 equiv.) in one portion, followed by the addition of iodomethane (0.13 mL, 2.09 mmol, 1 equiv.) dropwise *via* a 1 mL syringe. The vial was sealed with a PTFE-lined aluminium crimp cap and heated to 55 °C for 18 hours using a sand bath. After cooling to room temperature the mixture was poured into a 250 mL separating funnel containing distilled water (20 mL), to which 1 M aqueous hydrochloric acid (50 mL) was added. The mixture was extracted with ethyl acetate (3 x 50 mL) and the combined organic layers were washed with distilled water (3 x 100 mL) and subsequently brine (100 mL). The organic solution was dried over magnesium sulfate, filtered, and the solvent removed *in vacuo*. Purification *via* flash column chromatography on silica gel (eluent: dichloromethane / diethyl ether 5%;  $R_f$  = 0.31) afforded an orange oil whose physicochemical properties were consistent with those of the title compound **321** (449 mg, 1.49 mmol, 71% yield).

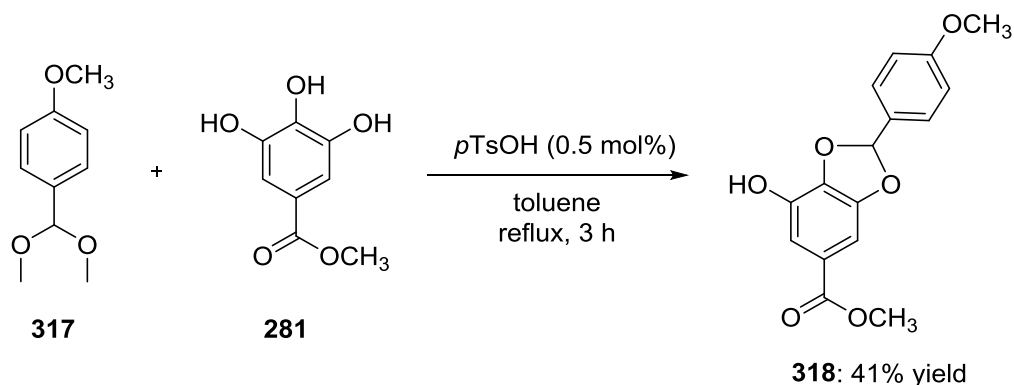
$^1\text{H-NMR}$  (500 MHz,  $\text{CDCl}_3$ )  $\delta$  9.94 (s, 1H,  $-\text{CHO}$ ), 7.87 (d,  $J$  = 8.8 Hz, 2H, Ar- $H$ ), 7.54 (d,  $J$  = 2.0 Hz, 1H, Ar- $H$ ), 7.32 (d,  $J$  = 2.0 Hz, 1H, Ar- $H$ ), 7.05 (d,  $J$  = 8.8 Hz, 2H, Ar- $H$ ), 5.94 (s, 1H,  $-\text{OH}$ ), 3.95 (s, 3H,  $-\text{OCH}_3$ ), 3.87 (s, 3H,  $-\text{OCH}_3$ );  $^{13}\text{C-NMR}$  (126 MHz,  $\text{CDCl}_3$ )  $\delta$  190.8 ( $-\text{CHO}$ ), 166.0 ( $-\text{CO}_2\text{CH}_3$ ), 162.4, 149.8, 145.9, 142.8, 132.2, 131.9, 126.3, 117.0, 115.7, 113.7, 61.6 (Ar- $\text{OCH}_3$ ), 52.5 ( $-\text{CO}_2\text{CH}_3$ ); FT-IR (thin film):  $\nu$  ( $\text{cm}^{-1}$ ) = 3384 (O-H), 2955, 2843 (C-H), 1709 (C=O), 1582, 1503, 1436, 1354, 1227, 1156; MS (MALDI-TOF)  $m/z$  325.03  $[\text{M}+\text{Na}]^+$ ; HRMS (NESI) exact mass calculated for  $\text{C}_{16}\text{H}_{15}\text{O}_6$   $[\text{M}+\text{H}]^+$  requires  $m/z$  303.0863, found  $m/z$  303.0866.

**Methyl 3-((*tert*-butyldiphenylsilyl)oxy)-5-(4-formylphenoxy)-4-methoxybenzoate (322)**



To a 5 mL round-bottom flask containing methyl 3-(4-formylphenoxy)-5-hydroxy-4-methoxybenzoate **321** (100 mg, 0.33 mmol, 1 equiv.) and a magnetic stirrer bar under a nitrogen atmosphere was added *N,N*-dimethylformamide (2 mL). To the stirred orange solution was added imidazole (50 mg, 0.73 mmol, 2.2 equiv.) in one portion, followed by the addition of *tert*-butyldiphenylchlorosilane (95  $\mu$ L, 0.36 mmol, 1.1 equiv.) *via* a 250  $\mu$ L syringe. The pale yellow solution was stirred at room temperature for 18 hours before being poured into a 50 mL separating funnel containing 5% aqueous sodium bicarbonate solution (10 mL) and the organics extracted with hexane (3 x 10 mL). The combined organic layers were washed with brine (30 mL), dried over magnesium sulfate, filtered, and the solvent removed *in vacuo*. Purification *via* flash column chromatography on silica gel (eluent: petroleum ether / diethyl ether 1:1;  $R_f$  = 0.56) afforded a colourless oil whose physicochemical properties were consistent with those of the title compound **322** (102 mg, 0.19 mmol, 57% yield).

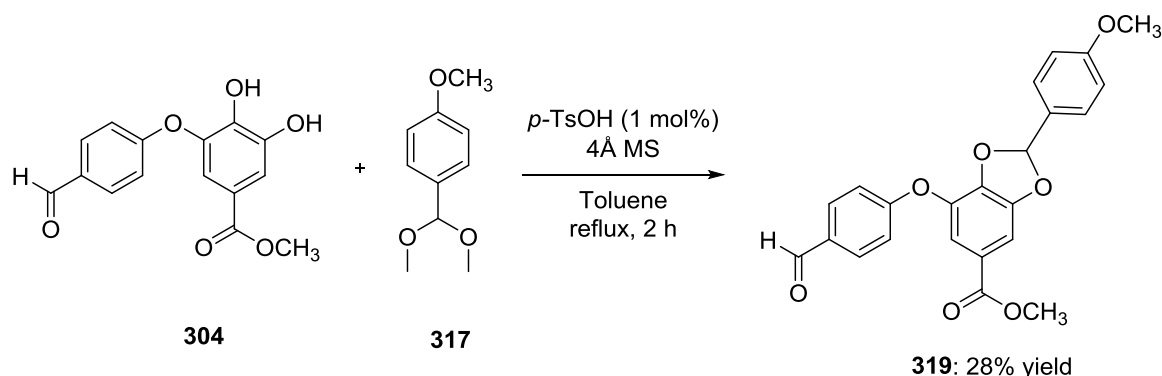
$^1\text{H-NMR}$  (500 MHz,  $\text{CDCl}_3$ )  $\delta$  9.91 (s, 1H,  $-\text{CHO}$ ), 7.80 (d,  $J$  = 8.6 Hz, 2H, Ar- $H$ ), 7.73 (d,  $J$  = 7.8 Hz, 4H, Ar- $H$ ), 7.46 (t,  $J$  = 7.4 Hz, 2H, Ar- $H$ ), 7.39 (t,  $J$  = 7.4 Hz, 4H, Ar- $H$ ), 7.36 – 7.31 (m, 2H, Ar- $H$ ), 6.83 (d,  $J$  = 8.6 Hz, 2H, Ar- $H$ ), 3.75 (s, 3H,  $-\text{CO}_2\text{CH}_3$ ), 3.65 (s, 3H,  $-\text{OCH}_3$ ), 1.14 (s, 9H,  $-\text{C}(\text{CH}_3)_3$ );  $^{13}\text{C-NMR}$  (126 MHz,  $\text{CDCl}_3$ )  $\delta$  190.8 ( $-\text{CHO}$ ), 165.8 ( $-\text{CO}_2\text{CH}_3$ ), 162.9, 149.9, 147.7, 147.3, 135.6, 132.4, 132.0, 131.3, 130.2, 127.9, 125.5, 119.6, 117.3, 116.4, 60.9 (Ar- $\text{OCH}_3$ ), 52.3 ( $-\text{CO}_2\text{CH}_3$ ), 26.7 ( $-\text{C}(\text{CH}_3)_3$ ), 19.8 ( $-\text{C}(\text{CH}_3)_3$ ); FT-IR (thin film):  $\nu$  ( $\text{cm}^{-1}$ ) = 3074 (C-H), 2956 (C-H), 2859 (C-H), 1726 (C=O), 1700 (C=O), 1603, 1582, 1506, 1430, 1345, 1227, 1155, 1109, 1071, 999; MS (MALDI-TOF)  $m/z$  579.28  $[\text{M}+\text{K}]^+$ ; HRMS (NESI) exact mass calculated for  $\text{C}_{32}\text{H}_{33}\text{O}_6\text{Si}$  requires  $m/z$  541.2041, found  $m/z$  541.2038  $[\text{M}+\text{H}]^+$ .

**Methyl 7-hydroxy-2-(4-methoxyphenyl)benzo[d][1,3]dioxole-5-carboxylate (**318**)**<sup>181</sup>

A flame-dried 250 mL two-necked round-bottom flask fitted with a Soxhlet apparatus containing 4Å molecular sieves was charged with a solution of *p*-anisaldehyde dimethyl acetal **317** (2.18 g, 12.0 mmol, 1.25 equiv.) in anhydrous toluene (100 mL) and a magnetic stirrer bar. Methyl gallate **281** (1.77 g, 9.60 mmol, 1 equiv.) and *para*-toluenesulfonic acid (8 mg, 0.046 mmol, 0.5 mol%) were added, and the solution heated at reflux for 3 hours. After cooling to room temperature the majority of the solvent was removed *in vacuo*. The residue was redissolved in dichloromethane (50 mL) and washed with saturated aqueous sodium carbonate solution (50 mL). The addition of hexane (50 mL) resulted in the precipitation of a pale yellow solid, which was filtered and recrystallised from dichloromethane / hexane (1:1) to afford a cream solid whose physicochemical properties matched those previously reported for this compound (1.20 g, 3.97 mmol, 41% yield).

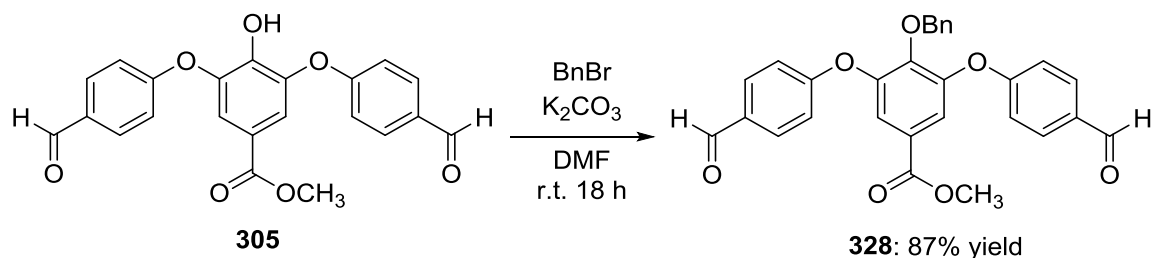
M.p. 130–132 °C (dichloromethane / hexane); <sup>1</sup>H-NMR (500 MHz, CDCl<sub>3</sub>) δ 7.50 (d, *J* = 8.8 Hz, 2H, Ar-*H*), 7.34 (d, *J* = 1.5 Hz, 1H, Ar-*H*), 7.18 (d, *J* = 1.5 Hz, 1H, Ar-*H*), 7.00 (s, 1H, -CH-), 6.96 (d, *J* = 8.8 Hz, 2H, Ar-*H*), 5.06 (s, 1H, -OH), 3.88 (s, 3H, -OCH<sub>3</sub>), 3.84 (s, 3H, -OCH<sub>3</sub>); FT-IR (thin film): ν (cm<sup>-1</sup>) = 3347 (O-H), 2920 (C-H), 2850 (C-H), 1696 (C=O), 1637, 1617, 1516, 1449, 1375, 1257, 1081; MS (MALDI-TOF) *m/z* 325.08 [M+Na]<sup>+</sup>.

**Methyl 7-(4-formylphenoxy)-2-(4-methoxyphenyl)benzo[d][1,3]dioxole-5-carboxylate (319)**



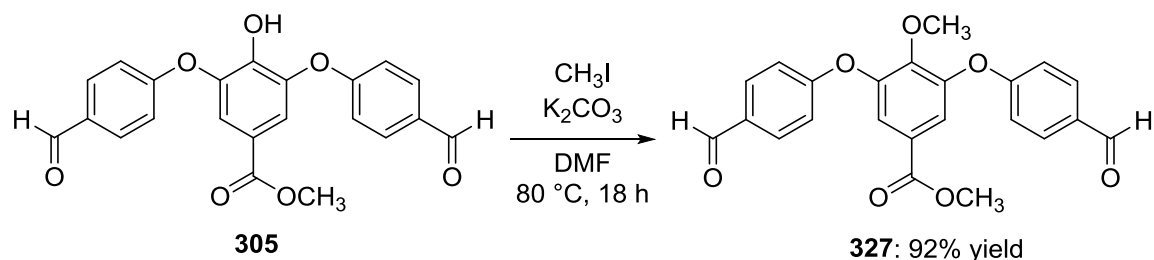
A 15 mL microwave vial containing 4Å molecular sieves was flame-dried and allowed to cool to room temperature under a flow of nitrogen. Methyl 3-(4-formylphenoxy)-4,5-dihydroxybenzoate **304** (100 mg, 0.347 mmol, 1 equiv.), anhydrous toluene (7 mL), *para*-anisaldehyde dimethyl acetal<sup>182</sup> **317** (66 mg, 0.364 mmol, 1.05 equiv.), and *para*-toluenesulfonic acid (0.7 mg, 0.0035 mmol, 1 mol%) were added. The vial was sealed with a PTFE-lined aluminium crimp cap and the stirred suspension was heated at 110 °C for 6 hours. After cooling to room temperature, sodium carbonate (0.4 mg, 0.0038 mmol, 1.09 mol%) was added and the mixture stirred at room temperature for one hour before being filtered to remove the molecular sieves. The solvent was removed *in vacuo*, and purification *via* flash column chromatography on silica gel (eluent: dichloromethane 100%;  $R_f$  = 0.30) afforded a pale yellow solid whose physicochemical properties were consistent with those of the title compound **319** (20 mg, 0.049 mmol, 28% yield).

M.p. 76–78 °C;  $^1\text{H-NMR}$  (400 MHz,  $\text{CDCl}_3$ )  $\delta$  9.93 (s, 1H,  $-\text{CHO}$ ), 7.85 (d,  $J$  = 8.7 Hz, 2H, Ar- $H$ ), 7.48 (d,  $J$  = 1.5 Hz, 1H, Ar- $H$ ), 7.46 – 7.40 (m, 3H, Ar- $H$ ), 7.09 (d,  $J$  = 8.7 Hz, 2H, Ar- $H$ ), 7.05 (s, 1H, Ar- $H$ ), 6.93 (d,  $J$  = 8.7 Hz, 2H, Ar- $H$ ), 3.88 (s, 3H,  $-\text{CO}_2\text{CH}_3$ ), 3.83 (s, 3H,  $-\text{OCH}_3$ );  $^{13}\text{C-NMR}$  (126 MHz,  $\text{CDCl}_3$ )  $\delta$  190.8 ( $-\text{CHO}$ ), 165.9 ( $-\text{CO}_2\text{CH}_3$ ), 162.0, 161.6, 150.1, 142.8, 136.5, 132.1, 131.8, 128.1, 127.0, 125.0, 118.4, 117.0, 114.2, 112.8, 106.9, 55.5 ( $-\text{OCH}_3$ ), 52.5 ( $-\text{CO}_2\text{CH}_3$ ); FT-IR (thin film):  $\nu$  ( $\text{cm}^{-1}$ ) = 3076 (C-H), 3011 (C-H), 2949 (C-H), 2843 (C-H), 2733 (C-H), 1717 (*ester* C=O), 1696 (*aldehyde* C=O), 1614, 1600, 1518, 1500, 1442, 1367, 1301, 1253, 1222, 1178, 1157, 1020, 1006; MS (MALDI-TOF)  $m/z$  405.25  $[\text{M-H}]^-$ ; HRMS (HNESP) exact mass calculated for  $\text{C}_{23}\text{H}_{19}\text{O}_7$  requires  $m/z$  407.1125, found  $m/z$  407.1128  $[\text{M+H}]^+$ .

**Methyl 4-(benzyloxy)-3,5-bis(4-formylphenoxy)benzoate (328)**

A 250 mL round-bottom flask was charged with a solution of methyl 3,5-bis(4-formylphenoxy)-4-hydroxybenzoate **305** (3.01 g, 7.65 mmol, 1 equiv.) in *N,N*-dimethylformamide (50 mL) under a nitrogen atmosphere. Potassium carbonate (712 mg, 11.5 mmol, 1.5 equiv.) was added in one portion, followed by the addition of benzyl bromide (0.91 mL, 7.65 mmol, 1 equiv.) *via* a 2 mL syringe. The mixture was stirred at room temperature for 18 hours before being transferred to a 250 mL separating funnel containing 1 M aqueous hydrochloric acid (100 mL). The organics were extracted with ethyl acetate (3 x 75 mL). The combined organic layers were washed with water (3 x 100 mL) and subsequently brine (100 mL). The organic layer was dried over magnesium sulfate, filtered, and the solvent removed *in vacuo*. Purification *via* flash column chromatography on silica gel (eluent: petroleum ether / ethyl acetate 30%;  $R_f$  0.38) afforded a pale yellow solid whose physicochemical characteristics were consistent with those of the title compound (**328**) (3.21 g, 6.64 mmol, 87% yield).

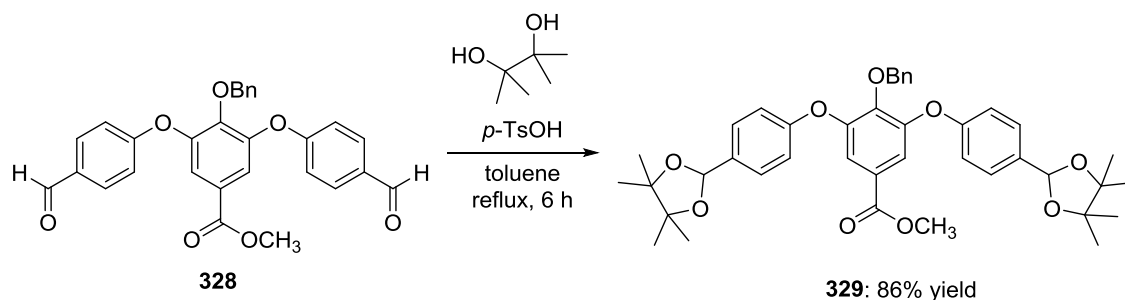
M.p. 80–82 °C;  $^1\text{H-NMR}$  (400 MHz,  $\text{CDCl}_3$ )  $\delta$  9.94 (s, 2H, -CHO), 7.86 (d,  $J$  = 8.8 Hz, 4H, Ar-*H*), 7.66 (s, 2H, Ar-*H*), 7.23 – 7.13 (m, 3H, Ar-*H*), 7.06 – 6.99 (m, 6H, Ar-*H*), 5.05 (s, 2H, -CH<sub>2</sub>Ph), 3.87 (s, 3H, -OCH<sub>3</sub>);  $^{13}\text{C NMR}$  (100 MHz,  $\text{CDCl}_3$ )  $\delta$  190.8 (-CHO), 165.3 (-CO<sub>2</sub>CH<sub>3</sub>), 162.3, 148.7, 147.2, 135.9, 132.2, 132.0, 128.6, 128.5, 128.3, 126.6, 120.5, 117.1, 75.7 (-CH<sub>2</sub>Ph), 52.7 (-CO<sub>2</sub>CH<sub>3</sub>); FT-IR (thin film):  $\nu$  (cm<sup>-1</sup>) = 3069 (C-H), 2956 (C-H), 2835 (C-H), 2745 (C-H), 1724 (d) (*ester and aldehyde C=O*), 1602, 1503, 1422, 1337, 1229, 1157; MS (MALDI-TOF)  $m/z$  505.0 [M+Na]<sup>+</sup>, 520.96 [M+K]<sup>+</sup>; HRMS (NESP) exact mass calculated for C<sub>29</sub>H<sub>22</sub>O<sub>7</sub>Na requires  $m/z$  505.1258, found  $m/z$  505.1250 [M+Na]<sup>+</sup>.

**Methyl 3,5-bis(4-formylphenoxy)-4-methoxybenzoate (327)**

To a 15 mL microwave vial was added methyl 3,5-bis(4-formylphenoxy)-4-hydroxybenzoate **305** (500 mg, 1.27 mmol, 1 equiv.), potassium carbonate (352 mg, 2.55 mmol, 2 equiv.) and a magnetic stirrer bar. *N,N'*-Dimethylformamide (6 mL) was added and the vial sealed with a PTFE-lined aluminium crimp cap. The suspension was stirred at room temperature for 15 minutes. Iodomethane (111  $\mu\text{L}$ , 1.78 mmol, 1.4 equiv.) was added *via* a 250  $\mu\text{L}$  syringe, and the mixture heated at 80  $^{\circ}\text{C}$  for 24 hours. After cooling to room temperature, the suspension was poured into a 250 mL separating funnel containing ethyl acetate (50 mL) and 1 M aqueous hydrochloric acid (50 mL). The aqueous layer was re-extracted with ethyl acetate (50 mL) and the combined organic layers were washed with distilled water (2 x 100 mL) and subsequently brine (100 mL) before being dried over magnesium sulfate and filtered. The solvent was removed *in vacuo* to afford a yellow oil whose physicochemical characteristics were consistent with those of the title compound (**327**) (478 mg, 1.18 mmol, 92%). **327** was used without further purification.

$^1\text{H}$ -NMR (500 MHz,  $\text{CDCl}_3$ )  $\delta$  9.94 (s, 2H,  $-\text{CHO}$ ), 7.88 (d,  $J = 8.7$  Hz, 4H, Ar- $H$ ), 7.68 (s, 2H, Ar- $H$ ), 7.07 (d,  $J = 8.7$  Hz, 4H, Ar- $H$ ), 3.88 (s, 3H,  $-\text{OCH}_3$ ), 3.78 (s, 3H,  $-\text{OCH}_3$ );  $^{13}\text{C}$ -NMR (126 MHz,  $\text{CDCl}_3$ )  $\delta$  190.7 ( $-\text{CHO}$ ), 165.3 ( $-\text{CO}_2\text{CH}_3$ ), 162.5, 148.7, 148.1, 132.2, 131.9, 126.2, 120.8, 117.0, 61.5 ( $-\text{OCH}_3$ ), 52.7 ( $-\text{CO}_2\text{CH}_3$ ); FT-IR (thin film):  $\nu$  ( $\text{cm}^{-1}$ ) = 2955 (C-H), 2836 (C-H), 2738 (C-H), 1727 (*ester* C=O), 1697 (*aldehyde* C=O), 1602, 1579, 1503, 1421, 1335, 1223, 1156; MS (MALDI-TOF)  $m/z$  429.2  $[\text{M}+\text{Na}]^+$ , 445.21  $[\text{M}+\text{K}]^+$ ; HRMS (NESP) exact mass calculated for  $\text{C}_{23}\text{H}_{19}\text{O}_7$  requires  $m/z$  407.1125, found  $m/z$  407.1125  $[\text{M}+\text{H}]^+$ .

**Methyl 4-(benzyloxy)-3,5-bis(4-(4,4,5,5-tetramethyl-1,3-dioxolan-2-yl)phenoxy)benzoate (**329**)**

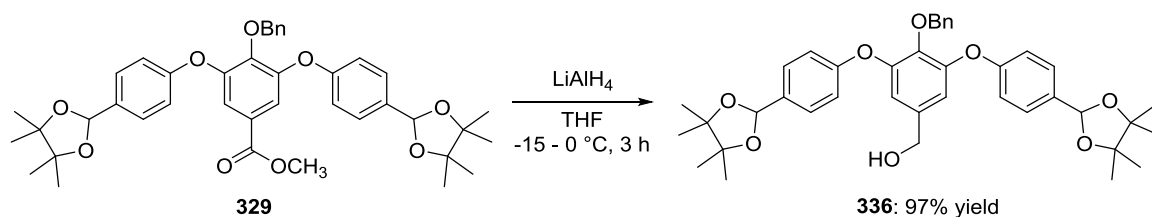


A 100 mL two-neck round-bottom flask was charged with a solution of methyl 4-(benzyloxy)-3,5-bis(4-formylphenoxy)benzoate **328** (1.0 g, 2.55 mmol, 1 equiv.) in dry toluene (40 mL). The flask was fitted with a Dean-Stark apparatus and reflux condenser under a nitrogen atmosphere. Pinacol (692 mg, 5.86 mmol, 2.3 equiv.) and *para*-toluenesulfonic acid (20 mg, 0.11 mmol, 5 mol%) were added, and the solution heated at reflux for 6 hours. After cooling to room temperature, triethylamine (0.1 mL, 0.72 mmol, 0.3 equiv.) was added *via* a 1 mL syringe and the solution was stirred for a further 30 minutes before the solvent was removed *in vacuo*. Purification *via* flash column chromatography on silica gel (eluent: petroleum ether / diethyl ether 1:1;  $R_f$  = 0.58) afforded a white solid whose physicochemical properties were consistent with those of the title compound (**329**) (1.50 g, 2.19 mmol, 86% yield).

M.p. 132–134 °C;  $^1\text{H-NMR}$  (500 MHz,  $\text{CDCl}_3$ )  $\delta$  7.47 (d,  $J$  = 8.7 Hz, 4H, Ar-*H*), 7.41 (s, 2H, Ar-*H*), 7.24 – 7.16 (m, 5H, Ar-*H*), 6.96 (d,  $J$  = 8.7 Hz, 4H, Ar-*H*), 5.98 (s, 2H, -*CH-pin.*), 5.12 (s, 2H, - $\text{CH}_2\text{Ph}$ ), 3.80 (s, 3H, - $\text{CO}_2\text{CH}_3$ ), 1.33 (s, 12H, - $\text{C}(\text{CH}_3)_2$ -), 1.30 (s, 12H, - $\text{C}(\text{CH}_3)_2$ -);  $^{13}\text{C-NMR}$  (126 MHz,  $\text{CDCl}_3$ )  $\delta$  165.8 (- $\text{CO}_2\text{CH}_3$ ), 157.4, 150.3, 146.0, 136.6, 134.9, 128.6, 128.3, 128.2, 128.2, 125.8, 117.8, 117.4, 99.7 (-*CH-pin.*), 82.8 (- $\text{C}(\text{CH}_3)_2$ -), 75.3 (- $\text{CH}_2\text{Ph}$ ), 52.3 (- $\text{CO}_2\text{CH}_3$ ), 24.6 (- $\text{C}(\text{CH}_3)_2$ -), 22.3 (- $\text{C}(\text{CH}_3)_2$ -); FT-IR (thin film):  $\nu$  ( $\text{cm}^{-1}$ ) = 2980 (C-H), 2932 (C-H), 2877 (C-H), 1727 (C=O), 1614, 1583, 1504, 1453, 1425, 1391, 1380, 1373, 1332, 1222, 1157, 1075, 1040, 1006; MS (MALDI-TOF)  $m/z$  681.7; HRMS (HNESP) exact mass calculated for  $\text{C}_{41}\text{H}_{50}\text{O}_9$  requires  $m/z$  700.3480, found  $m/z$  700.3496 [ $\text{M}+\text{NH}_4$ ] $^+$ .



**(4-(Benzyloxy)-3,5-bis(4-(4,4,5,5-tetramethyl-1,3-dioxolan-2-yl)phenoxy)phenyl) methanol (336)**

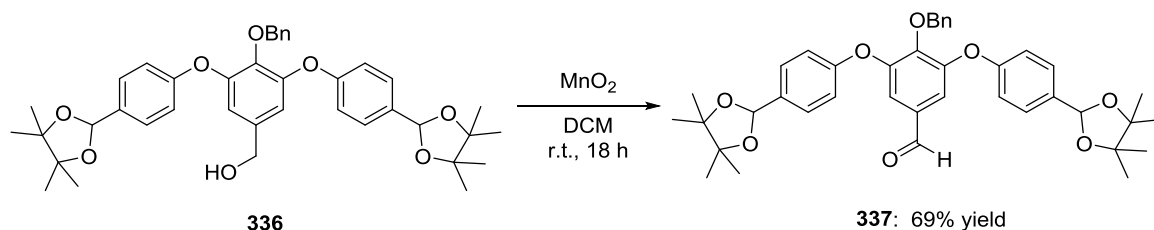


To a flame-dried 250 mL round-bottom flask was added lithium aluminium hydride (118 mg, 3.11 mmol, 2.5 equiv.) and dry tetrahydrofuran (40 mL) under a nitrogen atmosphere. The mixture was cooled to  $-15\text{ }^\circ\text{C}$  using an acetone / dry ice bath before a solution of methyl 4-(benzyloxy)-3,5-bis(4-(4,4,5,5-tetramethyl-1,3-dioxolan-2-yl)phenoxy)benzoate **329** (2.62 g, 4.56 mmol, 1 equiv.) in tetrahydrofuran (15 mL) was added dropwise *via* a 20 mL syringe. The mixture was allowed to warm to  $0\text{ }^\circ\text{C}$  and stirred for 2 hours. On complete disappearance of the starting material by thin layer chromatography (petroleum ether / diethyl ether 1:1), ethyl acetate (50 mL) and 1 M aqueous sodium hydroxide (50 mL) were added simultaneously in small portions while maintaining the temperature at  $0\text{ }^\circ\text{C}$ . The reaction mixture was transferred to a 500 mL separating funnel and the aqueous phase extracted with ethyl acetate (2 x 75 mL). The combined organic phases were washed with brine (150 mL), dried over magnesium sulfate, filtered, and the solvent removed *in vacuo* to afford a colourless oil whose physicochemical properties were consistent with those of the title compound (**336**) (2.42 g, 4.42 mmol, 97% yield); no further purification was required.

$R_f = 0.21$  (eluent: petroleum ether / diethyl ether 1:1);  $^1\text{H-NMR}$  (500 MHz,  $\text{CDCl}_3$ )  $\delta$  7.46 (d,  $J = 8.6\text{ Hz}$ , 4H, Ar-*H*), 7.22 – 7.15 (m, 5H, Ar-*H*), 6.97 (d,  $J = 8.6\text{ Hz}$ , 4H, Ar-*H*), 6.73 (s, 2H, Ar-*H*), 5.97 (s, 2H, -CH- *pin.*), 5.01 (s, 2H, -CH<sub>2</sub>Ph), 4.48 (s, 2H, -CH<sub>2</sub>OH), 1.33 (s, 12H, -C(CH<sub>3</sub>)<sub>2</sub>-), 1.29 (s, 12H, -C(CH<sub>3</sub>)<sub>2</sub>-);  $^{13}\text{C-NMR}$  (126 MHz,  $\text{CDCl}_3$ )  $\delta$  157.7, 150.8, 141.1, 137.2, 137.0, 134.5, 128.6, 128.3, 128.1, 128.1, 117.9, 114.4, 99.8 (-CH- *pin.*), 82.8 (-C(CH<sub>3</sub>)<sub>2</sub>-), 75.4 (-CH<sub>2</sub>Ph), 64.5 (-CH<sub>2</sub>OH), 24.6 (-C(CH<sub>3</sub>)<sub>2</sub>-), 22.3 (-C(CH<sub>3</sub>)<sub>2</sub>-); FT-IR (thin film):  $\nu$  ( $\text{cm}^{-1}$ ) = 3458 (O-H), 2984 (C-H), 2932 (C-H), 2877 (C-H), 1610, 1586, 1507, 1435, 1370, 1322, 1219, 1154, 1075, 1034, 989; MS (MALDI-TOF)  $m/z$

693.12  $[M+K]^+$ ; HRMS (HNESP) exact mass calculated for  $C_{40}H_{50}O_8N$  requires  $m/z$  672.3530, found  $m/z$  672.3531  $[M+NH_4]^+$ .

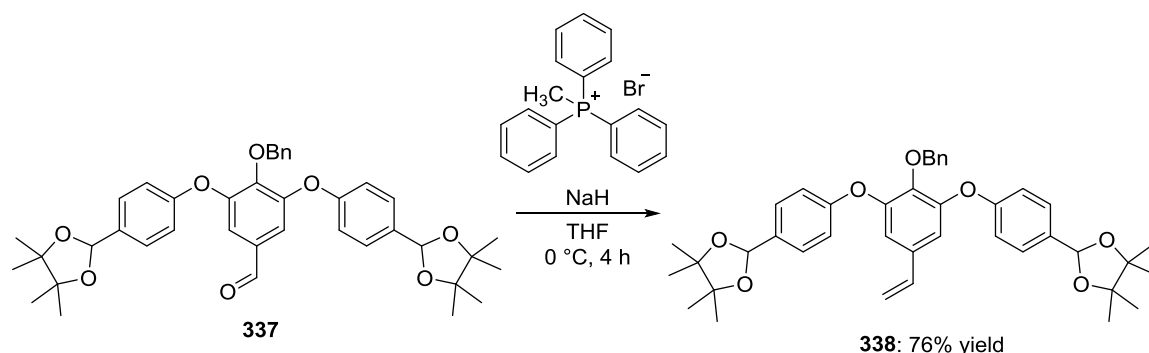
#### 4-(Benzyloxy)-3,5-bis(4-(dimethoxymethyl)phenoxy)benzaldehyde (**337**)



A 250 mL round-bottom flask was charged with a solution of 4-(benzyloxy)-3,5-bis(4-(dimethoxymethyl)phenoxy)benzyl alcohol **336** (447 mg, 0.68 mmol, 1 equiv.) in anhydrous dichloromethane (50 mL) under a nitrogen atmosphere. Activated manganese dioxide (1.19 g, 13.7 mmol, 20 equiv.) was added in small portions and the mixture stirred at room temperature for 18 hours. On complete disappearance of starting material **336** by thin layer chromatography (eluent: petroleum ether / ethyl acetate 20%), the mixture was filtered through celite and the solvent removed *in vacuo*. Purification *via* flash column chromatography on silica gel (eluent: petroleum ether / ethyl acetate 20%;  $R_f$  = 0.38) afforded a white solid whose physicochemical characteristics were consistent with those of the title compound **337** (307 mg, 0.47 mmol, 69% yield).

M.p. 118–120 °C;  $^1H$ -NMR (500 MHz,  $CDCl_3$ )  $\delta$  9.70 (s, 1H, -CHO), 7.49 (d,  $J$  = 8.6 Hz, 4H, Ar-*H*), 7.25 – 7.22 (m, 5H, Ar-*H*), 7.20 (s, 2H, Ar-*H*), 6.98 (d,  $J$  = 8.6 Hz, 4H, Ar-*H*), 5.98 (s, 2H, -CH- *pin.*), 5.19 (s, 2H, -CH<sub>2</sub>Ph), 1.34 (s, 12H, -C(CH<sub>3</sub>)<sub>2</sub>-), 1.29 (s, 12H, -C(CH<sub>3</sub>)<sub>2</sub>-);  $^{13}C$ -NMR (126 MHz,  $CDCl_3$ )  $\delta$  189.7 (-CHO), 156.7, 151.1, 146.6, 136.3, 135.2, 131.8, 128.4, 128.2, 128.1(1), 128.0(5), 117.9, 116.3, 99.3 (-CH- *pin.*), 82.6 (-C(CH<sub>3</sub>)<sub>2</sub>-), 75.2 (-CH<sub>2</sub>Ph), 24.3 (-C(CH<sub>3</sub>)<sub>2</sub>-), 22.1 (-C(CH<sub>3</sub>)<sub>2</sub>-); FT-IR (thin film):  $\nu$  (cm<sup>-1</sup>) = 2977 (C-H), 2936 (C-H), 2864 (C-H), 1696 (C=O), 1614, 1579, 1507, 1435, 1377, 1325, 1222, 1150, 1119, 1075, 1044; MS (MALDI-TOF)  $m/z$  691.44  $[M+K]^+$ ; HRMS (HNESP) exact mass calculated for  $C_{40}H_{48}O_8N$  requires  $m/z$  670.3374, found  $m/z$  670.3390  $[M+NH_4]^+$ .

**4,4'-((2-(Benzyloxy)-5-vinyl-1,3-phenylene)bis(oxy))bis((dimethoxymethyl)benzene) (338)**

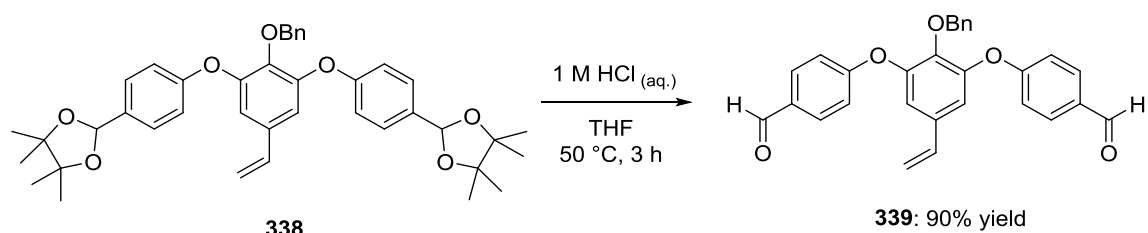


A 250 mL round-bottom flask under a nitrogen atmosphere was charged with methyl triphenylphosphonium bromide (1.09 g, 3.06 mmol, 4 equiv.) and tetrahydrofuran (40 mL). The suspension was stirred while being cooled to 0 °C in an ice bath before the addition of sodium hydride (60 % in mineral oil, 122 mg, 3.06 mmol, 4 equiv.). After 1 hour, a solution of 4-(benzyloxy)-3,5-bis(4-(dimethoxymethyl)phenoxy)benzaldehyde **337** (500 mg, 0.77 mmol, 1 equiv.) in tetrahydrofuran (10 mL) was added dropwise to the flask *via* a 20 mL syringe, and the resulting mixture stirred at 0 °C for a further 3 hours or until complete disappearance of the starting material by thin layer chromatography (eluent: petroleum ether / ethyl acetate 20%). Diethyl ether (75 mL) was added, and the mixture transferred to a 500 mL separating funnel containing cold distilled water (100 mL). The aqueous phase was extracted with diethyl ether (2 x 100 mL) and the combined organic layers washed with brine (150 mL) before being dried over magnesium sulfate, filtered, and the solvent removed *in vacuo*. Purification *via* flash column chromatography on silica gel (eluent: petroleum ether / ethyl acetate 20%;  $R_f$  = 0.53) afforded a white solid whose physicochemical properties were consistent with those of the title compound **338** (379 mg, 0.58 mmol, 76% yield).

M.p. 116–118 °C;  $^1\text{H-NMR}$  (500 MHz,  $\text{CDCl}_3$ )  $\delta$  7.46 (d,  $J$  = 8.6 Hz, 4H, Ar-*H*), 7.23 – 7.11 (m, 5H, Ar-*H*), 6.97 (d,  $J$  = 8.6 Hz, 4H, Ar-*H*), 6.81 (s, 2H, Ar-*H*), 6.47 (dd,  $J$  = 17.5, 11.0 Hz, 1H, -CH=CH<sub>2</sub>), 5.97 (s, 2H, -CH- *pin.*), 5.51 (dd,  $J$  = 17.5, 0.4 Hz, 1H, -CH=CH<sub>2</sub>), 5.16 (d,  $J$  = 11.0 Hz, 1H, -CH=CH<sub>2</sub>), 5.00 (s, 2H, -CH<sub>2</sub>Ph), 1.33 (s, 12H, -CH(CH<sub>3</sub>)<sub>2</sub>-), 1.29 (s, 12H, -CH(CH<sub>3</sub>)<sub>2</sub>-);  $^{13}\text{C-NMR}$  (126 MHz,  $\text{CDCl}_3$ )  $\delta$  157.9, 150.5, 141.8, 137.0, 135.4, 134.4, 133.9, 128.6, 128.3, 128.1, 128.0, 117.6, 114.5, 114.3, 99.8 (-CH- *pin.*), 82.8 (-C(CH<sub>3</sub>)<sub>2</sub>-), 75.4 (-CH<sub>2</sub>Ph), 24.6 (-CH(CH<sub>3</sub>)<sub>2</sub>-), 22.3 (-CH(CH<sub>3</sub>)<sub>2</sub>-); FT-

IR (thin film):  $\nu$  ( $\text{cm}^{-1}$ ) = 2983 (C-H), 2928 (C-H), 2855 (C-H), 1610, 1569, 1503, 1428, 1410, 1390, 1321, 1228, 1155, 1076, 1031, 990; MS (MALDI-TOF)  $m/z$  689.69  $[\text{M}+\text{K}]^+$ ; HRMS (HNESF) exact mass calculated for  $\text{C}_{41}\text{H}_{50}\text{O}_7\text{N}$  requires  $m/z$  668.3582, found  $m/z$  668.3581  $[\text{M}+\text{NH}_4]^+$ .

**4,4'-(2-(Benzyloxy)-5-vinyl-1,3-phenylene)bis(oxy)dibenzaldehyde (339)**

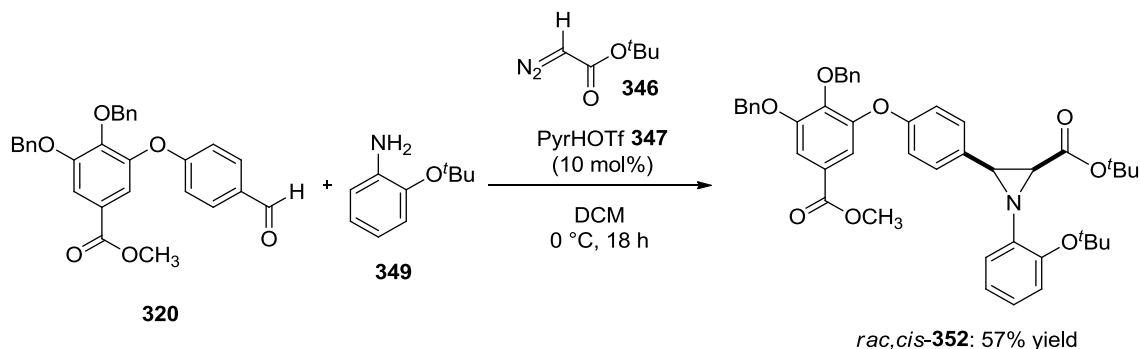


A 5 mL microwave vial was charged with a colourless solution of 4,4'-((2-(benzyloxy)-5-vinyl-1,3-phenylene)bis(oxy))bis((dimethoxymethyl)benzene) **338** (50 mg, 0.08 mmol, 1 equiv.) in tetrahydrofuran (1 mL). 1 M aqueous hydrochloric acid (1 mL) was added, and the solution was heated at 50 °C with stirring for 3 hours. On complete disappearance of the starting material by thin layer chromatography (eluent: petroleum ether / ethyl acetate 20%), the organic solvent was removed *in vacuo* and the residue extracted with dichloromethane (3 x 5 mL). The combined organic layers were washed with brine (20 mL) before being dried over magnesium sulfate, filtered, and the solvent removed *in vacuo*. Purification *via* flash column chromatography on silica gel (eluent: petroleum ether / diethyl ether 50%;  $R_f$  = 0.31) afforded a white solid whose physicochemical characteristics were consistent with those of the title compound (31 mg, 0.069 mmol, 90% yield).

M.p. 101–103 °C;  $^1\text{H}$ -NMR (400 MHz,  $\text{CDCl}_3$ )  $\delta$  9.92 (s, 2H, -CHO), 7.84 (d,  $J$  = 8.6 Hz, 4H, Ar-*H*), 7.22 – 7.10 (m, 3H, Ar-*H*), 7.06 (s, 2H, Ar-*H*), 7.03 (d,  $J$  = 8.6 Hz, 4H, Ar-*H*), 7.00 – 6.96 (m, 2H, Ar-*H*), 6.59 (dd,  $J$  = 17.5, 11.0 Hz, 1H, -CH=CH<sub>2</sub>), 5.65 (d,  $J$  = 17.5 Hz, 1H, -CH=CH<sub>2</sub>), 5.29 (d,  $J$  = 11.0 Hz, 1H, -CH=CH<sub>2</sub>), 4.92 (s, 2H, -CH<sub>2</sub>Ph);  $^{13}\text{C}$ -NMR (100 MHz,  $\text{CDCl}_3$ )  $\delta$  190.9 (-CHO), 162.9, 148.9, 142.8, 136.3, 134.9, 134.9, 132.2, 131.6, 128.4(1), 128.3(7), 117.2, 116.9, 115.6, 75.7 (-CH<sub>2</sub>Ph); FT-IR (thin film):  $\nu$  ( $\text{cm}^{-1}$ ) = 3070, 3033, 2834, 2741, 1696 (C=O), 1600, 1585, 1569, 1501, 1454, 1430, 1408, 1321, 1225, 1154, 1104, 1057, 1026; MS (MALDI-TOF)  $m/z$  473.32  $[\text{M}+\text{Na}]^+$ ; HRMS

(HNESP) exact mass calculated for  $C_{29}H_{26}O_5N$  requires  $m/z$  468.1805, found  $m/z$  468.1802  $[M+NH_4]^+$ .

***tert*-Butyl 3-(4-(2,3-bis(benzyloxy)-5-(methoxycarbonyl)phenoxy)phenyl)-1-(2-(*tert*-butoxy)phenyl)aziridine-2-carboxylate (*rac,cis*-**352**)**

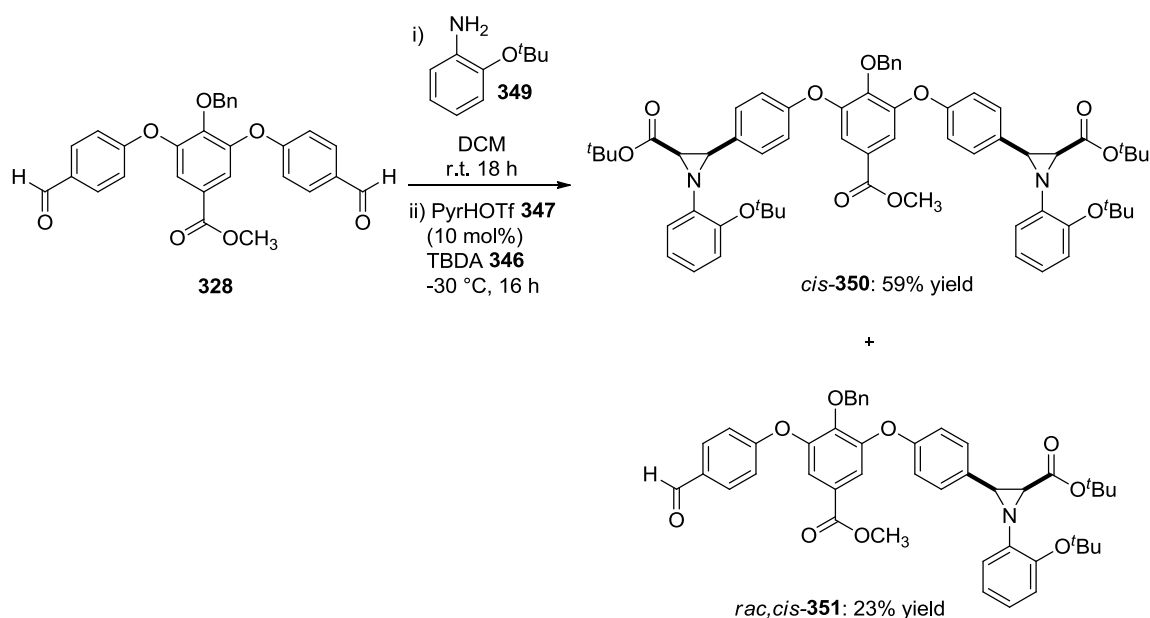


To a flame-dried 5 mL microwave vial containing crushed 4Å molecular sieves under a nitrogen atmosphere was added a solution of methyl 3,4-bis(benzyloxy)-5-(4-formylphenoxy)benzoate **320** (100 mg, 0.21 mmol, 1 equiv.) and 2-*tert*-butoxy aniline<sup>209</sup> **349** (33 mg, 0.20 mmol, 0.95 equiv.) in anhydrous dichloromethane (2 mL). The mixture was stirred slowly at room temperature for 18 hours. After the addition of pyridinium triflate **347** (5 mg, 0.02 mmol, 10 mol%), the vial was sealed with a PTFE-lined aluminium crimp cap and cooled to 0 °C. *Tert*-butyl diazoacetate **346** (30 µL, 0.21 mmol, 1 equiv.) was added dropwise *via* a 100 µL syringe. The solution was stirred at 0 °C for 18 hours before being filtered through a short plug of silica and eluted with diethyl ether (3 x 5 mL). The organic solvent was removed *in vacuo* to afford a dark yellow residue. Purification *via* flash column chromatography on silica gel (eluent: petroleum ether / diethyl ether / dichloromethane 8:1:1;  $R_f$  = 0.20), afforded a white solid whose physicochemical properties were consistent with those of the title compound **352** (89 mg, 0.12 mmol, 57% yield).

M.p. 39–41 °C;  $^1\text{H-NMR}$  (500 MHz,  $\text{CDCl}_3$ )  $\delta$  7.52 – 7.43 (m, 5H, Ar-*H*), 7.42 – 7.31 (m, 5H, Ar-*H*), 7.28 – 7.21 (m, 4H, Ar-*H*), 7.05 – 6.99 (m, 1H, Ar-*H*), 6.98 – 6.92 (m, 3H, Ar-*H*), 6.90 (d,  $J$  = 8.7 Hz, 2H, Ar-*H*), 5.17 (s, 2H,  $-\text{CH}_2\text{Ph}$ ), 5.13 (s, 2H,  $-\text{CH}_2\text{Ph}$ ), 3.84 (s, 3H,  $-\text{OCH}_3$ ), 3.46 (d,  $J$  = 6.7 Hz, 1H, *aziridine* C-*H*), 3.04 (d,  $J$  = 6.7 Hz, 1H, *aziridine* C-*H*), 1.38 (s, 9H,  $-\text{C}(\text{CH}_3)_3$ ), 1.23 (s, 9H,  $-\text{C}(\text{CH}_3)_3$ );  $^{13}\text{C-NMR}$  (126 MHz,  $\text{CDCl}_3$ )  $\delta$  167.3 ( $-\text{CO}_2^t\text{Bu}$ ), 166.3 ( $-\text{CO}_2\text{CH}_3$ ), 156.8, 153.1, 150.3, 148.1, 146.7, 144.2,

137.2, 136.5, 130.4, 129.6, 128.7, 128.6, 128.4, 128.3, 128.2, 127.8, 125.6, 123.3, 123.3, 123.1, 121.1, 117.5, 114.9, 110.8, 81.5 (-C(CH<sub>3</sub>)<sub>3</sub>), 80.5 (-C(CH<sub>3</sub>)<sub>3</sub>), 75.3 (-CH<sub>2</sub>Ph), 71.4 (-CH<sub>2</sub>Ph), 52.3 (aziridine C-H), 47.5 (-OCH<sub>3</sub>), 47.1 (aziridine C-H), 28.8 (-C(CH<sub>3</sub>)<sub>3</sub>), 28.0 (-C(CH<sub>3</sub>)<sub>3</sub>); FT-IR (thin film):  $\nu$  (cm<sup>-1</sup>) 3070, 3035, 2976, 2880, 1716 (C=O), 1585, 1490, 1424, 1367, 1338, 1210, 1164, 1077; HRMS (NESI) exact mass calculated for C<sub>45</sub>H<sub>48</sub>O<sub>8</sub>N requires  $m/z$  730.3374, found  $m/z$  730.3376 [M+H]<sup>+</sup>.

**Di-*tert*-butyl 3,3'-(((2-(benzyloxy)-5-(methoxycarbonyl)-1,3-phenylene))bis(oxy))bis(4,1-phenylene))bis(1-(2-(*tert*-butoxy)phenyl)aziridine-2-carboxylate) (*cis*-350)**



A 5 mL microwave vial containing 4Å molecular sieves was flame-dried and cooled under a flow of nitrogen. A solution of methyl 4-(benzyloxy)-3,5-bis(4-formylphenoxy)benzoate **328** (100 mg, 0.21 mmol, 1 equiv.) and 2-*tert*-butoxyaniline **349** (67 mg, 0.40 mmol, 1.95 equiv.) in dry chloroform (1.5 mL) was added, along with a magnetic stirrer bar. The vial was sealed with a PTFE-lined aluminium crimp cap and the reaction mixture was stirred slowly at room temperature for 18 hours. Pyridinium triflate **347** (5 mg, 0.021 mmol, 10 mol%) was added, and the vial was resealed before being cooled to -30 °C in a chiller bath. *Tert*-butyl diazoacetate **346** (32  $\mu$ L, 0.23 mmol, 2.2 equiv.) was added *via* a 100  $\mu$ L syringe and the mixture was stirred at -30 °C for 16 hours. After warming to room temperature, the solution was filtered through a short plug of silica, eluting with diethyl ether (3 x 5 mL). The solvent was removed *in vacuo*, and

purification *via* flash column chromatography on silica gel (eluent: petroleum ether / diethyl ether / dichloromethane 7:2:1;  $R_f$  = 0.26) afforded a white solid whose physicochemical properties were consistent with those of the title compound **350** (224 mg, 0.22 mmol, 59% yield).

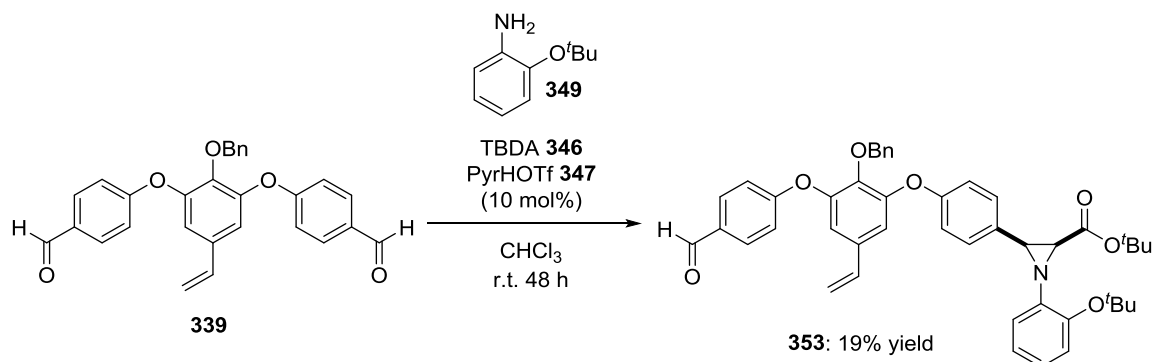
*cis*-**350**: M.p. 78–80 °C;  $^1\text{H-NMR}$  (300 MHz,  $\text{CDCl}_3$ )  $\delta$  7.52 (d,  $J$  = 8.6 Hz, 4H, Ar-*H*), 7.34 (s, 2H, Ar-*H*), 7.33 – 7.24 (m, 4H, Ar-*H*), 7.05 – 6.92 (m, 13H, Ar-*H*), 5.17 (s, 2H,  $-\text{CH}_2\text{Ph}$ ), 3.78 (s, 3H,  $-\text{CO}_2\text{CH}_3$ ), 3.47 (d,  $J$  = 6.7 Hz, 2H, *aziridine C-H*), 3.05 (d,  $J$  = 6.7 Hz, 2H, *aziridine C-H*), 1.38 (s, 18H,  $-\text{C}(\text{CH}_3)_3$ ), 1.24 (s, 18H,  $-\text{C}(\text{CH}_3)_3$ );  $^{13}\text{C-NMR}$  (126 MHz,  $\text{CDCl}_3$ )  $\delta$  167.2 ( $-\text{CO}_2^t\text{Bu}$ ), 165.8 ( $-\text{CO}_2\text{CH}_3$ ), 156.3, 150.8, 148.1, 146.6, 145.5, 136.8, 130.7, 129.7, 128.6, 128.4, 128.3, 125.7, 123.3, 123.3, 123.1, 121.1, 117.8, 116.5, 81.5 ( $-\text{C}(\text{CH}_3)_3$ ), 80.5 ( $-\text{C}(\text{CH}_3)_3$ ), 75.4 ( $-\text{CH}_2\text{Ph}$ ), 52.3 ( $-\text{CO}_2\text{CH}_3$ ), 47.5 (*aziridine C-H*), 47.1 (*aziridine C-H*), 28.8 ( $-\text{C}(\text{CH}_3)_3$ ), 28.0 ( $-\text{C}(\text{CH}_3)_3$ ); FT-IR (thin film):  $\nu$  ( $\text{cm}^{-1}$ ) = 2979 (C-H), 1721 (C=O), 1582, 1494, 1423, 1368, 1334, 1260, 1216, 1161, 1043, 978, 846; MS (MALDI-TOF)  $m/z$  1005.3  $[\text{M}]^+$ ; HRMS (NESP) exact mass calculated for  $\text{C}_{61}\text{H}_{72}\text{N}_3\text{O}_{11}$  requires  $m/z$  1022.5161, found  $m/z$  1022.5169  $[\text{M}+\text{NH}_4]^+$ .

A byproduct was isolated during the flash column chromatography ( $R_f$  = 0.23); this was identified as *rac*, *cis-tert*-butyl 3-(4-(2-(benzyloxy)-3-(4-formylphenoxy)-5-(methoxycarbonyl)phenoxy)phenyl)-1-(2-(*tert*-butoxy)phenyl)aziridine-2-carboxylate **351** (64 mg, 0.087 mmol, 23% yield;  $R_f$  = 0.23).

*rac,cis*-**351**:  $^1\text{H-NMR}$  (500 MHz,  $\text{CDCl}_3$ )  $\delta$  9.93 (s, 1H,  $-\text{CHO}$ ), 7.84 (d,  $J$  = 8.8 Hz, 2H, Ar-*H*), 7.56 – 7.53 (m, 3H, Ar-*H*), 7.46 (d,  $J$  = 2.0 Hz, 1H, Ar-*H*), 7.24 – 7.13 (m, 5H, Ar-*H*), 7.04 – 6.92 (m, 8H, Ar-*H*), 5.11 (s, 2H,  $-\text{CH}_2\text{Ph}$ ), 3.83 (s, 3H,  $-\text{CO}_2\text{CH}_3$ ), 3.48 (d,  $J$  = 6.7 Hz, 1H, *aziridine C-H*), 3.06 (d,  $J$  = 6.7 Hz, 1H, *aziridine C-H*), 1.38 (s, 9H,  $-\text{C}(\text{CH}_3)_3$ ), 1.24 (s, 9H,  $-\text{C}(\text{CH}_3)_3$ );  $^{13}\text{C-NMR}$  (126 MHz,  $\text{CDCl}_3$ )  $\delta$  190.9 ( $-\text{CHO}$ ), 167.1 ( $-\text{CO}_2^t\text{Bu}$ ), 165.5 ( $-\text{CO}_2\text{CH}_3$ ), 162.7, 156.0, 151.1, 148.3, 148.1, 146.5, 146.3, 136.3, 132.1, 131.6, 131.1, 129.8, 128.4(0), 128.3(8), 126.1, 123.2(4), 123.1(7), 121.0, 118.8, 118.1, 117.8, 116.9, 81.5 ( $-\text{C}(\text{CH}_3)_3$ ), 80.5 ( $-\text{C}(\text{CH}_3)_3$ ), 75.5 ( $-\text{CH}_2\text{Ph}$ ), 52.5 ( $-\text{CO}_2\text{CH}_3$ ), 47.5 (*aziridine C-H*), 47.0 (*aziridine C-H*), 28.8 ( $-\text{C}(\text{CH}_3)_3$ ), 28.0 ( $-\text{C}(\text{CH}_3)_3$ ); FT-IR (thin film):  $\nu$  ( $\text{cm}^{-1}$ ) = 3063 (C-H), 2978 (C-H), 1724 (*ester* C=O), 1699 (*aldehyde* C=O), 1580, 1504, 1491, 1452, 1422, 1392, 1368, 1333, 1306, 1223, 1157, 1040, 1005; MS (MALDI-

TOF)  $m/z$  782.1  $[M+K]^+$ ; HRMS (HNESP) exact mass calculated for  $C_{45}H_{46}NO_9$  requires  $m/z$  744.3167, found  $m/z$  744.3165  $[M+H]^+$ .

***tert*-Butyl 3-(4-(2-(benzyloxy)-3-(4-formylphenoxy)-5-vinylphenoxy)phenyl)-1-(2-*tert*-butoxyphenyl)aziridine-2-carboxylate (*rac*, *cis*-**353**)**



A 5 mL microwave vial containing crushed 4Å molecular sieves was flame-dried and cooled under nitrogen. The vial was charged with 4,4'-((2-(benzyloxy)-5-vinyl-1,3-phenylene)bis(oxy))dibenzaldehyde **339** (100 mg, 0.22 mmol, 1 equiv.) and a solution of 2-*tert*-butoxyaniline **349** (36 mg, 0.22 mmol, 0.98 equiv.) in chloroform (1 mL). The mixture was stirred at room temperature for 16 hours. Pyridinium triflate **347** (5 mg, 0.02 mmol, 10 mol%) was added, and the vial sealed with a PTFE-lined aluminium crimp cap. *Tert*-butyl diazoacetate **346** (31  $\mu$ L, 0.22 mmol, 1 equiv.) was added dropwise *via* syringe. The mixture was stirred at room temperature for a further 16 hours and filtered through a short plug of silica gel, eluting with diethyl ether (3 x 5 mL). The solvent was removed *in vacuo* to afford a brown oil. Purification *via* flash column chromatography on silica gel (eluent: petroleum ether / diethyl ether / dichloromethane (8:1:1);  $R_f$  0.20) afforded a pale red liquid whose physicochemical properties were consistent with those of the title compound **353** (18 mg, 0.025 mmol, 19%).

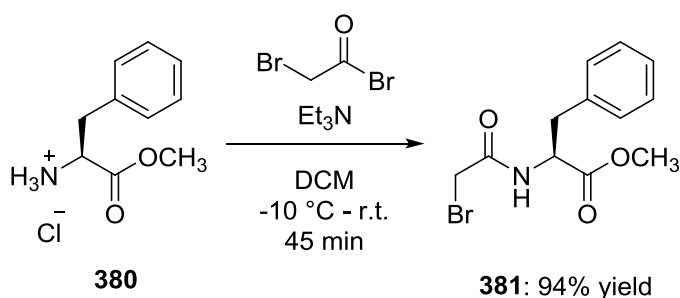
$^1H$ -NMR (500 MHz,  $CDCl_3$ )  $\delta$  9.91 (s, 1H, -CHO), 7.83 (d,  $J$  = 8.7 Hz, 2H, Ar-*H*), 7.53 (d,  $J$  = 8.7 Hz, 2H, Ar-*H*), 7.10 – 7.24 (m, 5H, Ar-*H*), 6.90 – 7.05 (m, 9H, Ar-*H*), 6.83 (d,  $J$  = 2.0 Hz, 1H, Ar-*H*), 6.50 (dd,  $J$  = 10.9, 17.5 Hz, 1H, -CH=CH<sub>2</sub>), 5.55 (d,  $J$  = 17.5 Hz, 1H, -CH=CH<sub>2</sub>), 5.21 (d,  $J$  = 10.9 Hz, 1H, -CH=CH<sub>2</sub>), 5.00 (s, 2H, -CH<sub>2</sub>Ph), 3.48 (d,  $J$  = 6.7 Hz, 1H, aziridine -CH-), 3.05 (d,  $J$  = 6.7 Hz, 1H, aziridine -CH-), 1.38 (s, 9H, -C(CH<sub>3</sub>)<sub>3</sub>), 1.23 (s, 9H, -C(CH<sub>3</sub>)<sub>3</sub>);  $^{13}C$ -NMR (100 MHz,  $CDCl_3$ )  $\delta$  190.9 (-CHO), 167.1 (-CO<sub>2</sub><sup>*t*</sup>Bu), 163.1, 156.4, 151.3, 148.5, 148.0, 146.5, 141.9, 136.7, 135.2, 134.3, 132.1, 131.3, 130.6, 129.6, 128.4, 128.3, 128.2, 123.2(4), 123.2(2), 123.1, 121.0, 117.7, 116.6,



115.2, 114.9, 114.8, 81.4 (-C(CH<sub>3</sub>)<sub>3</sub>), 80.5 (-C(CH<sub>3</sub>)<sub>3</sub>), 75.6 (-CH<sub>2</sub>Ph), 47.5 (aziridine -CH<sub>2</sub>-), 47.1 (aziridine -CH<sub>2</sub>-), 28.8 (-C(CH<sub>3</sub>)<sub>3</sub>), 28.0 (-C(CH<sub>3</sub>)<sub>3</sub>); FT-IR (thin film):  $\nu$  (cm<sup>-1</sup>) = 3065, 3033, 2976, 2930, 2733, 2250, 1744 (ester C=O), 1696 (aldehyde C=O), 1596, 1584, 1568, 1490, 1452, 1428, 1407, 1392, 1367, 1319, 1225, 1155, 1111, 1028;  $[\alpha]_D^{21} +6.1$  (c 1.0, CHCl<sub>3</sub>); HRMS (HNESP) exact mass calculated for C<sub>45</sub>H<sub>46</sub>NO<sub>7</sub> requires  $m/z$  712.3269, found  $m/z$  712.3265 [M+H]<sup>+</sup>.

**General procedure for the synthesis of amino acid bromoacetamides:**

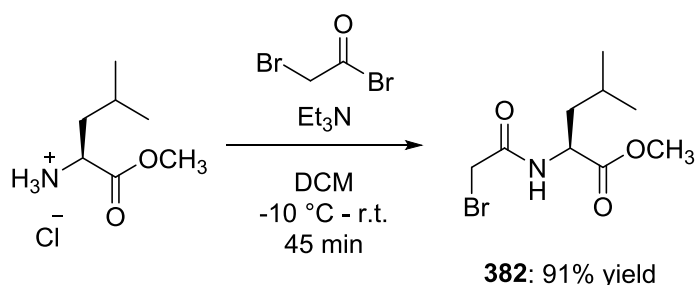
**(S)-Methyl 2-(2-bromoacetamido)-3-phenylpropanoate (**381**)**<sup>218</sup>



A 250 mL round-bottom flask containing a magnetic stirrer bar was flame-dried and allowed to cool to room temperature under a nitrogen atmosphere. To the flask was added (S)-phenylalanine methyl ester hydrochloride **380** (2 g, 9.27 mmol, 1 equiv.) and dry dichloromethane (70 mL). Triethylamine (1.3 mL, 9.27 mmol, 1 equiv.) was added dropwise *via* a 2.5 mL syringe and the suspension stirred at room temperature for 20 minutes. The reaction was cooled to -10 °C using an acetone / dry ice bath, and bromoacetyl bromide (0.8 mL, 9.27 mmol, 1 equiv.) was added dropwise *via* a 2 mL syringe followed by a further 1 equivalent of triethylamine (1.3 mL, 9.27 mmol, 1 equiv.). The solution continued to be stirred at -10 °C for 15 minutes before the cooling bath was removed and the reaction mixture was allowed to warm to room temperature. The solution was stirred for a further 30 minutes before the addition of distilled water (50 mL). The mixture was then poured into a 250 mL separating funnel and the aqueous layer extracted with dichloromethane (2 x 50 mL). The combined organic layers were washed with 1 M aqueous hydrochloric acid (100 mL), then half-saturated aqueous sodium bicarbonate solution (100 mL) and finally brine (100 mL), before being dried over magnesium sulfate and filtered. Removal of the solvent *in vacuo* afforded a pale brown solid (used without further purification) whose physicochemical properties matched those previously reported for the title compound (2.62 g, 8.71 mmol, 94% yield).

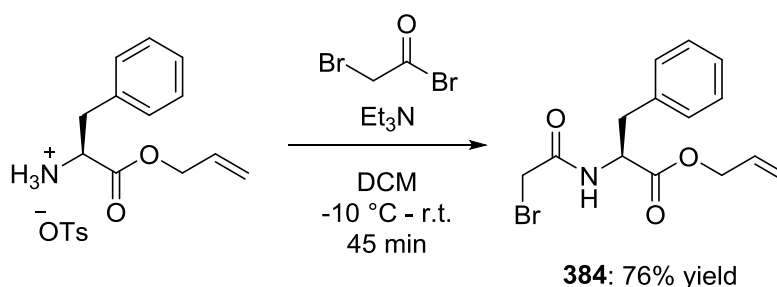
$^1\text{H}$ -NMR (500 MHz,  $\text{CDCl}_3$ )  $\delta$  = 7.33-7.24 (m, 3H, Ar-*H*), 7.14-7.10 (m, 2H, Ar-*H*), 6.83 (br d,  $J$  = 6.0 Hz, 1H, N-*H*), 4.85 (dt,  $J$  = 7.9, 5.8 Hz, 1H, -NHCH-), 3.86 (d,  $J$  = 13.7 Hz, 1H, **AB** - $\text{CH}_2\text{Br}$ ), 3.83 (d,  $J$  = 13.7 Hz, 1H, **AB** - $\text{CH}_2\text{Br}$ ), 3.74 (s, 3H, - $\text{OCH}_3$ ), 3.18 (dd,  $J$  = 13.9, 5.8 Hz, 1H, - $\text{CH}_2\text{Ph}$ ), 3.13 (dd,  $J$  = 13.9, 5.8 Hz, 1H, - $\text{CH}_2\text{Ph}$ );  $^{13}\text{C}$ -NMR (125 MHz,  $\text{CDCl}_3$ )  $\delta$  = 171.4 (-CONH-), 165.2 (- $\text{CO}_2\text{CH}_3$ ), 135.5, 129.4, 128.9, 127.5, 53.9 (-NHCH-), 52.6 (- $\text{OCH}_3$ ), 37.9 (- $\text{CH}_2\text{Ph}$ ), 28.8 (- $\text{CH}_2\text{Br}$ ); FT-IR (thin film,  $\text{cm}^{-1}$ )  $\nu$  = 3295 (N-H), 3033, 2959, 2854, 1746 (ester C=O), 1664 (amide C=O), 1533, 1440, 1365, 1216.

**(*S*)-Methyl 2-(2-bromoacetamido)-4-methylpentanoate (**382**)**<sup>250</sup>



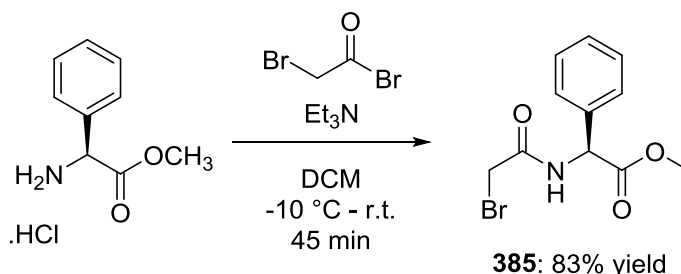
Compound **382** was prepared according to the general procedure described above to afford a white solid (1.33 g, 5.01 mmol, 91% yield) which was used without further purification. The physicochemical properties matched those previously reported for the title compound.

$^1\text{H}$ -NMR (500 MHz,  $\text{CDCl}_3$ )  $\delta$  = 6.79 (d,  $J$  = 6.8 Hz, 1H, N-*H*), 4.62 (dt,  $J$  = 8.5, 5.1 Hz, 1H, -NHCH-), 3.91 (d,  $J$  = 13.7 Hz, 1H, **AB** - $\text{CH}_2\text{Br}$ ), 3.87 (d,  $J$  = 13.7 Hz, 1H, **AB** - $\text{CH}_2\text{Br}$ ), 3.75 (s, 3H, - $\text{OCH}_3$ ), 1.74-1.55 (m, 3H, - $\text{CH}_2\text{CH}(\text{CH}_3)_2$ ), 0.95 (d,  $J$  = 6.3 Hz, 6H, - $\text{C}(\text{CH}_3)_2$ );  $^{13}\text{C}$ -NMR (125 MHz,  $\text{CDCl}_3$ )  $\delta$  = 172.9 (-CONH-), 165.4 (- $\text{CO}_2\text{CH}_3$ ), 52.6 (- $\text{OCH}_3$ ), 51.5 (-NHCH-), 41.5 (-CHCH<sub>2</sub>-), 28.9 (- $\text{CH}_2\text{Br}$ ), 25.0 (-CH(CH<sub>3</sub>)<sub>2</sub>), 22.9 (-CH(CH<sub>3</sub>)<sub>2</sub>), 22.1 (-CH(CH<sub>3</sub>)<sub>2</sub>); FT-IR (thin film,  $\text{cm}^{-1}$ )  $\nu$  = 3295 (N-H), 3074, 2959, 2873, 1746 (ester C=O), 1660 (amide C=O), 1544, 1440, 1208, 1156;  $[\alpha]_{\text{D}}^{21}$  +5.6 (c 1.0,  $\text{CHCl}_3$ ).

**(S)-Allyl 2-(2-bromoacetamido)-3-phenylpropanoate (384)**

Compound **384** was prepared according to the general procedure described above to afford a pale brown oil (1.26 g, 3.86 mmol, 76% yield) that was used without further purification.

$^1\text{H}$ -NMR (500 MHz,  $\text{CDCl}_3$ )  $\delta$  7.33 – 7.27 (m, 3H, Ar-*H*), 7.17 – 7.10 (m, 2H, Ar-*H*), 6.84 (br d,  $J = 7.6$  Hz, 1H, N-*H*), 5.88 (ddt,  $J = 17.2, 10.4, 5.9$  Hz, 1H, -CH=CH<sub>2</sub>), 5.32 (dd,  $J = 17.2, 1.4$  Hz, 1H, -CH=CH<sub>2</sub>), 5.27 (dd,  $J = 10.4, 1.4$  Hz, 1H, -CH=CH<sub>2</sub>), 4.87 (dt,  $J = 7.9, 5.9$  Hz, 1H, -NHCH-), 4.63 (dt,  $J = 5.9, 1.4$  Hz, 2H, -OCH<sub>2</sub>-), 3.87 (d,  $J = 13.7$  Hz, 1H, **AB** -CH<sub>2</sub>Br), 3.83 (d,  $J = 13.7$  Hz, 1H, **AB** -CH<sub>2</sub>Br), 3.19 (dd,  $J = 13.9, 5.9$  Hz, 1H, -CH<sub>2</sub>Ph), 3.14 (dd,  $J = 13.9, 5.9$  Hz, 1H, -CH<sub>2</sub>Ph);  $^{13}\text{C}$ -NMR (126 MHz,  $\text{CDCl}_3$ )  $\delta$  170.7 (*amide* C=O), 165.3 (*ester* C=O), 135.4, 131.4 (-CH=CH<sub>2</sub>), 129.5, 128.8, 127.5, 119.4 (-CH=CH<sub>2</sub>), 66.4 (-OCH<sub>2</sub>-), 53.9 (-NHCH-), 37.9 (-CH<sub>2</sub>Ph), 28.8 (-CH<sub>2</sub>Br); FT-IR (thin film):  $\nu$  ( $\text{cm}^{-1}$ ) = 3307 (N-H), 3032 (C-H), 2935 (C-H), 2863 (C-H), 1743 (*ester* C=O), 1662 (*amide* C=O), 1536, 1498, 1455, 1379, 1197, 1138, 1049;  $[\alpha]_{\text{D}}^{21} +22.3$  (c 1.0,  $\text{CHCl}_3$ ); MS (MALDI-TOF)  $m/z$  364.08, 366.07  $[\text{M}+\text{K}]^+$ ; HRMS (HNESF) exact mass calculated for  $\text{C}_{14}\text{H}_{17}\text{BrNO}_3$  requires  $m/z$  326.0386, 328.0366, found  $m/z$  326.0390, 328.0367  $[\text{M}+\text{H}]^+$ .

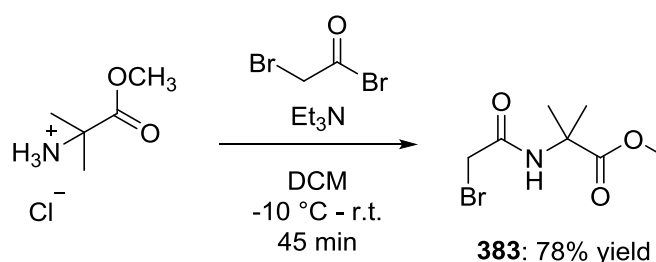
**(S)-Methyl 2-(2-bromoacetamido)-2-phenylacetate (385)<sup>220</sup>**

Compound **385** was prepared according to the general procedure described above to afford an orange solid (1.18 g, 4.12 mmol, 83% yield) which was used without further

purification. The physicochemical properties matched those previously reported for the title compound.

M.p. 74–76 °C;  $^1\text{H-NMR}$  (500 MHz,  $\text{CDCl}_3$ )  $\delta$  7.45 (br d,  $J = 6.1$  Hz, 1H, N-*H*), 7.41 – 7.31 (m, 5H, Ar-*H*), 5.54 (d,  $J = 7.1$  Hz, 1H, -CH-), 3.91 (d,  $J = 13.7$  Hz, 1H, **AB** - $\text{CH}_2\text{Br}$ ), 3.86 (d,  $J = 13.7$  Hz, 1H, **AB** - $\text{CH}_2\text{Br}$ ), 3.75 (s, 3H, - $\text{OCH}_3$ ); FT-IR (thin film):  $\nu$  ( $\text{cm}^{-1}$ ) = 3298 (N-H), 3041 (C-H), 2955 (C-H), 1746 (*ester* C=O), 1660 (*amide* C=O), 1529, 1339, 1216;  $[\alpha]_{\text{D}}^{19} +84.4$  (c 1.0,  $\text{CHCl}_3$ ).

### Methyl 2-(2-bromoacetamido)-2-methylpropanoate (**383**)

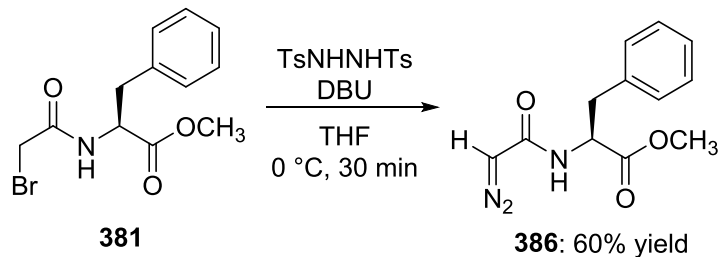


Compound **383** was prepared according to the general procedure described above to afford a white solid (1.27 g, 5.33 mmol, 78% yield) that was used without further purification.

M.p. 83–85 °C;  $^1\text{H-NMR}$  (500 MHz,  $\text{CDCl}_3$ )  $\delta$  7.06 (s, 1H, -NH-), 3.83 (s, 2H, - $\text{CH}_2\text{Br}$ ), 3.77 (s, 3H, - $\text{OCH}_3$ ), 1.59 (s, 6H, - $\text{C}(\text{CH}_3)_2$ );  $^{13}\text{C-NMR}$  (126 MHz,  $\text{CDCl}_3$ )  $\delta$  174.7 (*ester* -C=O), 164.9 (*amide* -C=O), 57.3 (- $\text{C}(\text{CH}_3)_2$ ), 53.0 (- $\text{OCH}_3$ ), 29.2 (- $\text{CH}_2\text{Br}$ ), 24.4 (- $\text{C}(\text{CH}_3)_2$ ); FT-IR (thin film):  $\nu$  ( $\text{cm}^{-1}$ ) = 3273 (N-H), 3074 (C-H), 2922 (C-H), 2859 (C-H), 1734 (*ester* C=O), 1650 (*amide* C=O), 1548, 1493, 1472, 1282, 1197, 1155, 1049; MS (MALDI-TOF)  $m/z$  261.92, 263.90  $[\text{M}+\text{Na}]^+$ ; HRMS (HNESP) exact mass calculated for  $\text{C}_7\text{H}_{13}\text{BrNO}_3$  requires  $m/z$  238.0073, 240.0053, found  $m/z$  238.0076, 240.0051  $[\text{M}+\text{H}]^+$ .

**General procedure for the synthesis of amino acid diazoacetamides (Method A: *N,N'*-Ditosylhydrazine):**

**(*S*)-Methyl 2-(2-diazoacetamido)-3-phenylpropanoate (**386**)<sup>217</sup>**

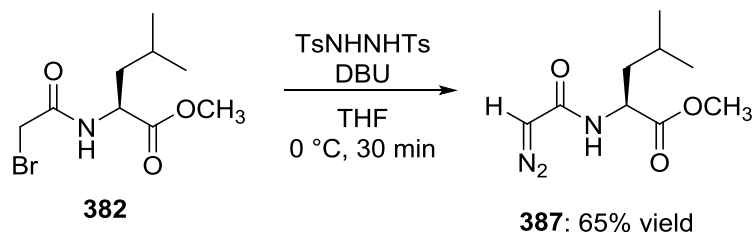


A 250 mL round-bottom flask containing (*S*)-methyl 2-(2-bromoacetamido)-3-phenylpropanoate **381** (1.23 g, 4.10 mmol, 1 equiv.) and a stirrer bar under a nitrogen atmosphere was cooled to 0 °C. Dry tetrahydrofuran (40 mL) was added *via* a 50 mL syringe, followed by the sequential addition of *N,N'*-ditosylhydrazine (2.79 g, 8.20 mmol, 2 equiv.) in one portion, and 1,8-diazabicycloundec[7]ene (3.1 mL, 20.5 mmol, 5 equiv.) *via* a 5 mL syringe. The resulting deep yellow solution was stirred at 0 °C for 30 minutes. The reaction was quenched by the addition of saturated sodium bicarbonate solution (20 mL) and poured into a 250 mL separating funnel containing distilled water (50 mL) and diethyl ether (50 mL). The mixture was extracted with diethyl ether (3 x 50 mL), and the combined organic layers were washed with brine (100 mL), dried over magnesium sulfate, filtered, and the solvent removed *in vacuo*. The yellow residue was redissolved in chloroform (50 mL) and the mixture filtered to remove the unreacted white solid *N,N'*-ditosylhydrazine. The yellow filtrate was concentrated *in vacuo*. Purification *via* flash column chromatography on silica gel (eluent: diethyl ether / petroleum ether 3:1,  $R_f$  = 0.28) afforded a yellow solid whose physicochemical properties were consistent with those of the title compound (598 mg, 0.24 mmol, 60% yield).

M.p. 126–128 °C (dichloromethane / diethyl ether / petroleum ether); <sup>1</sup>H-NMR (300 MHz, CD<sub>3</sub>CN)  $\delta$  = 7.39 – 7.15 (m, 5H, Ar-*H*), 6.33 (br s, 1H, -NH-), 5.03 (s, 1H, -CHN<sub>2</sub>), 4.68 (dt,  $J$  = 8.2, 5.6 Hz, 1H, -NHCH-), 3.65 (s, 3H, -OCH<sub>3</sub>), 3.11 (dd,  $J$  = 13.9, 5.6 Hz, 1H, -CH<sub>2</sub>Ph), 2.94 (dd,  $J$  = 13.9, 8.2 Hz, 1H, -CH<sub>2</sub>Ph); <sup>13</sup>C-NMR (100 MHz, CD<sub>3</sub>CN)  $\delta$  = 173.1 (-C=O *ester*), 166.3 (-C=O *amide*), 137.8, 130.2, 129.4, 127.8, 55.0 (-NHCH-), 52.7 (-OCH<sub>3</sub>), 47.5 (-CHN<sub>2</sub>), 38.4 (-CH<sub>2</sub>Ph); FT-IR (thin film, cm<sup>-1</sup>)  $\nu$  = 3106 (N-H), 3027, 2115 (*diazo* C=N<sub>2</sub>), 1748 (*ester* C=O), 1605 (*amide* C=O), 1527, 1385, 1208;  $[\alpha]_D^{21}$

+175.0 (c 1.0, CHCl<sub>3</sub>); MS (MALDI-TOF):  $m/z$  = 270.0 [M+Na]<sup>+</sup>; HRMS (ESI) exact mass calculated for C<sub>12</sub>H<sub>13</sub>N<sub>3</sub>NaO<sub>3</sub>  $m/z$  270.0849  $m/z$ , found  $m/z$  270.0850 [M+Na]<sup>+</sup>.

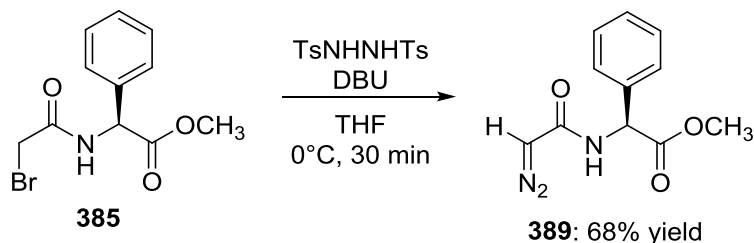
**(S)-Methyl 2-(2-diazoacetamido)-4-methylpentanoate (387)**



Compound **387** was prepared according to method A. Purification *via* flash column chromatography on silica gel (eluent: diethyl ether / petroleum ether 3:1; R<sub>f</sub> = 0.25) afforded a yellow oil whose physicochemical properties were consistent with those of the title compound (1.28 mg, 6.03 mmol, 65% yield).

<sup>1</sup>H-NMR (300 MHz, CD<sub>3</sub>CN) δ = 6.41 (br s, 1H, -NH-), 5.06 (s, 1H, -CHN<sub>2</sub>), 4.68 (m, 1H, -NHCH-), 3.65 (s, 3H, -OCH<sub>3</sub>), 1.69 – 1.49 (m, 3H, -CH<sub>2</sub>CH(CH<sub>3</sub>)<sub>2</sub>), 0.92 (d, *J* = 6.9 Hz, 3H, -CH(CH<sub>3</sub>)<sub>2</sub>), 0.89 (d, *J* = 6.9 Hz, 3H, -CH(CH<sub>3</sub>)<sub>2</sub>); <sup>13</sup>C-NMR (100 MHz, CD<sub>3</sub>CN) δ = 174.3 (-C=O *ester*), 166.5 (-C=O *amide*), 52.7 (-NHCH-), 52.0 (-OCH<sub>3</sub>), 47.5 (-CHN<sub>2</sub>), 41.4 (-CH<sub>2</sub>-), 25.5 (-CH(CH<sub>3</sub>)<sub>2</sub>), 23.1 (-CH(CH<sub>3</sub>)<sub>2</sub>), 21.8 (-CH(CH<sub>3</sub>)<sub>2</sub>); FT-IR (ATR, cm<sup>-1</sup>) ν = 3105 (N-H), 2959 (C-H), 2877 (C-H), 2100 (*diazo* C=N<sub>2</sub>), 1741 (C=O *ester*), 1616 (C=O *amide*), 1536, 1380, 1204, 1148 cm<sup>-1</sup>; [α]<sub>D</sub><sup>19</sup> -6.3 (c 1.0, CHCl<sub>3</sub>); MS (MALDI-TOF):  $m/z$  = 252.0 [M+K]<sup>+</sup>; HRMS (ESI) exact mass calculated for C<sub>9</sub>H<sub>16</sub>N<sub>3</sub>O<sub>3</sub> requires  $m/z$  214.1186, found  $m/z$  214.1187 [M+H]<sup>+</sup>.

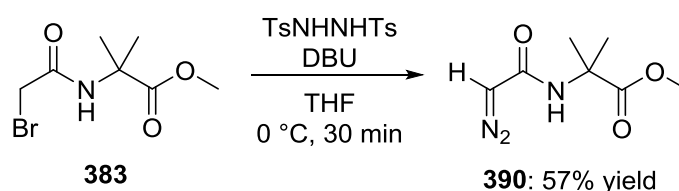
**(S)-Methyl 2-(2-diazoacetamido)-2-phenylacetate (389)**



Compound **389** was prepared according to method A. Purification *via* flash column chromatography on silica gel (eluent: diethyl ether / petroleum ether 3:1; R<sub>f</sub> = 0.31) afforded a yellow solid whose physicochemical properties were consistent with those of the title compound (1.00 g, 4.29 mmol, 68% yield).

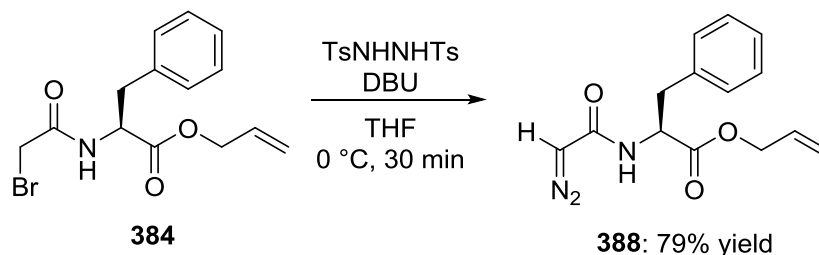
M.p. 87–89 °C;  $^1\text{H}$ -NMR (400 MHz,  $\text{CDCl}_3$ )  $\delta$  7.42 – 7.28 (m, 5H, Ar-*H*), 6.26 (br s, 1H, -NH-), 5.63 (d,  $J$  = 7.2 Hz, 1H, -CHN<sub>2</sub>), 4.83 (s, 1H, -NHCH-), 3.73 (s, 3H, -OCH<sub>3</sub>);  $^{13}\text{C}$ -NMR (100 MHz,  $\text{CDCl}_3$ )  $\delta$  171.6 (-C=O *ester*), 164.8 (-C=O *amide*), 136.6, 129.0, 128.6, 127.2, 56.7 (-NHCH-), 52.9 (-OCH<sub>3</sub>), 47.6 (-CHN<sub>2</sub>); FT-IR (thin film):  $\nu$  ( $\text{cm}^{-1}$ ) = 3307 (N-H), 3100 (C-H), 2965 (C-H), 2857 (C-H), 2111 (-HC=N<sub>2</sub>), 1746 (ester C=O), 1625 (amide C=O), 1535, 1386, 1265, 1211, 1174, 1103;  $[\alpha]_{\text{D}}^{20}$  +12.6 (c 1.0,  $\text{CHCl}_3$ ); MS (MALDI-TOF)  $m/z$  271.9  $[\text{M}+\text{K}]^+$ ; HRMS (HNESP) exact mass calculated for  $\text{C}_{11}\text{H}_{12}\text{N}_3\text{O}_3$  requires  $m/z$  234.0873, found  $m/z$  234.0876  $[\text{M}+\text{H}]^+$ .

### Methyl 2-(2-diazoacetamido)-2-methylpropanoate (**390**)



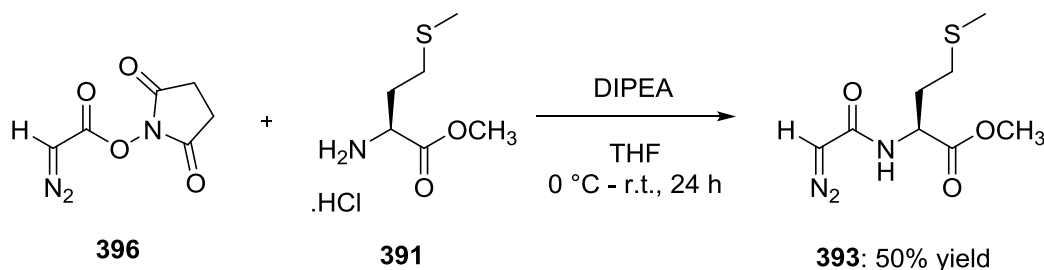
Compound **390** was prepared according to method A. Purification *via* flash column chromatography on silica gel (eluent: diethyl ether 100%;  $R_f$  = 0.55) afforded a yellow oil whose physicochemical properties were consistent with those of the title compound (829 mg, 4.48 mmol, 57% yield).

$^1\text{H}$ -NMR (500 MHz,  $\text{CDCl}_3$ )  $\delta$  5.65 (s, 1H, -NH-), 4.73 (s, 1H, -CHN<sub>2</sub>), 3.76 (s, 3H, -OCH<sub>3</sub>), 1.58 (s, 6H, -C(CH<sub>3</sub>)<sub>2</sub>);  $^{13}\text{C}$ -NMR (126 MHz,  $\text{CDCl}_3$ )  $\delta$  175.4 (C=O *ester*), 164.9 (C=O *amide*), 57.2 (-C(CH<sub>3</sub>)<sub>2</sub>), 53.0 (-OCH<sub>3</sub>), 47.8 (-CHN<sub>2</sub>), 25.3 (-C(CH<sub>3</sub>)<sub>2</sub>); FT-IR (thin film):  $\nu$  ( $\text{cm}^{-1}$ ) = 3319 (N-H), 3096, 2991, 2951, 2106 (*diazo* C=N<sub>2</sub>), 1739 (*ester* C=O), 1621 (*amide* C=O), 1539, 1383, 1289, 1246, 1152; MS (MALDI-TOF)  $m/z$  224.0  $[\text{M}+\text{K}]^+$ ; HRMS (HNESP) exact mass calculated for  $\text{C}_7\text{H}_{12}\text{N}_3\text{O}_3$  requires  $m/z$  186.0873, found  $m/z$  186.0873  $[\text{M}+\text{H}]^+$ .

**(S)-Allyl 2-(2-diazoacetamido)-3-phenylpropanoate (388)**

Compound **388** was prepared according to method A. Purification *via* flash column chromatography on silica gel (eluent: diethyl ether / petroleum ether 2:1;  $R_f$  = 0.37) afforded a yellow solid whose physicochemical properties were consistent with those of the title compound (836 mg, 3.06 mmol, 79% yield).

M.p. 66–68 °C;  $^1\text{H-NMR}$  (500 MHz,  $\text{CDCl}_3$ )  $\delta$  7.32 – 7.22 (m, 3H, Ar-*H*), 7.15 – 7.08 (m, 2H, Ar-*H*), 5.88 (ddt,  $J$  = 17.2, 10.4, 5.9 Hz, 1H, -CH=CH<sub>2</sub>), 5.46 (d,  $J$  = 7.5 Hz, 1H, -NH-), 5.32 (d,  $J$  = 17.2 Hz, 1H, -CH=CH<sub>2</sub>), 5.27 (d,  $J$  = 10.4 Hz, 1H, -CH=CH<sub>2</sub>), 4.98 (br s, 1H, -NHCH-), 4.73 (s, 1H, -CHN<sub>2</sub>), 4.62 (d,  $J$  = 5.9 Hz, 2H, -OCH<sub>2</sub>-), 3.18 (dd,  $J$  = 13.9, 5.7 Hz, 1H, -CH<sub>2</sub>Ph), 3.13 (dd,  $J$  = 13.9, 5.7 Hz, 1H, -CH<sub>2</sub>Ph);  $^{13}\text{C-NMR}$  (126 MHz,  $\text{CDCl}_3$ )  $\delta$  171.9 (C=O *ester*), 165.5 (C=O *amide*), 135.9, 131.4, 129.4, 128.6, 127.2, 119.2 (-CH=CH<sub>2</sub>), 66.2 (-OCH<sub>2</sub>-), 53.6 (-NHCH-), 47.4 (-CHN<sub>2</sub>), 38.3 (-CH<sub>2</sub>Ph); FT-IR (thin film):  $\nu$  (cm<sup>-1</sup>) = 3306 (N-H), 3092, 2953, 2108 (*diazo* C=N<sub>2</sub>), 1742 (*ester* C=O), 1625 (*amide* C=O), 1534, 1458, 1385, 1196;  $[\alpha]_D^{18}$  -47.4 (c 1.0,  $\text{CHCl}_3$ ); MS (MALDI-TOF)  $m/z$  312.05  $[\text{M}+\text{K}]^+$ ; HRMS (HNESP) exact mass calculated for  $\text{C}_{14}\text{H}_{16}\text{N}_3\text{O}_3$  requires  $m/z$  274.1186, found  $m/z$  274.1188  $[\text{M}+\text{H}]^+$ .

**General procedure for the synthesis of amino acid diazoacetamides (Method B):****(S)-Methyl 2-(2-diazoacetamido)-4-(methylthio)butanoate (393)**

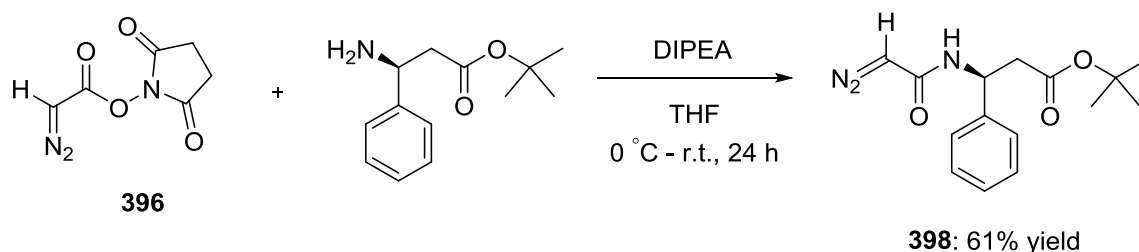
To a flame-dried 25 mL round-bottom flask containing (*S*)-methionine methyl ester hydrochloride **391** (218 mg, 1.09 mmol, 2 equiv.) and a magnetic stirrer bar was added dry tetrahydrofuran (5 mL) *via* syringe under a nitrogen atmosphere. The resulting



suspension was cooled to 0 °C using an ice bath and *N,N*-diisopropylethylamine (0.95 mL, 5.46 mmol, 3 equiv.) was added dropwise *via* a 2 mL syringe. The solution was stirred for 10 minutes while maintaining the temperature at 0 °C. A solution of succinimidyl diazoacetate<sup>222</sup> **396** (100 mg, 0.55 mmol, 1 equiv.) in tetrahydrofuran (10 mL) was added dropwise to the flask, and the solution was allowed to warm to room temperature. After stirring at room temperature for 24 hours, the solvent was removed *in vacuo* and the yellow residue extracted with dichloromethane (2 x 20 mL). The combined organic layers were washed with distilled water (3 x 30 mL), dried over magnesium sulfate, filtered, and the solvent removed *in vacuo*. Purification *via* flash column chromatography on silica gel (eluent: diethyl ether / petroleum ether;  $R_f$  = 0.24) afforded a yellow solid (63 mg, 0.27 mmol, 50% yield) whose physicochemical properties were consistent with those of the title compound.

M.p. = 40–42 °C; <sup>1</sup>H-NMR (500 MHz, CD<sub>3</sub>CN)  $\delta$  = 6.39 (br s, 1H, -NH-), 5.06 (s, 1H, -CHN<sub>2</sub>), 4.54 (dt,  $J$  = 8.9, 4.9 Hz, 1H, -NHCH-), 3.68 (s, 3H, -OCH<sub>3</sub>), 2.57 – 2.45 (m, 2H, -CH<sub>2</sub>S-), 2.06 (s, 3H, -SCH<sub>3</sub>), 2.05 – 2.00 (m, 1H, -CH<sub>2</sub>CH<sub>2</sub>S-), 1.92 – 1.85 (m, 1H, -CH<sub>2</sub>CH<sub>2</sub>S-); <sup>13</sup>C-NMR (125 MHz, CD<sub>3</sub>CN)  $\delta$  = 173.5 (C=O *ester*), 166.6 (C=O *amide*), 52.8 (-NHCH-), 52.6 (-OCH<sub>3</sub>), 47.6 (-CHN<sub>2</sub>), 32.2 (-CH<sub>2</sub>CH<sub>2</sub>S-), 30.6 (-CH<sub>2</sub>S-), 15.3 (-SCH<sub>3</sub>); FT-IR (thin film, cm<sup>-1</sup>)  $\nu$  = 3095 (N-H), 2925, 2111 (*diazo* C=N<sub>2</sub>), 1746 (*ester* C=O), 1620 (*amide* C=O), 1544, 1386, 1215;  $[\alpha]_D^{20}$  +5.31 (c 1.0, CHCl<sub>3</sub>); MS (MALDI-TOF)  $m/z$  269.9 [M+K]<sup>+</sup>; HRMS (HNESF) exact mass calculated for C<sub>8</sub>H<sub>14</sub>N<sub>3</sub>O<sub>3</sub>S requires  $m/z$  232.0750, found  $m/z$  232.0754 [M+H]<sup>+</sup>.

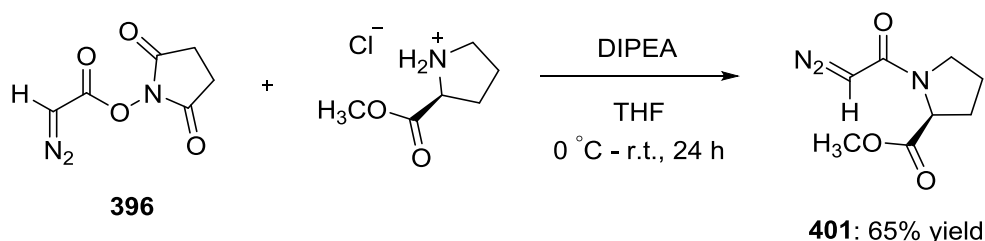
**(*S*)-tert-Butyl 3-(2-diazoacetamido)-3-phenylpropanoate (398)**



Compound **398** was prepared according to method B. Purification *via* flash column chromatography on silica gel (eluent: diethyl ether / petroleum ether 3:1;  $R_f$  = 0.31) afforded a yellow oil whose physicochemical properties were consistent with those of the title compound (33 mg, 0.114 mmol, 61% yield).

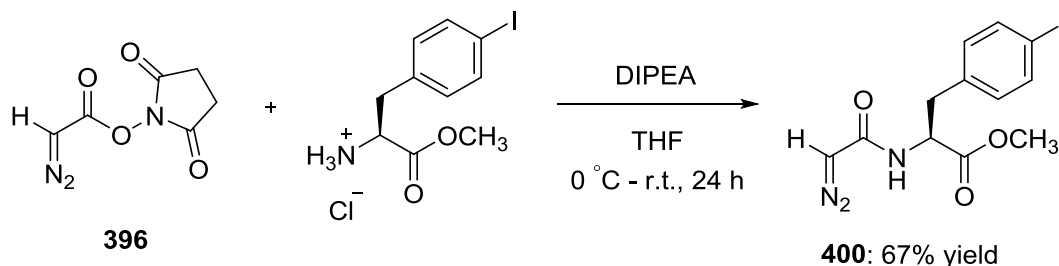
$^1\text{H}$ -NMR (300 MHz,  $\text{CD}_3\text{CN}$ )  $\delta$  7.49 – 7.20 (m, 5H, Ar-*H*), 6.66 (d,  $J$  = 6.7 Hz, 1H, -NH-), 5.28 (m, 1H, -NHCH-), 5.02 (s, 1H, -CHN<sub>2</sub>), 2.71 (dd,  $J$  = 14.5, 7.0 Hz, 1H, -CH<sub>2</sub>CO<sub>2</sub><sup>*t*</sup>Bu), 2.64 (dd,  $J$  = 14.5, 7.0 Hz, 1H, -CH<sub>2</sub>CO<sub>2</sub><sup>*t*</sup>Bu), 1.34 (s, 9H, -C(CH<sub>3</sub>)<sub>3</sub>);  $^{13}\text{C}$ -NMR (100 MHz,  $\text{CD}_3\text{CN}$ )  $\delta$  170.6 (*ester* -C=O), 165.7 (*amide* -C=O), 142.9, 129.4, 128.3, 127.5, 81.4 (-C(CH<sub>3</sub>)<sub>3</sub>), 51.6 (-NHCH-), 47.5 (-CHN<sub>2</sub>), 42.9 (-CH<sub>2</sub>CO<sub>2</sub><sup>*t*</sup>Bu), 28.1 (-C(CH<sub>3</sub>)<sub>3</sub>); FT-IR (ATR):  $\nu$  (cm<sup>-1</sup>) = 3277 (N-H), 3095 (C-H), 2983 (C-H), 2938 (C-H), 2099 (*diazo* C=N<sub>2</sub>), 1727 (*ester* C=O), 1619 (*amide* C=O), 1561, 1375, 1251, 1146, 701;  $[\alpha]_{\text{D}}^{19}$  -54.7 (c 1.5,  $\text{CHCl}_3$ ); MS (MALDI-TOF)  $m/z$  327.9  $[\text{M}+\text{K}]^+$ ; HRMS (HNESP) exact mass calculated for  $\text{C}_{15}\text{H}_{20}\text{N}_3\text{O}_3$  requires  $m/z$  290.1499, found  $m/z$  290.1503  $[\text{M}+\text{H}]^+$ .

**(*S*)-Methyl 1-(2-diazoacetyl)pyrrolidine-2-carboxylate (401)**



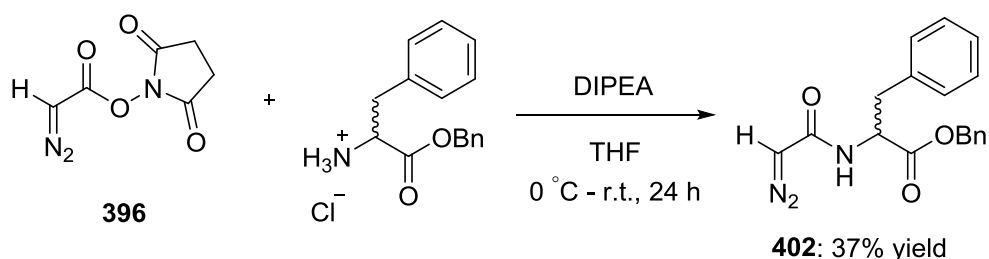
Compound **401** was prepared according to method B. Purification *via* flash column chromatography on silica (diethyl ether 100%;  $R_f$  = 0.19) afforded a yellow oil whose physicochemical properties were consistent with those of the title compound (70 mg, 0.35 mmol, 65% yield).

$^1\text{H}$ -NMR (500 MHz,  $\text{CDCl}_3$ )  $\delta$  4.88 (s, 1H, -CHN<sub>2</sub>), 4.53 (br s, 1H, -NCH-), 3.72 (s, 3H, -OCH<sub>3</sub>), 3.43 (br s, 1H, -NCH<sub>2</sub>-), 3.28 (br s, 1H, -NCH<sub>2</sub>-), 2.25–1.90 (m, 4H, -CH<sub>2</sub>-);  $^{13}\text{C}$ -NMR (101 MHz,  $\text{CD}_3\text{CN}$ )  $\delta$  174.0 (-C=O *ester*), 165.1 (-C=O *amide*), 59.8 (-NHCH-), 52.6 (-OCH<sub>3</sub>), 47.2 (-NCH<sub>2</sub>- + -CHN<sub>2</sub>), 30.0 (-CH<sub>2</sub>-), 25.2 (-CH<sub>2</sub>-); FT-IR (thin film):  $\nu$  (cm<sup>-1</sup>) = 3075 (C-H), 2861 (C-H), 2927 (C-H), 2855 (C-H), 2107 (*diazo* C=N<sub>2</sub>), 1736 (*ester* C=O), 1607 (*amide* C=O), 1413, 1163, 730;  $[\alpha]_{\text{D}}^{22}$  -11.4 (c 0.8,  $\text{CHCl}_3$ ); MS (MALDI-TOF)  $m/z$  220.9  $[\text{M}+\text{K}]^+$ ; HRMS (HNESP) exact mass calculated for  $\text{C}_8\text{H}_{12}\text{N}_3\text{O}_3$  requires  $m/z$  198.0873, found  $m/z$  198.0873  $[\text{M}+\text{H}]^+$ .

**(S)-Methyl 2-(2-diazoacetamido)-3-(4-iodophenyl)propanoate (400)**

Compound **400** was prepared according to method B. Purification *via* flash column chromatography on silica gel (eluent: diethyl ether / petroleum ether 3:1;  $R_f = 0.37$ ) afforded a yellow solid whose physicochemical properties were consistent with those of the title compound (89 mg, 0.24 mmol, 67% yield).

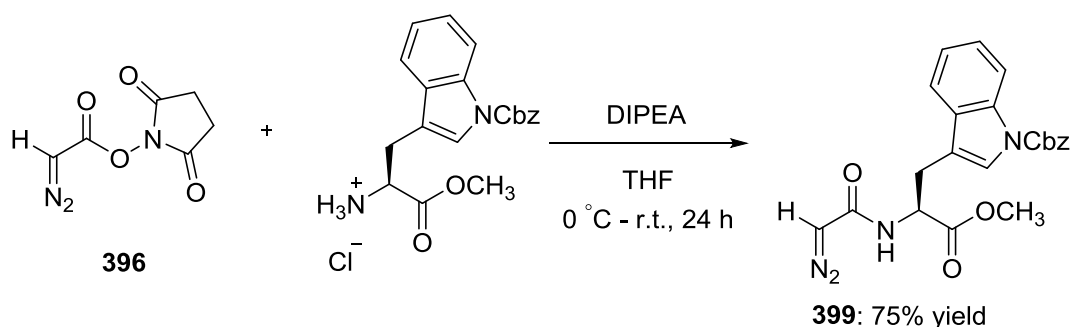
M.p. 73–75 °C;  $^1\text{H-NMR}$  (500 MHz,  $\text{CDCl}_3$ )  $\delta$  7.61 (d,  $J = 8.2$  Hz, 2H, Ar-*H*), 6.84 (d,  $J = 8.2$  Hz, 2H, Ar-*H*), 5.50 (d,  $J = 6.0$  Hz, 1H, -NH-), 4.93 (m, 1H, -NHCH-), 4.75 (s, 1H, -CHN<sub>2</sub>), 3.74 (s, 3H, -OCH<sub>3</sub>), 3.13 (dd,  $J = 13.9, 6.0$  Hz, 1H, -CH<sub>2</sub>Ph), 3.05 (dd,  $J = 13.9, 6.0$  Hz, 1H, -CH<sub>2</sub>Ph);  $^{13}\text{C-NMR}$  (126 MHz,  $\text{CDCl}_3$ )  $\delta$  172.3 (-C=O *ester*), 165.4 (-C=O *amide*), 137.7, 135.6, 131.4, 92.7 (C-I), 53.3 (-NHCH-), 52.6 (-OCH<sub>3</sub>), 47.5 (-CHN<sub>2</sub>), 37.7 (-CH<sub>2</sub>Ar); FT-IR (thin film):  $\nu$  ( $\text{cm}^{-1}$ ) = 3361 (N-H), 3091 (C-H), 3011 (C-H), 2922 (C-H), 2854 (C-H), 2106 (*diazo* C=N<sub>2</sub>), 1743 (*ester* C=O), 1620 (*amide* C=O), 1540, 1493, 1447, 1383, 1206, 1054;  $[\alpha]_D^{20} +151.8$  (c 1.0,  $\text{CHCl}_3$ ); MS (MALDI-TOF)  $m/z$  412.02  $[\text{M}+\text{K}]^+$ ; HRMS (HNESF) exact mass calculated for  $\text{C}_{12}\text{H}_{13}\text{IN}_3\text{O}_2$  requires  $m/z$  373.9996, found  $m/z$  373.9997  $[\text{M}+\text{H}]^+$ .

***rac*-Benzyl 2-(2-diazoacetamido)-3-phenylpropanoate (402)**

Compound **402** was prepared according to method B. Purification *via* flash column chromatography on silica gel (eluent: diethyl ether / petroleum ether 3:1;  $R_f = 0.47$ ) afforded a yellow solid whose physicochemical properties were consistent with those of the title compound (2.01 g, 6.22 mmol, 37% yield).

M.p. 78–80 °C;  $^1\text{H-NMR}$  (500 MHz,  $\text{CDCl}_3$ )  $\delta$  7.41 – 7.34 (m, 3H, Ar-*H*), 7.34 – 7.29 (m, 2H, Ar-*H*), 7.24 – 7.20 (m, 3H, Ar-*H*), 7.02 – 6.98 (m, 2H, Ar-*H*), 5.46 (d,  $J = 7.2$  Hz, 1H, -NH-), 5.18 (d,  $J = 12.1$  Hz, 1H, -OCH<sub>2</sub>Ph), 5.13 (d,  $J = 12.1$  Hz, 1H, -OCH<sub>2</sub>Ph), 4.99 (br s, 1H, -NHCH-), 4.72 (s, 1H, -CHN<sub>2</sub>), 3.15 (dd,  $J = 13.9, 5.9$  Hz, -CH<sub>2</sub>Ph), 3.12 (dd,  $J = 13.9, 5.9$  Hz, 1H, -CH<sub>2</sub>Ph);  $^{13}\text{C-NMR}$  (126 MHz,  $\text{CDCl}_3$ )  $\delta$  171.8 (-CO<sub>2</sub>Bn), 165.3 (-CONH-), 135.8, 135.1, 129.5, 128.8, 128.7, 128.7, 127.2, 67.5 (-CO<sub>2</sub>CH<sub>2</sub>Ph), 53.6 (-NHCH-), 47.5 (-CHN<sub>2</sub>), 38.3 (-CH<sub>2</sub>Ph); FT-IR (thin film):  $\nu$  ( $\text{cm}^{-1}$ ) = 3289 (N-H), 3094, 3070, 3035, 2946, 2108 (diazo C=N<sub>2</sub>), 1741 (ester C=O), 1621 (amide C=O), 1538, 1456, 1387, 1195, 1109, 1078, 1027, 992; MS (MALDI-TOF)  $m/z$  361.80 [ $\text{M}+\text{K}$ ]<sup>+</sup>; HRMS (HNESP) exact mass calculated for C<sub>18</sub>H<sub>18</sub>N<sub>3</sub>O<sub>3</sub> requires  $m/z$  324.1343, found  $m/z$  324.1344 [ $\text{M}+\text{H}$ ]<sup>+</sup>.

**(*S*)-Benzyl 3-(2-(2-diazoacetamido)-3-methoxy-3-oxopropyl)-1H-indole-1-carboxylate (399)**

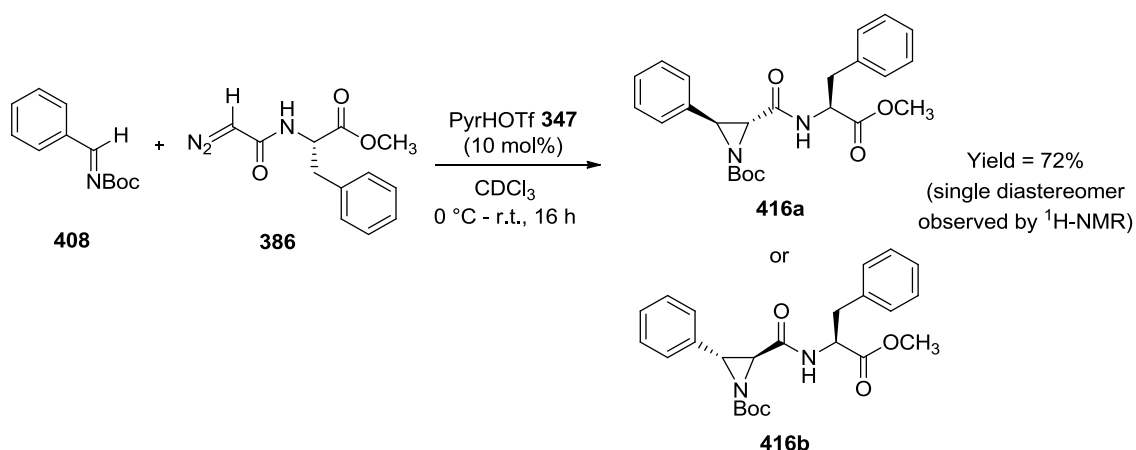


Compound **399** was prepared according to method A. Purification *via* flash column chromatography on silica gel (eluent: diethyl ether / dichloromethane / petroleum ether 7:1:2;  $R_f = 0.38$ ) afforded a pale yellow solid whose physicochemical properties were consistent with those of the title compound (876 mg, 2.08 mmol, 75% yield).

M.p. 120–122 °C;  $^1\text{H-NMR}$  (500 MHz,  $\text{CDCl}_3$ )  $\delta$  8.07 (br s, 1H, -CH<sub>ind</sub>), 7.45 – 7.39 (m, 3H, Ar-*H*), 7.38 – 7.28 (m, 4H, Ar-*H*), 7.25 (t,  $J = 7.3$  Hz, 1H, Ar-*H*), 7.21 – 7.16 (m, 1H, Ar-*H*), 5.52 (d,  $J = 7.6$  Hz, 1H, -NH-), 5.37 (s, 2H, -CH<sub>2</sub>Ph), 4.93 (m, 1H, -NHCH-), 4.62 (s, 1H, -CHN<sub>2</sub>), 3.60 (s, 3H, -OCH<sub>3</sub>), 3.28 (dd,  $J = 14.7, 5.6$  Hz, 1H, -CH<sub>2</sub>-indole), 3.22 (dd,  $J = 14.7, 5.6$  Hz, 1H, -CH<sub>2</sub>-indole);  $^{13}\text{C-NMR}$  (125 MHz,  $\text{CDCl}_3$ )  $\delta$  172.3 (-C=O ester), 165.2 (-C=O amide), 150.8 (-C=O carbamate), 135.2, 130.7, 128.9, 125.1, 123.9, 123.2, 119.1, 116.0, 115.5, 68.9 (-CH<sub>2</sub>Ph), 52.9 (-NHCH-), 52.7 (-OCH<sub>3</sub>), 47.7 (-CHN<sub>2</sub>), 27.9 (-CH<sub>2</sub>-indole); FT-IR (thin film,  $\text{cm}^{-1}$ )  $\nu$  = 3335 (N-H), 3092, 2920, 2106, 1739

(*ester* C=O), 1617 (*amide* C=O), 1539, 1457, 1394, 1250;  $[\alpha]_{\text{D}}^{25} +23.9$  (c 1.0, acetone); MS (MALDI-TOF):  $m/z = 443.12$   $[M+Na]^+$ ; HRMS (NSI) exact mass calculated for  $C_{22}H_{21}O_5N_4$  requires  $m/z$  421.1506, found  $m/z$  421.1505  $[M+H]^+$ .

***trans*-Tert-butyl 2-(((*S*)-1-methoxy-1-oxo-3-phenylpropan-2-yl)carbamoyl)-3-phenylaziridine-1-carboxylate (416a/b)**

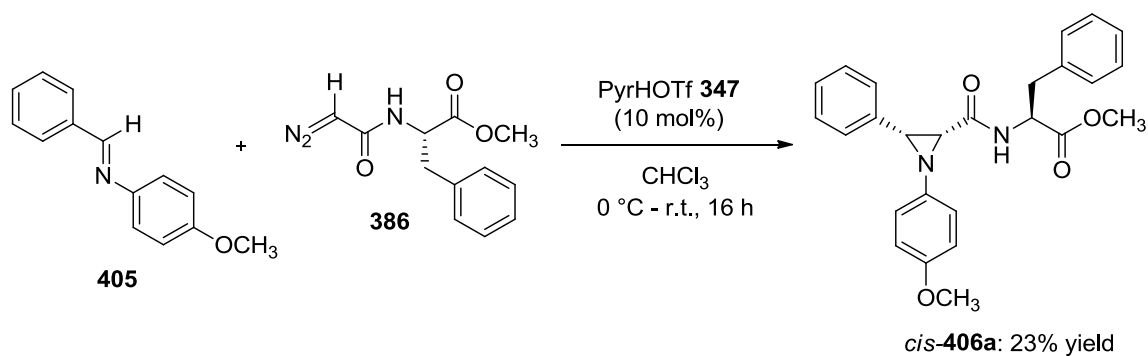


A 5 mL microwave vial containing crushed 4Å molecular sieves was flame-dried and cooled under a nitrogen atmosphere. The vial was charged with a solution of *tert*-butyl benzylidenecarbamate **408** (100 mg, 0.49 mmol, 1 equiv.) in chloroform- $d_3$  (1 mL) *via* syringe and a magnetic stirrer bar before being cooled to  $0\text{ }^{\circ}\text{C}$  using an ice bath. Pyridinium triflate (11 mg, 0.05 mmol, 10 mol%) was added, and the vial was sealed with a PTFE-lined aluminium crimp cap. A solution of (*S*)-methyl 2-(2-diazoacetamido)-3-phenylpropanoate **386** (145 mg, 0.59 mmol, 1.2 equiv.) in chloroform- $d_3$  (1 mL) was added dropwise *via* syringe, and the reaction was allowed to warm slowly to room temperature over 16 hours. On complete disappearance of imine **408** by  $^1\text{H-NMR}$ , the mixture was filtered through a short plug of silica, eluting with diethyl ether, and the solvent removed *in vacuo*. Purification *via* flash column chromatography on silica gel (eluent: petroleum ether / diethyl ether 1:1;  $R_f = 0.34$ ) afforded a white solid whose physicochemical properties were consistent with those of a single diastereomer of the title compound (149 mg, 0.35 mmol, 72% yield).

M.p.  $125\text{--}127\text{ }^{\circ}\text{C}$ ;  $^1\text{H-NMR}$  (500 MHz,  $CDCl_3$ )  $\delta$  7.39 – 7.22 (m, 8H, Ar-*H*), 7.11 (m, 2H, Ar-*H*), 6.56 (d,  $J = 8.0$  Hz, 1H, -NH-), 4.93 (dt,  $J = 8.0, 5.8$  Hz, 1H, -NHCH-), 3.73 (m, 4H,  $-\text{CO}_2\text{CH}_3$  + aziridine C-*H*), 3.19 (d,  $J = 2.2$  Hz, 1H, aziridine C-*H*), 3.18 (m, 1H, -

$\text{CH}_2\text{Ph}$ ), 3.14 (dd, 1H,  $J = 13.9, 5.8$  Hz,  $-\text{CH}_2\text{Ph}$ ), 1.33 (s, 9H,  $-\text{C}(\text{CH}_3)_3$ );  $^{13}\text{C}$ -NMR (126 MHz,  $\text{CDCl}_3$ )  $\delta$  171.6 ( $-\text{C}=\text{O}$  ester), 166.2 ( $-\text{C}=\text{O}$  amide), 158.3 ( $-\text{C}=\text{O}$  carbamate), 135.6, 134.3, 129.4, 128.8, 128.6(8), 128.6(6), 127.4, 127.2, 82.2 ( $-\text{C}(\text{CH}_3)_3$ ), 53.4 ( $-\text{NHCH}-$ ), 52.5 ( $-\text{OCH}_3$ ), 45.8 (*aziridine* C-H), 44.2 (*aziridine* C-H), 38.0 ( $-\text{CH}_2\text{Ph}$ ), 27.9 ( $-\text{C}(\text{CH}_3)_3$ ); FT-IR (thin film):  $\nu$  ( $\text{cm}^{-1}$ ) = 3323 (N-H), 2977 (C-H), 1726 (ester C=O), 1680 (amide C=O), 1535, 1455, 1367, 1321, 1215, 1152, 1086;  $[\alpha]_{\text{D}}^{23} +17.5$  (c 1.0,  $\text{CHCl}_3$ ); MS (MALDI-TOF)  $m/z$  463.27  $[\text{M}+\text{K}]^+$ ; HRMS (HNESF) exact mass calculated for  $\text{C}_{24}\text{H}_{28}\text{N}_2\text{O}_5\text{Na}$  requires  $m/z$  447.1890, found  $m/z$  447.1887  $[\text{M}+\text{Na}]^+$ .

***cis*-(2*S*)-Methyl 2-(1-(4-methoxyphenyl)-3-phenylaziridine-2-carboxamido)-3-phenylpropanoate (406a)**

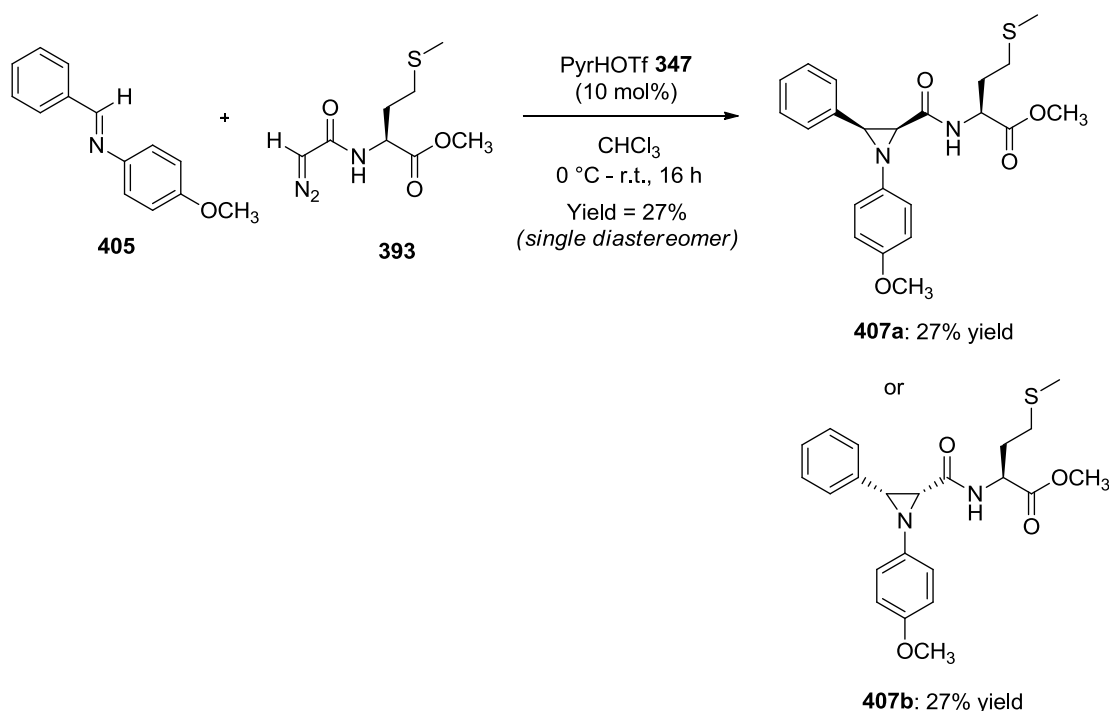


Compound **406a** was prepared according to the procedure for compound **416** above. Purification *via* flash column chromatography on silica gel (eluent: diethyl ether / petroleum ether 1:1;  $R_f = 0.13$ ) afforded a white solid whose physicochemical properties were consistent with those of the title compound (47 mg, 0.11 mmol, 23% yield).

M.p. 140–142 °C (petroleum ether / diethyl ether);  $^1\text{H}$ -NMR (500 MHz,  $\text{CDCl}_3$ )  $\delta$  7.42 – 7.36 (m, 2H, Ar-*H*), 7.32 – 7.21 (m, 6H, Ar-*H*), 7.14 – 7.06 (m, 2H, Ar-*H*), 6.92 (d,  $J = 9.0$  Hz, 2H, Ar-*H*), 6.88 – 6.81 (m, 3H, Ar-*H* + N-*H*), 4.60 (dt,  $J = 8.3, 6.0$  Hz, 1H,  $-\text{NHCH}-$ ), 3.80 (s, 3H, Ar- $\text{OCH}_3$ ), 3.57 (d,  $J = 7.0$  Hz, 1H, *aziridine* -CH-), 3.47 (s, 3H,  $-\text{CO}_2\text{CH}_3$ ), 3.10 (dd,  $J = 13.7, 6.0$  Hz, 1H,  $-\text{CH}_2\text{Ph}$ ), 3.05 (d,  $J = 7.0$  Hz, 1H, *aziridine* -CH-), 3.00 (dd,  $J = 13.7, 6.0$  Hz, 1H,  $-\text{CH}_2\text{Ph}$ );  $^{13}\text{C}$ -NMR (126 MHz,  $\text{CDCl}_3$ )  $\delta$  171.0 ( $-\text{C}=\text{O}$  ester), 166.7 ( $-\text{C}=\text{O}$  amide), 156.2 ( $-\text{COCH}_3$ ), 145.2, 136.0, 134.5, 129.5, 128.6, 128.4, 127.9, 127.7, 127.2, 120.9, 114.7, 55.8 ( $-\text{NHCH}-$ ), 52.7 (Ar- $\text{OCH}_3$ ), 52.2 ( $-\text{CH-aziridine}$ ), 48.0 ( $-\text{CO}_2\text{CH}_3$ ), 47.1 ( $-\text{CH-aziridine}$ ), 38.3 ( $-\text{CH}_2\text{Ph}$ ); FT-IR (thin film):  $\nu$  ( $\text{cm}^{-1}$ ) = 3393 (N-H), 3033, 2961, 1745 (ester C=O), 1673 (amide C=O), 1506, 1242,

1033;  $[\alpha]_D^{21}$  -21.7 (c 1.0,  $\text{CHCl}_3$ ); MS (MALDI-TOF)  $m/z$  453.08  $[\text{M}+\text{Na}]^+$ ; HRMS (HNESF) exact mass calculated for  $\text{C}_{26}\text{H}_{27}\text{N}_2\text{O}_4$  requires  $m/z$  431.1965, found  $m/z$  431.1973  $[\text{M}+\text{H}]^+$ .

***cis*-(2*S*)-Methyl 2-(1-(4-methoxyphenyl)-3-phenylaziridine-2-carboxamido)-4-(methylthio)butanoate (407a/b)**



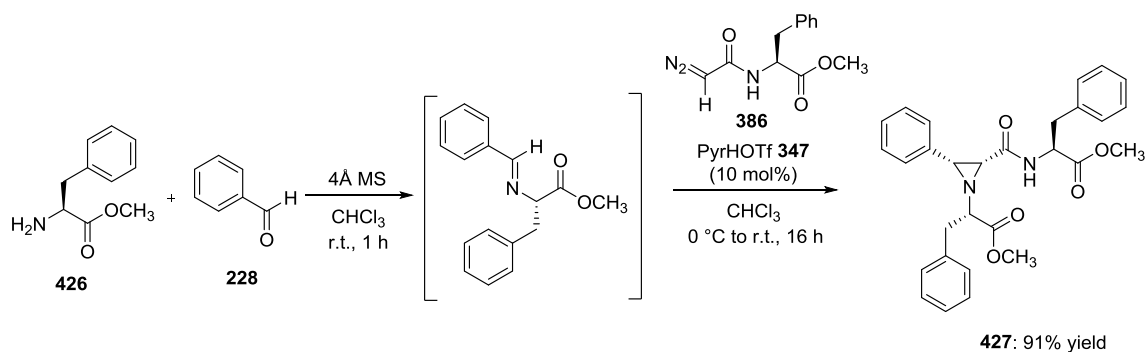
Compound **407a/b** was prepared according to the procedure for compound **416** above. Purification *via* flash column chromatography on silica gel (eluent: diethyl ether / petroleum ether 1:1;  $R_f$  = 0.10) afforded a colourless oil whose physicochemical properties were consistent with those of the title compound (18 mg, 0.04 mmol, 27% yield).

$^1\text{H}$ -NMR (400 MHz,  $\text{CDCl}_3$ )  $\delta$  7.46 (d,  $J$  = 7.1 Hz, 2H, Ar-*H*), 7.36 – 7.24 (m, 3H, Ar-*H*), 7.05 – 6.96 (m, 3H, Ar-*H* + -NH-), 6.85 (d,  $J$  = 8.9 Hz, 2H, Ar-*H*), 4.35 (dt,  $J$  = 6.1, 5.6 Hz, 1H, -NHCH-), 3.79 (s, 3H, - $\text{OCH}_3$ ), 3.59 (d,  $J$  = 7.0 Hz, 1H, aziridine -CH-), 3.54 (s, 3H, - $\text{CO}_2\text{CH}_3$ ), 3.13 (d,  $J$  = 7.0 Hz, 1H, aziridine -CH-), 2.38 (t,  $J$  = 7.8 Hz, 2H, - $\text{SCH}_2$ -), 2.12 – 2.00 (m, 1H, - $\text{SCH}_2\text{CH}_2$ -), 2.06 (s, 3H, - $\text{SCH}_3$ ), 1.98 – 1.84 (m, 1H, - $\text{SCH}_2\text{CH}_2$ -);  $^{13}\text{C}$ -NMR (126 MHz,  $\text{CDCl}_3$ )  $\delta$  171.3 (- $\text{CO}_2\text{CH}_3$ ), 167.2 (-CONH-), 156.3 (C- $\text{OCH}_3$ ), 145.1, 134.5, 128.5, 127.9, 127.8, 121.0, 114.8, 55.8 (Ar- $\text{OCH}_3$ ), 52.4 (-NHCH-), 51.1 (aziridine -CH-), 48.1 (- $\text{CO}_2\text{CH}_3$ ), 46.8 (aziridine -CH-), 32.0 (- $\text{SCH}_2\text{CH}_2$ -), 29.9 (- $\text{SCH}_2$ -

), 15.6 (-SCH<sub>3</sub>); FT-IR (thin film):  $\nu$  (cm<sup>-1</sup>) = 3312 (N-H), 2962 (C-H), 2923 (C-H), 1740 (ester C=O), 1653 (amide C=O), 1508, 1245, 1036;  $[\alpha]_D^{21}$  -23.8 (c 1.0, CHCl<sub>3</sub>); MS (MALDI-TOF)  $m/z$  452.8 [M+K]<sup>+</sup>; HRMS (ASAP, solid) exact mass calculated for C<sub>22</sub>H<sub>27</sub>N<sub>2</sub>O<sub>4</sub>S requires  $m/z$  415.1686, found  $m/z$  415.1687 [M+H]<sup>+</sup>.

**General procedure for the one-pot synthesis of peptide aziridines:**

**(S)-Methyl 2-((2R,3R)-1-((S)-1-methoxy-1-oxo-3-phenylpropan-2-yl)-3-phenylaziridine-2-carboxamido)-3-phenylpropanoate (**427**)**

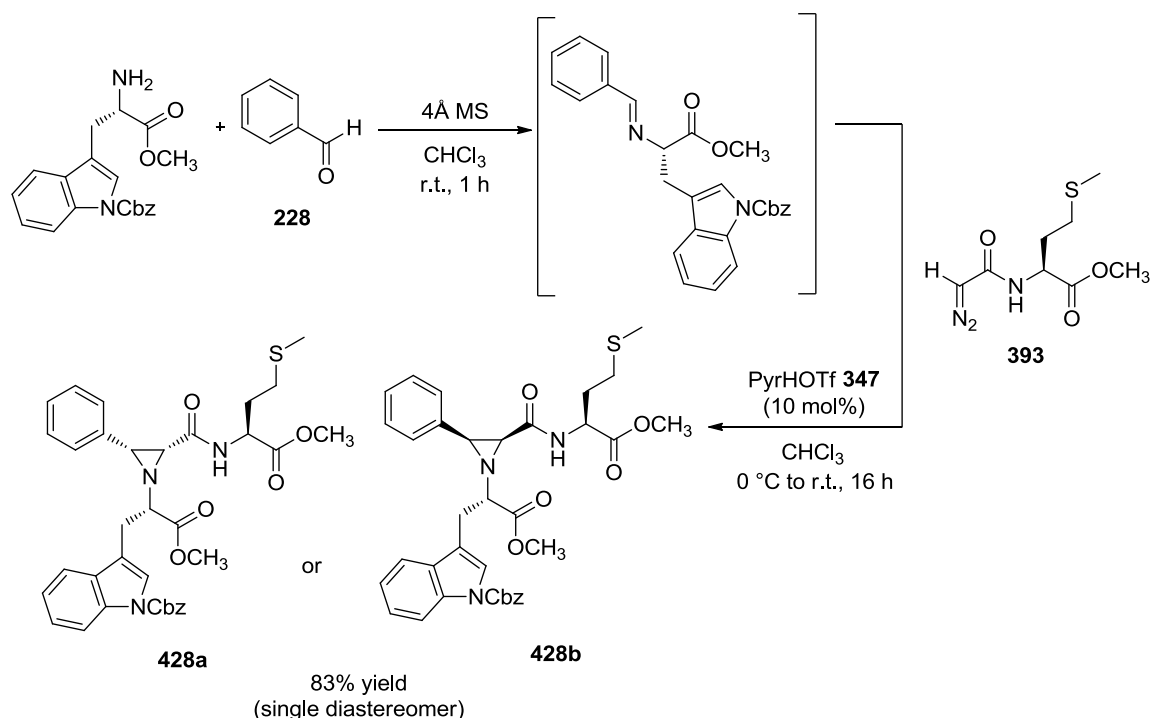


A 5 mL microwave vial containing crushed 4Å molecular sieves was flame-dried and cooled under a nitrogen atmosphere, followed by the addition of a magnetic stirrer bar. Benzaldehyde **228** (56 mg, 0.528 mmol, 1.1 equiv.) and (S)-phenylalanine methyl ester **426** (91 mg, 0.508 mmol, 1 equiv.) were weighed into a sample vial, dissolved in chloroform (1 mL) and transferred to the microwave vial *via* a 2 mL syringe. The solution was stirred at room temperature for 1 hour before being cooled to 0 °C using an ice-water bath. Pyridinium triflate **347** (12 mg, 0.0524 mmol, 10 mol%) was added and the vial was sealed with a PTFE-lined aluminium crimp cap. (S)-Methyl 2-(2-diazoacetamido)-3-phenylpropanoate **386** (150 mg, 0.607 mmol, 1.2 equiv.) was dissolved in chloroform (1 mL) and added dropwise to the reaction vial *via* a 2 mL syringe. Effervescence indicated the evolution of nitrogen gas during the reaction. The reaction was allowed to warm slowly to room temperature. After 16 hours the mixture was filtered through a short plug of silica, eluting with diethyl ether, and the solvent removed *in vacuo*. Purification *via* flash column chromatography on silica gel (eluent: diethyl ether / petroleum ether 3:1; R<sub>f</sub> = 0.17) afforded a colourless oil whose physicochemical properties were consistent with those of the title compound (224 mg, 0.460 mmol, 91% yield).



$^1\text{H}$ -NMR (500 MHz,  $\text{CDCl}_3$ )  $\delta$  = 7.32-7.10 (m, 15H, Ar-*H*), 4.57 (dt,  $J$  = 8.2, 6.2 Hz, 1H, -NHCH-), 3.64 (s, 3H, -OCH<sub>3</sub>), 3.47 (s, 3H, -OCH<sub>3</sub>), 3.29 (dd,  $J$  = 13.8, 6.2 Hz, 1H, -CH<sub>2</sub>Ph), 3.12 – 3.05 (m, 2H, -CH<sub>2</sub>Ph), 3.02 (dd,  $J$  = 13.8, 6.2 Hz, 1H, -CH<sub>2</sub>Ph), 2.90 (t,  $J$  = 6.6 Hz, 1H, -NCH(Bn)CO<sub>2</sub>CH<sub>3</sub>), 2.78 (d,  $J$  = 7.2 Hz, 1H, aziridine -CH-), 2.60 (d,  $J$  = 7.2 Hz, 1H, aziridine -CH-);  $^{13}\text{C}$ -NMR (125 MHz,  $\text{CDCl}_3$ )  $\delta$  = 171.7 (-C=O ester), 171.3 (-C=O ester), 166.4 (-C=O amide), 136.7, 136.1, 134.4, 129.5, 129.4, 128.6, 128.5, 128.0, 127.6, 127.5, 127.1, 126.9, 72.5 (-NCH-), 52.7 (-NHCH-), 52.2 (-OCH<sub>3</sub>), 52.1 (-OCH<sub>3</sub>), 47.4 (-CH- aziridine), 46.8 (-CH- aziridine), 39.2 (-CH<sub>2</sub>Ph), 38.3 (-CH<sub>2</sub>Ph); FT-IR (thin film,  $\text{cm}^{-1}$ )  $\nu$  = 3391 (N-H), 3035, 2955, 2935, 2867, 1745 (ester C=O), 1681 (amide C=O), 1521, 1497, 1217, 1181, 1125, 1053, 828;  $[\alpha]_{\text{D}}^{20}$  -48.3 (c 1.0,  $\text{CHCl}_3$ ); MS (MALDI-TOF):  $m/z$  = 509.4  $[\text{M}+\text{Na}]^+$ ; HRMS (NSI) exact mass calculated for  $\text{C}_{29}\text{H}_{31}\text{O}_5\text{N}_2$  requires  $m/z$  487.2227, found  $m/z$  487.2221  $[\text{M}+\text{H}]^+$ .

***cis*-Benzyl 3-((2*S*)-3-methoxy-2-(2-((*S*)-1-methoxy-4-(methylthio)-1-oxobutan-2-ylcarbamoyl)-3-phenylaziridin-1-yl)-3-oxopropyl)-1*H*-indole-1-carboxylate (428a/b)**

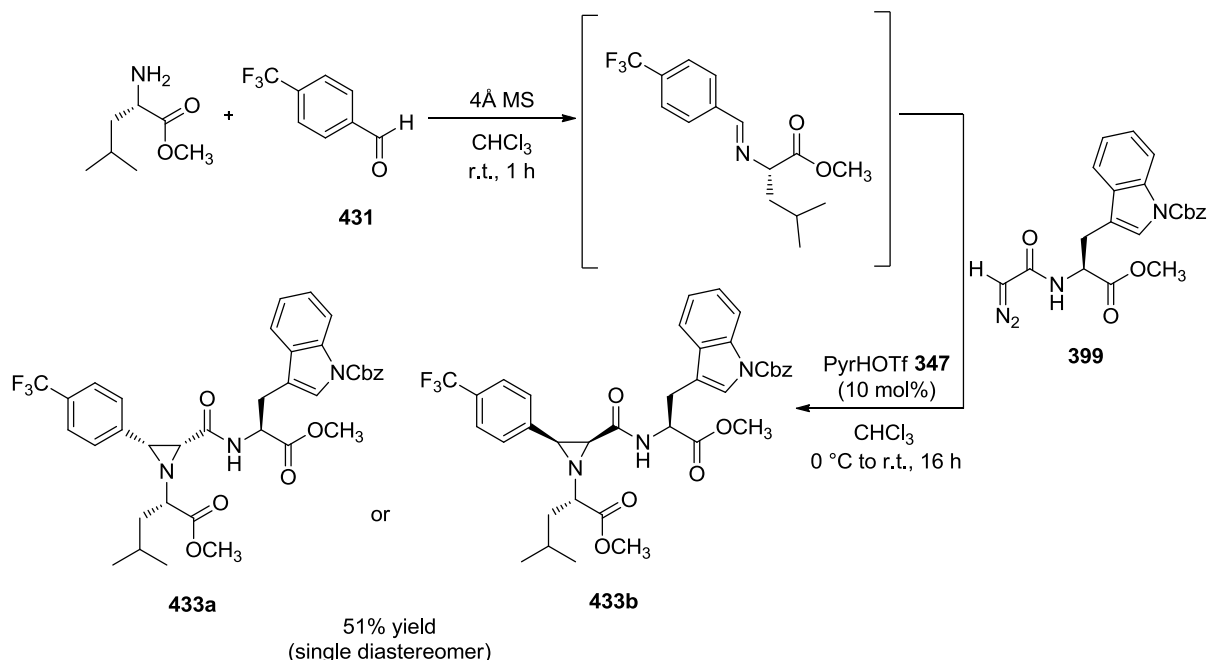


Compound **428a/b** was prepared according to the procedure for compound **427**. Purification *via* flash column chromatography on silica gel (eluent: diethyl ether / petroleum ether 1:1;  $R_f$  = 0.13) afforded a colourless oil whose physicochemical

properties were consistent with those of a single diastereomer of the title compound (188 mg, 0.292 mmol, 83% yield).

$^1\text{H}$ -NMR (500 MHz,  $\text{CD}_3\text{CN}$ )  $\delta$  = 8.06 (d,  $J$  = 8.0 Hz, 1H, -NH-), 7.55 (d,  $J$  = 7.7 Hz, 1H, Ar-*H*), 7.52 – 7.37 (m, 6H, Ar-*H*), 7.35 – 7.29 (m, 2H, Ar-*H*), 7.25 (t,  $J$  = 7.5, 1H, Ar-*H*), 7.16 – 7.04 (m, 5H, Ar-*H*), 5.34 (d,  $J$  = 12.2 Hz, 1H, -CH<sub>2</sub>Ph), 5.26 (d,  $J$  = 12.2 Hz, 1H, -CH<sub>2</sub>Ph), 4.34 (dt,  $J$  = 8.3, 5.0 Hz, 1H, -CONHCH-), 3.70 (s, 3H, -CO<sub>2</sub>CH<sub>3</sub>), 3.59 (s, 3H, -CO<sub>2</sub>CH<sub>3</sub>), 3.32 (dd,  $J$  = 14.4, 4.9 Hz, 1H, -CH<sub>2</sub>-indole), 3.25 – 3.14 (m, 1H, -CH<sub>2</sub>-indole, -NCH-), 2.68 (d,  $J$  = 7.2 Hz, 1H, -CH- aziridine), 2.61 (d,  $J$  = 7.2 Hz, 1H, -CH- aziridine), 2.04 – 1.99 (m, 2H, -CH<sub>2</sub>SCH<sub>3</sub>), 2.07-1.98 (m, 1H, -CH<sub>2</sub>CH<sub>2</sub>SCH<sub>3</sub>), 2.03 (s, 3H, -SCH<sub>3</sub>), 1.87 (ddt,  $J$  = 14.0, 8.2, 6.2 Hz, 1H, -CH<sub>2</sub>SCH<sub>3</sub>);  $^{13}\text{C}$ -NMR (126 MHz,  $\text{CD}_3\text{CN}$ )  $\delta$  = 173.4 (-C=O ester), 172.7 (-C=O ester), 167.3 (-C=O amide), 151.2 (-C=O carbamate), 136.6, 136.4, 136.3, 131.0, 129.7, 129.5, 129.3, 128.8, 128.2, 128.1, 125.7, 125.6, 123.7, 120.2, 117.1, 115.9, 70.0 (-NCH-), 69.3 (-CH<sub>2</sub>PH), 52.8(6) (-NHCH-), 52.8(5) (-OCH<sub>3</sub>), 51.5 (-OCH<sub>3</sub>), 48.0 (-CH- aziridine), 47.7 (-CH- aziridine), 32.6 (-NHCHCH<sub>2</sub>-), 30.1 (-CH<sub>2</sub>S-), 29.0 (-CH<sub>2</sub>-indole), 15.3 (-SCH<sub>3</sub>); FT-IR (thin film,  $\text{cm}^{-1}$ )  $\nu$  = 3385 (N-H), 2951, 2920, 2848, 1737 (ester C=O), 1677 (amide C=O), 1519, 1455, 1396, 1248, 1215, 1083;  $[\alpha]_{\text{D}}^{23}$  -41.4 (c 1.0,  $\text{CHCl}_3$ ); MS (MALDI-TOF):  $m/z$  = 666.5  $[\text{M}+\text{Na}]^+$ ; HRMS (NSI) exact mass calculated for  $\text{C}_{35}\text{H}_{38}\text{O}_7\text{N}_3\text{S}$  requires  $m/z$  644.2425, found  $m/z$  644.2440  $[\text{M}+\text{H}]^+$ .

***cis*-Benzyl 3-((2*S*)-3-methoxy-2-(1-((*S*)-1-methoxy-4-methyl-1-oxopentan-2-yl)-3-(4-(trifluoromethyl)phenyl)aziridine-2-carboxamido)-3-oxopropyl)-1*H*-indole-1-carboxylate (433a/b)**

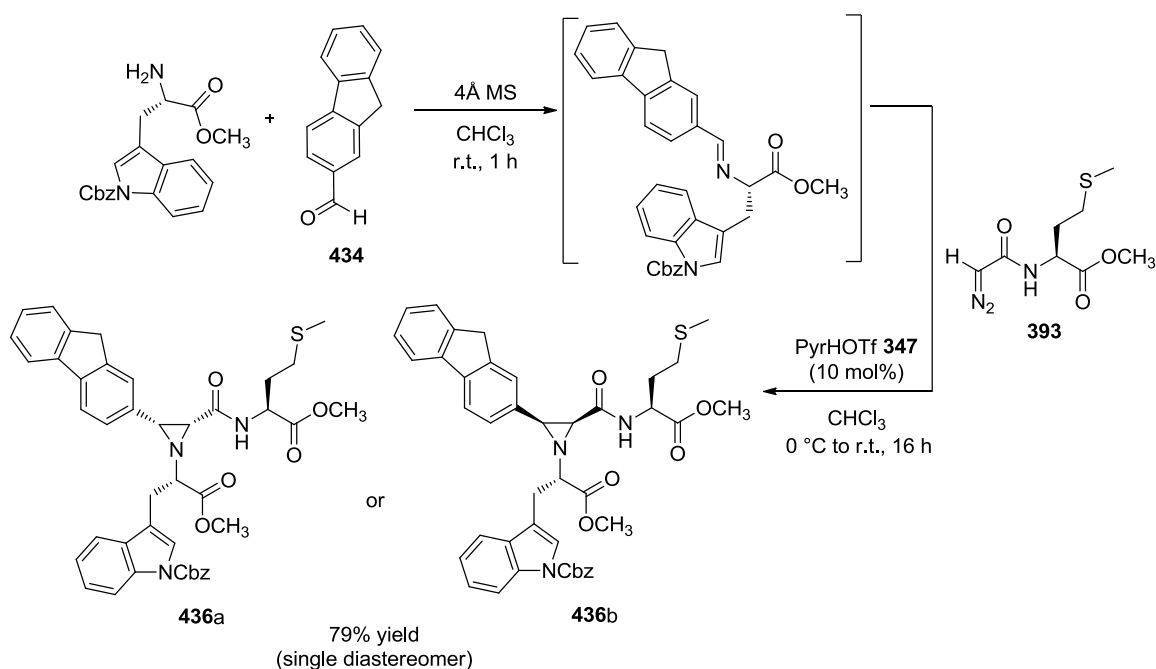


Compound **433a/b** was prepared according to the procedure for compound **427**. Purification *via* flash column chromatography on silica gel (eluent: diethyl ether / petroleum ether / dichloromethane 3:2:1;  $R_f$  = 0.16) afforded a colourless oil whose physicochemical properties were consistent with those of a single diastereomer of the title compound (122 mg, 0.18 mmol, 51% yield).

<sup>1</sup>H-NMR (500 MHz, CDCl<sub>3</sub>)  $\delta$  8.16 (br s, 1H, -NH-), 7.52 (d,  $J$  = 7.8 Hz, 2H, Ar-*H*), 7.50 – 7.46 (m, 2H, Ar-*H*), 7.43 – 7.36 (m, 5H, Ar-*H*), 7.34 – 7.29 (m, 4H, Ar-*H*), 7.28 – 7.23 (m, 1H, Ar-*H*), 5.47 (d,  $J$  = 12.1, 1H, -CH<sub>2</sub>Ph), 5.43 (d,  $J$  = 12.1, 1H, -CH<sub>2</sub>Ph), 4.59 (dt,  $J$  = 8.0, 5.9 Hz, 1H, -CONHCH-), 3.57 (s, 3H, -CO<sub>2</sub>CH<sub>3</sub>), 3.38 (s, 3H, -CO<sub>2</sub>CH<sub>3</sub>), 3.19 (dd,  $J$  = 14.8, 5.8 Hz, 1H, -CH<sub>2</sub>-indole), 3.13 (dd,  $J$  = 14.8, 5.8 Hz, 1H, -CH<sub>2</sub>-indole), 3.03 (d,  $J$  = 7.1 Hz, 1H, -CH- aziridine), 2.67 (t,  $J$  = 6.4 Hz, 1H, -NCH-), 2.61 (d,  $J$  = 7.1 Hz, 1H, -CH- aziridine), 1.85 – 1.78 (m, 1H, -CH(CH<sub>3</sub>)<sub>2</sub>), 1.75 – 1.62 (m, 2H, -CH<sub>2</sub>CH(CH<sub>3</sub>)<sub>2</sub>), 0.89 (d,  $J$  = 6.2 Hz, 3H, -CH(CH<sub>3</sub>)<sub>2</sub>), 0.88 (d,  $J$  = 6.2 Hz, 3H, -CH(CH<sub>3</sub>)<sub>2</sub>); <sup>19</sup>F-NMR (471 MHz, CDCl<sub>3</sub>)  $\delta$  -62.6; <sup>13</sup>C-NMR (125 MHz, CDCl<sub>3</sub>)  $\delta$  172.6 (-C=O ester), 171.4 (-C=O ester), 166.3 (-C=O amide), 150.9 (-C=O carbamate), 138.7, 135.2, 130.6, 129.8 (q,  $J$  =

32 Hz), 128.9, 128.8, 128.5, 128.0, 125.6, 125.2 (q,  $J = 3.7$  Hz), 125.0, 124.2 (q,  $J = 270$  Hz,  $-\text{CF}_3$ ), 124.1, 123.2, 119.1, 116.0, 115.4, 68.8 ( $-\text{NHCH}-$ ), 68.5 ( $-\text{CH}_2\text{Ph}$ ), 52.1 ( $-\text{NHCH}-$ ), 51.7 ( $-\text{OCH}_3$ ), 46.7 ( $-\text{OCH}_3$ ), 46.2 ( $-\text{CH}-\text{aziridine}$ ), 42.0 ( $-\text{CH}-\text{aziridine}$ ), 30.4 ( $-\text{CH}_2\text{CH}(\text{CH}_3)_2$ ), 27.8 ( $-\text{CH}_2\text{-indole}$ ), 24.8 ( $-\text{CH}(\text{CH}_3)_2$ ), 22.8 ( $-\text{CH}(\text{CH}_3)_2$ ), 22.7 ( $-\text{CH}(\text{CH}_3)_2$ ); FT-IR (thin film,  $\text{cm}^{-1}$ )  $\nu = 3385$  (N-H), 2956, 2872, 1747 (*ester* C=O), 1685 (*amide* C=O), 1622, 1520, 1457, 1399, 1358, 1325, 1249, 1164, 1131, 1095, 1065, 1018;  $[\alpha]_D^{20} -48.3$  (c 1.0,  $\text{CHCl}_3$ ); MS (MALDI-TOF):  $m/z = 732.55$   $[\text{M}+\text{K}]^+$ ; HRMS (NSI) exact mass calculated for  $\text{C}_{37}\text{H}_{38}\text{F}_3\text{O}_7\text{N}_3$  requires  $m/z$  694.2735, found  $m/z$  694.2730  $[\text{M}+\text{H}]^+$ .

**cis-Benzyl 3-((2*S*)-2-(2-(9*H*-fluoren-2-yl)-3-((*S*)-1-methoxy-4-(methylthio)-1-oxobutan-2-ylcarbamoyl)aziridin-1-yl)-3-methoxy-3-oxopropyl)-1*H*-indole-1-carboxylate (436a/b)**

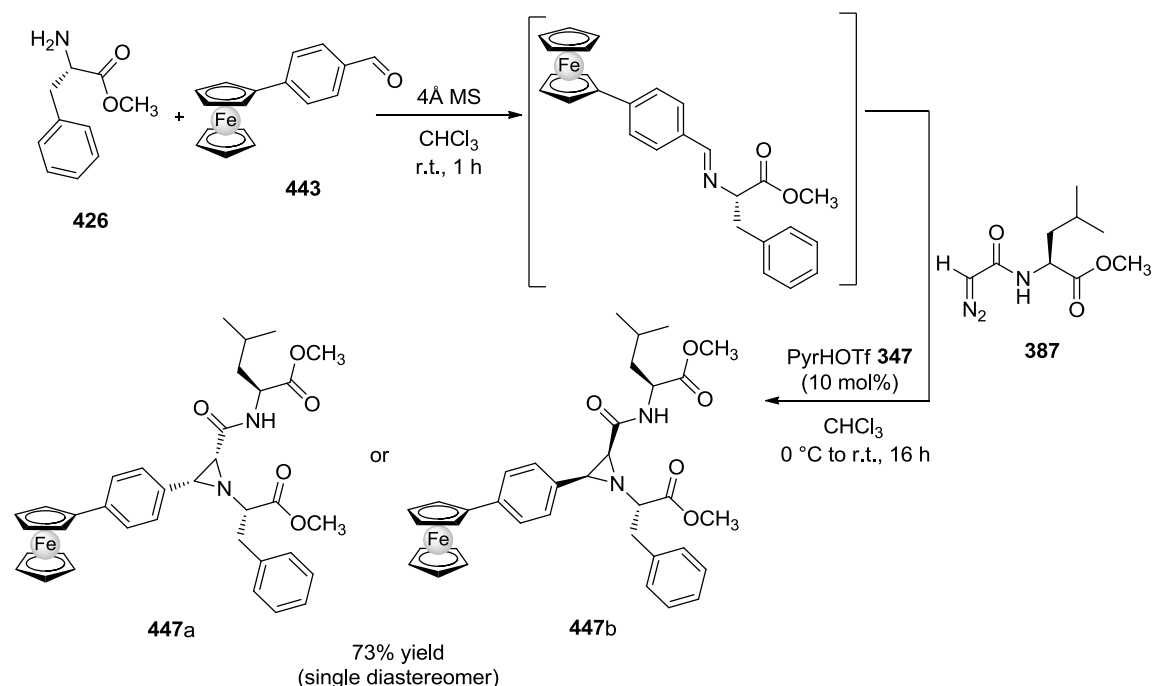


Compound **436a/b** was prepared according to the procedure for compound **427**. Purification *via* flash column chromatography on silica gel (eluent: diethyl ether / petroleum ether / dichloromethane 3:2:1;  $R_f = 0.16$ ) afforded a colourless oil whose physicochemical properties were consistent with those of a single diastereomer of the title compound (204 mg, 0.279 mmol, 79% yield).

$^1\text{H}$ -NMR (500 MHz,  $\text{CD}_3\text{CN}$ )  $\delta$  8.02 (br s, 1H, -NH-), 7.78 (d,  $J$  = 7.6 Hz, 1H, Ar-*H*), 7.60 – 7.55 (m, 4H, Ar-*H*), 7.39 – 7.25 (m, 8H, Ar-*H*), 7.22 – 7.20 (m, 2H, Ar-*H*), 7.17 (s, 1H, Ar-*H*), 6.98 (dd,  $J$  = 7.8, 1.7 Hz, 1H, Ar-*H*), 5.00 (d,  $J$  = 12.2 Hz, 1H, -CH<sub>2</sub>Ph), 4.78 (br d,  $J$  = 12.2 Hz, 1H, -CH<sub>2</sub>Ph), 4.38 (dt,  $J$  = 8.4, 4.9 Hz, 1H, -NHCH-), 3.80 (d,  $J$  = 21.0 Hz, 1H, **AB** -CH<sub>2</sub>- fluorene), 3.75 (s, 3H -OCH<sub>3</sub>), 3.74 (d,  $J$  = 21.0 Hz, 1H, **AB** -CH<sub>2</sub>- fluorene), 3.57 (s, 3H, -OCH<sub>3</sub>), 3.40 – 3.32 (m, 1H, -CH<sub>2</sub>-indole), 3.27 – 3.18 (m, 2H, -CH<sub>2</sub>-indole + -NCH-), 2.62 (d,  $J$  = 7.2 Hz, 1H, -CH- aziridine), 2.56 (d,  $J$  = 7.2 Hz, 1H, -CH- aziridine), 2.52 – 2.42 (m, 2H, -CH<sub>2</sub>S-), 2.07-2.00 (m, 1H, -CH<sub>2</sub>CH<sub>2</sub>SCH<sub>3</sub>), 2.03 (s, 3H, -SCH<sub>3</sub>), 1.92 – 1.86 (m, 1H, -CH<sub>2</sub>CH<sub>2</sub>SCH<sub>3</sub>);  $^{13}\text{C}$ -NMR (126 MHz,  $\text{CDCl}_3$ )  $\delta$  172.3 (-C=O ester), 172.0 (-C=O ester), 166.5 (-C=O amide), 150.1 (-C=O carbamate), 143.6, 143.2, 141.5, 141.1, 135.7, 135.1, 133.2, 129.7, 128.6, 128.5, 128.0, 126.9, 126.8, 126.1, 125.2, 125.0, 124.0, 123.1, 119.9, 119.3, 118.7, 115.7, 115.6, 70.0 (-NCH-), 68.3 (-CH<sub>2</sub>Ph), 52.5 (-NHCH-), 52.3 (-OCH<sub>3</sub>), 50.9 (-OCH<sub>3</sub>), 48.2 (-CH- aziridine), 47.3 (-CH- aziridine), 36.8 (-CH<sub>2</sub>- fluorene), 32.2 (-NHCHCH<sub>2</sub>-), 29.7 (-CH<sub>2</sub>S-), 29.1 (-CH<sub>2</sub>-indole), 15.5 (-SCH<sub>3</sub>); FT-IR (ATR,  $\text{cm}^{-1}$ )  $\nu$  = 3385 (N-H), 2925, 1737 (ester C=O), 1675 (amide C=O), 1519, 1455, 1398, 1253, 1212, 1088;  $[\alpha]_{\text{D}}^{23}$  -106.2 (c 1.0,  $\text{CHCl}_3$ ); MS (MALDI-TOF):  $m/z$  = 770.4  $[\text{M}+\text{K}]^+$ ; HRMS (NSI) exact mass calculated for  $\text{C}_{42}\text{H}_{41}\text{O}_7\text{N}_3\text{SO}_2\text{H}$  requires  $m/z$  764.2636, found  $m/z$  764.2654  $[\text{M}+\text{O}_2+\text{H}]^+$ .\*

\*Oxidation of methionine and/or tryptophan residues during MS analysis are commonly observed.

***cis*-Ferrocenyl-(*S*)-methyl 2-(1-((*S*)-1-methoxy-1-oxo-3-phenylpropan-2-yl)-3-phenylaziridine-2-carboxamido)-4-methylpentanoate (**447a/b**)**

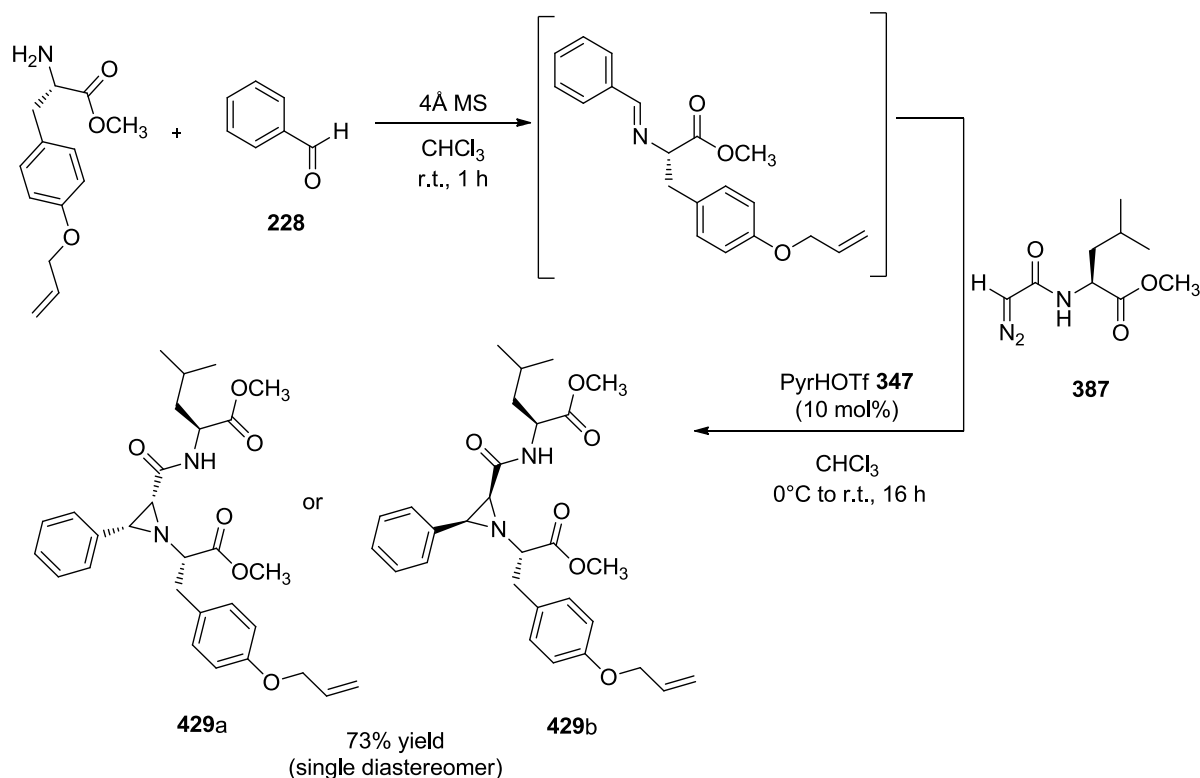


Compound **447a/b** was prepared according to the procedure for compound **427**. Purification *via* flash column chromatography on silica gel (eluent: diethyl ether / petroleum ether 1:1;  $R_f$  = 0.19) afforded a brown oil whose physicochemical properties were consistent with those of a single diastereomer of the title compound (160 mg, 0.252 mmol, 73% yield).

$^1\text{H}$ -NMR (500 MHz,  $\text{CDCl}_3$ )  $\delta$  7.33 (d,  $J$  = 8.3 Hz, 2H, Ar-*H*), 7.18 – 7.13 (m, 8H, Ar-*H*, -NH-), 4.59 (t,  $J$  = 1.5 Hz, 2H, Cp-*H*), 4.43 (dt,  $J$  = 8.7, 5.0 Hz, 1H, -NHCH-), 4.29 (t,  $J$  = 1.9 Hz, 2H, Cp-*H*), 4.03 (s, 5H, Cp-*H*), 3.71 (s, 3H, - $\text{CO}_2\text{CH}_3$ ), 3.53 (s, 3H, - $\text{CO}_2\text{CH}_3$ ), 3.33 (dd,  $J$  = 13.8, 6.1 Hz, 1H, - $\text{CH}_2\text{Ph}$ ), 3.13 (dd,  $J$  = 13.8, 7.2 Hz, 1H, - $\text{CH}_2\text{Ph}$ ), 2.91 (dd,  $J$  = 7.2, 6.1 Hz, 1H, -NCH-), 2.76 (d,  $J$  = 7.2 Hz, 1H, -CH- aziridine), 2.60 (d,  $J$  = 7.2 Hz, 1H, -CH- aziridine), 1.65 – 1.51 (m, 3H, - $\text{CH}_2\text{CH}(\text{CH}_3)_2$ ), 0.92 (d,  $J$  = 4.6 Hz, 3H, - $\text{CH}(\text{CH}_3)_2$ ), 0.91 (d,  $J$  = 4.6 Hz, 3H, - $\text{CH}(\text{CH}_3)_2$ );  $^{13}\text{C}$ -NMR (126 MHz,  $\text{CDCl}_3$ )  $\delta$  172.5 (-C=O ester), 171.8 (-C=O ester), 166.3 (-C=O amide), 138.4, 136.6, 131.9, 129.3, 128.4, 127.6, 126.9, 125.7, 85.2 (Cp), 72.6 (-NCH-), 69.6 (Cp), 68.8(9) (Cp), 68.8(7) (Cp), 66.6 (Cp), 66.3 (Cp), 52.1 (- $\text{OCH}_3$ ), 52.0 (- $\text{OCH}_3$ ), 50.0 (-NHCH-), 47.5 (-CH- aziridine), 46.9 (-CH- aziridine), 41.8 (- $\text{CH}_2\text{CH}(\text{CH}_3)_2$ ), 39.1 (- $\text{CH}_2\text{Ph}$ ), 24.6 (- $\text{CH}(\text{CH}_3)_2$ ), 22.8 (- $\text{CH}(\text{CH}_3)_2$ ), 22.1 (- $\text{CH}(\text{CH}_3)_2$ ); FT-IR (thin film,  $\text{cm}^{-1}$ )  $\nu$  = 3385 (N-H), 2951, 1742 (ester

C=O), 1677 (*amide* C=O), 1522, 1437, 1204, 1104, 1026, 819;  $[\alpha]_{\text{D}}^{23}$   $-93.1$  (c 1.0,  $\text{CHCl}_3$ ); MS (MALDI-TOF):  $m/z = 659.6$   $[\text{M}+\text{Na}]^+$ ; HRMS (NSI): exact mass calculated for  $\text{C}_{36}\text{H}_{41}\text{O}_5\text{N}_2\text{Fe}$  requires  $m/z$  635.2406, found  $m/z$  635.2406  $[\text{M}+\text{H}]^+$ .

***cis*-(*S*)-Methyl 2-(1-((*S*)-3-(4-(allyloxy)phenyl)-1-methoxy-1-oxopropan-2-yl)-3-phenylaziridine-2-carboxamido)-4-methylpentanoate (429a/b)**

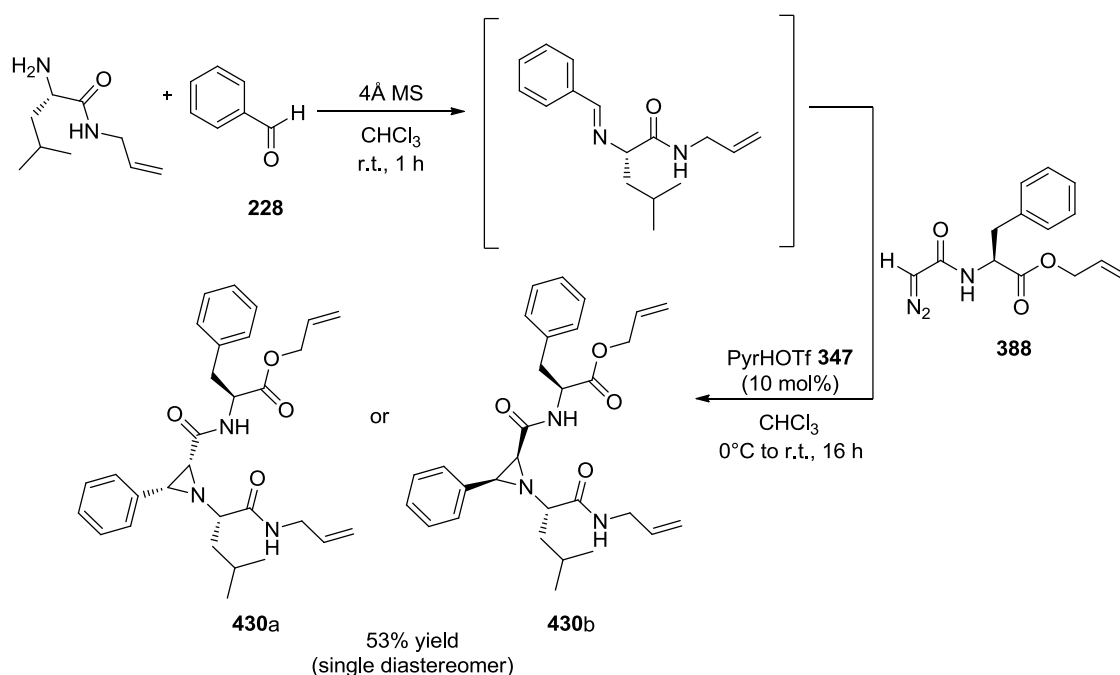


Compound **429a/b** was prepared according to the procedure for compound **427**. Purification *via* flash column chromatography on silica gel (eluent: diethyl ether / petroleum ether 1:1;  $R_f = 0.20$ ) afforded a colourless oil whose physicochemical properties were consistent with those of a single diastereomer of the title compound (320 mg, 0.63 mmol, 73% yield).

$^1\text{H}$ -NMR (500 MHz,  $\text{CDCl}_3$ )  $\delta$  7.25 – 7.18 (m, 5H, Ar-*H*), 7.15 (d,  $J = 8.9$  Hz, 1H, -NH-), 7.03 (d,  $J = 8.7$  Hz, 2H, Ar-*H*), 6.68 (d,  $J = 8.7$  Hz, 2H, Ar-*H*), 6.01 (ddt,  $J = 17.3, 10.5, 5.3$  Hz, 1H, -CH=CH<sub>2</sub>), 5.37 (dd,  $J = 17.3, 1.6$  Hz, 1H, -CH=CH<sub>2</sub>), 5.26 (dd,  $J = 10.5, 1.4$  Hz, 1H, -CH=CH<sub>2</sub>), 4.47 – 4.37 (m, 3H, -NHCH- + -OCH<sub>2</sub>-), 3.71 (s, 3H, -OCH<sub>3</sub>), 3.53 (s, 3H, -OCH<sub>3</sub>), 3.24 (dd,  $J = 13.9, 6.0$  Hz, 1H, -CH<sub>2</sub>Ph), 3.05 (dd,  $J = 13.9, 7.3$  Hz, 1H, -CH<sub>2</sub>Ph), 2.85 (dd,  $J = 7.2, 6.0$  Hz, 1H, -NCH-), 2.77 (d,  $J = 7.2$  Hz, 1H, -CH- aziridine),

2.57 (d,  $J = 7.2$  Hz, 1H, -CH- aziridine), 1.62 – 1.50 (m, 3H, -CH<sub>2</sub>CH(CH<sub>3</sub>)<sub>2</sub>), 0.91 (d,  $J = 6.4$  Hz, 3H, -CH(CH<sub>3</sub>)<sub>2</sub>), 0.90 (d,  $J = 6.4$  Hz, 3H, -CH(CH<sub>3</sub>)<sub>2</sub>); <sup>13</sup>C-NMR (126 MHz, CDCl<sub>3</sub>)  $\delta$  172.6 (-C=O ester), 172.0 (-C=O ester), 166.4 (-C=O amide), 157.6 (C-OAllyl), 134.6, 133.4, 130.4, 128.9, 128.0, 127.7, 127.6, 117.7, 114.8, 72.8 (-NCH-), 68.9 (-OCH<sub>2</sub>-), 52.2 (-OCH<sub>3</sub>), 52.1 (-OCH<sub>3</sub>), 50.1 (-NHCH-), 47.6 (-CH- aziridine), 47.0 (-CH- aziridine), 41.9 (-CH<sub>2</sub>CH(CH<sub>3</sub>)<sub>2</sub>), 38.4 (-CH<sub>2</sub>Ph), 24.8 (-CH(CH<sub>3</sub>)<sub>2</sub>), 22.9 (-CH(CH<sub>3</sub>)<sub>2</sub>), 22.2 (-CH(CH<sub>3</sub>)<sub>2</sub>); FT-IR (thin film):  $\nu$  (cm<sup>-1</sup>) = 3388, 2955, 1742, 1679, 1512, 1436, 1244, 1204, 1027;  $[\alpha]_D^{24}$  -25.4 (c 1.0, CHCl<sub>3</sub>); MS (MALDI-TOF)  $m/z$  531.5 [M+Na]<sup>+</sup>; HRMS (HNESF) exact mass calculated for C<sub>29</sub>H<sub>37</sub>N<sub>2</sub>O<sub>6</sub> requires  $m/z$  509.2646, found  $m/z$  509.2637 [M+H]<sup>+</sup>.

***cis*-(2*S*)-Allyl 2-(1-((*S*)-1-(allylamino)-4-methyl-1-oxopentan-2-yl)-3-phenylaziridine-2-carboxamido)-3-phenylpropanoate (430a/b)**



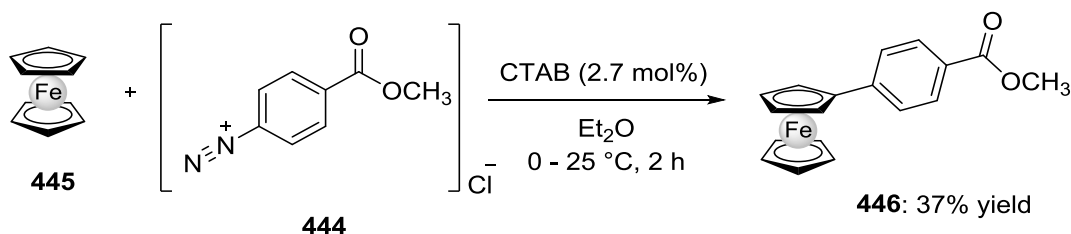
Compound **430a/b** was prepared according to the procedure for compound **427**. Purification *via* flash column chromatography on silica gel (eluent: diethyl ether / petroleum ether 3:1;  $R_f = 0.12$ ) afforded a colourless oil whose physicochemical properties were consistent with those of a single diastereomer of the title compound (78 mg, 0.16 mmol, 53% yield).

<sup>1</sup>H-NMR (500 MHz, CDCl<sub>3</sub>)  $\delta$  7.38 – 7.24 (m, 6H, Ar-*H*), 7.20 – 7.12 (m, 3H, Ar-*H* + -NH-), 6.69 – 6.64 (m, 2H, Ar-*H*), 6.16 (d,  $J = 7.5$  Hz, 1H, -NH-), 5.87 – 5.70 (m, 2H, -



$\text{CH}=\text{CH}_2$ ), 5.25 – 5.17 (m, 3H,  $-\text{CH}=\text{CH}_2$ ), 5.13 (dd,  $J = 10.3, 1.4$  Hz, 1H,  $-\text{CH}=\text{CH}_2$ ), 4.59 (dt,  $J = 7.5, 6.1$  Hz, 1H,  $-\text{NHCH}-$ ), 4.44 (dd,  $J = 5.9, 1.2$  Hz, 2H,  $-\text{OCH}_2-$ ), 3.98 – 3.90 (m, 1H,  $-\text{NCH}_2-$ ), 3.84 – 3.77 (m, 1H,  $-\text{NCH}_2-$ ), 3.09 (d,  $J = 6.9$  Hz, 1H,  $-\text{CH-aziridine}$ ), 2.91 (dd,  $J = 13.8, 5.1$  Hz, 1H,  $-\text{CH}_2\text{Ph}$ ), 2.72 (dd,  $J = 13.8, 6.2$  Hz, 1H,  $-\text{CH}_2\text{Ph}$ ), 2.61 (d,  $J = 6.9$  Hz, 1H,  $-\text{CH-aziridine}$ ), 2.55 (t,  $J = 6.5$  Hz, 1H,  $-\text{NCH}-$ ), 1.86 – 1.66 (m, 3H,  $-\text{CH}_2\text{CH}(\text{CH}_3)_2$ ), 0.90 (d,  $J = 3.4$  Hz, 3H,  $-\text{CH}(\text{CH}_3)_2$ ), 0.89 (d,  $J = 3.5$  Hz, 3H,  $-\text{CH}(\text{CH}_3)_2$ );  $^{13}\text{C}$ -NMR (126 MHz,  $\text{CDCl}_3$ )  $\delta$  172.3 ( $-\text{C}=\text{O}$  ester), 170.6 ( $-\text{C}=\text{O}$  ester), 166.3 ( $-\text{C}=\text{O}$  amide), 135.5, 134.9, 134.3, 131.4, 129.4, 128.6, 128.2, 127.5, 127.2, 119.2 ( $-\text{CH}=\text{CH}_2$ ), 116.5 ( $-\text{CH}=\text{CH}_2$ ), 71.0 ( $-\text{NCH}-$ ), 66.1 ( $-\text{OCH}_2-$ ), 53.1 ( $-\text{NHCH}-$ ), 47.3 ( $-\text{CH-aziridine}$ ), 46.9 ( $-\text{CH-aziridine}$ ), 43.2 ( $-\text{NCH}_2-$ ), 41.8 ( $-\text{CH}_2\text{CH}(\text{CH}_3)_2$ ), 38.2 ( $-\text{CH}_2\text{Ph}$ ), 24.7 ( $-\text{CH}(\text{CH}_3)_2$ ), 23.1 ( $-\text{CH}(\text{CH}_3)_2$ ), 23.0 ( $-\text{CH}(\text{CH}_3)_2$ ); FT-IR (ATR,  $\text{cm}^{-1}$ )  $\nu = 3310$  (N-H), 3066, 3032, 2956, 2936, 2860, 1744 (ester  $\text{C}=\text{O}$ ), 1662 (amide  $\text{C}=\text{O}$ ), 1531, 1452, 1422, 1384, 1367, 1342, 1322, 1260, 1191, 1092, 1027, 930;  $[\alpha]_D^{23} +31.1$  (c 1.0,  $\text{CHCl}_3$ ); MS (MALDI-TOF):  $m/z = 526.3$   $[\text{M}+\text{Na}]^+$ ; HRMS (NSI) exact mass calculated for  $\text{C}_{30}\text{H}_{38}\text{O}_4\text{N}_3$  requires  $m/z$  504.2857, found  $m/z$  504.2852  $[\text{M}+\text{H}]^+$ .

#### Methyl 4-(ferrocenyl)benzoate (**446**)<sup>254</sup>

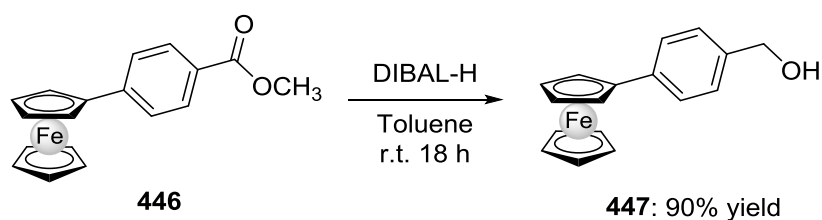


To a 250 mL round-bottom flask was added methyl-4-aminobenzoate (5 g, 33.1 mmol, 1 equiv.) and distilled water (16 mL). Concentrated hydrochloric acid (8 mL) was added, and the reaction mixture was cooled to 0 °C using an ice bath. A solution of sodium nitrite (2.28 g, 33.1 mmol, 1 equiv.) in distilled water (13 mL) was added dropwise *via* pipette. A colour change from pale brown to yellow indicated the formation of diazonium salt **444**. The solution was stirred for a further 30 minutes and the temperature maintained at 0 °C until use. To a 250 mL round-bottom flask containing a solution of ferrocene **445** (6.16 g, 33.1 mmol, 1 equiv.) in diethyl ether (50 mL) was added cetyltrimethylammonium bromide (330 mg, 0.906 mmol, 2.7 mol%). The mixture was cooled to 0 °C and the aqueous solution of diazonium salt **444** was added dropwise *via* pipette. The biphasic mixture was stirred vigorously for a further two hours before being

diluted with diethyl ether (50 mL). Saturated aqueous sodium bicarbonate solution (50 mL) was added, and the aqueous layer extracted with diethyl ether (2 x 100 mL). The combined organic layers were washed with distilled water (200 mL) and brine (150 mL), dried over magnesium sulfate, filtered, and the solvent removed *in vacuo*. Purification *via* flash column chromatography on silica gel (eluent: petroleum ether / diethyl ether 5%) afforded dark red crystals (3.92 g, 12.2 mmol, 37% yield); the physicochemical properties matched those previously reported.

M.p. 119–121 °C (petroleum ether / diethyl ether);  $^1\text{H-NMR}$  (500 MHz,  $\text{CDCl}_3$ )  $\delta$  7.94 (d,  $J = 7.6$  Hz, 2H, Ar-*H*), 7.48 (d,  $J = 7.6$  Hz, 2H, Ar-*H*), 4.77 (br s, 2H, Cp-*H*), 4.45 (br s, 2H, Cp-*H*), 4.09 (s, 5H, Cp-*H*), 3.92 (s, 3H,  $-\text{OCH}_3$ ); FT-IR (thin film,  $\text{cm}^{-1}$ )  $\nu = 2951$  (C-H), 1715 (C=O), 1609, 1430, 1281, 1183, 1105.

#### 4-(Ferrocenyl)benzyl alcohol (**447**)<sup>240</sup>

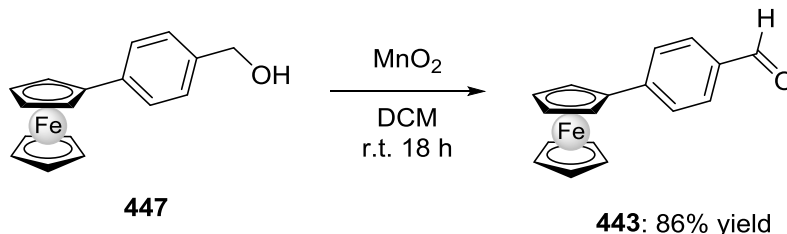


A flame-dried 250 mL round-bottom flask was cooled under nitrogen and charged with methyl 4-(ferrocenyl)benzoate **446** (290 mg, 0.91 mmol, 1 equiv.) and anhydrous toluene (10 mL). The resulting solution was cooled to  $-78$  °C using a dry ice/acetone bath. Diisobutylaluminium hydride (1.5 mL, 1.82 mmol, 2 equiv., 1.2 M in toluene) was added dropwise *via* a 2.5 mL syringe. The reaction was allowed to warm up slowly to room temperature over 18 hours. Ethyl acetate (20 mL) and distilled water (20 mL) were added to the reaction mixture, which was stirred vigorously for a further 30 minutes. The aqueous layer was extracted with ethyl acetate (30 mL) and the combined organic layers washed with distilled water (50 mL) and subsequently brine (50 mL). The orange solution was dried over magnesium sulfate, filtered, and the solvent removed *in vacuo* to afford an orange solid whose physicochemical properties matched those previously reported (238 mg, 0.82 mmol, 90% yield).

$R_f = 0.10$  (9:1 petroleum ether / ethyl acetate); m.p. 104–106 °C (hexane);  $^1\text{H-NMR}$  (500 MHz,  $\text{CDCl}_3$ )  $\delta = 7.48$  (d,  $J = 8.3$  Hz, 2H, Ar-*H*), 7.29 (d,  $J = 8.3$  Hz, 2H, Ar-*H*), 4.67 (d,

$J = 5.6$  Hz, 2H,  $\text{CH}_2\text{OH}$ ), 4.64 (t,  $J = 1.9$  Hz, 2H, Cp- $H$ ), 4.32 (t,  $J = 1.9$  Hz, 2H, Cp- $H$ ), 4.04 (s, 5H, Cp- $H$ ), 1.60 (t,  $J = 5.6$  Hz, 1H, -OH); MS (MALDI-TOF):  $m/z = 292.1$   $[\text{M}]^+$ .

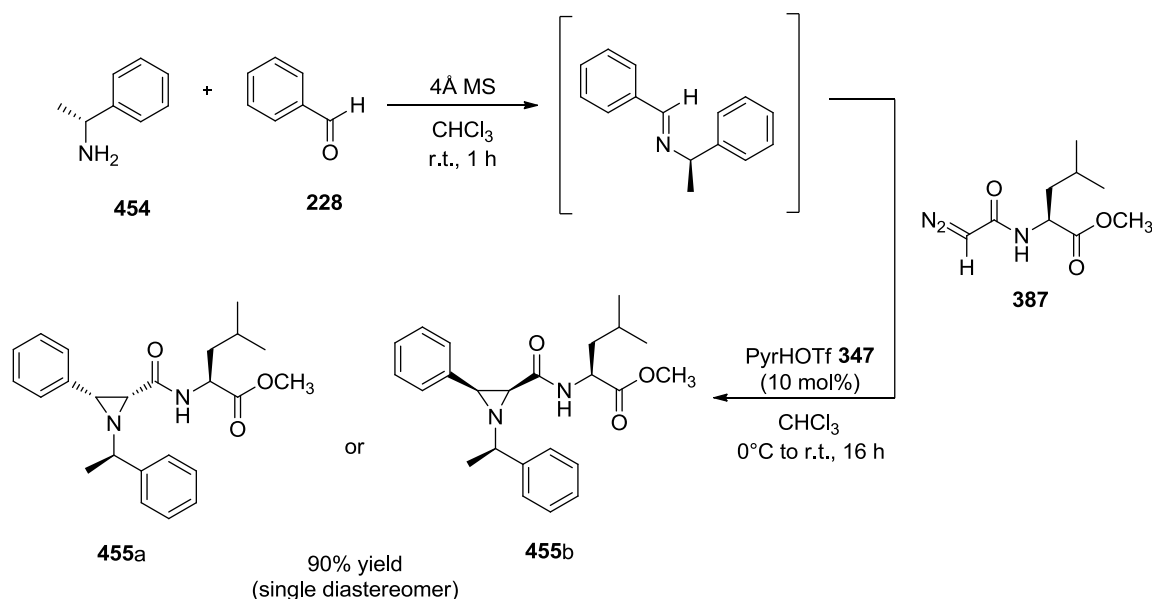
#### 4-(Ferrocenyl)benzaldehyde (**443**)<sup>254</sup>



To a 100 mL round-bottom flask containing 4-(ferrocenyl)benzyl alcohol **447** (237 mg, 0.81 mmol, 1 equiv.) dissolved in anhydrous dichloromethane (30 mL) under an atmosphere of nitrogen was added activated manganese dioxide (1.76 g, 20.3 mmol, 25 equiv.). The heterogeneous mixture was stirred at room temperature for 18 hours. The black solid manganese dioxide was removed by filtration and the solvent removed *in vacuo* to afford a red solid that was used without further purification (202 mg, 0.70 mmol, 86% yield); the physicochemical properties matched those previously reported for the title compound **443**.

M.p. 121–123 °C (hexane / ethyl acetate);  $^1\text{H}$ -NMR (500 MHz,  $\text{CDCl}_3$ )  $\delta = 9.97$  (s, 1H, -CHO), 7.79 (d,  $J = 8.3$  Hz, 2H, Ar- $H$ ), 7.60 (d,  $J = 8.3$  Hz, 2H, Ar- $H$ ), 4.74 (t,  $J = 1.9$  Hz, 2H, Cp- $H$ ), 4.44 (t,  $J = 1.9$  Hz, 2H, Cp- $H$ ), 4.05 (s, 5H, Cp- $H$ ); MS (MALDI-TOF):  $m/z = 290.05$   $[\text{M}]^+$ .

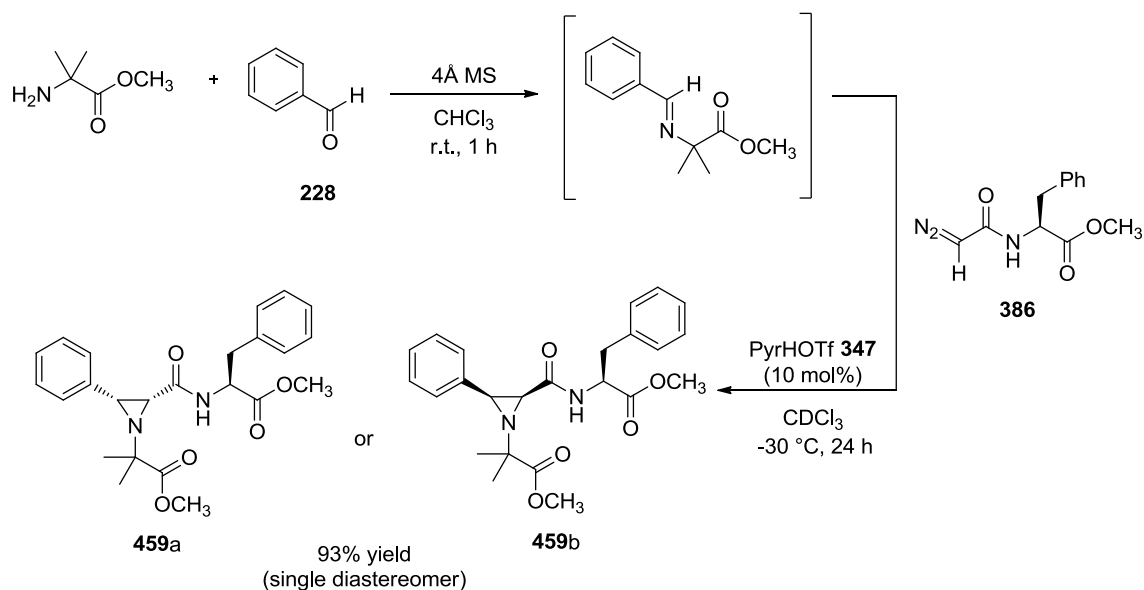
***cis*-(2*S*)-Methyl 4-methyl-2-(3-phenyl-1-((*R*)-1-phenylethyl)aziridine-2-carboxamido)pentanoate (455a/b)**



Compound **455a/b** was prepared according to the procedure for compound **427**. Purification *via* flash column chromatography on silica gel (eluent: diethyl ether / petroleum ether 3:1;  $R_f$  = 0.50) afforded a colourless oil whose physicochemical properties were consistent with those of a single diastereomer of the title compound (154 mg, 0.39 mmol, 91% yield).

$^1\text{H}$ -NMR (500 MHz,  $\text{CDCl}_3$ )  $\delta$  7.39 (d,  $J$  = 8.0 Hz, 2H, Ar-*H*), 7.28 (t,  $J$  = 7.5 Hz, 2H, Ar-*H*), 7.23 – 7.20 (m, 2H, Ar-*H*), 7.12 – 7.03 (m, 4H, Ar-*H*), 6.77 (br d,  $J$  = 8.6 Hz, 1H, -NH-), 4.32 – 4.26 (m, 1H, -NHCH-), 3.40 (s, 3H, - $\text{OCH}_3$ ), 3.01 (d,  $J$  = 7.1 Hz, 1H, -CH-aziridine), 2.85 (q,  $J$  = 6.5 Hz, 1H, -NCH-), 2.55 (d,  $J$  = 7.1 Hz, 1H, -CH-aziridine), 1.55 – 1.39 (m, 6H, - $\text{CH}_3$  + - $\text{CH}_2\text{CH}$ -), 0.85 (d,  $J$  = 3.5 Hz, 3H, - $\text{CH}(\text{CH}_3)_2$ ), 0.84 (d,  $J$  = 3.5 Hz, 3H, - $\text{C}(\text{CH}_3)_2$ );  $^{13}\text{C}$ -NMR (126 MHz,  $\text{CDCl}_3$ )  $\delta$  172.4 (-C=O ester), 167.5 (-C=O amide), 143.2, 134.9, 128.7, 128.1, 127.8, 127.7, 127.3, 127.0, 69.1 (-NCH-), 52.1 (-NHCH-), 50.2 (- $\text{OCH}_3$ ), 47.7 (-CH-aziridine), 46.7 (-CH-aziridine), 42.0 (- $\text{CH}_2$ -), 25.0 (- $\text{CH}(\text{CH}_3)_2$ ), 22.9 (- $\text{CH}(\text{CH}_3)_2$ ), 22.8 (- $\text{CH}(\text{CH}_3)_2$ ), 22.4 (- $\text{CH}_3$ ); FT-IR (thin film):  $\nu$  ( $\text{cm}^{-1}$ ) = 3392 (N-H), 3036 (C-H), 2960 (C-H), 2872 (C-H), 1744 (ester C=O), 1680 (amide C=O), 1516, 1452, 1372, 1328, 1260, 1204, 1156, 1100, 1028;  $[\alpha]_D^{18}$  -167.0 (c 0.5,  $\text{CHCl}_3$ ); MS (MALDI-TOF)  $m/z$  433.4  $[\text{M}+\text{K}]^+$ ; HRMS (HNESP) exact mass calculated for  $\text{C}_{24}\text{H}_{31}\text{N}_2\text{O}_3$  requires  $m/z$  395.2329, found  $m/z$  395.2320  $[\text{M}+\text{H}]^+$ .

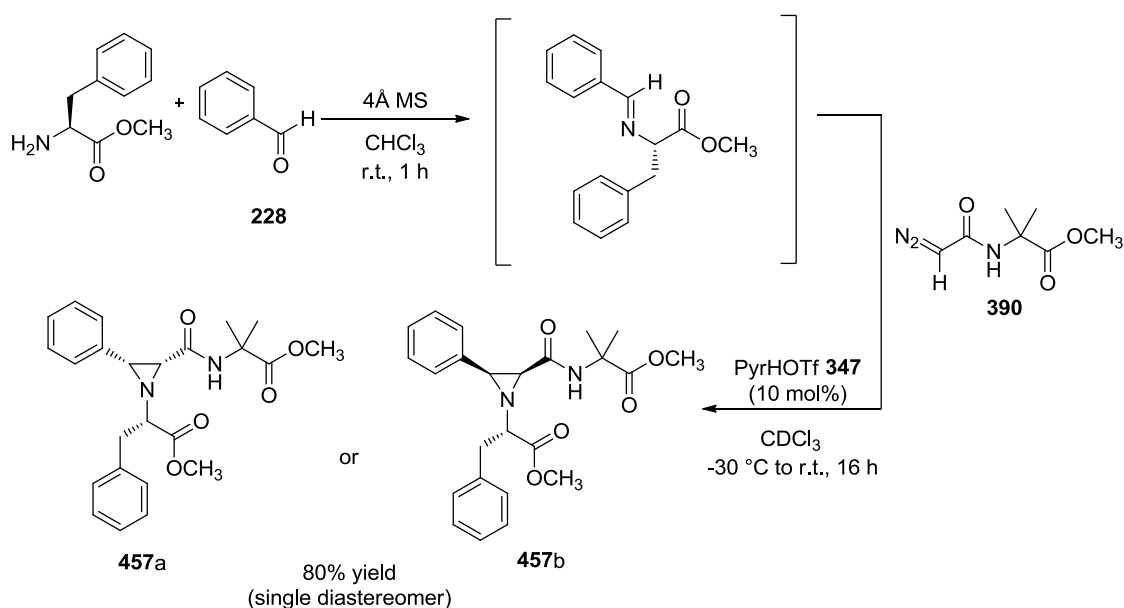
***cis*-Methyl 2-(2-(((*S*)-1-methoxy-1-oxo-3-phenylpropan-2-yl)carbamoyl)-3-phenylaziridin-1-yl)-2-methylpropanoate (**459a/b**)**



A 5 mL microwave vial containing crushed 4Å molecular sieves was flame-dried and cooled under a nitrogen atmosphere, followed by the addition of a magnetic stirrer bar. Benzaldehyde **228** (15 mg, 0.14 mmol, 1.1 equiv.) and methyl 2-amino-2-methylpropanoate (15 mg, 0.13 mmol, 1 equiv.) were weighed into a sample vial and dissolved in chloroform- $d_3$  (1 mL) before being transferred to the microwave vial *via* a 2 mL syringe. The solution was stirred at room temperature under nitrogen for 1 hour before pyridinium triflate (3 mg, 0.013 mmol, 10 mol%) was added and the vial was sealed with a PTFE-lined aluminium crimp cap. The reaction was cooled to  $-30\text{ }^\circ\text{C}$  using a chiller bath before the addition of a solution of (*S*)-methyl 2-(2-diazoacetamido)-3-phenylpropanoate **386** (38 mg, 0.15 mmol, 1.2 equiv.) in chloroform- $d_3$  (1 mL) was added dropwise to the reaction vial *via* a 2 mL syringe. The progress of the reaction was monitored by  $^1\text{H}$ -NMR until complete disappearance of the imine intermediate (~24 h). After being allowed to warm to room temperature, the mixture was filtered through a short plug of silica eluting with diethyl ether and the solvent was removed *in vacuo*. Purification *via* flash column chromatography on silica gel (eluent: diethyl ether / petroleum ether 3:1;  $R_f = 0.19$ ) afforded a colourless oil whose physicochemical properties were consistent with those of a single diastereomer of the title compound (51 mg, 0.12 mmol, 93% yield).

$^1\text{H-NMR}$  (500 MHz,  $\text{CDCl}_3$ )  $\delta$  7.34 – 7.16 (m, 8H, Ar-*H*), 7.12 – 7.06 (m, 2H, Ar-*H*), 6.94 (d,  $J$  = 7.9 Hz, 1H, -NH-), 4.51 (dt,  $J$  = 8.0, 5.9 Hz, 1H, -NHCH-), 3.68 (s, 3H, -OCH<sub>3</sub>), 3.44 (s, 3H, -OCH<sub>3</sub>), 3.35 (d,  $J$  = 6.9 Hz, 1H, -CH- aziridine), 3.07 (dd,  $J$  = 13.8, 6.1 Hz, 1H, -CH<sub>2</sub>Ph), 2.99 (dd,  $J$  = 13.8, 5.7 Hz, 1H, -CH<sub>2</sub>Ph), 2.86 (d,  $J$  = 6.9 Hz, 1H, -CH- aziridine), 1.36 (s, 3H, -CH<sub>3</sub>), 1.34 (s, 3H, -CH<sub>3</sub>);  $^{13}\text{C-NMR}$  (126 MHz,  $\text{CDCl}_3$ )  $\delta$  173.8 (-C=O ester), 171.1 (-C=O ester), 167.3 (-C=O amide), 136.0, 134.9, 129.4, 128.6, 128.1, 127.8, 127.4, 127.1, 61.4 (-NC-), 52.5 (-NHCH-), 52.2 (-OCH<sub>3</sub>), 52.1 (-OCH<sub>3</sub>), 42.1 (-CH- aziridine), 41.6 (-CH- aziridine), 38.1 (-CH<sub>2</sub>Ph), 23.7 (-CH<sub>3</sub>), 22.9 (-CH<sub>3</sub>); FT-IR (thin film):  $\nu$  ( $\text{cm}^{-1}$ ) = 3384 (N-H), 3062, 3033, 2990, 2953, 1738 (ester C=O), 1676 (amide C=O), 1512, 1450, 1366, 1279, 1195, 1147, 1078, 1031;  $[\alpha]_{\text{D}}^{23}$  -31.7 (c 1.0,  $\text{CHCl}_3$ ); MS (MALDI-TOF)  $m/z$  462.9  $[\text{M}+\text{K}]^+$ ; HRMS (HNESP) exact mass calculated for  $\text{C}_{24}\text{H}_{29}\text{N}_2\text{O}_5$  requires  $m/z$  425.2071, found  $m/z$  425.2069  $[\text{M}+\text{H}]^+$ .

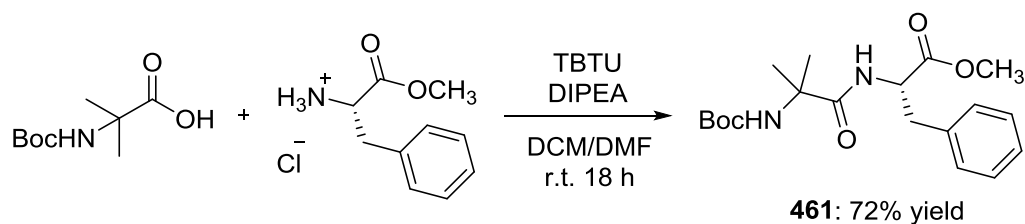
***cis*-Methyl 2-(1-((*R*)-1-methoxy-1-oxo-3-phenylpropan-2-yl)-3-phenylaziridine-2-carboxamido)-2-methylpropanoate (457a/b)**



Compound **457a/b** was prepared according to the procedure for compound **459** above. Purification *via* flash column chromatography on silica gel (eluent: diethyl ether / petroleum ether 3:1;  $R_f$  = 0.14) afforded a colourless oil whose physicochemical properties were consistent with those of a single diastereomer of the title compound (76 mg, 0.18 mmol, 80% yield).

$^1\text{H}$ -NMR (500 MHz,  $\text{CDCl}_3$ )  $\delta$  7.38 – 7.23 (m, 10H, Ar-*H*), 3.83 (s, 3H, - $\text{OCH}_3$ ), 3.68 (s, 3H, - $\text{OCH}_3$ ), 3.42 (dd,  $J = 13.9, 6.1$  Hz, 1H, - $\text{CH}_2\text{Ph}$ ), 3.22 (dd,  $J = 13.9, 7.1$  Hz, 1H, - $\text{CH}_2\text{Ph}$ ), 3.04 (dd,  $J = 7.0, 6.3$  Hz, 1H, - $\text{NCH-}$ ), 2.93 (d,  $J = 7.2$  Hz, 1H, - $\text{CH- aziridine}$ ), 2.63 (d,  $J = 7.2$  Hz, 1H, - $\text{CH- aziridine}$ ), 1.32 (s, 3H, - $\text{CH}_3$ ), 1.28 (s, 3H, - $\text{CH}_3$ );  $^{13}\text{C}$ -NMR (126 MHz,  $\text{CDCl}_3$ )  $\delta$  174.8 (-C=O ester), 171.9 (-C=O ester), 166.0 (-C=O amide), 136.8, 134.7, 129.4, 128.5, 127.9, 127.8, 127.6, 127.0, 72.1 (- $\text{NCH-}$ ), 55.8 (- $\text{C}(\text{CH}_3)_2$ ), 52.5 (- $\text{OCH}_3$ ), 52.3 (- $\text{OCH}_3$ ), 46.9 (- $\text{CH- aziridine}$ ), 46.6 (- $\text{CH- aziridine}$ ), 39.2 (- $\text{CH}_2\text{Ph}$ ), 24.7 (- $\text{CH}_3$ ), 24.0 (- $\text{CH}_3$ ); FT-IR (thin film):  $\nu$  ( $\text{cm}^{-1}$ ) = 3585 (N-H), 3375 (N-H), 3032, 2991, 2953, 2857, 1741 (ester C=O), 1676 (amide C=O), 1521, 1456, 1439, 1384, 1363, 1291, 1264, 1212, 1195, 1154, 1119, 1027;  $[\alpha]_{\text{D}}^{23}$  -39.2 (c 1.0,  $\text{CHCl}_3$ ); MS (MALDI-TOF)  $m/z$  462.9  $[\text{M}+\text{K}]^+$ ; HRMS (HNESF) exact mass calculated for  $\text{C}_{24}\text{H}_{29}\text{N}_2\text{O}_5$  requires  $m/z$  425.2071, found  $m/z$  425.2070  $[\text{M}+\text{H}]^+$ .

**(*S*)-Methyl 2-(2-(*tert*-butoxycarbonylamino)-2-methylpropanamido)-3-phenylpropanoate (461)<sup>251</sup>**

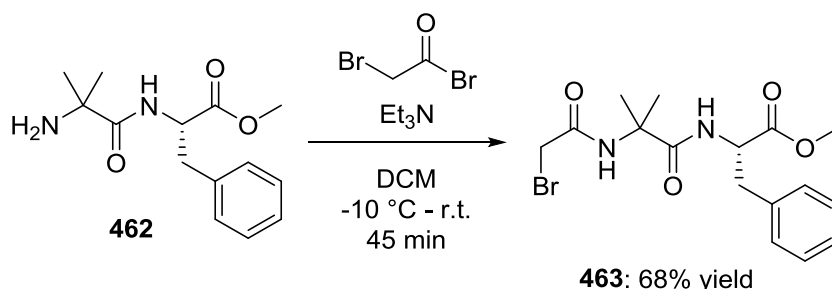


A 250 mL round-bottom flask was charged with 2-((*tert*-butoxycarbonyl)amino)-2-methylpropanoic acid (1 g, 4.92 mmol, 1 equiv.) and the solid dissolved in a mixture of dichloromethane and *N,N*-dimethylformamide (5:1, 30 mL) under a nitrogen atmosphere. (*S*)-Phenylalanine methyl ester hydrochloride (1.27 g, 5.90 mmol, 1.2 equiv.) was added in one portion, followed by the addition of *N,N*-diisopropylethylamine (3.9 mL, 22.1 mmol, 4.5 equiv.) *via* a 10 mL syringe. The solution was stirred at room temperature for 18 hours before the addition of distilled water (40 mL). The reaction mixture was extracted with dichloromethane (2 x 40 mL) and the combined organic layers washed with brine (50 mL), dried over magnesium sulfate, filtered, and the solvent removed *in vacuo*. Purification *via* flash column chromatography on silica gel (eluent: dichloromethane / ethyl acetate 9:1;  $R_f = 0.33$ ) afforded a white solid whose physicochemical properties matched those previously reported (1.29 g, 3.54 mmol, 72% yield).





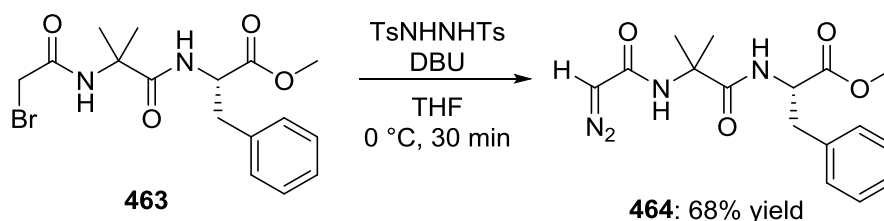
**(S)-Methyl 2-(2-(2-bromoacetamido)-2-methylpropanamido)-3-phenylpropanoate (463)**



Compound **463** was prepared according to the general procedure described above. Purification *via* flash column chromatography on silica gel (eluent: diethyl ether 100%;  $R_f$  = 0.23) afforded a white solid (514 mg, 1.34 mmol, 68% yield) whose physicochemical properties were consistent with those of the title compound.

M.p. 128–130 °C (diethyl ether);  $^1\text{H-NMR}$  (500 MHz,  $\text{CDCl}_3$ )  $\delta$  7.34 – 7.22 (m, 3H, Ar-*H*), 7.17 – 7.07 (m, 3H, Ar-*H* + -NH-), 6.50 (br d,  $J$  = 7.5 Hz, 1H, -NH-), 4.85 (dt,  $J$  = 7.6, 5.8 Hz, 1H, -NHCH-), 3.79 (s, 2H, -CH<sub>2</sub>Br), 3.75 (s, 3H, -OCH<sub>3</sub>), 3.19 (dd,  $J$  = 13.9, 5.7 Hz, 1H, -CH<sub>2</sub>Ph), 3.11 (dd,  $J$  = 13.9, 6.0 Hz, 1H, -CH<sub>2</sub>Ph), 1.55 (s, 3H, -C(CH<sub>3</sub>)<sub>2</sub>), 1.53 (s, 3H, -C(CH<sub>3</sub>)<sub>2</sub>);  $^{13}\text{C-NMR}$  (126 MHz,  $\text{CDCl}_3$ )  $\delta$  173.5 (C=O *amide*), 171.9 (C=O *amide*), 165.2 (C=O *ester*), 135.8, 129.4, 128.7, 127.4, 57.7 (-C(CH<sub>3</sub>)<sub>2</sub>), 53.5 (-NHCH-), 52.6 (-OCH<sub>3</sub>), 37.8 (-CH<sub>2</sub>Ph), 29.4 (-CH<sub>2</sub>Br), 24.7 (-C(CH<sub>3</sub>)<sub>2</sub>), 24.6 (-C(CH<sub>3</sub>)<sub>2</sub>); FT-IR (thin film):  $\nu$  (cm<sup>-1</sup>) = 3303 (N-H), 2931 (C-H), 2863 (C-H), 1734 (C=O), 1658 (C=O), 1544, 1493, 1455, 1219, 1117, 1058;  $[\alpha]_D^{19}$  +42.2 (c 1.0,  $\text{CHCl}_3$ ); MS (MALDI-TOF)  $m/z$  407.2, 409.2  $[\text{M}+\text{Na}]^+$ ; HRMS (HNESP) exact mass calculated for  $\text{C}_{16}\text{H}_{22}\text{BrN}_2\text{O}_4$  requires  $m/z$  385.0757, 387.0737 found  $m/z$  385.0762, 387.0740  $[\text{M}+\text{H}]^+$ .

**(S)-Methyl 2-(2-(2-diazoacetamido)-2-methylpropanamido)-3-phenylpropanoate (464)**

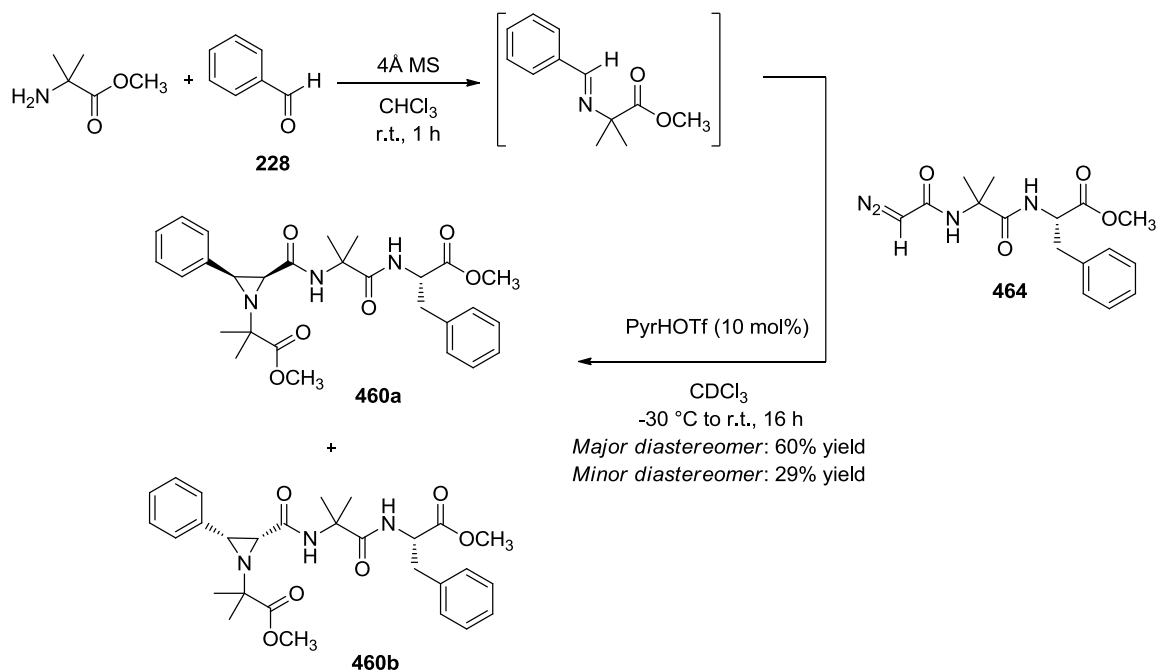


Compound **464** was prepared according to method A. Purification *via* flash column chromatography on silica gel (eluent: diethyl ether 100%;  $R_f$  = 0.17) afforded a pale

yellow solid whose physicochemical properties were consistent with those of the title compound (548 mg, 1.62 mmol, 68% yield).

M.p. 136–138 °C;  $^1\text{H-NMR}$  (500 MHz,  $\text{CDCl}_3$ )  $\delta$  7.33 – 7.21 (m, 3H, Ar-*H*), 7.14 – 7.10 (m, 2H, Ar-*H*), 6.79 (d,  $J$  = 7.5 Hz, 1H, -NH-), 5.61 (s, 1H, -NH-), 4.84 (dt,  $J$  = 7.6, 5.9 Hz, 1H, -NHCH-), 4.69 (s, 1H, -CHN<sub>2</sub>), 3.74 (s, 3H, -OCH<sub>3</sub>), 3.17 (dd,  $J$  = 13.9, 5.6 Hz, 1H, -CH<sub>2</sub>Ph), 3.11 (dd,  $J$  = 13.9, 6.2 Hz, 1H, -CH<sub>2</sub>Ph), 1.53 (s, 3H, -C(CH<sub>3</sub>)<sub>2</sub>), 1.51 (s, 3H, -C(CH<sub>3</sub>)<sub>2</sub>);  $^{13}\text{C-NMR}$  (126 MHz,  $\text{CDCl}_3$ )  $\delta$  174.2 (C=O *ester*), 172.1 (C=O *amide*), 165.3 (C=O *amide*), 135.9, 129.5, 128.6, 127.3, 57.9 (-C(CH<sub>3</sub>)<sub>2</sub>), 53.5 (-NHCH-), 52.5 (-OCH<sub>3</sub>), 48.1 (-CHN<sub>2</sub>), 37.9 (-CH<sub>2</sub>Ph), 25.9 (-C(CH<sub>3</sub>)<sub>2</sub>), 25.4 (-C(CH<sub>3</sub>)<sub>2</sub>); FT-IR (thin film):  $\nu$  (cm<sup>-1</sup>) = 3389 (N-H), 3252 (N-H), 3059, 2973, 2929, 2112 (*diazo* C=N<sub>2</sub>), 1734 (*ester* C=O), 1648 (*amide* C=O), 1631 (*amide* C=O), 1542, 1470, 1435, 1380, 1356, 1343, 1246, 1216, 1198, 1164, 1016, 972;  $[\alpha]_{\text{D}}^{20}$  +51.7 (c 1.0,  $\text{CHCl}_3$ ); MS (MALDI-TOF)  $m/z$  370.8  $[\text{M}+\text{K}]^+$ ; HRMS (HNESP) exact mass calculated for C<sub>16</sub>H<sub>21</sub>N<sub>4</sub>O<sub>4</sub> requires  $m/z$  333.1557, found  $m/z$  333.1557  $[\text{M}+\text{H}]^+$ .

***cis*-Methyl 2-(2-((1-(((*S*)-1-methoxy-1-oxo-3-phenylpropan-2-yl)amino)-2-methyl-1-oxopropan-2-yl)carbamoyl)-3-phenylaziridin-1-yl)-2-methylpropanoate (460a and 460b)**



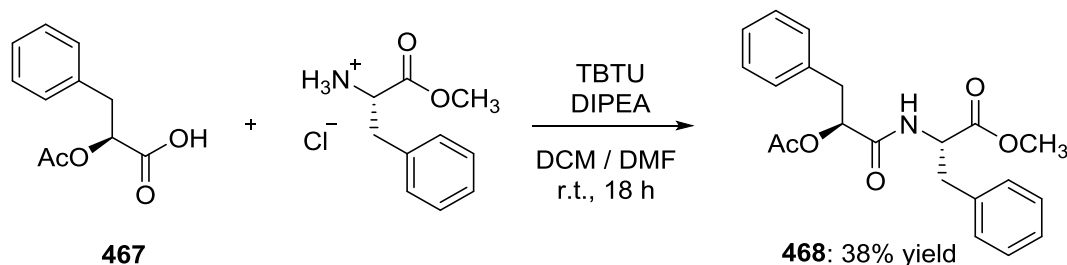
Compound **460a** and **460b** were prepared according to the procedure for compound **459** above. Purification *via* flash column chromatography on silica gel (eluent: diethyl ether 100%) afforded two separable diastereomers, (*S,S,S*)-**460a** and (*R,R,S*)-**460b** as colourless oils whose physicochemical properties were consistent with those of the title compound.

**R<sub>f</sub>** = **0.60** (diethyl ether 100%); 261 mg, 0.51 mmol, 60% yield; <sup>1</sup>H-NMR (500 MHz, CDCl<sub>3</sub>) δ 7.39 – 7.36 (m, 2H, Ar-*H*), 7.31 – 7.18 (m, 6H, Ar-*H*), 7.12 – 7.08 (m, 2H, Ar-*H*), 6.84 (d, *J* = 7.9 Hz, 1H, -NH-), 4.71 – 4.63 (m, 1H, -NHCH-), 3.68 (s, 3H, -OCH<sub>3</sub>), 3.67 (s, 3H, -OCH<sub>3</sub>), 3.37 (d, *J* = 6.9 Hz, 1H, -CH- aziridine), 3.06 (dd, *J* = 13.9, 5.8 Hz, 1H, -CH<sub>2</sub>Ph), 2.98 (dd, *J* = 13.8, 6.8 Hz, 1H, -CH<sub>2</sub>Ph), 2.77 (d, *J* = 6.9 Hz, 1H, -CH- aziridine), 1.43 (s, 3H, -CH<sub>3</sub>), 1.30 (s, 3H, -CH<sub>3</sub>), 1.05 (s, 3H, -CH<sub>3</sub>), 0.92 (s, 3H, -CH<sub>3</sub>); <sup>13</sup>C-NMR (126 MHz, CDCl<sub>3</sub>) δ 174.3 (-C=O ester), 173.8 (-C=O ester), 172.0 (-C=O amide), 167.7 (-C=O amide), 136.3, 135.2, 129.5, 128.5, 128.3, 128.0, 127.8, 127.0, 61.3 (-NC-), 56.7 (-NHC-), 53.4 (-NHCH-), 52.4 (-OCH<sub>3</sub>), 52.2 (-OCH<sub>3</sub>), 41.4 (-CH- aziridine), 41.3 (-CH- aziridine), 37.9 (-CH<sub>2</sub>Ph), 25.9 (-CH<sub>3</sub>), 24.5 (-CH<sub>3</sub>), 23.3 (-CH<sub>3</sub>), 21.4 (-CH<sub>3</sub>); FT-IR (thin film): ν (cm<sup>-1</sup>) = 3341 (N-H), 3066, 3033, 2985, 2952, 1743 (ester C=O), 1670 (amide C=O), 1512, 1457, 1388, 1366, 1278, 1212, 1150, 1029; [α]<sub>D</sub><sup>21</sup> +61.1 (c 1.0, CHCl<sub>3</sub>); MS (MALDI-TOF) *m/z* 547.76 [M+K]<sup>+</sup>; HRMS (HNESP) exact mass calculated for C<sub>28</sub>H<sub>36</sub>N<sub>3</sub>O<sub>6</sub> requires *m/z* 510.2599, found *m/z* 510.2589 [M+H]<sup>+</sup>.

**R<sub>f</sub>** = **0.36** (diethyl ether 100%); 126 mg, 0.25 mmol, 29% yield; <sup>1</sup>H-NMR (500 MHz, CDCl<sub>3</sub>) δ 7.39 – 7.34 (m, 2H, Ar-*H*), 7.30 – 7.18 (m, 6H, Ar-*H*), 7.13 – 7.05 (m, 3H, Ar-*H* + -NH-), 4.68 (dt, *J* = 7.2, 6.2 Hz, 1H, -NHCH-), 3.68 (s, 3H, -OCH<sub>3</sub>), 3.68 (s, 3H, -OCH<sub>3</sub>), 3.36 (d, *J* = 6.9 Hz, 1H, -CH- aziridine), 3.10 (dd, *J* = 13.8, 5.7 Hz, 1H, -CH<sub>2</sub>Ph), 2.96 (dd, *J* = 13.8, 6.8 Hz, 1H, -CH<sub>2</sub>Ph), 2.75 (d, *J* = 6.9 Hz, 1H, -CH- aziridine), 1.42 (s, 3H, -CH<sub>3</sub>), 1.31 (s, 3H, -CH<sub>3</sub>), 1.06 (s, 3H, -CH<sub>3</sub>), 0.97 (s, 3H, -CH<sub>3</sub>); <sup>13</sup>C-NMR (126 MHz, CDCl<sub>3</sub>) δ 174.3 (-C=O ester), 174.0 (-C=O ester), 172.0 (-C=O amide), 167.8 (-C=O amide), 136.5, 135.2, 129.5, 128.5, 128.3, 127.9, 127.8, 127.0, 61.3 (-NC-), 56.9 (-NHC-), 53.7 (-NHCH-), 52.4 (-OCH<sub>3</sub>), 52.3 (-OCH<sub>3</sub>), 41.4 (-CH- aziridine), 41.3 (-CH- aziridine), 37.9 (-CH<sub>2</sub>Ph), 25.9 (-CH<sub>3</sub>), 24.4 (-CH<sub>3</sub>), 23.4 (-CH<sub>3</sub>), 21.6 (-CH<sub>3</sub>); FT-IR (thin film): ν (cm<sup>-1</sup>) = 3341 (N-H), 3033, 2989, 2952, 2864, 1739 (ester C=O), 1666 (amide C=O), 1512, 1450, 1388, 1366, 1278, 1208, 1150, 1029; [α]<sub>D</sub><sup>21</sup> -5.1 (c 1.0,

CHCl<sub>3</sub>); MS (MALDI-TOF)  $m/z$  547.81 [M+K]<sup>+</sup>; HRMS (HNESP) exact mass calculated for C<sub>28</sub>H<sub>36</sub>N<sub>3</sub>O<sub>6</sub> requires  $m/z$  510.2599, found  $m/z$  510.2588 [M+H]<sup>+</sup>.

**(S)-Methyl 2-((S)-2-acetoxy-3-phenylpropanamido)-3-phenylpropanoate (468)**

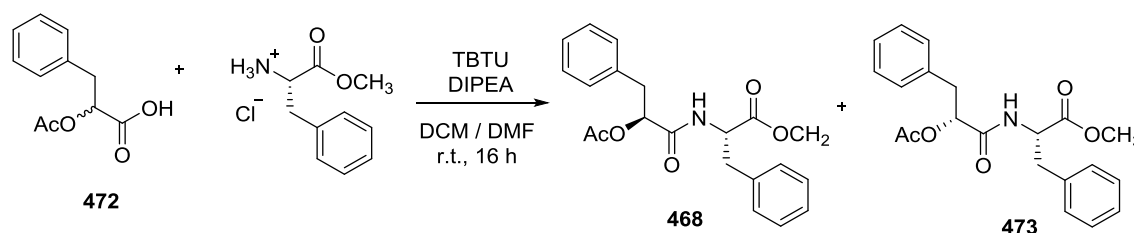


A 150 mL round-bottom flask containing (*S*)-2-acetoxy-3-phenylpropanoic acid **467** (500 mg, 2.40 mmol, 1 equiv.) under a nitrogen atmosphere was charged with dichloromethane (25 mL), *N,N*-dimethylformamide (5 mL) and a magnetic stirrer bar. (*S*)-Phenylalanine methyl ester hydrochloride (621 mg, 2.88 mmol, 1.2 equiv.) and *N,N,N',N'*-tetramethyl-*O*-(benzotriazol-1-yl)uronium tetrafluoroborate (1.08 g, 3.36 mmol, 1.4 equiv.) were added in one portion, followed by the addition of *N,N*-diisopropylethylamine (0.4 mL, 10.8 mmol, 4.5 equiv.) dropwise *via* a 1 mL syringe. The solution was stirred at room temperature for 18 hours before the addition of distilled water (30 mL). The mixture was extracted with dichloromethane (3 x 30 mL), washed with water (60 mL) and brine (60 mL). The organic phase was dried over magnesium sulfate, filtered and the solvent removed *in vacuo*. Purification *via* flash column chromatography on silica gel (eluent: dichloromethane / ethyl acetate 10%;  $R_f$  = 0.60) afforded a pale yellow oil whose physicochemical properties were consistent with those of the title compound (340 mg, 0.92 mmol, 38% yield).

<sup>1</sup>H-NMR (500 MHz, CDCl<sub>3</sub>)  $\delta$  7.33 – 7.27 (m, 2H, Ar-*H*), 7.25 – 7.20 (m, 4H, Ar-*H*), 7.20 – 7.17 (m, 2H, Ar-*H*), 6.87 – 6.82 (m, 2H, Ar-*H*), 6.38 (d,  $J$  = 8.2 Hz, 1H, -NH-), 5.37 (dd,  $J$  = 6.6, 4.8 Hz, 1H, AcOCH-), 4.85 (dt,  $J$  = 8.1, 5.5 Hz, 1H, -NHCH-), 3.68 (s, 3H, -CO<sub>2</sub>CH<sub>3</sub>), 3.19 (dd,  $J$  = 14.3, 4.7 Hz, 1H, -CH<sub>2</sub>Ph), 3.12 (dd,  $J$  = 14.3, 6.7 Hz, 1H, -CH<sub>2</sub>Ph), 3.07 (dd,  $J$  = 13.8, 5.2 Hz, 1H, -CH<sub>2</sub>Ph), 2.93 (dd,  $J$  = 13.8, 5.8 Hz, 1H, -CH<sub>2</sub>Ph), 2.03 (s, 3H, CH<sub>3</sub>CO<sub>2</sub>-); <sup>13</sup>C-NMR (126 MHz, CDCl<sub>3</sub>)  $\delta$  171.5 (-C=O ester), 169.4 (-C=O ester), 168.5 (-C=O amide), 135.9, 135.5, 129.9, 129.4, 128.64, 128.56, 127.3, 127.2, 74.2 (AcOCH-), 52.6, 52.5, 38.1 (-CH<sub>2</sub>Ph), 37.6 (-CH<sub>2</sub>Ph), 21.0 (CH<sub>3</sub>CO<sub>2</sub>-); FT-IR (thin film, cm<sup>-1</sup>)  $\nu$  = 3323 (N-H), 3030 (C-H), 2955 (C-H), 1746 (ester C=O), 1684

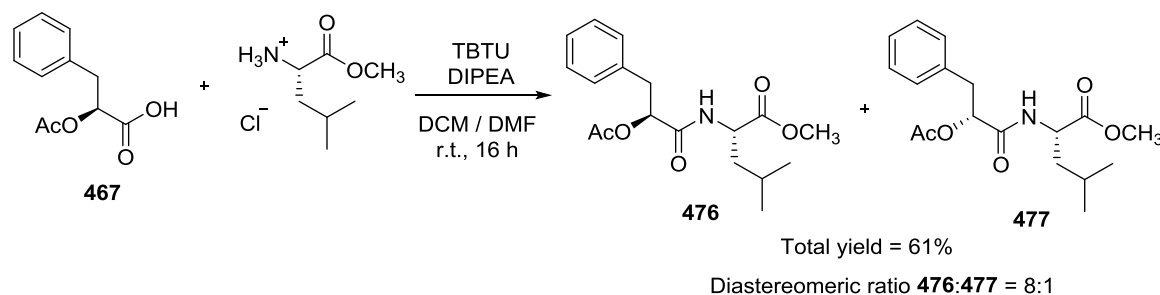
(amide C=O), 1531, 1457, 1371, 1226;  $[\alpha]_{\text{D}}^{22} +52.1$  (c 1.0,  $\text{CHCl}_3$ ); MS (MALDI-TOF):  $m/z = 392.2$   $[\text{M} + \text{Na}]^+$ ; HRMS (HNESF): exact mass calculated for  $\text{C}_{21}\text{H}_{24}\text{O}_5\text{N}$  requires  $m/z$  370.1649, found  $m/z$  370.1653  $[\text{M} + \text{H}]^+$ .

**(S)-Methyl 2-((S)-2-acetoxy-3-phenylpropanamido)-3-phenylpropanoate (468) and (S)-methyl 2-((R)-2-acetoxy-3-phenylpropanamido)-3-phenylpropanoate (473)**



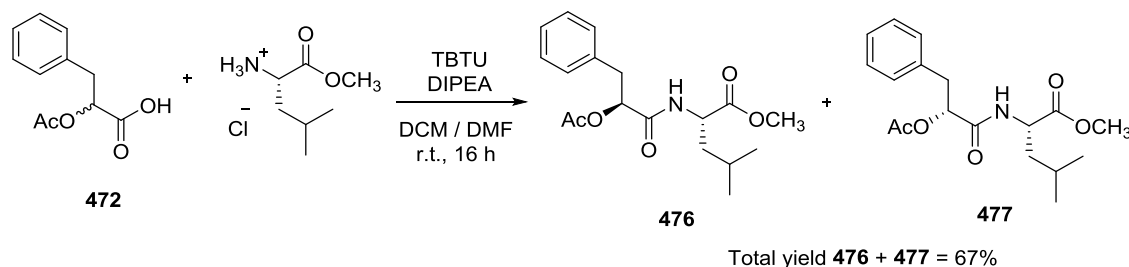
Compounds **468** and **473** were prepared according to the procedure for compound **468** above. Purification *via* flash column chromatography on silica gel (eluent: dichloromethane / ethyl acetate (10 %)  $R_f = 0.61$ ) afforded an inseparable mixture of two diastereomers **468** and **473** as a white solid whose physicochemical properties were consistent with those of the title compounds (318 mg, 0.86 mmol, 75% yield).

$^1\text{H}$ -NMR (500 MHz,  $\text{CDCl}_3$ )  $\delta$  7.33 – 7.15 (m, 16H, Ar-*H*), 7.00 – 6.96 (m, 2H, Ar-*H*), 6.87 – 6.82 (m, 2H, Ar-*H*), 6.39 (d,  $J = 7.9$  Hz, 1H, -NH-), 6.34 (d,  $J = 7.6$  Hz, 1H, -NH-), 5.40 – 5.35 (m, 2H, AcOCH-), 4.90 – 4.83 (m, 2H, -NHCH-), 3.72 (s, 3H, -CO<sub>2</sub>CH<sub>3</sub>), 3.68 (s, 3H, -CO<sub>2</sub>CH<sub>3</sub>), 3.24 – 2.99 (m, 7H, -CH<sub>2</sub>Ph), 2.93 (dd,  $J = 13.8, 5.9$  Hz, 1H, -CH<sub>2</sub>Ph), 2.02 (s, 3H, CH<sub>3</sub>CO<sub>2</sub>-), 1.96 (s, 3H, CH<sub>3</sub>CO<sub>2</sub>-);  $^{13}\text{C}$ -NMR (126 MHz,  $\text{CDCl}_3$ )  $\delta$  171.5 (-C=O), 171.5 (-C=O), 169.4 (-C=O), 169.4 (-C=O), 168.9 (-C=O), 168.5 (-C=O), 136.0, 135.9, 135.5(1), 135.4(7), 129.9, 129.6, 129.4, 128.7, 128.6, 128.5(3), 128.5(2), 127.4, 127.3, 127.2, 127.1, 74.3 (AcOCH-), 74.2 (AcOCH-), 52.7, 52.6, 52.5(2), 52.4(5), 38.0 (-CH<sub>2</sub>Ph), 37.9 (-CH<sub>2</sub>Ph), 37.8 (-CH<sub>2</sub>Ph), 37.6 (-CH<sub>2</sub>Ph), 20.9 (CH<sub>3</sub>CO<sub>2</sub>-), 20.8 (CH<sub>3</sub>CO<sub>2</sub>-); FT-IR (thin film):  $\nu$  ( $\text{cm}^{-1}$ ) = 3327 (N-H), 3066 (C-H), 3032 (C-H), 2949 (C-H), 2850 (C-H), 1748 (ester C=O), 1679 (amide C=O), 1528, 1497, 1452, 1439, 1370, 1219, 1119, 1061; MS (MALDI-TOF)  $m/z$  392.2  $[\text{M} + \text{Na}]^+$ .

**(S)-Methyl 2-((S)-2-acetoxy-3-phenylpropanamido)-4-methylpentanoate (476)**

Compound **476** was prepared according to the procedure for compound **468**. Purification *via* flash column chromatography on silica gel (eluent: dichloromethane / ethyl acetate (5%)  $R_f$  = 0.31) afforded a colourless oil whose physicochemical properties were consistent with a mixture of **476** and **477** in a diastereomeric ratio (*S,S/R,S*) of 8:1 by  $^1\text{H}$ -NMR (491 mg, 1.46 mmol, 61% yield).

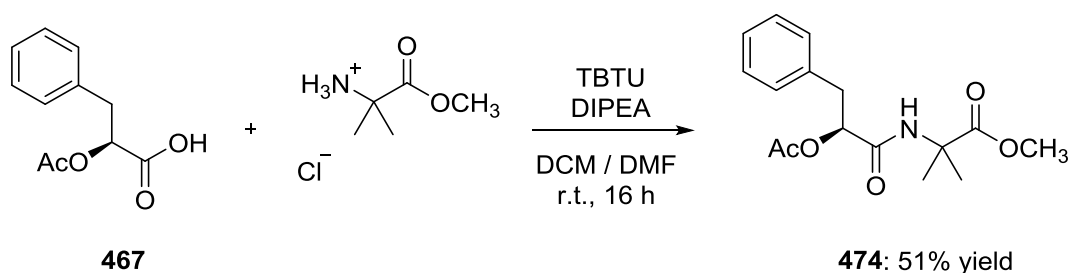
$^1\text{H}$ -NMR (500 MHz,  $\text{CDCl}_3$ )  $\delta$  7.29 – 7.20 (m, 3H, Ar-*H*), 7.20 – 7.14 (m, 2H, Ar-*H*), 6.31 (d,  $J$  = 8.5 Hz, 1H, -NH-), 5.40 (dd,  $J$  = 6.3, 4.8 Hz, 1H, AcOCH-), 4.62 – 4.56 (m, 1H, -NHCH-), 3.70 (s, 3H,  $-\text{CO}_2\text{CH}_3$ ), 3.20 (dd,  $J$  = 14.3, 4.8 Hz, 1H,  $-\text{CH}_2\text{Ph}$ ), 3.15 (dd,  $J$  = 14.3, 6.3 Hz, 1H,  $-\text{CH}_2\text{Ph}$ ), 2.12 (s, 3H,  $\text{CH}_3\text{CO}_2$ -), 1.57 – 1.49 (m, 1H,  $-\text{CH}_2\text{CH}(\text{CH}_3)_2$ ), 1.45 – 1.32 (m, 2H,  $-\text{CH}_2\text{CH}(\text{CH}_3)_2$  +  $-\text{CH}(\text{CH}_3)_2$ ), 0.87 (d,  $J$  = 6.5 Hz, 3H,  $-\text{CH}(\text{CH}_3)_2$ ), 0.85 (d,  $J$  = 6.5 Hz, 3H,  $-\text{CH}(\text{CH}_3)_2$ );  $^{13}\text{C}$ -NMR (126 MHz,  $\text{CDCl}_3$ )  $\delta$  173.2 ( $-\text{C}=\text{O}$ ), 169.4 ( $-\text{C}=\text{O}$ ), 168.6 ( $-\text{C}=\text{O}$ ), 135.8, 129.8, 128.5, 127.1, 74.3 (AcOCH-), 52.5, 50.4, 41.7, 37.6, 24.6 ( $-\text{CH}(\text{CH}_3)_2$ ), 22.8 ( $-\text{CH}(\text{CH}_3)_2$ ), 22.0 ( $-\text{CH}(\text{CH}_3)_2$ ), 21.1 ( $\text{CH}_3\text{CO}_2$ -); FT-IR (thin film):  $\nu$  ( $\text{cm}^{-1}$ ) = 3319 (N-H), 2959 (C-H), 1750 (*ester* C=O), 1668 (*amide* C=O), 1535, 1371, 1226, 1066;  $[\alpha]_D^{24}$  -3.2 (c 0.5,  $\text{CHCl}_3$ ); MS (MALDI-TOF)  $m/z$  374.39  $[\text{M}+\text{K}]^+$ ; HRMS (HNESP) exact mass calculated for  $\text{C}_{18}\text{H}_{26}\text{NO}_5$  requires  $m/z$  336.1807, found  $m/z$  336.1805  $[\text{M}+\text{H}]^+$ .

**(S)-Methyl 2-((S)-2-acetoxy-3-phenylpropanamido)-4-methylpentanoate (476) and (S)-methyl 2-((R)-2-acetoxy-3-phenylpropanamido)-4-methylpentanoate (477)**

Compounds **476** and **477** were prepared according to the procedure for compound **468**. Purification *via* flash column chromatography on silica gel (eluent: dichloromethane / ethyl acetate 5%;  $R_f = 0.31$ ) afforded an inseparable mixture of two diastereomers **476** and **477** as a colourless oil whose physicochemical properties were consistent with those of the title compound (540 mg, 1.61 mmol, 67% yield).

$^1\text{H}$ -NMR (500 MHz,  $\text{CDCl}_3$ )  $\delta$  7.24 – 7.08 (m, 10H, Ar-*H*), 6.27 – 6.20 (m, 2H, -NH-), 5.37 – 5.29 (m, 2H, AcOCH-), 4.56 – 4.50 (m, 2H, -NHCH-), 3.65 (s, 3H, -CO<sub>2</sub>CH<sub>3</sub>), 3.64 (s, 3H, -CO<sub>2</sub>CH<sub>3</sub>), 3.17 (dd,  $J = 14.2, 5.0$  Hz, 1H, -CH<sub>2</sub>Ph), 3.14 – 3.06 (m, 2H, -CH<sub>2</sub>Ph), 3.02 (dd,  $J = 14.2, 7.7$  Hz, 1H, -CH<sub>2</sub>Ph), 2.06 (s, 3H, CH<sub>3</sub>CO<sub>2</sub>-), 2.00 (s, 3H, CH<sub>3</sub>CO<sub>2</sub>-), 1.59 – 1.25 (m, 6H, -CH<sub>2</sub>CH(CH<sub>3</sub>)<sub>2</sub>), 0.83 (d,  $J = 4.4$  Hz, 3H, -CH(CH<sub>3</sub>)<sub>2</sub>), 0.82 (d,  $J = 4.4$  Hz, 3H, -CH(CH<sub>3</sub>)<sub>2</sub>), 0.81 (d,  $J = 6.5$  Hz, 3H, -CH(CH<sub>3</sub>)<sub>2</sub>), 0.79 (d,  $J = 6.5$  Hz, 3H, -CH(CH<sub>3</sub>)<sub>2</sub>);  $^{13}\text{C}$ -NMR (126 MHz,  $\text{CDCl}_3$ )  $\delta$  173.2 (-C=O), 173.0 (-C=O), 169.6 (-C=O), 169.4 (-C=O), 169.0 (-C=O), 168.6 (-C=O), 136.0, 135.8, 129.8, 129.6, 128.5(2), 128.4(6), 127.1, 127.0, 74.4 (AcOCH-), 74.3 (AcOCH-), 52.5, 50.6, 50.4, 41.7(3), 41.6(7), 37.8, 37.6, 24.9 (-CH(CH<sub>3</sub>)<sub>2</sub>), 24.6 (-CH(CH<sub>3</sub>)<sub>2</sub>), 22.8 (-CH(CH<sub>3</sub>)<sub>2</sub>), 22.1 (-CH(CH<sub>3</sub>)<sub>2</sub>), 22.0 (-CH(CH<sub>3</sub>)<sub>2</sub>), 21.1 (CH<sub>3</sub>CO<sub>2</sub>-), 20.9 (CH<sub>3</sub>CO<sub>2</sub>-); MS (MALDI-TOF)  $m/z$  358.6  $[\text{M}+\text{Na}]^+$ .

**(S)-Methyl 2-(2-acetoxy-3-phenylpropanamido)-2-methylpropanoate (474)**

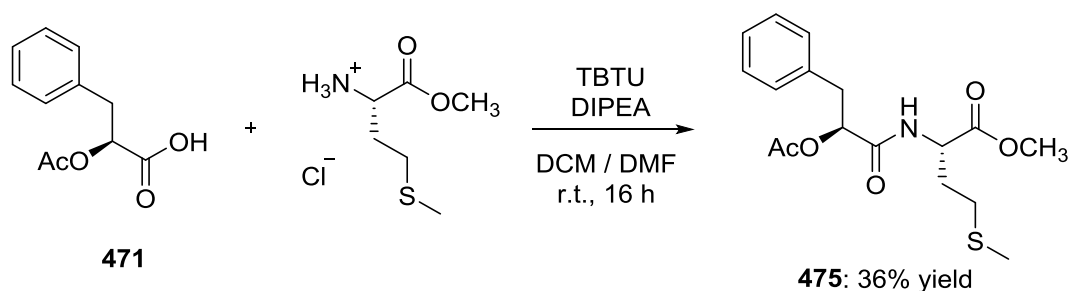


Compound **474** was prepared according to the procedure for compound **468**. Purification *via* flash column chromatography on silica gel (eluent: dichloromethane / ethyl acetate 10%;  $R_f = 0.56$ ) afforded a colourless oil whose physicochemical properties were consistent with those of the title compound (374 mg, 1.22 mmol, 51% yield).

$^1\text{H}$ -NMR (500 MHz,  $\text{CDCl}_3$ )  $\delta$  7.30 – 7.21 (m, 3H, Ar-*H*), 7.20 – 7.16 (m, 2H, Ar-*H*), 6.62 (s, 1H, -NH-), 5.32 (dd,  $J = 6.7, 5.0$  Hz, 1H, AcOCH-), 3.73 (s, 3H, -CO<sub>2</sub>CH<sub>3</sub>), 3.20 (dd,  $J = 14.3, 5.0$  Hz, 1H, -CH<sub>2</sub>Ph), 3.13 (dd,  $J = 14.3, 6.7$  Hz, 1H, -CH<sub>2</sub>Ph), 2.10 (s, 3H, -CH<sub>3</sub>CO<sub>2</sub>-), 1.52 (s, 3H, -C(CH<sub>3</sub>)<sub>2</sub>), 1.48 (s, 3H, -C(CH<sub>3</sub>)<sub>2</sub>);  $^{13}\text{C}$ -NMR (126 MHz,  $\text{CDCl}_3$ )

$\delta$  175.1 (-C=O), 169.5 (-C=O), 168.2 (-C=O), 136.0, 129.8, 128.5, 127.0, 74.4 (AcOCH-), 56.8, 52.9, 37.6, 24.5 (-C(CH<sub>3</sub>)<sub>2</sub>), 24.3 (-C(CH<sub>3</sub>)<sub>2</sub>), 21.1 (CH<sub>3</sub>CO<sub>2</sub>-); FT-IR (thin film):  $\nu$  (cm<sup>-1</sup>) = 3335 (N-H), 3034 (C-H), 2991 (C-H), 2955 (C-H), 1746 (ester C=O), 1676 (amide C=O), 1531, 1453, 1371, 1230, 1152, 1070;  $[\alpha]_D^{20}$  - 10.7 (c 1.0, CHCl<sub>3</sub>); MS (MALDI-TOF)  $m/z$  346.1 [M+K]<sup>+</sup>; HRMS (HNESP) exact mass calculated for C<sub>16</sub>H<sub>21</sub>NO<sub>5</sub> requires  $m/z$  308.1492, found  $m/z$  308.1496 [M+H]<sup>+</sup>.

**(S)-Methyl 2-((S)-2-acetoxy-3-phenylpropanamido)-4-(methylthio)butanoate (475)**

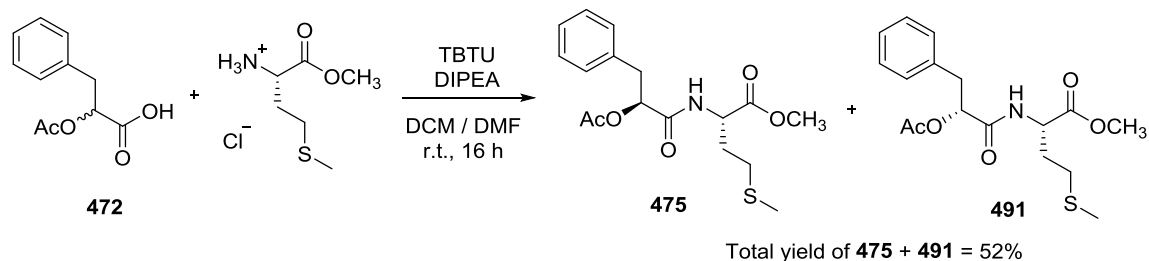


Compound **475** was prepared according to the procedure for compound **468**. Purification *via* flash column chromatography on silica gel (eluent: dichloromethane / ethyl acetate 10%;  $R_f$  = 0.44) afforded a colourless oil whose physicochemical properties were consistent with those of the title compound (302 mg, 0.85 mmol, 36% yield).

<sup>1</sup>H-NMR (500 MHz, CDCl<sub>3</sub>)  $\delta$  7.31 – 7.22 (m, 3H, Ar-*H*), 7.19 – 7.15 (m, 2H, Ar-*H*), 6.65 (d,  $J$  = 7.7 Hz, 1H, -NH-), 5.41 (t,  $J$  = 5.4 Hz, 1H, AcOCH-), 4.68 – 4.63 (m, 1H, -NHCH-), 3.73 (s, 3H, -CO<sub>2</sub>CH<sub>3</sub>), 3.19 (d,  $J$  = 5.9 Hz, 2H, -CH<sub>2</sub>Ph), 2.31 – 2.16 (m, 2H, -CH<sub>2</sub>S-), 2.14 (s, 3H, CH<sub>3</sub>CO<sub>2</sub>-), 2.07 – 2.00 (m, 1H, -CH<sub>2</sub>CH<sub>2</sub>S-), 2.03 (s, 3H, -SCH<sub>3</sub>), 1.93 – 1.84 (m, 1H, -CH<sub>2</sub>CH<sub>2</sub>S-); <sup>13</sup>C-NMR (126 MHz, CDCl<sub>3</sub>)  $\delta$  172.1 (-C=O), 169.4 (-C=O), 168.8 (-C=O), 135.7, 129.8, 128.5, 127.2, 74.3 (AcOCH-), 52.8, 51.3, 37.6 (-CH<sub>2</sub>Ph), 31.4 (-CH<sub>2</sub>CH<sub>2</sub>S-), 29.6 (-CH<sub>2</sub>S-), 21.1 (CH<sub>3</sub>CO<sub>2</sub>-), 15.4 (-SCH<sub>3</sub>); FT-IR (thin film):  $\nu$  (cm<sup>-1</sup>) = 3324 (N-H), 3030 (C-H), 2955 (C-H), 2921 (C-H), 2856 (C-H), 1746 (ester C=O), 1674 (amide C=O), 1531, 1439, 1374, 1227, 1063;  $[\alpha]_D^{20}$  + 20.5 (c 1.0, CHCl<sub>3</sub>); MS (MALDI-TOF)  $m/z$  376.3 [M+Na]<sup>+</sup>, 392.3 [M+K]<sup>+</sup>; HRMS (HNESP) exact mass calculated for C<sub>17</sub>H<sub>24</sub>NO<sub>5</sub>S requires  $m/z$  354.1370, found  $m/z$  354.1372 [M+H]<sup>+</sup>.

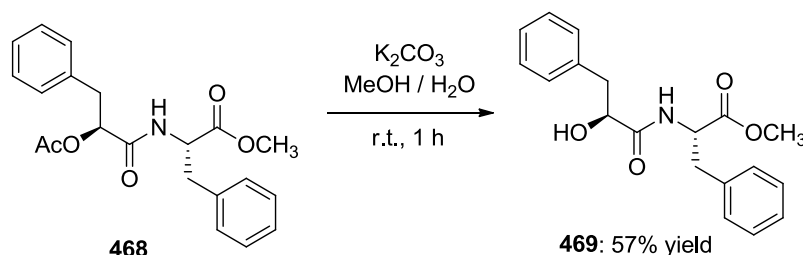


**(S)-Methyl 2-((S)-2-acetoxy-3-phenylpropanamido)-4-(methylthio)butanoate (475) and (S)-methyl 2-((R)-2-acetoxy-3-phenylpropanamido)-4-(methylthio)butanoate (491)**



Compounds **475** and **491** were prepared according to the procedure for compound **468**. Purification *via* flash column chromatography on silica gel (eluent: dichloromethane / ethyl acetate 10%;  $R_f$  = 0.44) afforded a colourless oil whose physicochemical properties were consistent with those of the title compound (441 mg, 1.25 mmol, 52% yield).

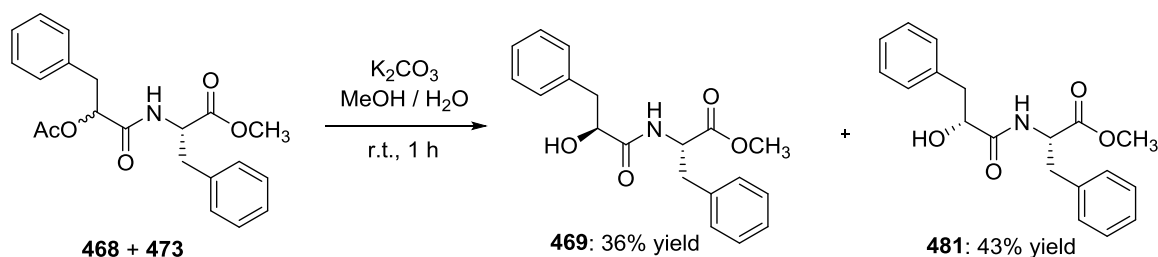
$^1\text{H}$ -NMR (500 MHz,  $\text{CDCl}_3$ )  $\delta$  7.26 (s, 6H, Ar-*H*), 7.21 – 7.16 (m, 4H, Ar-*H*), 6.65 (d,  $J$  = 7.3 Hz, 2H, -NH-), 5.41 (t,  $J$  = 5.4 Hz, 1H, AcOCH-), 5.39 – 5.36 (m, 1H, AcOCH-), 4.69 – 4.63 (m, 2H, -NHCH-), 3.74 (s, 3H, -CO<sub>2</sub>CH<sub>3</sub>), 3.73 (s, 3H, -CO<sub>2</sub>CH<sub>3</sub>), 3.24 (dd,  $J$  = 14.2, 4.9 Hz, 1H, -CH<sub>2</sub>Ph), 3.19 (d,  $J$  = 5.8 Hz, 2H, -CH<sub>2</sub>Ph), 3.09 (dd,  $J$  = 14.1, 7.7 Hz, 1H, -CH<sub>2</sub>Ph), 2.39 (m, 1H, -CH<sub>2</sub>S-), 2.30 – 2.16 (m, 2H, -CH<sub>2</sub>S-), 2.14 (s, 3H, CH<sub>3</sub>CO<sub>2</sub>-), 2.13 – 2.09 (m, 1H, -CH<sub>2</sub>S-), 2.09 (s, 3H, CH<sub>3</sub>CO<sub>2</sub>-), 2.06 (s, 3H, -SCH<sub>3</sub>), 2.05 – 2.00 (m, 4H, -SCH<sub>3</sub> + -CH<sub>2</sub>CH<sub>2</sub>S-), 1.96 (m, 2H, -CH<sub>2</sub>CH<sub>2</sub>S-), 1.88 (m, 1H, -CH<sub>2</sub>CH<sub>2</sub>S-);  $^{13}\text{C}$ -NMR (126 MHz,  $\text{CDCl}_3$ )  $\delta$  172.1 (-C=O), 172.0 (-C=O), 169.7 (-C=O), 169.4 (-C=O), 169.1 (-C=O), 168.8 (-C=O), 136.0, 135.7, 129.9, 129.6, 128.6, 128.6, 127.2, 127.1, 74.5 (AcOCH-), 74.3 (AcOCH-), 52.8, 51.5, 51.3, 37.8 (-CH<sub>2</sub>Ph), 37.6 (-CH<sub>2</sub>Ph), 31.4(4) (-CH<sub>2</sub>CH<sub>2</sub>S-), 31.3(5) (-CH<sub>2</sub>CH<sub>2</sub>S-), 30.0 (-CH<sub>2</sub>S-), 29.6 (-CH<sub>2</sub>S-), 21.1 (CH<sub>3</sub>CO<sub>2</sub>-), 21.0 (CH<sub>3</sub>CO<sub>2</sub>-), 15.6 (-SCH<sub>3</sub>), 15.4 (-SCH<sub>3</sub>); FT-IR (thin film):  $\nu$  (cm<sup>-1</sup>) = 3326 (N-H), 2950 (C-H), 2923 (C-H), 2852 (C-H), 1745 (ester C=O), 1677 (amide C=O), 1528, 1437, 1376, 1227, 1061; MS (MALDI-TOF)  $m/z$  376.33 [M+Na]<sup>+</sup>, 392.34 [M+K]<sup>+</sup>.

**(S)-Methyl 2-((S)-2-hydroxy-3-phenylpropanamido)-3-phenylpropanoate (469)**

A 150 mL round-bottom flask containing (S)-methyl 2-((S)-2-acetoxy-3-phenylpropanamido)-3-phenylpropanoate **468** (320 mg, 0.87 mmol, 1 equiv.) was charged with a mixture of methanol and distilled water (30 mL, 9:1), and a magnetic stirrer bar. Potassium carbonate (30 mg, 0.22 mmol, 0.25 equiv.) was added in one portion. The colourless solution was stirred at room temperature for 1 hour, and then concentrated by rotary evaporation. The aqueous residue was extracted with dichloromethane (3 x 25 mL) and the combined organic layers were washed with 1 M aqueous hydrochloric acid (50 mL) and subsequently brine (50 mL). The organic phase was dried over magnesium sulfate, filtered and the solvent removed *in vacuo*. Purification *via* flash column chromatography on silica gel (eluent: dichloromethane / ethyl acetate 10%;  $R_f = 0.22$ ) afforded a white solid whose physicochemical properties were consistent with those of the title compound (162 mg, 0.49 mmol, 57% yield).

M.p. 104–106 °C;  $^1\text{H-NMR}$  (500 MHz,  $\text{CDCl}_3$ )  $\delta$  7.36 – 7.30 (m, 2H, Ar-*H*), 7.29 – 7.20 (m, 6H, Ar-*H*), 6.96 (d,  $J = 7.9$  Hz, 2H, Ar-*H*), 6.91 (d,  $J = 8.4$  Hz, 1H, -NH-), 4.89 (dt,  $J = 8.2, 6.0$  Hz, 1H, -NHCH-), 4.30 (m, 1H, -CHOH), 3.71 (s, 3H, -OCH<sub>3</sub>), 3.15 (dd,  $J = 14.0, 4.0$  Hz, 1H, -CH<sub>2</sub>Ph), 3.05 (d,  $J = 6.0$  Hz, 2H, -CH<sub>2</sub>CHOH), 2.82 (dd,  $J = 13.9, 8.1$  Hz, 1H, -CH<sub>2</sub>Ph), 2.42 (d,  $J = 5.0$  Hz, 1H, -OH);  $^{13}\text{C-NMR}$  (126 MHz,  $\text{CDCl}_3$ )  $\delta$  172.2 (-C=O), 171.9 (-C=O), 136.7, 135.8, 129.8, 129.4, 128.9, 128.7, 127.2(8), 127.2(6), 72.9 (-CHOH), 52.8 (-NHCH-), 52.5 (-OCH<sub>3</sub>), 40.8 (-CH<sub>2</sub>Ph), 38.2 (-CH<sub>2</sub>Ph); FT-IR (thin film,  $\text{cm}^{-1}$ )  $\nu = 3398$  (N-H), 2967, 2854, 1739 (*ester* C=O), 1653 (*amide* C=O), 1539, 1441, 1093, 1030;  $[\alpha]_D^{19} +5.0$  (c 1.0,  $\text{CHCl}_3$ ); MS (MALDI-TOF):  $m/z = 350.2$   $[\text{M}+\text{Na}]^+$ ; HRMS (HNESF) exact mass calculated for  $\text{C}_{19}\text{H}_{22}\text{NO}_4$  requires  $m/z$  328.1543, found  $m/z$  328.1537  $[\text{M}+\text{H}]^+$ .

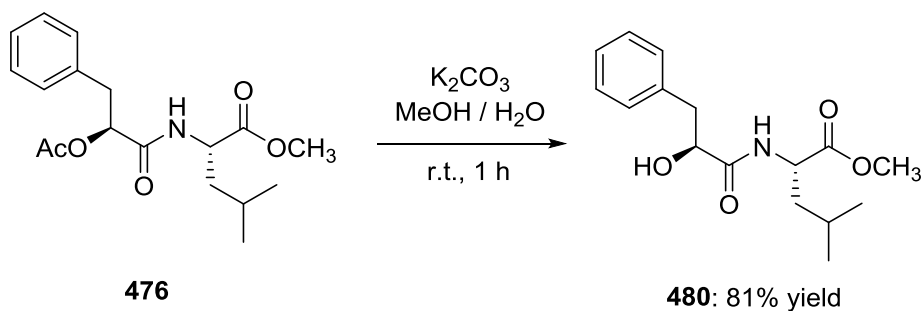
**(S)-Methyl 2-((S)-2-hydroxy-3-phenylpropanamido)-3-phenylpropanoate (469) and (S)-methyl 2-((R)-2-hydroxy-3-phenylpropanamido)-3-phenylpropanoate (481)**



Following the procedure for compound **469** above, a mixture of two diastereoisomers **469** and **481** were synthesised and separated *via* flash column chromatography on silica gel (eluent: dichloromethane / ethyl acetate (10%). Compound **469** was isolated as a colourless oil (278 mg, 0.85 mmol, 36% yield) whose physicochemical properties matched those reported above. Compound **481** was isolated as a colourless oil (332 mg, 1.01 mmol, 43% yield).

**316:**  $R_f = 0.43$ ;  $^1\text{H-NMR}$  (500 MHz,  $\text{CDCl}_3$ )  $\delta$  7.35 – 7.19 (m, 8H, Ar-*H*), 7.12 – 7.07 (m, 2H, Ar-*H*), 6.89 (d,  $J = 7.7$  Hz, 1H, -NH-), 4.88 (dt,  $J = 8.2, 6.1$  Hz, 1H, -NHCH-), 4.27 (dd,  $J = 9.0, 4.0$  Hz, 1H, -CHOH), 3.71 (s, 3H, -OCH<sub>3</sub>), 3.21 (dd,  $J = 14.0, 4.0$  Hz, 1H, -CH<sub>2</sub>Ph), 3.12 (qd,  $J = 13.9, 6.1$  Hz, 2H, -CH<sub>2</sub>Ph), 2.84 (dd,  $J = 14.0, 9.0$  Hz, 1H, -CH<sub>2</sub>Ph);  $^{13}\text{C-NMR}$  (126 MHz,  $\text{CDCl}_3$ )  $\delta$  172.3 (-C=O), 171.8 (-C=O), 136.8, 135.9, 129.6, 129.4, 129.0, 128.8, 127.3, 127.3, 73.0 (-CHOH), 53.0 (-NHCH-), 52.5 (-OCH<sub>3</sub>), 40.9 (-CH<sub>2</sub>Ph), 38.1 (-CH<sub>2</sub>Ph); FT-IR (thin film):  $\nu$  (cm<sup>-1</sup>) = 3390 (N-H), 3066, 3028, 2952, 2924, 1741 (ester C=O), 1655 (amide C=O), 1521, 1497, 1455, 1438, 1362, 1217, 1086;  $[\alpha]_D^{20} +86.4$  (c 1.0,  $\text{CHCl}_3$ ); MS (MALDI-TOF)  $m/z$  350.2  $[\text{M}+\text{Na}]^+$ ; HRMS (HNESP) exact mass calculated for  $\text{C}_{19}\text{H}_{22}\text{NO}_4$  requires  $m/z$  328.1543, found  $m/z$  328.1543  $[\text{M}+\text{H}]^+$ .

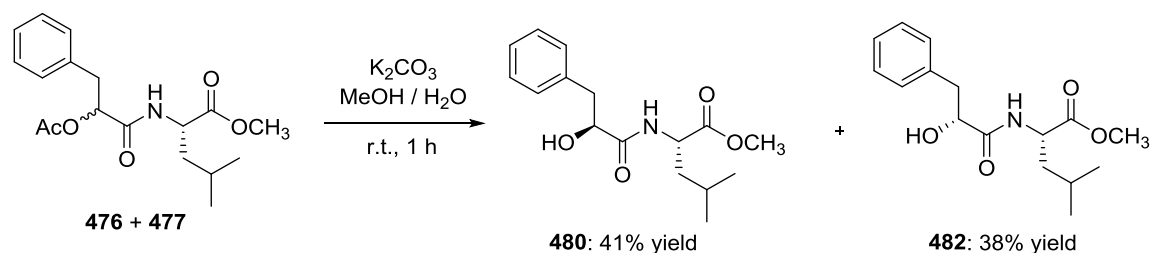
**(S)-Methyl 2-((R)-2-hydroxy-3-phenylpropanamido)-4-methylpentanoate (480)**



Compound **480** was prepared according to the procedure for compound **469**. Purification *via* flash column chromatography on silica (dichloromethane / ethyl acetate 10%;  $R_f = 0.42$ ) afforded a white solid whose physicochemical properties were consistent with those of the title compound (354 mg, 1.21 mmol, 81% yield).

M.p. 45–47 °C;  $^1\text{H-NMR}$  (500 MHz,  $\text{CDCl}_3$ )  $\delta$  7.37 – 7.31 (m, 2H, Ar-*H*), 7.30 – 7.23 (m, 3H, Ar-*H*), 6.77 (d,  $J = 8.3$  Hz, 1H, -NH-), 4.63 (dt,  $J = 8.8, 5.0$  Hz, 1H, -NHCH-), 4.36 – 4.30 (m, 1H, -CHOH), 3.73 (s, 3H, -OCH<sub>3</sub>), 3.25 (dd,  $J = 14.0, 4.2$  Hz, 1H-CH<sub>2</sub>Ph), 2.91 (dd,  $J = 14.0, 8.8$  Hz, 1H, -CH<sub>2</sub>Ph), 2.39 (s, 1H, -OH), 1.69 – 1.49 (m, 3H, -CH<sub>2</sub>CH(CH<sub>3</sub>)<sub>2</sub>), 0.91 (d,  $J = 2.7$  Hz, 3H, -CH(CH<sub>3</sub>)<sub>2</sub>), 0.90 (d,  $J = 2.8$  Hz, 3H, -CH(CH<sub>3</sub>)<sub>2</sub>);  $^{13}\text{C-NMR}$  (126 MHz,  $\text{CDCl}_3$ )  $\delta$  173.1 (-C=O), 172.9 (-C=O), 137.0, 129.6, 128.7, 126.9, 72.9 (-CHOH), 52.4 (-NHCH-), 50.4 (-OCH<sub>3</sub>), 41.5 (-CH<sub>2</sub>CH(CH<sub>3</sub>)<sub>2</sub>), 40.8 (-CH<sub>2</sub>Ph), 24.8 (-CH(CH<sub>3</sub>)<sub>2</sub>), 22.8 (-CH(CH<sub>3</sub>)<sub>2</sub>), 21.9 (-CH(CH<sub>3</sub>)<sub>2</sub>); FT-IR (thin film):  $\nu$  (cm<sup>-1</sup>) = 3389 (N-H), 3032, 2956, 2874, 1744 (ester C=O), 1658 (amide C=O), 1531, 1456, 1439, 1370, 1277, 1209, 1154, 1088;  $[\alpha]_D^{19} +48.6$  (c 1.0,  $\text{CHCl}_3$ ); MS (MALDI-TOF)  $m/z$  332.4  $[\text{M}+\text{K}]^+$ ; HRMS (HNESP) exact mass calculated for C<sub>16</sub>H<sub>24</sub>NO<sub>4</sub> requires  $m/z$  294.1700, found  $m/z$  294.1702  $[\text{M}+\text{H}]^+$ .

**(S)-Methyl 2-((S)-2-hydroxy-3-phenylpropanamido)-4-methylpentanoate (480) and (S)-methyl 2-((R)-2-hydroxy-3-phenylpropanamido)-4-methylpentanoate (482)**

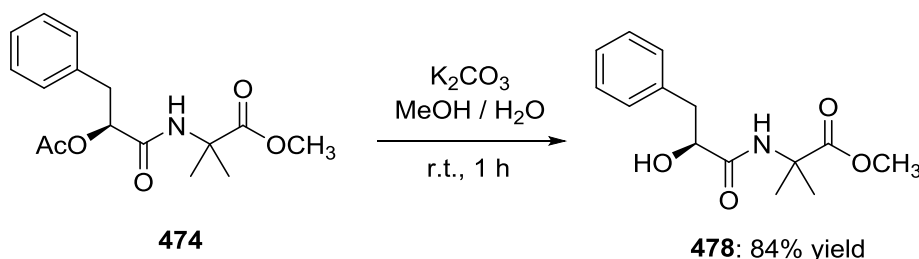


Following the procedure for compound **469**, a mixture of two diastereoisomers **480** and **482** were synthesised and separated *via* flash column chromatography on silica gel (eluent: dichloromethane / ethyl acetate 10 %). Compound **480** was isolated as a white solid (111 mg, 0.38 mmol, 41% yield) whose physicochemical properties matched those reported above. Compound **482** was isolated as a white solid (103 mg, 0.35 mmol, 38% yield).

**482:**  $R_f = 0.20$ ; M.p. 83–85 °C;  $^1\text{H-NMR}$  (500 MHz,  $\text{CDCl}_3$ )  $\delta$  7.31 – 7.25 (m, 2H, Ar-*H*), 7.25 – 7.19 (m, 3H, Ar-*H*), 6.93 (d,  $J = 8.5$  Hz, 1H, -NH-), 4.55 (dt,  $J = 8.9, 5.1$  Hz, 1H, -

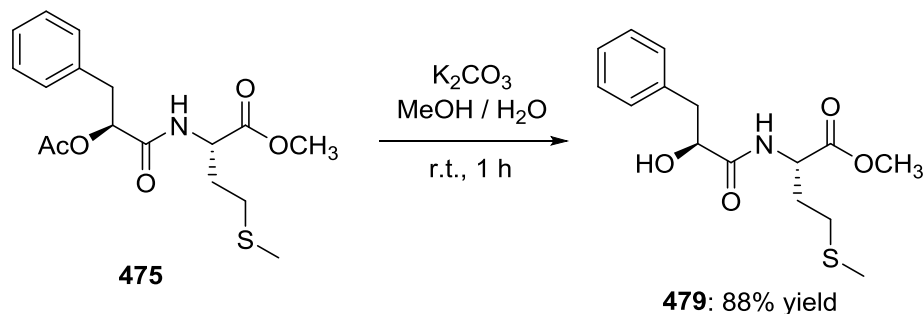
NHCH-), 4.33 (dt,  $J = 8.3, 4.4$  Hz, 1H, -CHOH), 3.68 (s, 3H, -OCH<sub>3</sub>), 3.43 (brs, 1H, -OH), 3.16 (dd,  $J = 14.0, 3.9$  Hz, 1H, -CH<sub>2</sub>Ph), 2.91 (dd,  $J = 14.0, 7.6$  Hz, 1H, -CH<sub>2</sub>Ph), 1.60 – 1.52 (m, 1H, -CH(CH<sub>3</sub>)<sub>2</sub>), 1.50 – 1.34 (m, 2H, -CH<sub>2</sub>CH(CH<sub>3</sub>)<sub>2</sub>), 0.87 (d,  $J = 2.8$  Hz, 3H, -CH(CH<sub>3</sub>)<sub>2</sub>), 0.86 (d,  $J = 2.9$  Hz, 3H, -CH(CH<sub>3</sub>)<sub>2</sub>); <sup>13</sup>C-NMR (126 MHz, CDCl<sub>3</sub>)  $\delta$  173.6 (-C=O), 173.1 (-C=O), 137.0, 129.8, 128.5, 126.9, 72.8 (-CHOH), 52.4 (-NHCH-), 50.3 (-OCH<sub>3</sub>), 41.3 (-CH<sub>2</sub>CH(CH<sub>3</sub>)<sub>2</sub>), 40.6 (-CH<sub>2</sub>Ph), 24.7 (-CH(CH<sub>3</sub>)<sub>2</sub>), 22.9 (-CH(CH<sub>3</sub>)<sub>2</sub>), 21.8 (-CH(CH<sub>3</sub>)<sub>2</sub>); FT-IR (thin film):  $\nu$  (cm<sup>-1</sup>) = 3372 (N-H), 3186, 2955, 2924, 2866, 1752 (ester C=O), 1662 (amide C=O), 1541, 1448, 1421, 1366, 1269, 1235, 1190, 1152, 1093;  $[\alpha]_D^{20} - 60.2$  (c 1.0, CHCl<sub>3</sub>); MS (MALDI-TOF)  $m/z$  332.37 [M+K]<sup>+</sup>; HRMS (HNESP) exact mass calculated for C<sub>16</sub>H<sub>24</sub>NO<sub>4</sub> requires  $m/z$  294.1700, found  $m/z$  294.1702 [M+H]<sup>+</sup>.

**(S)-Methyl 2-(2-hydroxy-3-phenylpropanamido)-2-methylpropanoate (478)**



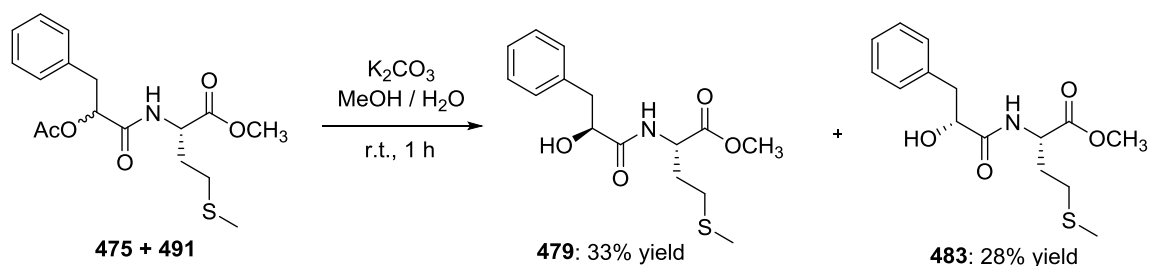
Compound **478** was prepared according to the procedure for compound **469**. Purification *via* flash column chromatography on silica gel (eluent: dichloromethane / ethyl acetate 10%;  $R_f = 0.13$ ) afforded a colourless oil whose physicochemical properties were consistent with those of the title compound (154 mg, 0.58 mmol, 84% yield).

<sup>1</sup>H-NMR (500 MHz, CDCl<sub>3</sub>)  $\delta$  7.36 – 7.29 (m, 2H, Ar-*H*), 7.29 – 7.23 (m, 3H, Ar-*H*), 6.89 (s, 1H, -NH-), 4.26 (dd,  $J = 8.1, 4.5$  Hz, 1H, -NHCH-), 3.74 (s, 3H, -OCH<sub>3</sub>), 3.17 (dd,  $J = 14.0, 4.4$  Hz, 1H, -CH<sub>2</sub>Ph), 2.93 (dd,  $J = 13.9, 8.1$  Hz, 1H, -CH<sub>2</sub>Ph), 2.55 (s, 1H, -OH), 1.52 (s, 3H, -CH<sub>3</sub>), 1.51 (s, 3H, -CH<sub>3</sub>); <sup>13</sup>C-NMR (126 MHz, CDCl<sub>3</sub>)  $\delta$  174.9 (-C=O), 172.4 (-C=O), 137.0, 129.8, 128.6, 127.0, 72.8 (-CHOH), 56.2 (-NHCH-), 52.7 (-OCH<sub>3</sub>), 40.7 (-CH<sub>2</sub>Ph), 25.0 (-CH<sub>3</sub>), 24.7 (-CH<sub>3</sub>); FT-IR (thin film):  $\nu$  (cm<sup>-1</sup>) = 3382 (N-H), 3033, 2991, 2953, 1742 (ester C=O), 1654 (amide C=O), 1528, 1456, 1385, 1296, 1162, 1090;  $[\alpha]_D^{20} - 49.1$  (c 1.0, CHCl<sub>3</sub>); MS (MALDI-TOF)  $m/z$  304.3 [M+K]<sup>+</sup>; HRMS (HNESP) exact mass calculated for C<sub>14</sub>H<sub>20</sub>NO<sub>4</sub> requires  $m/z$  266.1387, found  $m/z$  266.1390 [M+H]<sup>+</sup>.

**(S)-Methyl 2-((R)-2-hydroxy-3-phenylpropanamido)-4-(methylthio)butanoate (479)**

Compound **479** was prepared according to the procedure for compound **469**. Purification *via* flash column chromatography on silica gel (eluent: dichloromethane / ethyl acetate 10%;  $R_f$  = 0.10) afforded a white solid whose physicochemical properties were consistent with those of the title compound (166 mg, 0.53 mmol, 88% yield).

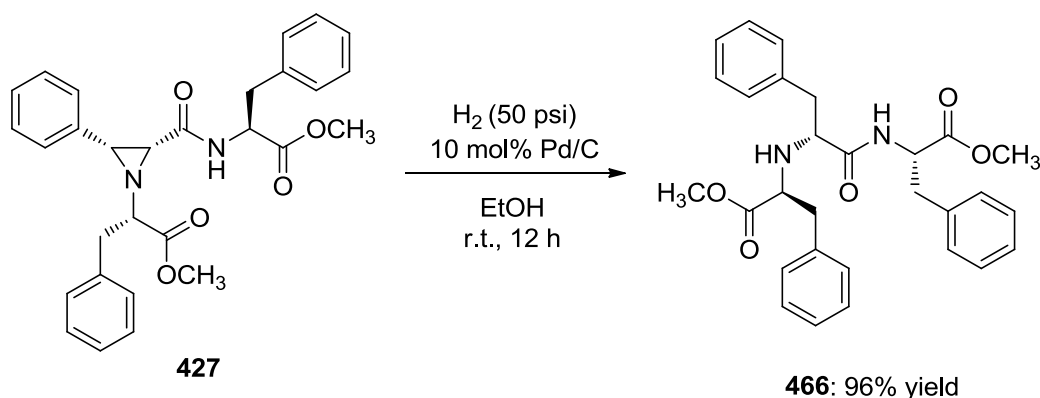
M.p. 60–62 °C;  $^1\text{H-NMR}$  (500 MHz,  $\text{CDCl}_3$ )  $\delta$  7.36 – 7.23 (m, 5H, Ar-*H*), 7.14 (d,  $J$  = 8.0 Hz, 1H, -*NH*-), 4.69 (dt,  $J$  = 7.9, 5.2 Hz, 1H, -*NHCH*-), 4.39 (dd,  $J$  = 7.6, 3.9 Hz, 1H, -*CHOH*), 3.74 (s, 3H, -*OCH*<sub>3</sub>), 3.20 (dd,  $J$  = 13.9, 4.0 Hz, 1H, -*CH*<sub>2</sub>Ph), 2.97 (dd,  $J$  = 13.9, 7.6 Hz, 2H, -*CH*<sub>2</sub>Ph), 2.38 – 2.26 (m, 2H, -*CH*<sub>2</sub>S-), 2.13 – 2.07 (m, 1H, -*CH*<sub>2</sub>CH<sub>2</sub>S-), 2.06 (s, 3H, -*SCH*<sub>3</sub>), 1.96 – 1.86 (m, 1H, -*CH*<sub>2</sub>CH<sub>2</sub>S-);  $^{13}\text{C-NMR}$  (126 MHz,  $\text{CDCl}_3$ )  $\delta$  173.0 (-C=O), 172.3 (-C=O), 136.6, 129.8, 128.7, 127.1, 72.7 (-*CHOH*), 52.7 (-*NHCH*-), 51.1 (-*OCH*<sub>3</sub>), 40.7 (-*CH*<sub>2</sub>Ph), 31.6 (-*CH*<sub>2</sub>CH<sub>2</sub>S-), 29.8 (-*CH*<sub>2</sub>S-), 15.5 (-*SCH*<sub>3</sub>); FT-IR (thin film):  $\nu$  ( $\text{cm}^{-1}$ ) = 3377 (N-H), 3255, 2957, 2913, 1752 (*ester* C=O), 1660 (*amide* C=O), 1542, 1447, 1352, 1274, 1223, 1196, 1189, 1169, 1125, 1088;  $[\alpha]_D^{20}$  – 29.5 (c 1.0,  $\text{CHCl}_3$ ); MS (MALDI-TOF)  $m/z$  334.3  $[\text{M}+\text{Na}]^+$ , 350.3  $[\text{M}+\text{K}]^+$ ; HRMS (HNESP) exact mass calculated for  $\text{C}_{15}\text{H}_{21}\text{NO}_4\text{S}$  requires  $m/z$  312.1264, found  $m/z$  312.1267  $[\text{M}+\text{H}]^+$ .

**(S)-Methyl 2-((S)-2-hydroxy-3-phenylpropanamido)-4-(methylthio)butanoate (479) and (S)-Methyl 2-((R)-2-hydroxy-3-phenylpropanamido)-4-(methylthio)butanoate (483)**

Using the procedure for compound **469**, a 1:1 mixture of diastereoisomers **479** and **483** were made and separated *via* flash column chromatography on silica gel (eluent: dichloromethane / ethyl acetate 20%). Compound **479** was isolated as a white solid (87 mg, 0.28 mmol, 33% yield) whose physicochemical properties matched those reported above. Compound **483** was isolated as a white solid (74 mg, 0.24 mmol, 28% yield).

**319**:  $R_f$  = 0.28;  $^1\text{H-NMR}$  (500 MHz,  $\text{CDCl}_3$ )  $\delta$  7.30 – 7.24 (m, 2H, Ar-*H*), 7.23 – 7.16 (m, 3H, Ar-*H*), 6.98 (d,  $J$  = 8.1 Hz, 1H, -NH-), 4.65 (dt,  $J$  = 7.8, 5.3 Hz, 1H, -NHCH-), 4.27 (dd,  $J$  = 8.8, 4.1 Hz, 1H, -CHOH), 3.68 (s, 3H, -OCH<sub>3</sub>), 3.18 (dd,  $J$  = 14.0, 4.1 Hz, 1H, -CH<sub>2</sub>Ph), 2.83 (dd,  $J$  = 14.0, 8.8 Hz, 1H, -CH<sub>2</sub>Ph), 2.40 (t,  $J$  = 7.4 Hz, 2H, -CH<sub>2</sub>S-), 2.14 – 2.04 (m, 1H, -CH<sub>2</sub>CH<sub>2</sub>S-), 2.02 (s, 3H, -SCH<sub>3</sub>), 1.97 – 1.86 (m, 1H, -CH<sub>2</sub>CH<sub>2</sub>S-);  $^{13}\text{C-NMR}$  (126 MHz,  $\text{CDCl}_3$ )  $\delta$  172.8 (-C=O), 172.1 (-C=O), 136.9, 129.6, 128.9, 127.1, 73.0 (-CHOH), 52.7 (-NHCH-), 51.3 (-OCH<sub>3</sub>), 40.9 (-CH<sub>2</sub>Ph), 31.7 (-CH<sub>2</sub>CH<sub>2</sub>S-), 30.0 (-CH<sub>2</sub>S-), 15.5 (-SCH<sub>3</sub>); FT-IR (thin film):  $\nu$  ( $\text{cm}^{-1}$ ) = 3382 (N-H), 3059, 3028, 2953, 2919, 2850, 1741 (*ester* C=O), 1658 (*amide* C=O), 1524, 1435, 1360, 1277, 1226, 1171, 1088, 1030;  $[\alpha]_D^{22}$  +33.1 (c 1.0,  $\text{CHCl}_3$ ); MS (MALDI-TOF)  $m/z$  349.7  $[\text{M}+\text{K}]^+$ ; HRMS (HNESF) exact mass calculated for  $\text{C}_{15}\text{H}_{22}\text{NO}_4\text{S}$  requires  $m/z$  312.1264, found  $m/z$  312.1265  $[\text{M}+\text{H}]^+$ .

**(*S*)-Methyl 2-((*R*)-2-((*S*)-1-methoxy-1-oxo-3-phenylpropan-2-ylamino)-3-phenylpropanamido)-3-phenylpropanoate (**466**)**

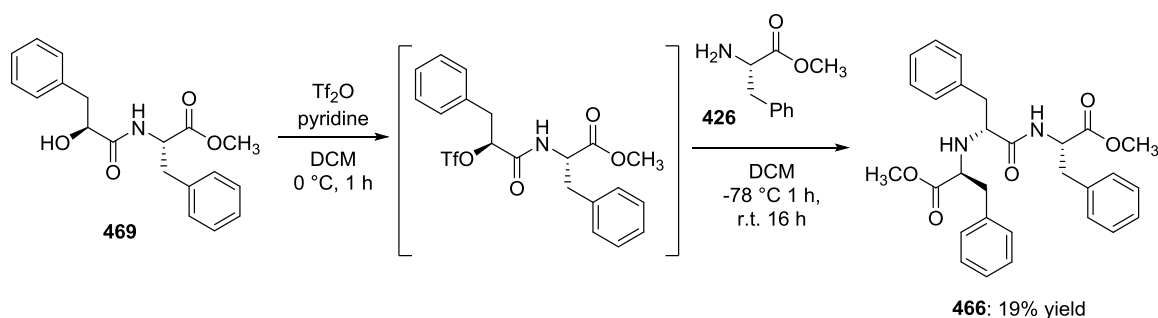


A Biotage Endeavor glass hydrogenation vial was charged with a solution of (*S*)-methyl 2-((2*R*,3*R*)-1-((*S*)-1-methoxy-1-oxo-3-phenylpropan-2-yl)-3-phenylaziridine-2-carboxamido)-3-phenylpropanoate **427** (100 mg, 0.21 mmol, 1 equiv.) in ethanol (4 mL). Palladium on carbon (10 wt%) (22 mg, 0.021 mmol, 10 mol%) was added, and the mixture stirred under 50 psi of hydrogen at room temperature for 12 hours. The mixture

was filtered through a short plug of celite and the solvent removed *in vacuo*. Purification *via* flash column chromatography on silica gel (eluent: dichloromethane / ethyl acetate 10%;  $R_f = 0.44$ ) afforded a colourless oil whose physicochemical properties were consistent with those of the title compound (96 mg, 0.20 mmol, 96% yield).

$^1\text{H-NMR}$  (500 MHz,  $\text{CDCl}_3$ )  $\delta$  7.71 (s, 1H, -NH-), 7.25 – 7.14 (m, 9H, Ar-H), 7.10 (d,  $J = 6.6$  Hz, 2H, Ar-H), 7.04 – 6.99 (m, 2H, Ar-H), 6.81 (d,  $J = 5.9$  Hz, 2H, Ar-H), 4.85 (dt,  $J = 8.3, 6.5$  Hz, 1H, -NHCH-), 3.70 (s, 3H, -OCH<sub>3</sub>), 3.56 (s, 3H, -OCH<sub>3</sub>), 3.34 (dd,  $J = 9.1, 4.3$  Hz, 1H, -NHCH-), 3.29 (t,  $J = 6.5$  Hz, 1H, -NHCH-), 3.18 – 3.03 (m, 3H, -CH<sub>2</sub>Ph), 2.76 – 2.63 (m, 3H, -CH<sub>2</sub>Ph);  $^{13}\text{C NMR}$  (126 MHz,  $\text{CDCl}_3$ )  $\delta$  173.3 (-C=O), 173.2 (-C=O), 172.0 (-C=O), 137.2, 136.4, 136.3, 129.4, 129.3, 129.2, 129.0, 128.8, 128.7, 127.1, 127.0(2), 126.9(6), 62.6 (-NHCH-), 61.6 (-NHCH-), 53.2 (-NHCH-), 52.3 (-OCH<sub>3</sub>), 52.0 (-OCH<sub>3</sub>), 39.1 (-CH<sub>2</sub>Ph), 38.1 (-CH<sub>2</sub>Ph), 38.0 (-CH<sub>2</sub>Ph); FT-IR (thin film):  $\nu$  (cm<sup>-1</sup>) = 3339, 2920, 2858, 1746, 1672, 1500, 1457, 1203, 1027;  $[\alpha]_D^{20} +11.9$  (c 1.0,  $\text{CHCl}_3$ ); MS (MALDI-TOF)  $m/z$  489.6  $[\text{M}+\text{Na}]^+$ ; HRMS (HNESF) exact mass calculated for  $\text{C}_{29}\text{H}_{33}\text{N}_2\text{O}_5$  requires  $m/z$  489.2384, found  $m/z$  489.2378  $[\text{M}+\text{H}]^+$ .

**(S)-Methyl 2-((R)-2-((S)-1-methoxy-1-oxo-3-phenylpropan-2-ylamino)-3-phenylpropanamido)-3-phenylpropanoate (466)**

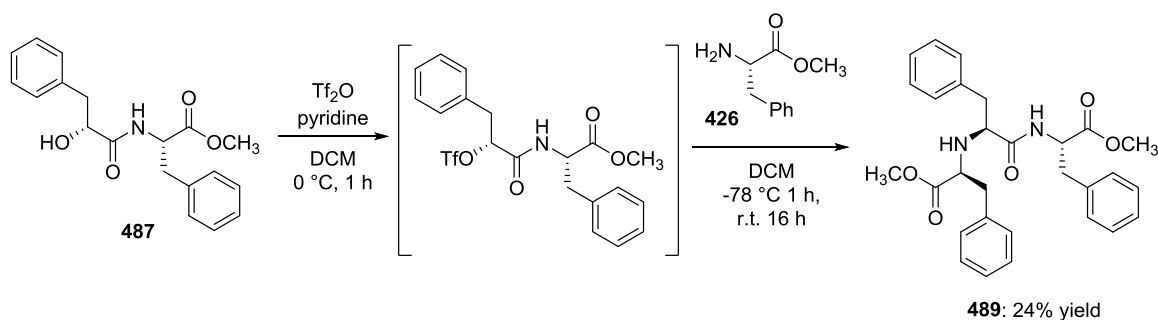


A flame-dried 5 mL microwave vial containing a magnetic stirrer bar was charged with a solution of trifluoromethanesulfonic anhydride (51  $\mu\text{L}$ , 0.31 mmol, 1 equiv.) in dry dichloromethane (1 mL) and cooled to 0 °C under a nitrogen atmosphere using an ice bath. A solution of (S)-methyl 2-((S)-2-hydroxy-3-phenylpropanamido)-3-phenylpropanoate **469** (100 mg, 0.31 mmol, 1 equiv.) and pyridine (25  $\mu\text{L}$ , 0.31 mmol, 1 equiv.) in dry dichloromethane (2 mL) was added dropwise *via* syringe over 1 hour. The reaction was allowed to warm slowly to room temperature, and the solvent removed *in vacuo*. Pentane (5 mL) was added and the resulting white precipitate was removed by



filtration. The filtrate was concentrated *in vacuo* before being redissolved in dry dichloromethane (2 mL) and added dropwise to a solution of L-phenylalanine methyl ester **426** (109 mg, 0.61 mmol, 2 equiv.) in dichloromethane (2 mL) at -70 °C in a 5 mL microwave vial under a nitrogen atmosphere. The reaction was stirred at -70 °C for one hour before being allowed to warm to room temperature and stirred for a further 16 hours. The white solid precipitate was removed by filtration and the filtrate concentrated *in vacuo*. Purification *via* flash column chromatography on silica gel (eluent: dichloromethane / ethyl acetate 10%;  $R_f$  = 0.44) afforded a colourless oil (28 mg, 0.058 mmol, 19% yield) whose physicochemical properties were consistent with those of the title compound and matched those obtained by hydrogenation of the corresponding aziridine **427** described above.

**(S)-Methyl 2-((S)-2-((S)-1-methoxy-1-oxo-3-phenylpropan-2-ylamino)-3-phenylpropanamido)-3-phenylpropanoate (489)**

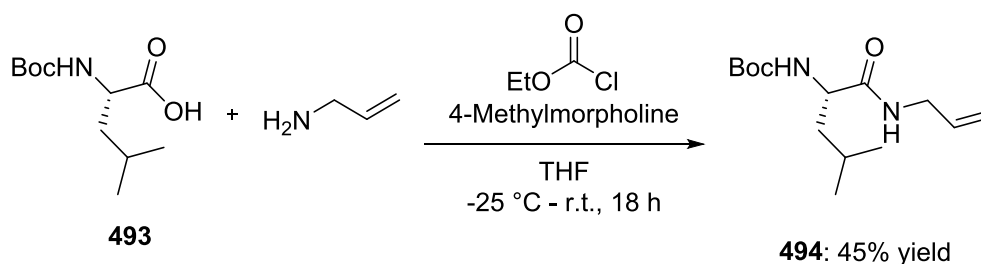


Compound **489** was prepared according to the procedure for compound **466**. Purification *via* flash column chromatography on silica (dichloromethane / ethyl acetate 10%;  $R_f$  = 0.32) afforded a colourless oil whose physicochemical properties were consistent with those of the title compound (36 mg, 0.073 mmol, 24% yield).

$^1\text{H-NMR}$  (500 MHz,  $\text{CDCl}_3$ )  $\delta$  7.32 – 7.20 (m, 10H, Ar-*H*), 7.11 – 7.05 (m, 4H, Ar-*H*), 6.96 (d,  $J$  = 7.2 Hz, 2H, Ar-*H*), 4.71 (td,  $J$  = 8.3, 5.3 Hz, 1H, -NHCH-), 3.73 (s, 3H, -OCH<sub>3</sub>), 3.48 (s, 3H, -OCH<sub>3</sub> + -NHCH-), 3.25 (dd,  $J$  = 8.8, 3.9 Hz, 1H, -NHCH-), 2.99 (dd,  $J$  = 13.9, 5.3 Hz, 1H, -CH<sub>2</sub>Ph), 2.94 (dd,  $J$  = 13.9, 4.1 Hz, 1H, -CH<sub>2</sub>Ph), 2.83 – 2.63 (m, 3H, -CH<sub>2</sub>Ph), 2.46 – 2.39 (m, 1H, -CH<sub>2</sub>Ph);  $^{13}\text{C-NMR}$  (126 MHz,  $\text{CDCl}_3$ )  $\delta$  173.3 (-C=O), 172.9 (-C=O), 171.8 (-C=O), 137.0, 136.7, 136.4, 129.7, 129.5, 129.3, 128.7(1), 128.6(7), 128.5, 127.2, 127.1, 127.0, 62.2 (-NHCH-), 61.1 (-NHCH-), 52.4 (-NHCH- + -OCH<sub>3</sub>), 51.9 (-OCH<sub>3</sub>), 40.0 (-CH<sub>2</sub>Ph), 39.6 (-CH<sub>2</sub>Ph), 37.4 (-CH<sub>2</sub>Ph); FT-IR (thin film):  $\nu$

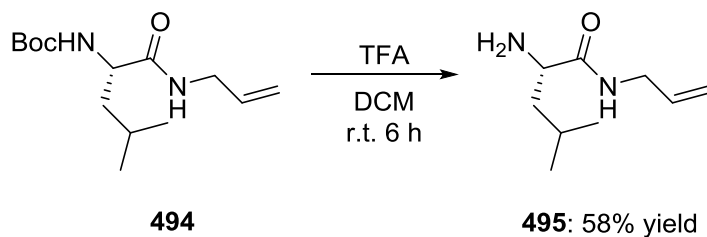
( $\text{cm}^{-1}$ ) = 3351 (N-H), 2924, 2854, 1743 (*ester* C=O), 1680 (*amide* C=O), 1504, 1453, 1203;  $[\alpha]_{\text{D}}^{20}$  -7.2 (c 0.6,  $\text{CHCl}_3$ ); MS (MALDI-TOF)  $m/z$  511.37  $[\text{M}+\text{Na}]^+$ ; HRMS (HNESF) exact mass calculated for  $\text{C}_{29}\text{H}_{33}\text{N}_2\text{O}_5$  requires  $m/z$  489.2384, found  $m/z$  489.2375  $[\text{M}+\text{H}]^+$ .

**(*S*)-tert-Butyl 1-(allylamino)-4-methyl-1-oxopentan-2-ylcarbamate (**494**)<sup>253</sup>**



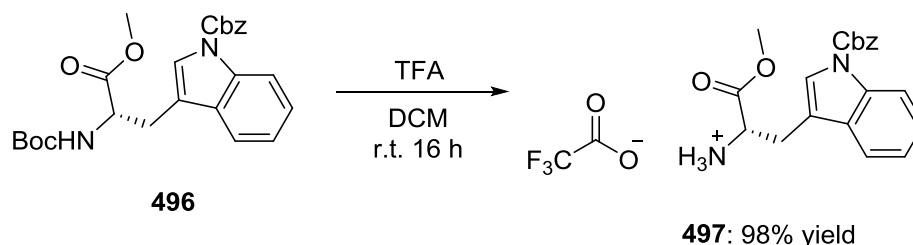
A 150 mL round-bottom flask was charged with a solution of (*S*)-2-((*tert*-butoxycarbonyl)amino)-4-methylpentanoic acid **493** (1.0 g, 4.32 mmol, 1 equiv.) in dry tetrahydrofuran (20 mL) and cooled to -25 °C under a nitrogen atmosphere. 4-Methylmorpholine (0.48 mL, 4.32 mmol, 1 equiv.), ethyl chloroformate (0.41 mL, 4.32 mmol, 1 equiv.) and allylamine (0.36 mL, 4.75 mmol, 1.1 equiv.) were added sequentially *via* syringe (3 x 1 mL) and with vigorous stirring of the reaction mixture. The resulting suspension was allowed to warm to room temperature and stirred for 18 hours. The solvent was removed *in vacuo* and the residue diluted with distilled water (15 mL) and adjusted to pH 1 with 1 M aqueous potassium hydrogen sulfate. The resulting mixture was extracted with ethyl acetate (3 x 30 mL) and the combined organic layers washed with distilled water (100 mL), then saturated aqueous sodium bicarbonate (100 mL) and finally brine (100 mL). The separated organic solution was dried over magnesium sulfate, filtered, and the solvent removed *in vacuo*. Purification *via* flash column chromatography on silica gel (eluent: petroleum ether / diethyl ether 1:1;  $R_f$  = 0.24) afforded a white solid whose physicochemical properties matched those previously reported (527 mg, 1.95 mmol, 45% yield).

M.p. 78–80 °C;  $^1\text{H}$ -NMR (500 MHz,  $\text{CDCl}_3$ )  $\delta$  = 6.19 (br s, 1H, -NH-), 5.87 – 5.78 (m, 1H, -CH=CH<sub>2</sub>), 5.19 (dd,  $J$  = 17.2, 1.4 Hz, 1H, -CH=CH<sub>2</sub>), 5.13 (dd,  $J$  = 10.3, 1.3 Hz, 1H, -CH=CH<sub>2</sub>), 4.85 (br s, 1H, BocNH-), 4.08 (br s, 1H, BocNHCH-), 3.88 (br s, 2H, -NHCH<sub>2</sub>-), 1.73 – 1.63 (m, 2H, -CH<sub>2</sub>CH(CH<sub>3</sub>)<sub>2</sub>), 1.52 – 1.40 (m, 1H, -CH(CH<sub>3</sub>)<sub>2</sub>), 1.44 (s, 9H, -C(CH<sub>3</sub>)<sub>3</sub>), 0.95 (d,  $J$  = 4.8 Hz, 3H, -CH(CH<sub>3</sub>)<sub>2</sub>), 0.93 (d,  $J$  = 4.8 Hz, 3H, -CH(CH<sub>3</sub>)<sub>2</sub>);



$[\alpha]_D^{17} -20.6$  (c 1.0,  $\text{CHCl}_3$ ); MS (MALDI-TOF):  $m/z = 209.1$   $[\text{M}+\text{K}]^+$ ; HRMS (HNESF) exact mass calculated for  $\text{C}_9\text{H}_{19}\text{N}_2\text{O}$  requires  $m/z$  171.1492, found  $m/z$  171.1491  $[\text{M}+\text{H}]^+$ .

**(S)-3-(1-((Benzyloxy)carbonyl)-1H-indol-3-yl)-1-methoxy-1-oxopropan-2-aminium trifluoroacetate (497)**



To a 500 mL two-necked round-bottom flask under a nitrogen atmosphere was added (S)-benzyl 3-(2-((*tert*-butoxycarbonyl)amino)-3-methoxy-3-oxopropyl)-1H-indole-1-carboxylate **329** (9.33 g, 20.6 mmol, 1 equiv.) and a magnetic stirrer bar. The white solid was dissolved in dichloromethane (60 mL) and trifluoroacetic acid (12.6 mL, 165 mmol, 8 equiv.) was added *via* a 20 mL syringe. The solution was stirred at room temperature for 16 hours, by which time complete disappearance of the starting material was observed by thin layer chromatography (eluent: petroleum ether / diethyl ether 1:1). The solvent was removed *in vacuo* to afford a colourless oil, and a white solid precipitate was formed on the addition of diethyl ether. The solid was filtered, washed with diethyl ether and dried *in vacuo*. The physicochemical properties were consistent with those of the title compound (6.71 g, 20.2 mmol, 98% yield).

M.p. 138–140 °C;  $^1\text{H}$ -NMR (500 MHz, MeOD)  $\delta$  8.18 (d,  $J = 8.1$  Hz, 1H, Ar-*H*), 7.66 (s, 1H, *ind.* C-2 *H*), 7.60 – 7.56 (m, 1H, Ar-*H*), 7.55 – 7.51 (m, 2H, Ar-*H*), 7.46 – 7.33 (m, 4H, Ar-*H*), 7.30 (t,  $J = 7.5$  Hz, 1H, Ar-*H*), 5.48 (s, 2H,  $-\text{CH}_2\text{Ph}$ ), 4.39 (br s, 1H,  $-\text{CHNH}_2$ ), 3.78 (s, 3H,  $-\text{OCH}_3$ ), 3.42 (dd,  $J = 15.2, 5.1$  Hz, 1H,  $-\text{CH}_2\text{-ind}$ ), 3.34 – 3.25 (m, 1H,  $-\text{CH}_2\text{-ind}$ );  $^{13}\text{C}$ -NMR (126 MHz, MeOD)  $\delta$  170.5 ( $-\text{C}=\text{O}$ ), 162.2 ( $-\text{C}=\text{O}$ ), 151.8 ( $-\text{C}=\text{O}$ ), 137.0, 136.6, 130.9, 129.8, 129.7, 129.6, 126.1, 126.1, 124.2, 119.7, 116.3, 114.9, 69.9 ( $-\text{CH}_2\text{Ph}$ ), 53.7 ( $-\text{OCH}_3$ ), 27.0 ( $-\text{CH}_2\text{-ind}$ ); FT-IR (thin film):  $\nu$  ( $\text{cm}^{-1}$ ) = 3441 (N-H), 3038 (C-H), 2959 (C-H), 2921 (C-H), 2855 (C-H), 1741 (*ester* C=O), 1679 (*carbamate* C=O), 1610, 1521, 1462, 1403, 1362, 1345, 1303, 1255, 1203, 1135, 1093, 1024, 945;  $[\alpha]_D^{19} +4.8$  (c 1.0, MeOH); MS (MALDI-TOF)  $m/z$  352.5  $[\text{M}]^+$  (*free amine*); HRMS (HNESF) exact mass calculated for  $\text{C}_{20}\text{H}_{21}\text{N}_2\text{O}_4$  requires  $m/z$  353.1496, found  $m/z$  353.1494  $[\text{M}+\text{H}]^+$  (*free amine*).

## BIBLIOGRAPHY

## **Bibliography**

1. M. H. McCormick, W. M. Stark, G. E. Pittenger, R. C. Pittenger and G. M. McGuire, *Antibiot. Annu.*, **1955–56**, 606; D. P. Levine, *Clin. Infect. Dis.*, **2006**, 42, S5.
2. C. Watanakunakorn, *J. Antimicrob. Chemother.*, **1984**, 14 (Suppl. D), 7.
3. R. C. Moellering, *Clin. Infect. Dis.*, **2006**, 42, S3.
4. N. H. Cynamon and P. A. Granato, *Antimicrob. Agents Chemother.*, **1982**, 21, 504; C. H. Wallas and J. L. Strominger, *J. Biol. Chem.*, **1963**, 238, 2264.
5. F. M. Aarestrup, A. M. Seyfarth, H.-D. Emborg, K. Pedersen, R. S. Hendriksen and F. Bager, *Antimicrob. Agents Chemother.*, **2001**, 45, 2054.
6. K. Hiramatsu, *Drug Resist. Updates*, **1998**, 1, 135.
7. Review of the “Chemistry, biology and medicine of the glycopeptide antibiotics”, K. C. Nicolaou, C. N. C. Boddy, S. Braïse and N. Winssinger, *Angew. Chem., Int. Ed.*, **1999**, 38, 2096.
8. D. H. Williams and J. R. Kalman, *J. Am. Chem. Soc.*, **1977**, 99, 2768.
9. G. M. Sheldrick, P. G. Jones, O. Kennard, D. H. Williams and G. A. Smith, *Nature*, **1978**, 271, 223.
10. C. M. Harris and T. M. Harris, *J. Am. Chem. Soc.*, **1982**, 104, 4295.
11. D. H. Williams, U. Gerhard, J. P. Mackay and R. A. Maplestone, *J. Am. Chem. Soc.*, **1993**, 115, 232.
12. M. Schäfer, T. R. Schneider and G. M. Sheldrick, *Structure*, **1996**, 4, 1510.
13. D. L. Boger, S. Miyazaki, S. Heon Kim, J. H. Wu, S. L. Castle, O. Loiseleur and Q. Jin, *J. Am. Chem. Soc.*, **1999**, 121, 10004.
14. J. P. Mackay, U. Gerhard, R. A. Maplestone and D. H. Williams, *J. Am. Chem. Soc.*, **1994**, 116, 4573.
15. J. P. Mackay, U. Gerhard, D. A. Beauregard, D. H. Williams, M. S. Westwell and M. S. Searle, *J. Am. Chem. Soc.*, **1994**, 116, 4581.
16. B. M. Crowley and D. L. Boger, *J. Am. Chem. Soc.*, **2006**, 128, 2885.
17. D. Kahne, C. Leimkuhler, W. Lu and C. Walsh, *Chem. Rev.*, **2005**, 105, 425.
18. Y. Nitnai, T. Kikuchi, K. Kakoi, S. Hanamaki, I. Fujisawa and K. Aoki, *J. Mol. Biol.*, **2009**, 385, 1422.
19. R. Nagarajan, *J. Antibiot.*, **1993**, 46, 1181.

20. A. Leighton, A. B. Gottlieb, M.-B. Dorr, D. Jabes, G. Mosconi, C. Van Saders, E. J. Mroszczak, K. C. M. Campbell and E. Kelly, *Antimicrob. Agents Chemother.*, **2004**, 48, 940.
21. R. A. Blouin, L. A. Bauer, D. D. Miller, K. E. Record and W. O. Griffen Jr., *Antimicrob. Agents Chemother.*, **1982**, 21, 575.
22. A. Belley, G. A. McKay, F. F. Arhin, I. Sarmiento, S. Beaulieu, I. Fadhil, T. R. Parr Jr. and G. Moeck, *Antimicrob. Agents Chemother.*, **2010**, 12, 5369.
23. E. Bouza and A. Burillo, *Int. J. Antimicrob. Agents*, **2010**, 6, 401.
24. M. R. Leadbetter, S. M. Adams, B. Bazzini, P. R. Fatheree, D. E. Karr, K. M. Krause, B. M. T. Lam, M. S. Linsell, M. B. Nodwell, J. L. Pace, K. Quast, J.-P. Shaw, E. Soriano, S. G. Trapp, J. D. Villena, T. X. Wu, B. G. Christensen and J. K. Judice, *J. Antibiot.*, **2004**, 5, 326.
25. J. L. Pace and G. Yang, *Biochem. Pharmacol.*, **2006**, 71, 968.
26. D. L. Boger, R. T. Beresis, O. Loiseleur, J. H. Wu and S. L. Castle, *Bioorg. Med. Chem. Lett.*, **1998**, 8, 721.
27. J. Jeffrey McAfee, S. L. Castle, Q. Jin and D. L. Boger, *Bioorg. Med. Chem. Lett.*, **2002**, 12, 1319.
28. C. C. McComas, B. M. Crowley, I. Hwang and D. L. Boger, *Bioorg. Med. Chem. Lett.*, **2003**, 13, 2933.
29. C. M. Crane and D. L. Boger, *J. Med. Chem.*, **2009**, 52, 1471.
30. S. Weist, B. Bister, O. Puk, D. Bischoff, S. Pelzer, G. J. Nicholson, W. Wohlleben, G. Jung and R. D. Süßmuth, *Angew. Chem., Int. Ed.*, **2002**, 41, 3383.
31. B. Bister, D. Bischoff, G. J. Nicholson, S. Stockert, J. Wink, C. Brumati, S. Donadio, S. Pelzer, W. Wohlleben and R. D. Süßmuth, *ChemBioChem*, **2003**, 4, 649.
32. O. Yoshida, T. Yasukata, Y. Sumino, T. Munekage, Y. Narukawa and Y. Nishitani, *Bioorg. Med. Chem. Lett.*, **2002**, 12, 3031.
33. T. Yasukata, H. Shindo, O. Yoshida, Y. Sumino, T. Munekage, Y. Narukawa and Y. Nishitani, *Bioorg. Med. Chem. Lett.*, **2002**, 12, 3033.
34. (a) T. I. Nicas, D. L. Mullen, J. E. Flokowitsch, D. A. Preston, N. J. Snyder, R. E. Stratford and R. D. G. Cooper, *Antimicrob. Agents Chemother.*, **1995**, 39, 2585;  
(b) N. E. Allen, D. L. Le Tourneau and J. N. Hobbs Jr., *Antimicrob. Agents Chemother.*, **1997**, 41, 66; (c) T. I. Nicas, D. L. Mullen, J. E. Flokowitsch, D. A.

- Preston, N. J. Snyder, M. J. Zweifel, M. J. Rodriguez, R. C. Thompson and R. D. G. Cooper, *Antimicrob. Agents Chemother.*, **1996**, *40*, 2194.
35. O. Yoshida, T. Yasukata, Y. Sumino, T. Munekage, Y. Narukawa and Y. Nishitani, *Bioorg. Med. Chem. Lett.*, **2002**, *12*, 3027.
  36. A. Y. Pavlov, M. N. Preobrazhenskaya, A. Malabarba, R. Ciabatti and L. Colombo, *J. Antibiot.*, **1998**, *51*, 73.
  37. A. Y. Pavlov, E. I. Lazhko and M. N. Preobrazhenskaya, *J. Antibiot.*, **1997**, *50*, 509.
  38. X. Fu, C. Albermann, C. Zhang and J. S. Thorson, *Org. Lett.*, **2005**, *7*, 1513.
  39. G. Pinter, G. Batta, S. Keki, A. Mandi, I. Komaromi, K. Takacs-Novak, F. Sztaricskai, E. Roth, E. Ostorhazi, F. Rozgonyi, L. Naesens and P. Herczegh, *J. Med. Chem.*, **2009**, *59*, 564.
  40. G. Pinter, I. Bereczki, G. Batta, R. Otvos, F. Sztaricskai, E. Roth, E. Ostorhazi, F. Rozgonyi, L. Naesens, M. Szarvas, Z. Boda and P. Herczegh, *Bioorg. Med. Chem. Lett.*, **2010**, *20*, 2713.
  41. L. Naesens, E. Vanderlinden, E. Roth, J. Jeko, G. Andrei, R. Snoeck, C. Pannecouque, E. Illyes, G. Batta, P. Herczegh and F. Sztaricskai, *Antiviral Res.*, **2009**, *82*, 89.
  42. S. S. Printsevskaya, A. Y. Pavlov, E. N. Olsufyeva, E. P. Mirchink, E. B. Isakova, M. I. Reznikova, R. C. Goldman, A. A. Branstrom, E. R. Baizman, C. B. Longley, F. Sztaricskai, G. Batta and M. N. Preobrazhenskaya, *J. Med. Chem.*, **2002**, *45*, 1340.
  43. K. R. Maples, C. Wheeler, E. Ip, J. J. Plattner, D. Chu, Y.-K. Zhang, M. N. Preobrazhenskaya, S. S. Printsevskaya, S. E. Solovieva, E. N. Olsufyeva, H. Heine, J. Lovchik and C. R. Lyons, *J. Med. Chem.*, **2007**, *50*, 3681.
  44. Y. Nakama, O. Yoshida, M. Yoda, K. Araki, Y. Sawada, J. Nakamura, S. Xu, K. Miura, H. Maki and H. Arimoto, *J. Med. Chem.*, **2010**, *53*, 2528.
  45. K. W. Anderson and S. L. Buchwald, *Angew. Chem., Int. Ed.*, **2005**, *44*, 6173.
  46. D. H. Williams and M. A. Cooper, *Chem. Biol.*, **1999**, *6*, 892.
  47. K. C. Nicolaou, R. Hughes, S. Young Cho, N. Winssinger, C. Smethurst, H. Labischinski and R. Endermann, *Angew. Chem. Int. Ed.*, **2000**, *39*, 3823.
  48. R. K. Jain, J. Trias and J. A. Ellman, *J. Am. Chem. Soc.*, **2003**, *125*, 8740.
  49. M. Mammen, S.-K. Choi and G. M. Whitesides, *Angew. Chem., Int. Ed.*, **1998**, *37*, 2754.



50. J. Lu, O. Yoshida, S. Hayashic and H. Arimoto, *Chem. Commun.*, **2007**, 251.
51. B. Xing, C.-W. Yu, K.-H. Chow, P.-L. Ho, D. Fu and B. Xu, *J. Am. Chem. Soc.*, **2002**, *124*, 14846.
52. B. Xing, C.-W. Yu, P.-L. Ho, K.-H. Chow, T. Cheung, H. Gu, Z. Cai and B. Xu, *J. Med. Chem.*, **2003**, *46*, 4904.
53. B. Xing, T. Jiang, W. Bi, Y. Yang, L. Li, M. Ma, C.-K. Chang, B. Xu and E. Kok Lee Yeow, *Chem. Commun.*, **2011**, *47*, 1601.
54. A notable exception: O. A. Mirgorodskaya, E. N. Olsufyeva, D. E. Kolume, T. J. D. Joergensen, P. Roepstorff, A. Yu. Pavlov, O. V. Miroshnikova and M. N. Preobrazhenskaya, *Russ. J. Bioorg. Chem.*, **2000**, *26*, 566.
55. J. H. Griffin, M. S. Linsell, M. B. Nodwell, Q. Chen, J. L. Pace, K. L. Quast, K. M. Krause, L. Farrington, T. X. Wu, D. L. Higgins, T. E. Jenkins, B. G. Christensen and J. K. Judice, *J. Am. Chem. Soc.*, **2003**, *125*, 6517.
56. O. Yoshida, J. Nakamura, H. Yamashiro, K. Miura, S. Hayashi, K. Umetsu, S. Xu, H. Maki and Hirokazu Arimoto, *Med. Chem. Commun.*, **2011**, *2*, 278.
57. I. Kaneko, D. T. Fearon and K. F. Austen, *J. Immunol.*, **1980**, *124*, 1194.
58. H. Seto, K. Fujioka, K. Furihata, I. Kaneko and S. Takashashi, *Tetrahedron Lett.*, **1989**, *42*, 236.
59. (a) K. Matsuzaki, H. Ikeda, T. Ogino, A. Matsumoto, H. B. Woodruff, H. Tanaka and S. Omura, *J. Antibiot.*, **1994**, *47*, 1173; (b) H. Gouda, K. Matsuzaki, H. Tanaka, S. Hirono, S. Omura, J. A. McCauley, P. A. Sprengeler, G. T. Furst and A. B. Smith III, *J. Am. Chem. Soc.*, **1996**, *118*, 13087.
60. T. Shinohara, H. Deng, M. L. Snapper and A. H. Hoveyda, *J. Am. Chem. Soc.*, **2005**, *127*, 7334.
61. H. Jayasuriya, G. M. Salituro, S. K. Smith, J. V. Heck, S. J. Gould, S. B. Singh, C. F. Homnick, M. K. Holloway, S. M. Pitzenberger and M. A. Patane, *Tetrahedron Lett.*, **1998**, *39*, 2247.
62. For a review of the anti-HIV behaviour of the compounds discussed in this paper: M. N. Preobrazhenskaya and E. N. Olsufyeva, *Antiviral Res.*, **2006**, *71*, 227.
63. S. B. Singh, H. Jayasuriya, G. M. Salituro, D. L. Zink, A. Shafiee, B. Heimbuch, K. C. Silverman, R. B. Lingham, O. Genilloud, A. Teran, D. Vilella, P. Felock and D. Hazuda, *J. Nat. Prod.*, **2001**, *64*, 874.
64. G. Roussi, E. G. Zamora, A.-C. Carbonnelle and R. Beugelmans, *Tetrahedron Lett.*, **1997**, *38*, 4401.

65. M. K. Gurjar and N. K. Tripathy, *Tetrahedron Lett.*, **1997**, 38, 2163.
66. A. M. Elder and D. H. Rich, *Org. Lett.*, **1999**, 1, 1443.
67. H. Deng, J.-K. Jung, T. Liu, K. W. Kuntz, M. L. Snapper and A. H. Hoveyda, *J. Am. Chem. Soc.*, **2003**, 125, 9032.
68. A. F. Littke, L. Schwarz and G. C. Fu, *J. Am. Chem. Soc.*, **2002**, 124, 6343.
69. Z. Wang, M. Bois-Choussy, Y. Jia and J. Zhu, *Angew. Chem. Int. Ed.*, **2010**, 49, 2018.
70. H. Shimamura, S. P. Breazzano, J. Garfinkle, F. S. Kimball, J. D. Trzupek and D. L. Boger, *J. Am. Chem. Soc.*, **2010**, 132, 7776.
71. R. C. Larock and E. K. Yum, *J. Am. Chem. Soc.*, **1991**, 113, 6689.
72. R. C. Larock, E. K. Yum and M. D. Refvik, *J. Org. Chem.*, **1998**, 63, 7652.
73. B. M. Crowley, Y. Mori, C. C. McComas, D. Tang and D. L. Boger, *J. Am. Chem. Soc.*, **2004**, 126, 4310.
74. C. A. Lewis, K. E. Longcore, S. J. Miller and P. A. Wender., *J. Nat. Prod.*, **2009**, 72, 1864.
75. S. J. Miller and T. P. Pathak, *J. Am. Chem. Soc.*, **2012**, 134, 6120.
76. R. H. Mitchell, Y.-H. Lai and R. V. Williams, *J. Org. Chem.*, **1979**, 44, 4733.
77. S. J. Miller and Tejas P. Pathak, *J. Am. Chem. Soc.*, **2013**, 135, 8415.
78. A. Sipos, G. Máté, E. Róth, A. Borbás, G. Batta, I. Bereczki, S. Kéki, I. Jóna, E. Ostorházi, F. Rozgonyi, E. Vanderlinden, L. Naesens and P. Herczegh, *Eur. J. Med. Chem.*, **2012**, 58, 361; A. Sipos, Z. Török, E. Róth, A. Kiss-Szikszai, G. Batta, I. Bereczki, Z. Fejes, A. Borbás, E. Ostorházi, F. Rozgonyi, L. Naesens, P. Herczegh, *Bioorg. Med. Chem. Lett.*, **2012**, 22, 7092.
79. Michael Zasloff, *Nature*, **2002**, 415, 389.
80. V. Yarlagadda, P. Akkapeddi, G. B. Manjunath and J. Haldar, *J. Med. Chem.*, **2013**, 57, 4558.
81. T. Warne, M. J. Serrano-Vega, J. G. Baker, R. Moukhametzianov, P. C. Edwards, R. Henderson, A. G. W. Leslie, C. G. Tate and G. F. X. Schertler, *Nature*, **2008**, 454, 486.
82. J. Clayden and N. Vassiliou, *Org. Biomol. Chem.*, **2006**, 4, 2667; J. Clayden, L. Vallverdú and M. Helliwell, *Chem. Commun.*, **2007**, 2357; J. Clayden, M. Pickworth and L. H. Jones, *Chem. Commun.*, **2009**, 547; J. Clayden, A. Castellanos, J. Solà and G. A. Morris, *Angew. Chemie Int. Ed.*, **2009**, 8, 5962; J. Solà, S. P. Fletcher, A. Castellanos and J. Clayden, *Angew. Chemie Int. Ed.*,

- 2010**, *49*, 6836; J. Solà, M. Helliwell and J. Clayden, *J. Am. Chem. Soc.*, **2010**, *132*, 4548; T. Boddaert, J. Solà, M. Helliwell and J. Clayden, *Chem. Commun.*, **2012**, *48*, 3397; R. A. Brown, V. Diemer, S. J. Webb and J. Clayden, *Nature Chem.*, **2013**, *5*, 853; L. Byrne, J. Solà, T. Boddaert, T. Marcelli, R. W. Adams, G. A. Morris and J. Clayden, *Angew. Chemie Int. Ed.*, **2014**, *53*, 151.
83. S. Dutt, C. Wilch and T. Schrader, *Chem. Commun.*, **2011**, *47*, 5376; T. R. Simmons, G. Berggren, M. Bacchi, M. Fontecave and V. Artero, *Coordination Chem. Rev.*, **2014**, *270*, 127.
  84. For a comprehensive review see D. Parmar, E. Sugiono, S. Raja and M. Rueping, *Chem. Rev.*, **2014**, *114*, 9047.
  85. Y. Zhang, Z. Lu, W. D. Wulff, *Synlett*, **2009**, *17*, 2715.
  86. J. Bao, W. D. Wulff, J. B. Dominy, M. J. Fumo, E. B. Grant, A. C. Rob, M. C. Whitcomb, S.-M. Yeung, R. L. Ostrander and A. L. Rheingold, *J. Am. Chem. Soc.*, **1996**, *118*, 3392.
  87. E. J. Corey and H. E. Ensley, *J. Am. Chem. Soc.*, **1975**, *97*, 6908; D. A. Evans, K. T. Chapman, and J. Bisaha, *J. Am. Chem. Soc.*, **1988**, *110*, 1238.
  88. M. M. Heravi and V. Zadsirjan, *Tetrahedron: Asymmetry*, **2013**, *24*, 1149.
  89. B. Huang, L. Wang, L. Gong and E. Meggers, *Chem. Asian J.*, **2013**, *8*, 2274.
  90. M. M. Heravi and V. Zadsirjan, *Tetrahedron: Asymmetry*, **2014**, *25*, 1061.
  91. S. G. Davies, H. J. Sanganee and P. Szolcsanyi, *Tetrahedron*, **1999**, *55*, 3337.
  92. A. B. Smith and A. S. Thompson, *J. Org. Chem.*, **1984**, *49*, 1469.
  93. J. K. Whitesell, *Chem. Rev.*, **1992**, *92*, 953; H.-U. Blaser, *Chem. Rev.*, **1992**, *92*, 935.
  94. A. H. Hoveyda, D. A. Evans and G. C. Fu, *Chem. Rev.*, **1993**, *93*, 1307.
  95. J. Clayden, *Chem. Soc. Rev.*, **2009**, *38*, 817.
  96. A. J. Frontiera and C. Collison, *Tetrahedron*, **2005**, *61*, 7577.
  97. L. N. Pridgen, K. Huang, S. Shilcrat, A. Tickner-Eldridge, C. DeBrosse and R. Curtis Haltiwanger, *Synlett*, **1999**, *10*, 1612.
  98. R. Hayashi, M. C. Walton, R. P. Hsung, J. H. Schwab and X. Yu, *Org. Lett.*, **2010**, *12*, 5768.
  99. S. V. Ley, L. R. Cox, G. Meek, K.-H. Metten, C. Piqué and J. M. Worrall, *J. Chem. Soc., Perkin Trans. 1*, **1997**, 3299.
  100. C. J. Hollowood, S. V. Ley and E. A. Wright, *Org. Biomol. Chem.*, **2003**, *1*, 3208.

101. C. J. Hollowood and S. V. Ley, *Chem. Commun.*, **2002**, 2130.
102. G. A. Molander and K. L. Bobbitt, *J. Am. Chem. Soc.*, **1993**, *115*, 7517.
103. C. Aurisicchio, E. Baciocchi, M. F. Gerini and O. Lanzalunga, *Org. Lett.*, **2007**, *9*, 1939.
104. F. M. Hauser and S. R. Ellenberger, *J. Am. Chem. Soc.*, **1984**, *106*, 2458.
105. G. Solladié, F. Colobert and F. Somny, *Tetrahedron Lett.*, **1999**, *40*, 1227; Y. Arai, A. Suzuki, T. Masuda, Y. Masaki and M. Shiro, *Chem. Pharm. Bull.*, **1996**, *44*, 1765; C. Iwata, Y. Moritani, K. Sugiyama, M. Fujita and T. Imanishi, *Tetrahedron Lett.*, **1987**, *28*, 2255.
106. P. C. B. Page, M. J. McKenzie, S. M. Allin, E. W. Collington and R. A. E. Carr, *Tetrahedron*, **1995**, *51*, 1285.
107. N. Maezaki, T. Shogaki, T. Imamura, K. Tokuno, K. Ohkubo, T. Tanaka and C. Iwata, *Chem. Pharm. Bull.*, **1998**, *46*, 837.
108. J. L. G. Ruano, M. Á. Fernández-Ibáñez and M. C. Maestro, *Tetrahedron*, **2006**, *62*, 12297.
109. J. L. García Ruano, J. Alemán, M. Teresa Aranda, M. A. Fernández-Ibáñez, M. Mercedes Rodríguez-Fernández and M. C. Maestro, *Tetrahedron*, **2004**, *60*, 10067.
110. Y. Arai, T. Masuda and Y. Masaki, *J. Chem. Soc., Perkin Trans. I*, **1999**, 2165.
111. K. Mikami, M. Shimizu, H.-C. Zhang and B. E. Maryanoff, *Tetrahedron*, **2001**, *57*, 2917.
112. W. Xuan, C. Zhu, Y. Liu and Y. Cui, *Chem. Soc. Rev.*, **2012**, *41*, 1677.
113. H. Otsuka and S. Shinkai, *Supramol. Sci.*, **1996**, *3*, 189.
114. U. Boas, J. B. Christensen and P. M. H. Heegaard, *J. Mater. Chem.*, **2006**, *16*, 3785.
115. H. C. Kolb, M. G. Finn, and K. B. Sharpless, *Angew. Chem. Int. Ed.*, **2001**, *40*, 2004.
116. S. E. Bode, M. Wolberg and M. Müller, *Synthesis*, **2006**, *4*, 557.
117. A. Lorente, K. Makowski and F. Albericio and M. Álvarez, *Ann. Mar. Biol. Res.*, **2014**, *1*, 1003.
118. L. C. Dias and A. M. Aguilar, *Chem. Soc. Rev.*, **2008**, *37*, 451.
119. Y. Zhang, C. C. Arpin, A. J. Cullen, M. J. Mitton-Fry and T. Sammakia, *J. Org. Chem.*, **2011**, *76*, 7641; F. Wu, M. E. Green and P. E. Floreancig, *Angew. Chem. Int. Ed.*, **2011**, *50*, 1131.

120. D. A. Evans, J. L. Duffy and M. J. Dart, *Tetrahedron Lett.* **1994**, 35, 8537; D. A. Evans, M. J. Dart, J. L. Duffy and M. G. Yang, *J. Am. Chem. Soc.*, **1996**, 118, 4322.
121. D. A. Evans, P. J. Coleman and B. Côté, *J. Org. Chem.*, **1997**, 62, 788.
122. J. M. Goodman and R. S. Paton, *Chem. Commun.*, **2007**, 2124.
123. D. A. Evans, B. Côté, P. J. Coleman and B. T. Connell, *J. Am. Chem. Soc.*, **2003**, 125, 10895.
124. I. Paterson, O. Delgado, G. J. Florence, I. Lyothier, J. P. Scott and N. Sereinig, *Org. Lett.*, **2003**, 5, 35.
125. L. C. Dias, P. K. Kuroishi, E. C. Polo and E. C. de Lucca Jr, *Tetrahedron Lett.*, **2013**, 54, 980.
126. M. Akakura, M. B. Boxer and H. Yamamoto, *ARKIVOC*, **2007**, 10, 337.
127. Y. Yamaoka and H. Yamamoto, *J. Am. Chem. Soc.*, **2010**, 132, 5354.
128. S. E. Denmark and J. Fu, *Chem. Rev.*, **2003**, 103, 2763.
129. E. J. Thomas, *Chem Rec.*, **2007**, 7, 115.
130. A. H. MacNeill and E. J. Thomas, *Synthesis*, **1994**, 322; J. C. Carey and E. J. Thomas, *Tetrahedron Lett.*, **1993**, 34, 3935; J. C. Carey and E. J. Thomas, *J. Chem. Soc. Chem. Commun.*, **1994**, 283.
131. E. K. Hoegenauer and E. J. Thomas, *Org. Biomol. Chem.*, **2012**, 10, 6995.
132. M. Hoch, *Appl. Geochem.*, **2001**, 16, 719.
133. E. J. Thomas and A. P. Weston, *Tetrahedron Lett.*, **2007**, 48, 341.
134. Y. Tamai, T. Hattori, M. Date, H. Takayama, Y. Kamikubo, Y. Minato and S. Miyano, *J. Chem. Soc. Perkin Trans. 1*, **1999**, 1141.
135. H. Takahashi, K. Tanahashi, K. Higashiyama and H. Onishi, *Chem. Pharm. Bull.*, **1986**, 34, 479.
136. H. Takahashi, K. Hattori, K. Higashiyama and Y. Ueno, *Chem. Pharm. Bull.*, **1990**, 38, 1062.
137. A. W. Frank, *Crit. Rev. Biochem.*, **1984**, 16, 51.
138. G. Castelot-Deliencourt, E. Roger, X. Pannecoucke and J.-C. Quirion, *Eur. J. Org. Chem.*, **2001**, 3031.
139. P. Linnane, N. Magnus and P. Magnus, *Nature*, **1997**, 385, 799.
140. N. Magnus and P. Magnus, *Tetrahedron Lett.*, **1997**, 38, 3491.
141. J. Clayden, M. Darbyshire, J. H. Pink, N. Westlund and F. X. Wilson, *Tetrahedron Lett.*, **1997**, 38, 8587.

142. J. Clayden, J. H. Pink and S. A. Yasin, *Tetrahedron Lett.*, **1998**, 39, 105.
143. S. D. Bull, S. G. Davies, S. W. Epstein and J. V. A. Ouzman, *Chem. Commun.*, **1998**, 659.
144. J. Clayden, A. Lund, L. Vallverdú and M. Helliwell, *Nature*, **2004**, 431, 966.
145. L. Byrne, J. Solà, T. Boddaert, T. Marcelli, R. W. Adams, G. A. Morris and J. Clayden, *Angew. Chem. Int. Ed.*, **2014**, 53, 151.
146. R. Crabtree, *Acc. Chem. Res.*, **1979**, 12, 331.
147. P. Li, E. M. Forbeck, C. D. Evans and M. M. Joullié, *Org. Lett.*, **2006**, 8, 5106.
148. A. Alam, Y. Takaguchi, S. Tsuboi, H. Ito and T. Yoshida, *Tetrahedron*, **2005**, 61, 1909.
149. Y. Yilmaz and R. T. Toledo, *J. Agric. Food Chem.*, **2004**, 52, 255.
150. F. Ullmann and P. Sponagel, *Chem. Ber.*, **1905**, 38, 2212.
151. A. A. Moroz and M. S. Shvartsberg, *Russ. Chem. Rev.*, **1974**, 43, 679.
152. S. Verma, N. Kumar and S. L. Jain, *Tetrahedron Lett.*, **2012**, 35, 4665.
153. D. A. Evans, J. L. Katz and T. R. West, *Tetrahedron Lett.*, **1998**, 39, 2937.
154. C. H. Burgos, T. E. Barder, X. Huang and S. L. Buchwald, *Angew. Chem. Int. Ed.*, **2006**, 45, 4321.
155. D. L. Boger, R. M. Borzilleri, S. Nukui and R. T. Beresis, *J. Org. Chem.*, **1997**, 62, 4721.
156. M. J. Mann, N. Pant and A. D. Hamilton, *J. Chem. Soc., Chem. Commun.*, **1986**, 158.
157. K. C. Nicolaou, C. N. C. Boddy, S. Natarajan, T.-Y. Yue, H. Li, S. Bräse and J. M. Ramanjulu, *J. Am. Chem. Soc.*, **1997**, 119, 3421.
158. K. C. Nicolaou, N. F. Jain, S. Natarajan, R. Hughes, M. E. Solomon, H. Li, J. M. Ramanjulu, M. Takayanagi, A. E. Koumbis and T. Bando, *Angew. Chem. Int. Ed.*, **1998**, 37, 2714.
159. T. P. Petersen, A. F. Larsen, A. Ritzén and T. Ulven, *J. Org. Chem.*, **2013**, 78, 4190.
160. CRC Handbook of Chemistry and Physics, 66<sup>th</sup> Ed., R. C. Weast, Ed.; CRC Press: Boca Raton, FL, 1985; F-165.
161. J. A. Cella and S. W. Bacon, *J. Org. Chem.*, **1984**, 49, 1122.
162. Theoretical pKa values were calculated in MarvinSketch 15.1.19 using the protonation plugin.
163. T. Okazoe, *Proc. Jpn. Acad., Ser. B*, **2009**, 85, 276.

164. F. H. Allen, O. Kennard, D. G. Watson, L. Brammer, A. G. Orpen and R. Taylor, *J. Chem. Soc., Perkin Trans. 2*, **1987**, S1.
165. S. J. Blanksby and G. B. Ellison, *Acc. Chem. Res.*, **2003**, 36, 255.
166. A. L. Allred, *J. Inorg. Nucl. Chem.*, **1961**, 17, 215.
167. P. J. Loll, A. E. Bevivino, B. D. Korty and P. H. Axelsen, *J. Am. Chem. Soc.*, **1997**, 119, 1516.
168. R. J. Abraham and M. Mobli, *Modelling <sup>1</sup>H NMR Spectra of Organic Compounds: Theory, Applications and NMR Prediction Software*, 1<sup>st</sup> ed.; John Wiley & Sons, Ltd, Chichester, 2008, p. 56.
169. Brian C. Smith, *Infrared Spectral Interpretation: A Systematic Approach*, 1<sup>st</sup> ed.; CRC Press: Boca Raton, FL, 1999, p 93.
170. J. Wegner, S. Ceylan and A. Kirschning, *Adv. Synth. Catal.*, **2012**, 354, 17.
171. C. Wiles and P. Watts, *Green Chem.*, **2012**, 14, 38.
172. C. F. Carter, H. Lange, S. V. Ley, I. R. Baxendale, B. Wittkamp, J. G. Goode and N. L. Gaunt, *Org. Process Res. Dev.*, **2010**, 14, 393.
173. J. Bart, A. J. Kolkman, A. J. Oosthoek-de Vries, K. Koch, P. J. Nieuwland, H. J. W. G. Janssen, J. P. J. M. van Bentum, K. A. M. Ampt, F. P. J. T. Rutjes, S. S. Wijmenga, H. J. G. E. Gardeniers and A. P. M. Kentgens, *J. Am. Chem. Soc.*, **2009**, 131, 5014.
174. For examples, see J. Hartwig, J. B. Metternich, N. Nikbin, A. Kirschning and S. V. Ley, *Org. Biomol. Chem.*, **2014**, 12, 3611; J.-I Yoshida, Y. Takahashi and A. Nagaki, *Chem. Commun.*, **2013**, 49, 9896.
175. J. Yoshida, *Flash Chemistry: Fast Organic Synthesis in Microsystems*, 1<sup>st</sup> ed.; John Wiley & Sons, Ltd, Chichester, 2008.
176. C. Wiles and P. Watts, *Beilstein J. Org. Chem.* **2011**, 7, 1372.
177. J. A. Marafie and J. D. Moseley, *Org. Biomol. Chem.*, **2010**, 8, 2219.
178. For examples see: D. L. Boger, R. M. Borzilleri, S. Nukui and R. T. Beresis, *J. Org. Chem.*, **1997**, 62, 4721; A. J. Pearson and D. V. Ciurea, *J. Org. Chem.* **2008**, 73, 760.
179. M. Schelhaas and H. Waldmann, *Angew. Chem. Int. Ed.*, **1996**, 35, 2056.
180. A. Alam, Y. Takaguchi, H. Ito, T. Yoshida and S. Tsuboi, *Tetrahedron*, **2005**, 61, 1909.
181. K.-F. Chan, Y. Zhao, L. M. C. Chow and T. H. Chan, *Tetrahedron*, **2005**, 61, 4149.

182. R. Johansson and B. Samuelsson, *J. Chem. Soc. Perkin Trans. 1*, **1984**, 2371.
183. M. Kodama, Y. Shiobara, H. Sumitomo, K. Matsumura, M. Tsukamoto and C. Harada, *J. Org. Chem.*, **1988**, 53, 72.
184. Nagase and Company, Ltd., **2007**, EU Patent EP1870403 A1
185. P. K. Mandal and J. S. McMurray, *J. Org. Chem.*, **2007**, 72, 6599.
186. Y. Nishihama, Y. Ishikawa and S. Nishiyama, *Tetrahedron Lett.*, **2009**, 50, 2801.
187. A. M. DiLauro, W. Seo and S. T. Phillips, *J. Org. Chem.*, **2011**, 76, 7352.
188. C.-E. Yeom, H. W. Kim, S. Y. Lee and B. M. Kim, *Synlett*, **2007**, 146.
189. R. S. Porto, M. L. A. A. Vasconcellos, E. Ventura and F. Coelho, *Synthesis*, **2005**, 14, 2297.
190. A. Bartoszewicz, M. Kalek, J. Nilsson, R. Hiresova and J. Stawinski, *Synlett*, **2008**, 1, 37.
191. T. J. Barton, R. Rogido and J. C. Clardy, *Tetrahedron*, **2011**, 11, 2081.
192. F. Huet, A. Lechevallier, M. Pellet and J. M. Conia, *Synthesis*, **1978**, 1, 63.
193. P. G. M. Wuts and T. W. Greene, *Greene's Protective Groups in Organic Synthesis*, 4th Ed., John Wiley & Sons, Ltd, Chichester, **2007**, p. 448.
194. H. M. H. G. Albers, L. J. D. Hendrickx, R. J. P. van Tol, J. Hausmann, A. Perrakis and H. Ovaa, *J. Med. Chem.*, **2011**, 54, 4619.
195. Z. Yongpeng and X. Jiayi, *Prog. Chem.*, **2014**, 26, 1471.
196. V. Percec, H.-J. Sun, P. Leowanawat, M. Peterca, R. Graf, H. W. Spiess, X. Zeng, G. Ungar and P. A. Heiney, *J. Am. Chem. Soc.*, **2013**, 135, 4129.
197. P. Garner and J. M. Park, *J. Org. Chem.*, **1987**, 52, 2361.
198. D. S. Seferos, D. A. Banach, N. A. Alcantar, J. N. Israelachvili and G. C. Bazan, *J. Org. Chem.*, **2004**, 69, 1110; V. Leandri, R. Ruffo, V. Trifiletti and A. Abbotto, *Eur. J. Org. Chem.* **2013**, 30, 6793; J. McNulty, C. Zepeda-Velázquez and D. McLeod, *Green Chem.*, **2013**, 15, 3146.
199. Y. Seeleib, G. Nemecek, D. Pfaff, B. D. Sueveges, J. Podlech, *Synth. Comm.*, **2014**, 44, 2966.
200. D. S. Seferos, D. A. Banach, N. A. Alcantar, J. N. Israelachvili and G. C. Bazan, *J. Org. Chem.*, **2004**, 69, 1110.
201. M. Firstenberg, K. Nanjunda Shivananda, I. Cohen, O. Solomeshch, V. Medvedev, N. Tessler and Y. Eichen, *Adv. Funct. Mater.* **2011**, 21, 634.
202. S. P. Bew, R. Carrington, D. L. Hughes, J. Liddle and Paolo Pesce, *Adv. Synth. Catal.*, **2009**, 351, 2579.



203. R. K. Bansal, *Heterocyclic Chemistry*, 3<sup>rd</sup> Ed.; New Age International (P) Ltd., New Delhi, 1999, p 11.
204. Graph based on the equation  $^3J_{\text{HH}'} = A + B \cos \phi + C \cos 2 \phi$  where  $A = 4.22$ ,  $B = -0.5$  and  $C = 4.5$  Hz from M. Karplus, *J. Am. Chem. Soc.*, **1963**, 85, 2870.
205. J. Crugeiras, A. Rios, E. Riveiros and J. P. Richard, *J. Am. Chem. Soc.*, **2009**, 131, 15815.
206. L. Chmurzynski, *J. Heterocyclic Chem.*, **2000**, 37, 71.
207. M. Regitz, *Diazo Compounds: Properties and Synthesis*, 1<sup>st</sup> Ed., Academic Press Inc., Orlando, FL, 1986, p 13.
208. D. L. Wright and M. C. McMills, *Org. Lett.*, 1999, 1, 667.
209. P. Pesce, *Organocatalytic methods towards the synthesis of chiral racemic and chiral non-racemic C<sub>2,3</sub>-functionalised N-alkyl and N-arylaziridines*, Ph.D. Thesis, University of East Anglia, UK, 2010.
210. T. Curtius, *Chem. Ber.*, **1883**, 16, 2230.
211. L. Giraldi, C. Monti-Bragadin, and R. Della-Loggia, *Experientia*, **1974**, 30, 496.
212. L. Baldini and G. Brambilla, *Cancer Res.*, **1966**, 26, 1754.
213. T. Curtius and A. Darapsky, *Chem. Ber.*, **1906**, 39, 1378.
214. V. K. Antonov, *Russ. Chem. Bull. (Int. Ed.)*, **1963**, 1030; M. Mokotoff, J. F. Bagaglio and B. S. Parikh, *J. Med. Chem.*, **1975**, 18, 354; A. Ouhia, L. René and B. Badet, *Tetrahedron Lett.*, **1992**, 33, 5509.
215. T. Toma, J. Shimokawa and T. Fukuyama, *Org. Lett.*, **2007**, 9, 3195.
216. U. Ragnarsson and L. Grehn, *Tetrahedron Lett.*, **2012**, 53, 1045.
217. A. Trabocchi, G. Menchi, N. Cini, F. Bianchini, S. Raspanti, A. Bottoncetti, A. Pupi, L. Calorini and A. Guarna, *J. Med. Chem.*, **2010**, 19, 7119; S. P. Bew, P. Ashford and D. U. Bachera, *Synthesis*, **2013**, 45, 903
218. E. Vaz, M. Fernandez-Suarez and L. Munoz, *Tetrahedron: Asymmetry.*, **2003**, 13, 1935.
219. V. Haridas, S. Sadanandan, Y. Sharma, S. Chinthalapalli and A. Shandilya, *Tetrahedron Lett.*, **2012**, 6, 623.
220. M. Ordonez, E. Hernandez-Fernandez, M. Montiel-Perez, R. Bautista, P. Bustos, H. Rojas-Cabrera, M. Fernandez-Zertuche and O. Garcia-Barradas, *Tetrahedron: Asymmetry*, **2007**, 20, 2427.
221. R. A. Franich, G. Lowe and J. Parker, *J. Chem. Soc., Perkin Trans. 1*, **1972**, 2034.

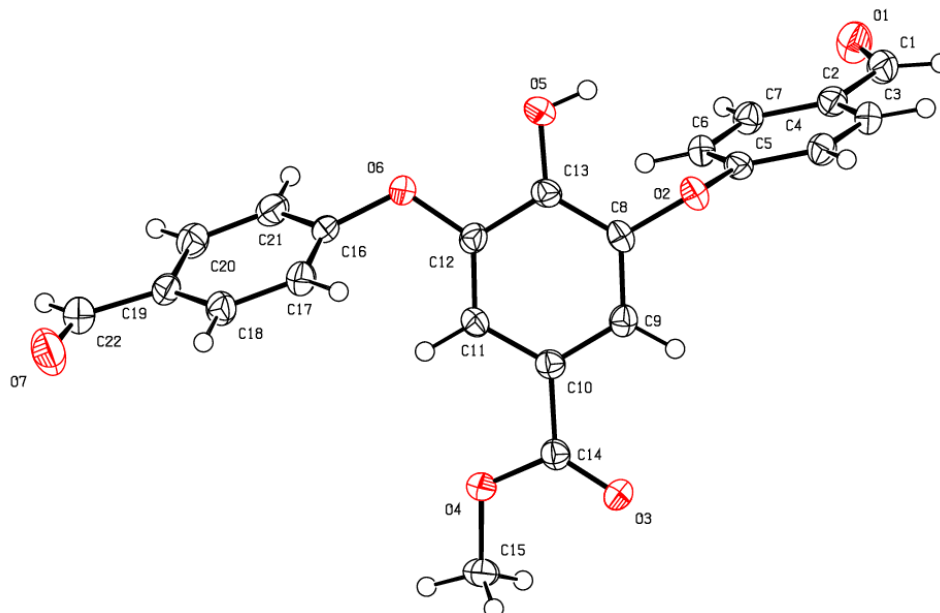
222. A. Ouïhia, L. Rene, J. Guilhem, C. Pascard and B. Badet, *J. Org. Chem*, **1993**, 58, 1641.
223. S. P. Bew, S. A. Fairhurst, D. L. Hughes, L. Legentil, J. Liddle, P. Pesce, S. Nigudkar and M. A. Wilson, *Org. Lett.*, **2009**, 20, 4552.
224. A. Mazumdar, Z. Xue, M. F. Mayer, *Synlett*, **2007**, 13, 2025.
225. N. G. Anderson, Practical Process Research & Development, 2<sup>nd</sup> Ed., Academic Press Inc., Oxford, 2012, p. 329.
226. A. A. Desai and W. D. Wulff, *J. Am. Chem. Soc.*, **2010**, 132, 13100.
227. T. Hashimoto, N. Uchiyama and K. Maruoka, *J. Am. Chem. Soc.*, **2008**, 130, 14380.
228. T. Schirmeister, *J. Med. Chem.*, **1999**, 42, 560; T. Schirmeister and M. Peric, *Bioorg. Med. Chem.*, **2000**, 6, 1281.
229. N. Yoichi, F. Masaki, W. Kaoru, M. Shigeki and F. Nobuhiro, *J. Am. Chem. Soc.*, **2000**, 122, 10462.
230. B. K. W. Chung, J. L. Hickey, C. C. G. Scully, S. Zaretsky, A. Yudin, *Med. Chem. Commun.*, **2013**, 4, 1124; C. J. White, J. L. Hickey, C. C. G. Scully and A. K. Yudin, *J. Am. Chem. Soc.*, **2014**, 136, 3728.
231. N. D. Ide, D. P. Galonić, W. A. van der Donk and D. Y. Gin, *Synlett*, **2005**, 13, 2011; F. B. Dyer, C.-M. Park, R. Joseph and P. Garner, *J. Am. Chem. Soc.*, **2011**, 133, 20033.
232. C. Büchold, Y. Hemberger, C. Heindl, A. Welker, B. Degel, T. Pfeuffer, P. Staib, S. Schneider, P. J. Rosenthal, J. Gut, J. Morschhäuser, G. Bringmann and T. Schirmeister, *ChemMedChem*, **2011**, 6, 141.
233. G. L. Thomas, R. J. Spandl, F. G. Glansdorp, M. Welch, A. Bender, J. Cockfield, J. A. Lindsay, C. Bryant, D. F. J. Brown, O. Loiseleur, H. Rudyk, M. Ladlow and D. R. Spring, *Angew. Chem. Int. Ed.*, **2008**, 15, 2808.
234. A. N. Tkachenko, P. K. Mykhailiuk, S. Afonin, D. S. Radchenko, V. S. Kubyshkin, A. S. Ulrich and I. V. Komarov, *Angew. Chem. Int. Ed.*, **2013**, 52, 1486.
235. K. J. Schafer-Hales, K. D. Belfield, S. Yao, P. K. Frederiksen, J. M. Hales, P. E. Kolattukudy, *J. Biomed. Opt.*, **2005**, 5, 051402.
236. E. Hillard, A. Vessièrès, L. Thouin, G. Jaouen and C. Amatore, *Angew. Chem. Int. Ed.*, **2006**, 45, 285; F. Dubar, T. J. Egan, B. Pradines, D. Kuter, K. K. Ncokazi, D. Forge, J.-F. Paul, C. Pierrot, H. Kalamou, J. Khalife, E. Buisine, C. Rogier, H.

- Vezin, I. Forfar, C. Slomianny, X. Trivelli, S. Kapishnikov, L. Leiserowitz, D. Dive and C. Biot, *ACS Chem. Biol.*, **2011**, 6, 275.
237. K. Kerman and H.-B. Kraatz, *Analyst*, **2009**, 134, 2400.
238. R. S. Herrick, C. J. Ziegler, M. Precopio, K. Crandall, J. Shaw and R. M. Jarret, *J. Organomet. Chem.*, **2008**, 693, 619.
239. T. D. Turbitt and W. E. Watts, *J. Chem. Soc., Perkin Trans. 2*, **1974**, 185.
240. C. Imrie, C. Loubser, P. Engelbrecht and C. W. McClelland, *J. Chem. Soc., Perkin Trans. 1*, **1999**, 2513.
241. For a review of the use of  $\alpha$ -methylbenzylamine in asymmetric synthesis, see: E. Juaristi, J. L. León-Romo, A. Reyes and J. Escalante, *Tetrahedron: Asymmetry*, **1999**, 10, 2441.
242. M. Ziółkowski, Z. Czarnocki, A. Leniewski and J. K. Maurin, *Tetrahedron: Asymmetry*, **1999**, 10, 3371.
243. G. Knupp and A. W. Frahm, *Chem. Ber.*, **1984**, 6, 2076.
244. S. H. Lee, I. W. Song, *Bull. Korean Chem. Soc.*, **2005**, 26, 223.
245. L. Huang, Y. Zhang, R. J. Staples, R. H. Huang and W. D. Wulff, *Chem. Eur. J.*, **2012**, 18, 5302.
246. L. Byrne, J. Sol, T. Boddaert, T. Marcelli, R. W. Adams, G. A. Morris and J. Clayden, *Angew. Chem. (Int. Ed.)*, **2014**, 1, 151.
247. M. Poterala and J. Pleniewicz, *Tetrahedron: Asymmetry*, **2011**, 3, 294.
248. D. Yang, B. Li, F.-F. Ng, Y.-L. Yan, J. Qu and Y. D. Wu, *J. Org. Chem.*, **2001**, 22, 7303.
249. C. Abalain and M. Langlois, *Eur. J. Med. Chem.*, **1998**, 33, 155.
250. K. Sivasubramanian, L. S. Kaanumalle, S. Uppili and V. Ramamurthy, *Org. Biomol. Chem.*, **2007**, 5, 1569.
251. D. Crich, K. Sana and S. Guo, *Org. Lett.*, **2007**, 9, 4423.
252. P. Zajdel, G. Nomezine, N. Masurier, M. Amblard, M. Pawłowski, J. Martinez and G. Subra, *Chem. Eur. J.*, **2010**, 16, 7547.
253. V. Balraju, R. Vasu Dev, D. Srinivasa Reddy and J. Iqbal, *Tetrahedron Lett.*, **2006**, 47, 3569.
254. D. Savage, J. F. Gallagher, Y. Ida and P. T.M. Kenny, *Inorg. Chem. Comm.*, **2002**, 12, 1034.

## APPENDIX

### X-ray crystallographic data

**Appendix 1: X-ray crystal structure and crystallographic data for methyl 3,5-bis(4-formylphenoxy)-4-hydroxybenzoate **305**<sup>i</sup>**



**Figure 1** • An Ortep representation of the crystal structure of **305**. Thermal ellipsoids are drawn at 50% probability level.

**Crystal data and structure refinement details:**

Identification code	2011src0044 (PA298)	
Empirical formula	C <sub>22</sub> H <sub>16</sub> O <sub>7</sub>	
Formula weight	392.35	
Temperature	120(2) K	
Wavelength	0.71073 Å	
Crystal system	Monoclinic	
Space group	<i>P</i> 2 <sub>1</sub> / <i>n</i>	
Unit cell dimensions	<i>a</i> = 11.2899(5) Å	$\alpha = 90^\circ$
	<i>b</i> = 8.8623(4) Å	$\beta = 99.367(2)^\circ$
	<i>c</i> = 17.9619(9) Å	$\gamma = 90^\circ$
Volume	1773.20(14) Å <sup>3</sup>	
<i>Z</i>	4	
Density (calculated)	1.470 Mg / m <sup>3</sup>	
Absorption coefficient	0.111 mm <sup>-1</sup>	
<i>F</i> (000)	816	
Crystal	Fragment; Pale Brown	
Crystal size	0.20 × 0.18 × 0.07 mm <sup>3</sup>	

<sup>i</sup> All x-ray crystallographic data collection and structure analysis carried out by Dr Mateusz B. Pitak, UK National Crystallography Service, Southampton.

$\theta$ range for data collection	2.94 – 24.99°
Index ranges	$-13 \leq h \leq 13, -10 \leq k \leq 10, -21 \leq l \leq 21$
Reflections collected	13357
Independent reflections	3079 [ $R_{int} = 0.0355$ ]
Completeness to $\theta = 24.99^\circ$	98.7 %
Absorption correction	Semi-empirical from equivalents
Max. and min. transmission	0.9923 and 0.9782
Refinement method	Full-matrix least-squares on $F^2$
Data / restraints / parameters	3079 / 0 / 264
Goodness-of-fit on $F^2$	1.101
Final $R$ indices [ $F^2 > 2\sigma(F^2)$ ]	$R1 = 0.0456, wR2 = 0.1014$
$R$ indices (all data)	$R1 = 0.0574, wR2 = 0.1108$
Largest diff. peak and hole	0.351 and $-0.276 \text{ e } \text{\AA}^{-3}$

**Table 1** • Atomic coordinates [ $\times 10^4$ ], equivalent isotropic displacement parameters [ $\text{\AA}^2 \times 10^3$ ] and site occupancy factors.  $U_{eq}$  is defined as one third of the trace of the orthogonalized  $U^{ij}$  tensor.

Atom	$x$	$y$	$z$	$U_{eq}$	$S.o.f.$
C1	8061(2)	3839(3)	8764(1)	31(1)	1
C2	8627(2)	3187(2)	8164(1)	26(1)	1
C3	9391(2)	1959(2)	8318(1)	28(1)	1
C4	9919(2)	1303(2)	7757(1)	26(1)	1
C5	9699(2)	1909(2)	7036(1)	23(1)	1
C6	8956(2)	3156(2)	6872(1)	24(1)	1
C7	8413(2)	3785(2)	7434(1)	26(1)	1
C8	10364(2)	1974(2)	5843(1)	23(1)	1
C9	11390(2)	2828(2)	5852(1)	24(1)	1
C10	11568(2)	3597(2)	5205(1)	23(1)	1
C11	10707(2)	3496(2)	4553(1)	24(1)	1
C12	9698(2)	2626(2)	4551(1)	24(1)	1
C13	9503(2)	1839(2)	5199(1)	23(1)	1
C14	12657(2)	4552(2)	5240(1)	24(1)	1
C15	13613(2)	6438(3)	4613(1)	33(1)	1
C16	8929(2)	3063(2)	3245(1)	26(1)	1
C17	9795(2)	2454(2)	2868(1)	28(1)	1
C18	9836(2)	2925(2)	2140(1)	29(1)	1
C19	9022(2)	3995(2)	1793(1)	27(1)	1
C20	8179(2)	4602(2)	2188(1)	31(1)	1
C21	8125(2)	4131(3)	2915(1)	31(1)	1
C22	8997(2)	4421(3)	998(1)	36(1)	1
O1	7287(1)	4813(2)	8660(1)	38(1)	1
O2	10212(1)	1165(2)	6490(1)	25(1)	1
O3	13455(1)	4629(2)	5775(1)	30(1)	1
O4	12649(1)	5351(2)	4604(1)	30(1)	1
O5	8488(1)	1022(2)	5156(1)	30(1)	1
O6	8765(1)	2525(2)	3951(1)	33(1)	1
O7	9629(2)	3859(2)	588(1)	52(1)	1

**Table 2** • Bond lengths [Å] and angles [°].

---

C1–O1	1.221(3)
C1–C2	1.460(3)
C1–H1	0.9500
C2–C3	1.388(3)
C2–C7	1.398(3)
C3–C4	1.380(3)
C3–H3	0.9500
C4–C5	1.387(3)
C4–H4	0.9500
C5–O2	1.384(2)
C5–C6	1.389(3)
C6–C7	1.381(3)
C6–H6	0.9500
C7–H7	0.9500
C8–C9	1.381(3)
C8–C13	1.389(3)
C8–O2	1.401(2)
C9–C10	1.390(3)
C9–H9	0.9500
C10–C11	1.397(3)
C10–C14	1.485(3)
C11–C12	1.374(3)
C11–H11	0.9500
C12–O6	1.382(2)
C12–C13	1.406(3)
C13–O5	1.347(2)
C14–O3	1.208(2)
C14–O4	1.343(2)
C15–O4	1.451(2)
C15–H15A	0.9800
C15–H15B	0.9800
C15–H15C	0.9800
C16–C21	1.378(3)
C16–C17	1.386(3)
C16–O6	1.394(2)
C17–C18	1.381(3)
C17–H17	0.9500
C18–C19	1.395(3)
C18–H18	0.9500
C19–C20	1.384(3)
C19–C22	1.473(3)
C20–C21	1.382(3)
C20–H20	0.9500
C21–H21	0.9500
C22–O7	1.212(3)
C22–H22	0.9500
O5–H5	0.8400

---

O1–C1–C2	123.7(2)
O1–C1–H1	118.1
C2–C1–H1	118.1
C3–C2–C7	119.46(19)
C3–C2–C1	119.63(19)
C7–C2–C1	120.91(19)
C4–C3–C2	120.81(19)
C4–C3–H3	119.6
C2–C3–H3	119.6
C3–C4–C5	119.04(19)
C3–C4–H4	120.5
C5–C4–H4	120.5
O2–C5–C4	116.41(18)
O2–C5–C6	122.39(17)
C4–C5–C6	121.13(18)
C7–C6–C5	119.34(18)
C7–C6–H6	120.3
C5–C6–H6	120.3
C6–C7–C2	120.19(19)
C6–C7–H7	119.9
C2–C7–H7	119.9
C9–C8–C13	121.99(18)
C9–C8–O2	119.09(17)
C13–C8–O2	118.85(17)
C8–C9–C10	119.59(18)
C8–C9–H9	120.2
C10–C9–H9	120.2
C9–C10–C11	119.53(18)
C9–C10–C14	118.39(18)
C11–C10–C14	122.05(18)
C12–C11–C10	120.13(18)
C12–C11–H11	119.9
C10–C11–H11	119.9
C11–C12–O6	124.38(18)
C11–C12–C13	121.17(18)
O6–C12–C13	114.31(17)
O5–C13–C8	124.70(18)
O5–C13–C12	117.71(17)
C8–C13–C12	117.58(18)
O3–C14–O4	123.19(19)
O3–C14–C10	124.86(18)
O4–C14–C10	111.94(16)
O4–C15–H15A	109.5
O4–C15–H15B	109.5
H15A–C15–H15B	109.5
O4–C15–H15C	109.5
H15A–C15–H15C	109.5
H15B–C15–H15C	109.5



---

C21–C16–C17	121.66(19)
C21–C16–O6	116.80(19)
C17–C16–O6	121.30(19)
C18–C17–C16	118.67(19)
C18–C17–H17	120.7
C16–C17–H17	120.7
C17–C18–C19	120.5(2)
C17–C18–H18	119.7
C19–C18–H18	119.7
C20–C19–C18	119.52(19)
C20–C19–C22	119.4(2)
C18–C19–C22	121.0(2)
C21–C20–C19	120.4(2)
C21–C20–H20	119.8
C19–C20–H20	119.8
C16–C21–C20	119.2(2)
C16–C21–H21	120.4
C20–C21–H21	120.4
O7–C22–C19	124.3(2)
O7–C22–H22	117.9
C19–C22–H22	117.9
C5–O2–C8	117.81(15)
C14–O4–C15	116.10(16)
C13–O5–H5	109.5
C12–O6–C16	119.33(15)

---

**Table 3 •** Anisotropic displacement parameters [ $\text{\AA}^2 \times 10^3$ ]. The anisotropic displacement factor exponent takes the form:  $-2\pi^2[h^2a^{*2}U^{11} + \dots + 2hk a^* b^* U^{12}]$ .

Atom	$U^{11}$	$U^{22}$	$U^{33}$	$U^{23}$	$U^{13}$	$U^{12}$
C1	29(1)	40(1)	24(1)	-3(1)	6(1)	0(1)
C2	23(1)	30(1)	24(1)	-2(1)	4(1)	0(1)
C3	28(1)	34(1)	21(1)	2(1)	2(1)	-1(1)
C4	25(1)	27(1)	26(1)	4(1)	2(1)	4(1)
C5	22(1)	26(1)	22(1)	-2(1)	6(1)	-2(1)
C6	26(1)	27(1)	21(1)	2(1)	3(1)	0(1)
C7	25(1)	28(1)	25(1)	0(1)	2(1)	4(1)
C8	28(1)	24(1)	20(1)	2(1)	8(1)	3(1)
C9	24(1)	25(1)	22(1)	0(1)	3(1)	5(1)
C10	22(1)	25(1)	24(1)	0(1)	6(1)	2(1)
C11	24(1)	28(1)	20(1)	1(1)	7(1)	0(1)
C12	22(1)	31(1)	19(1)	-4(1)	3(1)	1(1)
C13	22(1)	26(1)	23(1)	-2(1)	8(1)	0(1)
C14	23(1)	29(1)	23(1)	2(1)	6(1)	4(1)
C15	25(1)	36(1)	38(1)	6(1)	6(1)	-6(1)
C16	26(1)	32(1)	20(1)	-1(1)	-1(1)	-11(1)
C17	29(1)	29(1)	25(1)	2(1)	1(1)	3(1)
C18	30(1)	34(1)	23(1)	-1(1)	5(1)	2(1)
C19	27(1)	29(1)	23(1)	0(1)	-1(1)	-3(1)
C20	30(1)	30(1)	31(1)	2(1)	0(1)	2(1)
C21	24(1)	40(1)	28(1)	-7(1)	3(1)	0(1)
C22	37(1)	41(1)	28(1)	4(1)	2(1)	-2(1)
O1	37(1)	48(1)	31(1)	-6(1)	7(1)	10(1)
O2	31(1)	26(1)	21(1)	4(1)	9(1)	4(1)
O3	24(1)	41(1)	24(1)	2(1)	-1(1)	-4(1)
O4	24(1)	39(1)	27(1)	8(1)	1(1)	-7(1)
O5	28(1)	36(1)	26(1)	2(1)	8(1)	-8(1)
O6	28(1)	53(1)	19(1)	4(1)	0(1)	-13(1)
O7	59(1)	67(1)	33(1)	11(1)	13(1)	6(1)

**Table 4** • Hydrogen coordinates [ $\times 10^4$ ] and isotropic displacement parameters [ $\text{\AA}^2 \times 10^3$ ].

Atom	<i>x</i>	<i>y</i>	<i>z</i>	<i>U</i> <sub>eq</sub>	<i>S.o.f.</i>
H1	8309	3485	9265	37	1
H3	9552	1566	8817	33	1
H4	10426	447	7864	31	1
H6	8823	3571	6378	29	1
H7	7892	4626	7324	32	1
H9	11970	2888	6298	28	1
H11	10819	4028	4111	29	1
H15A	13675	7059	5069	49	1
H15B	13442	7087	4166	49	1
H15C	14371	5903	4609	49	1
H17	10349	1726	3106	34	1
H18	10423	2518	1874	35	1
H20	7635	5347	1957	37	1
H21	7540	4538	3183	37	1
H22	8449	5185	792	43	1
H5	8436	666	5582	45	1

**Table 5** • Hydrogen bonds [ $\text{\AA}$  and  $^\circ$ ].

<i>D</i> –H... <i>A</i>	<i>d</i> ( <i>D</i> –H)	<i>d</i> (H... <i>A</i> )	<i>d</i> ( <i>D</i> ... <i>A</i> )	$\angle$ ( <i>DHA</i> )
O5–H5...O1 <sup>i</sup>	0.84	1.86	2.654(2)	157.8
Possible intramolecular H-bond				
O5–H5...O2	0.84	2.41	2.834(2)	112.0
Symmetry transformations used to generate equivalent atoms:				
(i) $-x+3/2, y-1/2, -z+3/2$				

**Diffractometer:** *Nonius KappaCCD* area detector ( $\phi$  scans and  $\omega$  scans to fill *asymmetric unit* sphere).

**Cell determination:** DirAx (Duisenberg, A.J.M.(1992). *J. Appl. Cryst.* 25, 92-96.)

**Data collection:** Collect (Collect: Data collection software, R. Hooft, Nonius B.V., 1998).

**Data reduction and cell refinement:** *Denzo* (Z. Otwinowski & W. Minor, *Methods in Enzymology* (1997) Vol. **276: Macromolecular Crystallography**, part A, pp. 307–326; C. W. Carter, Jr. & R. M. Sweet, Eds., Academic Press).

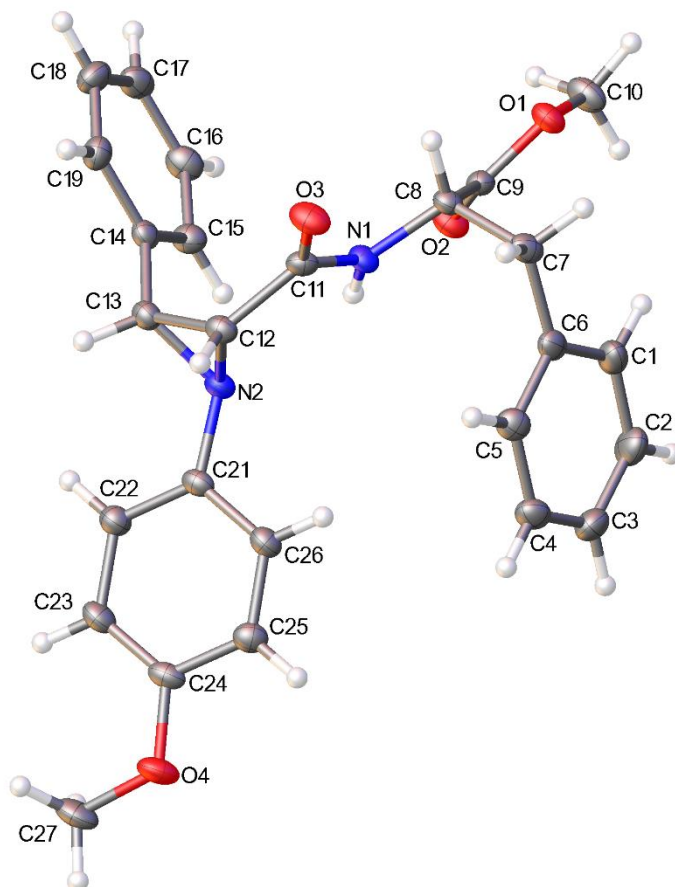
**Absorption correction:** *SADABS* (Sheldrick, G. M. (2007). *SADABS*. Version 2007/2. Bruker AXS Inc., Madison, Wisconsin, USA.).

**Structure solution:** *SHELXS97* (Sheldrick, G.M. (2008). *Acta Cryst.* A64, 112-122.).

**Structure refinement:** *SHELXL97* (G Sheldrick, G.M. (2008). *Acta Cryst.* A64, 112-122.).

**Graphics:** *OLEX2* (Dolomanov, O. V., Bourhis, L. J., Gildea, R. J., Howard, J. A. K. & Puschmann, H. (2009). *J. Appl. Cryst.* 42, 339-341.)

**Appendix 2: X-ray crystal structure and crystallographic data for *cis*-(S)-methyl 2-(1-(4-methoxyphenyl)-3-phenylaziridine-2-carboxamido)-3-phenylpropanoate 406a**



**Figure 1 •** Molecular structure of *rac,cis*-406a. Displacement ellipsoids – 50% probability.

**Crystal data and structure refinement details:**

Identification code	2012ncs0332 (PA531)	
Empirical formula	$C_{26}H_{26}N_2O_4$	
Formula weight	430.49	
Temperature	120(2) K	
Wavelength	0.71075 Å	
Crystal system	Triclinic	
Space group	<i>P</i> -1	
Unit cell dimensions	$a = 9.6355(2)$ Å	$\alpha = 98.751(7)^\circ$
	$b = 9.9156(2)$ Å	$\beta = 97.164(7)^\circ$
	$c = 12.9883(9)$ Å	$\gamma = 113.516(8)^\circ$
Volume	$1100.83(8)$ Å <sup>3</sup>	
<i>Z</i>	2	
Density (calculated)	1.299 Mg / m <sup>3</sup>	

---

Absorption coefficient	0.088 mm <sup>-1</sup>
<i>F</i> (000)	456
Crystal	Prism; colourless
Crystal size	0.60 × 0.37 × 0.17 mm <sup>3</sup>
$\theta$ range for data collection	2.99 – 27.45°
Index ranges	–12 ≤ <i>h</i> ≤ 12, –12 ≤ <i>k</i> ≤ 12, –16 ≤ <i>l</i> ≤ 14
Reflections collected	19839
Independent reflections	5019 [ <i>R</i> <sub>int</sub> = 0.0140]
Completeness to $\theta = 27.45^\circ$	99.7 %
Absorption correction	Semi-empirical from equivalents
Max. and min. transmission	0.9852 and 0.9491
Refinement method	Full-matrix least-squares on <i>F</i> <sup>2</sup>
Data / restraints / parameters	5019 / 0 / 295
Goodness-of-fit on <i>F</i> <sup>2</sup>	1.045
Final <i>R</i> indices [ <i>F</i> <sup>2</sup> > 2σ( <i>F</i> <sup>2</sup> )]	<i>R</i> 1 = 0.0348, <i>wR</i> 2 = 0.0926
<i>R</i> indices (all data)	<i>R</i> 1 = 0.0377, <i>wR</i> 2 = 0.0948
Largest diff. peak and hole	0.325 and –0.198 e Å <sup>-3</sup>

**Special details:**

The crystal structure of 2012ncs0332 (PA531) crystallises in centrosymmetric spacegroup triclinic P-1. This means, that the crystal structure is a 50/50 racemic mixture of two enantiomers.

**Table 1** • Atomic coordinates [ $\times 10^4$ ], equivalent isotropic displacement parameters [ $\text{\AA}^2 \times 10^3$ ] and site occupancy factors.  $U_{eq}$  is defined as one third of the trace of the orthogonalized  $U^{ij}$  tensor.

Atom	$x$	$y$	$z$	$U_{eq}$	$S.o.f.$
C1	8253(1)	−260(1)	7885(1)	30(1)	1
C2	9479(1)	−80(2)	7373(1)	35(1)	1
C3	9319(1)	−46(1)	6303(1)	30(1)	1
C4	7925(1)	−186(1)	5740(1)	26(1)	1
C5	6708(1)	−340(1)	6262(1)	24(1)	1
C6	6851(1)	−376(1)	7339(1)	22(1)	1
C7	5546(1)	−473(1)	7904(1)	23(1)	1
C8	5753(1)	1088(1)	8512(1)	18(1)	1
C9	7150(1)	1779(1)	9425(1)	18(1)	1
C10	8185(1)	1492(1)	11077(1)	29(1)	1
C11	4723(1)	2108(1)	7163(1)	19(1)	1
C12	5120(1)	3240(1)	6474(1)	20(1)	1
C13	5796(1)	4927(1)	6906(1)	20(1)	1
C14	6133(1)	5642(1)	8062(1)	19(1)	1
C15	7570(1)	6070(1)	8713(1)	24(1)	1
C16	7866(1)	6776(1)	9781(1)	27(1)	1
C17	6723(1)	7041(1)	10208(1)	27(1)	1
C18	5281(1)	6593(1)	9565(1)	28(1)	1
C19	4988(1)	5912(1)	8496(1)	24(1)	1
C21	7298(1)	4414(1)	5578(1)	19(1)	1
C22	7773(1)	5783(1)	5271(1)	23(1)	1
C23	8367(1)	5952(1)	4343(1)	24(1)	1
C24	8490(1)	4742(1)	3731(1)	22(1)	1
C25	8036(1)	3371(1)	4050(1)	23(1)	1
C26	7442(1)	3210(1)	4963(1)	22(1)	1
C27	9606(1)	6166(1)	2475(1)	32(1)	1
N1	5929(1)	2150(1)	7829(1)	19(1)	1
N2	6765(1)	4214(1)	6550(1)	19(1)	1
O1	6916(1)	959(1)	10170(1)	23(1)	1
O2	8307(1)	2895(1)	9473(1)	26(1)	1
O3	3370(1)	1207(1)	7093(1)	27(1)	1
O4	9032(1)	4765(1)	2801(1)	29(1)	1

**Table 2** • Bond lengths [Å] and angles [°].

---

C1–C2	1.3911(16)
C1–C6	1.3982(15)
C1–H1	0.9500
C2–C3	1.3857(16)
C2–H2	0.9500
C3–C4	1.3904(15)
C3–H3	0.9500
C4–C5	1.3940(14)
C4–H4	0.9500
C5–C6	1.3962(14)
C5–H5	0.9500
C6–C7	1.5114(13)
C7–C8	1.5497(13)
C7–H7A	0.9900
C7–H7B	0.9900
C8–N1	1.4510(11)
C8–C9	1.5181(13)
C8–H8	1.0000
C9–O2	1.2038(12)
C9–O1	1.3395(11)
C10–O1	1.4482(12)
C10–H10A	0.9800
C10–H10B	0.9800
C10–H10C	0.9800
C11–O3	1.2330(12)
C11–N1	1.3412(12)
C11–C12	1.5025(13)
C12–N2	1.4715(12)
C12–C13	1.5136(13)
C12–H12	1.0000
C13–N2	1.4565(12)
C13–C14	1.4943(13)
C13–H13	1.0000
C14–C15	1.3936(13)
C14–C19	1.3966(13)
C15–C16	1.3943(15)
C15–H15	0.9500
C16–C17	1.3891(15)
C16–H16	0.9500
C17–C18	1.3889(16)
C17–H17	0.9500
C18–C19	1.3892(15)
C18–H18	0.9500
C19–H19	0.9500
C21–C22	1.3876(13)
C21–C26	1.3974(14)

---

C21–N2	1.4326(11)
C22–C23	1.4010(14)
C22–H22	0.9500
C23–C24	1.3899(15)
C23–H23	0.9500
C24–O4	1.3747(12)
C24–C25	1.3971(14)
C25–C26	1.3838(13)
C25–H25	0.9500
C26–H26	0.9500
C27–O4	1.4276(13)
C27–H27A	0.9800
C27–H27B	0.9800
C27–H27C	0.9800
N1–H1N	0.855(14)
C2–C1–C6	120.71(10)
C2–C1–H1	119.6
C6–C1–H1	119.6
C3–C2–C1	120.47(10)
C3–C2–H2	119.8
C1–C2–H2	119.8
C2–C3–C4	119.73(10)
C2–C3–H3	120.1
C4–C3–H3	120.1
C3–C4–C5	119.61(10)
C3–C4–H4	120.2
C5–C4–H4	120.2
C4–C5–C6	121.37(10)
C4–C5–H5	119.3
C6–C5–H5	119.3
C5–C6–C1	118.09(9)
C5–C6–C7	120.66(9)
C1–C6–C7	121.20(9)
C6–C7–C8	112.83(8)
C6–C7–H7A	109.0
C8–C7–H7A	109.0
C6–C7–H7B	109.0
C8–C7–H7B	109.0
H7A–C7–H7B	107.8
N1–C8–C9	108.21(7)
N1–C8–C7	112.53(8)
C9–C8–C7	111.36(8)
N1–C8–H8	108.2
C9–C8–H8	108.2
C7–C8–H8	108.2
O2–C9–O1	124.67(9)
O2–C9–C8	125.14(8)
O1–C9–C8	110.19(8)



---

O1–C10–H10A	109.5
O1–C10–H10B	109.5
H10A–C10–H10B	109.5
O1–C10–H10C	109.5
H10A–C10–H10C	109.5
H10B–C10–H10C	109.5
O3–C11–N1	123.93(9)
O3–C11–C12	120.75(8)
N1–C11–C12	115.32(8)
N2–C12–C11	117.86(8)
N2–C12–C13	58.39(6)
C11–C12–C13	123.55(8)
N2–C12–H12	115.0
C11–C12–H12	115.0
C13–C12–H12	115.0
N2–C13–C14	117.63(8)
N2–C13–C12	59.36(6)
C14–C13–C12	123.57(8)
N2–C13–H13	114.9
C14–C13–H13	114.9
C12–C13–H13	114.9
C15–C14–C19	119.21(9)
C15–C14–C13	121.60(9)
C19–C14–C13	119.17(9)
C14–C15–C16	120.34(9)
C14–C15–H15	119.8
C16–C15–H15	119.8
C17–C16–C15	120.15(10)
C17–C16–H16	119.9
C15–C16–H16	119.9
C18–C17–C16	119.63(10)
C18–C17–H17	120.2
C16–C17–H17	120.2
C17–C18–C19	120.44(10)
C17–C18–H18	119.8
C19–C18–H18	119.8
C18–C19–C14	120.21(9)
C18–C19–H19	119.9
C14–C19–H19	119.9
C22–C21–C26	119.34(9)
C22–C21–N2	122.37(9)
C26–C21–N2	118.12(8)
C21–C22–C23	120.50(9)
C21–C22–H22	119.7
C23–C22–H22	119.7
C24–C23–C22	119.66(9)
C24–C23–H23	120.2
C22–C23–H23	120.2
O4–C24–C23	124.97(9)

---

O4–C24–C25	115.14(9)
C23–C24–C25	119.89(9)
C26–C25–C24	120.09(9)
C26–C25–H25	120.0
C24–C25–H25	120.0
C25–C26–C21	120.49(9)
C25–C26–H26	119.8
C21–C26–H26	119.8
O4–C27–H27A	109.5
O4–C27–H27B	109.5
H27A–C27–H27B	109.5
O4–C27–H27C	109.5
H27A–C27–H27C	109.5
H27B–C27–H27C	109.5
C11–N1–C8	122.31(8)
C11–N1–H1N	117.6(9)
C8–N1–H1N	120.0(9)
C21–N2–C13	120.15(8)
C21–N2–C12	117.80(7)
C13–N2–C12	62.25(6)
C9–O1–C10	115.43(8)
C24–O4–C27	117.50(8)

---

**Table 3** • Anisotropic displacement parameters [ $\text{\AA}^2 \times 10^3$ ]. The anisotropic displacement factor exponent takes the form:  $-2\pi^2[h^2a^{*2}U^{11} + \dots + 2hk a^* b^* U^{12}]$ .

Atom	$U^{11}$	$U^{22}$	$U^{33}$	$U^{23}$	$U^{13}$	$U^{12}$
C1	44(1)	35(1)	23(1)	11(1)	9(1)	27(1)
C2	39(1)	45(1)	33(1)	11(1)	7(1)	31(1)
C3	35(1)	31(1)	32(1)	7(1)	14(1)	20(1)
C4	34(1)	25(1)	20(1)	3(1)	8(1)	12(1)
C5	25(1)	23(1)	20(1)	2(1)	3(1)	8(1)
C6	30(1)	16(1)	22(1)	4(1)	7(1)	10(1)
C7	28(1)	17(1)	21(1)	4(1)	8(1)	5(1)
C8	19(1)	19(1)	17(1)	7(1)	7(1)	6(1)
C9	21(1)	19(1)	18(1)	6(1)	8(1)	10(1)
C10	25(1)	37(1)	23(1)	13(1)	2(1)	9(1)
C11	20(1)	21(1)	15(1)	3(1)	6(1)	7(1)
C12	18(1)	23(1)	16(1)	6(1)	3(1)	7(1)
C13	20(1)	22(1)	19(1)	8(1)	5(1)	9(1)
C14	23(1)	16(1)	20(1)	7(1)	6(1)	7(1)
C15	22(1)	27(1)	22(1)	6(1)	6(1)	9(1)
C16	26(1)	28(1)	22(1)	5(1)	2(1)	7(1)
C17	37(1)	22(1)	21(1)	4(1)	8(1)	11(1)
C18	33(1)	25(1)	31(1)	4(1)	13(1)	16(1)
C19	24(1)	21(1)	27(1)	5(1)	5(1)	12(1)
C21	17(1)	24(1)	16(1)	7(1)	3(1)	7(1)
C22	24(1)	22(1)	22(1)	7(1)	6(1)	9(1)
C23	25(1)	24(1)	23(1)	12(1)	7(1)	7(1)
C24	18(1)	28(1)	16(1)	7(1)	4(1)	5(1)
C25	22(1)	24(1)	19(1)	4(1)	4(1)	7(1)
C26	23(1)	21(1)	21(1)	8(1)	5(1)	7(1)
C27	31(1)	38(1)	26(1)	17(1)	12(1)	7(1)
N1	17(1)	19(1)	20(1)	8(1)	5(1)	5(1)
N2	19(1)	21(1)	17(1)	7(1)	5(1)	7(1)
O1	22(1)	25(1)	20(1)	10(1)	4(1)	7(1)
O2	21(1)	26(1)	26(1)	10(1)	5(1)	4(1)
O3	18(1)	32(1)	25(1)	10(1)	4(1)	3(1)
O4	33(1)	32(1)	20(1)	9(1)	12(1)	8(1)

**Table 4** • Hydrogen coordinates [ $\times 10^4$ ] and isotropic displacement parameters [ $\text{\AA}^2 \times 10^3$ ].

Atom	<i>x</i>	<i>y</i>	<i>z</i>	<i>U</i> <sub>eq</sub>	<i>S.o.f.</i>
H1	8370	−305	8615	36	1
H2	10433	21	7758	41	1
H3	10158	72	5955	36	1
H4	7803	−175	5004	32	1
H5	5762	−423	5876	29	1
H7A	5481	−1134	8413	28	1
H7B	4558	−942	7374	28	1
H8	4812	944	8815	22	1
H10A	9080	1402	10845	43	1
H10B	7872	884	11606	43	1
H10C	8462	2551	11393	43	1
H12	4471	2876	5739	24	1
H13	5520	5504	6411	24	1
H15	8352	5881	8427	28	1
H16	8852	7075	10219	33	1
H17	6925	7526	10935	33	1
H18	4490	6753	9859	34	1
H19	4006	5629	8058	28	1
H22	7695	6611	5692	27	1
H23	8684	6890	4134	29	1
H25	8135	2548	3638	27	1
H26	7131	2274	5174	26	1
H27A	8792	6520	2394	48	1
H27B	9923	6024	1793	48	1
H27C	10497	6914	3013	48	1
H1N	6830(16)	2804(15)	7818(10)	27(3)	1

**Diffractometer:** *Rigaku R-Axis Spider* including curved Fujifilm image plate and a graphite monochromated sealed tube Mo generator.

**Cell determination and data collection:** *CrystalClear-SM Expert 2.0 r11* (Rigaku, 2011).

**Data reduction, cell refinement and absorption correction:** *CrystalClear-SM Expert 2.0 r13* (Rigaku, 2011).

**Structure solution:** *SHELXS97* (Sheldrick, G.M. (2008). Acta Cryst. A64, 112-122).

**Structure refinement:** *SHELXL97* (Sheldrick, G.M. (2008). Acta Cryst. A64, 112-122).

**Graphics:** *OLEX2* (Dolomanov, O. V., Bourhis, L. J., Gildea, R. J., Howard, J. A. K. & Puschmann, H. (2009). J. Appl. Cryst. 42, 339-341).